

Four new erythroneurine leafhopper species from karst areas in Southwestern China (Hemiptera, Cicadellidae, Typhlocybinae, Erythroneurini)

Jinxiu Wang^{1,2}, Wenming Xu^{1,2}, Tianyi Pu^{1,2}, Ni Zhang^{1,2}, Yuehua Song^{1,2}

¹ School of Karst Science, Guizhou Normal University, Guiyang 550001, China

² State Engineering Technology Institute for Karst Desertification Control, Guiyang 550001, China

Corresponding author: Yuehua Song (songyuehua@163.com)

Abstract

Four new erythroneurine leafhopper species, *Empoascanara aparoides* Wang & Song, **sp. nov.**, *Motaga mengyangensis* Wang & Song, **sp. nov.**, *Motaga acicularis* Wang & Song, **sp. nov.**, and *Tautoneura qingxiuensis* Wang & Song, **sp. nov.** from karst areas in Southwestern China, are described and illustrated.

Key words: Homoptera, morphology, new taxa, taxonomy

Introduction

Erythroneurini is the largest tribe of Typhlocybinae (Yuan et al. 2014). Erythroneurine leafhoppers are rich in diversity and have a body length of less than 5 mm. There are approximately 2,000 species worldwide, which are difficult to identify (Song and Li 2014). They feed on the leaf parenchyma cell contents and can cause harm to agricultural crops and forest trees of economic importance (Lu et al. 2021).

The genus *Empoascanara* was established by Distant (1918) with *Empoascanara prima* Distant, 1918 as its type species. Subsequently, other researchers have described many new species. There are currently 92 *Empoascanara* species known, most of which are found in the Australian, Afrotropical, and Oriental regions. The genus *Motaga* was established by Dworakowska (1979) with *Motaga rokfa* Dworakowska, 1979 as its type species. Only five species are known, and the genus is currently known only from the Oriental region. The genus *Tautoneura* was established by Anufriev (1969) with *Tautoneura tricolor* Anufriev, 1969 as its type species. It contains 64 species, of which 22 were previously known from China until now.

As part of this work, some interesting erythroneurine leafhopper materials from karst areas of Southwestern China were collected. Following examination and comparison of these materials, four new species, *Empoascanara aparoides* Wang & Song, **sp. nov.**, *Motaga mengyangensis* Wang & Song, **sp. nov.**, *Motaga acicularis* Wang & Song, **sp. nov.**, and *Tautoneura qingxiuensis* Wang & Song, **sp. nov.**, were discovered, and these are described and illustrated in this paper.



Academic editor: Allen Sanborn

Received: 1 March 2024

Accepted: 5 May 2024

Published: 3 June 2024

ZooBank: <https://zoobank.org/C881A211-879C-438A-9B89-27A4698492E1>

Citation: Wang J, Xu W, Pu T, Zhang N, Song Y (2024) Four new erythroneurine leafhopper species from karst areas in Southwestern China (Hemiptera, Cicadellidae, Typhlocybinae, Erythroneurini). ZooKeys 1204: 1–13. <https://doi.org/10.3897/zookeys.1204.122042>

Copyright: © Jinxiu Wang et al.
This is an open access article distributed under terms of the Creative Commons Attribution License (Attribution 4.0 International – CC BY 4.0).

Materials and methods

Specimens were collected by sweeping-net method. Male genitalia and abdominal apodemes were dissected and cleared in a 10% NaOH solution. Morphological terminology used in this study follows Dietrich (2005) and Song and Li (2013). The specimens were observed and drawn under Olympus SZX16 and Olympus BX53 microscopes, respectively. A Keyence VHX-5000 digital microscope was used for photography. The length of erythroneurine leafhoppers was measured from the apex of the head to the tip of the folded forewing. All specimens examined are deposited in the collection of the School of Karst Science, Guizhou Normal University, China (GZNU).

Taxonomy

Empoascanara (Empoascanara) Distant, 1918

Empoascanara Distant, 1918: 94.

Type species. *Empoascanara prima* Distant, 1918, by original designation.

Description. Dorsum yellow, white, pale red or brown. Crown broadly rounded medially. Vertex unicolorous, with a single dark median apical spot or a pair of spots. Crown nearly equal, slightly wider or narrower than widest part of pronotum. Pronotum pale, with darker posterior margin. Forewings with or without markings.

Male genitalia. Pygofer microtrichia well developed. Pygofer lobe with caudal margin rounded or angulate. Dorsal pygofer appendage movably articulated, with or without ventral pygofer appendage. Subgenital plate expanded subbasally, with 2–4 basal macrosetae and numerous short stout setae along upper margin in lateral view. Style with preapical lobe prominent. Aedeagus with dorsal apodeme not or slightly expanded in lateral view. Aedeagal shaft usually symmetrical, slender in lateral view. Aedeagus with or without apical, subapical, or basal processes, and with or without preatrial ventral process or processes. Connective with median anterior lobe and arms short.

Distribution. Oriental, Afrotropical, and Australian regions.

Empoascanara (Empoascanara) aparaoides Wang & Song, sp. nov.

<https://zoobank.org/33509E60-DC24-4BDD-9B8E-6ECDA5536AEE>

Figs 1–12

Diagnosis. The new species can be distinguished from other species by the aedeagal shaft with one pair of longer subapical processes and one pair of shorter apical processes; the aedeagus without any basal process; the subgenital plate provided with three macrosetae on lateral surface; the pygofer dorsal appendage tapering towards apex; the connective with body strong, but lateral arms and central lobe short.

Description. Body small, ochraceous with brown markings. Vertex ochre-yellow; with one large, irregular, brown spot in middle of anterior margin (Figs 1, 3). Crown nearly equal to widest part of pronotum. Pronotum with anterior part



Figures 1–4. *Empoascanara (Empoascanara) aparaoides* Wang & Song, sp. nov. 1 habitus, dorsal view 2 habitus, lateral view 3 head and thorax, dorsal view 4 face.

ochraceous and brownish posterior part; posterior margin concave (Figs 1, 3). Crown with coronal suture short. Eyes black. Mesonotum ochraceous. Face milky yellow (Figs 2, 4). Forewing hyaline with brownish tinge (Figs 1, 3).

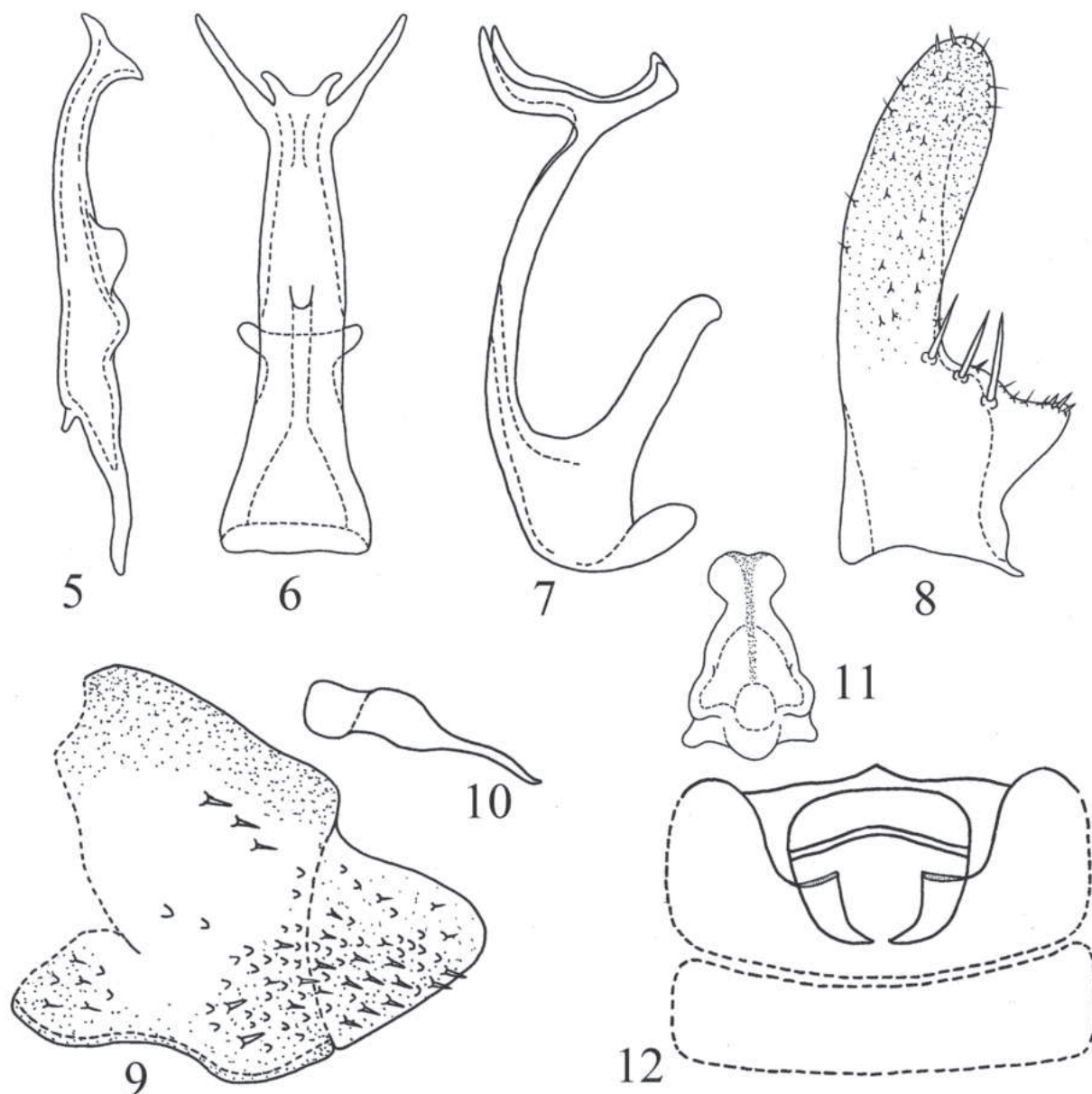
Male abdominal apodemes small, not exceeding 3rd sternite (Fig. 12).

Male genitalia. Pygofer lobe with numerous microsetae distributed densely at ventrolateral area and caudal part; three peg-like setae located on subdorsal area (Fig. 9). Dorsal pygofer appendage long, tapering towards apex (Fig. 10). Style slim (Fig. 5). Subgenital plate subbasally broadened, with three macrosetae on lateral surface, several peg-like setae distributed at subbase and apex; several microsetae scattered on apical part (Fig. 8). Aedeagal shaft long, provided with longer pair of subapical processes and a shorter apical pair of processes. Gonopore located at about mid-length of shaft on ventral surface (Figs 6, 7). Connective Y-shaped, with robust central lobe and two short lateral arms (Fig. 11).

Specimens examined. Holotype: ♂; CHINA, Yunnan Prov., Jinghong; 6 August 2021; Jinqiu Wang leg.; GZNU-2021-YN-JH-11-001. **Paratypes:** 18 ♂♂, 24 ♀♀; same data as holotype; GZNU-2021-YN-JH-11-002 to 043.

Measurements. Male length 2.3–2.4 mm, female length 2.4–2.5 mm.

Remarks. This species is similar to *Empoascanara apara* Dworakowska, 1979, but can be distinguished by its differently shaped pygofer dorsal process



Figures 5–12. *Empoascanara (Empoascanara) aparaoides* Wang & Song, sp. nov. 5 style 6 aedeagus, ventral view 7 aedeagus, lateral view 8 subgenital plate 9 pygofer lobe 10 dorsal pygofer appendage, lateral view 11 connective 12 abdominal apodemes.

and an aedeagal shaft with one pair of long and one pair of short apical processes compared to only one pair of long processes in *E. apara*; also, the aedeagal shaft in *E. aparaoides* is without the medial hook-like process of *E. apara*.

Etymology. The new species is named from the similar species, *E. apara*, the Greek suffix *-oides* denotes the similarity of the new species to *E. apara*.

***Motaga* Dworakowska, 1979**

Motaga Dworakowska, 1979: 12.

Type species. *Motaga rokfa* Dworakowska, 1979, by original designation.

Description. Body gray to brown, without or with markings. Eyes gray to black. Crown fore margin weakly produced, broadly rounded apically. Pronotum usually without conspicuous pits. Mesonotum grayish brown. Forewing transparent or semitransparent. Peripheral vein at costal margin of hind wing absent.

Male genitalia. Pygofer lobe broad, sparse setae on outer surface. Pygofer dorsal appendage curved ventrally in lateral view. Pygofer ventral appendage absent. Subgenital plate with 2–4 basal macrosetae; numerous short and stout setae forming continuous row from subbase to apex; several microsetae scattered on apical disc. Style apex truncated or expanded, foot-like. Connective with central lobe large. Aedeagus with dorsal apodeme expanded in lateral view; aedeagal shaft slender, curved dorsad in lateral view, with paired processes arising from base and shorter than shaft.

Distribution. Oriental region.

***Motaga mengyangensis* Wang & Song, sp. nov.**

<https://zoobank.org/F4C1D37F-9AA3-4108-B407-937E4BCC7DBF>

Figs 13–24

Diagnosis. The new species can be distinguished from other species by the aedeagal shaft bifurcated at apex, crab claw-like, with one pair $\frac{1}{2}$ length of aedeagal shaft basal processes; pygofer dorsal appendage expanded at base and tapering towards apex; subgenital plate with row of four macrosetae medially on outer surface; connective with central lobe broad and stem well developed.

Description. Body brown (Figs 13, 16). Head slightly narrower than pronotum (Fig. 15). Crown fore margin strongly produced, with two irregular, medial, amber-colored patches (Figs 13, 15). Anterior part of pronotum light brown; posterior margin slightly darkened, with one nearly V-shaped, milky-white stripe. Coronal suture well developed. Eyes black (Figs 13, 14). Mesonotum brown. Forewing grayish brown (Fig. 14).

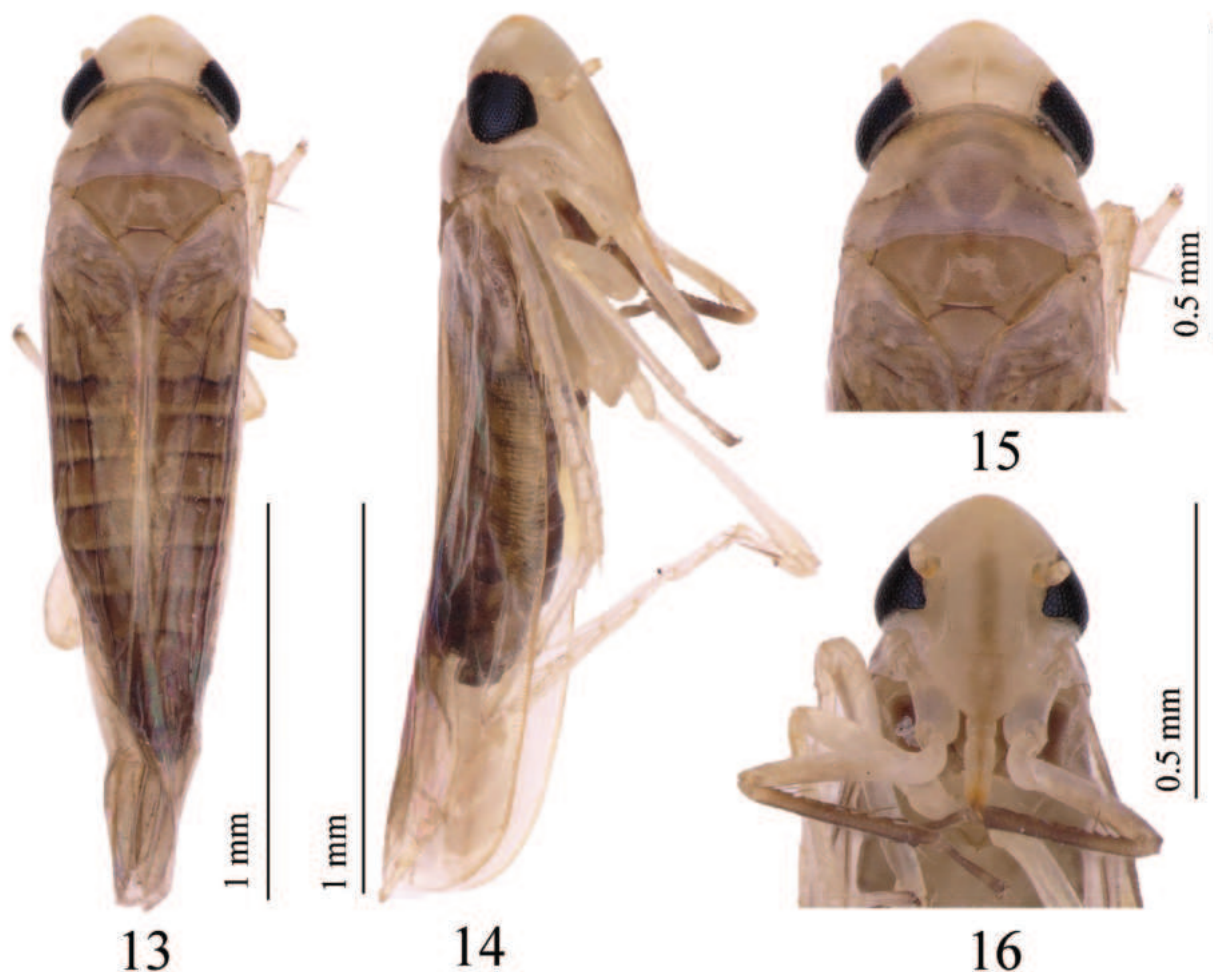
Male abdominal apodemes broad, extending to anterior margin of 4th sternite (Fig. 24).

Male genitalia. Pygofer lobe broad, with numerous microtrichia scattered along caudal edge and dorsal margin (Fig. 21). Dorsal pygofer appendage with wide base and sharp apex (Fig. 22). Subgenital plate with a row of four macrosetae in middle and with marginal peg-like setae from subbase to apex forming continuous row (Fig. 20). Style long and slender (Fig. 17). Connective with lateral arms strong, central lobe broad and stem well developed (Fig. 23). Aedeagal shaft long, straight in ventral view, curved dorsad in lateral view, bifurcated at apex; crab claw-like and with pair of basal long processes; gonopore located at $\frac{1}{2}$ height of aedeagal shaft, ventrad (Figs 18, 19).

Specimens examined. *Holotype*: ♂; CHINA, Yunnan Prov., Jinghong City, Mnegyang Town; 2 August 2021; Tianyi Pu leg.; GZNU-2021-YN-JH-6-001. *Paratypes*: 41 ♂♂, 58 ♀♀, same data as holotype; GZNU-2021-YN-JH-6-002 to 100.

Measurements. Male length 2.3–2.4 mm, female length 2.4–2.5 mm (including wings).

Remarks. This species is very similar to *Motaga fara* Dworakowska, 1980, but it differs from *M. fara* in having the dorsal pygofer process with a stouter base, the length of the aedeagal shaft proportionally longer compared to the



Figures 13–16. *Motaga mengyangensis* Wang & Song, sp. nov. 13 habitus, dorsal view 14 habitus, lateral view 15 head and thorax, dorsal view 16 face.

basal processes, and the gonopore located at about halfway along the length of the aedeagal shaft.

Etymology. The new species is named after its type locality, Mengyang Town.

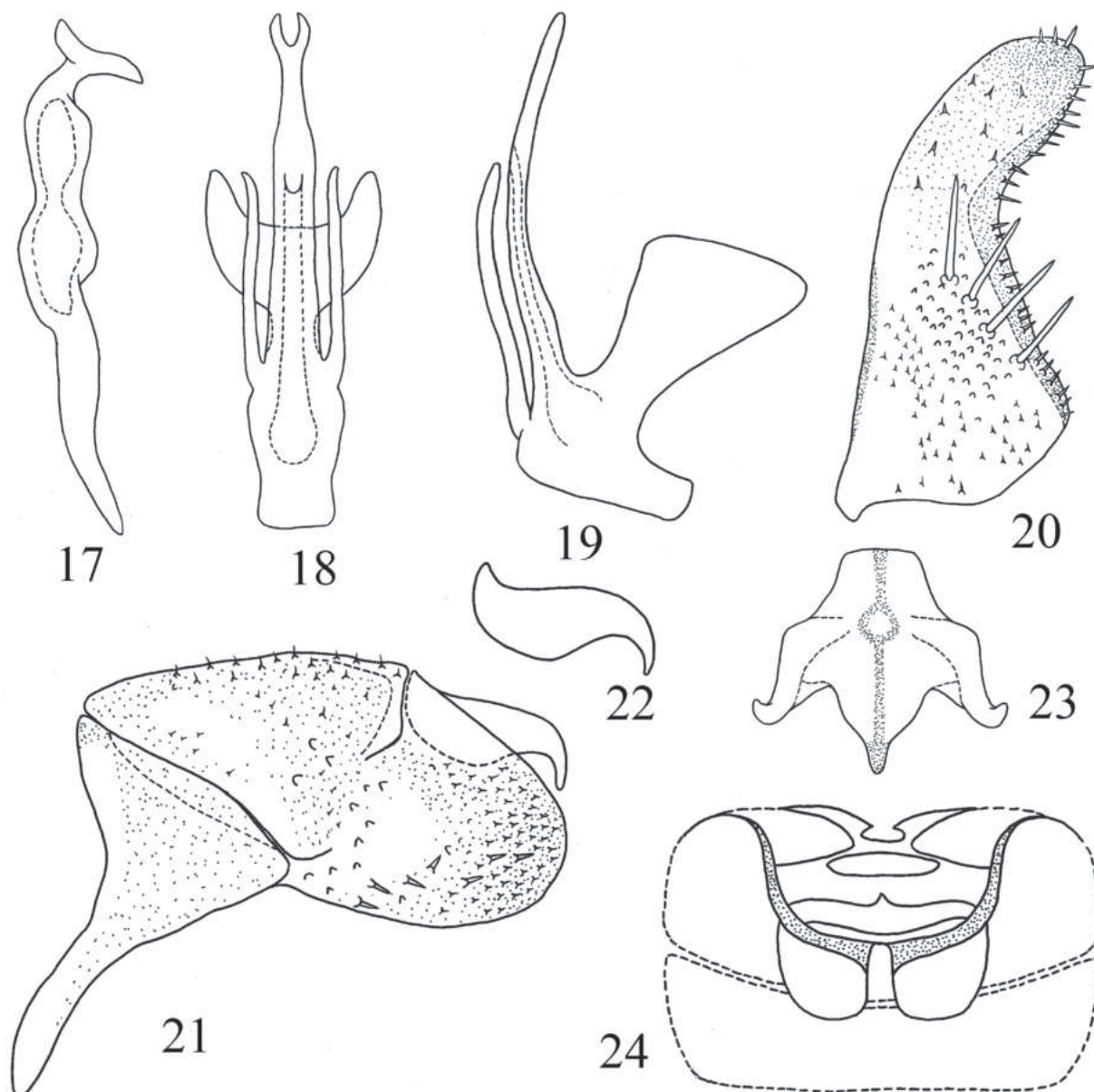
***Motaga acicularis* Wang & Song, sp. nov.**

<https://zoobank.org/4F5E5783-D358-4D31-82CE-C3E376DF6E64>

Figs 25–36

Diagnosis. The new species can be distinguished from other *Motaga* species by its extremely long and slender in lateral view aedeagal shaft, which has a pair of short basal processes that are not bifurcated at apex; the pygofer dorsal appendage, which tapers to the apex and is bent ventrad and hook-like apically; the connective with two long arms; the subgenital plate with four macrosetae; and the very small male abdominal apodemes.

Description. Vertex light brown (Figs 25, 27). Crown fore margin strongly produced, median length of crown slightly less than width between eyes (Figs 25, 27). Crown nearly equal to width of pronotum. Pronotum and mesonotum

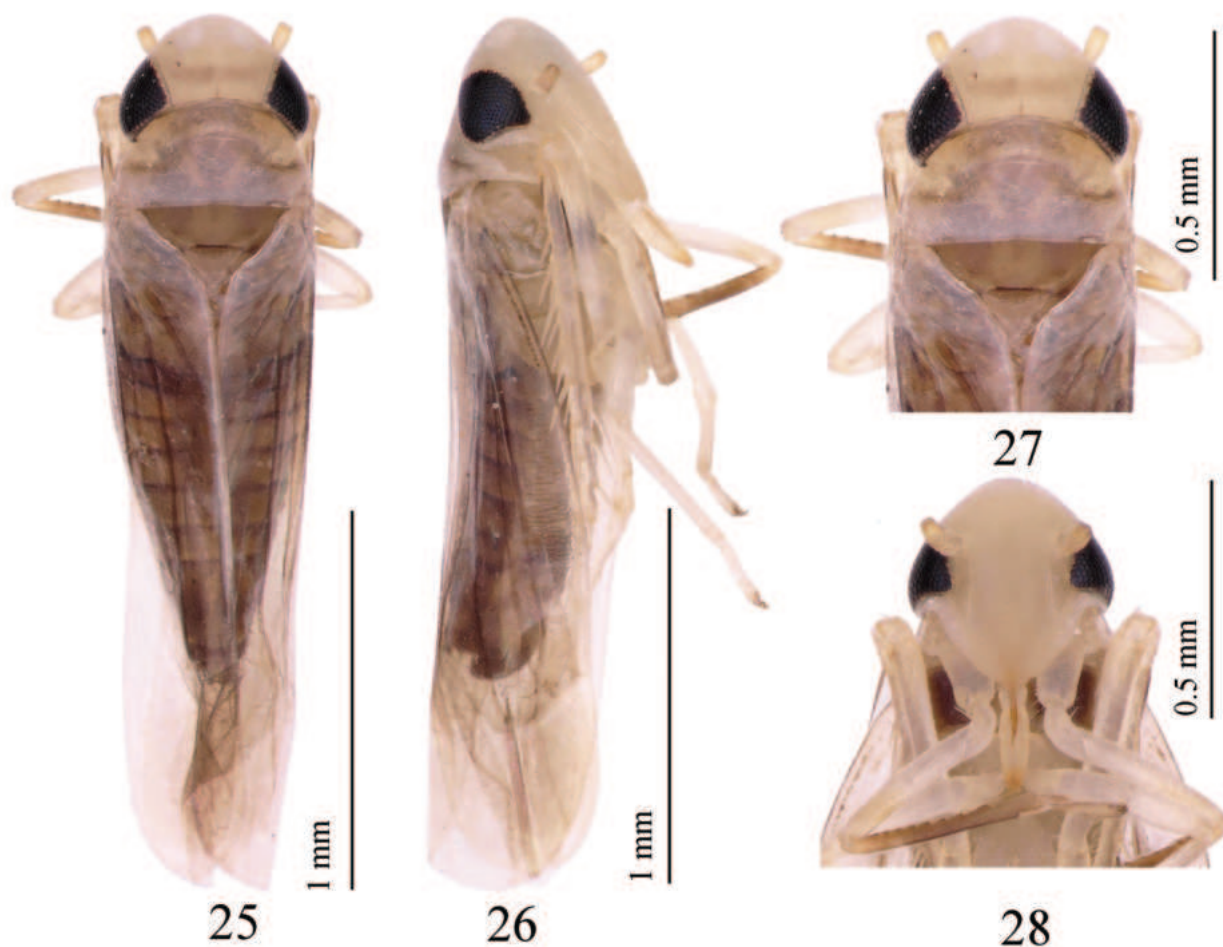


Figures 17–24. *Motaga mengyangensis* Wang & Song, sp. nov. 17 style 18 aedeagus, ventral view 19 aedeagus, lateral view 20 subgenital plate 21 pygofer lobe 22 dorsal pygofer appendage, lateral view 23 connective 24 abdominal apodemes.

brownish yellow, posterior margin of pronotum almost straight (Figs 25, 27). Eyes black (Fig. 26). Forewings without spots, semitransparent (Figs 25, 26).

Male abdominal apodemes extremely small, not exceeding 3rd sternite (Fig. 36).

Male genitalia. Pygofer lobe broad, with numerous microtrichia; several peg-like setae scattered on middle area and hind edge (Fig. 33). Dorsal pygofer appendage with base expanded, with hook-like apex (Fig. 34). Subgenital plate with four macrosetae medially on lateral margin and numerous microsetae distributed along upper margin (Fig. 32). Style apex truncate and slightly expanded (Fig. 29). Connective with lateral arms robust, with obvious central lobe (Fig. 35). Aedeagal shaft long, slender, with paired processes at base (Figs 30, 31). Preatrium short; dorsal apodeme well developed, with apex bifurcate; gonopore located at basal 1/3 of aedeagal shaft (Figs 30, 31).



Figures 25–28. *Motaga acicularis* Wang & Song, sp. nov. 25 habitus, dorsal view 26 habitus, lateral view 27 head and thorax, dorsal view 28 face.

Specimens examined. Holotype: ♂; CHINA, Guangxi Prov., Liuzhou; 18 July 2021; Ni Zhang leg.; GZNU-2021-GX-LZ-8-001. **Paratypes:** 96 ♂♂, 144 ♀♀; same data as holotype; GZNU-2021-GX-LZ-8-002 to 241.

Measurements. Male length 2.3–2.4 mm, female length 2.4–2.5 mm (including wings).

Remarks. This species is very similar to *Motaga rokfa* Dworakowska, 1979 but can be distinguished by having the aedeagal shaft without a bifurcated apex, the preatrium expanded but short, and the paired basal processes approximately 1/3 length of aedeagal shaft.

Etymology. The species epithet is the Latin word *acicularis*, which means slender, as a needle and refers to the needle-like aedeagal shaft.

***Tautoneura* Anufriev, 1969**

Tautoneura Anufriev, 1969: 186. Type species: *Tautoneura tricolor* Anufriev, 1969.

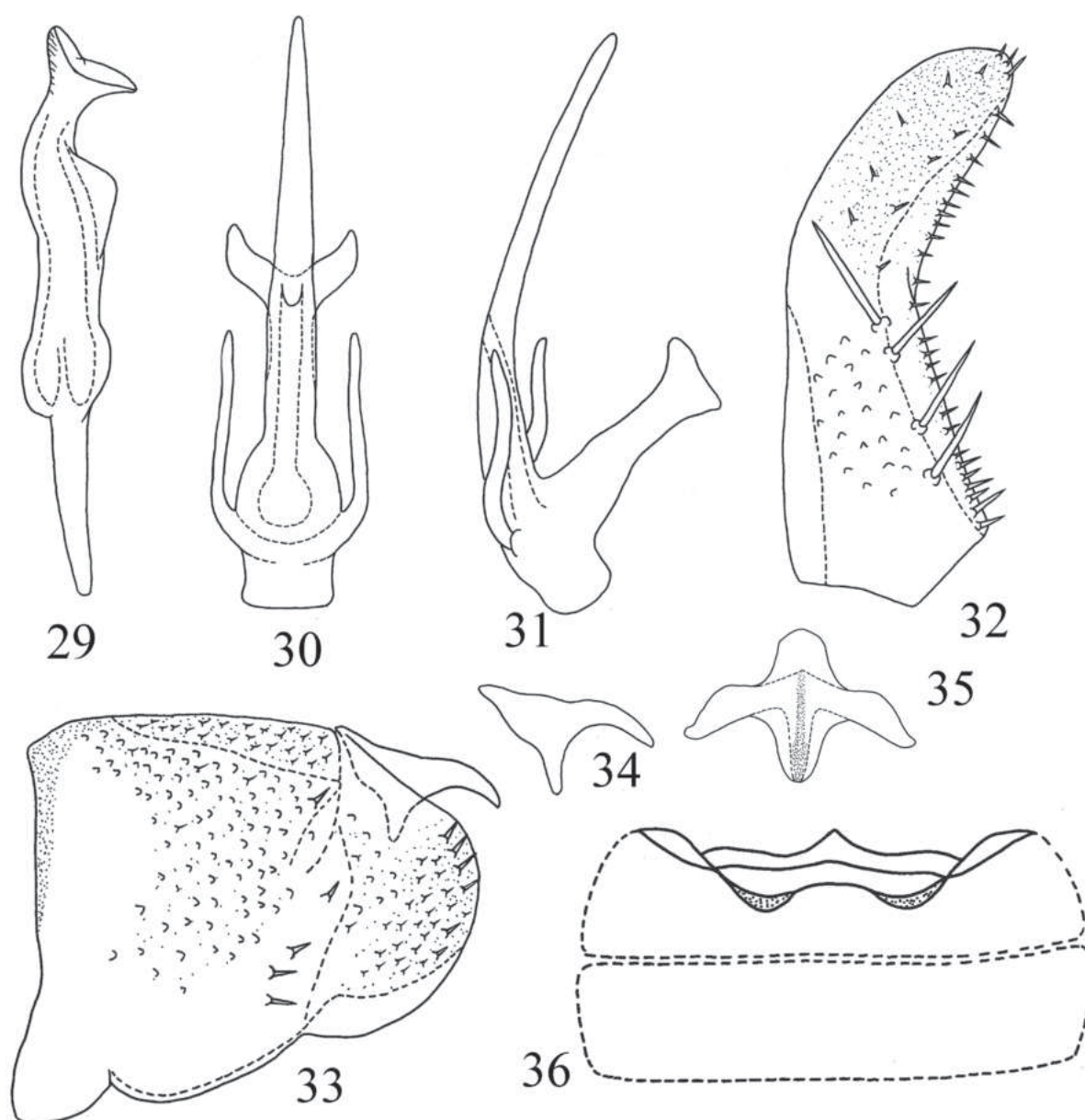
Erythroneura (*Balila*) Dworakowska, 1970: 347. Type species: *Chlorita mori* Matsuura, 1906.

Havelia Ahmed, 1971: 277. Type species: *Havelia alba* Ahmed, 1971.

Description. Body white to yellow. Crown fore margin strongly produced medially, and slightly narrower or slightly wider than pronotum. Pronotum broad, with or without irregular spots. Mesonotum white to yellow, with basal triangles dark or indistinct. Forewing transparent, usually with single or multiple patches.

Male genitalia. Pygofer lobe rounded, usually with several macrosetae at basal ventral angle and few peg-like setae at distal part on inner surface. Pygofer dorsal appendage slender and apically tapering, ventral appendage absent or present. Subgenital plate lateral margin distinctly widened subbasally, with 2–4 basal macrosetae. Style preapical lobe prominent, apex slender or truncate and expanded or with three points. Connective M- or Y-shaped, with slender median anterior lobe. Aedeagus dorsal apodeme usually expanded in lateral view; aedeagal shaft usually with single or paired processes apically and of variable length.

Distribution. Palaearctic and Oriental regions.



Figures 29–36. *Motaga acicularis* Wang & Song, sp. nov. 29 style 30 aedeagus, ventral view 31 aedeagus, lateral view 32 subgenital plate 33 pygofer lobe 34 dorsal pygofer appendage, lateral view 35 connective 36 abdominal apodemes.

***Tautoneura qingxiuensis* Wang & Song, sp. nov.**

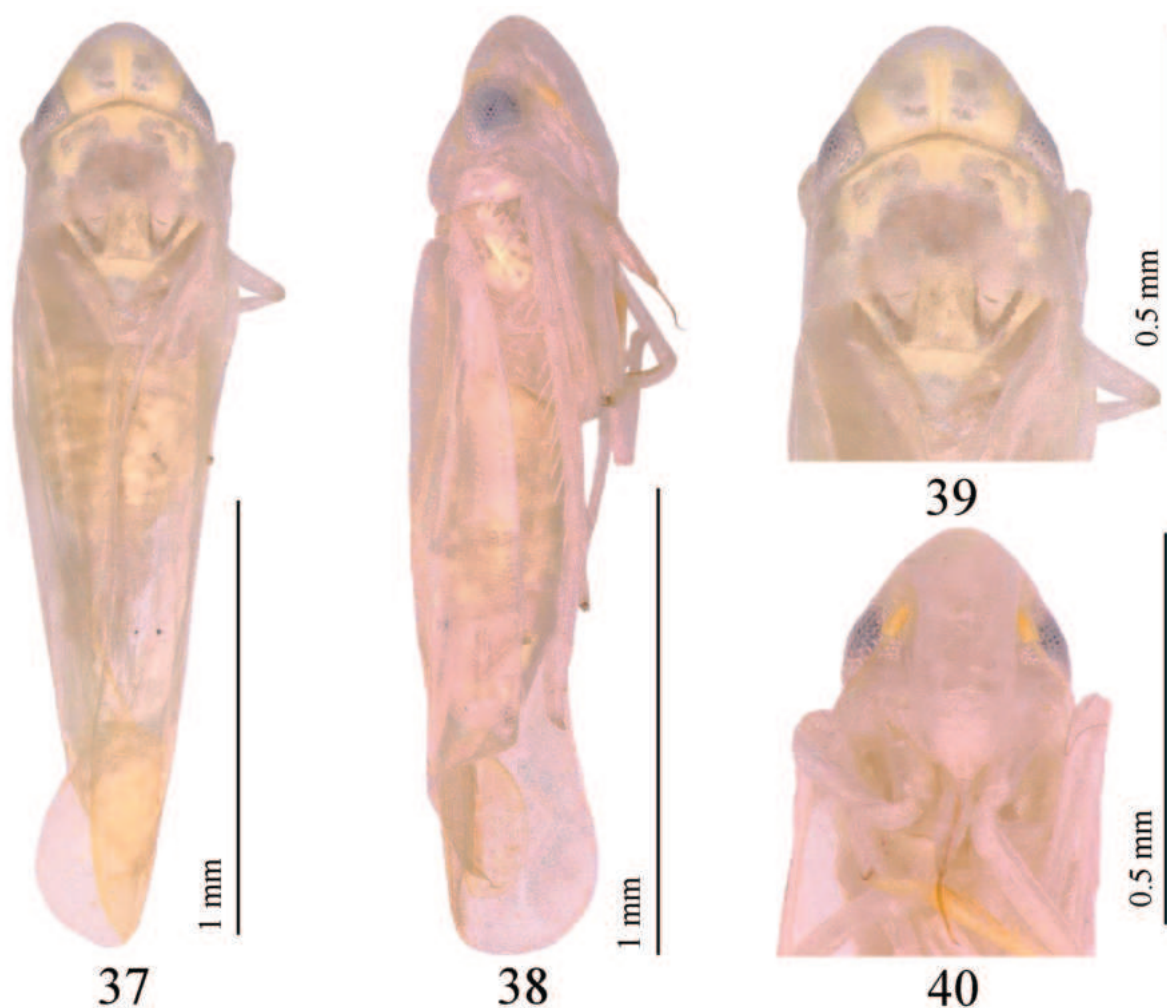
<https://zoobank.org/F0B7D9BC-841C-4816-A9A2-0BD3B59BC2A7>

Figs 37–48

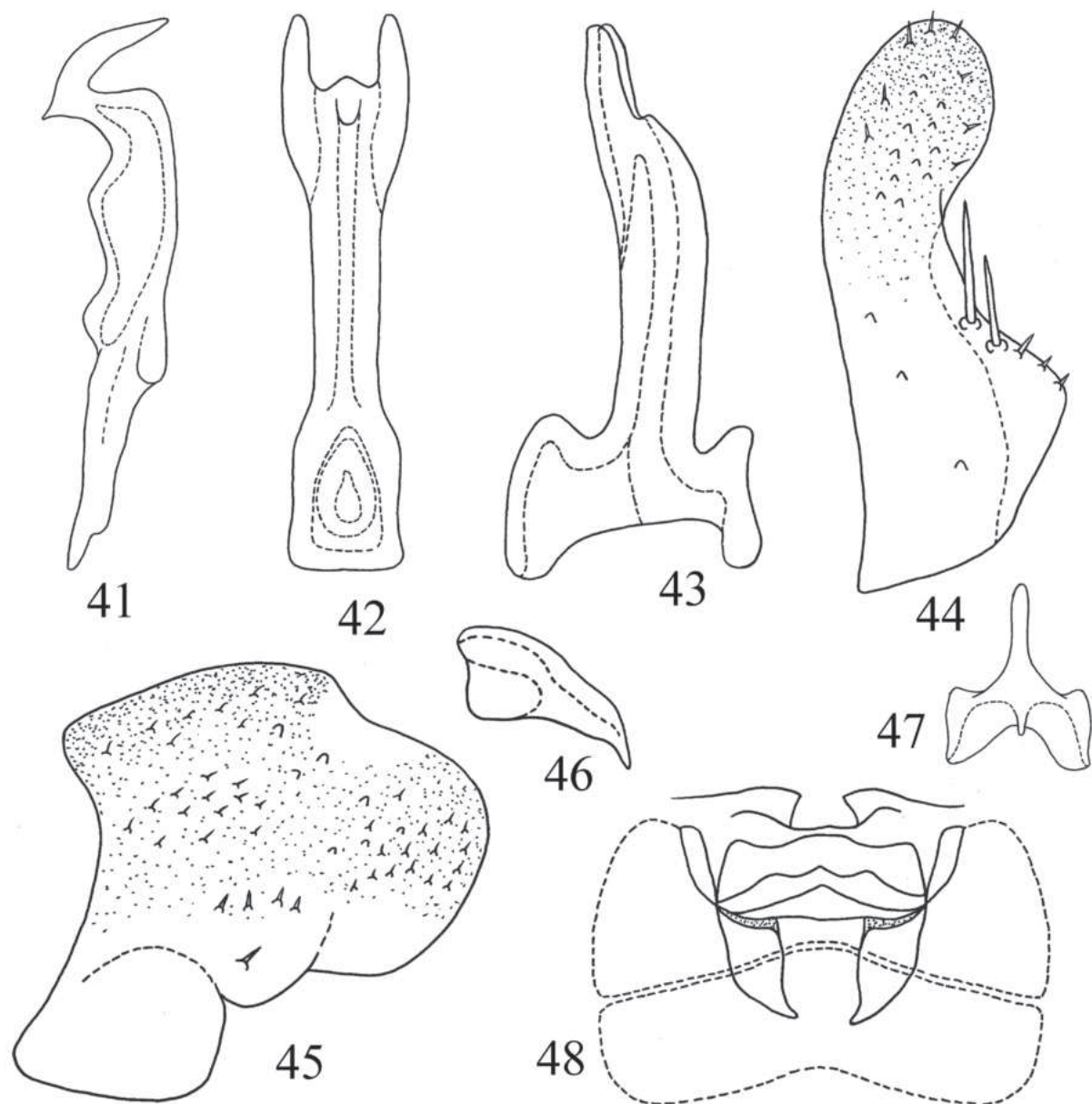
Diagnosis. The new species can be distinguished from other *Tautoneura* species by subapically broadened the aedeagal shaft in ventral view, with one pair of processes at apex; the extremely short preatrium; the apical gonopore; the dorsal pygofer appendage with base expanded; and the Y-shaped connective, with long, slim stem.

Description. Body milky-yellow (Figs 37, 40). Vertex milky-yellow, with pair of gray-yellow spots on either side of coronal suture (Figs 37, 39). Crown yellowish, with fore margin strongly produced medially (Figs 37, 39). Eyes gray. Face milky-white, with base of antenna yellow (Fig. 40). Pronotum milky-yellow, with posterior margin whitish gray (Figs 37, 39). Mesonotum with basal triangles brownish yellow, but inside milky yellow (Fig. 39). Forewing transparent (Fig. 38).

Male abdominal apodemes narrow and extending to midlength of 4th sternite (Fig. 48).



Figures 37–40. *Tautoneura qingxiuensis* Wang & Song, sp. nov. **37** habitus, dorsal view **38** habitus, lateral view **39** head and thorax, dorsal view **40** face.



Figures 41–48. *Tautoneura qingxiuensis* Wang & Song, sp. nov. **41** style **42** aedeagus, ventral view **43** aedeagus, lateral view **44** subgenital plate **45** pygofer lobe **46** dorsal pygofer appendage, lateral view **47** connective **48** abdominal apodemes.

Male genitalia. Pygofer lobe with a few fine setae scattered on lateral surface; pygofer microtrichia conspicuous, well developed; dorsal pygofer appendage distally tapered and basally expanded (Figs 45, 46). Subgenital plate with two macrosetae near middle area of outer margin and some stout setae scattered near apex (Fig. 44). Style with prominent preapical lobe (Fig. 41). Connective Y-shaped, with long stem, two lateral arms strong, and central lobe rather small (Fig. 47). Aedeagal shaft nearly straight, subapically broadened in ventral view, with pair of processes at apex; gonopore near apex on ventral surface; dorsal apodeme slightly broadened in lateral view; preatrium extremely short (Figs 42, 43).

Specimens examined. Holotype: ♂; CHINA, Guangxi Prov., Nanning, Qingxiu Mountain; 21 July 2021; Wenming Xu leg.; GZNU-2021-GX-NN-3-001. **Paratypes:** 2 ♂♂, 3 ♀♀; same data as holotype; GZNU-2021-GX-NN-3-002 to 006.

Measurements. Male length 2.1–2.2 mm, female length 2.2–2.3 mm (including wings).

Remarks. This species closely resembles *Tautoneura maculosa* Sohi, Mann & Shenhmar, 1987, but it can be distinguished by the absence of prominent, dark markings on head, pronotum, and mesonotum (present in *T. maculosa*), the subgenital plate bearing two macrosetae (vs three), and the much stouter aedeagus than in *T. maculosa*.

Etymology. The new species is named after its type locality, Qingxiu Mountain.

Additional information

Conflict of interest

The authors declare that they have no known competing financial interests or personal relationships that could have appeared to influence the work reported in this paper.

Ethical statement

No ethical statement was reported.

Funding

This study was supported by the National Natural Science Foundation of China (32260120), the Training Program for High-level Innovative Talents of Guizhou Province (Qiankehepingtairencai-GCC [2023]032), the Natural Science Foundation of Guizhou Province (Qiankehejichu-ZK [2023] General 257), and the Science and Technology Innovation Talent Team Building Project of Guizhou Province (Qiankehepingtairencai-CXTD [2023]010).

Author contributions

Data curation: JW, WX. Funding acquisition: YS. Investigation: JW, TP, WX, NZ. Methodology: JW. Resources: YS. Software: WX, NZ, TP, JW. Supervision: YS. Validation: YS. Visualization: TP, NZ, JW, WX. Writing – original draft: JW. Writing – review and editing: YS.

Author ORCIDs

Jingju Wang  <https://orcid.org/0000-0003-0675-8245>

Wenming Xu  <https://orcid.org/0009-0004-8936-1650>

Tianyi Pu  <https://orcid.org/0000-0002-6867-1527>

Ni Zhang  <https://orcid.org/0000-0002-8604-8448>

Yuehua Song  <https://orcid.org/0000-0003-3567-3056>

Data availability

All of the data that support the findings of this study are available in the main text.

References

- Anufriev GA (1969) New and little known leaf-hoppers of the subfamily Typhlocybinae from the Soviet Maritime Territory (Homopt., Auchenorrhyncha). *Acta Faunistica Entomologica Musei Nationalis Pragae* 13(153): 163–190.
- Dietrich CH (2005) Keys to the families of Cicadomorpha and subfamilies and tribes of Cicadellidae (Hemiptera: Auchenorrhyncha). *The Florida Entomologist* 88(4): 502–517. [https://doi.org/10.1653/0015-4040\(2005\)88\[502:KTTFOC\]2.0.CO;2](https://doi.org/10.1653/0015-4040(2005)88[502:KTTFOC]2.0.CO;2)

- Distant WL (1918) Rhynchota. VII. Homoptera: appendix. Heteroptera: addenda. In: The Fauna of British India, Including Ceylon and Burma. Vol. 7. Taylor and Francis, London, 210 pp.
- Dworakowska I (1979) On some Erythroneurini from Vietnam (Typhlocybae, Cicadellidae). *Annotationes Zoologicae et Botanicae* 131: 1–50.
- Dworakowska I (1980) On some Typhlocybae from India (Homoptera, Auchenorrhyncha, Cicadellidae). *Entomologische Abhandlungen und Berichte aus dem Staatlichen Museum für Tierkunde in Dresden* 43(8): 151–201. <https://doi.org/10.1515/9783112653227-010>
- Lu L, Dietrich CH, Cao Y, Zhang Y (2021) A multi-gene phylogenetic analysis of the leafhopper subfamily Typhlocybae (Hemiptera: Cicadellidae) challenges the traditional view of the evolution of wing venation. *Molecular Phylogenetics and Evolution* 165: 107299. <https://doi.org/10.1016/j.ympev.2021.107299>
- Sohi AS, Mann JS, Shenhmar M (1987) Eight new species of Typhlocybae from India (Insecta, Homoptera, Auchenorrhyncha, Cicadellidae). *Reichenbachia* 25(11): 37–45.
- Song YH, Li ZZ (2013) Two new species of *Empoasca* Distant (Hemiptera: Cicadellidae: Typhlocybae) from Yunnan Province, China. *Zootaxa* 3637(1): 089–093. <https://doi.org/10.11646/zootaxa.3637.1.11>
- Song YH, Li ZZ (2014) Erythroneurini and Zyginellini from China (Hemiptera: Cicadellidae: Typhlocybae). Science and Technology Publishing House, Guiyang, China, 12–209.
- Yuan S, Huang M, Wang XS, Ji LQ, Zhang YL (2014) Centers of endemism and diversity patterns for typhlocybinae leafhoppers (Hemiptera: Cicadellidae: Typhlocybae) in China. *Insect Science* 21(4): 523–536. <https://doi.org/10.1111/1744-7917.12040>

Ribbon worms (phylum Nemertea) from Bodega Bay, California: A largely undescribed diversity

Christina I. Ellison¹, Madeline R. Frey², Eric Sanford^{2,3}, Svetlana Maslakova¹

¹ Department of Biology, Oregon Institute of Marine Biology, University of Oregon, Charleston, OR, USA

² Bodega Marine Laboratory, Bodega Bay, CA 94923, USA

³ Department of Evolution and Ecology, University of California, Davis, CA 95616, USA

Corresponding author: Christina I. Ellison (cellison@uoregon.edu)

Abstract

The diversity of nemerteans along the Pacific coast of the United States is regarded as well characterized, but there remain many cryptic, undescribed, and “orphan” species (those known only in their larval form). Recent sampling of nemerteans in Oregon and Washington has begun to fill in these taxonomic gaps, but nemertean diversity in California has received relatively little attention over the past 60 years. During the summers of 2019 and 2020, nemertean specimens were collected from 20 locations in the Bodega Bay region of northern California, USA, including rocky intertidal shores, sandy beaches, mudflats, and other habitats. Based on morphological assessment and DNA sequence analysis (partial Cytochrome Oxidase I and 16S rRNA genes), our surveys identified 34 nemertean species. Only 13 of these (38%) can be confidently assigned to described species. Another 11 represent species that are new to science, including members of the genera *Riserius*, *Nipponnemertes*, *Poseidonemertes*, *Zygonemertes*, *Nemertellina*, *Oerstedia*, and three species of uncertain affiliation. The remaining ten species include undescribed or cryptic species of uncertain status that have been found previously along the Pacific Coast of North America. Our surveys also document extensions of known geographic ranges for multiple species, including the first records in California of *Antarctonemertes phyllospadicola*, *Cephalothrix hermaphroditica*, and *Maculaura oregonensis*. This is the first report of the genus *Nemertellina* in the northeast Pacific and *Riserius* in California. Overall, our findings highlight how much remains to be learned about the diversity and distribution of nemerteans in the northeast Pacific.

Key words: Biodiversity, cryptic species, Hoplonemertea, invertebrate, marine, Palaeonemertea, Pilidiophora



Academic editor: Jon Norenburg

Received: 27 December 2023

Accepted: 25 February 2024

Published: 4 June 2024

ZooBank: <https://zoobank.org/86BD3637-DE34-4E25-B236-8B076B94F29B>

Citation: Ellison CI, Frey MR, Sanford E, Maslakova S (2024) Ribbon worms (phylum Nemertea) from Bodega Bay, California: A largely undescribed diversity. ZooKeys 1204: 15–64. <https://doi.org/10.3897/zookeys.1204.117869>

Copyright: © Christina I. Ellison et al.
This is an open access article distributed under terms of the Creative Commons Attribution License (Attribution 4.0 International – CC BY 4.0).

Introduction

Nemerteans, or ribbon worms, are a phylum of approximately 1300 species (Gibson 1995; Kajihara et al. 2008; WoRMS Editorial Board 2023) of soft-bodied, non-segmented worms with an eversible proboscis housed within a fluid-filled rhynchocoel. They are found in all the world’s oceans, with most species known from benthic marine habitats, although some have adapted to pelagic, fresh-water, and terrestrial environments as well. Most nemerteans

are predators that feed on annelids, crustaceans, and mollusks (McDermott and Roe 1985), some throughout their life cycle, i.e., even in the plankton as larvae (Maslakova and Hiebert 2014; von Dassow et al. 2022; Maslakova et al. 2024). Some nemertean species impact commercially important crab, clam, and eel fisheries (e.g., Kuris and Wickham 1987; Bourque et al. 2001; Park et al. 2019), and some have been shown to produce compounds with biomedical potential (Kem et al. 2006; Whelan et al. 2014; Göransson et al. 2019; Verdes et al. 2022). Despite their ecological and applied importance, nemerteans remain understudied as a group, and the vast majority of the phylum's diversity has yet to be characterized (e.g., Mahon et al. 2010; Chernyshev and Lutaenko 2011; Kajihara 2017; Maslakova et al. 2022).

Nemerteans are challenging to identify given their relatively small number of external features, many of which do not fall into discrete character states (e.g., color and shape of body), and the fact that many species have been described and are known only from histological study of formalin-preserved material. The phylum is known to possess large numbers of cryptic species, that is, morphologically indistinguishable, but nevertheless distinct, species (e.g., Chen et al. 2010; Leasi and Norenburg 2014; Hao et al. 2015; Hiebert and Maslakova 2015a). Given that morphological approaches often fail to distinguish between look-alikes, DNA-based approaches are increasingly used to identify and delimit species, resolve phylogenies, and infer biogeographical patterns (e.g., Chernyshev et al. 2021a; Mendes et al. 2021; Kajihara et al. 2022a, 2022b).

The nemertean fauna of the Cold Temperate Northern Pacific province (as per Spalding et al. 2007) is among the best-characterized in the world, as it has been studied by several nemertologists during the course of the past century and a half (e.g., Stimpson 1857; Griffin 1898; Coe 1901, 1904, 1905, 1940; Corrêa 1964). However, new nemertean species are routinely discovered by researchers working in this region as molecular techniques are applied, and as new locations, life stages, habitats and depths are sampled and living specimens studied (e.g., Maslakova and von Dassow 2012; Hiebert et al. 2013; Hao et al. 2015; Hiebert and Maslakova 2015a, 2015b; Hunt and Maslakova 2017; Chernyshev et al. 2021b). Roe et al. (2007) report 65 intertidal nemertean species for the Oregonian Biogeographic Province (Oregon to Central California). However, recent sampling and DNA-barcoding of adults and planktonic larvae increased the known number of nemertean species in Oregon alone to more than a hundred (Hiebert 2016; Maslakova et al. 2022). In contrast, the diversity of nemerteans in California has received relatively little attention during the past 60 years, and molecular methods have not been applied broadly to the nemertean fauna of California.

The Bodega Bay region in northern California supports biodiverse ecosystems including rocky shores, kelp forests, sandy beaches, seagrass beds, and mudflats. The diversity of nemerteans in the Bodega Bay region has received some attention historically. A student report by Tamura (1957) identified 12 nemertean species in this region. Corrêa (1964) surveyed the southern end of Bodega Bay, including Dillon Beach, Tomales Point, and Tomales Bay, and identified 18 nemertean species. A pair of surveys conducted of Bodega Harbor (Standing et al. 1975) and the open coast of Bodega Marine Reserve (Ristau et al. 1978) identified seven nemertean species. Collectively, these previous studies identified a total of 21 different species of nemerteans in this region. The goal of this study was to extend the geographic scope of recent investigations

of nemertean diversity in the northeast Pacific (Hiebert 2016; Maslakova et al. 2022) to include northern California. In particular, we collected nemerteans from a variety of habitats in the Bodega Bay region and used DNA barcoding to examine this fauna for the first time.

Materials and methods

Specimen collection and preservation

During the summers of 2019 and 2020, we collected samples from 20 locations around Bodega Bay, California (Fig. 1, Tables 1, 2).

We selected the locations to encompass a variety of habitat types, including rocky substrate and soft sediments in both wave-exposed/outer coast and wave-protected, estuarine/harbor environments. Most of our collections were from the intertidal zone, but some subtidal collections were made as well. In the field, we haphazardly searched for visible nemerteans and additionally collected complex habitat material to extract small worms in the laboratory. Complex material (e.g., sedentary/colonial animals, algal holdfasts, surfgrass roots, sand, mud, etc.) was collected in the field and placed into sealed plastic bags. In the laboratory, we transferred these materials into clear aquaria, and covered the material with seawater. These samples were left for several days and checked regularly to remove any nemerteans observed crawling on the walls or water's surface. After several days, we broke apart and sorted through complex habitat material to remove hidden worms. Colonial ascidians and other invertebrates from samples of benthic communities tended to deteriorate rapidly in the laboratory and caused any nemertean specimens to become unusable, so these materials were sorted soon after collection.

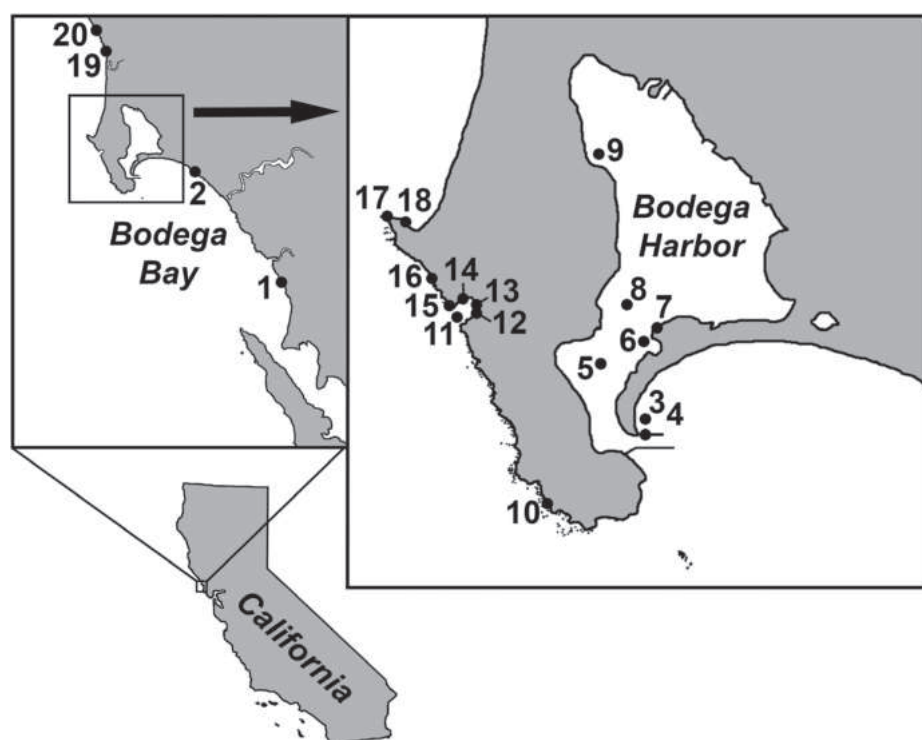


Figure 1. Map of collection stations (1–20) within Bodega Bay, California, USA.

Table 1. Nemertean collection locations in the Bodega Bay region. Locations #8 and #11–#18 are within the Bodega Marine Reserve.

Station	GPS Coordinates	Site Description
1	38.2573, -122.9713	Dillon Beach: wave-exposed, intertidal habitat with boulders and rocky outcrops
2	38.3055, -123.0171	Pinnacle Gulch: wave-exposed, intertidal habitat with boulders and rocky outcrops
3	38.3064, -123.0514	Doran Beach: subtidal, soft sediment habitat
4	38.3059, -123.0524	Bodega Harbor North Jetty: intertidal jetty with boulders
5	38.3106, -123.0556	Bodega Harbor: intertidal flats with soft sediments
6	38.3131, -123.0514	Bodega Harbor, near Coast Guard dock: intertidal breakwater with boulders
7	38.3141, -123.0515	Bodega Harbor, near Coast Guard dock: intertidal breakwater with boulders
8	38.3135, -123.0543	Bodega Harbor, Gaffney Point: intertidal flats with soft sediments
9	38.3289, -123.0573	Bodega Harbor, Spud Point Marina: subtidal fouling community on floating docks
10	38.3002, -123.0617	Bodega Head, south end: wave-exposed, rocky intertidal habitat with shaded caves
11	38.3150, -123.0712	Bodega Head, Horseshoe Cove: subtidal holdfasts of bull kelp (<i>Nereocystis luetkeana</i>)
12	38.3159, -123.0693	Bodega Head, south side of Horseshoe Cove: rocky intertidal benches, among the roots of surfgrass (<i>Phyllospadix</i> sp.)
13	38.3162, -123.0691	Bodega Head, Horseshoe Cove Beach: intertidal sandy beach with coarse sediments
14	38.3168, -123.0709	Bodega Head, north side of Horseshoe Cove: rocky intertidal benches, among the roots of surfgrass (<i>Phyllospadix</i> sp.)
15	38.3161, -123.0719	Bodega Head, Horseshoe Cove Point: wave-exposed rocky intertidal benches at northern edge of the cove
16	38.3185, -123.0740	Bodega Head: wave-exposed rocky intertidal benches
17	38.3235, -123.0785	Bodega Head, Mussel Point: wave-exposed rocky intertidal benches
18	38.3231, -123.0766	Bodega Head: rocky intertidal benches south of Salmon Creek Beach
19	38.3631, -123.0709	Coleman Beach: wave-exposed, intertidal habitat with boulders and rocky outcrops
20	38.3747, -123.0789	Schoolhouse Beach: wave-exposed, intertidal habitat with boulders and rocky outcrops

Table 2. Species identity, collection location, and accession numbers of nemertean specimens from Bodega Bay, CA. “Station” refers to collection location (Fig. 1, Table 1), USNM (United States National Museum) numbers refers to vouchers deposited at the Smithsonian Institution’s National Museum of Natural History.

Specimen ID	OTU (ASAP subset)	Species ID	Station	BOLD process ID	GenBank accession number	USNM voucher
B01	BOBA001	<i>Maculaura oregonensis</i> Hiebert & Maslakova, 2015a	6	NONEP001-21	COI: QQ075685 16S: QQ075747	USNM 1673940
B02	BOBA009	<i>Paranemertes</i> sp. BOBA009	6	NONEP002-21	COI: QQ075698 16S: QQ075759	USNM 1673941
B03	BOBA011	<i>Nemertellina</i> sp. BOBA011	6	NONEP003-21	COI: QQ075690 16S: QQ075753	N/A
B04	BOBA029	<i>Tetrastemma</i> sp. BOBA029	6	NONEP004-21	COI: QQ075707	N/A
B05	BOBA012	<i>Zygonemertes</i> sp. BOBA012	6	NONEP005-21	COI: QQ075710 16S: QQ075767	N/A
B06	BOBA012	<i>Zygonemertes</i> sp. BOBA012	6	NONEP006-21	COI: QQ075709	N/A
B07	BOBA014	<i>Zygonemertes</i> sp. BOBA014	6	NONEP007-21	COI: QQ075721 16S: QQ075778	N/A
B08	BOBA014	<i>Zygonemertes</i> sp. BOBA014	6	NONEP008-21	COI: QQ075717 16S: QQ075774	N/A
B09	BOBA012	<i>Zygonemertes</i> sp. BOBA012	6	NONEP009-21	16S: QQ075773	N/A
B10	BOBA031	<i>Tubulanus sexlineatus</i> (Griffin, 1898)	10	NONEP010-21	COI: QQ075708 16S: QQ075766	USNM 1673942
B11	BOBA007	<i>Riserius</i> sp. BOBA007	13	NONEP011-21	COI: QQ075703 16S: QQ075764	USNM 1673943
B12	BOBA025	<i>Cephalothrix simula</i> (Iwata, 1952)	9	NONEP012-21	COI: QQ075671 16S: QQ075732	USNM 1673944
B13	BOBA026	<i>Cephalothrix hermaphroditica</i> (Gibson, Sánchez & Méndez, 1990)	15	NONEP013-21	COI: QQ075668 16S: QQ075729	USNM 1673945

Specimen ID	OTU (ASAP subset)	Species ID	Station	BOLD process ID	GenBank accession number	USNM voucher
B14	BOBA010	<i>Poseidonemertes</i> sp. BOBA010	3	NONEP014-21	COI: QQ075700 16S: QQ075761	USNM 1673946
B15	BOBA016	<i>Eumonostilifera</i> sp. BOBA016	9	NONEP015-21	COI: QQ075687 16S: QQ075750	USNM 1673947
B16	BOBA027	<i>Emplectonema viride</i> Stimpson, 1857	1	NONEP016-21	COI: QQ075674 16S: QQ075735	USNM 1673948
B18	BOBA021	<i>Tetrastemma bilineatum</i> Coe, 1904	1	NONEP017-21	COI: QQ075705	USNM 1673949
B19	BOBA006	<i>Maculaura cerebrosa</i> Hiebert & Maslakova, 2015	16	NONEP018-21	COI: QQ075682 16S: QQ075743	USNM 1673950
B20	BOBA017	<i>Amphiporus</i> sp. BOBA017	16	NONEP019-21	COI: QQ075662 16S: QQ075723	USNM 1673951
B21	BOBA011	<i>Nemertellina</i> sp. BOBA011	9	NONEP020-21	COI: QQ075691 16S: QQ075754	N/A
BON01	BOBA019	<i>Tetrastemma nigrifrons</i> Coe, 1904	17	NONEP021-21	COI: QQ075706	USNM 1673952
BON02	BOBA002	<i>Micrura verrilli</i>	18	NONEP022-21	COI: QQ075686 16S: QQ075748	USNM 1673953
BON03	BOBA003	<i>Kulikovia</i> sp. BOBA003	10	NONEP023-21	COI: QQ075675 16S: QQ075736	USNM 1673954
BON04	BOBA026	<i>Cephalothrix hermaphroditica</i> (Gibson, Sánchez & Méndez, 1990)	10	NONEP024-21	COI: QQ075670 16S: QQ075731	USNM 1673955
BON06	BOBA005	<i>Lineus flavescens</i> Coe, 1904	6	NONEP025-21	COI: QQ075679 16S: QQ075740	USNM 1673956
BON10	BOBA001	<i>Maculaura oregonensis</i> Hiebert & Maslakova, 2015a	8	NONEP026-21	16S: QQ075746	USNM 1673957
BON11	BOBA005	<i>Lineus flavescens</i> Coe, 1904	8	NONEP027-21	COI: QQ075681 16S: QQ075742	USNM 1673958
BON13	BOBA028	<i>Nipponnemertes</i> sp. BOBA028	7	NONEP028-21	COI: QQ075693 16S: QQ075756	USNM 1673959
BON16	BOBA018	<i>Amphiporus</i> sp. BOBA018	19	NONEP029-21	COI: QQ075660 16S: QQ075722	USNM 1673960
BON24	BOBA032	<i>Carinomella lactea</i> Coe, 1905	8	NONEP030-21	COI: QQ075667 16S: QQ075728	USNM 1673961
BON27	BOBA013	<i>Zygonemertes</i> sp. BOBA013	7	NONEP031-21	COI: QQ075716 16S: QQ075772	N/A
BON32	BOBA022	<i>Oerstedtia</i> sp. BOBA022	4	NONEP032-21	COI: QQ075694 16S: QQ075757	N/A
BON33	BOBA022	<i>Oerstedtia</i> sp. BOBA022	4	NONEP033-21	COI: QQ075695 16S: QQ075758	N/A
BON35	BOBA033	<i>Poseidonemertes</i> sp. BOBA033	8	NONEP034-21	COI: QQ075699 16S: QQ075760	USNM 1673962
BON36	BOBA024	<i>Amphiporus</i> sp. BOBA024	18	NONEP035-21	COI: QQ075658	USNM 1673963
BON38	BOBA026	<i>Cephalothrix hermaphroditica</i> (Gibson, Sánchez & Méndez, 1990)	18	NONEP036-21	COI: QQ075669 16S: QQ075730	USNM 1673964
BON40	BOBA005	<i>Lineus flavescens</i> Coe, 1904	2	NONEP037-21	COI: QQ075680 16S: QQ075741	USNM 1673965
BON41	BOBA034	<i>Micrura wilsoni</i> (Coe, 1904)	7	NONEP038-21	16S: QQ075749	USNM 1673966
BON44	BOBA018	<i>Amphiporus</i> sp. BOBA018	18	NONEP039-21	COI: QQ075663	USNM 1673967
BON47	BOBA017	<i>Amphiporus</i> sp. BOBA017	18	NONEP040-21	COI: QQ075661	USNM 1673968
BON50	BOBA005	<i>Lineus flavescens</i> Coe, 1904	2	NONEP041-21	COI: QQ075676 16S: QQ075737	USNM 1673969
BON51	BOBA025	<i>Cephalothrix simula</i> (Iwata, 1952)	9	NONEP042-21	COI: QQ075672 16S: QQ075733	USNM 1673970
BON59	BOBA004	Siphonenteron gen. sp. BOBA004	15	NONEP043-21	COI: QQ075704 16S: QQ075765	USNM 1673971
BON60	BOBA005	<i>Lineus flavescens</i> Coe, 1904	15	NONEP044-21	COI: QQ075677 16S: QQ075738	USNM 1673972
BON61	BOBA024	<i>Amphiporus</i> sp. BOBA024	14	NONEP045-21	COI: QQ075659	USNM 1673973
BON62	BOBA015	<i>Zygonemertes</i> sp. BOBA015	14	NONEP046-21	COI: QQ075715	USNM 1673974

Specimen ID	OTU (ASAP subset)	Species ID	Station	BOLD process ID	GenBank accession number	USNM voucher
BON63	BOBA015	<i>Zygonemertes</i> sp. BOBA015	14	NONEP047-21	COI: OQ075714 16S: OQ075771	N/A
BON64	BOBA007	<i>Riserius</i> sp. BOBA007	13	NONEP048-21	COI: OQ075701 16S: OQ075762	USNM 1673975
BON65	BOBA007	<i>Riserius</i> sp. BOBA007	13	NONEP049-21	COI: OQ075702 16S: OQ075763	USNM 1673976
BON67	BOBA023	<i>Antarctonemertes phyllospadicola</i> (Stricker, 1985)	14	NONEP050-21	COI: OQ075664 16S: OQ075724	USNM 1673977
BON68	BOBA023	<i>Antarctonemertes phyllospadicola</i> (Stricker, 1985)	14	NONEP051-21	COI: OQ075665 16S: OQ075725	USNM 1673978
BON69	BOBA011	<i>Nemertellina</i> sp. BOBA011	14	NONEP052-21	COI: OQ075689 16S: OQ075752	N/A
BON70	BOBA008	<i>Cerebratulus</i> sp. BOBA008	5	NONEP053-21	COI: OQ075673 16S: OQ075734	USNM 1673979
BON75	BOBA020	<i>Tetrastemma</i> sp. BOBA020	13	NONEP054-21	COI: OQ075688 16S: OQ075751	N/A
BON76	BOBA013	<i>Zygonemertes</i> sp. BOBA013	10	NONEP055-21	COI: OQ075718 16S: OQ075775	USNM 1673986
BON77	BOBA030	<i>Ototyphlonemertes</i> sp. BOBA030	13	NONEP056-21	COI: OQ075696	N/A
BON78	BOBA030	<i>Ototyphlonemertes</i> sp. BOBA030	13	NONEP057-21	COI: OQ075697	N/A
BON80	BOBA013	<i>Zygonemertes</i> sp. BOBA013	10	NONEP058-21	COI: OQ075719 16S: OQ075776	USNM 1673980
BON81	BOBA015	<i>Zygonemertes</i> sp. BOBA015	10	NONEP059-21	COI: OQ075720 16S: OQ075777	USNM 1673981
BON83	BOBA006	<i>Maculaura cerebrosa</i> Hiebert & Maslakova, 2015a	12	NONEP060-21	COI: OQ075684 16S: OQ075745	USNM 1673982
BON85	BOBA006	<i>Maculaura cerebrosa</i> Hiebert & Maslakova, 2015a	12	NONEP061-21	COI: OQ075683 16S: OQ075744	USNM 1673983
BON86	BOBA005	<i>Lineus flavescens</i> Coe, 1904	10	NONEP062-21	COI: OQ075678 16S: OQ075739	USNM 1673984
BON87	BOBA013	<i>Zygonemertes</i> sp. BOBA013	11	NONEP063-21	COI: OQ075711 16S: OQ075768	N/A
BON88	BOBA014	<i>Zygonemertes</i> sp. BOBA014	6	NONEP064-21	COI: OQ075712 16S: OQ075769	USNM 1673985
BON91	BOBA014	<i>Zygonemertes</i> sp. BOBA014	6	NONEP065-21	COI: OQ075713 16S: OQ075770	N/A
BON93	BOBA032	<i>Carinomella lactea</i> Coe, 1905	8	NONEP066-21	16S: OQ075726	USNM 1673987
BON94	BOBA032	<i>Carinomella lactea</i> Coe, 1905	8	NONEP067-21	COI: OQ075666 16S: OQ075727	USNM 1673988
BON95	BOBA028	<i>Nipponnemertes</i> sp. BOBA028	7	NONEP068-21	COI: OQ075692 16S: OQ075755	USNM 1673989

Photographs and videos of worms were taken using a Leica MC170HD digital camera mounted to a Leica M125 dissecting microscope or a Leica DM1000 compound microscope, with accompanying software (Leica Application Suite v. 4.4). For hoplonemerteans, the stylet and basis of living specimens were photographed, when possible, using a compound microscope. We made initial species identifications using available morphological keys and geographically relevant inventories of Nemertea (Coe 1905; Roe et al. 2007; Hiebert 2016). Tissue samples were then preserved in 95% ethanol for DNA extraction, and some specimens were preserved in 4% formalin as morphological vouchers. Specimens collected in 2019 were identified with numbers preceded by the letter “B” and those collected in 2020 were given identifiers beginning with the label “BON.” Morphological and tissue vouchers have been deposited in the National Museum of Natural History, Smithsonian Institution, Washington, D.C. (Table 2, see also BOLD dataset <https://dx.doi.org/10.5883/DS-NEMBBCA>).

DNA extraction, PCR, sequence analysis, and species delimitation

We extracted DNA from 76 individuals using DNEasy Blood and Tissue Kit (Qiagen) following the manufacturer's protocol. We attempted to PCR-amplify portions of two mitochondrial genes, cytochrome c oxidase subunit I (COI) and 16S rRNA, from each individual, using universal and nemertean-specific primers (Table 3).

Each PCR was performed in a 20 µl volume, with 1 unit per reaction of Go Taq Polymerase (Promega) with supplied buffer, 200 µM dNTPs, and 500 nM of each primer. We used the following thermocycle profile: 95 °C 2 min; 34 cycles of: 95 °C 40 s, 45 °C (COI) 48–50 °C (16S) 40 s, and 72 °C 1 min; followed by final extension for 2 min (72 °C). Some DNA extracts required dilution (~ 1:20) for PCR success. PCR products were assessed with gel electrophoresis, purified with Wizard SV Gel and PCR Clean Up Kit (Promega), and sequenced at Sequetech (Mountain View, CA) in both directions using PCR primers. We used Geneious Prime for sequence analysis. Sequences with initial HQ < 50% were discarded. Each sequence was manually trimmed to eliminate primers and low-quality end regions. Forward and reverse strands were aligned, proofread against each other using quality PHRED scores and chromatograms, and contigs used to generate consensus sequences. Nucleotides with combined PHRED score of less than 20 in consensus sequences were trimmed off or converted to "N". We translated each COI nucleotide sequence into amino acids using the Invertebrate Mitochondrial translation table and checked for the presence of stop codons.

Consensus sequences were checked against the NCBI database (GenBank) using nucleotide BLAST to screen for contamination and to aid with specimen identification. A 4% p-distance divergence was previously identified as appropriate for species delineation in large scale COI-barcoding studies of nemertean (e.g., Kvist et al. 2014; Maslakova et al. 2022), and thus was used here as a criterion for selection of conspecific reference sequences. When available, conspecific sequences from GenBank were added to the alignment. Reference sequences from closely related species were added where no conspecific reference sequences were available (Suppl. material 1). All newly generated sequences have been deposited in BOLD and GenBank (Table 2, see also BOLD dataset <https://dx.doi.org/10.5883/DS-NEMBBCA>). We aligned sequences using the MAFFT plug-in within Geneious, using default parameters, visually inspected alignments for gaps and irregularities, then used them to construct unrooted neighbor-joining trees (Tamura Nei substitution model). Final COI alignment

Table 3. PCR primers used in this study.

Locus	Primer name	Primer sequence	Reference
COI	LCO1490 HCO2198	5' GGTCAACAAATCATAAAGATATTGG 5' TAAACTTCAGGGTGACCAAAAAATCA	Folmer et al. 1994
COI	COI LF COI DR	5' TTTCAACAAATCATAAAGATAT 5' GAGAAATAATACCAAAACCAGG	Cherneva et al. 2023
16S	16SARL 16SBRH	5' CGCCTGTTTATCAAAAACAT 5' CCGGTCTGAACTCAGATCACGT	Palumbi et al. 1991
16S	16S AF 16S KR	5' TCGTCTGTTTATCAAAAACATAGY 5' AATAGATAGAAACCAACCTGGC	Cherneva et al. 2023

was trimmed to 658 bp and contained a total of 107 sequences (including 64 generated in this study), and 16S alignment was 568 bp long, and contained 93 sequences (57 generated in this study). We used ASAP (Assembling Species by Automatic Partitioning) analysis (Puillandre et al. 2021) of the COI data to partition the dataset into Operational Taxonomic Units (OTUs), putative species. The 16S rRNA sequences were used to verify species identity, where we lacked COI sequence data, but were not used for species delineation, because they are more conservative and can fail to differentiate between closely related species. Below we refer to reference sequences by either GenBank accession number or BOLD Process ID, where accession numbers are not available.

Results

Of the 76 specimens from which DNA was extracted, we were able to successfully obtain sequences from 68; a total of 64 COI sequences and 57 16S sequences (see Table 2, BOLD dataset <https://dx.doi.org/10.5883/DS-NEMBB-CA>). Results of the ASAP analysis of the COI data suggested the presence of a barcoding gap (i.e., the separation between the maximum intraspecific and the minimum interspecific variation) between 3–5%, similar to previous large-scale DNA-barcoding studies of nemerteans (e.g., Kvist et al. 2014; Sundberg et al. 2016; Maslakova et al. 2022). Using 0.038 simple p-distance as the threshold, ASAP partitioned the dataset into 52 OTUs, 33 of which contained all our samples (Table 4). BOLD species delineation algorithm partitioned our sequences into 34 barcode index numbers (BINs, Table 4), splitting *Zygonemertes* sp. BOBA015 into two separate BINs. Of the 34 BINs, ten are unique, meaning they lacked representation in BOLD (likely not previously sequenced). We were not able to obtain a COI sequence from specimen BON41, but its identity was determined morphologically as *Micrura wilsoni* (Coe, 1904) and was confirmed by the 16S rRNA sequence data. There is no evidence of cryptic species of *M. wilsoni* in the region thus far. Hence, we report a total of 34 putative species of nemerteans from Bodega Bay, CA (Table 4). COI sequences were obtained for 33/34 species, and 16S sequences for 28/34 species. Neighbor-Joining trees of the COI and 16S rRNA sequence alignments are shown on Figs 2, 3, respectively.

Because of the ubiquitous presence of cryptic species among nemerteans, species distributions listed below refer to reports verified by DNA sequence data, unless otherwise noted. Undescribed species, as well as species of uncertain status, were assigned temporary alphanumeric OTU codes (e.g., BOBA0XX) for tracking purposes, until their taxonomy is resolved.

Class PALAEONEMERTEA

Order Archinemertea Iwata, 1960

Family Cephalotrichidae McIntosh, 1873

Genus Cephalothrix Örsted, 1843

A species-rich genus of mostly white, thread-like worms, which have a long pre-oral region and lack ocelli as adults. Given their general lack of distinguishing features, the species therein are difficult to differentiate morphologically

Table 4. Nemertean species identified from Bodega Bay, California. The term “unresolved” refers to cryptic species of uncertain taxonomic status.

Class	Species	Status	OTU code (this study)	BOLD Barcode Identification Number (BIN)	Maslakova et al. (2022) OTU
Palaeonemertea	<i>Cephalothrix hermaphroditica</i> (Gibson, Sánchez & Méndez, 1990)	described	BOBA026	BOLD:ADM3467	-
Palaeonemertea	<i>Cephalothrix simula</i> (Iwata, 1952)	described	BOBA025	BOLD:AAM5519	-
Palaeonemertea	<i>Carinomella lactea</i> Coe, 1905	described	BOBA032	BOLD:AEJ8707	-
Palaeonemertea	<i>Tubulanus sexlineatus</i> (Griffin, 1898)	described	BOBA031	BOLD:ADM0945	OTU 83
Pilidiophora	<i>Cerebratulus</i> sp. BOBA008	previously reported, undescribed	BOBA008	BOLD:AAE9633	OTU 62
Pilidiophora	<i>Kulikovia</i> sp. BOBA003	previously reported, undescribed	BOBA003	BOLD:ADX1401	OTU 49
Pilidiophora	<i>Maculaura cerebrosa</i> Hiebert & Maslakova, 2015a	described	BOBA006	BOLD:AAP1201	OTU 54
Pilidiophora	<i>Maculaura oregonensis</i> Hiebert & Maslakova, 2015a	described	BOBA001	BOLD:ADM2641	OTU 61
Pilidiophora	<i>Riserius</i> sp. BOBA007	new to science	BOBA007	BOLD:AEJ1230	-
Pilidiophora	<i>Lineus flavescens</i> Coe, 1904	described	BOBA005	BOLD:ADS0049	OTU 45
Pilidiophora	<i>Micrura verrilli</i> Coe, 1901	described	BOBA002	BOLD:ADW4746	OTU 65
Pilidiophora	<i>Micrura wilsoni</i> (Coe, 1904)	described	BOBA034	BOLD:ADW9830	OTU 90
Pilidiophora	Siphonenteron gen. sp. BOBA004	new to science	BOBA004	BOLD:ADR9817	-
Hoplonemertea	<i>Nipponnemertes</i> sp. BOBA028	new to science	BOBA028	BOLD:AEJ7531	-
Hoplonemertea	<i>Amphiporus</i> sp. BOBA024	new to science	BOBA024	BOLD:AEI5687	-
Hoplonemertea	<i>Amphiporus</i> sp. BOBA017	previously reported, undescribed	BOBA017	BOLD:ADR7530	OTU 6
Hoplonemertea	<i>Amphiporus</i> sp. BOBA018	previously reported, undescribed	BOBA018	BOLD:AEA1922	OTU 5
Hoplonemertea	<i>Emplectonema viride</i> Stimpson, 1857	described	BOBA027	BOLD:AAP1200	OTU 17
Hoplonemertea	<i>Ototyphlonemertes</i> sp. BOBA030	previously reported, unresolved	BOBA030	BOLD:ADM3126	-
Hoplonemertea	<i>Paranemertes</i> sp. BOBA009	previously reported, undescribed	BOBA009	BOLD:ADM0221	OTU 10
Hoplonemertea	<i>Poseidonemertes</i> sp. BOBA010	new to science	BOBA010	BOLD:AEK1697	-
Hoplonemertea	<i>Poseidonemertes</i> sp. BOBA033	new to science	BOBA033	BOLD:AEK1698	-
Hoplonemertea	<i>Tetrastemma nigrifrons</i> Coe, 1904	described	BOBA019	BOLD:ADX0572	OTU 18
Hoplonemertea	<i>Tetrastemma</i> sp. BOBA029	previously reported, undescribed	BOBA029	BOLD:ADW8618	OTU 20
Hoplonemertea	<i>Tetrastemma</i> sp. BOBA020	new to science	BOBA020	BOLD:AEJ7493	-
Hoplonemertea	<i>Zygonemertes</i> sp. BOBA012	previously reported, unresolved	BOBA012	BOLD:ADL9636	OTU 23
Hoplonemertea	<i>Zygonemertes</i> sp. BOBA013	previously reported, unresolved	BOBA013	BOLD:ADW7912	OTU 26
Hoplonemertea	<i>Zygonemertes</i> sp. BOBA014	new to science	BOBA014	BOLD:AEK0256	-
Hoplonemertea	<i>Zygonemertes</i> sp. BOBA015	new to science	BOBA015	BOLD:AEJ0120, BOLD:ADR7155	-
Hoplonemertea	<i>Eumonostilifera</i> sp. BOBA016	previously reported, undescribed	BOBA016	BOLD:AEJ6897	OTU 13
Hoplonemertea	<i>Antarctonemertes phyllospadicola</i> (Stricker, 1985)	described	BOBA023	BOLD:ACH3602	-
Hoplonemertea	<i>Nemertellina</i> sp. BOBA011	new to science	BOBA011	BOLD:AEJ4336	-
Hoplonemertea	<i>Oerstedtia</i> sp. BOBA022	new to science	BOBA022	BOLD:AEJ2779	-
Hoplonemertea	<i>Tetrastemma bilineatum</i> Coe, 1904	described	BOBA021	BOLD:ADW8130	OTU 29

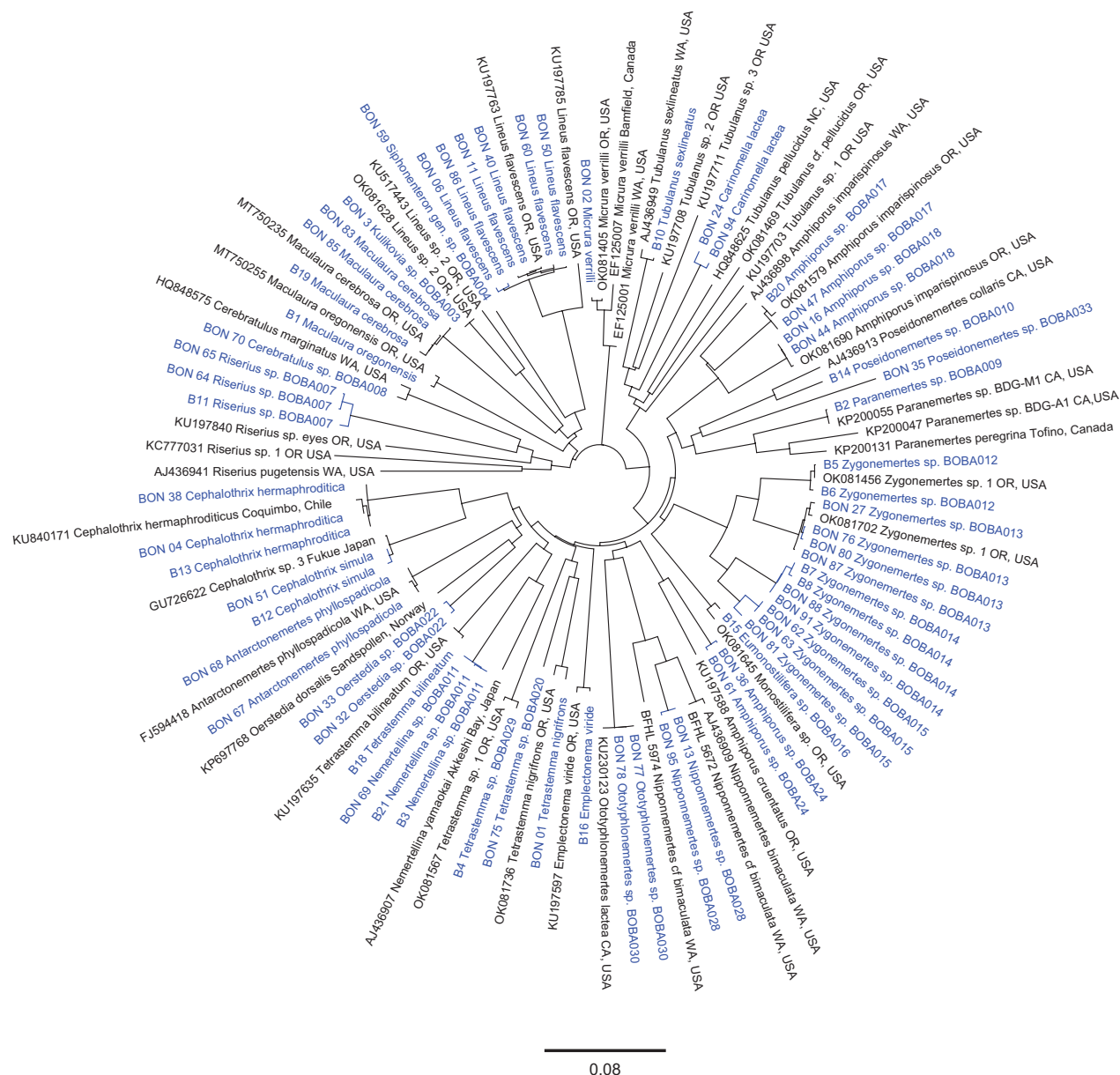


Figure 2. Neighbor-joining tree of COI sequences. Sequences generated in this study are shown in blue. BOBA numbers reflect subsets (OTUs) from the ASAP analysis.

(e.g., Chen et al. 2010; Leasi and Norenburg 2014; Kajihara 2019; Sagorny et al. 2019). COI sequences are available for at least ten species from Oregon and California, most of which have not been described and some are only known in their larval form (Hiebert 2016; Maslakova et al. 2022).

Cephalothrix hermaphroditica (Gibson, Sánchez & Méndez, 1990)

Procephalothrix hermaphroditicus Gibson et al., 1990: 279, figs 1–15; Sundberg and Hylbom 1994: 358; McDermott 2001: 12; Carroll et al. 2003: 52; Sundberg et al. 2003: 281.

Cephalothrix hermaphroditicus: Paule et al. 2021: 5.

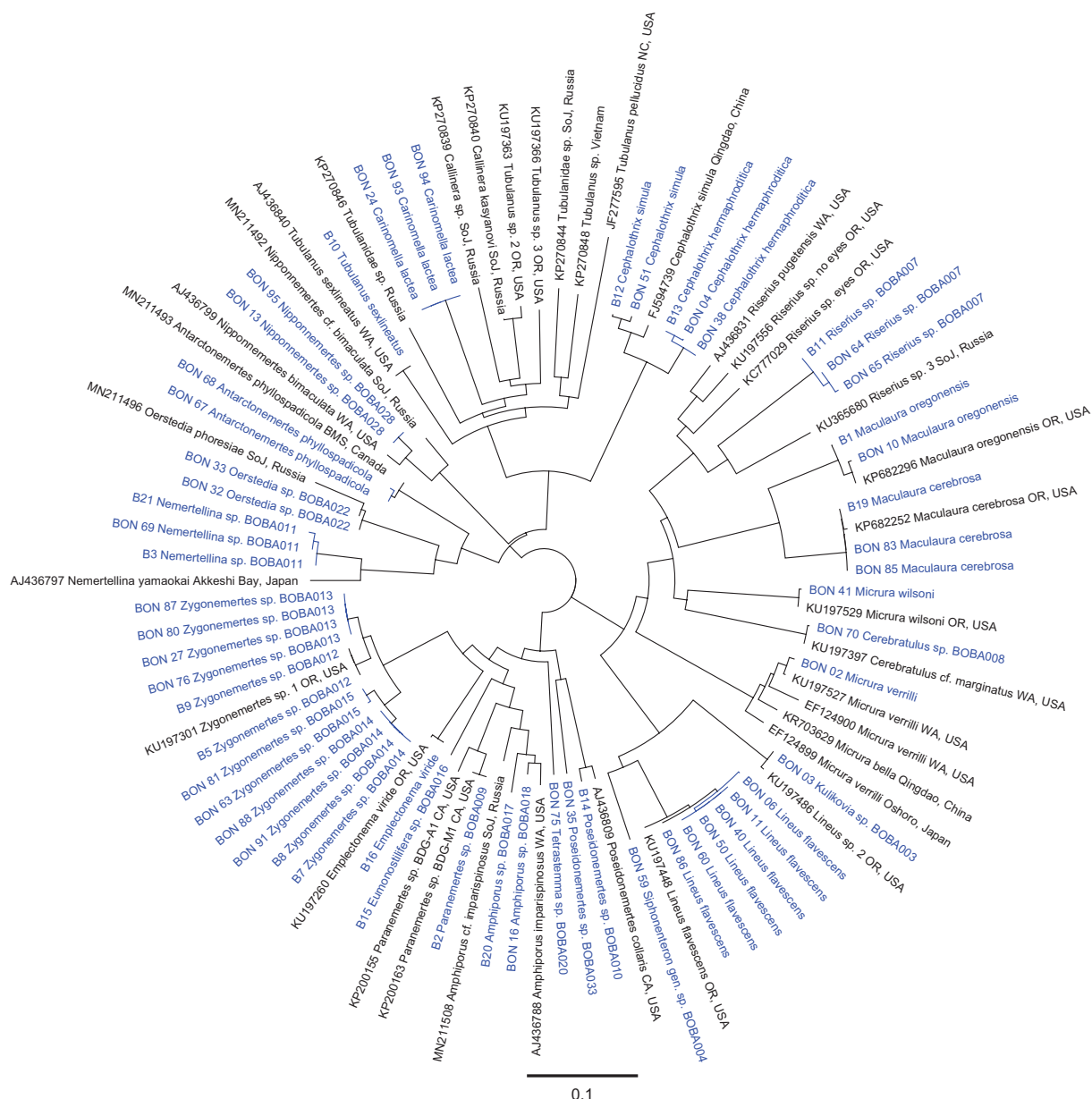


Figure 3. Neighbor-joining tree of 16S sequences. Sequences generated in this study are shown in blue. BOBA numbers reflect subsets (OTUs) from ASAP analysis on COI data.

BIN. BOLD:ADM3467.

Material examined. B13, BON4, BON38.

Morphology. Filiform body, 15–51 mm long. Body color orange with translucent margins, somewhat paler ventrally, with a deeper orange anterior tip (Fig. 4A). Preoral region relatively shorter than in other *Cephalothrix* species.

Identification. Our specimens share high sequence similarity (99–100% COI) with specimens reported as *C. hermaphroditicus* from Chile (KU840171), France (MH681952), Spain (KM230034), and Argentina (KM230037). The type locality of the species is Cocholgue, Chile, but given the comparatively low haplotype diversity in Chile, and high haplotype diversity in France, Sagorny et al. (2019) suggested the species may have been introduced to Chile from Europe.



Figure 4. Palaeonemertean worms of Bodega Bay **A** *Cephalothrix hermaphroditica*, individual B13 **B** *Cephalothrix simula*, individual BON51 **C** *Carinomella lactea*, individual BON24 **D** *Tubulanus sexlineatus*, individual B10.

COI barcodes for the Bodega Bay specimens are identical to the Chilean ones, consistent with the idea of a single introduction to the Pacific from the Atlantic.

Habitat. Collected from wave-exposed, rocky intertidal habitats, among colonial ascidians. Stations 10, 15, 18 (Fig. 1, Table 1).

Distribution. Bodega Bay, CA, USA (this study); Coquimbo, Chile (Sundberg et al. 2016); Camarones Bay, Argentina; Vilan Cape, Spain (Fernández-Álvarez et al., unpublished); Roscoff, France (Sagorny et al. 2019; Paule et al. 2021).

Notes. The only available sequences of *Cephalothrix hermaphroditica* from Chile were collected ~ 1,000 km north of its type locality. Given that biogeographical patterns among nemertean species are variable, we tentatively include the species as synonymous with the species we encountered in our surveys. This is the first report of the species in the Cold Temperate Northern Pacific, and first 16S barcode for the species. *Cephalothrix hermaphroditica* provides the only known example of hermaphroditism among the Palaeonemertea. Reproductive features were not observed by us.

***Cephalothrix simula* (Iwata, 1952)**

Procephalothrix simulus Iwata, 1952: 132.

Cephalothrix simula: Kajihara et al. 2013: 987, figs 2–11 (see publication for full synonymy up through 2013).

Cephalothrix simula: Chernyshev and Polyakova 2021: 586.

Cephalothrix sp.: Nam and Rhee 2020: 2012.

BIN. BOLD:AAM5519.

Material examined. B12, BON51.

Morphology. Filiform body, ~ 50 mm long, pale yellowish to orange, color brighter in the head and foregut regions, paler and somewhat translucent posteriorly (Fig. 4B).

Identification. Our specimens share high (99.6% COI) sequence similarity to the topogenotype of *C. simula* (GU726622), and other *C. simula* sequences, as defined by Kajihara et al. (2013). The type locality of *C. simula* is Japan, but it has since been reported from the Pacific coast of the U.S., the Atlantic, and the Mediterranean. Remarkably, and in contrast to many other reported cases of such widespread distribution among nemertean species, these reports refer to the same species, as assessed by genetic data (Chen et al. 2010; Kajihara et al. 2013; Sagorny et al. 2019). This suggests that *C. simula* has been broadly introduced to many geographic regions.

Habitat. Collected among fouling organisms on marina docks (station 9).

Distribution. Changdao, China (Chen et al. 2010, 2011); South Korea (Chen et al. 2010; Nam and Rhee 2020; Chernyshev and Polyakova 2021); Japan: Fukue, Hiroshima, Oshoro, Seto, Shimoda (Thollesson and Norenburg 2003; Chen et al. 2010; Kajihara et al. 2013); Iturup Island, Russia (Chernyshev and Polyakova 2021); Bodega Bay, CA, USA (this study); San Diego, CA, USA (Chen et al. 2010); Spain: Aramar, Blanes, Cap de Creus, Islares, San Vicente do Mar (Fernández-Álvarez and Machordom 2013; Sagorny et al. 2019); France: Concarneau, Roscoff (Sagorny et al. 2019); Italy: Giglio, Trieste (Chen et al. 2010; Sagorny et al. 2019); Netherlands: Sint Annaland, Zierikzee (Faasse and Turbeville 2015).

Notes. Previously reported from southern California (Chen et al. 2010), this is the first report of the species from northern California. Following the detection of *C. simula* in the Mediterranean, the species was identified as non-native (Fernández-Álvarez and Machordom 2013), likely introduced to locations outside of East Asia in the 21st century via transport of larvae and juveniles in the ballast water of ships (Chernyshev 2014) or with oyster aquaculture (e.g., Ruesink et al. 2005). Apart from being one of the few known cases of species introductions amongst the nemerteans (but see Moore et al. 2001), *C. simula* has attracted interest for the high levels of neurotoxin tetrodotoxin (TTX) found in its tissues, sparking concern about potential contamination of shellfish (e.g., Kajihara et al. 2013; Turner et al. 2018).

Order Tubulaniformes Chernyshev, 1995

Family Carinomellidae Chernyshev, 1995

Genus *Carinomella* Coe, 1905

A monotypic genus. Morphology resembles *Tubulanus*; likely related to *Carinella*, *Parahubrechtia* and other unpigmented tubulanids (Chernyshev et al. 2021b).

***Carinomella lactea* Coe, 1905**

Carinomella lactea Coe, 1905: 127, pls V–XI, figs 45–61, 63–72.

BIN. BOLD:AEJ8707.

Material examined. BON24, BON93, BON94.

Morphology. Eyeless white worm 65–87 mm long (Fig. 4C); spatulate head demarcated from the body by width and an indistinct transverse furrow; the mouth a small slit just posterior to the furrow on the ventral side. With large, oblong, conspicuous lateral sense organs located posterior to the tubulanid ring.

Identification. Specimens at hand most resemble *Carinomella lactea* described by Coe (1905) from San Pedro, California and, to a lesser extent, *Tubulanus pellucidus* (Coe, 1895). The latter was described from the coast of New England, but later also reported from Monterey Bay, San Pedro, and San Diego, California by Coe (1905). In his description of the species, Coe (1905) notes that *T. pellucidus* often co-occurs with *C. lactea* in southern California, but the former is smaller in size (10–25 mm long). The species encountered here did not locate any close sequence matches within GenBank, and there are no previously published sequences of *C. lactea*. A COI sequence (OK081469) derived from a small unpigmented tubulanid reported from Oregon by Maslakova et al. (2022: OTU 89), is distinct from those of Bodega Bay specimens, and so is the only available COI sequence (HQ848625) purported to belong to an Atlantic *T. pellucidus*, from North Carolina (Andrade et al. 2012). The 16S sequences place Bodega Bay specimens within a clade of other unpigmented tubulanids including species of *Tubulanus*, *Carinella*, and *Parahubrechtia* (Fig. 3).

Habitat. Mudflats. Collected among polychaete tubes on intertidal mudflats, just below the surface of the sediments (station 8).

Distribution. Bodega Bay, CA, USA (this study). The species has been reported from the Atlantic (Corrêa 1961), but it is unlikely this report refers to the same species.

Notes. Species not previously sequenced.

Family Tubulanidae sensu Chernyshev, 2022

Genus *Tubulanus* Renier, 1804

Tubulanus sexlineatus (Griffin, 1898)

Carinella sexlineata Griffin, 1898: 201, fig. 15; Coe 1904: 118; 1905: 85, pl. I, figs 2, 3.
Carinella dinema Coe, 1901: 15, pl. I, figs 2, 3.

BIN. BOLD:ADM0945.

Material examined. B10.

Morphology. Slender reddish brown worm with elaborate white markings (Fig. 4D), including a series of transverse rings, six longitudinal lines (one mid-dorsal, originating from the first ring; two paired lateral and one mid-ventral originating from the second ring), and small white dots. Paler ventrally. Spatulate head well demarcated from the body by width and a pair of transverse cerebral organ furrows; with tubulanid ring and lateral sense organs. No ocelli.

Identification. Morphology agrees with *Tubulanus sexlineatus*, a species described from Puget Sound, Washington and Alaska, and DNA sequences show high percent similarity to previously published sequences of *T. sexlineatus*. Also resembles *T. punctatus* (Takakura, 1898) from Japan, and *T. superbus* (Kölliker, 1845) from the Mediterranean. Two described *Tubulanus* species from

the northeast Pacific with similar coloration have no published sequences but can be differentiated from *T. sexlineatus* by pattern: *T. cingulatus* (Coe, 1904) is deep brown, with four dorsal longitudinal white lines, and *T. capistratus* (Coe, 1901) is brown with many narrow white rings, and only three white longitudinal lines (Coe 1901; Corrêa 1964).

Habitat. Relatively common in the Bodega Bay region. Collected from the wave-exposed, rocky intertidal zone, among colonial ascidians (stations 2, 10, 15), and observed among surfgrass roots (stations 12, 14), kelp holdfasts (station 7), and on the underside of rocks in pale cellophane-like tubes of its own secretion (station 2, 7).

Distribution. Discovery Island, BC, Canada (QHAK2597-22, QHAK2649-22 in BOLD); Puget Sound, WA, USA (Thollesson and Norenburg 2003; Andrade et al. 2012; Charleston, OR, USA (Hiebert 2016; Maslakova et al. 2022); Bodega Bay, CA, USA (this study); Malibu, CA, USA (DISA603-19 in BOLD).

Class PILIDIOPHORA Thollesson & Norenburg, 2003

Order Heteronemertea Bürger, 1892

Family Lineidae

Genus *Cerebratulus* Renier, 1804

Cerebratulus is one of three non-monophyletic mega-genera in the Class Pilidiophora, with *Lineus* and *Micrura* (e.g., see Kajihara et al. 2022b). The morphological diagnosis of the genus is based on combinations of non-unique characters (Schwartz 2009). However, since *Cerebratulus marginatus* is the type species of the genus, and the species below is closely related (Verdes et al. 2021), it will likely retain the generic affiliation.

Cerebratulus sp. BOBA008

Cerebratulus marginatus: Andrade et al. 2012: 6; Thollesson and Norenburg 2003: 408; Roe et al. 2007: 224, pl. 88, figs C, D.

Cerebratulus cf. *marginatus*: Hiebert 2016: 48; Verdes et al. 2021: 898; Maslakova et al. 2022.

BIN. BOLD:AAE9633.

Material examined. BON70.

Morphology. Large (25 cm long), dorsoventrally flattened dull reddish brown worm with lateral margins distinct both in color (pale) and shape (flattened). Spade-shaped head bordered by deep cephalic slits, with a long slit-like mouth located posterior to their endings on the ventral side (Fig. 5C). Capable of swimming. Young individuals have a pair of inconspicuous ocelli near the anterior tip of the head.

Identification. A common intertidal mudflat species, previously reported from Washington and Oregon as *Cerebratulus marginatus* or *Cerebratulus* cf. *marginatus* (Thollesson and Norenburg 2003; Roe et al. 2007; Andrade et al. 2012; Hiebert 2016; Maslakova et al. 2022). The type locality of *C. marginatus* is Naples, Italy, but the closest available sequenced specimens are from Spain. Although the nominal species *C. marginatus* is reported from the eastern and

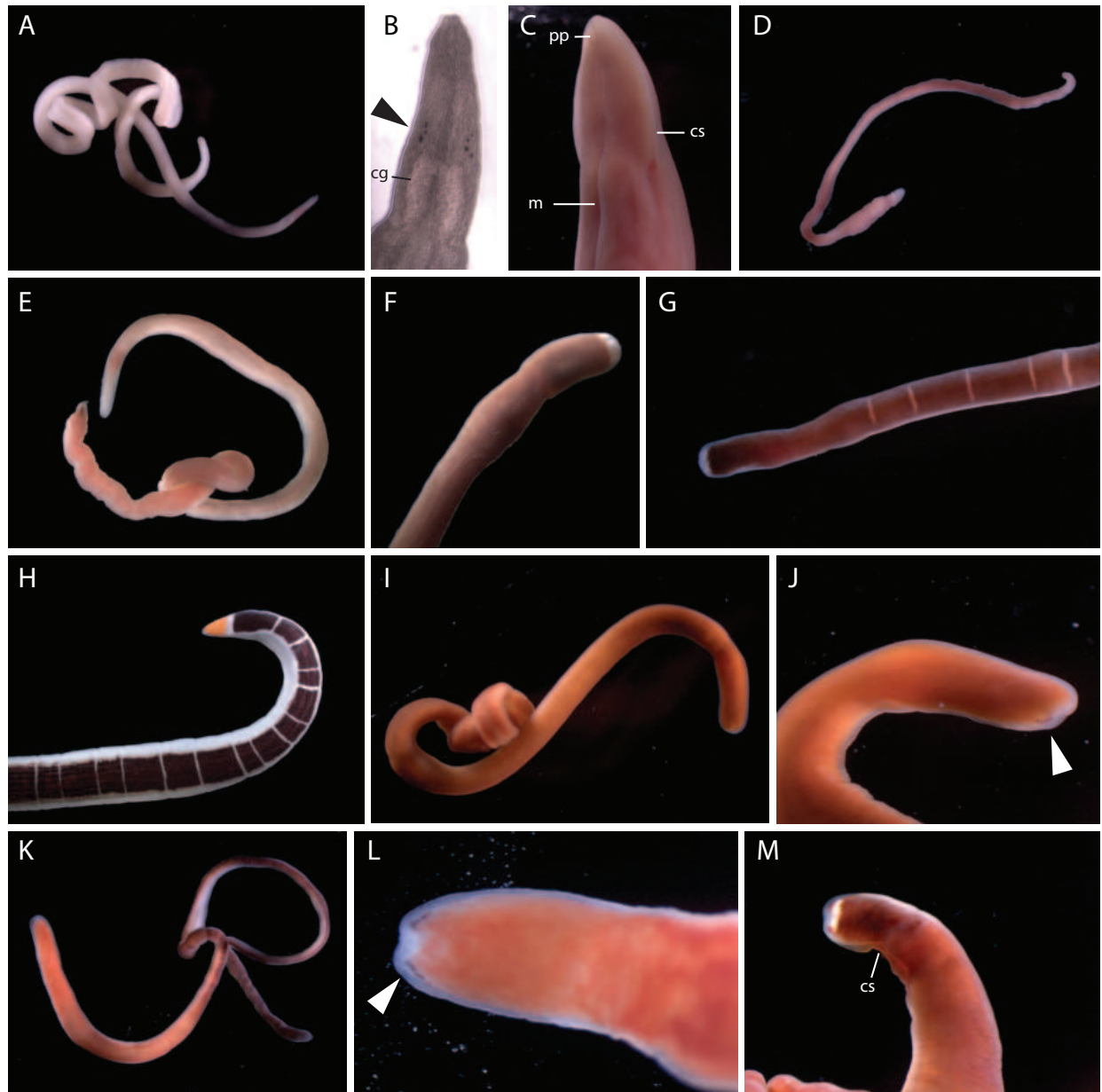


Figure 5. Pilidiophoran nemerteans of Bodega Bay **A, B** *Riserius* sp. BOBA007, a new species, individual BON064 **B** close up of head in transmitted light showing ocelli (arrowhead) **C** *Cerebratulus* sp. BOBA008, individual BON070, ventrolateral view of head **D** *Maculaura cerebrosa*, individual BON085 **E** *Maculaura oregonensis*, individual B1 **F** *Kulikovia* sp. BOBA003, anterior end of individual BON003 **G** *Micrura wilsoni*, individual BON041 **H** *Micrura verrilli*, individual BON002 **I, J** Siphonenteron gen. sp. BOBA004, a new species, individual BON059 **J** close up of anterior end, showing ocelli (arrowhead) **K–M** *Lineus flavescens* **K, L** individual BON040 **L** close up of head showing ocelli (arrowhead) **M** individual BON006, a color morph with a white anterior patch and reddish ocelli. Abbreviations: cg – cerebral ganglia, cs – cephalic slit, m – mouth, pp – proboscis pore.

western Pacific and Atlantic oceans, and the Baltic, North, and Mediterranean seas, it has been shown to constitute a large cryptic species complex with at least six lineages in Europe (Verdes et al. 2021). The seventh, NE Pacific, lineage most certainly represents an undescribed species. At least one closely related look-alike, *Cerebratulus* sp. "spade head", occurs in southern Oregon (Hiebert 2016; Maslakova et al. 2022: OTU 63) and another, recently re-described as *Cerebratulus orochi* Kajihara, 2020, in the Sea of Japan.

Habitat. Intertidal mudflats in areas with sandy sediments; often > 30 cm below the surface (station 5).

Distribution. Discovery Islands, BC, Canada (QHAK2554-22 in BOLD), Puget Sound, WA, USA (Thollesson and Norenburg 2003; Andrade et al. 2012; Verdes et al. 2021); Charleston, OR, USA (Hiebert 2016; Maslakova et al. 2022); Bodega Bay, CA, USA (this study).

Genus *Kulikovia* Chernyshev et al. 2018

***Kulikovia* sp. BOBA003**

Lineus sp.: Maslakova et al. 2022.

Lineus sp. 2: Hiebert 2016: 54, fig. 4.16.

BIN. BOLD:ADX1401.

Material examined. BON3.

Morphology. Body 27 cm long, reddish brown with a white anterior tip (Fig. 5F).

Identification. Resembles *Kulikovia* spp., and several other species in the Siphonenteron clade (see Lineidae incertae sedis below). COI sequences show that it is conspecific (99–100% similarity) with one of two sister lineages previously reported from southern Oregon in their larval form as *Lineus* sp. 2 by Hiebert (2016) and as *Lineus* sp. by Maslakova et al. (2022: OTU 49) in both larval and adult form. Phylogenetic analysis based on five genetic markers places this species within the Siphonenteron clade, more specifically within the genus *Kulikovia* (Chernyshev et al. 2018; Kajihara et al. 2022b). Two other members of the genus are reported from the northeast Pacific: *K. montgomeryi* from Kachemak, Alaska and San Juan Island, Washington (as *Cerebratulus montgomeryi* in Schwartz 2009; Hiebert 2016), and an undescribed species reported from southern Oregon as *Lineus* sp. 'red' by Hiebert and Maslakova (2015b) and as *Kulikovia* sp. by Maslakova et al. (2022: OTU 59).

Habitat. Collected from a sandy, low intertidal pool, under stones (station 10).

Distribution. Charleston, OR, USA (Hiebert 2016; Maslakova et al. 2022); Bodega Bay, CA, USA (this study).

Notes. This is the first record of the species in California.

Genus *Maculaura* Hiebert & Maslakova, 2015a

The genus *Maculaura* was erected for five cryptic species occurring in NE Pacific that were previously recognized under the name *Micrura alaskensis* Coe, 1901. A phylogenetic analysis by Kajihara et al. (2022b) shows *Maculaura* as a well-supported lineid clade.

***Maculaura cerebrosa* Hiebert & Maslakova, 2015a**

Maculaura cerebrosa Hiebert & Maslakova, 2015a: 628, fig. 4G–J.

BIN. BOLD:AAP1201.

Material examined. B19, BON83, BON85.

Morphology. Body 15–18 mm long. Anterior tip white, with lateral cephalic slits, no ocelli, and pink cerebral ganglia visible through the body wall (Fig. 5D). One individual quite pink, with color beginning near the brain, another white throughout the foregut region, with brown coloration beginning in the intestinal area.

Identification. Bodega Bay individuals conform to the morphological description of *Maculaura* spp., and COI sequences exhibit 99–100% similarity to those of *M. cerebrosa* from Oregon (Hiebert and Maslakova 2015a; Maslakova et al. 2022: OTU 54).

Habitat. Collected from the open coast among the roots of surfgrass (*Phyllospadix* sp., station 12) and in mid-intertidal mussel beds (station 16). In southern Oregon, this species has also been found within estuaries, especially under rocks at the edges of mudflats (Hiebert and Maslakova 2015a).

Distribution. Wrangell, AK, USA (MOBIL9484-19 in BOLD); Bamfield, BC, Canada (OPQCS038-10 in BOLD); Charleston, OR, USA; Crescent City, CA, USA (Hiebert and Maslakova 2015a; Maslakova et al. 2022); Bodega Bay, CA, USA (this study).

***Maculaura oregonensis* Hiebert & Maslakova, 2015a**

Maculaura oregonensis Hiebert & Maslakova, 2015a: 630, 4L–Q.

BIN. BOLD:ADM2641.

Material examined. B1.

Morphology. Body ~ 18 mm long; anterior tip white, eyeless, with lateral cephalic slits, the rest of the body pink. Anterior tip rounded in extension, head not demarcated from the body. Cerebral ganglia rosy and visible through the body wall (Fig. 5E). Body somewhat transparent. Posterior end with translucent, somewhat thickened caudal cirrus.

Identification. Bodega Bay individuals conform to the morphological description of *Maculaura* spp., and COI sequences exhibit > 99% similarity to those of *M. oregonensis* from Oregon (Hiebert and Maslakova 2015a; Maslakova et al. 2022: OTU 61).

Habitat. Collected from Bodega Harbor within the holdfast of subtidal Giant Kelp (*Macrocystis pyrifera*) at a depth of 3–4 m (station 6). In Oregon, individuals have also been found intertidally in sand and mud (Hiebert and Maslakova 2015a).

Distribution. Charleston, OR, USA (Hiebert and Maslakova 2015a; Maslakova et al. 2022); Bodega Bay, CA, USA (this study).

Notes. This is the first record of the species in California.

Genus *Riserius* Norenburg, 1993

Riserius is the only known genus of Pilidiophora to exhibit a mesopsammic lifestyle, i.e., living interstitially among sand grains. Its members display a curious suite of features: lack of cutis, cerebral organs opening via lateral pits rather than longitudinal slits, and a transverse cephalic furrow that encircles the body in front of the mouth. Possesses a unique sock-like pilidium recurvatum larva (Hiebert et al. 2013). A single species, *Riserius pugetensis* Norenburg, 1993, is described from coarse marine sediments of Puget Sound, Washington. Two additional, undescribed species, *R. sp.* “eyes” and *R. sp.* “no eyes,” are known from southern Oregon, and two others, *R. sp.* 3 and *R. sp.* 4, from the Sea of Japan

(Vostok Bay, Russia), all collected exclusively in larval form, but some raised in the laboratory to sexual maturity (Hiebert et al. 2013; Hiebert 2016). Similar larval forms are reported from other parts of the world, but sequence data are lacking (reviewed in Hiebert et al. 2013). Phylogenetic analysis by Kajihara et al. (2022b) suggests *Riserius* is a derived lineid that lost the lateral cephalic slits.

***Riserius* sp. BOBA007**

BIN. BOLD:AEJ1230.

Material examined. B11, BON64, BON65.

Morphology. Thread-like cream-colored worm, 50–100 mm long (Fig. 5A), with a long and narrow pointed head not well demarcated from the body, except by the cerebral organ pits. With four ocelli in a small cluster on each side of the head just in front of the pink tinged cerebral ganglia (Fig. 5B). Cerebral organs just posterior to the brain, opening via conspicuous lateral pits. With a V-shaped transverse furrow located posteriorly ~ 3/4 of the length from the tip of the head to the cerebral organs.

Identification. Morphology of our specimens agrees with that of *Riserius* spp. (Norenburg 1993; Hiebert et al. 2013), though specimens observed here are much longer than *R. pugetensis*, which is ~ 15 mm. Sequences from Bodega Bay specimens are distinct from those of the previously reported species, and 16S rRNA tree places these individuals within a monophyletic *Riserius* clade (Fig. 3). Specimens from Bodega Bay represent a new species of *Riserius*.

Habitat. Collected on wave-exposed, sandy beaches from among very coarse sand in the low intertidal zone at ~ -0.15 m to +0.30 m above Mean Lower Low Water (MLLW, station 13). Small numbers of individuals were also observed on other local beaches among very coarse sand (station 20).

Distribution. Bodega Bay, CA, USA (this study).

Notes. Species new to science. First record of the genus in California.

LINEIDAE incertae sedis

Lineus and *Micrura* are non-monophyletic mega-genera within the family Lineidae (e.g., see Kajihara et al. 2022b). The morphological diagnoses of these genera are based on combinations of non-unique characters (Schwartz 2009). Here we use names *Lineus* and *Micrura* as taxonomic artifacts, and not to imply shared common ancestry.

***Lineus flavescens* Coe, 1904**

Lineus flavescens Coe, 1904: 184, pl. XVII, figs 3, 4.

BIN. BOLD:ADS0049.

Material examined. BON6, BON11, BON40, BON50, BON60, BON86.

Morphology. Body 8–52 mm long, with significant variation in color: pale (semi-transparent), tan, reddish brown, and rosy-orange varieties observed (Fig. 5K), with lighter coloration ventrally, and smaller individuals appearing paler in color. Head not demarcated from the body, with pale margins, and 3–7

red, purple, or black ocelli arranged closely in a single row on each side of the anterior tip along the head margin (Fig. 5L, M). In some individuals, there is an irregular transverse band of white pigment granules just posterior to and between the two rows of ocelli (Fig. 5M). Cerebral ganglia are rosy, but this is faint in some individuals. Mouth just posterior to the end of the lateral cephalic slits on the ventral side. Body tapers posteriorly.

Identification. The six individuals included here match closely (99–100% similarity, COI) to *Lineus flavescens* reported from southern Oregon (Hiebert 2016; Maslakova et al. 2022: OTU 45) and agree with Coe’s description of the species. A closely related species (5–6% divergence, COI) is reported from Dutch Harbor, Alaska (OR590584), Puget Sound, Washington (BBPS027-19 in BOLD) and Charleston, Oregon (Fig. 2; Maslakova et al. 2022: OTU 46). The two species closely resemble each other, but one is known to occur from Alaska to Oregon, while the other from Puget Sound, Washington to Long Beach, California. Because the type locality of *L. flavescens* Coe, 1904 is San Pedro, California, we assume that we encountered the “real” *L. flavescens*, and not its more northerly look-alike.

Habitat. Collected from among colonial ascidians, algae, and other low intertidal organisms on rocky intertidal shores (stations 2, 6, 10, 15). Also collected just below the surface on intertidal mudflats (station 8).

Distribution. Puget Sound, WA, USA (BBPS722-19 in BOLD); Charleston, OR, USA (Hiebert 2016; Maslakova et al. 2022); Bodega Bay (this study), Point Mugu (DISA800-19 in BOLD) and Long Beach, CA, USA (DISA619-19 in BOLD).

Notes. With *Kulikovia* sp. BOBA003 (above) and Siphonenteron gen. sp. BOBA004 (below), this species belongs to the Siphonenteron clade, defined by Chernyshev et al. (2018), also referred to as “lineid lineage N” by Kajihara et al. (2022b), and not closely related to the type species of the genus, *Lineus longissimus* (Gunnerus, 1770).

***Micrura verrilli* Coe, 1901**

Lineus striatus Griffin, 1898: 214.

Micrura verrilli Coe, 1901: 68, pl. V, figs 1–3.

BIN. BOLD:ADW4746.

Material examined. BON2.

Morphology. Body ~ 12 cm long, margins and ventral surface white, dorsally with an orange patch at the anterior tip, bordered posteriorly by white, and followed by a broad purple stripe, which is interrupted at intervals by thin, transverse white lines (Fig. 5H). With lateral cephalic slits and a slender caudal cirrus.

Identification. Morphologically, specimens from Bodega Bay resemble *Lineus striatus* briefly described by Griffin (1898) from Puget Sound, Washington and *Micrura verrilli* described by Coe (1901) from Prince William Sound, Alaska. In addition, three similar species have been reported from the western Pacific: *Micrura bella* (Stimpson, 1857), *Micrura impressa* (Stimpson, 1857), and *Micrura festiva* Takakura, 1898. Coe synonymized Griffin’s taxon with his own (despite Griffin’s having priority), and *M. impressa* and *M. festiva* and have been treated as synonyms of *M. bella* (Crandall and Norenburg 2001), although *M. impressa*

is still listed as an accepted species in WoRMS (WoRMS Editorial Board 2023). ASAP analysis of the COI data suggests that all available *M. verrilli* sequences from the west coast of USA and Canada comprise a single OTU (Fig. 2). A closely related species is reported by Chernyshev and Polyakova (2022) from the Bering Sea as *Evelineus* sp., but there is no mention of its appearance, and it has only been encountered at depths 350 m and below. COI sequences suggest that Bodega Bay specimens are conspecific (97–99% similarity COI) with *M. verrilli* reported from Bamfield, BC, Canada (EF125007), Puget Sound, Washington (KF935508), and Charleston, Oregon (Maslakova et al. 2022: OTU 65). One additional available COI sequence (EF125001) of *M. verrilli* from Puget Sound, Washington contains many ambiguities, which causes some algorithms (e.g., Geneious Prime distance calculations) to interpret it as substantially different from the others, however ASAP analysis places it within the same OTU. A COI sequence of *M. bella* reported from the Sea of Japan (NC_027727) is ~ 10% different from that of *M. verrilli*, and thus belongs to a separate species.

Crandall and Norenburg (2001) suggest the extent of the anterior orange patch may help differentiate the eastern (exclusively dorsal) and western (extends onto ventral side) Pacific forms, however one of the *M. verrilli* specimens found in Washington had pigmentation on both sides (Schwartz 2009).

Habitat. Collected from the low intertidal zone among colonial ascidians (station 18) and observed among kelp holdfasts washed ashore in the Bodega Bay region.

Distribution. Bamfield, BC, Canada (Schwartz 2009); Puget Sound, WA, USA (Kvist et al. 2014); Charleston, OR, USA (Maslakova et al. 2022); Bodega Bay, CA, USA (this study).

Notes. The species reported here belongs to a clade of lineids with orange or magenta red anterior tip that may be synonymous with *Evelineus* (Schwartz 2009), also referred to as “lineid lineage A” (Kajihara et al. 2022b) and is not closely related to the type species of the genus, *Micrura fasciolata* Ehrenberg, 1828 (Chernyshev et al. 2018; Chernyshev and Polyakova 2019).

***Micrura wilsoni* (Coe, 1904)**

Lineus wilsoni Coe, 1904: 195, pl. XVI, figs 10, 11.

BIN. BOLD:ADW9830.

Material examined. BON41.

Morphology. Dark brown worm, ~ 45 mm long, slightly paler ventrally, cephalic lobe bordered by white at the anterior tip and along the lateral cephalic slits; thin white transverse bands at irregular intervals along most of the body length (Fig. 5G). No ocelli; rosy cerebral ganglia visible through the body wall. With a small white caudal cirrus.

Identification. Conforms to the description of *Micrura wilsoni* (Coe, 1904), described from Monterey and San Pedro, California. No look-alikes are currently known in the northeast Pacific. Although we were not able to obtain a high-quality COI sequence, 16S rRNA sequence from the Bodega Bay individual is 99–100% identical to those of *M. wilsoni* reported by Hiebert (2016) from southern Oregon. These individuals correspond to the COI-delimited *M. wilsoni* of Maslakova et al. (2022: OTU 90).

Habitat. Collected from kelp holdfasts (*Macrocystis pyrifera*) in the subtidal (station 6) and very low intertidal zones (station 7), also among holdfasts of subtidal bull kelp (*Nereocystis luetkeana*) washed ashore. In southern Oregon found on the exposed rocky shore under boulders and in rock crevices of the low intertidal zone.

Distribution. British Columbia, Canada (Gustav Paulay et al., unpublished BOLD records), Charleston, OR, USA (Hiebert 2016; Maslakova et al. 2022); Bodega Bay, CA, USA (this study). Records from San Juan Islands, WA (Maslakova, unpublished) and south to Mexico (Roe et al. 2007) are not currently substantiated by DNA data.

Notes. According to a recent phylogenetic analysis of the family Lineidae this species is not closely related to the type species of the genus, *Micrura fasciolata*, but is a member of a clade called “lineid lineage G” by Kajihara et al. (2022b).

Siphonenteron gen. sp. BOBA004

BIN. BOLD:ADR9817.

Material examined. BON59.

Morphology. Body 97 mm long, uniformly orange (Fig. 5I). Head the same width as the body, with pale margins, lateral cephalic slits. Ocelli arranged in two rows, one along each anterolateral margin (Fig. 5J), ~ 7 ocelli each, but it is difficult to know the true number as the pigment granules appear broken up and irregular.

Identification. BON59 resembles other species from the Siphonenteron clade (defined by Chernyshev et al. 2018), such as *Lineus flavescens*, *Kulikovia* spp. (Kajihara et al. 2022b; this study), and several undescribed representatives of the Siphonenteron clade from southern Oregon previously reported as *Lineus* sp. 1, *Lineus* sp. 2, *Lineus* sp. crescent, *Lineus* sp. red (Hiebert and Maslakova 2015b; Hiebert 2016) or *Lineus* sp. and *Kulikovia* sp. (Maslakova et al. 2022: OTUs 47, 49–51, 59). Among our collections from Bodega Bay, it most resembles *Lineus flavescens* and *Kulikovia* sp. BOBA003 (above). COI and 16S sequences do not have any species-level matches in GenBank; both place this species within the Siphonenteron clade (Figs 2, 3).

Habitat. Collected from a wave-exposed, rocky intertidal habitat among colonial ascidians and coralline algae (station 15).

Distribution. Discovery Island, Canada (QHAK2948-23 in BOLD); Bodega Bay, CA, USA (this study).

Notes. Species new to science.

Class HOPLONEMERTEA Hubrecht, 1879

Order Monostilifera Brinkmann, 1917

Suborder Cratenemertea

Familial classification suspended as per Kajihara, 2021

Genus *Nipponnemertes* Friedrich, 1968

Of the seven *Nipponnemertes* species described from the northeast Pacific, *N. bi-maculata* (Coe, 1901), *N. drepanophoroides* (Griffin, 1898), *N. fernaldi* Iwata, 2001, *N. occidentalis* (Coe, 1905), *N. pacifica* (Coe, 1905), *N. punctatula* (Coe, 1905), and *N. rubella* (Coe, 1905), only two have been reported and/or barcoded in recent

years, *N. bimaculata* and *N. punctatula*. The type locality of the latter species is southern California, but the only available barcodes are from Japan (Thollesson and Norenburg 2003; Hookabe et al. 2022), so the two may represent distinct species. An unknown species was reported from southern California (Andrade et al. 2012), from 360–390 m, but its identity and relationship to the above species is not yet known. Clearly, there is a diversity of *Nipponnemertes* species along the Pacific coast of North America, including several cryptic species.

Hookabe et al. (2022), in their revision of the genus that includes descriptions of ten new species, reported three clades of *Nipponnemertes* that are supported by molecular data as well as morphology: degree of head demarcation and presence/absence of a cephalic patch. The species we encountered at Bodega Bay most closely resembles *N. bimaculata* (Coe, 1901), which belongs to Clade B of Hookabe et al. (2022), with the northwest Pacific species *N. jambio* Hookabe et al., 2022, *N. neonilae* Hookabe et al., 2022, *N. ojimaorum* Hookabe et al., 2022, *N. crypta* Hookabe et al., 2022, and a potential trans-Pacific complex of species currently known as *N. punctatula* (Coe, 1905). Species in this complex vary in the degree of development of dorsal and cephalic pigmentation, but most have more or less distinct cephalic pigment patch(es).

***Nipponnemertes* sp. BOBA028**

BIN. BOLD:AEJ7531.

Material examined. BON13, BON95.

Morphology. Body 55–67 mm long, broad, reddish brown dorsally, much paler (almost white) ventrally. Head white, pointed, narrower than the body, with two maroon, triangular pigment patches placed symmetrically on either side of a mid-dorsal ridge (Fig. 6A). Numerous large ocelli lie in the space between the anterolateral margins and the pigment patches, ~ 20 per side. With two pairs of cephalic furrows. The anterior, cerebral organ furrows are equipped with numerous secondary furrows, as is characteristic of other members of the genus (Fig. 6A, inset). The posterior neck furrow forms a posteriorly directed V on the dorsal surface. Pink cerebral ganglia are discernible from the ventral side, just posterior to the cerebral organ furrows (Fig. 6A, inset). Proboscis and stylet apparatus not observed.

Identification. The specimens from Bodega Bay conform to the description of *Nipponnemertes bimaculata* (Coe, 1901) except for the shape of the cephalic patches, which are triangular in our specimens as opposed to oval in the original description. However, Coe (1905) later reported triangular patches in other specimens. COI sequences from Bodega Bay individuals form a separate OTU from those of the species previously reported as *N. bimaculata* from Washington and Oregon (Thollesson and Norenburg 2003; Maslakova et al. 2022: OTU 28), as well as an additional species collected in Puget Sound, Washington by CIE (BHFL_5974, Fig. 2), which can be distinguished from other northeast Pacific look-alikes by mottling on the dorsum. The *N. bimaculata* reported from Washington and Oregon seems to have narrower cephalic patches than the species from Bodega Bay. We have not observed any individuals with oval cephalic patches. The type locality of *N. bimaculata* is Alaska and Puget Sound, Washington (Coe 1901), although the species was later reported south to Ensenada, Mexico (Coe 1940). We suggest to reserve the name *N. bimaculata* for the northern form with solid dorsal pigmentation (Maslakova et al. 2022: OTU 28), and to treat Bodega Bay specimens as a new species.

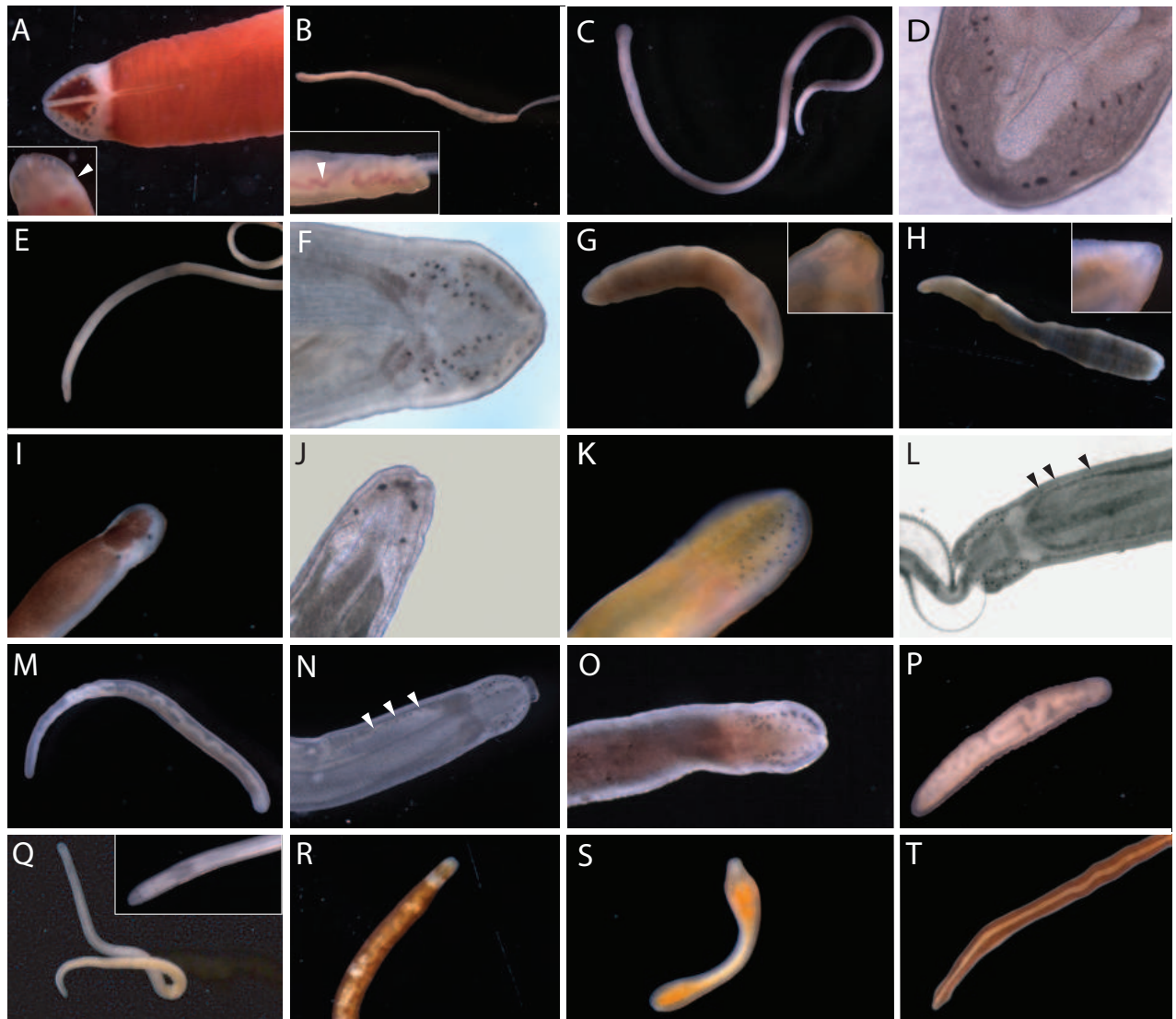


Figure 6. Hoplonemertean of Bodega Bay **A** *Nipponnemertes* sp. BOBA028, a new species, individual BON95. Dorsal and ventral (inset) view of the anterior, showing cerebral organ furrows with numerous secondary furrows (arrowhead) and pink cerebral ganglia **B** *Amphiporus* sp. BOBA024, a new species, individual BON61. Inset a close up lateral view of the anterior, showing red blood vessels (arrowhead) **C**, **D** *Amphiporus* sp. BOBA018 individual BON44 **D** close up of head in transmitted light, showing pattern of ocelli **E**, **F** *Amphiporus* sp. BOBA017 individual B20 **F** close up of head in transmitted light, showing pattern of ocelli **G** *Poseidonemertes* sp. BOBA010, a new species, individual B14. Inset a close up of the head showing ocelli **H** *Poseidonemertes* sp. BOBA033, a new species, individual BON35, full body. Inset a close up of the head showing ocelli **I** *Tetrastemma nigrifrons*, anterior end of BON01 **J** *Tetrastemma* sp. BOBA029, close up of head of B04 in transmitted light **K** *Zygonemertes* sp. BOBA012, individual B09 **L** *Zygonemertes* sp. BOBA014, a new species, close up of anterior of BON88 in reflected light, showing post-cerebral ocelli (arrowheads) **M**, **N** *Zygonemertes* sp. BOBA013, individual BON87 **N** close up of anterior showing post cerebral ocelli (arrowheads) **O** *Zygonemertes* sp. BOBA015, a new species, individual BON63 **P** *Antarctonemertes phyllospadicola*, individual BON67 **Q** *Nemertellina* sp. BOBA011, new to science, individual BON69 **R–S** *Oerstedtia* sp. BOBA022, new to science, showing differences in color pattern **R** individual BON32 **S** individual BON33 **T** *Tetrastemma bilineatum*, individual B18.

Habitat. Collected from the holdfasts of kelp (*Macrocystis pyrifera*) in the very low intertidal zone (station 7).

Distribution. Bodega Bay, CA, USA (this study).

Notes. Species new to science.

Suborder EUMONOSTILIFERA Kajihara, 2021

Infraorder AMPHIPORINA Kajihara, 2021

Familial classification suspended as per Kajihara (2021)

Genus *Amphiporus* Ehrenberg, 1831

A diverse and non-monophyletic genus of the class Hoplonemertea with 74 species listed in the WoRMS database, many more having been declared *nomen dubium*, or transferred to other genera (Gibson and Crandall 1989). We refer to the species below as *Amphiporus* merely to emphasize the close relationship to previously described species within the genus, not to imply that they constitute a monophyletic group.

Amphiporus sp. BOBA024

BIN. BOLD:AEI5687.

Material examined. BON36, BON61.

Morphology. Body slender, 13 mm long, yellowish white (Fig. 6B). Red blood vessels show prominently through the body wall (Fig. 6B, inset). Head narrow, with a single row of ~ 8 ocelli on either side (Fig. 6B, inset). Very slender, cylindrical basis slightly longer than the central stylet (Fig. 7A), with two accessory stylet pouches.

Identification. Specimens from Bodega Bay resemble *Amphiporus cruentatus* Verrill, 1879, originally described from Vineyard Sound, Massachusetts, but later reported from Puget Sound, Washington to San Diego, California (Coe 1905, 1940), in having a small and slender pale yellow body, a single row of ocelli on each side of head, red blood, and a very slender basis of central stylet, with ratio of stylet length to basis length (S/B ratio) close to 1. DNA sequence data are not available for *A. cruentatus* from the Atlantic Coast of North America. Maslakova et al. (2022) published COI sequences of two other Pacific *A. cruentatus* look-alikes: one from southern Oregon (OTU 27), and another from the Bay of Panama (OTU 143), and a third from the Caribbean coast of Panama (OTU 274, as *Monostilifera* gen. sp.). Given this abundance of cryptic species, it seems likely that the Pacific forms are distinct from the originally described Atlantic *A. cruentatus*. Bodega Bay individuals form a separate OTU from the Oregon individuals (Fig. 2; Maslakova et al. 2022: OTU 27).

Habitat. Collected from wave-exposed rocky shores among surfgrass roots and other low intertidal organisms (stations 14, 18).

Distribution. Bodega Bay, CA, USA (this study).

Notes. Species new to science.

Amphiporus imparispinosus Griffin, 1898 species complex

Amphiporus sp. BOBA017

Amphiporus imparispinosus: Maslakova et al. 2022.

BIN. BOLD:ADR7530.

Material examined. B20, BON47.

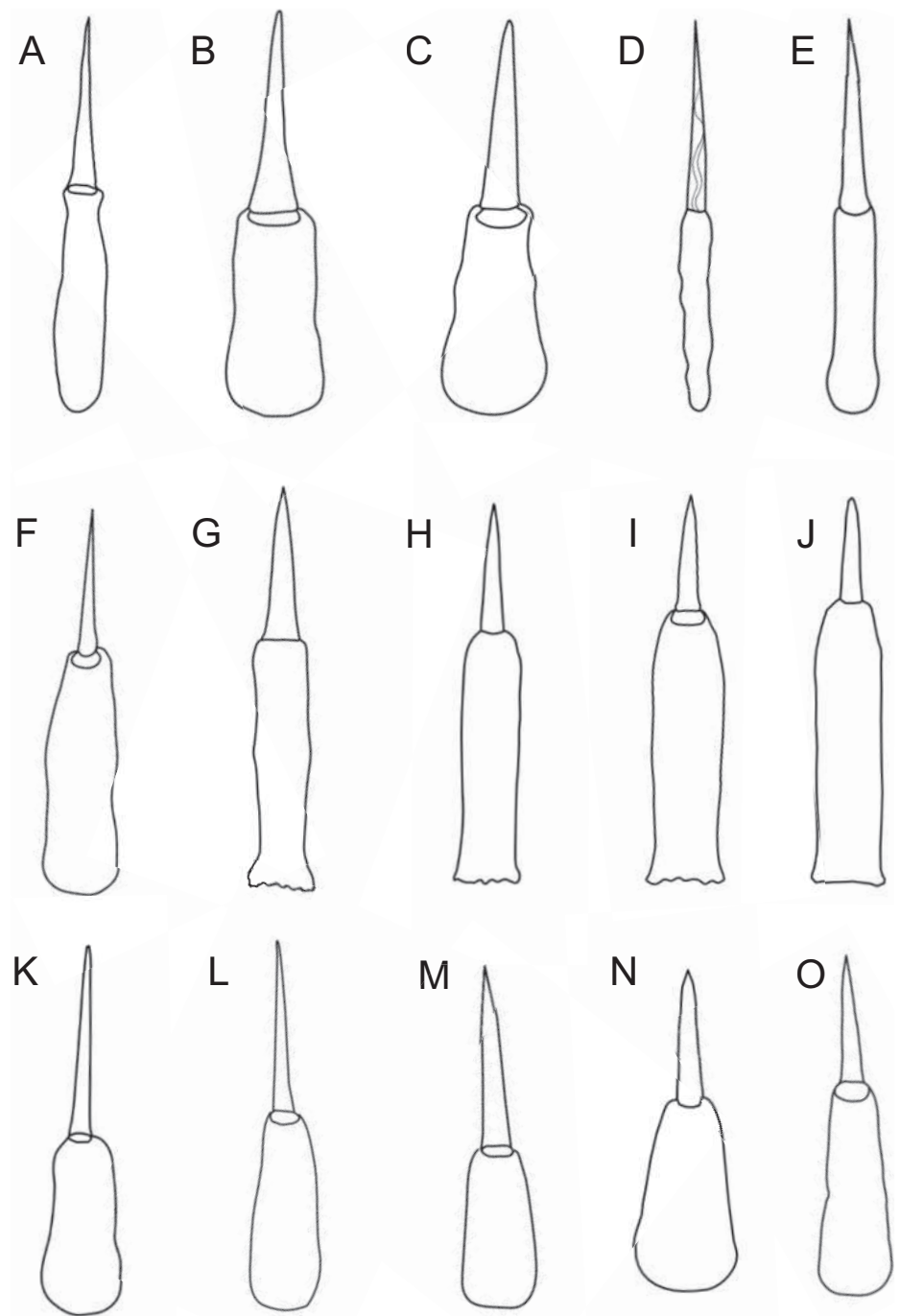


Figure 7. Stylets of Hoplonemerteans of Bodega Bay **A** *Amphiporus* sp. BOBA024, individual BON61 **B** *Amphiporus* sp. BOBA018, individual BON16 **C** *Amphiporus* sp. BOBA017, individual B20 **D** *Ototyphlonemertes* sp. BOBA030, individual BON78 **E** *Poseidonemertes* sp. BOBA010, individual B14 **F** *Tetrastemma nigrifrons*, individual BON01 **G** *Zygonemertes* sp. BOBA012, individual B06 **H** *Zygonemertes* sp. BOBA014, individual B07 **I** *Zygonemertes* sp. BOBA013, individual BON76 **J** *Zygonemertes* sp. BOBA015, individual BON62 **K** *Antarctonemertes phyllospadicola*, individual BON67 **L** *Nemertellina* sp. BOBA011, individual BON69 **M** *Oerstedia* sp. BOBA022, individual BON32 **N** *Eumonostilifera* sp. BOBA016, individual B15 **O** *Tetrastemma* sp. BOBA020, individual BON75.

Morphology. Body 63 mm long, pale yellow to pale peach color (Fig. 6E). Head rounded and wider than the adjacent body, with 20–25 ocelli on each side, arranged as a row along the anterior margin, and another, more irregular grouping, medially (Fig. 6F). Cerebral ganglia pinkish in color. Basis pear-shaped, broadening posteriorly, S/B ~ 1 (Fig. 7C). With three accessory stylet pouches.

Identification. Specimens from Bodega Bay conform to the description of *Amphiporus imparispinosus* Griffin, 1898 from Port Townsend, Washington and Sitka, Alaska. Two similar species have been described from the northeast Pacific: *Amphiporus leuciodus* Coe, 1901, from Victoria, BC, Canada and New Metlakatla and Glacier Bay, Alaska, and *Amphiporus similis* Coe, 1905, from Monterey, California, though Coe later treated the former as a synonym (1905), and the latter as a variety (1940) of *A. imparispinosus*. Subsequent authors retained all three as valid species (Gibson and Crandall 1989; Crandall and Norenburg 2001; WoRMS; but see Roe et al. 2007). Coe (1905) notes that *A. imparispinosus* has a pink brain, small cerebral sense organs, three accessory stylet pouches, and is longer (to 75 mm) than *A. similis*, which is 10–15 mm, with a clear brain, large cerebral sense organs, fewer ocelli and two accessory stylet pouches. Griffin (1898) does not mention color of the cerebral ganglia in *A. imparispinosus*.

Maslakova et al. (2022) report, based on COI sequence data, three distinct *A. imparispinosus*-like species (OTUs 4–6) from the northeast Pacific. One of those (OTU 4) is distributed from Dutch Harbor, AK to Charleston, OR, and overlaps the original range of *A. imparispinosus* (including samples from Puget Sound, WA), so may represent the true *A. imparispinosus*. The other two OTUs have not been reported north of Oregon (Maslakova et al. 2022: OTUs 5 and 6). Another look-alike is reported from the Sea of Japan (Chernyshev and Polyakova 2019: MN211508). The pinkish color of cerebral ganglia and the three accessory stylet pouches in our specimens suggests that it is not *A. similis*, but an undescribed cryptic species.

Habitat. Collected from wave-exposed, rocky intertidal habitats (stations 16, 18), including on holdfasts of the kelp *Egregia menziesii* and within mid-intertidal mussel beds; among algal turf.

Distribution. Charleston, OR, USA (Maslakova et al. 2022: OTU 6); Bodega Bay (this study); Point Mugu, CA, USA (DISA798-19 in BOLD).

***Amphiporus* sp. BOBA018**

Amphiporus imparispinosus: Maslakova et al. 2022.

BIN. BOLD:AEA1922.

Material examined. BON16, BON44.

Morphology. Body 38–70 mm long, white. Head rounded and wider than body (Fig. 6C). Four clusters of ocelli; two rows following the anterolateral margins, and two more located posteriorly and medially, above the colorless cerebral ganglia (Fig. 6D). The posterior clusters of ocelli appear reddish, while the anterior rows appear brown in reflected light. The neck furrow is obvious and forms a dorsal V-shape posterior to the cerebral ganglia. Basis with rounded posterior margin and slight medial constriction. Central stylet equal in length to the basis (Fig. 7B). Proboscis with three accessory stylet pouches.

Identification. See *Amphiporus* sp. BOBA018 above. The presence of three pouches of accessory stylets and the length of the worms suggest that this is not *A. similis*, but an undescribed cryptic species.

Habitat. Collected from wave-exposed, rocky intertidal habitats (stations 18, 19), including on holdfasts of the kelp *Egregia menziesii* and crawling across other low intertidal surfaces.

Distribution. Charleston, OR, USA (Maslakova et al. 2022: OTU 5); Bodega Bay, CA, USA (this study).

Notes. This is the first record of the species in California.

Genus *Emplectonema* Stimpson, 1857

Emplectonema viride Stimpson, 1857

Emplectonema viride Stimpson, 1857: 163.

Emplectonema gracile: Coe 1901: 23, pl. VIII, fig. 3; 1905: 207, pl. I, figs 14, 15; 1940: 279, pl. XXX, fig. 40; Roe et al. 2007: 229, pl. 89, fig. I.

BIN. BOLD:AAP1200.

Material examined. B16.

Morphology. Body long and slender, green dorsally, cream-colored ventrally. Head not especially demarcated from the body. With numerous ocelli distributed along the colorless anterolateral margins of the head. Pink cerebral ganglia. Basis of central stylet much longer than the slightly curved central stylet.

Identification. Specimens from Bodega Bay conform to the description of *Emplectonema viride* Stimpson, 1857, as redescribed by Mendes et al. (2021). There are no known look-alikes in the northeast Pacific. For years, the species has been reported as a synonym of its Atlantic look-alike *Emplectonema gracile* (Johnston, 1837) (e.g., Roe et al. 2007 and references therein). The two species were recently shown to be distinct, the name *E. viride* resurrected, and the Pacific species redescribed (Mendes et al. 2021).

Habitat. Collected from a mid-intertidal mussel bed (station 1), and commonly observed in many intertidal habitats throughout the Bodega Bay region. Typically associated with acorn barnacles, which it preys upon.

Distribution: Amaknak (MZ580909) and Fox (MZ580901) Islands, AK, USA; Bamfield (MG423290) and Discovery Islands (QHAK2422-22, QHAK2449-22 in BOLD), BC, Canada; Charleston, OR, USA (Hiebert 2016; Mendes et al. 2021; Maslakova et al. 2022; von Dassow et al. 2022); Bodega Bay, CA, USA (this study). The species is reported as far south as Mexico (Roe et al. 2007), but so far, there are no DNA sequence data to confirm.

Notes. For photographs of this species, see Mendes et al. (2021: fig. 3)

Genus *Ototyphlonemertes* Diesing, 1863

Species of *Ototyphlonemertes* are exclusively mesopsammic, living in the interstices of well-sorted, coarse marine sediments. They are easily distinguished from other small, slender, white eumonostiliferans by the presence of a pair of statocysts in the cerebral ganglia, and the lack of ocelli in adults, but most of the described species appear to represent cryptic species complexes (e.g., Leasi and Norenburg

2014; Leasi et al. 2016). Two species of *Ototyphlonemertes* with spirally sculpted stylets are described from the Pacific coast of the U.S.: *O. americana* Gerner, 1969 and *O. spiralis* Coe, 1940, and a third species, with a smooth stylet, was reported near San Francisco (Roe et al. 2007). However, the *Ototyphlonemertes* spp. of the Pacific coast are not well sampled, and “forms that key out to either of the known species have a reasonable probability of not being those species” (Roe et al. 2007).

***Ototyphlonemertes* sp. BOBA030**

Ototyphlonemertes lactea: Leasi et al. 2016.

BIN. BOLD:ADM3126.

Material examined. BON77, BON78.

Morphology. Body 3.5 mm long and less than 1 mm wide, white; foregut region transparent, intestinal region cream-colored. Head slightly demarcated from the body by a transverse cephalic groove. With a pair of statocysts, one in each of the two ventral cerebral ganglia. Statocysts of the polygranular type. Basis slender, irregularly cylindrical, and longer than the spirally sculpted central stylet (Fig. 7D). Proboscis diaphragm not especially long, middle chamber bulbous.

Identification. Specimens from Bodega Bay conform to the description of *O. americana* Gerner, 1969 from Puget Sound, Washington, but DNA sequence data are not available from Puget Sound region to confirm identification. COI sequences from Bodega Bay specimens in this study match closely (> 99% similarity, COI) with a species previously reported from San Diego, California as *Ototyphlonemertes lactea* by Leasi et al. (2016: KU230123). *O. lactea* was described from Brazil (Corrêa 1954), but the name was later used to refer to a group of species with similar morphologies and presumed shared ancestry, called phylomorphs (Envall and Norenburg 2001). *O. americana* belongs to the lactea type, which was later synonymized with the macintoshi type (Kajihara et al. 2018), a decision supported by a multigene phylogenetic analysis (Leasi et al. 2016). Relative to macintoshi type worms, *O. americana* and *O. lactea* have a shorter proboscis diaphragm and a bulbous middle chamber, as opposed to a long, tubular one. Another OTU of a lactea type reported from Half Moon Bay, California by Leasi et al. (2016: KU230128) is likely to be confused with the Bodega Bay species. Sampling of *Ototyphlonemertes* in Puget Sound is needed to resolve the specific identity of these lineages.

Habitat. Collected from low intertidal, coarse marine sediments on a wave-exposed sandy beach (station 13).

Distribution. Wright’s Beach, CA, USA (Leasi et al. 2016); Bodega Bay, CA, USA (this study).

Genus *Paranemertes* Coe, 1901

***Paranemertes* sp. BOBA009**

Paranemertes peregrina: Hiebert 2016: 78.

Paranemertes sp.: Hao et al. 2015: 572, fig. 1J.

BIN. BOLD:ADM0221.

Material examined. B2.

Morphology. Body ~ 5 cm long, orangish purple dorsally, paler ventrally. Head slightly demarcated from the body, with red cerebral ganglia visible through the body wall. Stylet apparatus not observed.

Identification. *Paranemertes peregrina* is a cryptic species complex composed of at least seven distinct lineages (Hao et al. 2015). A single widely distributed lineage likely corresponding to the *P. peregrina* Coe, 1901 originally described from Alaska has been identified on the basis of proximity to the type locality and habitat, and is confirmed by DNA sequence data to occur from British Columbia, Canada to southern Oregon, USA on the northeast Pacific coast, and from Kuril Islands, Russia to Shandong, China on the northwest Pacific coast (Hao et al. 2015). The remaining six species, including the two previously reported from Bodega Bay, remain undescribed.

Habitat. Collected from kelp holdfasts in shallow subtidal zone within Bodega Harbor (station 6).

Distribution. Unalaska Island, AK, USA (DUTCH345-19 in BOLD); Discovery Islands, BC, Canada (QHAK177-20 in BOLD); Charleston, OR, USA (Hiebert 2016; Maslakova et al. 2022: OTU 10); Bodega Bay, CA, USA (Hao et al. 2015; this study).

Notes. Hao et al. (2015) report that the two *Paranemertes* cf. *peregrina* OTUs from Bodega Bay are well-separated by habitat, with one occurring in mudflats and the other in rocky intertidal contexts, under stones, among algae, etc. Interestingly, the species encountered in this survey came from among kelp holdfasts but matches the one previously found in mudflats by Hao et al. (2015). This might not be as surprising as it appears at first because the kelp holdfasts collected by us (station 6) were from a small kelp bed within Bodega Harbor immediately adjacent to extensive mudflats. For photographs of this species, see Hao et al. (2015: fig. 1J).

Genus *Poseidonemertes* Kirsteuer, 1967

Poseidonemertes sp. BOBA010

BIN. BOLD:AEK1697.

Material examined. B14.

Morphology. Stout, pale, rust-colored worm with thick, clear margins; body widens posteriorly. Anterior end sharply pointed, with two ocelli near its tip (Fig. 6G). Basis cylindrical, slender, of a similar length as the central stylet (Fig. 7E). With two accessory stylet pouches.

Identification. The two *Poseidonemertes* specimens from this study (B14 and BON35 listed below) resemble *Poseidonemertes collaris* Roe & Wickham, 1984 described from Bodega Bay, California, and other light-colored members of the genus, e.g., *Poseidonemertes maslakovae* Chernyshev, 2002 and *Poseidonemertes* sp. 508 from the Sea of Japan. *P. collaris* is the only member of the genus previously reported from the Pacific coast of the U.S. COI sequence data suggest B14 represents a distinct OTU (8.2% divergent) from what was reported as *P. collaris* by Tholleson and Norenburg (2003) and from BON35 (described below, 19% divergent), or any other previously sequenced members of the genus.

Habitat. Collected just offshore, < 200 m from an open coast beach, among subtidal sand/mud sediments from a depth of 6–7 m (station 3).

Distribution. Bodega Bay, CA, USA (this study).

Notes. Species new to science.

***Poseidonemertes* sp. BOBA033**

BIN. BOLD:AEK1698.

Material examined. BON35.

Morphology. Stout, cream-colored worm, ~ 25 mm long, with branched intestinal diverticula, greenish in color, highly visible through the body wall (Fig. 6H). Body widens posteriorly. Head pointed, with two ocelli near its tip (Fig. 6H, inset). Stylet apparatus not observed.

Identification. See B14 above.

Habitat. Collected from an intertidal mudflat, just below the surface of the sediment, among polychaete tubes (station 8).

Distribution. Bodega Bay, CA, USA (this study).

Notes. Species new to science.

Genus *Tetrastemma* Ehrenberg, 1831

This non-monophyletic genus of small four eyed eumonostiliferans containing > 100 species was recently redefined by Chernyshev et al. (2021a) based on a multigene phylogenetic analysis. *Tetrastemma nigrifrons* is part of the *Tetrastemma* clade sensu Chernyshev et al. 2021a. The other two species are included here tentatively.

***Tetrastemma nigrifrons* Coe, 1904**

Tetrastemma nigrifrons Coe, 1904: 159, pl. XV, fig. 7, pl. XVI, figs 6–9, pl. XVII, fig. 1, pl. XX, fig. 16, pl. XXI, figs 15–23; Maslakova et al. 2022.

Quasitetrastemma nigrifrons Chernyshev, 2004: 154; Chernyshev et al. 2021a.

BIN. BOLD:ADX0572.

Material examined. BON1.

Morphology. Body 27 mm long, brown dorsally, pale ventrally. Head rounded with colorless margins and a broad brown patch, differentiated only slightly from the body by the colorless transverse band (Fig. 6I). With four eyes; the anterior pair halfway between the anterior tip and the cerebral organ furrows, the posterior pair just below the posterior furrow. With bright red blood vessels. Cylindrical basis, slightly longer than the central stylet (Fig. 7F). With two accessory stylet pouches.

Identification. Fits the description of *Tetrastemma nigrifrons* Coe, 1904, described from Monterey Bay, California. A look-alike, *Tetrastemma stimpsoni* Chernyshev, 1992 occurs in the northwest Pacific and the Sea of Japan (Chernyshev et al. 2021a). A third, closely related species has been documented from Dutch Harbor, Alaska (6–7% divergence, BIN: BOLD:AEC4254). No pictures are available, but the description (“brown dorsally, white band separates head, 2 prs eye spots”) matches that of this species.

Habitat. Collected from the low intertidal zone among red algal blades and colonies of the kamptozoan *Barentsia conferta* (station 17). Similar specimens also observed intertidally among low zone tunicates and algae (station 2), kelp holdfasts (station 7), and surfgrass roots (station 14). Subtidally, among organisms on marina docks (station 9).

Distribution. Unalaska, AK, USA (DUTCH209-19 in BOLD); Canada (Chernyshev et al. 2021a); Charleston, OR, USA (Chernyshev et al. 2021a; Maslakova et al. 2022); CA, USA (Chernyshev et al. 2021a); Bodega Bay, CA, USA (this study).

Notes. This species has variable coloration, both in terms of pattern and the amount of pigmentation (Roe et al. 2007; Maslakova, unpublished). Some specimens are almost completely dark brown dorsally with a colorless transverse bar separating the cephalic patch from the dorsum, while others have much less dorsal pigment (e.g., it may be separated into two more or less continuous stripes by a pigment-less mid-dorsal region). Some specimens may be almost entirely devoid of pigment, except for the cephalic patch (which may be broken into two by a mid-dorsal gap). With four ocelli. Blood vessels are red, and clearly show through the body wall.

***Tetrastemma* sp. BOBA029**

Tetrastemma sp. 1: Hiebert 2016: 84, fig. 2.14.

Tetrastemma sp.: Maslakova et al. 2022.

BIN. BOLD:ADW8618.

Material examined. B4.

Morphology. Small and slender, transparent, fast-moving worm; internal structures appear yellowish through the body wall. Anterior tip with a small white patch. With four ocelli (Fig. 6J). Stylet apparatus not observed.

Identification. Anterior white patch and otherwise featureless body distinguishes this from other species of *Tetrastemma* reported from northeast Pacific (Roe et al. 2007). DNA sequences from the Bodega Bay specimen match those of *Tetrastemma* sp. 1 first reported from southern Oregon by Hiebert (2016) and Maslakova et al. (2022: OTU 19 as *Tetrastemma* sp.). Two other overall similar species lacking the anterior white patch occur in southern Oregon (Maslakova et al. 2022: OTUs 15 and 20).

Habitat. Collected from Bodega Harbor within the holdfasts of subtidal Giant Kelp (*Macrocystis pyrifera*) at a depth of 3–4 m (station 6). In Oregon, collected from among surfgrass (*Phyllospadix* spp.) in the rocky intertidal zone (Hiebert 2016).

Distribution. Charleston, OR, USA (Maslakova et al. 2022); Bodega Bay, CA, USA (this study).

Notes. First record of the species in California. This species is very common in southern Oregon. Reproductive individuals were found in July in southern Oregon, and deposited egg masses in laboratory dishes upon collection, with crawl-away juveniles hatching a week or two later.

***Tetrastemma* sp. BOBA020**

BIN. BOLD:AEJ7493.

Material examined. BON75.

Morphology. Body 1.7 mm long, transparent, with an orange gut. With four eyes and two pairs of cephalic furrows: cerebral organ furrows at the level of the posterior pair of eyes, and a V-shaped neck furrow posteriorly, overlying the

anterior portion of the cerebral ganglia. Conical basis, significantly longer than the central stylet (Fig. 70).

Identification. Resembles other featureless species of *Tetrastemma*. COI sequences show it to be distinct from any previously sequenced species.

Habitat. Collected from low intertidal, coarse marine sediments on a wave-exposed sandy beach (station 13).

Distribution. Bodega Bay, CA, USA (this study).

Notes. Species new to science.

Genus *Zygonemertes* Montgomery, 1897

Members of the genus *Zygonemertes* are distinct from other eumonostiliferans in having a single row of post cerebral ocelli on each side, along the lateral nerve cords, in addition to the more typical ocelli found in rows or groups on the head. In addition, all species we have had the opportunity to examine possess sickle-shaped microscopic inclusions in the epidermis, and most have a characteristically truncated basis of the central stylet.

Three species of *Zygonemertes* are reported from the northeast Pacific coast: *Z. albida* Coe, 1901, *Z. thalassina* Coe, 1901, and *Z. virescens* (Verrill, 1879). The first two were described by Coe from British Columbia and Alaska, respectively. *Zygonemertes thalassina* has never been reported outside its type locality, *Z. albida* was subsequently reported by Coe to occur as far south as Ensenada, Mexico (Coe 1944), and *Z. virescens* is reported to have a very wide geographic distribution including Pacific (British Columbia to Mexico), Atlantic (Maine to Florida) and Gulf coasts of North America, as well as Curaçao (Coe 1940; Gibson 1995; Roe et al. 2007), but clearly represents a large cryptic species complex (Maslakova, unpublished). The type locality of *Z. virescens* is New England. Presently we are aware of several genetically distinct Atlantic look-alikes (e.g., from Florida, Colombia, and Caribbean Panama); these are also distinct from several Pacific *Z. virescens*-like forms. Based on this, it seems most reasonable to exclude *Z. virescens* from the list of Pacific fauna, and to describe the Pacific forms as new species.

Zygonemertes thalassina was regarded as being extremely similar to *Z. virescens*, except often longer (to 60 mm), darker in color (olive green), with a smaller S/B ratio, a shorter, stubbier central stylet, and with five stylets per accessory pouch, rather than two or three (Coe 1901, 1905). *Zygonemertes albida* was distinguished on the basis of its small size, lack of color, longer proboscis, and differences in the stylet apparatus, appearing similar to juveniles of the other two species. Among individuals of *Z. virescens*, Coe noted variation in color, number and arrangement of ocelli, and relative proportions of central stylet and basis. While some of these features may be variable (e.g., with age or environment), we consider it likely that he encountered more than one species, as there are at least four *Z. virescens*-like species in southern Oregon alone (Maslakova et al. 2022: OTUs 23–26), and we identified an additional two species in this study. The increasing number of *Zygonemertes* species uncovered with genetic data, and the lack of barcodes from type localities make it difficult to assign existing names to these species. For now, we refer to them as *Zygonemertes* spp. until formal descriptions are made. We consider reports of *Z. albida* from the Atlantic coast dubious (Zattara et al. 2019).

Zygonemertes sp. BOBA012

Zygonemertes sp. 1: Hiebert 2016: 70.

Zygonemertes sp.: Maslakova et al. 2022.

Nemertea sp.: Leray and Paulay unpublished (MH242861).

BIN. BOLD:ADL9636.

Material examined. B5, B6, B9.

Morphology. Body somewhat transparent, greenish yellow with clear margins; 15–25 ocelli arranged in two irregular rows on each side of the head, with a single row of post cerebral ocelli on each side along the lateral nerve cords. Cerebral ganglia pink, visible through the body wall (Fig. 6K). With two pairs of cephalic furrows; cerebral organ furrows are simple ventrolateral arches located 1/2 to 2/3 of the way between the anterior tip and the neck furrow, which overlays the anterior portion of the cerebral ganglia. Specimens B5 and B9 had long slender basis with a slightly concave to flat posterior margin, B6 had a flared stylet basis similar to the illustration for *Z. virescens* in Roe et al. (2007). Central stylet shorter than basis, S/B ~ 0.5 (Fig. 7G); two accessory stylet pouches, with two stylets each.

Identification. See above on species of *Zygonemertes*. COI sequences from Bodega Bay specimens match those of *Nemertea* sp. from Puget Sound, Washington (Paulay and Leray, unpublished, MH242862) and those reported as *Zygonemertes* sp. 1 (Hiebert 2016) or *Zygonemertes* sp. (Maslakova et al. 2022: OTU 23) from southern Oregon.

Habitat. Collected from Bodega Harbor within the holdfasts of subtidal Giant Kelp (*Macrocystis pyrifera*) at a depth of 3–4 m (station 6).

Distribution. Puget Sound, WA, USA (MH242861; Maslakova, unpublished); Charleston, OR, USA (Maslakova et al. 2022); Bodega Bay, CA, USA (this study).

Notes. Species not previously reported from California. In the first round of PCR with universal primers, we apparently amplified the gut contents of these worms, the barnacle *Balanus glandula*. Like another barnacle-eating nemertean, *Emplectonema viride*, some specimens of this species have a long, slender basis of central stylet. The basis in this species appears slightly narrower than in other species of *Zygonemertes*.

Zygonemertes sp. BOBA013

Zygonemertes sp. 1: Hiebert 2016: 70.

Zygonemertes sp.: Maslakova et al. 2022; O'Mahoney et al. unpublished (MZ580839).

BIN. BOLD:ADW7912.

Material examined. BON27, BON76, BON80, BON87.

Morphology. Body 4–15 mm long; color ranging from white with a tinge of yellow to orange, sometimes with dark pigment spots along the sides of the body or at the posterior (Fig. 6M). 25–50+ ocelli arranged in four irregular rows on the head, a single row of ~ 10 post-cerebral ocelli along the lateral nerve cords (Fig. 6N). With two pairs of cephalic furrows: cerebral organ furrows are simple ventrolateral arches located 2/3 of the distance from the tip of the head

to the V-shaped neck furrow, which overlies the cerebral ganglia. Basis slender, much longer than the central stylet, $S/B \sim 0.5\text{--}0.65$, sometimes with slight medial constriction posteriorly, and with flat or slightly concave posterior margin (Fig. 7I). Two accessory stylet pouches with two or three stylets each.

Identification. See above on species of *Zygonemertes*. COI sequences from Bodega Bay specimens match a subset of those reported as *Zygonemertes* sp. 1 (Hiebert 2016) and *Zygonemertes* sp. (Maslakova et al. 2022: OTU 26) from southern Oregon, and two specimens from Dutch Harbor, Alaska. This species may correspond to *Z. albid*a or a cryptic undescribed species.

Habitat. Collected from the low intertidal zone among colonial ascidians and polychaete worm tubes (stations 7, 10). Collected subtidally from within holdfasts of bull kelp (*Nereocystis luetkeana*), station 11.

Distribution. Amaknak (MZ580839) and Unalaska Islands, AK, USA (MZ580813); San Juan Island, WA, USA (Maslakova, unpublished), Charleston, OR, USA (Hiebert 2016; Maslakova et al. 2022); Bodega Bay, CA, USA (this study).

Notes. First record of the species in California. Reproductive individuals encountered in August in Bodega Bay.

***Zygonemertes* sp. BOBA014**

BIN. BOLD:AEK0256.

Material examined. B7, B8, BON88, BON91.

Morphology. Body up to 31 mm long, greenish yellow, digestive tract appearing bright reddish orange ventrally. With ~ 15 ocelli on each side of the head, arranged in four irregular rows, and a single row of post-cerebral ocelli (~ 8) along each lateral nerve cord (Fig. 6L). Cerebral organ furrows $2/3$ the distance between the anterior tip and the posterior V-shaped neck furrow. Cylindrical basis, longer than the central stylet, with truncated posterior margin (Fig. 7H). $S/B \sim 0.5\text{--}0.65$. Two accessory stylet pouches, with two or three stylets each.

Identification. See above on species of *Zygonemertes*.

Habitat. Collected from Bodega Harbor within the holdfasts of subtidal Giant Kelp (*Macrocystis pyrifera*) in the shallow subtidal zone (< 5 m depth, station 6).

Distribution. Bodega Bay, CA, USA (this study).

Notes. Species new to science. Closely related to *Zygonemertes* sp. BOBA015 (6% divergence, COI).

***Zygonemertes* sp. BOBA015**

BIN. BOLD:AEJ0120, BOLD:ADR7155.

Material examined. BON62, BON63, BON81.

Morphology. Body 4–15 mm long, brownish, with numerous ocelli arranged in four irregular rows on the head, $\sim 25+$ on each side (Fig. 6O). Basis quite massive compared to central stylet, in terms of length and width (Fig. 7J), though this is not as obvious in smaller specimens (BON63). $S/B 0.4\text{--}0.75$. One individual (BON81) had an unusual triangle-shaped basis, widening significantly posteriorly, with a flat posterior margin. Two accessory stylet pouches with two or three stylets each.

Identification. See above on species of *Zygonemertes*.

Habitat. Low intertidal zone among surfgrass roots (station 14) and colonial ascidians (station 10).

Distribution. Calvert Island, BC, Canada (BHAK2541-20 in BOLD). Bodega Bay, CA, USA (this study); Point Mugu, CA, USA (DISA797-19 in BOLD).

Notes. Species new to science. Closely related to *Zygonemertes* sp. BOBA014 (6% divergence, COI).

Amphiporina incertae sedis

Eumonostilifera sp. BOBA016

Monostilifera sp.: Maslakova et al. 2022.

BIN. BOLD:AEJ6897.

Material examined. B15.

Morphology. Body orange, with 15 ocelli on each side of the cephalic lobe. Basis nearly conical, rounded at the bottom, a bit shorter than the central stylet (Fig. 7N). Two accessory stylet pouches with two stylets each.

Identification. Resembles individuals of *Amphiporus* sp. BOBA017 and BOBA018 described above, but COI sequences do not match any previously sequenced species, and do not group closely with *Amphiporus* cf. *imparispinosus*. Taxonomic affiliation is uncertain until a more thorough phylogenetic analysis (with more conservative markers than COI and 16S) is carried out. Overall morphology and 16S tree (Fig. 3) suggest it belongs within Amphiporina.

Habitat. Among fouling organisms on marina docks (station 9).

Distribution. San Juan Island, WA, USA (Maslakova, unpublished); Charleston, OR, USA (Maslakova et al. 2022); Bodega Bay, CA, USA (this study).

Notes. First record of the species in California. The eggs of this species (which have a polyhedral chorion) have been collected in the plankton in Charleston, OR (Maslakova et al. 2022: OTU 13) and matching COI barcodes have been obtained from adults collected from Friday Harbor, WA (Maslakova, unpublished).

Infraorder Oerstediiina Kajihara, 2021

Family Oerstediidae Chernyshev, 1993

Genus *Antarctonemertes* Friedrich, 1955

***Antarctonemertes phyllospadicola* (Stricker, 1985)**

Tetrastemma phyllospadicola Stricker, 1985: 682, figs 1–28; Stricker and Cavey 1986: 2188; McDermott 1997: 254; Stricker and Folsom 1997: 57; Stricker et al. 2001: 214.

BIN. BOLD:ACH3602.

Material examined. BON67, BON68.

Morphology. Body short and stout, pale yellow to pale peach color, 6–7 mm long (Fig. 6P), with four eyes occupying the corners of a square, and a prominent pointed snout (not apparent on Fig. 6P). Cephalic lobe at its widest at the level of cerebral organ furrow, between the first and second pairs of eyes. Cerebral organ furrows are limited to the ventral side. Transverse neck furrow posterior to the second pair of eyes. Rounded in cross section, proboscis extending

to posterior end of the body. Basis oval, widening a bit posteriorly, with a slender central stylet, $S > B$ (Fig. 7K). With two accessory stylet pouches, with one or two stylets each.

Identification. Specimens from Bodega Bay conform to the description of *Antarctonemertes phyllospadicola* (Stricker, 1985) described from San Juan Island, Washington, and the COI sequences match those of *A. phyllospadicola* from San Juan Island, Washington (Thollessen and Norenburg 2003) and southern Oregon (Maslakova, unpublished).

Habitat. Collected with intertidal samples of surfgrass, *Phyllospadix scouleri* (station 14). In the San Juan Islands, WA this species is found on blades and inside female inflorescences of *P. scouleri* in the low intertidal zone.

Distribution. Bamfield Marine Science Centre, Canada (Chernyshev and Polyakova 2019); Puget Sound, WA, USA (Maslakova and von Döhren 2009); Charleston, OR (Maslakova, unpublished); Bodega Bay, CA, USA (this study).

Notes. This is the first record of this genus and species for California.

Genus *Nemertellina* Friedrich, 1935

The genus *Nemertellina* has never been reported from the northeast Pacific and currently contains five valid species, three occurring in Kiel Bay, Germany, and one each in Madagascar and Japan. Members of this genus have four eyes, with the anterior and posterior pairs widely separated; small and simple cerebral organs located far anterior to the brain and opening ventrally near the tip of the head; short rhynchocoel; conical or pear-shaped basis, with 2–4 accessory stylet pouches. *Nemertellina canea* Friedrich, 1935b, *N. minuta* Friedrich, 1935a, *N. oculata* Friedrich, 1935b and *N. tropica* Kirsteuer, 1965 are reported to completely lack cephalic furrows, while *N. yamaokai* Kajihara, Gibson & Mawatari, 2000 has two pairs.

Nemertellina sp. BOBA011

BIN. BOLD:AEJ4336.

Material examined. B3, B21, BON69.

Morphology. Body small and slender, ~ 15 mm long, cylindrical in cross-section (Fig. 6Q). Head the same width as adjacent body. Four eyes occupy the corners of a rectangle, the distance between the anterior and posterior pairs of eyes is considerably larger than the distance between the two eyes of each pair. With two pairs of cephalic furrows: cerebral organ furrows are just posterior to the anterior pair of eyes, and the posterior neck furrow overlies the anterior margin of the cerebral ganglia, which are translucent. Stylet basis cylindrical, rounded posteriorly, $S/B \sim 1$ (Fig. 7L); two accessory stylet pouches. The rhynchocoel extends 3/4 of the body length.

Identification. The species encountered here is most similar to *Nemertellina yamaokai* in possessing two sets of cephalic furrows. The Bodega Bay specimens are ~ 10% divergent (COI) from *N. yamaokai*, suggesting the presence of a sixth *Nemertellina* species, and the first reported from the northeast Pacific.

Habitat. Collected subtidally in Bodega Harbor from kelp holdfasts (station 6) and among fouling organisms on boat marina docks (station 9). Collected intertidally from rocky shores on the open coast among surfgrass roots (station 14).

Distribution. Charleston, OR, USA (Maslakova, unpublished); Bodega Bay, CA, USA (this study).

Notes. Species new to science, and new record of the genus for North America.

Genus *Oerstedtia* Quatrefages, 1846

Oerstedtia sp. BOBA022

BIN. BOLD:AEJ2779.

Material examined. BON32, BON33.

Morphology. Short and stout cylindrical body, 3–6 mm long, with a head narrower than the body. One individual pale, with a bright orange gut (Fig. 6S), the other with the dorsal surface completely covered with blotches of various shades of brown (Fig. 6R). With four large eyes. Basis conical, rounded posteriorly, shorter than the slender central stylet (Fig. 7M). Two accessory stylet pouches, with three or four stylets each.

Identification. The only species of *Oerstedtia* reported to occur in the northeast Pacific (from Washington to Mexico) is *Oerstedtia dorsalis* (Abildgaard, 1806). The type locality of *O. dorsalis* is northern Europe, but the species has been reported throughout the northern hemisphere and is famously polymorphic. Sundberg et al. (2009) demonstrated that there are at least nine cryptic species within *O. dorsalis* in northern Europe alone, each exhibiting color polymorphism. Reports of *Oerstedtia* on this coast likely refer to undescribed species. Bodega Bay specimens are sufficiently divergent from any previously sequenced *Oerstedtia*, including a species occurring in southern Oregon (Maslakova, unpublished).

Habitat. Collected among low intertidal red algae on the rocky boulders of a breakwater (station 4).

Distribution. Bodega Bay, CA, USA (this study).

Notes. Species new to science.

Oerstedtiina incertae sedis

Tetrastemma bilineatum Coe, 1904

Tetrastemma bilineatum Coe, 1904: 164, pl. XIV, fig. 6, pl. XXI, figs 13, 14, pl. XXII, fig. 4.

BIN. BOLD:ADW8130.

Material examined. B18.

Morphology. Small, slender worm with two dorsal longitudinal brown stripes, each 1/3 of the body width, upon a cream-colored background (Fig. 6T). Brown stripes narrow and terminate towards the anterior tip. Head triangular in shape, with four eyes; the anterior pair located halfway between the tip of the head and the posterior pair.

Identification. Specimens from Bodega Bay conform to the description of *Tetrastemma bilineatum* Coe, 1904, originally from San Diego, California, though sequence data are not available from southern California. COI sequence of the Bodega Bay specimen matches those of *T. bilineatum* individuals reported from southern Oregon (Hiebert 2016; Maslakova et al. 2022: OTU 29).

Habitat. Collected from a wave-exposed mussel bed (station 1) and found in similar habitat in southern Oregon.

Distribution. Bamfield Marine Science Centre, Canada (Chernyshev et al. 2021a); Charleston, OR, USA (Hiebert 2016; Maslakova et al. 2022); Bodega Bay, CA, USA (this study).

Notes. Coe's (1904) original record of the species from San Diego, California is not verified by DNA sequence data, but given the distinctiveness of this species, and the absence of known look-alikes on this coast, the reported distribution seems likely. According to a recent molecular phylogeny of *Tetrastemma* and its allies (Chernyshev et al. 2021a) this species does not belong to *Tetrastemma* sensu stricto or the infraorder Amphiporina, but instead is a member of Oerstedina. Its generic placement remains uncertain.

Discussion

The geographic distributions and abundances of coastal species are changing in response to a variety of human impacts (O'Hara et al. 2021), including warming oceans (Sagarin et al. 1999; Sorte et al. 2010; Lonhart et al. 2019; Sanford et al. 2019). Evaluation of these ecological changes is hindered by our incomplete knowledge of the fauna and flora of coastal ecosystems, pointing to a critical need for assessment of biodiversity (Gray 1997). Currently, up to 90% of marine eukaryotic species are estimated to remain undescribed (Mora et al. 2011; Appeltans et al. 2012). Lesser-studied groups, such as nemerteans, have an especially high fraction of undescribed and undetected species (e.g., Hiebert 2016; Maslakova et al. 2022).

Our study extends the geographic focus of recent taxonomic work on nemerteans to include northern California where relatively little work has been done on nemertean diversity during the past 60 years. Notably, only 13 of the 34 species (38%) we collected and barcoded can be unambiguously assigned to described species. This highlights that nemertean diversity remains poorly known in the northeast Pacific despite more than a century of study. That the majority of the observed diversity cannot be assigned to described species renders the few existing geographically relevant identification guides (e.g., Coe 1940; Corrêa 1964; Kozloff 1996; Roe et al. 2007) inadequate.

Eleven species (32%) reported here are new to science, and ten (29%) comprise previously reported undescribed species, or cryptic species whose taxonomic status cannot be resolved with data at hand (Table 4). Some of the newly discovered species were likely overlooked or set aside because of their relatively small size and evident cryptic morphology (e.g., *Tetrastemma* sp. BOBA020, *Nemertellina* sp. BOBA011). Others represent cryptic lineages of previously described species (e.g., *Amphiporus cruentatus*, *Amphiporus imparispinosus*, *Lineus flavescens*, *Nipponnemertes bimaculata*, *Oerstedina dorsalis*, *Poseidonemertes collaris*, *Zygonemertes virescens*). Yet others may have escaped notice due to their rarity or cryptic habits.

Twenty two of the 34 species have not been previously confirmed by DNA barcodes to occur in northern California. This includes two species that appear to have been introduced from other parts of the world (*Cephalothrix simula* from the northwest Pacific, and *Cephalothrix hermaphroditica* from European waters, possibly via Chile or another point of entry along the Pacific Coast of the Americas).

In fact, our study is the first to report *C. hermaphroditica* from the northeast Pacific. Introduction of *C. simula* may be of concern to aquaculture due to its association with oysters, and high levels of tetrodotoxin in its tissues (Kajihara et al. 2013; Turner et al. 2018). These are the first reports in California of two previously described species, *Antarctonemertes phyllospadicola* and *Maculaura oregonensis*, and six previously reported but undescribed species (*Kulikovia* sp. BOBA003, *Amphiporus* sp. BOBA018, *Tetrastemma* sp. BOBA029, *Zygonemertes* sp. BOBA012, 13, *Eumonostilifera* sp. BOBA016). This is also the first record of the genus *Riserius* in California and *Nemertellina* in the northeast Pacific.

Historical surveys of nemertean diversity in the Bodega Bay region (Tamura 1957; Corrêa 1964; Standing et al. 1975; Ristau et al. 1978) identified 21 different species. The majority of these species were also found in our surveys, although in some cases, taxonomic uncertainty makes a direct comparison difficult.

Several species recorded in historical surveys of the Bodega Bay region were absent from our surveys. For example, Corrêa (1964) reported a single specimen of *Lineus pictifrons*, a species we did not locate. Corrêa (1964) also reported several species (e.g., *Tubulanus cingulatus*, *Cerebratulus longiceps*) that were dredged with soft sediments at 6 m depth in Tomales Bay, a subtidal habitat that we did not survey. Perhaps the most conspicuous absence in our survey was the lack of *Tubulanus ruber* (Griffin, 1898), which was reported under the name *Tubulanus polymorphus* in three of the historical studies cited above and was described as “rather common” in the Bodega Bay region by Corrêa (1964). DNA barcodes suggest that *T. ruber*, originally described from Alaska, is distinct from *Tubulanus polymorphus* Renier, 1804, an Atlantic species with which it was previously synonymized by Coe (1940) (Hiebert 2016). The geographic range of *T. ruber* (as *T. polymorphus*) has been reported as San Luis Obispo, CA to Alaska (Morris et al. 1980), and from Monterey, CA to the Aleutian Islands (Roe et al. 2007). iNaturalist documents only two clear records of *Tubulanus “polymorphus”* from central California (San Mateo County, iNaturalist 19743045; and San Luis Obispo County, iNaturalist 84371695), and many records from northern California (Mendocino County) to Alaska. While seasonality could potentially explain the absence of some previously documented species in our surveys, one of us (ES) has conducted intertidal fieldwork in this region throughout the year for the past 20 years and has never observed *T. ruber* in Sonoma County. The scarcity of recent observations of this large and conspicuous red/orange ribbon worm from Bodega Bay and the southern portion of its geographic range is consistent with a geographic range contraction.

Conclusions

Our findings demonstrate how much there is to learn about the diversity and distribution of nemerteans of the northeast Pacific, particularly among southern regions that have received the least amount of attention. Lack of baseline occurrence data (supported by DNA barcodes) hinders our ability to detect shifts in the distribution and abundance of these species. Further sampling and DNA barcoding along the west coast of North America is needed to obtain a more accurate picture of the diversity in this region. Sampling type localities of previously described species will help resolve some of the taxonomic ambiguities associated with species already encountered.

Acknowledgments

For field assistance in the Bodega Bay region, we thank Isaiah Bluestein, Michael Brito, Erin de Leon Sanchez, Jason Herum, Shelby Kawana, Helen Killeen, John Liu, Gabriel Ng, Sarah Merolla, Alisha Saley, Jackie Sones, Evan Tjeerde-ma, and Jenna Quan. The authors acknowledge the students of the Marine Molecular Biology classes at the Oregon Institute of Marine Biology taught by S.M. in Fall 2019 and 2020, for their help with DNA extraction and PCR. We are grateful to the University of California Natural Reserve System for access to Bodega Marine Reserve. We extend our gratitude to an anonymous reviewer and Jon L Norenburg for their thoughtful reviews of this manuscript.

Additional information

Conflict of interest

The authors have declared that no competing interests exist.

Ethical statement

No ethical statement was reported.

Funding

This project was supported by a Field Science Fellowship from the University of California Natural Reserve System to M.F. and E.S. Additional support was provided by NSF grant OCE-1851462 to E.S. C.I.E. was partially supported by the NSF grant DEB-1856363 to S.M.

Author contributions

CIE Data curation, Formal Analysis, Validation, Visualization, Writing – original draft; MRF Funding acquisition, Conceptualization, Investigation, Visualization; ES Funding acquisition, Investigation, Visualization, Writing – review and editing; SM Funding acquisition, Methodology, Formal Analysis, Validation, Visualization, Writing – review and editing.

Author ORCIDs

Christina I. Ellison  <https://orcid.org/0000-0002-1856-386X>

Eric Sanford  <https://orcid.org/0000-0001-9053-6826>

Svetlana Maslakova  <https://orcid.org/0000-0002-3629-6638>

Data availability

All of the data that support the findings of this study are available in the main text or Supplementary Information.

References

- Andrade SCS, Strand M, Schwartz M, Chen H, Kajihara H, von Döhren J, Sun S, Junoy J, Thiel M, Norenburg JL, Turbeville JM, Giribet G, Sundberg P (2012) Disentangling ribbon worm relationships: Multi-locus analysis supports traditional classification of the phylum Nemertea. *Cladistics* 28(2): 141–159. <https://doi.org/10.1111/j.1096-0031.2011.00376.x>
- Appeltans W, Ah Yong ST, Anderson G, Angel MV, Artois T, Bailly N, Bamber R, Barber A, Bartsch I, Berta A, Błażewicz-Paszkowycz M, Bock P, Boxshall G, Boyko CB, Brandão

- SN, Bray RA, Bruce NL, Cairns SD, Chan T-Y, Cheng L, Collins AG, Cribb T, Curini-Galletti M, Dahdouh-Guebas F, Davie PJF, Dawson MN, De Clerck O, Decock W, De Grave S, de Voogd NJ, Domning DP, Emig CC, Erséus C, Eschmeyer W, Fauchald K, Fautin DG, Feist SW, Franssen CHJM, Furuya H, Garcia-Alvarez O, Gerken S, Gibson D, Gittenberger A, Gofas S, Gómez-Daglio L, Gordon DP, Guiry MD, Hernandez F, Hoeksema BW, Hopcroft RR, Jaume D, Kirk P, Koedam N, Koenemann S, Kolb JB, Kristensen RM, Kroh A, Lambert G, Lazarus DB, Lemaitre R, Longshaw M, Lowry J, Macpherson E, Madin LP, Mah C, Mapstone G, McLaughlin PA, Mees J, Meland K, Messing CG, Mills CE, Molodtsova TN, Mooi R, Neuhaus B, Ng PKL, Nielsen C, Norenburg J, Opresko DM, Osawa M, Paulay G, Perrin W, Pilger JF, Poore GCB, Pugh P, Read GB, Reimer JD, Rius M, Rocha RM, Saiz-Salinas JI, Scarabino V, Schierwater B, Schmidt-Rhaesa A, Schnabel KE, Schotte M, Schuchert P, Schwabe E, Segers H, Self-Sullivan C, Shenkar N, Siegel V, Sterrer W, Stöhr S, Swalla B, Tasker ML, Thuesen EV, Timm T, Todaro MA, Turon X, Tyler S, Uetz P, van der Land J, Vanhoorne B, van Ofwegen LP, van Soest RWM, Vanaverbeke J, Walker-Smith G, Walter TC, Warren A, Williams GC, Wilson SP, Costello MJ (2012) The magnitude of global marine species diversity. *Current Biology* 22(23): 2189–2202. <https://doi.org/10.1016/j.cub.2012.09.036>
- Bourque D, Miron G, Landry T (2001) Predation on soft-shell clams (*Mya arenaria*) by the nemertean *Cerebratulus lacteus* in Atlantic Canada: Implications for control measures. *Hydrobiologia* 456(1/3): 33–44. <https://doi.org/10.1023/A:1013061900032>
- Carroll S, McEvoy EG, Gibson R (2003) The production of tetrodotoxin-like substances by nemertean worms in conjunction with bacteria. *Journal of Experimental Marine Biology and Ecology* 288(1): 51–63. [https://doi.org/10.1016/S0022-0981\(02\)00595-6](https://doi.org/10.1016/S0022-0981(02)00595-6)
- Chen H, Strand M, Norenburg JL, Sun S, Kajihara H, Chernyshev AV, Maslakova SA, Sundberg P (2010) Statistical parsimony networks and species assemblages in cephalotrichid nemerteans (Nemertea). *PLoS ONE* 5(9): e12885. <https://doi.org/10.1371/journal.pone.0012885>
- Chen H-X, Sundberg P, Wu H-Y, Sun S-C (2011) The mitochondrial genomes of two nemerteans, *Cephalothrix* sp. (Nemertea: Palaeonemertea) and *Paranemertes* cf. *pergrina* (Nemertea: Hoplonemertea). *Molecular Biology Reports* 38(7): 4509–4525. <https://doi.org/10.1007/s11033-010-0582-4>
- Cherneva I, Ellison CI, Zattara EE, Norenburg JL, Schwartz ML, Junoy J, Maslakova SA (2023) Seven new species of Tetranemertes Chernyshev, 1992 (Monostilifera, Hoplonemertea, Nemertea) from the Caribbean Sea, western Pacific, and Arabian Sea, and revision of the genus. *ZooKeys* 1181: 167–200. <https://doi.org/10.3897/zookeys.1181.109521>
- Chernyshev AV (2002) Description of a new species of the genus *Poseidonemertes* (Nemertea, Monostilifera) with establishment of the family Poseidonemertidae. *Zoologicheskij Zhurnal* 81: 909–916.
- Chernyshev AV (2004) Two new genera of nemertean worms of the family Tetrastemma-tidae (Nemertea: Monostilifera). *Zoosystematica Rossica* 12(2): 151–156. <https://doi.org/10.31610/zsr/2003.12.2.151>
- Chernyshev AV (2014) Nemertean biodiversity in the Sea of Japan and adjacent areas. In: *Marine biodiversity and ecosystem dynamics of the north-western Pacific Ocean*. Publishing House of Science, Beijing, 119–135. <https://www.elibrary.ru/item.asp?id=26149928&pff=1>
- Chernyshev AV, Lutaenko KA (2011) Nemertean worms (Nemertea) of the Vietnamese coastal waters. In: *Coastal marine biodiversity and bioresources of Vietnam and adjacent areas to the South China Sea*. Nha Trang, Vietnam, 21–25.

- Chernyshev AV, Polyakova NE (2019) Nemerteans from the deep-sea expedition KuramBio II with descriptions of three new hoplonemerteans from the Kuril-Kamchatka Trench. *Progress in Oceanography* 178: 102148. <https://doi.org/10.1016/j.pocean.2019.102148>
- Chernyshev AV, Polyakova N (2021) An integrative description of a new *Cephalothrix* species (Nemertea: Palaeonemertea) from the South China Sea. *Zootaxa* 4908(4): 584–594. <https://doi.org/10.11646/zootaxa.4908.4.10>
- Chernyshev AV, Polyakova NE (2022) Nemerteans collected in the Bering Sea during the research cruises aboard the R/V Akademik M.A. Lavrentyev in 2016, 2018, and 2021 with an analysis of deep-sea heteronemertean and hoplonemertean species. *Deep-sea Research. Part II, Topical Studies in Oceanography* 199: 105081. <https://doi.org/10.1016/j.dsr2.2022.105081>
- Chernyshev AV, Polyakova NE, Turanov SV, Kajihara H (2018) Taxonomy and phylogeny of *Lineus torquatus* and allies (Nemertea, Lineidae) with descriptions of a new genus and a new cryptic species. *Systematics and Biodiversity* 16(1): 55–68. <https://doi.org/10.1080/14772000.2017.1317672>
- Chernyshev AV, Polyakova NE, Norenburg JL, Kajihara H (2021a) A molecular phylogeny of *Tetrastemma* and its allies (Nemertea, Monostilifera). *Zoologica Scripta* 50(6): 824–836. <https://doi.org/10.1111/zsc.12511>
- Chernyshev AV, Polyakova NE, Hiebert TC, Maslakova SA, Chernyshev AV, Polyakova NE, Hiebert TC, Maslakova SA (2021b) Evaluation of the taxonomic position of the genus *Carinina* (Nemertea: Palaeonemertea), with descriptions of two new species. *Invertebrate Systematics* 35(3): 245–260. <https://doi.org/10.1071/IS20061>
- Coe WR (1895) Descriptions of three new species of New England palaeonemerteans. *Transactions of the Connecticut Academy of Arts and Sciences* 9: 515–522.
- Coe WR (1901) Papers from the Harriman Alaska Expedition xx. The Nemerteans. *Proceedings of the Washington Academy of Sciences* 3: 1–110.
- Coe WR (1904). Nemerteans of the Pacific Coast of North America 11(Pt. II): 111–220.
- Coe WR (1905) Nemerteans of the West and Northwest Coasts of America. *Museum of Comparative Zoology at Harvard College*.
- Coe WR (1940) Revision of the nemertean fauna of the Pacific coasts of North, Central and northern South America. *Allan Hancock Pacific Expeditions* 2: 247–322.
- Coe WR (1944) Geographical distribution of the nemerteans of the Pacific coast of North America, with descriptions of two new species. *Journal of the Washington Academy of Sciences* 34: 27–32.
- Corrêa DD (1954) Nemertinos do litoral brasileiro. *Boletim da Faculdade de Filosofia, Ciências e Letras, Universidade de São Paulo. Zoologia* 19(19): 1–121. <https://doi.org/10.11606/issn.2526-3382.bffclzoologia.1954.120084>
- Corrêa DD (1961) Nemerteans from Florida and Virgin Islands. *Bulletin of Marine Science* 11: 1–44.
- Corrêa DD (1964) Nemerteans from California and Oregon. *Proceedings of the California Academy of Sciences* 31: 515–558.
- Crandall FB, Norenburg JL (2001) Checklist of the nemertean fauna of the United States.
- Ehrenberg CG (1828) Phytozoa turbellaria Africana et Asiatica in *Phytozoorum Tabula IV et V delineata*. In: Hemprich FG, Ehrenberg CG (Eds) *Symbolae physicae, seu icones et descriptiones corporum naturalium novorum aut minus cognitorum quae ex itineribus per Libyam, Aegyptium, Nubiam, Dongalam, Syriam, Arabiam et Habessiniam, pars zoologica II, anima*. *Officina Academica, Berlin*. Vol. 2, 515 pp. <https://doi.org/10.5962/bhl.title.107403>

- Envall M, Norenburg JL (2001) Morphology and systematics in mesopsammic nemerteans of the genus *Ototyphlonemertes* (Nemertea, Hoplonemertea, Ototyphlonemertidae). *Hydrobiologia* 456(1/3): 145–163. <https://doi.org/10.1023/A:1013029310452>
- Faasse MA, Turbeville JM (2015) The first record of the north-west Pacific nemertean *Cephalothrix simula* in northern Europe. *Marine Biodiversity Records* 8: e17. <https://doi.org/10.1017/S1755267214001523>
- Fernández-Álvarez FÁ, Machordom A (2013) DNA barcoding reveals a cryptic nemertean invasion in Atlantic and Mediterranean waters. *Helgoland Marine Research* 67(3): 599–605. <https://doi.org/10.1007/s10152-013-0346-3>
- Folmer O, Black M, Hoeh W, Lutz R, Vrijenhoek R (1994) DNA primers for amplification of mitochondrial cytochrome c oxidase subunit I from diverse metazoan invertebrates. *Molecular Marine Biology and Biotechnology* 3: 294–299.
- Friedrich F (1935a) Studien zur morphologie, systematik und Oekologie der nemertinen der Kieler Bucht. *Archiv für Naturgeschichte* 4: 293–375.
- Friedrich H (1935b) Neue Hoplonemertinen der Kieler Bucht. *Schr naturw Ver Schlesw-Holst* 21: 10–19.
- Gerner L (1969) Nemertinen der gattungen *Cephalothrix* und *Ototyphlonemertes* aus dem marinen mesopsammal. *Helgoländer Wissenschaftliche Meeresuntersuchungen* 19(1): 68–110. <https://doi.org/10.1007/BF01625860>
- Gibson R (1995) Nemertean genera and species of the world: An annotated checklist of original names and description citations, synonyms, current taxonomic status, habitats and recorded zoogeographic distribution. *Journal of Natural History* 29(2): 271–561. <https://doi.org/10.1080/00222939500770161>
- Gibson R, Crandall FB (1989) The genus *Amphiporus* Ehrenberg (Nemertea, Enopla, Monostiliferoidea). *Zoologica Scripta* 18(4): 453–470. <https://doi.org/10.1111/j.1463-6409.1989.tb00140.x>
- Gibson R, Sánchez M, Méndez M (1990) A new species of *Procephalothrix* (Nemertea, Anopla, Archinemertea) from Chile. *Journal of Natural History* 24(2): 277–287. <https://doi.org/10.1080/00222939000770201>
- Göransson U, Jacobsson E, Strand M, Andersson HS (2019) The toxins of nemertean worms. *Toxins* 11(2): 120. <https://doi.org/10.3390/toxins11020120>
- Gray JS (1997) Marine biodiversity: Patterns, threats and conservation needs. *Biodiversity and Conservation* 6(1): 153–175. <https://doi.org/10.1023/A:1018335901847>
- Griffin BB (1898) Description of some marine nemerteans of Puget Sound and Alaska. *Annals of the New York Academy of Sciences* 11(1): 193–217. <https://doi.org/10.1111/j.1749-6632.1898.tb54969.x>
- Gunnerus JE (1770) Nogle smaa rare og mestendeelen nye norske sødyr. *Skrifter som udi det Kiøbenhavnske Selskab af Lærdoms og Videnskabers Elskere ere fremlagte og oplæste* 10: 166–176.
- Hao Y, Kajihara H, Chernyshev AV, Okazaki RK, Sun S-C (2015) DNA taxonomy of *Paranemertes* (Nemertea: Hoplonemertea) with spirally fluted stylets. *Zoological Science* 32(6): 571–578. <https://doi.org/10.2108/zs140275>
- Hiebert TC (2016) New nemertean diversity discovered in the Northeast Pacific, using surveys of both planktonic larvae and benthic adults. Ph.D. University of Oregon. <https://www.proquest.com/docview/1780588156/abstract/5DD5117979CC4585PQ/1>
- Hiebert TC, Maslakova S (2015a) Integrative taxonomy of the *Micrura alaskensis* Coe, 1901 species complex (Nemertea: Heteronemertea), with descriptions of a new genus *Maculaura* gen. nov. and four new species from the NE Pacific. *Zoological Science* 32(6): 615–637. <https://doi.org/10.2108/zs150011>

- Hiebert TC, Maslakova SA (2015b) Larval development of two N. E. Pacific Pilidiophoran nemerteans (Heteronemertea; Lineidae). *The Biological Bulletin* 229(3): 265–275. <https://doi.org/10.1086/BBLv229n3p265>
- Hiebert TC, von Dassow G, Hiebert LS, Maslakova S (2013) The peculiar nemertean larva pilidium recurvatum belongs to *Riserius* sp., a basal heteronemertean that eats *Carcinonemertes errans*, a hoplonemertean parasite of Dungeness crab. *Invertebrate Biology* 132(3): 207–225. <https://doi.org/10.1111/ivb.12023>
- Hookabe N, Kajihara H, Chernyshev AV, Jimi N, Hasegawa N, Kohtsuka H, Okanishi M, Tani K, Fujiwara Y, Tsuchida S, Ueshima R (2022) Molecular phylogeny of the genus *Nipponnemertes* (Nemertea: Monostilifera: Cratenemertidae) and descriptions of 10 new species, with notes on small body size in a newly discovered clade. *Frontiers in Marine Science* 9: 906383. <https://doi.org/10.3389/fmars.2022.906383>
- Hunt MK, Maslakova SA (2017) Development of a lecithotrophic pilidium larva illustrates convergent evolution of trochophore-like morphology. *Frontiers in Zoology* 14(1): 7. <https://doi.org/10.1186/s12983-017-0189-x>
- Iwata F (1952) Nemertini from the coasts of Kyusyu (with 18 text-figures). *Journal of the Faculty of Science, Hokkaido University. Series 6, Zoology* 11: 126–148.
- Iwata F (2001) *Nipponnemertes fernaldi*, a new species of swimming monostiliferous hoplonemertean from the San Juan Archipelago, Washington, U.S.A. *Proceedings of the Biological Society of Washington* 114: 833–857.
- Johnston G (1837) *Miscellanea zoologica. II. A description of some planarian worms. Magazine of Zoology and Botany* 1: 529–538.
- Kajihara H (2017) Species diversity of Japanese ribbon worms (Nemertea). In: Motokawa M, Kajihara H (Eds), *Species Diversity of Animals in Japan. Diversity and Commonality in Animals*. Springer Japan, Tokyo, 419–444. https://doi.org/10.1007/978-4-431-56432-4_16
- Kajihara H (2019) Resolving a 200-year-old taxonomic conundrum: neotype designation for *Cephalothrix linearis* (Nemertea: Palaeonemertea) based on a topotype from Bergen, Norway. *Fauna Norvegica* 39: 39–76. <https://doi.org/10.5324/fn.v39i0.2734>
- Kajihara H (2020) Redescription of *Cerebratulus marginatus* auct. (Nemertea: Pilidiophora) from Hokkaido, Japan, as a new species. *Zootaxa* 4819(2): 295–315. <https://doi.org/10.11646/zootaxa.4819.2.4>
- Kajihara H (2021) Higher classification of the Monostilifera (Nemertea: Hoplonemertea). *Zootaxa* 4920(2): 151–199. <https://doi.org/10.11646/zootaxa.4920.2.1>
- Kajihara H, Chernyshev AV, Sun S-C, Sundberg P, Crandall FB (2008) Checklist of nemertean genera and species published between 1995 and 2007. *Species Diversity: An International Journal for Taxonomy, Systematics, Speciation, Biogeography, and Life History Research of Animals* 13(4): 245–274. <https://doi.org/10.12782/specdiv.13.245>
- Kajihara H, Sun S-C, Chernyshev AV, Chen H-X, Ito K, Asakawa M, Maslakova SA, Norenburg JL, Strand M, Sundberg P, Iwata F (2013) Taxonomic identity of a tetrodotoxin-accumulating ribbon-worm *Cephalothrix simula* (Nemertea: Palaeonemertea): a species artificially introduced from the Pacific to Europe. *Zoological Science* 30(11): 985–997. <https://doi.org/10.2Fio108/zsj.30.985>
- Kajihara H, Tamura K, Tomioka S (2018) Histology-free descriptions for seven species of interstitial ribbon worms in the genus *Ototyphlonemertes* (Nemertea: Monostilifera) from Vietnam. *Species Diversity: An International Journal for Taxonomy, Systematics, Speciation, Biogeography, and Life History Research of Animals* 23(1): 13–37. <https://doi.org/10.12782/specdiv.23.13>

- Kajihara H, Abukawa S, Chernyshev AV (2022a) Exploring the basal topology of the heteronemertean tree of life: establishment of a new family, along with turbotaxonomy of Valenciniidae (Nemertea: Pilidiophora: Heteronemertea). *Zoological Journal of the Linnean Society* 196(1): 503–548. <https://doi.org/10.1093/zoolinnean/zlac015>
- Kajihara H, Ganaha I, Kohtsuka H (2022b) Lineid Heteronemerteans (Nemertea: Pilidiophora) from Sagami Bay, Japan, with Some Proposals for the Family-Level Classification System. *Zoological Science* 39(1): 62–80. <https://doi.org/10.2108/zs210059>
- Kem W, Soti F, Wildeboer K, LeFrancois S, MacDougall K, Wei D-Q, Chou K-C, Arias HR (2006) The nemertine toxin anabaseine and its derivative DMXBA (GTS-21): Chemical and Pharmacological Properties. *Marine Drugs* 4(3): 255–273. <https://doi.org/10.3390/md403255>
- Kirsteuer E (1965) Über das vorkommen von nemertinen in einem tropischen korallenriff. 4. Hoplonemertini monostilifera. *Zoologische Jahrbucher. Abteilung für Systematik, Ökologie und Geographie der Tiere* 92: 289–326.
- Kölliker A (1845) Lineola, Chloriane, Polycystis, neue Wurmgattungen und neue arten von Nemertes. *Verhandlungen der schweizerischen naturforschenden Gesellschaft* 29: 86–99.
- Kozloff EN (1996) *Marine Invertebrates of the Pacific Northwest*, Second Printing. University of Washington Press, Seattle and London.
- Kuris AM, Wickham DE (1987) Effect of nemertean egg predators on crustaceans. *Bulletin of Marine Science* 41: 151–164.
- Kvist S, Laumer CE, Junoy J, Giribet G (2014) New insights into the phylogeny, systematics and DNA barcoding of Nemertea. *Invertebrate Systematics* 28(3): 287–308. <https://doi.org/10.1071/IS13061>
- Leasi F, Andrade SC da S, Norenburg J (2016) At least some meiofaunal species are not everywhere. Indication of geographic, ecological and geological barriers affecting the dispersion of species of *Ototyphlonemertes* (Nemertea, Hoplonemertea). *Molecular Ecology* 25: 1381–1397. <https://doi.org/10.1111/mec.13568>
- Leasi F, Norenburg JL (2014) The necessity of DNA taxonomy to reveal cryptic diversity and spatial distribution of meiofauna, with a focus on Nemertea. *PLoS ONE* 9(8): e104385. <https://doi.org/10.1371/journal.pone.0104385>
- Lonhart SI, Jeppesen R, Beas-Luna R, Crooks JA, Lorda J (2019) Shifts in the distribution and abundance of coastal marine species along the eastern Pacific Ocean during marine heatwaves from 2013 to 2018. *Marine Biodiversity Records* 12(1): 13. <https://doi.org/10.1186/s41200-019-0171-8>
- Mahon AR, Thornhill DJ, Norenburg JL, Halanych KM (2010) DNA uncovers Antarctic nemertean biodiversity and exposes a decades-old cold case of asymmetric inventory. *Polar Biology* 33(2): 193–202. <https://doi.org/10.1007/s00300-009-0696-0>
- Maslakova SA, Hiebert TC (2014) From trochophore to pilidium and back again - a larva's journey. *The International Journal of Developmental Biology* 58(6–7–8): 585–591. <https://doi.org/10.1387/ijdb.140090sm>
- Maslakova SA, von Dassow G (2012) A non-feeding pilidium with apparent prototroch and telotroch. *Journal of Experimental Zoology. Part B, Molecular and Developmental Evolution* 318(7): 586–590. <https://doi.org/10.1002/jezb.22467>
- Maslakova SA, von Döhren J (2009) Larval development with transitory epidermis in *Paranemertes peregrina* and other hoplonemerteans. *The Biological Bulletin* 216(3): 273–292. <https://doi.org/10.1086/BBLv216n3p273>
- Maslakova S, Ellison CI, Hiebert TC, Conable F, Heaphy MC, Venera-Pontón DE, Norenburg JL, Schwartz ML, Moss ND, Boyle MJ, Driskell AC, Macdonald KS III, Zattara EE, Collin

- R (2022) Sampling multiple life stages significantly increases estimates of marine biodiversity. *Biology Letters* 18(4): 20210596. <https://doi.org/10.1098/rsbl.2021.0596>
- Maslakova SA, Hiebert TC, Von Dassow G (2024) Nemertea. In: *Atlas of Marine Invertebrate Larvae*. Elsevier Science, United Kingdom, 691 pp.
- McDermott JJ (1997) Observations on feeding in a South African suctorial hoplonemertean, *Nipponnemertes* sp. (Family Cratenemertidae). *Hydrobiologia* 365(1/3): 251–256. <https://doi.org/10.1023/A:1003114117397>
- McDermott JJ (2001) Status of the Nemertea as prey in marine ecosystems. *Hydrobiologia* 456(1/3): 7–20. <https://doi.org/10.1023/A:1013001729166>
- McDermott JJ, Roe P (1985) Food, feeding behavior and feeding ecology of nemerteans. *American Zoologist* 25(1): 113–125. <https://doi.org/10.1093/icb/25.1.113>
- Mendes CB, Delaney P, Turbeville JM, Hiebert T, Maslakova S (2021) Redescription of *Emplectonema viride* – a ubiquitous intertidal hoplonemertean found along the West Coast of North America. *ZooKeys* 1031: 1–17. <https://doi.org/10.3897/zookeys.1031.59361>
- Moore J, Gibson R, Jones HD (2001) Terrestrial nemerteans thirty years on. *Hydrobiologia* 456(1/3): 1–6. <https://doi.org/10.1023/A:1013052728257>
- Mora C, Tittensor DP, Adl S, Simpson AGB, Worm B (2011) How many species are there on earth and in the ocean? *PLoS Biology* 9(8): 1–8. <https://doi.org/10.1371/journal.pbio.1001127>
- Morris RH, Abbott DP, Haderlie EC (1980) *Intertidal Invertebrates of California*. Stanford University Press, Stanford.
- Nam S-E, Rhee J-S (2020) Characterization and phylogenetic analysis of the complete mitochondrial genome of the marine ribbon worm *Cephalothrix* species (nemertea: Palaeonemertea). *Mitochondrial DNA. Part B, Resources* 5(2): 2012–2014. <https://doi.org/10.1080/23802359.2020.1756967>
- Norenburg JL (1993) *Riserius pugetensis* gen. n., sp. n. (Nemertina: Anopla), a new mesopsammic species, and comments on phylogenetics of some anoplan characters. In: Gibson R, Moore J, Sundberg P (Eds) *Advances in Nemertean Biology*. Developments in Hydrobiology. Springer Netherlands, Dordrecht, 203–218. https://doi.org/10.1007/978-94-011-2052-4_15
- O'Hara CC, Frazier M, Halpern BS (2021) At-risk marine biodiversity faces extensive, expanding, and intensifying human impacts. *Science* 372(6537): 84–87. <https://doi.org/10.1126/science.abe6731>
- Palumbi S, Martin A, Romano S, McMillan WO, Stice L, Grabowski G (1991) *The simple fools guide to PCR* Version 2.0. Department of Zoology Kewalo Marine Laboratory, University of Hawaii, Honolulu.
- Park T, Lee S-H, Sun S-C, Kajihara H (2019) Morphological and molecular study on *Yininemertes pratensis* (Nemertea, Pilidiophora, Heteronemertea) from the Han River Estuary, South Korea, and its phylogenetic position within the family Lineidae. *ZooKeys* 852: 31–51. <https://doi.org/10.3897/zookeys.852.32602>
- Paule J, von Döhren J, Sagorny C, Nilsson MA (2021) Genome size dynamics in marine ribbon worms (Nemertea, Spiralia). *Genes* 12(9): 1347. <https://doi.org/10.3390/genes12091347>
- Puillandre N, Brouillet S, Achaz G (2021) ASAP: Assemble species by automatic partitioning. *Molecular Ecology Resources* 21(2): 609–620. <https://doi.org/10.1111/1755-0998.13281>
- Ristau DA, Tarp C, Hand C (1978) A survey of the biota of the open coast at Bodega Marine Life Refuge (area of special biological significance). A report to the California State Department of Fish and Game.

- Roe P, Wickham DE (1984) *Poseidonemertes collaris*, n. sp. (Nemertea Amphiporidae) from California, with notes on its biology. *Proceedings of the Biological Society of Washington* 97: 60–70.
- Roe P, Norenburg JL, Maslakova S (2007) Nemertea. In: *The Light and Smith Manual*. University of California Press, 221–233. <https://doi.org/10.1525/9780520930438-019>
- Ruesink JL, Lenihan HS, Trimble AC, Heiman KW, Micheli F, Byers JE, Kay MC (2005) Introduction of non-native oysters: Ecosystem effects and restoration implications. *Annual Review of Ecology, Evolution, and Systematics* 36(1): 643–689. <https://doi.org/10.1146/annurev.ecolsys.36.102003.152638>
- Sagarin RD, Barry JP, Gilman SE, Baxter CH (1999) Climate-related change in an intertidal community over short and long time scales. *Ecological Monographs* 69(4): 465–490. [https://doi.org/10.1890/0012-9615\(1999\)069\[0465:CRCIAI\]2.0.CO;2](https://doi.org/10.1890/0012-9615(1999)069[0465:CRCIAI]2.0.CO;2)
- Sagoriny C, Wesseler C, Krämer D, von Döhren J (2019) Assessing the diversity and distribution of *Cephalothrix* species (Nemertea: Palaeonemertea) in European waters by comparing different species delimitation methods. *Journal of Zoological Systematics and Evolutionary Research* 57(3): 497–519. <https://doi.org/10.1111/jzs.12266>
- Sanford E, Sones JL, García-Reyes M, Goddard JHR, Largier JL (2019) Widespread shifts in the coastal biota of northern California during the 2014–2016 marine heatwaves. *Scientific Reports* 9(1): 4216. <https://doi.org/10.1038/s41598-019-40784-3>
- Schwartz ML (2009) Untying a Gordian knot of worms: Systematics and taxonomy of the Pilidiophora (phylum Nemertea) from multiple data sets. Ph.D. The George Washington University. <https://www.proquest.com/docview/288078184/abstract/23E2D19A677A40C5PQ/1> [October 3, 2023]
- Sorte CJB, Williams SL, Carlton JT (2010) Marine range shifts and species introductions: Comparative spread rates and community impacts. *Global Ecology and Biogeography* 19(3): 303–316. <https://doi.org/10.1111/j.1466-8238.2009.00519.x>
- Spalding MD, Fox HE, Allen GR, Davidson N, Ferdaña ZA, Finlayson M, Halpern BS, Jorge MA, Lombana A, Lourie SA, Martin KD, McManus E, Molnar J, Recchia CA, Robertson J (2007) Marine ecoregions of the world: A bioregionalization of coastal and shelf areas. *Bioscience* 57(7): 573–583. <https://doi.org/10.1641/B570707>
- Standing J, Speth JW, Browning BM (1975) The natural resources of Bodega Harbor. State of California, Dept. of Fish and Game, Sacramento, i, 183, [40 p.] pp. <https://catalog.hathitrust.org/Record/007158184>
- Stimpson W (1857) *Prodromus descriptionis animalium evertibratorum, quae in Expeditione ad Oceanum Pacificum Septentrionalem, a Republica Federata missa, Cadwaladaro Ringgold et Johanne Rodgers Ducibus, observavit et descripsit, Pars II, Turbellarieorum Nemertineorum*. *Proceedings of the Academy of Natural Sciences of Philadelphia* 9. <https://doi.org/10.5962/bhl.title.51447>
- Stricker SA (1985) A new species of *Tetrastemma* (Nemertea, Monostilifera) from San Juan Island, Washington, U.S.A. *Canadian Journal of Zoology* 63(3): 682–690. <https://doi.org/10.1139/z85-098>
- Stricker SA, Cavey MJ (1986) An ultrastructural study of spermatogenesis and the morphology of the testis in the nemertean worm *Tetrastemma phyllospadicola* (Nemertea, Hoplonemertea). *Canadian Journal of Zoology* 64(10): 2187–2202. <https://doi.org/10.1139/z86-333>
- Stricker SA, Folsom MW (1997) A comparative ultrastructural analysis of spermatogenesis in nemertean worms. *Hydrobiologia* 365(1/3): 55–72. <https://doi.org/10.1023/A:1003186611254>

- Stricker SA, Smythe TL, Miller L, Norenburg JL (2001) Comparative biology of oogenesis in nemertean worms. *Acta Zoologica* (Stockholm, Sweden) 82(3): 213–230. <https://doi.org/10.1046/j.1463-6395.2001.00080.x>
- Sundberg P, Hylbom R (1994) Phylogeny of the Nemertean Subclass Palaeonemertea (Anopla, Nemertea). *Cladistics* 10(4): 347–402. <https://doi.org/10.1111/j.1096-0031.1994.tb00185.x>
- Sundberg P, Gibson R, Olsson U (2003) Phylogenetic analysis of a group of palaeonemerteans (Nemertea) including two new species from Queensland and the Great Barrier Reef, Australia. *Zoologica Scripta* 32(3): 279–296. <https://doi.org/10.1046/j.1463-6409.2002.00032.x>
- Sundberg P, Vodoti E, Zhou H, Strand M (2009) Polymorphism hides cryptic species in *Oerstedtia dorsalis* (Nemertea, Hoplonemertea). *Biological Journal of the Linnean Society. Linnean Society of London* 98(3): 556–567. <https://doi.org/10.1111/j.1095-8312.2009.01310.x>
- Sundberg P, Kvist S, Strand M (2016) Evaluating the Utility of Single-Locus DNA Barcoding for the Identification of Ribbon Worms (Phylum Nemertea). *PLoS ONE* 11(5): e0155541. <https://doi.org/10.1371/journal.pone.0155541>
- Takakura U (1898) A classification of the nemerteans of the Misaki region. *Zoological Magazine, Tokyo* 10: 424–429.
- Tamura M (1957) A distributional study of some nemerteans of the Bodega Bay region. *Zoology* S112. [UC Berkeley Student Report]
- Thollessen M, Norenburg JL (2003) Ribbon worm relationships: a phylogeny of the phylum Nemertea. *Proceedings of the Royal Society of London. Series B: Biological Sciences* 270: 407–415. <https://doi.org/10.1098/rspb.2002.2254>
- Turner AD, Fenwick D, Powell A, Dhanji-Rapkova M, Ford C, Hatfield RG, Santos A, Martinez-Urtaza J, Bean TP, Baker-Austin C, Stebbing P (2018) New invasive nemertean species (*Cephalothrix simula*) in England with high levels of tetrodotoxin and a microbiome linked to toxin metabolism. *Marine Drugs* 16(11): 452. <https://doi.org/10.3390/md16110452>
- Verdes A, Arias MB, Junoy J, Schwartz ML, Kajihara H (2021) Species delimitation and phylogenetic analyses reveal cryptic diversity within *Cerebratulus marginatus* (Nemertea: Pilidiophora). *Systematics and Biodiversity* 19(7): 895–905. <https://doi.org/10.1080/14772000.2021.1950231>
- Verdes A, Taboada S, Hamilton BR, Undheim EAB, Sonoda GG, Andrade SCS, Morato E, Marina AI, Cárdenas CA, Riesgo A (2022) Evolution, expression patterns, and distribution of novel ribbon worm predatory and defensive toxins. *Molecular Biology and Evolution* 39(5): msac096. <https://doi.org/10.1093/molbev/msac096>
- Verrill AE (1879) Notice of recent additions to the marine Invertebrata of the north-eastern coast of America, with descriptions of new genera and species and critical remarks on others. Part I. Annelida, Gephyraea, Nemertina, Nematoda, Polyzoa, Tunicata, Mollusca, Anthozoa, Echinodermata, Porifera. *Proceedings of the United States National Museum* 2(76): 165–205. <https://doi.org/10.5479/si.00963801.76.165>
- von Dassow G, Mendes CB, Robbins K, Andrade SCS, Maslakova SA (2022) Hoplonemertean larvae are planktonic predators that capture and devour active animal prey. *Invertebrate Biology* 141(1): e12363. <https://doi.org/10.1111/ivb.12363>
- Whelan NV, Kocot KM, Santos SR, Halanych KM (2014) Nemertean toxin genes revealed through transcriptome sequencing. *Genome Biology and Evolution* 6(12): 3314–3325. <https://doi.org/10.1093/gbe/evu258>

WoRMS Editorial Board (2023). World Register of Marine Species. <https://doi.org/10.14284/170>

Zattara EE, Fernández-Álvarez FA, Hiebert TC, Bely AE, Norenburg JL (2019) A phylum-wide survey reveals multiple independent gains of head regeneration in Nemer-
tea. *Proceedings of the Royal Society B: Biological Sciences* 286: 20182524. <https://doi.org/10.1098/rspb.2018.2524>

Supplementary material 1

Reference sequences used in species delimitation (ASAP), alignments, and trees

Authors: Christina I. Ellison, Madeline R. Frey, Eric Sanford, Svetlana Maslakova

Data type: xlsx

Copyright notice: This dataset is made available under the Open Database License (<http://opendatacommons.org/licenses/odbl/1.0/>). The Open Database License (ODbL) is a license agreement intended to allow users to freely share, modify, and use this Dataset while maintaining this same freedom for others, provided that the original source and author(s) are credited.

Link: <https://doi.org/10.3897/zookeys.1204.117869.suppl1>

Four new species of *Marphysa* (Annelida, Eunicida, Eunicidae) from the east coast of Peninsular Malaysia

Che Engku Siti Mariam Che Engku Abdullah¹, Izwandy Idris^{2,3}, Afiq Durrani Mohd Fahmi⁴,
Beth Flaxman^{5,6}, Pat Hutchings^{6,7}

1 Institute of Oceanography and Environment, Universiti Malaysia Terengganu, 21030 Kuala Nerus, Terengganu, Malaysia

2 South China Sea Repository and Reference Centre, Institute of Oceanography and Environment, Universiti Malaysia Terengganu, 21030 Kuala Nerus, Terengganu, Malaysia

3 Mangrove Research Unit, Institute of Oceanography and Environment, Universiti Malaysia Terengganu, 21030 Kuala Nerus, Terengganu, Malaysia

4 Faculty of Science and Marine Environment, Universiti Malaysia Terengganu, 21030 Kuala Nerus, Terengganu, Malaysia

5 Australian Museum Research Institute, Australian Museum, NSW 2010, Sydney, Australia

6 School of Life and Environmental Sciences, The University of Sydney, NSW 2006, Sydney, Australia

7 Marine Ecology Group, School of Natural Sciences, Wallumattagal Campus, Macquarie University, NSW 2109, North Ryde, Australia

Corresponding author: Izwandy Idris (izwandy.idris@umt.edu.my)

Abstract

Four new species of *Marphysa* are described from Terengganu state on the east coast of Peninsular Malaysia, using morphological and molecular (cytochrome oxidase subunit I (COI) gene) data. These species belong to different groups of *Marphysa*: *Marphysa kertezensis* **sp. nov.** belongs to Group A (Mossambica), *Marphysa merchangensis* **sp. nov.** and *Marphysa setiuense* **sp. nov.** belong to Group B (Sanguinea) and *Marphysa ibaiensis* **sp. nov.** belongs to Group E (Gravellyi). *Marphysa kertezensis* **sp. nov.** is characterised by having only limbate chaetae, absence of subaciclar hooks, three types of pectinate chaetae including wide, thick isodont with short and slender inner teeth, and pectinate branchiae with up to nine branchial filaments. *Marphysa merchangensis* **sp. nov.** is characterised by the presence of eyes, unidentate subaciclar hooks, four types of pectinate chaetae including wide, thick anodont pectinate chaetae with five long and thick inner teeth, and pectinate branchiae with up to six branchial filaments. *Marphysa setiuense* **sp. nov.** has mostly unidentate subaciclar hooks (bidentate on several posterior chaetigers), four types of pectinate chaetae including wide, thick anodont pectinate chaetae with seven thick and long inner teeth, and pectinate branchiae with up to five branchial filaments. *Marphysa ibaiensis* **sp. nov.** has bidentate subaciclar hooks throughout, five types of pectinate chaetae, including a heterodont with 12 short and slender inner teeth, and pectinate branchiae with up to eight branchial filaments. The designation of these new species based on morphology is fully supported by molecular data. Habitat descriptions of each species are also included.

Key words: Bloodworm, COI, identification key, mangrove bait worm, *Marphysa*, South China Sea



Academic editor: Christopher Glasby

Received: 12 December 2023

Accepted: 22 April 2024

Published: 4 June 2024

ZooBank: <https://zoobank.org/0704A2BB-6173-44BD-A1F7-CB3EDCFDC5DC>

Citation: Che Engku Abdullah CESM, Idris I, Fahmi ADM, Flaxman B, Hutchings P (2024) Four new species of *Marphysa* (Annelida, Eunicida, Eunicidae) from the east coast of Peninsular Malaysia. ZooKeys 1204: 65–103. <https://doi.org/10.3897/zookeys.1204.117261>

Copyright: © C. E. S. M. Che Engku Abdullah et al.
This is an open access article distributed under terms of the Creative Commons Attribution License (Attribution 4.0 International – CC BY 4.0).

Introduction

Marphysa de Quatrefages 1866, currently with 83 accepted species, is the second most speciose genus in the family Eunicidae, after the genus *Eunice* Cuvier, 1817 (Read and Fauchald 2023). *Marphysa* species inhabit a wide range of habitats, either in soft sediments or rocky ground, from intertidal to shallow subtidal depth, and are commonly found in estuarine or sheltered habitats (Abdullah et al. in review; Zanol et al. 2016; Martin et al. 2020). Three species have recently been described from the deep sea (Lavesque et al. 2023). Taxonomic studies of *Marphysa* species have increased considerably since the redescription of the type species, *M. sanguinea* (Montagu, 1813) and the designation of a neotype by Hutchings and Karageorgopoulos (2003); and later by molecular sequencing (Zanol et al. 2010). Since then, many more species have been described or previously synonymised species resurrected, using molecular data and additional morphological characters such as the types and distributions of chaetae.

According to Fauchald (1970) and Glasby and Hutchings (2010), *Marphysa* can be divided into five informal groups (Groups A–E) depending on their type of chaetae. Group A (Mossambica) without compound chaetae, Group B (Sanguinea) with only compound spinigers present, Group C (Aenea) with only compound falcigers present, Group D (Belli) with both spinigers and falcigers present, and Group E (Teretiuscula; renamed Gravelyi by Molina-Acevedo and Idris 2021) with only compound spinigers and subacicular chaetae in anterior parapodia and limbate chaetae throughout.

In Malaysia, Paxton and Chou (2000) suggested that the low number of polychaete species identified in Malaysia is an underestimate due to the limited sampling of polychaetes. Idris et al. (2014) described *Marphysa moribidii* Idris, Hutchings & Arshad, 2014 from the west coast of Peninsular Malaysia. The species is currently the only *Marphysa* described from Malaysia, occurring in *Rhizophora* and *Sonneratia* spp. mangroves. *Marphysa moribidii* is regularly used as fishing bait by local fishermen. In addition, recent studies (Ee Pei et al. 2020; Rapi et al. 2020; Rosman et al. 2020) reported the potential applications of *M. moribidii* as a wound-healing agent and bio-catalyst of gold and silver nanoparticles. This study investigated *Marphysa* species from the mangrove forest on the east coast of Peninsular Malaysia, specifically Terengganu, as they may also have potential applications similar to *M. moribidii*. We found four new *Marphysa* species using an integrated approach to taxonomy, including morphological and molecular analyses.

Materials and methods

Study area and sampling

Marphysa specimens were collected from the rivers, lagoon and estuary of the Terengganu mangrove forests during spring low tides from September 2021 until March 2022. A total of four mangrove areas were chosen, i.e. Setiu wetlands, Kuala Ibai, Merchang, and Kerteh (Fig. 1A, B). At each site, sediments were dug using a shovel to approximately 30 cm depth at several points along the river (upper course to lower course) and carefully broken into small pieces

to search for the worms. Worms suspected to be *Marphysa* were fixed and preserved in 95% ethanol. Sediments where the *Marphysa* worms were found were also collected and kept in labelled plastic bags for sediment analysis. All material was collected by the first author.

Morphological analyses

Preserved specimens were examined under AmScope SM-2 Series stereo and 120 Series compound microscopes. Additionally, the specimens were also examined under Leica M165 C stereo and Nikon Labophot-2 compound microscopes, and photographed with a Nikon D610 camera at the Natural History Museum of Los Angeles County, USA (NHMLAC). Drawings of parapodia and pectinate chaetae were made using a Wacom Intuos Pro drawing tablet. Length at chaetiger 10 (L10) and width at chaetiger 10 (W10) without parapodia of all specimens were measured and recorded. Morphological terminology, including diagnostic features of *Marphysa* species, follows Molina-Acevedo and Carrera-Parra (2017). Terminology of pectinate chaetae is derived and modified from Carrera-Parra and Salazar-Vallejo (1998) for the relative length of outer and inner teeth, Zanol et al. (2014, 2016) for the thickness of the



Figure 1. Map showing sampling sites of four new *Marphysa* species in Terengganu mangrove forest, east coast of Peninsular Malaysia **A** location of Terengganu on the east of Peninsular Malaysia **B** symbols indicate each sampling site; Setiu Wetlands (red star), Kuala Ibai (red rhombus), Merchang (red triangle), and Kerteh (red oval).

blade and Glasby et al. (2019) for the size of the inner teeth: isodont means outer teeth much longer than inner teeth; anodont means outer teeth more or less the same length as inner teeth; heterodont refers to when one long and one short (same length as inner teeth) lateral tooth is present. The thickness of the shaft is thin when it is thinner than the limbate chaetae on the same parapodium, thick when the shaft is as thick or thicker than limbate chaetae on the same parapodium. The width of the pectinate blade is wide when the blade is $\geq 30 \mu\text{m}$ and narrow below this threshold; length of the inner teeth is long when they are $\geq 12 \mu\text{m}$ and thick when $\geq 2 \mu\text{m}$; below these thresholds, the teeth are defined as short and slender, respectively. Table 1 and Fig. 2 summarises and illustrates the types of pectinate chaetae present in species of *Marphysa* from Terengganu.

Terminology of maxillary apparatus followed Molina-Acevedo and Carreira-Parra (2015). Several parapodia from the anterior, median, and posterior regions were removed from the type material of each species, dehydrated in ethanol and hexamethyldisilazane (HMDS), coated with 20 nm of silver-gold, examined under the scanning electron microscope JEOL JSM-6360LA, and imaged with a secondary detector at SEM laboratories of Universiti Malaysia Terengganu and Macquarie University, Sydney, Australia.

Repositories

Materials were deposited at the institution and museums listed below:

- South China Sea Repository and Reference Centre (**RRC**), Universiti Malaysia Terengganu, Malaysia, as holotype (**UMT**) (UMTAnn 2149, UMTAnn 2177, UMTAnn 2179, UMTAnn 2181) and paratypes (UMTAnn 2150 to 2176, UMTAnn 2178, UMTAnn 2180, UMTAnn 2182 to 2193)
- Australian Museum, Sydney, Australia (**AM**) as paratypes (AM W.54041 to W.54060)
- Natural History Museum of Los Angeles County, USA (**NHMLAC**) as paratypes (LACM-AHF 13494 to 13505)
- Lee Kong Chian Natural History Museum, Singapore (**LKCNHM**) as paratypes (ZRC.ANN.1604 to ZRC.ANN.1612, ZRC.ANN.1614 to 1615)
- Iziko South African Museum, South Africa (**ISAM**) as paratypes (SAM-MB-A096021 to A096023)

Table 1. Type of pectinate chaetae present in *Marphysa* from Terengganu.

Type of pectinate chaetae	Description
Type 1	Thin, narrow isodont with short and slender inner teeth
Type 2	Thin, wide isodont with short and slender inner teeth
Type 3	Thin, narrow heterodont with short and slender inner teeth
Type 4	Thick, wide isodont with short and slender inner teeth
Type 5	Thick, wide isodont with long and slender inner teeth
Type 6	Thick, narrow anodont with long and thick inner teeth
Type 7	Thick, wide anodont with long and slender inner teeth
Type 8	Thick, wide anodont with long and thick inner teeth

Molecular analyses

Molecular analyses were done at the Universiti Malaysia Terengganu (UMT) and the Australian Museum Research Institute, Australian Museum, Sydney (AMRI). At UMT, extractions of DNA were done using the xanthogenate method (Tillett and Neilan 2000). Approximately 600 bp of cytochrome oxidase subunit 1 (COI) gene were amplified using universal primer pair LCO1490 and HCO2198 (Folmer et al. 1994). Polymerase Chain Reaction (PCR) amplifications were carried out using 12.5 μ L of OneTaq Quick-Load Master mix, 9.5 μ L of biology grade water, 0.5 μ L of primers (10 μ M), 1 μ L of 1% bovine serum albumin (BSA) and 1 μ L DNA template. The temperature profile was as follows: 95 °C / 180 s – (94 °C / 20 s – 45 °C / 30 s – 72 °C / 60 s)*35 cycles and final extension time at 72 °C / 300 s. PCR success was verified by electrophoresis in a 1% p/v agarose gel stained with GelRed. Amplified products were sent to Apical Scientific Sdn. Bhd. for Sanger sequencing using forward primer (LCO1490).

Meanwhile, at AMRI, extractions of DNA were done with an ISOLATE II Genomic DNA kit (BIOLINE) following the protocol supplied by the manufacturers. Approximately 600 bp of COI gene were amplified using primers polyLCO and polyHCO (Carr et al. 2011). PCR was performed with Taq DNA Polymerase QIAGEN Kit in 20 μ L mixtures containing: 2 μ L of 10 \times CoralLoad PCR Buffer (final concentration of 1 \times), 1.5 μ L of MgCl₂ (25 Mm) solution, 1.5 μ L of PCR nucleotide mix (final concentration of 0.2 mM each dNTP), 0.4 μ L of each primer (final concentration of 0.2 μ M), 0.1 μ L of Taq DNA Polymerase (5U/ μ L), 1 μ L template DNA and 13.1 μ L of nuclease-free water. The temperature profile was as follows; 94 °C / 60 s – (94 °C / 40 s – 45 °C / 40 s – 72 °C / 60 s)*5 cycles – (94 °C / 40 s – 51 °C / 40 s – 72 °C / 60 s)*35 cycles – 72 °C / 300 s. PCR success was verified by electrophoresis in a 1% p/v agarose gel stained with GelRed. Amplified products were sent to Macrogen Company for Sanger sequencing using the same set of primers used for PCR.

A total of 63 COI sequences were downloaded from GenBank or obtained during this study; 60 COI sequences of *Marphysa* species and three out-group species from closely related genera in the order Eunicida (Table 2). All COI sequences were aligned in MEGA v. 11.0.10 using ClustalW plugin with default settings. The best DNA/Protein Models (ML) test was conducted, and the GTR model of molecular evolution was chosen as the best evolutionary model for the COI gene alignment. The phylogenetic analysis was performed in MEGA v. 11.0.10 (Tamura et al. 2021). The analysis was run for 1000 replicates. Pair-wise Kimura 2-parameter (K2P) genetic distance was performed using MEGA v. 11.0.10.

Habitat description and sediment analyses

Habitats of identified *Marphysa* were described based on the observations made during sampling including mangrove vegetations and sediment analyses. The particle size of the sediments was determined using dry-sieving techniques. Sediments were oven-dried at 60 °C for ~ 72 h. Then, 100 g of sub-samples were gently dry-sieved through a series of 4, 2, 1, 0.5, 0.25, 0.125, and 0.063 mm mesh openings of an Octagon D200 Digital mechanical shaker.

Table 2. Terminal taxa used in molecular part of the study (COI), with type localities, collection localities, GenBank accession numbers and references.

Species	Type locality	Collection locality	GenBank accession number	Reference
<i>Ophryotrocha marinae</i> Zhang, Zhou, Yen, Hiley & Rouse, 2023	Gulf of California, Mexico	Hydrothermal vents of Pescadero and Guaymas Basin, Gulf of California, Mexico	OP561817	Zhang et al. (2023)
<i>Diopatra aciculata</i> Knox & Cameron, 1971	Port Phillip Bay, Victoria, Australia	Port Phillip Bay, Victoria, Australia	AY838867	Struck et al. (2006)
<i>Oenone fulgida</i> (Lamarck, 1818)	Coast of Red Sea, Egypt	Coast of Red Sea, Egypt	AY838872	Struck et al. (2006)
<i>Marphysa aegypti</i> Elgetany, El-Ghobashy, Ghoneim & Struck, 2018	Suez Canal, Egypt	Suez Canal, Egypt	MF196968	Elgetany et al. (2018)
<i>Marphysa bifurcata</i> Kott, 1951	Western Australia, Australia	Queensland, Australia	KX172177	Zanol et al. (2016)
			KX172178	
<i>Marphysa brevitentaculata</i> Treadwell, 1921	Tobago Island, Trinidad and Tobago	Quintana Roo, Mexico	GQ497548	Zanol et al. (2010)
<i>Marphysa californica</i> Moore, 1909	California, USA	California, USA	GQ497552	Zanol et al. (2010)
<i>Marphysa chirigota</i> Martin, Gil & Zanol, 2020	Bay of Cadiz, Spain	Bay of Cadiz, Spain	MN816443	Martin et al. (2020)
<i>Marphysa davidattenboroughi</i> Lavesque, Zanol, Daffe, Flaxman & Hutchings, 2023	Bass Strait, Australia	Bass Strait, Australia	OQ622195	Lavesque et al. (2023)
			OQ622196	
<i>Marphysa disjuncta</i> Hartman, 1961	California, USA	California, USA	GQ497549	Zanol et al. (2010)
<i>Marphysa fauchaldi</i> Glasby & Hutchings, 2010	Northern Territory, Australia	Northern Territory, Australia	KX172165	Zanol et al. (2016)
<i>Marphysa gaditana</i> Martin, Gil & Zanol, 2020	Bay of Cadiz, Spain	Bay of Cadiz, Spain	MN816441	Martin et al. (2020)
<i>Marphysa hongkongensa</i> Wang, Zhang & Qiu, 2018	Hong Kong	Hong Kong	MH598525	Wang et al. (2018)
			MH598526	
<i>Marphysa ibaiensis</i> sp. nov.	Kuala Ibai, Terengganu, Malaysia	Kuala Ibai Lagoon and estuary, Terengganu, Malaysia	OR995540	This study
			OR995541	
			OR995542	
			OR995543	
			OR995544	
<i>Marphysa iloiloensis</i> Glasby, Mandario, Burghardt, Kupriyanova, Gunton & Hutchings, 2019	Iloilo, Philippines	Iloilo, Philippines	MN106279	Glasby et al. (2019)
			MN106280	
<i>Marphysa kertehensis</i> sp. nov.	Kerteh, Terengganu, Malaysia	Kerteh mangrove river, Terengganu, Malaysia	OR981603	This study
			OR981604	
			OR981605	
			OR995527	
			OR995528	
			OR995529	
			OR995530	
OR995531				
<i>Marphysa kristiani</i> Zanol, da Silva & Hutchings, 2016	New South Wales, Australia	New South Wales, Australia	KX172160	Zanol et al. (2016)
			KX172161	
<i>Marphysa madrasi</i> Hutchings, Lavesque, Priscilla, Daffe, Malathi & Glasby, 2020	Chennai, India	Chennai, India	MT813506	Hutchings et al. (2020)
			MT813507	
<i>Marphysa merchangensis</i> sp. nov.	Merchang, Terengganu, Malaysia	Merchang mangrove estuary, Terengganu, Malaysia	OR995532	This study
			OR995533	
			OR995534	
			OR995535	
<i>Marphysa mossambica</i> (Peters, 1854)	Mozambique	Iloilo, Philippines	KX172164	Zanol et al. (2016)
<i>Marphysa mullawa</i> Hutchings & Karageorgopoulos, 2003	Queensland, Australia	New South Wales, Australia	KX172166	Zanol et al. (2016)
			KX172167	

Species	Type locality	Collection locality	GenBank accession number	Reference
<i>Marphysa papuaensis</i> Lavesque, Daffe, Glasby, Hourdez & Hutchings, 2022	Solomon Sea, Papua New Guinea	Solomon Sea, Papua New Guinea	OP184050	Lavesque et al. (2022)
<i>Marphysa pseudosessilola</i> Zanol, da Silva & Hutchings, 2017	New South Wales, Australia	New South Wales, Australia	KY605405	Zanol et al. (2010)
			KY605406	
<i>Marphysa regalis</i> Verill, 1900	Bermuda, British Overseas Territory	Ceara, Brazil (Lavesque et al. 2023)	GQ497562	Zanol et al. (2010)
<i>Marphysa sanguinea</i> (Montagu, 1813)	Devon, UK	Callot Island, France	GQ497547	Zanol et al. (2010)
<i>Marphysa sanguinea</i> (Montagu, 1813)	Devon, UK	Cornwall, UK	MK950853	Lavesque et al. (2019)
<i>Marphysa sanguinea</i> (Montagu, 1813)	Arcachon Bay, France	Arcachon Bay, France	MK541904	Lavesque et al. (2019)
<i>Marphysa setiuense</i> sp. nov.	Setiu Wetlands, Terengganu, Malaysia	Setiu Wetland estuary, Terengganu Malaysia	OR995536	This study
			OR995537	
			OR995538	
			OR995539	
<i>Marphysa sherlockae</i> Kara, Molina-Acevedo, Zanol, Simon & Idris, 2020	Durban, South Africa	Strand, South Africa	MT840349	Kara et al. (2020)
			MT840350	
<i>Marphysa tripectinata</i> Liu, Hutchings & Sun, 2017	Beihai, China	Beihai, China	MN106271	Liu et al. (2017)
			MN106272	
<i>Marphysa victori</i> Lavesque, Daffe, Bonifácio & Hutchings, 2017	Arcachon Bay, France	Arcachon Bay, France	MG384996	Lavesque et al. (2017)
<i>Marphysa victori</i> Lavesque, Daffe, Bonifácio & Hutchings, 2017	Mangoku-ura Inlet, Japan	Mangoku-ura Inlet, Japan	LC467767	Abe et al. (2019)
<i>Marphysa victori</i> Lavesque, Daffe, Bonifácio & Hutchings, 2017	Arcachon, France	Ena Bay, Japan	LC467772	Abe et al. (2019)
<i>Marphysa viridis</i> Treadwell, 1917	Florida, USA	Ceara, Brazil	GQ497553	Zanol et al. (2010)
<i>Marphysa zanolae</i> Lavesque, Daffe, Glasby, Hourdez & Hutchings, 2022	Solomon Sea, Papua New Guinea	Solomon Sea, Papua New Guinea	OP184049	Lavesque et al. (2023)

Sediments retained on each sieve were weighed and recorded. Sediment grain size was classified according to grain size classifications by Blair and McPherson (1999), modified after Udden (1914) and Wentworth (1922). The percentage of particle size compositions was calculated, and the texture of sediments was determined based on the sediment textural classification scheme of Blair and McPherson (1999), modified after Folk et al. (1970).

Furthermore, total organic matter was determined using the loss on ignition (LOI) method which calculates the weight loss after combustion (Dean 1974). A total of 5 g of oven-dried sediments were placed in ceramic crucibles and ashed at 550 °C for six h in a muffle furnace. Then, sediments were cooled in a desiccator and weighed. The percentage of total organic matter (TOM) was analysed by the percentage loss of weight on ignition at 550 °C.

Results

Molecular analyses

DNA sequences of COI (460 bp) (Fig. 3) were used for phylogenetic analysis based on the maximum likelihood (ML) method. Results based on the COI showed that the four *Marphysa* species from Terengganu were well separated from other sequences of *Marphysa* and formed four different clades. Nodal support ranges from 97–100%, showing strong support for the clades. The interspecific divergence between these new species and all their sister taxa pair is high (pair-wise Kimura 2-parameter – COI K2P range from 6.14%–19.16%) (see Suppl. material 1).

Ecological analyses

Particle size analyses of sediment from sampling sites in Terengganu mangrove forest estuary, lagoon and river are shown in Table 3. Generally, sediments from all sampling sites were mainly composed of sand. However, sites can be differentiated by the composition of different particle sizes, sediment texture, and percentage of organic matter content. Sediments collected from Setiu Wetlands, Kuala Ibai mangrove estuary, and Kerteh mangrove river were dominated by fine sand; meanwhile, sediments from Merchang mangrove estuary and Kuala Ibai lagoon were dominated by a mixture of fine pebble + granule and medium size sand, respectively.

All sampling sites were located less than 1 km from the river mouth except for Kerteh station, which is 3.12 km from the river mouth. The sediment texture of sampling sites in Terengganu mangrove forest was classified as slightly gravelly sand, gravelly sand, and gravelly muddy sand (Fig. 4, Table 4). Total organic matter content indicated in Table 4; ranges from $0.29 \pm 0.05\%$ – $5.11 \pm 0.91\%$.

Taxonomic account

Family Eunicidae Berthold, 1827

Order Eunicida Dales, 1962

Genus *Marphysa* Quatrefages, 1866

Type species. *Nereis sanguinea* Montagu, 1813.

Diagnosis (after Molina-Acevedo and Carrera-Parra 2017). Prostomium slightly or completely bilobed; five prostomial appendages without articulations; eyes present or absent. Peristomium without peristomial cirri. Maxillary apparatus with four pairs of maxillae, an unpaired on the left side; M1 with falcal arch developed, extended, with the outer edge of the base arched; MIII curved, forming part of distal arc, with attachment lamella of rectangular or

Table 3. Particle size composition (%) of sediments from four sampling sites in Terengganu mangrove forest. Asterisk (*) indicates the largest particle size composition.

	Particle size composition (%)				
	Setiu Wetlands	Merchang mangrove estuary	Kuala Ibai		Kerteh mangrove river
			Mangrove estuary	Lagoon	
Fine pebble + granule (gravel)	3.06	*24.59	2.9	3.94	7.99
Very coarse sand	8.64	19.77	4.34	12.49	9.4
Coarse sand	15.21	21.33	7.59	23.89	8.24
Medium sand	26.29	17.6	21.28	*46.03	12.78
Fine sand	*32.08	7.05	*49.92	13.2	*33.16
Very fine sand	11.51	7.38	12.55	0.45	20.89
Silt + clay (mud)	3.21	2.28	1.42	0	7.54
Total	100	100	100	100	100
Percentage sand	93.73	73.13	95.68	96.06	84.47

Table 4. Distance of sampling sites from river mouth, type of sediment textures and total organic matter content of sampling sites in Terengganu mangrove forest.

Sampling sites	Distance from river mouth (km)	Type of sediment texture	Organic matter content (%)
Setiu Wetlands	0.9	Slightly gravelly sand	1.02 ± 0.17
Merchang mangrove estuary	0.85	Gravelly sand	5.11 ± 0.91
Kuala Ibai mangrove estuary	0.83	Slightly gravelly sand	1.66 ± 0.89
Kuala Ibai lagoon	0.53	Slightly gravelly sand	1.97 ± 0.29
Kerteh mangrove river	3.12	Gravelly muddy sand	0.29 ± 0.05

irregular shape, situated at centre of posterior edge of maxilla; MIV with circular or rectangular attachment lamella. Branchiae distributed along entire body. Dorsal cirri without articulation; postchaetal lobe well developed in anterior region. Ventral cirri with swollen, oval, or circular base. All sub-aciculae dark. Supracicular chaetae include limbate, pectinate isodont chaetae with slender teeth, pectinate anodont chaetae with long teeth. Subacicular chaetae include compound falcigers or spinigers, or only limbate chaetae. Subacicular hook dark or translucent, bidentate or unidentate. Pygidium with two pairs of anal cirri, without articulation.

***Marphysa kertehensis* sp. nov.**

<https://zoobank.org/73FBB175-0342-4A83-AF27-36A1DCD5EB66>

Figs 1, 2, 5–7

Material examined. Holotype. UMTAnn 2181, complete (regenerated posterior), antero-ventrally dissected, some parapodia removed and mounted for SEM. **Paratypes.** AM W.54059, complete, some parapodia removed and mounted for SEM; LACM-AHF 13503 to 13505, complete, some parapodia removed; ZRC. ANN.1614 to 1615, incomplete, some parapodia removed; SAM-MB-A096023, incomplete, some parapodia removed. All material was collected from the east coast of Peninsular Malaysia, Terengganu, Kerteh mangrove forest river (04°32.142'N, 103°26.363'E), March 2022.

Diagnosis. Prostomium completely bilobed, five prostomial appendages without articulations; eyes absent. Peristomium without peristomial cirri. Maxillary apparatus with four pairs of maxillae, an unpaired one on the left side, MI with falcular arch extended at sub-right angle, basal outer edge arched, basal inner edge lacking curvature. MII with triangular teeth and without attachment lamella. MIII slightly curved, with equal-sized triangular teeth, without attachment lamella. MIV with dark and curved attachment lamella. Branchiae distributed along entire body. Dorsal cirri without articulations; postchaetal lobe well developed in anterior regions. Ventral cirri with swollen, inflated base. Sub-aciculae black, blunt and translucent at distal end, pale brown in posterior-most parapodia. Supra-acicular chaetae include limbate, pectinate thin, narrow and wide isodont with short and slender inner teeth, and pectinate thick, wide isodont with short and slender inner teeth. Subacicular chaetae include only limbate chaetae. Subacicular hook absent. Pygidium with two pairs of anal cirri, without articulation.

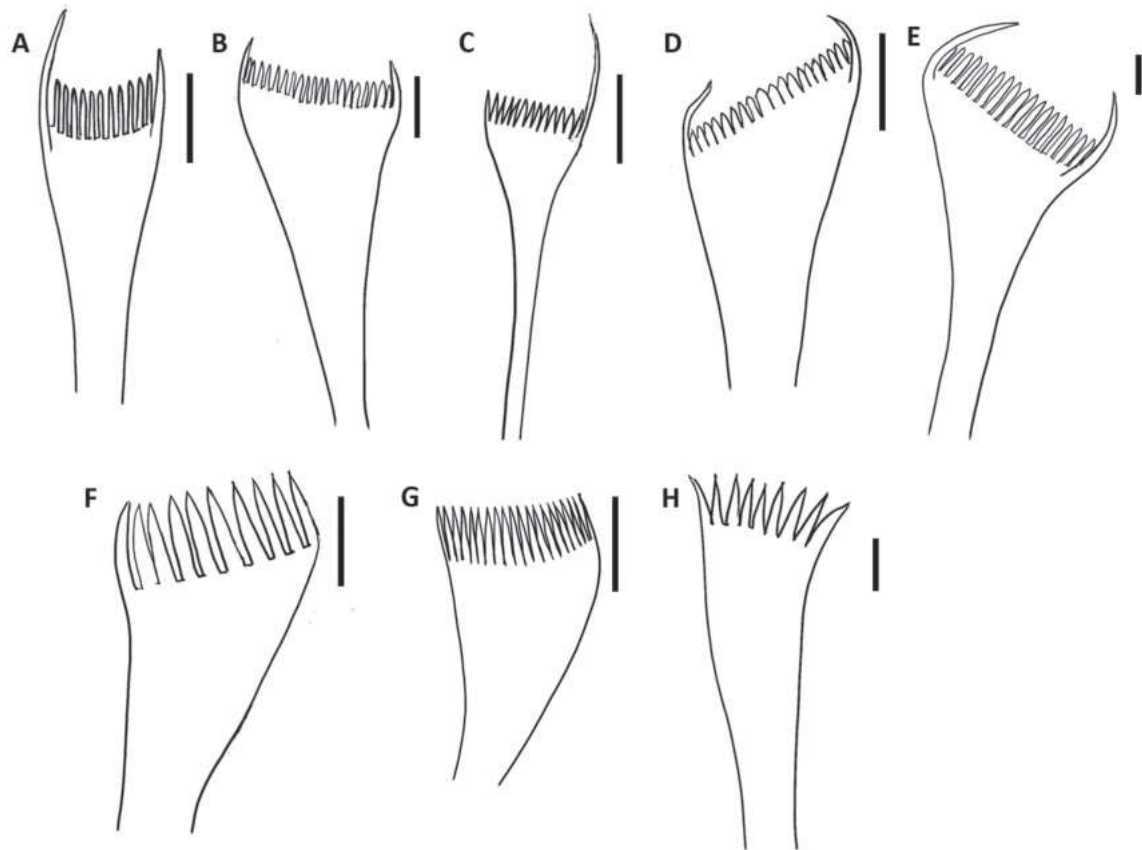


Figure 2. The schematic drawing of type of pectinate chaetae present in *Marphysa* from Terengganu **A** thin, narrow isodont with short and slender inner teeth (type 1) **B** thin, wide isodont with short and slender inner teeth (type 2) **C** thin, narrow heterodont with short and slender inner teeth (type 3) **D** thick, wide isodont with short and slender inner teeth (type 4) **E** thick, wide isodont with short and slender inner teeth (type 5) **F** thick, narrow anodont with long and thick inner teeth (type 6) **G** thick, wide anodont with long and slender inner teeth (type 7) **H** thick, wide anodont with long and thick inner teeth (type 8). Scale bars: 18 µm (**A**); 35 µm (**B**, **G**); 20 µm (**C**); 38 µm (**D**); 32 µm (**E**); 13 µm (**F**); 30 µm (**H**).

Description (based on holotype, with variation in parentheses for paratypes). Preserved specimens beige (Fig. 5A), with 518 (135–578) chaetigers, ~ 413 mm (173–295) total length, 12 mm (6–10.8) in length to chaetiger 10 (L10), 4.8 mm (3.15–5.1 mm) width at chaetiger 10 (W10), excluding parapodia. Body with dorsum convex and flat ventrum (Fig. 5A), without groove; body elongated, rounded in cross-section at anterior and median regions, and dorsoventrally flattened thereafter. Live specimens red (Fig. 7D).

Prostomium bilobed, anteriorly rounded with two dorsoventrally flattened lobes separated by an anterior notch between (Fig. 5B). Prostomial appendages in a semicircle, median antennae separated by a gap (Fig. 5B). Palps reach to first ring of peristomium; lateral and median antennae to second ring of peristomium. Palpophores and ceratophores are ring-shaped, short, thin; palpostyles and ceratostyles tapering and slender. Prostomial peduncles absent. Peristomium larger and wider than prostomium; first ring 3× longer than second ring, separation between rings distinct on all sides.

Maxillae dark (Fig. 5C), and maxillary formula (MF) as follows: 1+1, 5+5 (4–5), 8 (7–8)+0, 3 (3–4)+9 (8–9), 1+1. Maxillary carrier ~ 2.8× shorter than MI, rectangular anteriorly, triangular posteriorly. MI forceps-like, without

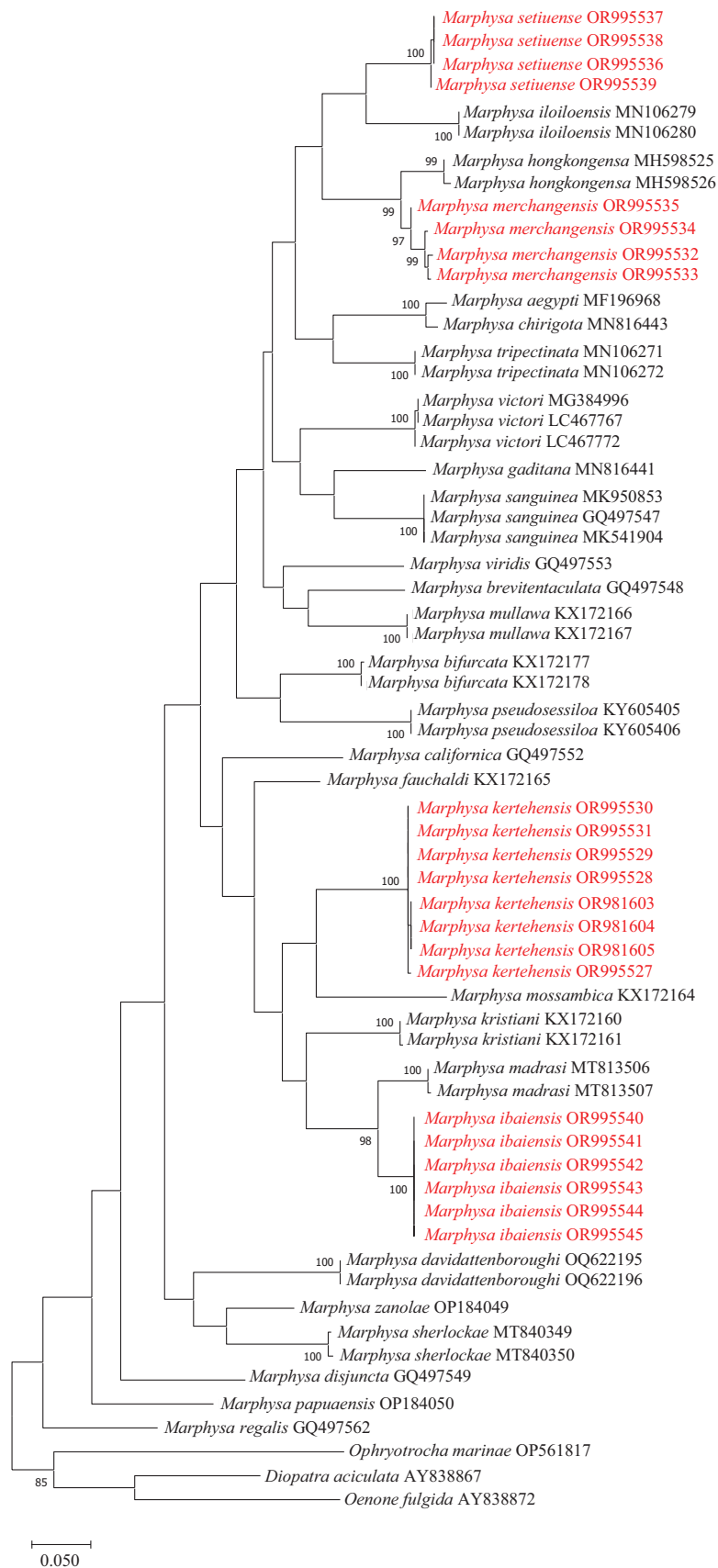


Figure 3. Phylogenetic tree generated by maximum likelihood (ML) method based on COI (460 bp). The sequences of the four new species of *Marphysa* obtained in this study are marked in red. Numbers beside the branches indicate ML bootstrap values of 80 (maximum: 100) based on 1000 bootstrap replications.

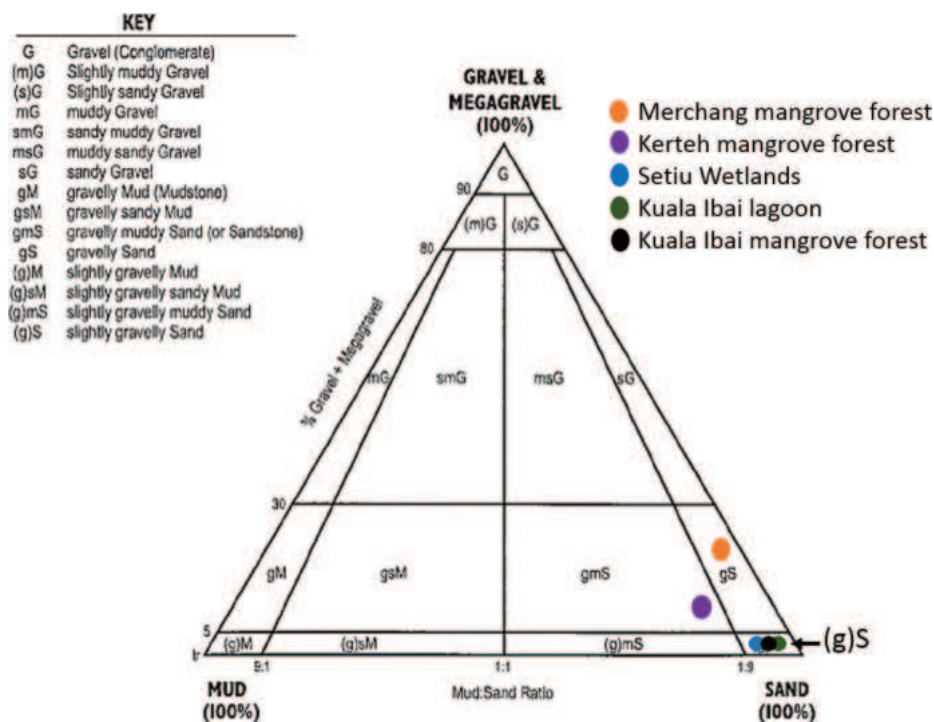


Figure 4. Sediment classification from sampling sites of Terengganu mangrove forest, according to sediment classification scheme by Blair and McPherson (1999), modified after Folk et al. (1970).

attachment lamellae, falcular arch extended at sub-right angle, basal outer edge arched, basal inner edge lacking a curvature. Closing system ~ 4.2x shorter than MI. Ligament between MI and MII dark. MII without attachment lamella, teeth triangular, distributed on < 1/2 of plate length. Ligament between MII and MIII dark. MIII single, longer than left MIV, slightly curved, with equal-sized triangular teeth, without attachment lamella. Left MIV short (< 1/2 the size of right MIV), attachment lamella dark, curved. Right MIV long, with teeth triangular, decreasing in size and teeth curved posteriorly; attachment lamella curved, dark. MV paired, longer than high. Mandible dark, longer than MI; cutting plates whitish (Fig. 5D).

First and second parapodia located ventrolaterally but gradually positioned dorsolaterally on subsequent segments. Chaetal lobes conical and directed to ventral cirri in anterior chaetigers, conical in median and posterior chaetigers (Fig. 5E–G). Prechaetal lobe shorter than chaetal lobe throughout body. Post-chaetal lobe rounded and longer than chaetal lobe in anterior chaetigers, conical in mid-body onwards and absent in the posterior-most chaetigers. Dorsal cirri digitiform with slender and tapering tips longer than ventral cirri anteriorly, digitiform and slightly longer from mid-body, digitiform and approximately similar length in posterior-most chaetigers (Fig. 5E–G). Ventral cirri digitiform in first chaetigers, basally inflated with digitiform tip from chaetiger 15 onwards (Fig. 5E–G). Branchiae pectinate, from chaetiger 41 (27–58), branchial filaments 3x longer than dorsal cirri where best developed; number of filaments increasing from five anteriorly to nine in mid-body, decreasing to three in last several chaetigers. Black dot present at the base of dorsal cirri from median chaetigers toward posterior chaetigers (Fig. 5F–H).

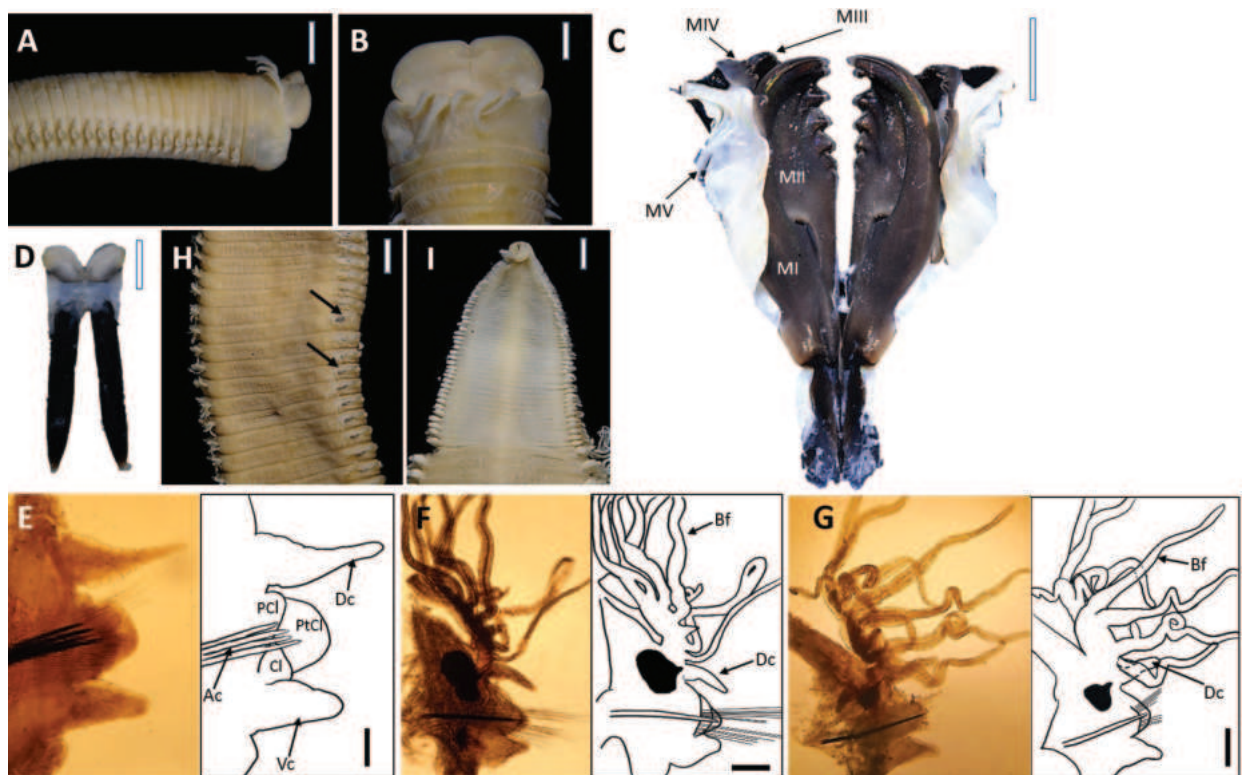


Figure 5. *Marphysa kertehensis* sp. nov. Holotype UMTAnn 2181 (A–I). Light microscopy images and digital drawing **A** anterior end, lateral view **B** anterior end, dorsal view **C** maxillae, dorsal view **D** mandibles, dorsal view **E** parapodium, chaetiger 10 **F** parapodium, chaetiger 295 **G** parapodium, chaetiger 462 **H** median region, dorsal view. Arrows indicate black dot at the base of dorsal cirri **I** posterior segments and pygidium, ventral view. Abbreviations; MI–MV: maxillae I–V, Ac: aciculae, Dc: dorsal cirrus, Vc: ventral cirrus, PCl: prechaetal lobe, Cl: chaetal lobe, PtCl: postchaetal lobe, Bf: branchial filament. Scale bars: 2 mm (A, H, I); 1 mm (B–D); 0.1 mm (E–G).

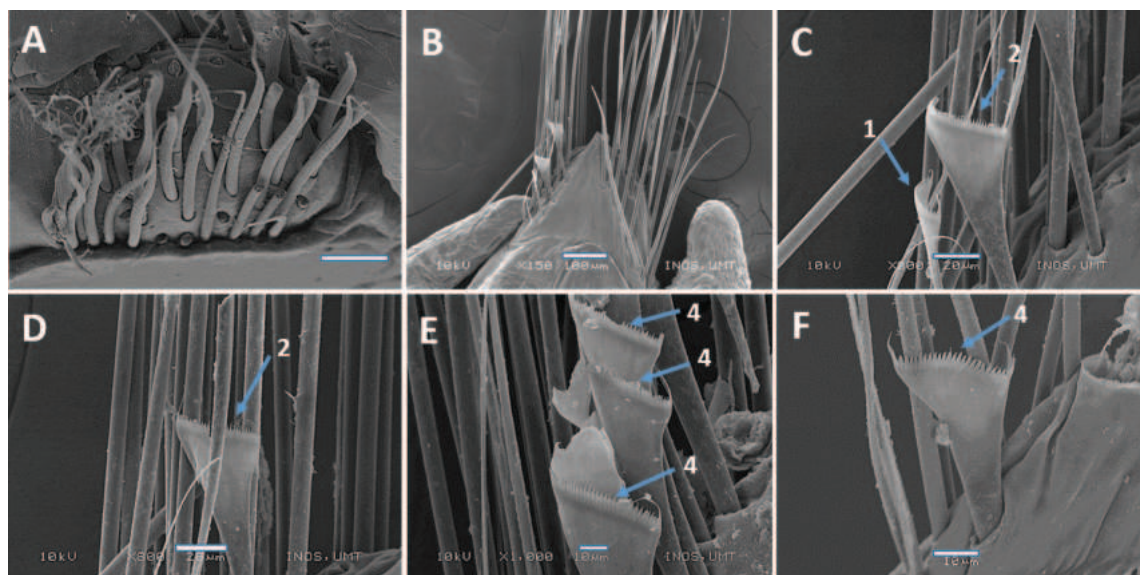


Figure 6. Scanning Electron Microscopy (SEM) images of *Marphysa kertehensis* sp. nov. Holotype UMTAnn 2181 (B–E), paratype AM W.54059 (A, F) **A** limbate chaetae, chaetiger 10 **B** parapodia, chaetiger 300 **C–D** pectinate chaetae, chaetiger 300 **E** pectinate chaetae, chaetiger 462 **F** pectinate chaetae, chaetiger 525. Numbers denoted by arrows indicate the type of pectinate chaetae: 1. Thin, narrow isodont; 2. Thin, wide isodont; 4. Thick, wide isodont. Scale bars: 50 μ m (A); 100 μ m (B); 20 μ m (C–D); 10 μ m (E–F).



Figure 7. Sampling site in Kerteh mangrove forest (river area) **A** habitat of *Marphysa kertehensis* sp. nov. **B** *Marphysa kertehensis* sp. nov. found inside driftwood and **C** in the sediment **D** live and complete *M. kertehensis* sp. nov.

Notoaciculae absent, neuroaciculae black, blunt, and translucent at distal end along most of body, pale brown in posterior-most parapodia; three or four per parapodium in anterior, one or two per parapodium in median and posterior chaetigers (Fig. 5E–G). Supra-acicular chaetae with limbate capillaries and pectinates, subacicular chaetae with limbate capillaries, compound chaetae absent (Fig. 6A, B). Three types of pectinate chaetae were identified (types 1, 2, 4; see Fig. 2): type 1: thin, narrow isodont with 28 short and slender inner teeth, outer teeth longer on one side, present only in the anterior body region (Fig. 6C); type 2: thin, wide isodont with ~ 30–32 short and slender teeth, present only in median and posterior region (Fig. 6C, D); type 4: thick, wide isodont with ~ 23 short and slender inner teeth, present only in posterior region (Fig. 6E, F). Anodont pectinate chaetae and subacicular hooks ($n = 30$) completely absent. Pygidium with crenulated margin, with two pairs of pygidial cirri attached (Fig. 5I).

Etymology. The new name denotes the type locality (Kerteh River) where the specimens were collected.

Type locality. South China Sea, Malaysia, east coast of Peninsular, Terengganu, Kerteh River (see Fig. 1).

Distribution. Known only from the type locality.

Habitat. Gravelly muddy sand (Table 4), burrowing inside driftwood, in mangroves, intertidal (Fig. 7A–C) with salinity 3.18‰ during spring low tide.

Remarks. With the presence of only limbate chaetae in both supra- and subacicular chaetae bundles, *Marphysa kertezensis* sp. nov. belongs to *Marphysa* Group A (Mossambica). Comparing *Marphysa* Group A from Malaysia's coastal water bodies, *M. kertezensis* sp. nov. is similar to *M. moribidii* (type locality: Morib, Malaysia) in lacking eyes. Table 5 lists the characteristics of Group A species, such as the presence or absence of peduncle in the prostomial appendages, the number of types of pectinate chaetae, chaetiger from where the branchiae commence and finish, number of branchial filaments and subacicular hooks and all differ from the new species. *Marphysa kertezensis* sp. nov. has three types of pectinate chaetae (types 1, 2, 4) but lacks any wide anodont chaetae (types 6, 7, 8), while *M. moribidii* has four types, including wide anodont (types 1, 4, 5, 8). Although they all have the same type of pectinate branchiae and the chaetiger where the branchiae emerge, *M. moribidii* (TL: 333 mm) has a wider range variation of chaetiger where the branchiae emerge; they occur from chaetiger 35 (4–63) whereas in *M. kertezensis* sp. nov. (TL: 413 (173–295) mm), the branchiae are present from chaetiger 41 (27–58). There are no subacicular hooks present in all specimens of *M. kertezensis* sp. nov., but there are

Table 5. Morphological features comparison between *Marphysa* Group A (Mossambica) described in this study and species occurring within Malaysian water bodies. The features for new species are based on holotype, with variation in parentheses for paratypes. Abbreviations: MF: maxillary formula, roman numerals refer to number of maxilla; PR-I: first peristomial ring; PR-II: second peristomial ring; p/a: present/absent; NIA: no information available. The major feature's differences between the species are mark with asterisk (*).

Morphological feature	<i>M. moribidii</i> Idris, Hutchings & Arshad, 2014	<i>M. kertezensis</i> sp. nov.
Source of Information	Paratypes AM W.38690; additional material (Idris et al. 2014)	Holotype UMTAnn 2181 (this study)
Size (mm): L10, W10	12.2–20, 6.3–8.2	12 (6–10.8), 4.8 (3.15–5.1)
Prostomium: shape	Bilobed	Bilobed
Palps: reaching	PR-II	PR-I
Lateral antennae:reaching	PR-II or Chaetiger 1	PR-II
Median antennae: reaching	Chaetiger 1 or 2	PR-II
Peduncle in prostomial appendages*	Present	Absent
Eyes	Absent	Absent
MF: MII, MIII, MIV*	5–6+4–6, 7–8+0, 6+8–10	5+5 (4–5), 8 (7–8)+0, 3 (3–4)+9 (8–9)
Branchiae: shaped	Pectinate	Pectinate
Branchiae: start chaetiger; last chaetiger before pygidium*	27–39; 15–37	41 (27–58), until pygidium
Branchial filaments: numbers	7–10	9
Dorsal cirri: shaped	Conical	Digitiform
Prechaetal lobe: shaped	Transverse fold	Transverse fold
Chaetal lobe: shaped	Rounded	Conical and directed to ventral cirri, conical
Aciculae: shape; colour	Blunt, dark	Black, dark and translucent at distal end
Subacicular limbate chaetae: (p/a); distribution	Present; all chaetigers	Present; all chaetigers
Pectinate chaetae: number of type*	4	3
Subacicular hook: shape; colour*	Bidentate, translucent	No subacicular hook
Subacicular hook: start chaetiger*	56–65	No subacicular hook
Subacicular hook: distribution*	Scattered	No subacicular hook

a few subacicular hooks present in the paratype of *M. moribidii* AM W.38690. Additionally, *M. kertezensis* sp. nov. has a black dot at the base of dorsal cirri in median and posterior chaetigers, possibly a reservoir of blood to irrigate the branchiae, which is absent in *M. moribidii*. It is worth mentioning that comparisons between the two species were based only on morphological features as there is no sequence data published for *M. moribidii*. Furthermore, each species lives in a different habitat. *Marphysa kertezensis* sp. nov. was found in the driftwood within the mangrove area dominated by *Exoecaria agallocha*, meanwhile *M. moribidii* inhabits mangrove forest with *Rhizophora* spp., *Avicennia alba* and *Sonneratia caseolaris* (Idris et al. 2014).

***Marphysa merchangensis* sp. nov.**

<https://zoobank.org/AD77E9BF-8D3D-458F-8AEA-BAC2E7AAF7CB7>

Figs 1, 2, 8–10

Material examined. Holotype. UMTAnn 2149, complete, antero-ventrally dissected, some parapodia mounted for SEM. **Paratypes.** AM W.54044, complete, some parapodia mounted for SEM. LACM-AHF 13494 to 13496, complete, some parapodia removed; ZRC.ANN.1604 to 1606, complete, some parapodia removed; SAM-MB-A096021, complete, some parapodia removed. All material was collected from the east coast of Peninsular Malaysia, Terengganu, Merchang mangrove estuary (05°01.393'N, 103°17.994'E), October 2021.

Diagnosis. Prostomium completely bilobed, five prostomial appendages without articulations; eyes present. Peristomium without peristomial cirri. Maxillary apparatus with four pairs of maxillae, an unpaired on the left side, MI with falcate arch extended at sub-right angle, basal outer edge arched, basal inner edge lacking curvature. MII with triangular teeth and without attachment lamella. MIII slightly curved, with equal-sized triangular teeth, without attachment lamella. MIV with rectangular and curved attachment lamella. Branchiae distributed along entire body. Dorsal cirri without articulations; postchaetal lobe well developed in anterior regions. Ventral cirri with swollen, inflated base. Sub-aciculae black, blunt, and translucent at distal end, pale brown in posterior-most parapodia. Supra-acicular chaetae include limbate, pectinate thin, narrow isodont with short and slender inner teeth, pectinate thick, wide isodont with short or long and slender inner teeth, and pectinate thick, narrow and wide anodont with long and thick inner teeth. Subacicular chaetae include only compound spinigers. Subacicular hook unidentate throughout chaetigers. Pygidium with two pairs of anal cirri, without articulation.

Description (based on holotype, with variation in parentheses for paratypes). Preserved specimen beige (Fig. 8A), 257 (165–294) chaetigers, 94 mm (37–144 mm) long, L10 - 5.25 mm (3.45–5.85 mm), W10 - 2.85 mm (1.95–3.15 mm), excluding parapodia. Anterior region of body with dorsum convex and flat ventrum, without groove (Fig. 8A); body depressed from chaetiger 25, elongated and tapering at distal end. Live specimens pink with red branchiae (Fig. 10D).

Prostomium bilobed, anteriorly rounded with two dorsoventrally flattened lobes with an anterior notch between them (Fig. 8A, B). Prostomial appendages in a semicircle, median antenna isolated by a gap (Fig. 8B). Palps reach middle of second peristomial ring; lateral antennae reaching chaetiger 2; medi-

an antenna reaching chaetiger 3. Palpophores and ceratophores ring-shaped, short, and thick; palpostyles and ceratostyles tapering, and slender. Prostomial appendage peduncles absent. A pair of faded brown eyes present at posterior base of prostomium, between palps and lateral antennae (Fig. 8B). Peristomium larger and wider than prostomium; first ring is 2.5× longer than second ring, separation between rings distinct on all sides.

Maxillae pale brown (Fig. 8C), and maxillary formula as follows: MF = 1+1, 5 (4–5)+5 (5–6), 7 (6–7)+0, 4 (4–5)+8 (5–8), 1+1. Maxillary carrier ~ 2.5× shorter than MI, rectangular anteriorly, triangular posteriorly. MI forceps-like, without attachment lamellae, falcate arch extended at sub-right angle, basal outer edge arched, basal inner edge lacking a curvature. Closing system ~ 3× shorter than MI. Ligament between MI and MII pale brown. MII without attachment lamella, teeth triangular, distributed on < 1/2 length of the plate. Ligament between MII and MIII pale brown. MIII single, longer than left MIV slightly curved, with equal-sized triangular teeth, without attachment lamella. Left MIV short (< 1/2 the size of right MIV) with rectangular attachment lamellae. Right MIV long with curved attachment lamellae, teeth triangular, decreasing in size and teeth curved posteriorly. MV paired. Mandible pale brown, with concentric stripes, longer than MI; cutting plates whitish (Fig. 8D).

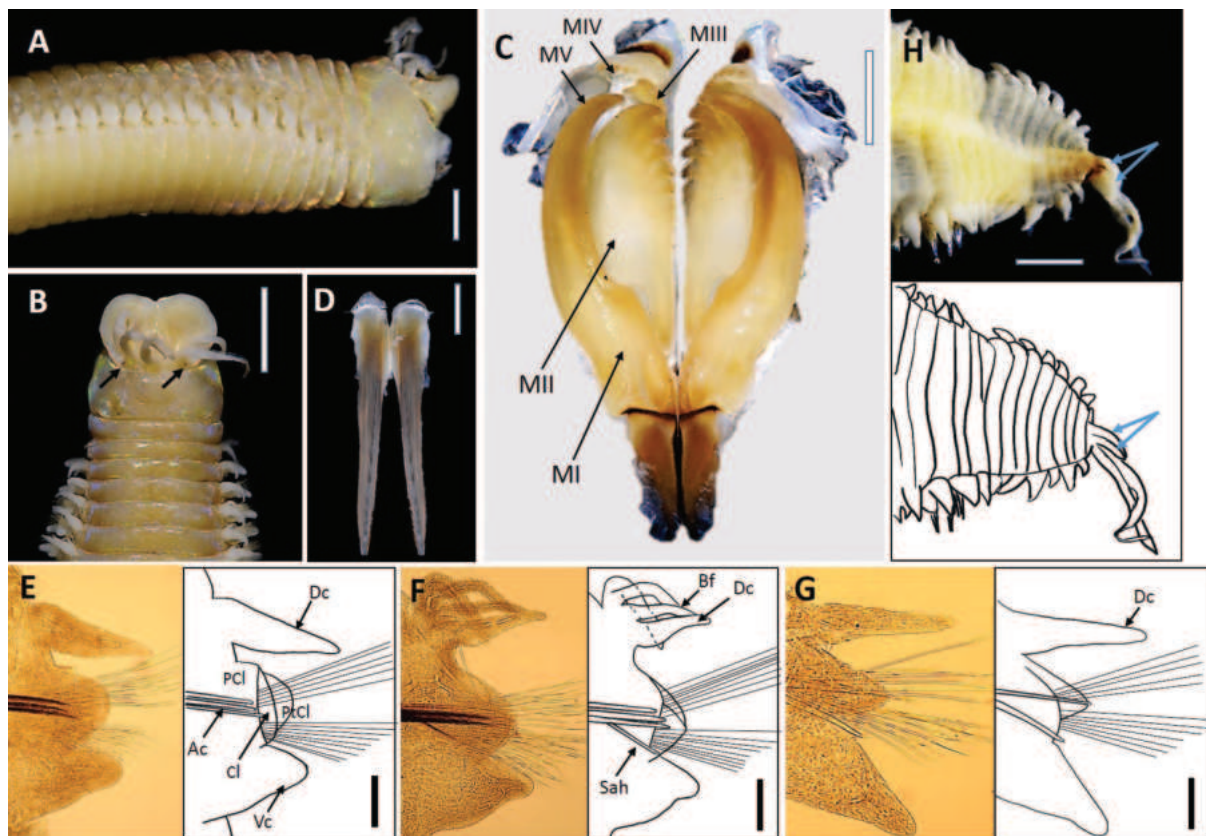


Figure 8. *Marphysa merchangensis* sp. nov. Holotype UMTAnn 2149 (B–H), paratype UMTAnn 2148 (A). Light microscopy images and digital drawing **A** anterior end, lateral view **B** anterior end, dorsal view. Arrows indicate eyes **C** maxillae, dorsal view **D** mandibles, dorsal view **E** parapodium, chaetiger 10 **F** parapodium, chaetiger 134 **G** parapodium, chaetiger 250 **H** posterior segments and pygidium, ventral view. Arrows show the short pair of pygidial cirri. Abbreviations; MI–MV: maxillae I–V, Ac: aciculae, Dc: dorsal cirrus, Vc: ventral cirrus, PCl: prechaetal lobe, Cl: chaetal lobe, PtCl: postchaetal lobe, Sah: subacicular hook, Bf: branchial filament. Scale bars: 1 mm (A–D, H); 0.1 mm (E–G).

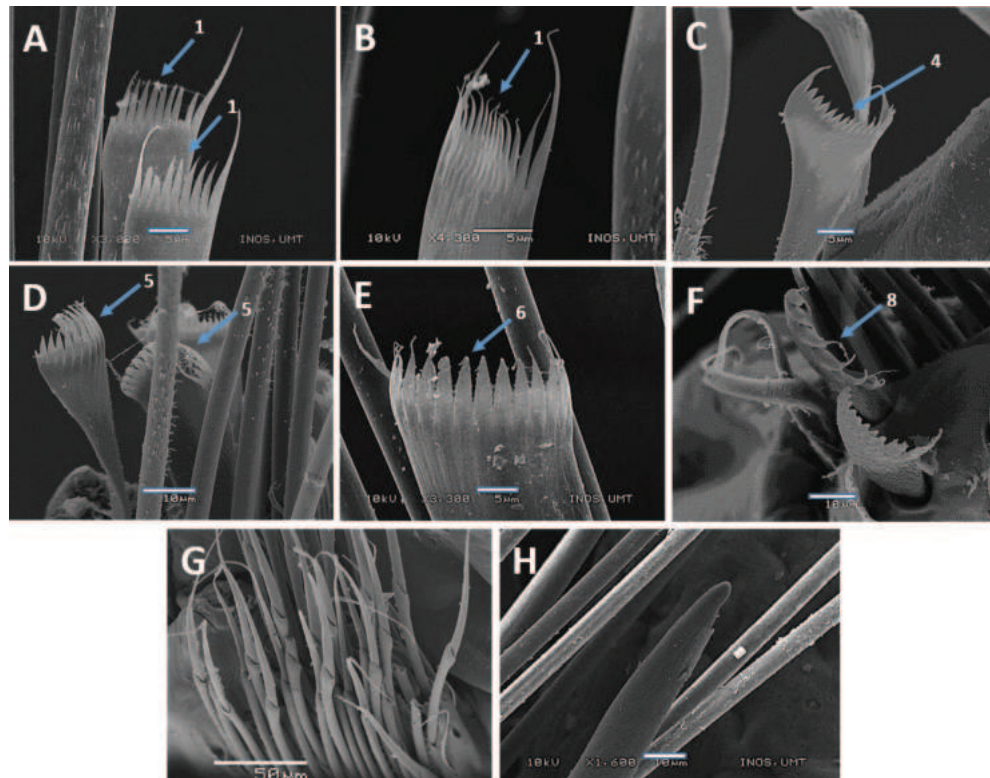


Figure 9. SEM images of *Marphysa merchangensis* sp. nov. Holotype UMTAnn 2149 (**A, B, E, H**), paratype AM W.54044 (**C, D, F, G**) **A, B** pectinate chaetae, chaetiger 10 **C** pectinate chaetae, chaetiger 164 **D** pectinate chaetae, chaetiger 245 **E** pectinate chaetae, chaetiger 250 **F** pectinate chaetae, chaetiger 265 **G** spiniger chaetae, chaetiger 10 **H** subacicular hook, chaetiger 128. Numbers denoted by arrows indicate the type of pectinate chaetae; 1. Thin, narrow isodont; 4, 5. Thick, wide isodont; 6. Thick, narrow anodont; 8. Thick, wide anodont. Scale bars: 5 μ m (**A–C, E**); 10 μ m (**D, F, H**); 50 μ m (**G**).

First few parapodia located ventrolaterally but gradually becoming dorsolateral in subsequent segments. Chaetal lobes rounded in anterior and posterior chaetigers, conical in median chaetigers (Fig. 8E–G). Prechaetal lobe shorter than chaetal lobe throughout body. Postchaetal lobe digitiform in first three chaetigers then rounded thereafter; longer than chaetal lobe in median chaetigers onwards, become shorter and absent in the posterior-most chaetigers. Dorsal cirri digitiform and slender, longer than ventral cirri anteriorly, slightly longer or similar from mid-body towards posterior-most chaetigers (Fig. 8E–G). Ventral cirri thumb-shaped with rounded wide tips in first few chaetigers, basally inflated with digitiform tip from chaetiger 15, and gradually becoming conical posteriorly (Fig. 8E–G). Branchiae pectinate, from chaetiger 24 (16–27) and continuing to last \sim 10 chaetigers, branchial filaments 4 \times longer than dorsal cirri where best developed; number of filaments increasing from three anteriorly to six in mid-body, decreasing to one in last several chaetigers.

Notoaciaculae absent, neuroaciaculae black, blunt, and translucent at distal end along most of body, pale brown in posterior-most parapodia; \sim 2 or 3 per parapodium in anterior, one per parapodium in median and posterior chaetigers (Fig. 8E–G). Supra-aciacular chaetae with limbate capillaries and pectinates. Five types of pectinate chaetae present (types 1, 4, 5, 6, 8) (see Fig. 2): type 1: thin, narrow isodont with 7–12 short and slender inner teeth, outer teeth longer, but with varying lengths, present in anterior and median body



Figure 10. Sampling site in Merchang mangrove estuary **A** habitat of *M. merchangensis* sp. nov. **B–C** worm found in decayed root of *Exoecaria agallocha* (Malay: Bebuta) **D** live worms.

region (Fig. 9A, B); type 4: thick, wide isodont with 12–15 short and slender inner teeth, present only in median and posterior region (Fig. 9C); type 5: thick, wide isodont, with 15–18 long and slender inner teeth, only present in posterior region (Fig. 9D); type 6: thick, narrow anodont with 11 or 12 long thick teeth, only present in posterior region (Fig. 9E); type 8: thick, wide anodont, with five inner long and thick teeth, only present in the posterior region (Fig. 9F). Subacicular chaetae with compound spinigers (Fig. 9G). Subacicular hooks pale brown, translucent at distal end, emerge from chaetiger 37 (26–42) and then present on all chaetigers, one per parapodium; subacicular hooks unidentate throughout chaetigers (Fig. 9H). Pygidium with crenulated margin, with two pairs of tapering pygidial cirri attached to ventral side of pygidium, dorsal pair ~ 4× longer than ventral (Fig. 8H).

Etymology. The name denotes the type locality (Merchang estuary) where the specimens were collected.

Type locality. South China Sea, Malaysia, east coast of Peninsular, Terengganu, Merchang mangrove estuary (see Fig. 1).

Distribution. Known only from the type locality and Setiu Wetlands, Terengganu, Malaysia.

Habitat. Gravelly and slightly gravelly sand (Table 4), burrowing in decayed roots of the mangrove *E. agallocha* (Malay: Bebuta) (Fig. 10A–C), burrowing in the sediments within an area populated with *Talipariti tiliaceum* (Fig. 13C) with salinity 26‰ during spring low tide.

Remarks. With the presence of only compound spinigers along the whole body and branchiae along most of the body, *Marphysa merchangensis* sp. nov. belongs to the *Marphysa* Group B (Sanguinea). Other *Marphysa* species from Sanguinea-group occurring in the same water body (South China Sea) as *M. merchangensis* sp. nov. are *M. setiuense* sp. nov., *M. hongkongensa* Wang, Zhang & Qiu, 2018 (type locality: Hong Kong), *M. iloiloensis* Glasby, Mandario, Burghardt, Kupriyanova, Gunton & Hutchings, 2019 (type locality: Philippines), *M. multipectinata* Liu, Hutchings & Sun, 2017 (type locality: Shimen, Taiwan of China), *M. orientalis* Treadwell, 1936 (type locality: Xiamen, China), *M. tribranchiata* Liu, Hutchings & Sun, 2017 (type locality: Wanli, Taiwan of China), and *M. tripectinata* Liu, Hutchings & Sun, 2017 (type locality: Beihai, China).

Marphysa merchangensis sp. nov. is similar to *M. setiuense* sp. nov. in having a pair of eyes and the absence of peduncle on the prostomial appendages. However, they can be differentiated by the number of types of pectinate chaetae, maxillary formula, chaetiger on which the branchiae and subacicular hooks occur, shape of dorsal cirri, chaetal lobes and subacicular hooks. Number of types of pectinate chaetae in *M. merchangensis* sp. nov. is five (types 1, 4, 5, 6, 8), whereas in *M. setiuense* sp. nov. there are four (types 1, 2, 7, 8), and they lack the thick, wide isodont pectinate chaetae (types 4, 5). *Marphysa merchangensis* sp. nov. (L10: 5.25 (3.45–5.85) mm) has more denticles on MIII 7 (6–7)+0 compared to *M. setiuense* sp. nov. (L10: 2.7 (2.85–4.8) mm) which has MIII: 5 (4–6)+0. Branchiae and subacicular hook of *M. merchangensis* sp. nov. occur later (chaetiger 24 (16–27) and 37 (26–42)), respectively) compared to *M. setiuense* sp. nov., where they occur from chaetiger 20 (15–25) and 25 (21–38), respectively. *Marphysa merchangensis* sp. nov. has digitiform dorsal cirri along the whole body, while *M. setiuense* sp. nov. has both thumb-shaped and digitiform dorsal cirri. *Marphysa merchangensis* sp. nov. has rounded shaped chaetal lobe in the anterior and posterior, and conical in the median region, whereas *M. setiuense* sp. nov. has rounded chaetal lobes on all parapodia. Finally, *M. merchangensis* sp. nov. has unidentate subacicular hook, whereas *M. setiuense* sp. nov. has unidentate and a few bidentate subacicular hooks present in posterior chaetigers.

Marphysa merchangensis sp. nov. and *M. hongkongensa* can be differentiated by the presence or absence of eyes, number of types of pectinate chaetae, maximum number of branchial filaments, and the shape of subacicular hooks. *Marphysa merchangensis* sp. nov. has a pair of eyes but they are absent in *M. hongkongensa*. *Marphysa merchangensis* sp. nov. has five types of pectinate chaetae (types 1, 4, 5, 6, 8) compared to four types present in *M. hongkongensa* (types 1, 2, 7, 8). *Marphysa hongkongensa* lacks thick, wide isodont and thick, narrow anodont pectinate chaetae (types 4, 5, 6) which are present in the new

species. The maximum number of branchial filaments in *M. merchangensis* sp. nov. (L10: 5.25 (3.45–5.85) mm) is six and they begin from chaetiger 24 (16–27) whereas *M. hongkongensis* (L10: 3.3–7 mm) has a maximum of ten branchial filaments, beginning from chaetiger 15–35. Finally, *M. merchangensis* sp. nov. only has unidentate subacicular hooks while both unidentate and bidentate subacicular hooks are present in *M. hongkongensis*.

Marphysa merchangensis sp. nov. is similar to *M. iloiloensis* and *M. multiplectinata* in having a pair of eyes. However, they can be distinguished by the number of types of pectinate chaetae present, the chaetiger on which branchiae and subacicular hooks occur, number of branchial filaments, shape of subacicular hooks and the maxillae formula. *Marphysa merchangensis* sp. nov. has five types of pectinate chaetae (types 1, 4, 5, 6, 8) whereas *M. iloiloensis* and *M. multiplectinata* have three (types 1, 4, 6) and four (types 1, 4, 7, 8) respectively. *Marphysa merchangensis* sp. nov. and *M. iloiloensis* have the same type of pectinate branchiae (beginning on the same chaetiger with different range of variation) (chaetiger 24 (16–27) for the new species, and chaetiger 19 (16–20) for *M. iloiloensis*). The maximum number of branchial filaments in *M. merchangensis* sp. nov. (TL: 94 (37–144) mm) is six, while *M. iloiloensis* (TL: 99 (95–165+) mm) has a maximum of seven branchial filaments. *Marphysa multiplectinata* (L10: 13.9 mm) has palmate branchiae with maximum of five branchial filaments from chaetiger 32. Finally, all these species have different formulae for MII, MIII and MIV (see Table 6).

The other species from the Sanguinea complex, *M. tribranchiata* and *M. tripectinata* differ from *M. merchangensis* sp. nov. by the absence of eyes. Both *M. tribranchiata* and *M. tripectinata* have three types of pectinate chaetae, whereas *M. merchangensis* sp. nov. has five types. *Marphysa tribranchiata* lacks thick, wide isodont and thick, narrow anodont pectinate chaetae (types 4, 6), while *M. tripectinata* lacks thin, narrow isodont pectinate chaetae (type 1) which are present in the new species (types 1, 4, 5, 6, 8). While *M. merchangensis* sp. nov. and *M. tripectinata* only have unidentate subacicular hooks, they begin much later (chaetiger 170) in the latter species. *Marphysa tribranchiata* has both unidentate and bidentate subacicular hooks whereas only unidentate hooks are present in *M. merchangensis* sp. nov. The maximum number of branchiae filaments present in *M. tribranchiata* (L10: 8.7 mm) and *M. tripectinata* (L10: 12.7 mm) are three and eight respectively, differs from *M. merchangensis* sp. nov. (L10: 5.25 (3.45–5.85) mm), which has a maximum of six.

Finally, *M. merchangensis* sp. nov. is similar to *M. orientalis* by having unidentate subacicular hooks. *Marphysa merchangensis* sp. nov. has a pair of eyes and two pairs of anal cirri, while *M. orientalis* has no eyes and only one pair of anal cirri. Also, branchiae in *M. merchangensis* sp. nov. begin earlier from chaetiger 24 (16–27) compared to *M. orientalis* (chaetiger 45). The maximum number of branchial filaments in *M. merchangensis* sp. nov. is six, while *M. orientalis* has a maximum of three branchial filaments. Nevertheless, the original description of *M. orientalis* is incomplete and does not include certain important features such as the number and type of pectinate chaetae. Fresh material of *M. orientalis* should be collected and redescribed from the type locality at Gulf of Mannar, Sri Lanka.

Table 6. Morphological features comparison between *Marphysa* Group B (Sanguinea) described in this study and species occurring within Malaysian water bodies (South China Sea). The features for new species are based on the holotype, with variation in parentheses for paratypes. Abbreviations: MF: maxillary formula, roman numerals refer to number of maxilla; PR-I: first peristomial ring; PR-II: second peristomial ring; p/a: present/absent; NIA: no information available. The major differences between the species are marked with asterisk (*).

Morphological feature	<i>M. hongkongensis</i> Wang, Zhang & Qiu, 2018	<i>M. iloiloensis</i> Glasby, Mandario, Burghardt, Kupriyanova, Gunton & Hutchings, 2019	<i>M. multipectinata</i> Liu, Hutchings & Sun, 2017	<i>M. orientalis</i> , Treadwell, 1936	<i>M. tribranchiata</i> Liu, Hutchings & Sun, 2017	<i>M. tripectinata</i> Liu, Hutchings & Sun, 2017	<i>M. merchangensis</i> sp. nov.	<i>M. setiuense</i> sp. nov.
Source of information	Holotype: SWIMS-ANN-18-012; Paratypes: SWIMS-ANN-18-013. (Wang et al. 2018)	Holotype: NTM W29624; Paratypes: NTM W29619 – NTM W29623 (Glasby et al. 2019)	Holotype: ASIZW0000345-1 (Liu et al. 2017)	Type: USNM. No. 20114 (Treadwell 1936)	Holotype: ASIZW0000348-2 (Liu et al. 2017)	Holotype: AM W49069 (Liu et al. 2017)	Holotype: UMTAnn 2149 (this study)	Holotype: UMTAnn 2177 (this study)
Size (mm): L:T0, W:10	3.3–7.0, 2.2–5.3	NIA, 2.6	13.9, 5.7	NIA	8.7, 3.9	12.7, 5.95	5.25 (3.45–5.85), 2.85 (1.95–3.15)	2.7 (2.85–4.8), 1.8 (1.65–2.55)
Prostomium: shape	Bilobed	Bilobed	Bilobed	Bilobed	Bilobed	Bilobed	Bilobed	Bilobed
Palps: reaching	Chaetiger 1	Chaetiger 1	PR-I	NIA	Chaetiger 1	PR-I	PR-II	Chaetiger 3
Lateral antennae:reaching	Chaetiger 1	Chaetiger 1 or 2	PR-I	NIA	Chaetiger 2	PR-II	Chaetiger 2	Chaetiger 4
Median antennae: reaching	Chaetiger 1 or 2	Chaetiger 1 or 2	PR-II	NIA	Chaetiger 3	Chaetiger 1	Chaetiger 3	Chaetiger 5
Peduncle in prostomial appendages	Absent	Absent	Absent	Absent	Absent	Absent	Absent	Absent
Eyes*	Absent	Present	Present	Absent	Absent	Absent	Present	Present
MF: MII, MIII, MIV*	5-6+5-6, 7+0, 4+8	4+5, 4-5+0, 3-4+5-6	3+3, 4+0, 4+5	3+3, 4+0, 4+3	4+4, 5+0, 4+8	5+5, 5+0, 4+8	5 (4-5)+5 (5-6), 7 (6-7)+0, 4 (4-5)+8 (5-8)	5 (4-5)+5 (4-6), 5 (4-6)+0, 3 (3-4)+6 (7-8)
Branchiae: shape	Pectinate	Pectinate	Palmate	NIA	Pectinate	Pectinate	Pectinate	Pectinate
Branchiae: start chaetiger; last chaetiger before pygidium	15–35; until pygidium	16–20; until pygidium	32; end at chaetiger 281	45; end ~30 last chaetiger	26; end at chaetiger 181	15; end at chaetiger 399	24 (16–27); end ~10 last chaetiger	20 (15–25); until pygidium
Branchial filaments: numbers	5–10	6–7	5	3	3	8	6	5
Dorsal cirri: shaped	Conical	Conical	NIA	Conical	NIA	NIA	Digitiform	Thumb-shape, digitiform
Prechaetal lobe: shaped	Transverse fold	Transverse fold	NIA	NIA	NIA	NIA	Transverse fold	Transverse fold
Chaetal lobe: shaped	Rounded	Rounded	NIA	Rounded	NIA	NIA	Rounded and conical	Rounded
Aciculae: shape; colour	NIA; black with paler tips	Blunt; black with paler tips	NIA; brown	Blunt; black	NIA; brown	NIA; black	Blunt; black and translucent at distal end	Blunt; black and translucent at distal end
Subacicular limbate chaetae: (p/a); distribution	Absent; all chaetigers	Absent; all chaetigers	Absent; all chaetigers	Absent; all chaetigers	Absent; all chaetigers	Absent; all chaetigers	Absent; all chaetigers	Absent; all chaetigers
Pectinate chaetae: number of type*	4	3	4	NIA	3	3	5	4
Subacicular hook: shape; colour*	Unidentate and bidentate; amber	Unidentate; amber to black	Unidentate and bidentate; yellow	Unidentate; NIA	Unidentate and bidentate; brown	Unidentate	Unidentate; light brown and translucent at distal end	Unidentate and bidentate; light brown and translucent at distal end
Subacicular hook: start chaetiger*	26–58	30–38	20	Present in posterior region (No information on start chaetiger)	20	170	37 (26–42)	25 (21–38)
Subacicular hook: distribution	Continuous	Continuous	Continuous	NIA	Continuous	Continuous	Continuous	Continuous

***Marphysa setiuense* sp. nov.**

<https://zoobank.org/46E5DB0B-5F17-45D6-A57E-56AD91799411>

Figs 1, 2, 11–13

Material examined. Holotype. UMTAnn 2177, complete, antero-ventrally dissected, some parapodia mounted for SEM. **Paratypes.** AM W.54050, complete, some parapodia mounted for SEM. LACM-AHF 13497 to 13499, complete, some parapodia removed; ZRC.ANN.1607 to 1609, complete, some parapodia removed. All material was collected from the east coast of Peninsular Malaysia, Terengganu, Setiu Wetlands (05°39.183'N, 102°45.194'E), October 2021.

Diagnosis. Prostomium completely bilobed, five prostomial appendages without articulations; eyes present. Peristomium without Peristomial cirri. Maxillary apparatus with four pairs of maxillae, an unpaired on the left side, MI with falcal arch extended at sub-right angle, basal outer edge arched, basal inner edge lacking curvature. MII with triangular teeth and without attachment lamella. MIII slightly curved, with equal-sized triangular teeth, without attachment lamella, MIV with curved attachment lamella. Branchiae distributed along entire body. Dorsal cirri without articulations; postchaetal lobe well developed in anterior regions. Ventral cirri with swollen, inflated base. Sub-aciculae black, blunt, and translucent at distal end, pale brown in posterior-most parapodia. Supra-acicular chaetae include limbate, pectinate thin, narrow and wide isodont with short and slender inner teeth, and pectinate thick, wide anodont with long and slender or thick inner teeth. Subacicular chaetae include only compound spinigers. Subacicular hook unidentate, and a few bidentate present in posterior chaetigers. Pygidium with two pairs of anal cirri, without articulation.

Description (based on holotype, with variation in parentheses for paratypes). Preserved specimens beige (Fig. 11A), ~ 154 (141–259) chaetigers, ~ 51 mm (27–75 mm) long, L10 - 2.7 mm (2.85–4.8 mm), W10 - 1.8 mm (1.65–2.55 mm), excluding parapodia. Anterior region of the body with dorsum convex and flat ventrum, without groove; body depressed from chaetiger 11, elongated and tapering at the distal end. Live specimens pink (Fig. 13B, D).

Prostomium bilobed, anteriorly rounded with two dorsoventrally flattened lobes separated by an anterior notch (Fig. 11A, B). Prostomial appendages in a semi-circle, median antenna isolated by a gap (Fig. 11B). Palps reaching chaetiger 3; lateral antennae reaching chaetiger 4; median antenna reaching chaetiger 5. Palpophores and ceratophores ring-shaped, short, and thick; palpostyles and ceratostyles tapering and slender. Prostomial appendage peduncles absent. Pair of faded brown eyes at posterior base of prostomium, between palps and lateral antennae. Peristomium similar in size (width and length) to prostomium; the first ring is 1.5× longer than second ring, and separation between rings distinct on all sides.

Maxillae dark brown (Fig. 11C) and maxillary formula as follows: MF = 1+1, 5 (4–5)+5 (4–6), 5 (4–6)+0, 3 (3–4)+6 (7–8), 1+1. Maxillary carrier ~ 2.4× shorter than MI, rectangular anteriorly, triangular posteriorly. MI forceps-like, without attachment lamellae, falcal arch extended at sub-right angle, basal outer edge arched, basal inner edge lacking a curvature. Closing system ~ 5× shorter than MI. Ligament between MI and MII pale brown. MII without attachment lamella, teeth triangular, distributed along half of plate length. Ligament between MII and MIII pale brown. MIII single, longer than left MIV, slightly curved, with equal-sized triangular teeth, without attachment lamella. Left MIV short (< 1/2

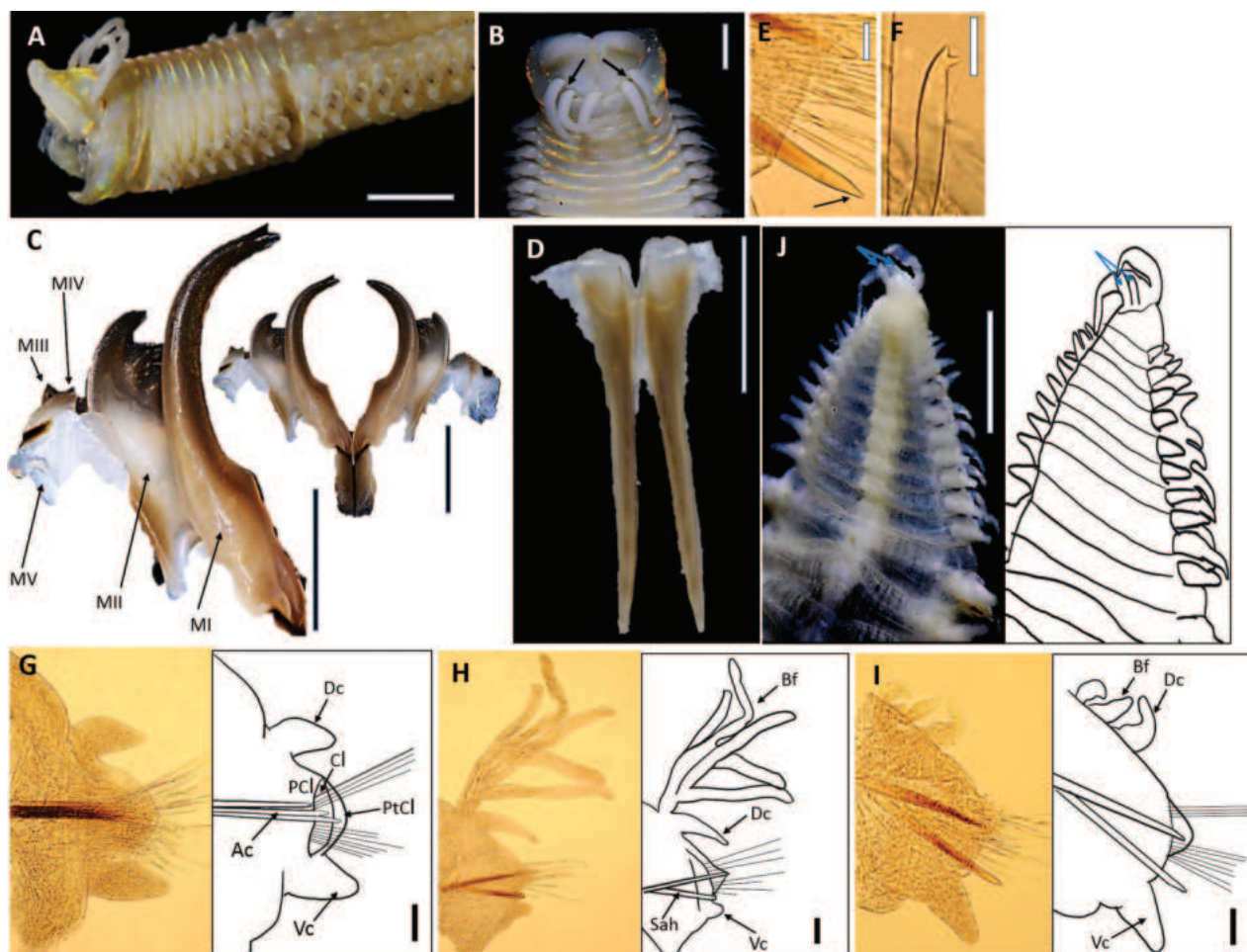


Figure 11. *Marphysa setiuense* sp. nov. Holotype UMTAnn 2177 (A–J). Light microscopy images and digital drawing **A** anterior end, lateral view **B** anterior end, dorsal view. Arrows indicate eyes **C** maxillae, dorsal view **D** mandibles, dorsal view **E** unidentate hook, chaetiger 136 **F** bidentate hooded hook, chaetiger 140 **G** parapodium, chaetiger 10 **H** parapodium, chaetiger 77 **I** parapodium, chaetiger 136 **J** posterior segments and pygidium, dorsal view. Arrows show the short pair of pygidial cirri. Abbreviations; MI–MV: maxillae I–V, Ac: aciculae, Dc: dorsal cirrus, Vc: ventral cirrus, PCL: prechaetal lobe, Cl: chaetal lobe, PtCl: postchaetal lobe, Sah: subacicular hook, Bf: branchial filament. Scale bars: 1 mm (A, C, D, J); 1 mm (B); 20 μ m (E–F); 0.1 mm (G–I).

the size of right MIV) with curved attachment lamellae. Right MIV long, with teeth triangular with curved attachment lamellae, decreasing in size and teeth curved posteriorly. MV paired. Mandibles dark brown (Fig. 11D), with concentric stripes; longer than MI; cutting plates whitish.

First parapodia occur ventrolaterally, gradually becoming dorsolateral in following segments. Chaetal lobes rounded in all chaetigers (Fig. 11G–I). Prechaetal lobe shorter than chaetal lobe along whole body. Postchaetal lobe digitiform in first three chaetigers and rounded thereafter; conical and longer than chaetal lobe in median and posterior chaetigers, becoming shorter and absent in the posterior-most chaetigers. Dorsal cirri thumb-shaped with digitiform tips, shorter than ventral cirri in anterior, digitiform with slender and tapering tips; slightly longer or similar length from mid-body onwards and shorter in posterior-most chaetigers (Fig. 11G–I). Ventral cirri thumb-shaped with digitiform tips in the first few chaetigers, basally inflated with digitiform tip from chaetiger 15 onwards, and gradually becoming conical posteriorly (Fig. 11G–I). Branchiae

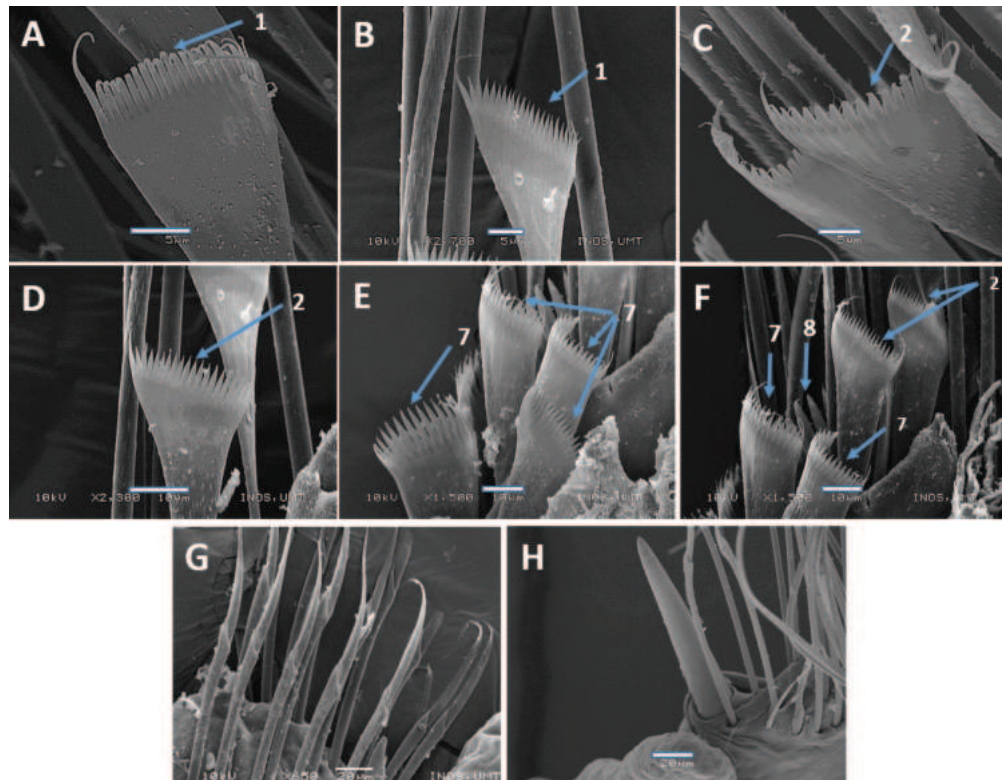


Figure 12. SEM images of *Marphysa setiuense* sp. nov. Holotype UMTAnn 2177 (**B, D–G**), paratype AM W.54050 (**A, C, H**) **A** pectinate chaetae, chaetiger 30 **B** pectinate chaetae, chaetiger 77 **C** pectinate chaetae, chaetiger 203 **D** pectinate chaetae, chaetiger 77 **E, F** pectinate chaetae, chaetiger 136 **G** spiniger chaetae, chaetiger 25 **H** subacicular hook, chaetiger 183. Numbers denoted by arrows indicate the type of pectinate chaetae; 1. Thin, narrow isodont; 2. Thin, wide isodont; 7, 8. Thick, wide anodont. Scale bars: 5 μ m (**A–C**); 10 μ m (**D–F**); 20 μ m (**G, H**).

pectinate, from chaetiger 20 (15–25) and continuing to near the end (~ 8 last chaetigers without branchiae), branchial filament 4 \times longer than dorsal cirri where best developed; number of filaments increasing from two anteriorly to five in mid-body, decreasing to one in last several chaetigers.

Notoacaculae absent, neuroacaculae black, blunt, and translucent at distal end on most of body, pale brown in posterior-most parapodia; ~ 2 or 3 per parapodium in anterior, one per parapodium in median and posterior chaetigers (Fig. 11G–I). Supra-acicular chaetae with limbate capillaries and pectinates. Four types of pectinate chaetae were identified (types 1, 2, 7, 8) (see Fig. 2): type 1: thin, narrow isodont with ~ 18–22 short and slender inner teeth, outer teeth longer, but of varying lengths, present in anterior and median body region (Fig. 12A, B); type 2: thin, wide isodont with 14–21 short and slender teeth, outer teeth same length as inner teeth, present only in anterior and posterior region (Fig. 12C, D); type 7: thick, wide anodont with 15–18 long and slender inner teeth, only present in posterior region (Fig. 12E, F); type 8: thick, wide anodont, with seven inner long and thick teeth, only present in posterior region (Fig. 12F). Subacicular chaetae with compound spinigers (Fig. 12G). Subacicular hooks unidentate (Figs 11E, 12H), pale brown, translucent at distal end, commencing from chaetiger 25 (21–38) and then present on all subsequent chaetigers, one per parapodium and with a few bidentate hooks in posterior chaetigers (Fig. 11F). Pygidium with crenulated margin, with two pairs of tapering pygidial cirri attached to ventral side of pygidium, dorsal pair ~ 4 \times longer than ventral one (Fig. 11J).



Figure 13. Sampling in Setiu Wetlands (river area) **A, C** habitat of *M. setiuense* sp. nov. and *M. merchangensis* sp. nov. within *Talipariti tiliaceum* **B** *Marphysa setiuense* sp. nov. in situ **D** live *M. setiuense* sp. nov.

Etymology. The name refers to the type locality Setiu Wetlands.

Type locality. South China Sea, Malaysia, east coast of Peninsular, Terengganu, Setiu Wetlands (see Fig. 1).

Distribution. Known only from the type locality.

Habitat. Slightly gravelly sand sediment (Table 4), burrowing in decayed roots of mangrove trees (*Sonneratia* spp.) and area within *Talipariti tiliaceum* (Fig. 13A–C), with salinity 26‰ during spring low tide.

Remarks. With the presence of only compound spiniger along the whole body and branchiae along most of the body, *Marphysa setiuense* sp. nov. belongs to Group B (Sanguinea). As mentioned earlier, there are seven other Sanguinea-group *Marphysa* species described from the South China Sea; *M. merchangensis* sp. nov., *M. hongkongensis*, *M. iloiloensis*, *M. multipectinata*, *M. orientalis*, *M. tribranchiata* and *M. tripectinata*. The most morphologically-similar species to *M. setiuense* sp. nov. is *M. hongkongensis*. Both species have four types of pectinate chaetae (two isodont and two anodont; types 1, 2, 7, 8) and have both unidentate and bidentate subacicular hooks in posterior chaetigers. However, they differ in the number of branchial filaments and the distribution of branchiae. *Marphysa setiuense* sp. nov. (L10: 2.7 (2.85–4.8) mm) has a maximum of five branchial filaments while *M. hongkongensis* (L10: 3.3–7 mm) has up to ten. Also, the species have different maxillae formulae. *Marphysa setiuense* sp. nov.

has fewer denticles on MIII (5 (4–6)+0) compared to *M. hongkongensa* which has MIII (7+0) (see Table 6).

Marphysa setiuense sp. nov. is similar to *M. iloiloensis* and *M. multipectinata* in having a pair of eyes, but they can be distinguished by the number of types of pectinate chaetae, the chaetiger on which branchiae and subacicular hooks begin, number of branchial filaments, shape of subacicular hooks and maxillae formula. *Marphysa setiuense* sp. nov. has four types of pectinate chaetae (types 1, 2, 7, 8) compared to three types present in *M. iloiloensis* (types 1, 4, 6). *Marphysa multipectinata* also has four types of pectinate chaetae (types 1, 4, 7, 8), but they are only present on median and posterior chaetigers, whereas in *M. setiuense* sp. nov., the pectinate chaetae are present throughout the body. The maximum number of branchial filament in *M. setiuense* sp. nov. (L10: 2.7 (2.85–4.8) mm) is five, and up to seven for *M. iloiloensis*. *Marphysa multipectinata* (L10: 13.9 mm) has palmate branchiae with maximum five branchial filaments and begin from chaetiger 32 whereas *Marphysa setiuense* sp. nov. also has a maximum of five branchial filaments but they begin from chaetiger 20 (15–25). *Marphysa setiuense* sp. nov. and *M. multipectinata* have unidentate and bidentate subacicular hooks from chaetiger 25 (21–38) and chaetiger 20, whereas *M. iloiloensis* has unidentate subacicular hooks only from chaetiger 30–38. All these species have different formulae for MII, MIII, and MIV (see Table 6).

The other two *Marphysa* species of the Sanguinea complex occurring within the South China Sea, *M. tribranchiata* and *M. tripectinata* differ from *M. setiuense* sp. nov. by having no eyes. They also can be differentiated by the number of types of pectinate chaetae. *Marphysa tribranchiata* and *M. tripectinata* have three types of pectinate chaetae, while *M. setiuense* sp. nov. has four (types 1, 2, 7, 8). *Marphysa tribranchiata* lacks thin, wide isodont (type 2), while *M. tripectinata* lacks thin, narrow isodont pectinate chaetae (type 1). Also, *M. tripectinata* (L10: 12.7 mm) only has unidentate subacicular hooks, whereas *M. tribranchiata* (L10: 8.7 mm) and *M. setiuense* sp. nov. (L10: 2.7 (2.85–4.8) mm) have both unidentate and bidentate subacicular hooks.

Marphysa setiuense sp. nov. and *M. orientalis* differ by the presence or absence of eyes, shape of subacicular hooks, pair of anal cirri, the chaetiger on which the branchiae begin and the maximum number of branchial filaments. *Marphysa setiuense* sp. nov. has a pair of eyes and two pairs of anal cirri, while *M. orientalis* has no eyes and only one pair of anal cirri. The new species has unidentate and bidentate subacicular hooks while *M. orientalis* has only unidentate subacicular hooks. Branchiae in *M. setiuense* sp. nov. begin from chaetiger 20 (15–25) whereas in *M. orientalis* they occur from chaetiger 45. The maximum number of branchial filaments in *M. setiuense* sp. nov. is five, while *M. orientalis* only has three branchial filaments.

***Marphysa ibaiensis* sp. nov.**

<https://zoobank.org/EFD572B1-A215-49FF-9C42-76DA2561E4D9>

Figs 1, 2, 14–16

Material examined. Holotype. UMTAnn 2179, complete, antero-ventrally dissected, some parapodia mounted for SEM. **Paratypes.** AM W.54052, complete, some parapodia mounted for SEM. LACM-AHF 13500 to 13502, complete,

some parapodia removed; ZRC.ANN.1610 to 1612, complete, some parapodia removed; SAM-MB-A096022, complete, some parapodia removed. All material was collected from the east coast of Peninsular Malaysia, Terengganu, Kuala Ibai lagoon (05°17.198'N, 103°10.194'E) and estuary (05°16.780'N, 103°10.137'E), October 2021.

Diagnosis. Prostomium completely bilobed, five prostomial appendages without articulations; eyes absent. Peristomium without Peristomial cirri. Maxillary apparatus with four pairs of maxillae, an unpaired on the left side, MI with falcate arch extended at sub-right angle, basal outer edge arched, basal inner edge lacking curvature. MII with triangular teeth and without attachment lamella. MIII slightly curved, with equal-sized triangular teeth, without attachment lamella. MIV with curved attachment lamella. Branchiae distributed along entire body. Dorsal cirri without articulations; postchaetal lobe well developed in anterior regions. Ventral cirri with swollen, inflated base. Sub-aciculae black, blunt, and translucent at distal end, pale brown in posterior-most parapodia. Supra-acicular chaetae include limbate, pectinate, thin, narrow isodont with short and slender inner teeth, pectinate thin, narrow heterodont with short and slender inner teeth, pectinate thick, wide isodont with long or short and slender inner teeth, and pectinate thick, wide anodont with long and slender inner teeth. Subacicular chaetae include limbate and compound spinigers. Subacicular hook bidentate. Pygidium with two pairs of anal cirri, without articulation.

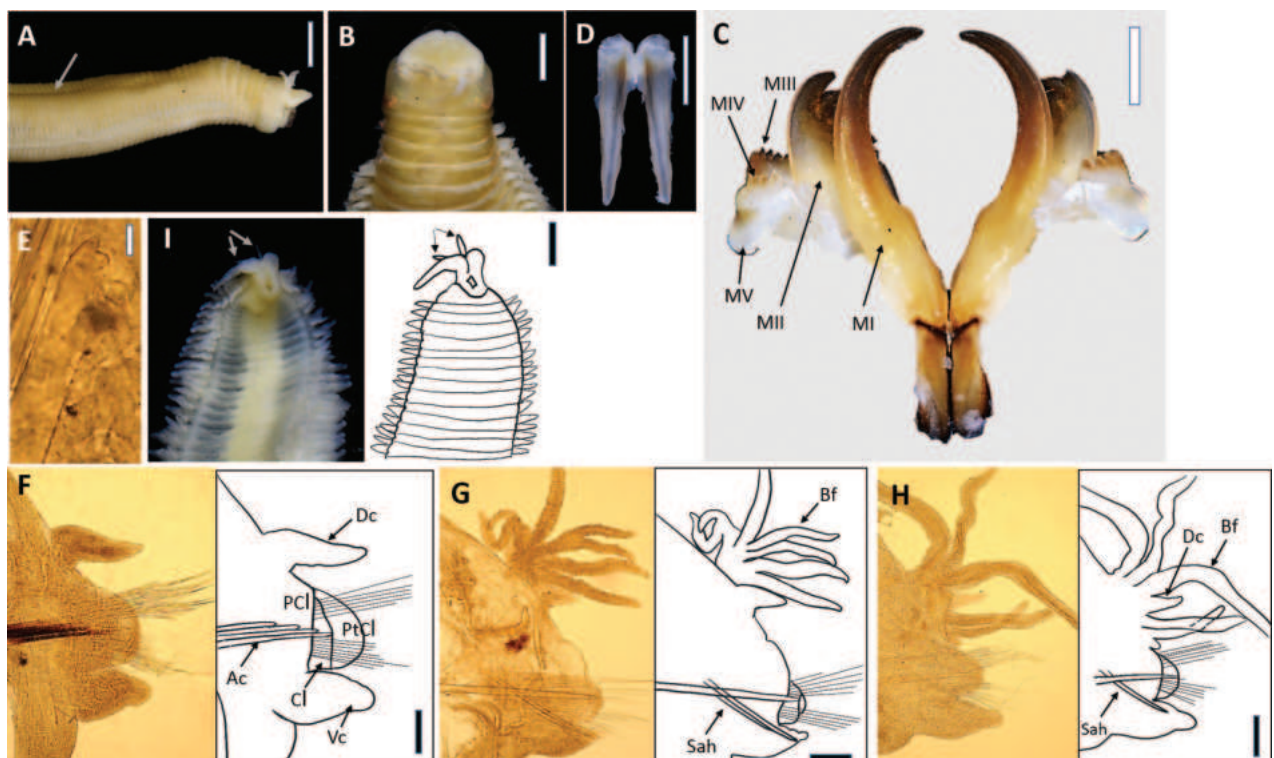


Figure 14. *Marphysa ibaiensis* sp. nov. Holotype UMTAnn 2179 (A–I). Light microscopy images and digital drawing **A** anterior end, lateral view. Arrow shows shallow groove **B** anterior end, dorsal view **C** maxillae, dorsal view **D** mandibles, dorsal view **E** bidentate hook, chaetiger 97 **F** parapodium, chaetiger 10 **G** parapodium, chaetiger 97 **H** parapodium chaetiger 145 **I** posterior segments and pygidium, dorsal view. Arrows show the short pair of pygidial cirri. Abbreviations; MI–MV: maxillae I–V, Ac: aciculae, Dc: dorsal cirrus, Vc: ventral cirrus, PCl: prechaetal lobe, Cl: chaetal lobe, PtCl: postchaetal lobe, Sah: subacicular hook, Bf: branchial filament. Scale bars: 2 mm (A, D); 1 mm (B, C, I); 20 µm (E), 0.1 mm (F–H).

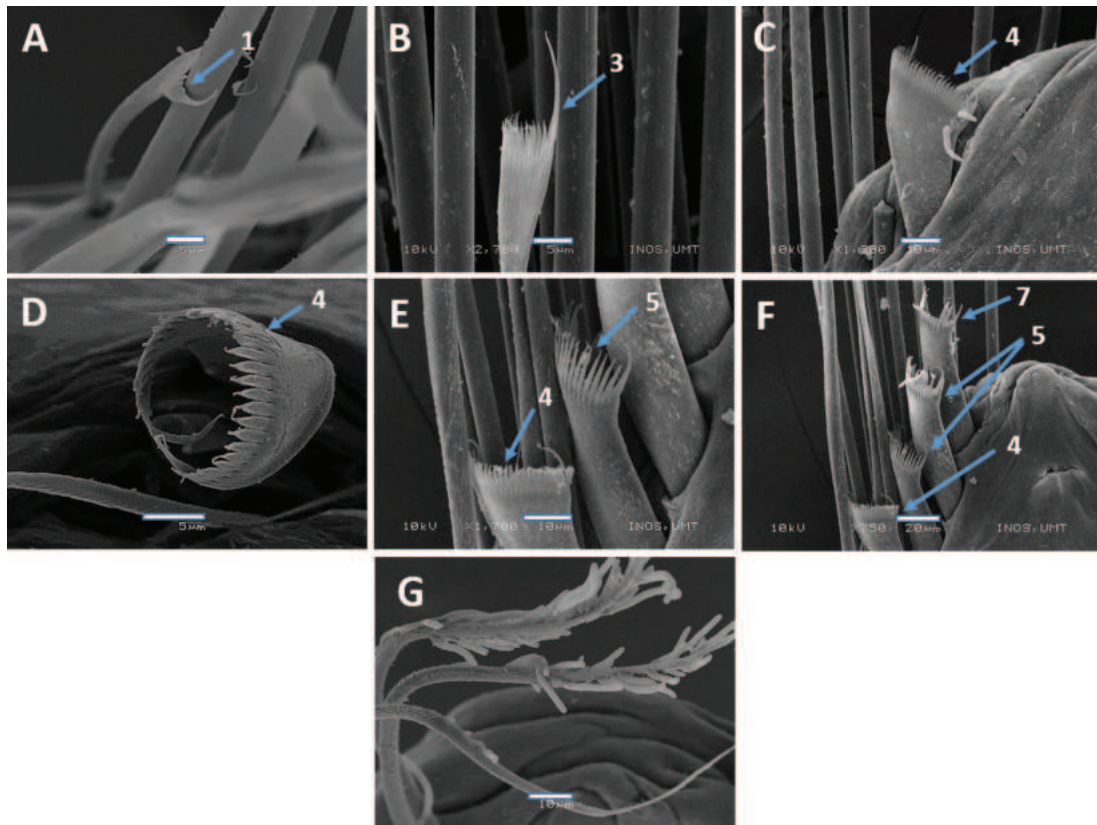


Figure 15. SEM images of *Marphysa ibaiensis* sp. nov. Holotype UMTAnn 2179 (**B, C, E, F**), paratype AM W.54052 (**A, D, G**) **A** pectinate chaetae, chaetiger 97 **B** pectinate chaetae, chaetiger 10 **C** pectinate chaetae, chaetiger 88 **D** pectinate chaetae, chaetiger 88 **E–F** pectinate chaetae, chaetiger 125 **G** serrations and projections on limbate chaetae, chaetiger 31. Numbers denoted by arrows indicate the type of pectinate chaetae; 1. Thin, narrow isodont; 3. Thin, narrow heterodont; 4, 5. Thick, wide isodont; 7. Thick, wide anodont. Scale bars: 5 μ m (**A–B, D**); 10 μ m (**C, F–H**); 20 μ m (**E**).

Description (based on holotype, with variation in parentheses for paratypes). Preserved specimens beige (Fig. 14A), ~ 195 (66–401) chaetigers and 52 mm (20–91 mm) long, L10: 4.5 mm (2.25–6.3 mm), W10: 2.85 mm (1.2–3.75 mm), excluding parapodia. Anterior region of body cylindrical, with shallow groove until median chaetigers (Fig. 14A); body depressed from chaetiger 30, elongated, and tapering at distal end. Live specimens red (Fig. 16C).

Prostomium conically bilobed, with two dorsoventrally lobes separated by an anterior notch (Fig. 14A, B). Prostomial appendages in a semicircle, median antennae separated by a gap. Palps, lateral and median antennae reaching first peristomium. Palpophores and ceratophores ring-shaped, short, and thin; palpostyles and ceratostyles tapering and slender. Prostomial appendage peduncles absent. Peristomium wider than prostomium; first ring 3 \times longer than second ring, separation between rings distinct on all sides.

Maxillae pale brown (Fig. 14C) and maxillary formula as follows: MF = 1+1, 6 (5–6)+7 (6–7), 7 (7–8)+0, 4+10 (9–10), 1+1. Maxillary carrier ~ 2.2 \times shorter than MI, rectangular anteriorly, triangular posteriorly. MI forceps-like, without attachment lamellae, falcate arch extended at sub-right angle, basal outer edge arched, basal inner edge lacking a curvature. Closing system is ~ 5.5 \times shorter than MI. Ligament between MI and MII pale brown. MII without attachment lamella, teeth triangular, present on < 1/2 of plate length. Ligament between MII and MIII pale brown. MIII single, longer than left MIV, slightly curved, with equal-



Figure 16. Sampling site in Kuala Ibai (estuary and lagoon area) **A** habitat of *Marphysa ibaiensis* **B** found in sediment deposited inside driftwood **C** live *M. ibaiensis* sp. nov.

sized triangular teeth, without attachment lamella. Left MIV short ($< 1/2$ the size of right MIV) with curved attachment lamellae. Right MIV long, with teeth triangular and curved attachment lamellae, decreasing in size and teeth curved posteriorly. MV paired. Mandibles whitish with pale brown core, longer than MI; cutting longer than MI; cutting plates whitish (Fig. 14D).

First few parapodia inserted ventrolaterally, but then becoming lateral in anterior region and dorsolaterally in subsequent segments. Chaetal lobes rounded on all chaetigers (Fig. 14F–H). Prechaetal lobe shorter than chaetal lobe along the entire body. Postchaetal lobe rounded and longer than chaetal lobe in anterior chaetigers and mid-body onwards (Fig. 14F–H), becoming shorter and absent in the posterior-most chaetigers. Dorsal cirri digitiform and slender, longer than ventral cirri anteriorly, as long as or shorter from mid-body and shorter in posterior chaetigers (Fig. 14F–H). Ventral cirri digitiform in first chaetigers, basally inflated with digitiform tip from chaetiger six onwards (Fig. 14F–H). Branchiae pectinate, starting from chaetiger 20 (11–65) and continuing to near end (~ 13 last chaetigers without branchiae), branchial filament 3× longer than dorsal cirri where best developed; number of filaments increasing from one anteriorly to eight in mid-body, decreasing to six in last several chaetigers. Pygidial cirri attached to ventral side of pygidium, dorsal pair ~ 4× longer than ventral (Fig. 14I).

Notoaciculae absent. Neuroaciculae black, blunt, and translucent at distal end along most of body, pale brown in posterior-most parapodia; ~ 3 or 4 per parapodium in anterior, one or two per parapodium in median and one per parapodium in posterior chaetigers (Fig. 14F–H). Supra-acicular chaetae with lim-

bate capillaries and pectinates. Five types of pectinate chaetae were identified (types 1, 3, 4, 5, 7) (see Fig. 2): type 1: thin, narrow isodont with 12–15 short and slender inner teeth, present in anterior and median region (Fig. 15A); type 3: thin, narrow heterodont with 12 short and slender inner teeth, outer teeth longer on one side, present in the anterior body region (Fig. 15B); type 4: thick, wide isodont with 18–29 short and slender teeth, outer teeth different length to inner teeth, only present in median and posterior region (Fig. 15C–F); type 5: thick, wide isodont with 15–18 long and slender inner teeth, present only posteriorly (Fig. 15E, F); type 7: thick, wide anodont with ~ 15 long and slender inner teeth, only present in posterior parapodia (Fig. 15F). Subacicular chaetae with compound spinigers and limbate capillaries in median and posterior chaetigers. Some limbate chaetae with inconspicuous serrations and numerous projections (Fig. 15G). Subacicular hooks pale brown, translucent at distal end, from chaetiger 22 (22–46), 1–3 per parapodium; subacicular hooks bidentate present throughout (Fig. 14E). Pygidium with crenulated margin, with two pairs of tapering pygidial cirri attached to ventral side of pygidium, dorsal pair ~ 4× longer than ventral one (Fig. 14I).

Etymology. Name refers to the type locality Kuala Ibai River.

Type locality. South China Sea, Malaysia, east coast of Peninsular, Terengganu, Kuala Ibai river estuary and lagoon (see Fig. 1).

Distribution. Known only from the type locality.

Habitat. Slightly gravelly sand sediment (Table 4) associated with oyster clumps within *Rhizophora* spp. (Fig. 16A), burrowing in sediment deposited inside driftwood bark (Fig. 16B) with salinity 26‰ (estuary) and 18‰ (lagoon) during spring low tide.

Remarks. With the presence of subacicular limbate and compound spinigers in the median and posterior region, *M. ibaiensis* sp. nov. belongs to Group E (Gravelly). There are four *Marphysa* species belonging to this group; *M. borradalei* Pillai, 1958 (type locality: Negombo Lagoon, Sri Lanka), *M. fauchaldi* Glasby & Hutchings, 2010 (type locality: Ardatek Barrumundi farm, Darwin, Australia), *M. gravellyi* Southern, 1921 (type locality: Chilka Lake, India) and *M. mdrasi* Hutchings, Lavesque, Priscilla, Daffe, Malathi & Glasby, 2020 (type locality: Chennai, India). The morphological features of these species are given in Table 7.

Marphysa ibaiensis sp. nov. can be distinguished from *M. borradalei* by the number of branchial filaments, shape of the subacicular hooks, chaetiger where the branchiae and subacicular hook occur, and the shape of postchaetal lobe in the anterior region. *Marphysa ibaiensis* sp. nov. (TL: 52 (20–91) mm) has a maximum of eight branchial filaments whereas *M. borradalei* (TL: 1–8 mm) has up to 20 branchial filaments. The subacicular hook of *M. ibaiensis* sp. nov. is bidentate and occurs from chaetiger 22 (22–46) onwards while *M. borradalei* has a strongly hooded unidentate hook that occur from chaetiger 50 onwards. *Marphysa ibaiensis* sp. nov. has rounded postchaetal lobe in anterior region, while *M. borradalei* has sub-conical shaped postchaetal lobes in the anterior region. The original description of *M. borradalei* makes it challenging to undertake a detailed morphological comparison and additional material from the type locality (Sri Lanka) needs to be collected and redescribed.

The new species can also be differentiated from *M. gravelyi* and *M. madrasi* by the absence of eyes, number of types of pectinate chaetae, number of branchial filaments, chaetiger where subacicular hooks begin and the length of the pygidial cirri. *Marphysa ibaiensis* sp. nov. has no eyes, while both *M. gravelyi* and *M. madrasi* have a pair of eyes. *Marphysa ibaiensis* sp. nov. has five types of pectinate chaetae (types 1, 3, 4, 5, 7), whereas *M. madrasi* has only two (types 4, 5). While all these species have bidentate hooks, they begin on chaetiger 22 (22–46) in *M. ibaiensis* sp. nov. (L10: 4.5 (2.25–6.3) mm), 26–35 in *M. gravelyi* and 33–72 in *M. madrasi* (L10: 6 (4–9) mm). *Marphysa ibaiensis* sp. nov. has short and long pairs of pygidial cirri attached to the pygidium, whereas *M. madrasi* only has one pair of short pygidial cirri.

Table 7. Morphological features comparison between *Marphysa* Group E (Gravelyi) described in this study and species occurring worldwide. The features for new species are based on the holotype, with variation in parentheses for paratypes. Abbreviations: MF: maxillary formula, roman numerals refer to number of maxilla; PR-I: first peristomial ring; PR-II: second peristomial ring; p/a: present/absent; NIA: no information available. The major differences between the species are marked with asterisk (*).

Morphological feature	<i>M. borradalei</i> Pillai, 1958	<i>M. gravelyi</i> Southern, 1921	<i>M. fauchaldi</i> Glasby & Hutchings, 2010	<i>M. madrasi</i> Hutchings, Lavesque, Priscilla, Daffe, Malathi & Glasby, 2020	<i>M. ibaiensis</i> sp. nov.
Source of Information	Lectotype BMNH 1960.3.13.6 (Glasby and Hutchings 2010)	Paratypes 1938.5.7.55 and the type description (Hutchings et al. 2020)	Holotype NTM W23040 (Glasby and Hutchings 2010)	Holotype NL-ENNORE_01 (ZSI); Paratypes: ZSI-HQ/GNC/AN6072/1 (Hutchings et al. 2020)	Holotype: UMTAnn 2179 (this study)
Size (mm): L10, W10	NIA	NIA	NIA	6 (4–9), 2.5 (2–3.9)	4.5 (2.25–6.3), 2.85 (1.2–3.75)
Prostomium: shape	Bilobed	Bilobed	Bilobed	Bilobed	Bilobed
Palps: reaching	NIA	NIA	NIA	NIA	PR-I
Lateral antennae:reaching	NIA	PR-I	NIA	NIA	PR-I
Median antennae: reaching	NIA	PR-I	NIA	NIA	PR-I
Peduncle in prostomial appendages	NIA	Absent	Present	Absent	Absent
Eyes*	NIA	Present	Absent	Present	Absent
MF: MII, MIII, MIV*	6, NIA	5+6, 12–13+0, 4+8	5+6, 7+0, 4+9	8+9, 10+0, 7+11	6 (5–6)+7 (6–7), 7 (7–8)+0, 4+10 (9–10)
Branchiae: shape		Pectinate	Pectinate	Pectinate	Pectinate
Branchiae: start chaetiger; last chaetiger before pygidium	7–60; end ~ 10 last chaetiger	22–52; end ~ 20 last chaetiger	31; end ~ 10 last chaetiger	48–50, end ~ 10 last chaetiger	20 (11–65); end ~ 13 last chaetiger
Branchial filaments: numbers	20	9	9	9	8
Dorsal cirri: shaped	NIA	NIA	Conical	Digitiform	Digitiform
Prechaetal lobe: shaped	NIA	NIA	Ridge	Transverse fold	Transverse fold
Chaetal lobe: shaped	NIA	NIA	NIA	Rounded, conical	Rounded
Aciculae: shape; colour	NIA; black	NIA; black	NIA; oblique	Blunt, black with paler tips	Blunt; black and translucent at distal end
Subacicular limbate chaetae: (p/a); distribution	Present; NIA	Present; all chaetigers	Present; posterior chaetigers	Present; all chaetigers	Present; in median and posterior chaetigers
Pectinate chaetae: number of type*	NIA	NIA	2	2	5
Subacicular hook: shape; colour*	Unidentate, strongly hooded; NIA	Bidentate; NIA	Bidentate, close-fitting hood; dark brown	Bidentate; NIA	Bidentate; light brown and translucent at distal end
Subacicular hook: start chaetiger*	50	26–35	40	33–72	22 (22–46)
Subacicular hook: distribution	Continuous	Continuous	Continuous	Continuous	Continuous

Marphysa ibaiensis sp. nov. differs from *M. fauchaldi* by the absence of peduncle in prostomial appendages, the chaetiger on which the branchiae and subacicular hook occur and the distribution of subacicular limbate chaetae. Subacicular hooks and branchiae of *M. ibaiensis* sp. nov. (TL: 52 (20–91) mm) have a wide range variation of chaetiger where they begin; from chaetiger 22 (22–46) and 20 (11–65), respectively compared to *M. fauchaldi* (TL: 190 (78–155) mm); they begin from chaetiger 40 (31–50) and 31 (22–32), respectively. The subacicular limbate chaetae in *M. ibaiensis* sp. nov. occur from mid-chaetigers onwards whereas in *M. fauchaldi*, they are restricted to posterior chaetigers.

Key to *Marphysa* species occurring in coastal water bodies of Malaysia and nearby areas (South China Sea and Andaman Sea)

- 1 Compound chaetae present 2
- Compound chaetae absent 4
- 2 Two types of compound chaetae present; spinigers and falcigers
..... ***Marphysa digitibranchia* Hoagland, 1920**
- One type of compound chaetae present; spinigers 3
- 3 One pair of anal cirri ***M. orientalis* Treadwell, 1936**
- Two pairs of anal cirri 5
- 4 Subacicular hook absent ***M. kertehensis* sp. nov.**
- Subacicular hook present ***M. moribidii* Idris, Hutchings & Arshad, 2014**
- 5 Subacicular limbate chaetae present 6
- Subacicular limbate chaetae absent 8
- 6 Eyes absent, branchiae pectinate with ≤ 8 number of filaments
..... ***M. ibaiensis* sp. nov.**
- Eyes present, branchiae pectinate with ≤ 9 number of filaments 7
- 7 Subacicular hook bidentate and emerge from chaetiger 26–35
..... ***M. gravelyi* Southern, 1921**
- Subacicular hook bidentate and emerge from chaetiger 33–72
..... ***M. madrasi* Hutchings, Lavesque, Priscilla, Daffe, Malathi & Glasby, 2020**
- 8 Branchiae palmate ***M. multipectinata* Liu, Hutchings & Sun, 2017**
- Branchiae pectinate 9
- 9 Eyes present 10
- Eyes absent 12
- 10 Subacicular hook unidentate and bidentate ***M. setiuense* sp. nov.**
- Subacicular hook unidentate 11
- 11 Maximum number of branchial filaments seven, three types of pectinate chaetae ***M. iloiloensis* Glasby, Mandario, Burghardt, Kupriyanova, Gunton & Hutchings, 2019**
- Maximum number of branchial filaments five, five types of pectinate chaetae ***M. merchangensis* sp. nov.**
- 12 Four types of pectinate chaetae
..... ***M. hongkongensa* Wang, Zhang & Qiu, 2018**
- Three types of pectinate chaetae 13
- 13 Maximum number of branchial filaments three
..... ***M. tribranchiata* Liu, Hutchings & Sun, 2017**
- Maximum number of branchial filaments eight
..... ***M. tripectinata* Liu, Hutchings & Sun, 2017**

Discussion

Prior to this study, a total of ten *Marphysa* species were described from Malaysia and nearby coastal waters (South China Sea and Andaman Sea) including one species from Group A (Mossambica) – *Marphysa moribidii*, six species from Group B (Sanguinea) – *M. iloiloensis*, *M. hongkongensa*, *M. multipectinata*, *M. orientalis*, *M. tribranchiata*, and *M. tripectinata*, one species from Group D (Belli) – *M. digitibranchia* Hoagland, 1920 (type locality: Hong Kong), and two species from Group E (Gravelly) – *M. madrasi* and *M. gravellyi*. This study increases the number of *Marphysa* species from these water regions to 14.

Characteristics such as the distribution of different types of chaetae, including pectinate chaetae, branchial distribution and number of filaments, and jaw formula, allowed us to describe four new species. These characters have also been used recently by Lavesque et al. (2020) and Martin et al. (2020) in their studies of species of *Marphysa*.

All these new species occur in slightly different types of habitats, but share several general characteristics: all are found in mangrove areas, tolerate a wide range of salinity (euryhaline), and live in high percentage of sand. According to Glasby and Hutchings (2010), habitat type is a useful character to recognise species in a particular area. Therefore, describing a species' habitat is important for taxonomic studies and conservation strategy management.

Phylogenetic analysis from COI data placed *M. merchangensis* sp. nov. as sister to *M. hongkongensa*, *M. setiuense* sp. nov. as sister to *M. iloiloensis*, *M. ibaiensis* sp. nov. as sister to *M. madrasi*, and *M. kertehensis* sp. nov. as sister to *M. mossambica* (Peters, 1854). Nevertheless, the interspecific divergence between these new species and all their sister taxa pair is high (Pair-wise Kimura 2-parameter – COI K2P range 6.14%–19.16% (see Suppl. material 1), which clearly showed the distinct genetic separation. Additionally, obtaining sequence data for *M. moribidii* is imperative to investigate the genetic difference between *M. moribidii* and *M. kertehensis* sp. nov. as they possessed a few similar morphological features and occur within Malaysian water bodies. The molecular analysis in this study aligns with the morphological analysis and confirms the presence of four new *Marphysa* species in the Terengganu mangrove area.

Conclusions

Four species of *Marphysa* from Terengganu mangrove forests (lagoon, river, and estuary) were described and confirmed by morphology and molecular data and can also be separated based on their habitat. This study increases the species in the genus *Marphysa* and the number of polychaetes described from Malaysia. In addition, data provided in this study can also provide insight for future research on the potential use of *Marphysa* species in Malaysia as the only described species in Malaysia, *M. moribidii* has revealed a wide potential application for commercial use.

Acknowledgements

We would like to thank all people involved directly or indirectly (especially our polychaete team members at Institute of Oceanography and Environ-

ment, INOS, UMT) in the collection of type specimens of *Marphysa* species from Terengganu mangrove river, lagoon, and estuary. Also, we are very thankful for the assistance from INOS and South China Sea Repository and Reference (RRC) staff throughout the research journey and for all the facilities provided by Universiti Malaysia Terengganu. We extend our gratitude to Sue Lindsay from the Macquarie University for mounting the parapodia and taking the SEM photos of paratypes. We also would like to thank the Natural History of Los Angeles County (NHMLAC) for awarding the Anne Baker-Hayes Polychaete Student Fund to the first author. Our deepest gratitude goes to Ms Leslie Harris and Dr. Kirk Fitzhugh (Polychaete Department of NHMLAC) for providing facilities to photograph the type material, research experience and hospitality for the first author during her visit. Finally, our sincere appreciation goes to the Academic Editor (Chris Glasby) and two expert reviewers (you know who you are) for their meticulous comments and editing this manuscript.

Additional information

Conflict of interest

The authors have declared that no competing interests exist.

Ethical statement

No ethical statement was reported.

Funding

This research was funded by Talent and Publication Enhancement-Research Grant (TAPE-RG) sponsored by Universiti Malaysia Terengganu (UMT/TAPE-RG/2020/55231).

Author contributions

Che Engku Siti Mariam Che Engku Abdullah conceived and designed the experiments, performed the experiments, analysed the data, prepared figures and/or tables, authored drafts of the article, and approved the final draft. Izwandy Idris authored drafts of the article, approved the final draft, supervised and acquired funds for the project. Afiq Durrani Mohd Fahmi reviewed drafts of the article, approved the final draft, supervised the project. Beth Flaxman performed the experiments, authored and reviewed the drafts of the articles. Pat Hutchings analysed the data, authored and reviewed drafts of the article, and approved the final draft.

Author ORCIDs

Che Engku Siti Mariam Che Engku Abdullah  <https://orcid.org/0009-0002-8371-1141>

Izwandy Idris  <https://orcid.org/0000-0003-1516-8175>

Afiq Durrani Mohd Fahmi  <https://orcid.org/0000-0002-5131-0098>

Beth Flaxman  <https://orcid.org/0000-0002-0329-9525>

Pat Hutchings  <https://orcid.org/0000-0001-7521-3930>

Data availability

The data underpinning the analysis reported in this paper are deposited at GBIF, the Global Biodiversity Information Facility, and are available at <https://www.gbif.org/dataset/f3e0c6b6-0bcc-4a3b-9ee6-1ca8d1098f7c>.

References

- Abdullah CESMCE, Hutchings P, Mohd-Fahmi AD, Turni H, Idris I (in review) *Marphysa* species (Annelida: Eunicidae) with potential economic applications: A preliminary assessment. *Journal of Sustainability Science and Management*.
- Abe H, Tanaka M, Taru M, Abe S, Nishigaki A (2019) Molecular evidence for the existence of five cryptic species within the Japanese species of *Marphysa* (Annelida: Eunicidae) known as Iwa-mushi. *Plankton & Benthos Research* 14(4): 303–314. <https://doi.org/10.3800/pbr.14.303>
- Blair TC, McPherson J (1999) Grain-size and textural classification of coarse sedimentary particles. *Journal of Sedimentary Research* 69(1): 6–19. <https://doi.org/10.2110/jsr.69.6>
- Carr CM, Hardy SM, Brown TM, Macdonald TA, Hebert PD (2011) A Tri-Oceanic Perspective: DNA Barcoding Reveals Geographic Structure and Cryptic Diversity in Canadian Polychaetes. *PLOS ONE* 6(7): e22232. <https://doi.org/10.1371/journal.pone.0022232>
- Carrera-Parra LF, Salazar-Vallejo SI (1998) A new genus and 12 new species of Eunicidae (Polychaeta) from the Caribbean Sea. *Journal of the Marine Biological Association of the United Kingdom* 78(1): 145–182. <https://doi.org/10.1017/S0025315400040005Cu>
- Cuvier G (1817) Les Annélides. In: Cuvier G, Laurillard CL, Pierron JA, Louvet GP, Latreille PA (Eds) *Le règne animal distribué d'après son organisation: pour servir de base à l'histoire naturelle des animaux et d'introduction à l'anatomie comparée*. Chez Déterville, Paris, 515–532. <https://doi.org/10.5962/bhl.title.41460>
- Dean WE (1974) Determination of carbonate and organic matter in calcareous sediments and sedimentary rocks by loss on ignition; comparison with other methods. *Journal of Sedimentary Research* 44: 242–248. <https://doi.org/10.1306/74D729D2-2B21-11D7-8648000102C1865D>
- Ee Pei AU, Huai PC, Adhwa Masimen MA, Wan Ismail WI, Idris I, Harun NA (2020) Biosynthesis of gold nanoparticles (AuNPs) by marine baitworm *Marphysa moribidii* Idris, Hutchings & Arshad, 2014 (Annelida: Polychaeta) and its antibacterial activity. *Advances in Natural Sciences: Nanoscience and Nanotechnology* 11(1): 015001. <https://doi.org/10.1088/2043-6254/ab6291>
- Elgetany AH, El-Ghobashy AE, Ghoneim AM, Struck TH (2018) Description of a new species of the genus *Marphysa* (Eunicidae), *Marphysa aegypti* sp. n., based on molecular and morphological evidence. *Zoologia Bespozvonocnyh* 15(1): 71–84. <https://doi.org/10.15298/invertzool.15.1.05>
- Fauchald K (1970) Polychaetous annelids of the families Eunicidae, Lumbrineridae, Lphitimidae, Arabellidae, Lysaretidae and Dorvilleidae from western Mexico. *Allan Hancock Monographs in marine biology* 5: 1–335. <http://repository.si.edu/xmlui/handle/10088/3457> [February 5, 2021]
- Folk RL, Andrews PB, Lewis DW (1970) Detrital sedimentary rock classification and nomenclature for use in New Zealand. *New Zealand Journal of Geology and Geophysics* 13(4): 937–968. <https://doi.org/10.1080/00288306.1970.10418211>
- Folmer O, Black M, Hoeh W, Lutz R, Vrijenhoek R (1994) DNA primers for amplification of mitochondrial cytochrome c oxidase subunit I from diverse metazoan invertebrates. *Molecular Marine Biology and Biotechnology* 3: 294–299.
- Glasby CJ, Hutchings P (2010) A new species of *Marphysa* Quatrefages, 1865 (Polychaeta: Eunicidae) from Northern Australia and a review of similar taxa from the Indo-West Pacific, including the genus *Nauphanta* Kinberg, 1865. *Zootaxa* 2352(1): 29–45. <https://doi.org/10.11646/zootaxa.2352.1.2>

- Glasby CJ, Mandario MAE, Burghardt I, Kupriyanova E, Gunton LM, Hutchings P (2019) A new species of the sanguinea-group Quatrefages, 1866 (Annelida: Eunicidae: *Marphysa*) from the Philippines. *Zootaxa* 4674(2): 264–282. <https://doi.org/10.11646/zootaxa.4674.2.7>
- Hoagland RA (1920) Polychaetous annelids collected by the United States fisheries steamer Albatross during the Philippine expedition of 1907–1909. *Bulletin - United States National Museum* 1001: 603–635.
- Hutchings P, Karageorgopoulos P (2003) Designation of a neotype of *Marphysa sanguinea* (Montagu, 1813) and a description of a new species of *Marphysa* from eastern Australia. *Advances in Polychaete Research* 170: 87–94. https://doi.org/10.1007/978-94-017-0655-1_9
- Hutchings P, Lavesque N, Priscilla L, Daffe G, Malathi E, Glasby CJ (2020) A new species of *Marphysa* (Annelida: Eunicida: Eunicidae) from India, with notes on previously described or reported species from the region. *Zootaxa* 4852(3): 285–308. <https://doi.org/10.11646/zootaxa.4852.3.2>
- Idris I, Hutchings P, Arshad A (2014) Description of a new species of *Marphysa* Quatrefages, 1865 (Polychaeta: Eunicidae) from the west coast of Peninsular Malaysia and comparisons with species from *Marphysa* Group A from the Indo-West Pacific and Indian Ocean. *Memoirs of the Museum of Victoria* 71: 109–121. <https://doi.org/10.24199/j.mmv.2014.71.11>
- Kara J, Molina-Acevedo IC, Zanol J, Simon C, Idris I (2020) Morphological and molecular systematic review of *Marphysa* Quatrefages, 1865 (Annelida: Eunicidae) species from South Africa. *PeerJ* 8: e10076. <https://doi.org/10.7717/peerj.10076>
- Lavesque N, Daffe G, Bonifácio P, Hutchings P (2017) A new species of the *Marphysa sanguinea* complex from French waters (Bay of Biscay, NE Atlantic) (Annelida, Eunicidae). *ZooKeys* 2017: 1–17. <https://doi.org/10.3897/zookeys.716.14070>
- Lavesque N, Daffe G, Grall J, Zanol J, Gouillieux B, Hutchings P (2019) Guess who? On the importance of using appropriate name: Case study of *Marphysa sanguinea* (Montagu, 1803). *ZooKeys* 2019: 1–15. <https://doi.org/10.3897/zookeys.859.34117>
- Lavesque N, Hutchings P, Abe H, Daffe G, Gunton LM, Glasby CJ (2020) Confirmation of the exotic status of *Marphysa victori* Lavesque, Daffe, Bonifácio & Hutchings, 2017 (Annelida) in French waters and synonymy of *Marphysa bulla* Liu, Hutchings & Kupriyanova, 2018. *Aquatic Invasions* 15(3): 355–366. <https://doi.org/10.3391/ai.2020.15.3.01>
- Lavesque N, Daffe G, Glasby C, Hourdez S, Hutchings P (2022) Three new deep-sea species of *Marphysa* (Annelida, Eunicida, Eunicidae) from Papua New Guinea (Bismarck and Solomon seas). *ZooKeys* 1122: 81–105. <https://doi.org/10.3897/zookeys.1122.89990>
- Lavesque N, Zanol J, Daffe G, Flaxman B, Hutchings P (2023) Two new species of *Marphysa* (Annelida, Eunicidae) from southern Australia. *Zootaxa* 5277(1): 113–130. <https://doi.org/10.11646/zootaxa.5277.1.5>
- Liu Y, Hutchings P, Sun S-C (2017) Three new species of *Marphysa* Quatrefages, 1865 (Polychaeta: Eunicida: Eunicidae) from the south coast of China and redescription of *Marphysa sinensis* Monro, 1934. *Zootaxa* 4263(2): 228–250. <https://doi.org/10.11646/zootaxa.4263.2.2>
- Martin D, Gil J, Zanol J, Meca MA, Pérez Portela R (2020) Digging the diversity of Iberian bait worms *Marphysa* (Annelida, Eunicidae). *PLOS ONE* 15(1): e0226749. <https://doi.org/10.1371/journal.pone.0226749>
- Molina-Acevedo IC, Carrera-Parra LF (2015) Reinstatement of three species of the *Marphysa sanguinea* complex (Polychaeta: Eunicidae) from the Grand Caribbean Region. *Zootaxa* 3925(1): 37–55. <https://doi.org/10.11646/zootaxa.3925.1.3>

- Molina-Acevedo IC, Carrera-Parra LF (2017) Revision of *Marphysa* de Quatrefages, 1865 and some species of *Nicidion* Kinberg, 1865 with the erection of a new genus (Polychaeta: Eunicidae) from the Grand Caribbean. *Zootaxa* 4241(1): 1–62. <https://doi.org/10.11646/zootaxa.4241.1.1>. <https://doi.org/10.11646/zootaxa.4241.1.1>
- Molina-Acevedo IC, Idris I (2021) Unravelling the convoluted nomenclature of *Marphysa simplex* (Annelida, Eunicidae) with the proposal of a new name and the re-description of species. *Zoosystematics and Evolution* 97(1): 121–139. <https://doi.org/10.3897/zse.97.59559>
- Montagu G (1813) Descriptions of several new or rare animals, principally marine, discovered on the South Coast of Devonshire. *Transactions of the Linnean Society of London* 11(1): 1–26. <https://doi.org/10.1111/j.1096-3642.1813.tb00035.x>
- Paxton H, Chou L (2000) Polychaetous annelids from the South China Sea. *The Raffles Bulletin of Zoology* 48: 209–232.
- Peters WCH (1854) Über die Gattung *Bdella*, Savigny, (Limnatis, Moquin-Tandon) und die in Mossambique beobachteten Anneliden, wovon hier eine Mittheilung folgt. Bericht über die zur Bekanntmachung geeigneten Verhandlungen der Königl. Preuss. Akademie der Wissenschaften zu Berlin 1854: 607–614. <https://www.biodiversitylibrary.org/part/82566>
- Pillai TG (1958) Studies on a brackish-water polychaetous annelid, *Marphysa borradailei* sp. n. from Ceylon. *Ceylon Journal of Science* 1: 94–106.
- Rapi HS, Che Soh N, Mohd Azam NS, Maulidiani M, Assaw S, Haron MN, Ali AM, Idris I, Ismail WIW (2020) Effectiveness of aqueous extract of marine baitworm *Marphysa moribidii* Idris, Hutchings & Arshad, 2014 (Annelida, Polychaeta), on acute wound healing using Sprague Dawley rats. *Evidence-Based Complementary and Alternative Medicine* 2020: 1–15. <https://doi.org/10.1155/2020/1408926>
- Read G, Fauchald K (2023) World Polychaeta Database. *Marphysa* Quatrefages 1866. World Register of Marine Species. <https://www.marinespecies.org/aphia.php?p=tax-details&id=129281> [September 19, 2021]
- Rosman NSR, Harun NA, Idris I, Wan Ismail WI (2020) Eco-friendly silver nanoparticles (AgNPs) fabricated by green synthesis using the crude extract of marine polychaete, *Marphysa moribidii*: Biosynthesis, characterisation, and antibacterial applications. *Heliyon* 6(11): e05462. <https://doi.org/10.1016/j.heliyon.2020.e05462>
- Southern R (1921) Polychaeta of the Chilka Lake, and also of fresh and brackish waters in other parts of India. *Memoirs of the Indian Museum* 5: 563–659. Available from: <https://www.biodiversitylibrary.org/part/168161>
- Struck T, Purschke G, Halanych K (2006) Phylogeny of Eunicida (Annelida) and exploring data congruence using a partition addition bootstrap alteration (PABA) approach. *Systematic Biology* 55(1): 1–20. <https://doi.org/10.1080/10635150500354910>
- Tamura K, Stecher G, Kumar S (2021) MEGA11: Molecular Evolutionary Genetics Analysis Version 11. *Molecular Biology and Evolution* 38(7): 3022–3027. <https://doi.org/10.1093/molbev/msab120>
- Tillett D, Neilan BA (2000) Xanthogenate nucleic acid isolation from cultured and environmental cyanobacteria. *Journal of Phycology* 36(1): 251–258. <https://doi.org/10.1046/j.1529-8817.2000.99079.x>
- Treadwell AL (1936) Polychaetous annelids from Amoy, China. *Proceedings of the United States National Museum* 83(2984): 261–278. <https://doi.org/10.5479/si.00963801.83-2984.261>

- Udden J (1914) Mechanical Composition of Clastic Sediments. Geological Society of America Bulletin 25(1): 655–744. <https://doi.org/10.1130/GSAB-25-655>
- Wang Z, Zhang Y, Qiu JW (2018) A new species in the *Marphysa sanguinea* complex (Annelida, Eunicidae) from Hong Kong. Zoological Studies 57. <https://doi.org/10.6620/ZS.2018.57-48>
- Wentworth CK (1922) A Scale of Grade and Class Terms for Clastic Sediments. The Journal of Geology 30(5): 377–392. <https://doi.org/10.1086/622910>
- Zanol J, Halanych KM, Struck TH, Fauchald K (2010) Phylogeny of the bristle worm family Eunicidae (Eunicida, Annelida) and the phylogenetic utility of noncongruent 16S, COI and 18S in combined analyses. Molecular Phylogenetics and Evolution 55(2): 660–676. <https://doi.org/10.1016/j.ympev.2009.12.024>
- Zanol J, Halanych KM, Fauchald K (2014) Reconciling taxonomy and phylogeny in the bristleworm family Eunicidae (polychaete, Annelida). Zoologica Scripta 43(1): 79–100. <https://doi.org/10.1111/zsc.12034>
- Zanol J, da Silva TSC, Hutchings P (2016) *Marphysa* (Eunicidae, Polychaeta, Annelida) species of the Sanguinea group from Australia, with comments on pseudo-cryptic species. Invertebrate Biology 135(4): 328–344. <https://doi.org/10.1111/ivb.12146>
- Zhang D, Zhou Y, Yen N, Hiley AS, Rouse GW (2023) *Ophryotrocha* (Dorvilleidae, Polychaeta, Annelida) from deep-sea hydrothermal vents, with the description of five new species. European Journal of Taxonomy 864: 167–194. <https://doi.org/10.5852/ejt.2023.864.2101>

Supplementary material 1

Pair-wise patristic distances between pairs of sequences of *Marphysa* species

Authors: Che Engku Siti Mariam Che Engku Abdullah, Izwandy Idris, Afiq Durrani Mohd Fahmi, Beth Flaxman, Pat Hutchings

Data type: xlsx

Copyright notice: This dataset is made available under the Open Database License (<http://opendatacommons.org/licenses/odbl/1.0/>). The Open Database License (ODbL) is a license agreement intended to allow users to freely share, modify, and use this Dataset while maintaining this same freedom for others, provided that the original source and author(s) are credited.

Link: <https://doi.org/10.3897/zookeys.1204.117261.suppl1>

Three new *Stenohya* species with sexually dimorphic leg I from China (Pseudoscorpiones, Neobisiidae)

Jiaqi Zhao¹, Xiangbo Guo^{1,2}, Feng Zhang^{1,2}¹ Key Laboratory of Zoological Systematics and Application, College of Life Sciences, Hebei University, Baoding, Hebei 071002, China² Hebei Basic Science Center for Biotic Interaction, Hebei University, Baoding, Hebei 071002, ChinaCorresponding authors: Xiangbo Guo (xiangboguo@126.com); Feng Zhang (dudu06042001@163.com)

Abstract

Three new species of the genus *Stenohya* Beier, 1967 from China are described: *Stenohya gibba* **sp. nov.** and *S. papillata* **sp. nov.** from Hunan Province, and *S. guangmingensis* **sp. nov.** from Jiangxi Province. In addition to their sexually dimorphic pedipalp, these three new species also have a uniquely sexual dimorphic leg I, which has not been reported in other *Stenohya* species. Additionally, an updated key to the Chinese *Stenohya* species is provided.

Key words: Diversity, fused podomeres, sexual dimorphism, taxonomy

Introduction

Stenohya Beier, 1967, originally placed in the family Hyidae (Beier 1967), was erected with the type species *S. vietnamensis* Beier, 1967 and transferred to the family Neobisiidae by Harvey (1991), based on the presence of venom apparatus only in the fixed chelal finger and the presence of a non-lanceolate trichobothrium *t.* Of the 23 *Stenohya* species known, 14 of them occur in China (WPC 2022; Li and Shi 2023). These 14 species mainly occur in the southern region of China, except for *S. xiningensis*, which lives in the northern region. *Stenohya* mainly lives in leaf litter and soil, under rocks, bark, and fern fronds.

Sexual dimorphism is common in *Stenohya* species and is mainly reflected in the morphology of the pedipalps. Male pedipalps are distinctly thinner than the female ones in *S. huangi* Hu & Zhang, 2012, *S. martensi* (Schawaller, 1987), and *S. pengae* Hu & Zhang, 2012 (Schawaller 1987; Hu and Zhang 2012; Zhan et al. 2023). The shapes of pedipalpal femora differ in males and females in *S. arcuata* Guo, Zang & Zhang, 2019 and *S. tengchongensis* Yang & Zhang, 2013 (Yang and Zhang 2013; Guo et al. 2019). Male pedipalpal chelal hands have special prominences near the base of the fingers in *S. bicornuta* Guo, Zang & Zhang, 2019, *S. curvata* Zhao, Zhang & Jia, 2011, *S. hamata* (Leclerc & Mahnert, 1988), and *S. meiacantha* Yang & Zhang, 2013 (Leclerc and Mahnert 1988; Zhao et al. 2011; Yang and Zhang 2013; Guo et al. 2019). The males of *S. spinata* Zhan, Feng & Zhang, 2023 have spinous apophyses on the dorsal side of the median pedipalpal chelal hand, and



Academic editor: Jana Christophoryová

Received: 18 March 2024

Accepted: 7 May 2024

Published: 4 June 2024

ZooBank: <https://zoobank.org/OCA13BC5-54AD-4782-A883-F282ADA4CDCE>

Citation: Zhao J, Guo X, Zhang F (2024) Three new *Stenohya* species with sexually dimorphic leg I from China (Pseudoscorpiones, Neobisiidae). ZooKeys 1204: 105–133. <https://doi.org/10.3897/zookeys.1204.123294>

Copyright: © Jiaqi Zhao et al.
This is an open access article distributed under terms of the Creative Commons Attribution License (Attribution 4.0 International – CC BY 4.0).

strong thorns on the femur and patella but these are absent in the females (Zhan et al. 2023).

In this study, three new *Stenohya* species with sexually dimorphic pedipalps and leg I are described from China: *S. gibba* sp. nov., *S. papillata* sp. nov., and *S. guangmingensis* sp. nov.

Materials and methods

All specimens were preserved in 75% alcohol. Temporary slide mounts were prepared in glycerol. Detailed examinations were carried out with an Olympus BX53 general optical microscope. Photographs and measurements were taken using a Leica M205A stereomicroscope equipped with a Leica DFC550 camera. Drawings were made using the Inkscape ver. 1.0.2.0. Figures were edited and formatted using Adobe Photoshop 2022. The specimens were deposited in the Museum of Hebei University (**MHBU**), Baoding, China.

Terminology and measurements largely follow Chamberlin (1931), except for the nomenclature of the pedipalps and legs, and the terminology of trichobothria (Harvey 1992); the term “rallum” (for flagellum) is adopted from Judson (2007). The following abbreviations are used in the text for the trichobothria: **b** = basal; **sb** = sub-basal; **st** = sub-terminal; **t** = terminal; **ib** = interior basal; **isb** = interior sub-basal; **ist** = interior sub-terminal; **it** = interior terminal; **eb** = exterior basal; **esb** = exterior sub-basal; **est** = exterior sub-terminal; **et** = exterior terminal.

Taxonomy

Family Neobisiidae Chamberlin, 1930

Subfamily Microcreagrinae Balzan, 1892

Genus *Stenohya* Beier, 1967

***Stenohya gibba* sp. nov.**

<https://zoobank.org/96FB4752-3A00-430C-9F00-7EC80CA53888>

Figs 1–6

Chinese name. 驼峰狭伪蝎

Type material. **Holotype** male (Ps.-MHBU-HN2023111901), China: Hunan Province, Suining County, Huangsang Nature Reserve in Nanshan National Park [26°24'32"N, 110°05'38"E], 460 m a.s.l., 19 November 2023, in leaf litter (Fig. 2C, D), Jiaqi Zhao, Jianzhou Sun, Tao Zheng & Songtao Shi leg. **Paratypes:** three males (Ps.-MHBU-HN2023111902–04), four females (Ps.-MHBU-HN2023013105–08), same data as for holotype.

Etymology. The specific name is derived from the Latin word “*gibbus*”, meaning hump-shaped, which refers to the shape of the projections on the basitarsus and telotarsus of the male leg I.

Diagnosis. Carapace with four well-developed eyes, epistome triangular (Figs 3A, 4A, 5A, 6A). Male pedipalpal trochanter with a process and small frosted projections on the prolateral position (Figs 3G, 4E); femur with three projections (Figs 3G, 4E); patella with a small projection medially on the prolateral position (Figs 3G, 4E); chelal hand concaved distally at the dorsal side, with 15–18 small, triangular apophyses on the dorsal side, extending into the dorsal face of

fixed finger (Figs 3H, 4C). Male leg I specialized, femur and patella enlarged, basitarsus and telotarsus semi-fused, the dividing line between the two limb segments visible, basitarsus and telotarsus each with a large columnar projection laterally (Figs 3I, K, 4F–H). Female pedipalpal movable chelal finger with 79–87 teeth; female pedipalpal chela (with pedicel) 4.67–4.98 times longer than wide.

Description. Adult male (holotype and male paratypes) (Figs 1A, 2A).

Carapace (Figs 3A, 4A). Carapace 1.30–1.36 times longer than broad, with a total of 30–32 setae, including six near anterior margin and 6–7 near posterior margin; eight lyrifissures near the eyes, four lyrifissures near posterior margin; epistome small, triangular, with rounded top; with four corneate eyes. Carapace divided into three parts by two transverse, shallow grooves, the anterior part uplifted, the median part smooth, the posterior part uplifted, and with microgrooves.

Chelicera (Figs 3B, 4B). Hand with 6–7 setae and two lyrifissures, movable finger with one seta; fixed finger with 13–15 teeth; movable finger with 7–9 teeth; serrula exterior with 44–46 lamellae; serrula interior with 36–37 lamellae; galea developed, divided into two main branches, one branch five, while the other two (Fig. 3D); rallum consisting of 7–8 blades, all with anteriorly directed spinules, the basal-most blade shortest (Fig. 3C).

Pedipalps (Figs 3G, H, 4C, E). Apex of pedipalpal coxa rounded, with seven long setae. Trochanter with a process on the median prolateral position, as well as some small frosted projections; femur with a curved cylindrical process on the median prolateral position, as well as a projection on the subdistal prolateral surface, and with a columnar process adjacent to this projection; patella with a small projection on the median prolateral position and two lyrifissures (Figs 3G, 4E); chelal hand deeply concaved at the dorsal side of distal half, with 15–18 small, triangular, spinous apophyses arranged in a row on the dorsal side, each spinous apophysis with a seta at the base, a few spinous apophyses extended into the dorsal face of fixed finger. On the posterior side, several small granular processes located at the distal of the hand and near the base of the fixed finger, at the ventral of the hand from the distal to two-thirds with shallow invagination. Fixed chelal finger slightly curved upward at median to distal part (Figs 3H, 4C). Trochanter 1.46–1.65, femur 3.96–4.37, patella 3.47–3.71, chela with pedicel 3.98–4.16, chela without pedicel 3.71–3.89 times longer than broad, movable finger 1.98–2.35 times longer than hand without pedicel. Fixed chelal finger with eight, movable chelal finger with four trichobothria: *eb* and *esb* situated on the base of hand, grouped very closely with *ib* and *isb*; *est*, *et* and *it* grouped distally; *ist* closer to *est-et-it* than to *isb-ib-esb-eb* in fixed chelal finger; *b* and *sb* situated closer to each other in basal half, *st* and *t* close to each other in distal half of movable finger. Venom apparatus present only in fixed chelal finger, venom duct short. Fixed chelal finger with 117 pointed teeth, movable finger with 103–108 teeth, 47–51 rounded teeth at base, and 56–57 pointed teeth at distal position.

Abdomen. Pleural membrane granulated. Tergites and sternites undivided, tergal chaetotaxy (I–XI): 4–5: 7–8: 7–11: 9–10: 9–10: 10–12: 11–12: 11–12: 11–12: 12: 11, sternal chaetotaxy (IV–XI): 22–28: 21–24: 19–24: 18–19: 19: 17–19: 12–15: 4, sternites VI–VIII with 3–6 medial scattered glandular setae, anal cone with two dorsal and two ventral setae. Genital area (Figs 3F, 4D): anterior genital sternite with 75–80 setae and two lyrifissures; posterior genital sternite with 55–59 setae and two lyrifissures.



Figure 1. *Stenohya gibba* sp. nov. **A** holotype male (dorsal view) **B** paratype female (dorsal view). Scale bars: 2 mm.

Legs (Figs 3I–K, 4F–I). Leg I specialized, femur and patella enlarged, basitarsus and telotarsus semi-fused, the dividing line between the two limb segments visible, basitarsus and telotarsus each with a large columnar projection on the lateral side (Figs 3I, K, 4F–H), femur with three lyrifissures. Leg IV generally typical, long, and sinewy, trochanter with three lyrifissures (Figs 3J, 4I). Leg I: trochanter 1.40–1.55, femur 2.06–2.24, patella 2.61–3.27, tibia 3.25–3.43, basitarsus 2.31–2.52, telotarsus 2.52–2.89 times longer than deep. Leg IV: trochanter 2.23–2.73, femur + patella 4.08–4.72, tibia 6.96–7.52, basitarsus 4.19–4.38, telotarsus 6.67–7.15 times longer than deep; tibia with two submedial tactile setae (TS = 0.60–0.67, 0.96), basitarsus with two tactile setae (TS = 0.12–0.14, 0.82–0.83), telotarsus with two tactile setae (TS = 0.20, 0.55–0.58); subterminal tarsal seta bifurcate (Fig. 3E). Arolium not divided, shorter than the slender and simple claws.

Adult female (paratype females) (Figs 1B, 2B): mostly same as males, except where noted.

Carapace (Figs 5A, 6A). Carapace 1.02–1.19 times longer than broad, with a total of 29–30 setae, including six near anterior margin and 4–5 near posterior margin; ten lyrifissures near the eyes, five lyrifissures near posterior margin; the front half of carapace uplifted, the back half smooth and with triangular invagination at 1/3 and 2/3 positions.

Chelicera (Figs 5B, 6B). Fixed finger with 14–15 teeth; movable finger with 6–7 teeth; serrula exterior with 45–51 lamellae; serrula interior with 38–40

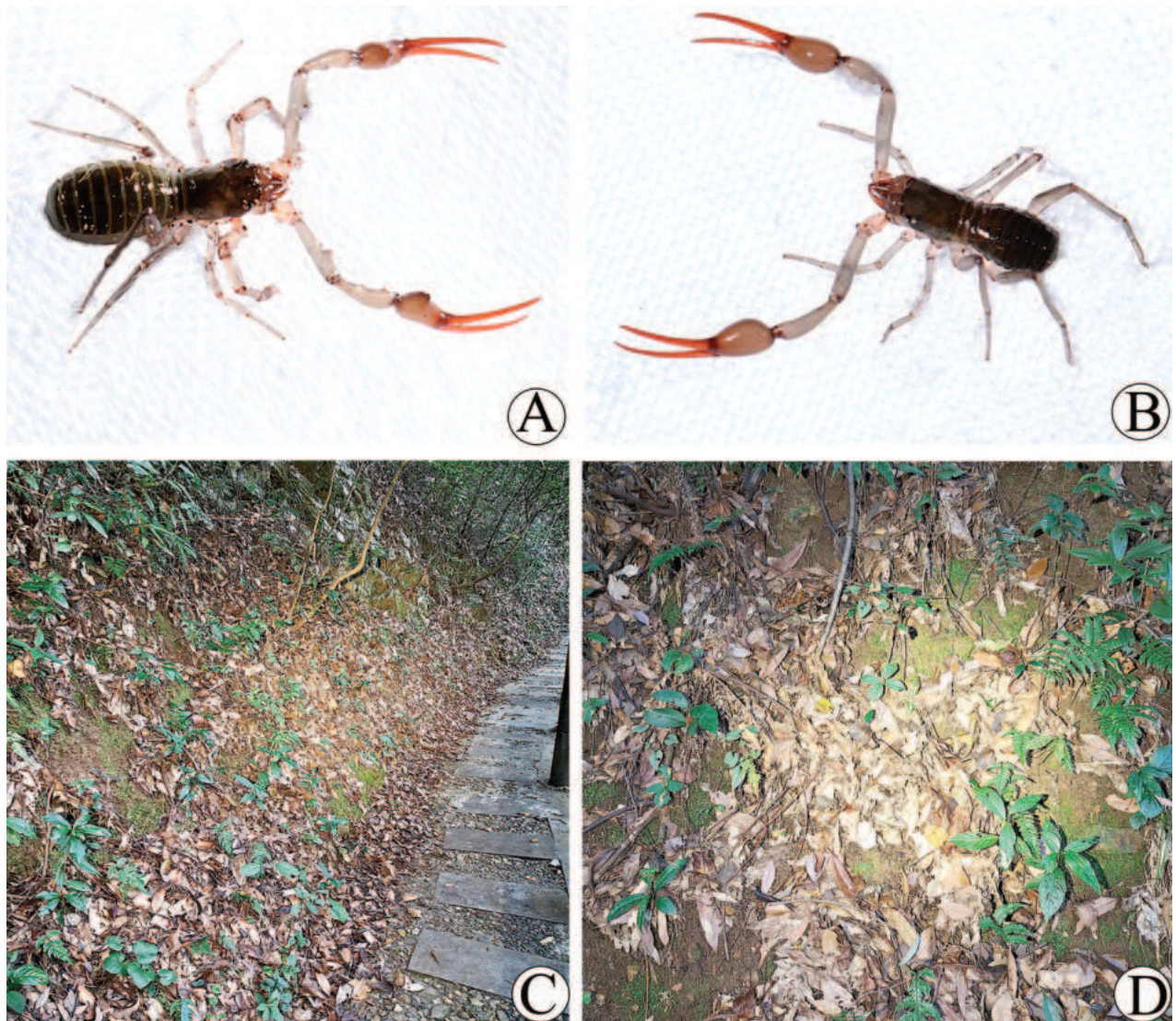


Figure 2. Type locality and habitus of *Stenohya gibba* sp. nov. **A** male habitus **B** female habitus **C, D** litter layer inhabited by habitus.

lamellae; galea divided into two main branches, one branch five, while the other three (Fig. 5D); rallum consisting of 8–9 blades, all with anteriorly directed spinules, the basal-most blade shortest (Fig. 5C).

Pedipalps (Figs 5G, H, 6C, E). Apex of pedipalpal coxa with six long setae. Femur with a few tubercles prolaterally. Trochanter 1.87–1.94, femur 4.56–4.80, patella 3.15–3.71, chela with pedicel 4.67–4.98, chela without pedicel 3.94–4.14 times longer than broad, movable finger 1.60–1.72 times longer than hand without pedicel. Fixed chelal finger with 99–100 pointed teeth, movable finger with 79–87 teeth, 39–44 rounded teeth at base, and 40–43 pointed ones.

Abdomen. Tergal chaetotaxy (I–XI): 3–5: 7–8: 8–10: 9–10: 11: 10–11: 10–13: 11–12: 11–12: 11–13: 8–10, sternal chaetotaxy (IV–XI): 22–24: 21–24: 18–20: 18–20: 16–18: 16–18: 13–14: 4–6, sternites VI–VIII with two medial scattered glandular setae; genital area (Figs 5F, 6D): sternite II with total of 29–34 setae and two lyrifissures; sternite III with a row of 31–34 setae and two lyrifissures along posterior margin.

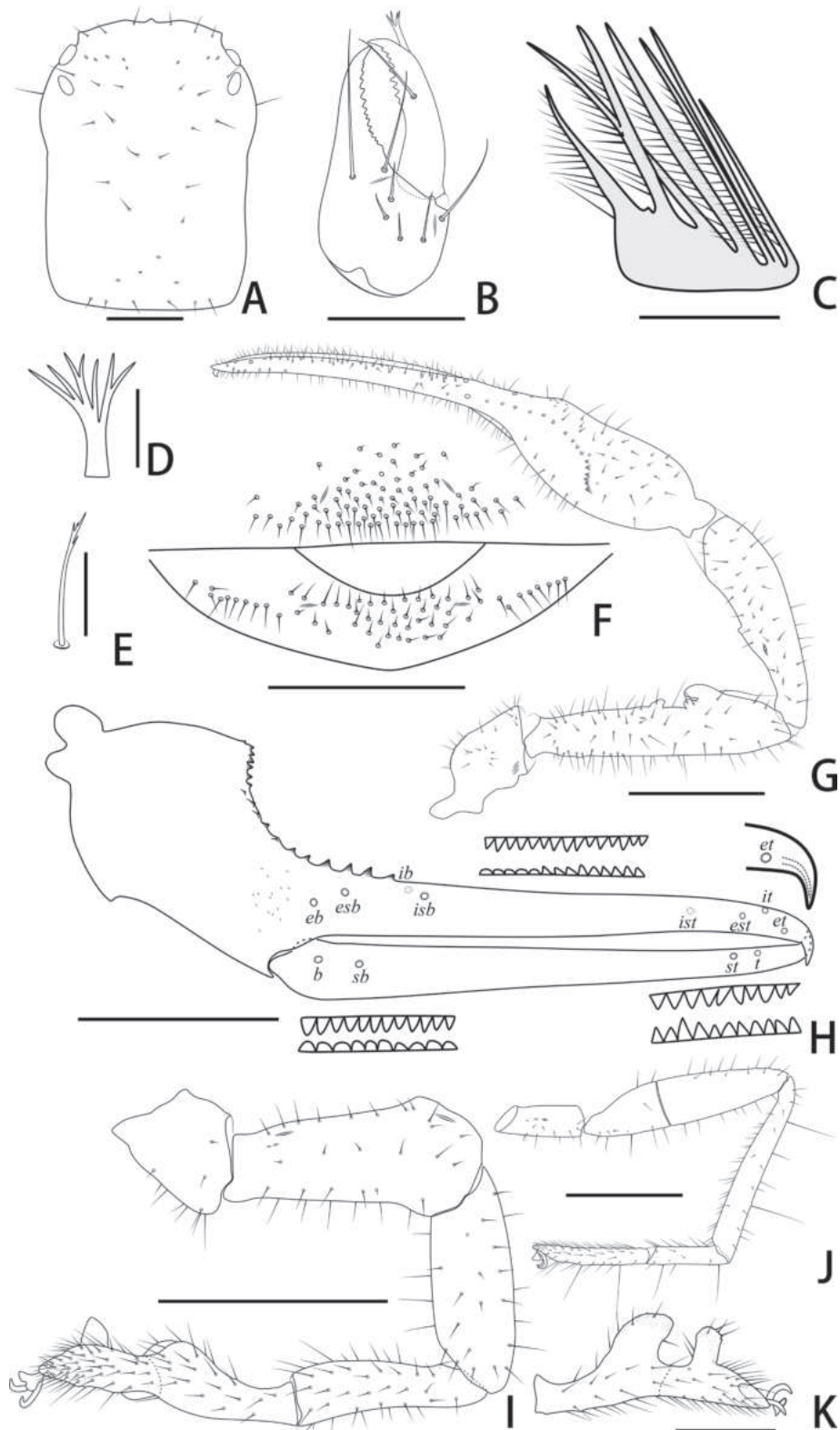


Figure 3. Holotype male of *Stenohya gibba* sp. nov. **A** carapace, dorsal view **B** right chelicera, dorsal view **C** rallum **D** galea **E** subterminal tarsal seta **F** chaetotaxy of genital area, ventral view **G** right pedipalp, dorsal view **H** right chela, lateral view, showing trichobothriotaxy, teeth and venom apparatus **I** right leg I, lateral view **J** right leg IV, lateral view **K** right leg I (basitarsus and telotarsus), retrolateral view. Scale bars: 0.5 mm (**A**, **B**, **F**, **K**); 0.1 mm (**C**–**E**); 1 mm (**G**–**J**).

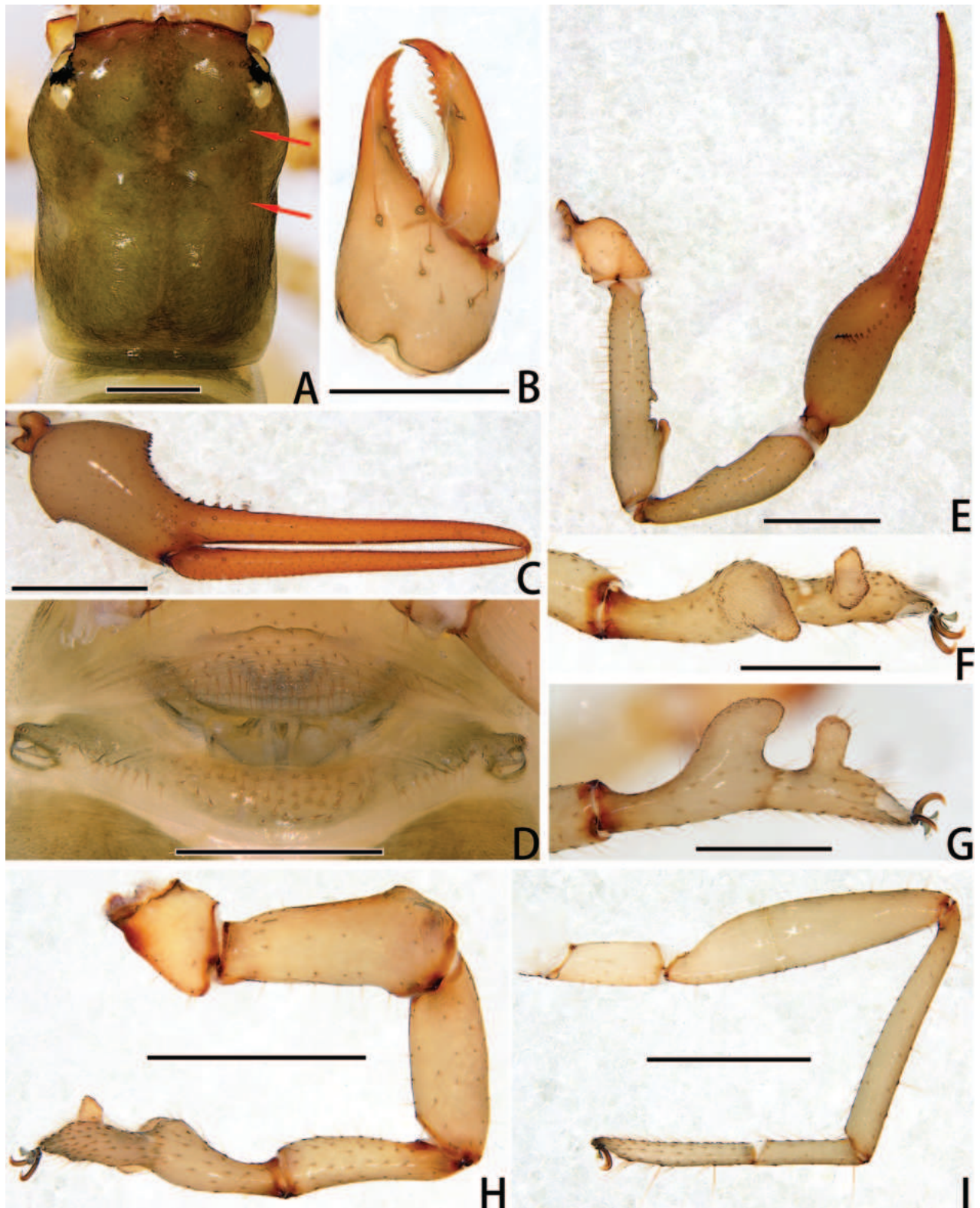


Figure 4. Holotype male of *Stenohya gibba* sp. nov. **A** carapace, dorsal view (red arrows showing two transverse grooves) **B** right chelicera, dorsal view **C** right chela, lateral view **D** genital area, ventral view **E** right pedipalp, dorsal view **F** right leg I (basitarsus and telotarsus), prolateral view **G** right leg I (basitarsus and telotarsus), retrolateral view. **H** right leg I, lateral view **I** right leg IV, lateral view. Scale bars: 0.5 mm (**A**, **B**, **D**, **F**, **G**); 1 mm (**C**, **E**, **H**, **I**).

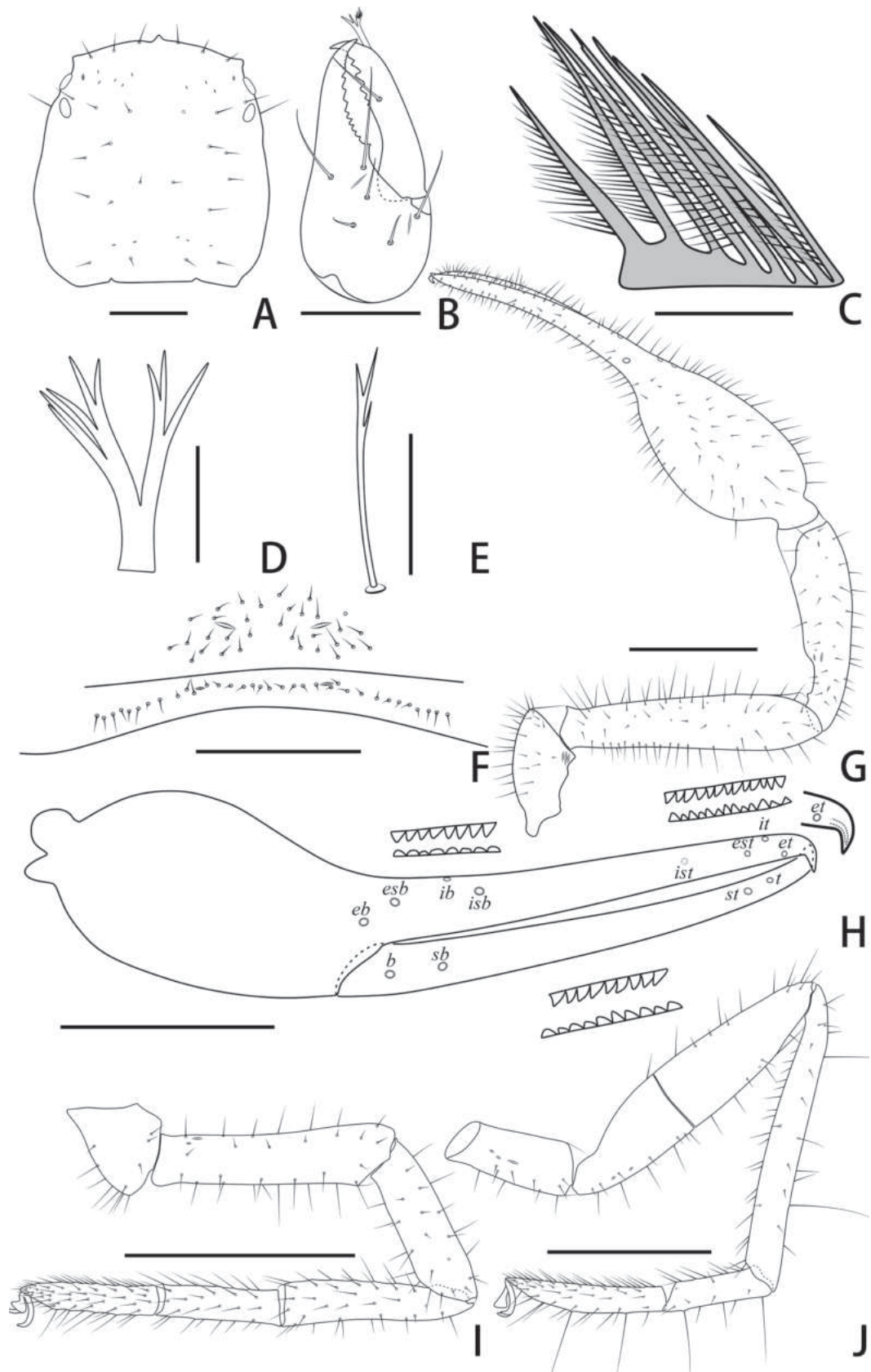


Figure 5. Paratype female of *Stenohya gibba* sp. nov. **A** carapace, dorsal view **B** right chelicera, dorsal view **C** rallum **D** galea **E** subterminal tarsal seta **F** chaetotaxy of genital area, ventral view **G** right pedipalp, dorsal view **H** right chela, lateral view, showing trichobothriotaxy, teeth and venom apparatus **I** right leg I, lateral view **J** right leg IV, lateral view. Scale bars: 0.5 mm (**A**, **B**, **F**); 0.1 mm (**C**–**E**); 1 mm (**G**–**J**).

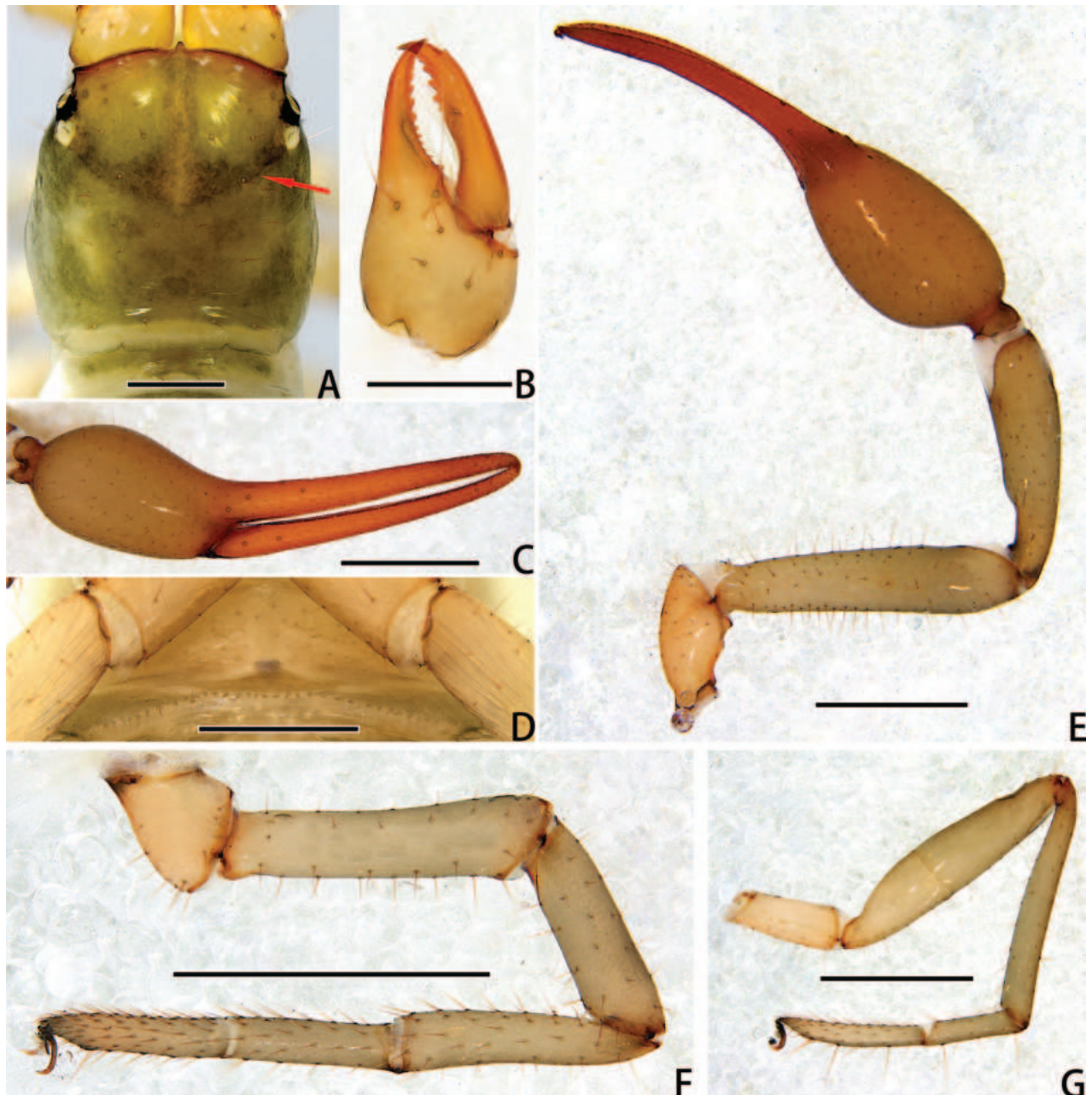


Figure 6. Paratype female of *Stenohya gibba* sp. nov. **A** carapace, dorsal view (red arrow showing transverse groove) **B** right chelicera, dorsal view **C** right chela, lateral view **D** genital area, ventral view **E** right pedipalp, dorsal view **F** right leg I, lateral view **G** right leg IV, lateral view. Scale bars: 0.5 mm (**A**, **B**, **D**); 1 mm (**C**, **E–G**).

Legs (Figs 5I, J, 6F, G). Leg I: trochanter 1.25–1.37, femur 3.64–3.96, patella 3.00–3.45, tibia 3.79–4.56, basitarsus 3.29–4.00, telotarsus 4.77–4.85 times longer than deep. Leg IV: trochanter 2.55–2.79, femur + patella 4.30–4.72, tibia 6.68–7.29, basitarsus 3.93–4.40, telotarsus 6.53–6.79 times longer than deep; tibia with two submedial tactile setae (TS = 0.22–0.29, 0.72–0.76), basitarsus with two tactile setae (TS = 0.12–0.13, 0.80), telotarsus with two tactile setae (TS = 0.20–0.22, 0.59).

Measurements (in mm; length/breadth or, for legs, length/depth). Male (holotype and paratypes). Body length 4.55–5.30. Carapace 1.84–1.90/1.40–1.42. Pedipalpal trochanter 0.76–0.86/0.48–0.57, femur 1.82–2.01/0.46, patella

1.56–1.67/0.45–0.46, chela with pedicel 3.80–3.87/0.92–0.99, chela without pedicel 3.58–3.67/0.92–0.99, hand without pedicel length 1.15–1.30, movable finger length 2.58–2.70. Leg I: trochanter 0.56–0.59/0.38–0.40, femur 1.03–1.14/0.50–0.52, patella 0.92–1.08/0.33–0.36, tibia 0.78–0.83/0.23–0.25, basitarsus 0.53–0.60/0.21–0.26, telotarsus 0.55–0.58/0.19–0.23. Leg IV: trochanter 0.69–0.81/0.26–0.31, femur + patella 1.63–1.84/0.39–0.40, tibia 1.58–1.64/0.21–0.23, basitarsus 0.64–0.70/0.15–0.16, telotarsus 0.93–1.00/0.13–0.15.

Female (paratypes). Body length 4.45–5.65. Carapace 1.48–1.64/1.24–1.55. Pedipalpal trochanter 0.83–0.91/0.43–0.47, femur 1.96–2.06/0.41–0.44, patella 1.45–1.66/0.41–0.48, chela with pedicel 3.56–3.72/0.84–0.90, chela without pedicel 3.38–3.55/1.39–1.52, hand without pedicel length 1.27–1.37, movable finger length 2.17–2.30. Leg I: trochanter 0.41–0.46/0.30–0.36, femur 0.95–1.02/0.24–0.28, patella 0.66–0.78/0.22–0.24, tibia 0.72–0.82/0.18–0.19, basitarsus 0.46–0.60/0.14–0.15, telotarsus 0.58–0.63/0.12–0.13. Leg IV: trochanter 0.74–0.87/0.29–0.34, femur + patella 1.74–1.85/0.38–0.43, tibia 1.47–1.56/0.21–0.22, basitarsus 0.59–0.70/0.15–0.16, telotarsus 0.95–0.98/0.14–0.15.

Distribution. China (Hunan).

Remarks. The male of this new species differs from all other species of the genus *Stenohya* by the presence of a large columnar projection on the lateral side of basitarsus and telotarsus. The female can be distinguished from other *Stenohya* species reported from China by the presence of 79–87 teeth on pedipalpal movable chelal finger (115–118 in *S. arcuata*; 68 in *S. bomica*; 96–98 in *S. hainanensis*; 46–51 in *S. huangji*; 45–55 in *S. pengae*), the pedipalpal chela with pedicel 4.67–4.98 times longer than wide (4.20 in *S. bicornuta*; 4.19–4.37 in *S. curvata*; 4.16–4.27 in *S. hainanensis*; 3.56 in *S. meiacantha*; 4.09–4.25 in *S. pengae*; 4.02–4.10 in *S. spinata*; 3.44–4.50 in *S. tengchongensis*) (Zhao and Zhang 2011; Zhao et al. 2011; Hu and Zhang 2012; Yang and Zhang 2013; Guo and Zhang 2016; Guo et al. 2019; Zhan et al. 2023).

***Stenohya papillata* sp. nov.**

<https://zoobank.org/50230EC7-A562-4638-AA98-DA00F4B0F59A>

Figs 7–12

Chinese name. 乳突狭伪蝎

Type material. **Holotype** male (Ps.-MHBU-HN2023111909), China: Hunan Province, Suining County, Ganchong Village [26°29'59"N, 110°08'01"E], 460 m a.s.l., 19 November 2023, in leaf litter (Fig. 8C, D), Jiaqi Zhao, Jianzhou Sun, Tao Zheng & Songtao Shi leg. **Paratypes:** two males (Ps.-MHBU-HN2023111910–11), three females (Ps.-MHBU-HN2023111912–14), same data as for holotype.

Etymology. The specific name is derived from the Latin word “*papillatus*” and refers to the presence of a papillary projection on the ventral face of the pedipalpal chela hand in male.

Diagnosis. Carapace with four well-developed eyes, epistome triangular (Figs 9A, 10A, 11A, 12A). Male pedipalpal trochanter with a small process and small frosted projections on the median prolateral position; femur with several big tubercles and a projection on the prolateral position, a few small tubercles at the

retrolateral surface; patella with a triangular protuberance on the prolateral position (Figs 9G, 10E); chelal hand concaved distally at the dorsal side, with 30–33 triangular spinous apophyses on the dorsal side and a papillary projection at the median of ventral side (Figs 9H, 10C). Male leg I femur and patella enlarged and basitarsus and telotarsus semi-fused (Figs 9I, 10F). Female pedipalpal fixed chelal finger with 99–102 teeth; pedipalpal femur 4.76–4.98 times longer than wide.

Description. Adult male (holotype and male paratypes) (Figs 7A, 8A).

Carapace (Figs 9A, 10A). Carapace 1.23–1.36 times longer than broad, with a total of 36–37 setae, including six near anterior margin and 6–7 near posterior margin; five lyrifissures near the eyes, four lyrifissures near posterior margin; epistome small, triangular, with rounded apex; four well-developed eyes; carapace divided into three parts by two transverse, shallow grooves, the anterior part uplifted, the median part with microgrooves, the posterior part uplifted and with microgrooves.

Chelicera (Figs 9B, 10B). Hand with 6–7 setae and two lyrifissures, movable finger with one seta; fixed finger with 16–17 teeth; movable finger with six teeth; serrula exterior with 48–55 lamellae; serrula interior with 39–42 lamellae; galea developed, one branch four, while the other three (Fig. 9D); rallum consisting of eight blades, all with anteriorly directed spinules, the basal-most blade shortest (Fig. 9C).

Pedipalps (Figs 9G, H, 10C, E). Apex of pedipalpal coxa rounded, with six long setae. Trochanter with a small process on the median prolateral position, as well as some small frosted projections; femur with several big tubercles on the prolateral position, as well as a projection on the subdistal prolateral surface, few small tubercles placed at the retrolateral surface; patella with a projection on the prolateral position and three lyrifissures (Figs 9G, 10E); chelal hand concaved at the dorsal side of distal half, and with 30–33 triangular-shaped, spinous apophyses on the dorsal side, every apophyse with a setae at the base (Figs 9H, 10C). A few spinous apophyses extended to the subbase of fixed finger. A papillary projection in the middle of the ventral aspect of the pedipalpal chelal hand. On the posterior side, a few small granular processes dispersedly located at the distal of the hand and near the base of the fingers. Fixed chelal finger slightly curved upward at median to distal part (Figs 9H, 10C). Trochanter 1.46–1.63, femur 4.48–5.02, patella 3.67–4.78, chela with pedicel 4.58–4.60, chela without pedicel 3.53–3.71 times longer than broad, movable finger 1.68–1.84 times longer than hand without pedicel. Fixed chelal finger with eight, movable chelal finger with four trichobothria: *eb* and *esb* situated on the base of hand, grouped very closely with *ib* and *isb*; *est*, *et* and *it* grouped distally; *ist* closer to *est-et-ist* than to *isb-ib-esb-eb* in fixed chelal finger; *b* and *sb* situated closer to each other in basal half, *st* and *t* close to each other in distal half of movable finger. Venom apparatus present only in fixed chelal finger, venom duct short. Fixed chelal finger with 93–105 pointed teeth, movable finger with 87–94 teeth, 34–42 rounded teeth at base, and 52–53 pointed ones.

Abdomen. Pleural membrane granulated. Tergites and sternites undivided, tergal chaetotaxy (I–XI): 5: 7: 9–10: 10–11: 10–11: 11: 11: 11–12: 12: 11–12: 12–13, sternal chaetotaxy (IV–XI): 26–30: 19–24: 17: 15–18: 16–18: 14–16: 11–14: 5, sternites VI–VIII with 11 medial scattered glandular setae, anal cone with two dorsal and two ventral setae. Genital area (Figs 9F, 10D): anterior genital sternite with 39–40 setae and two lyrifissures; posterior genital sternite with 31–37 setae and two lyrifissures.

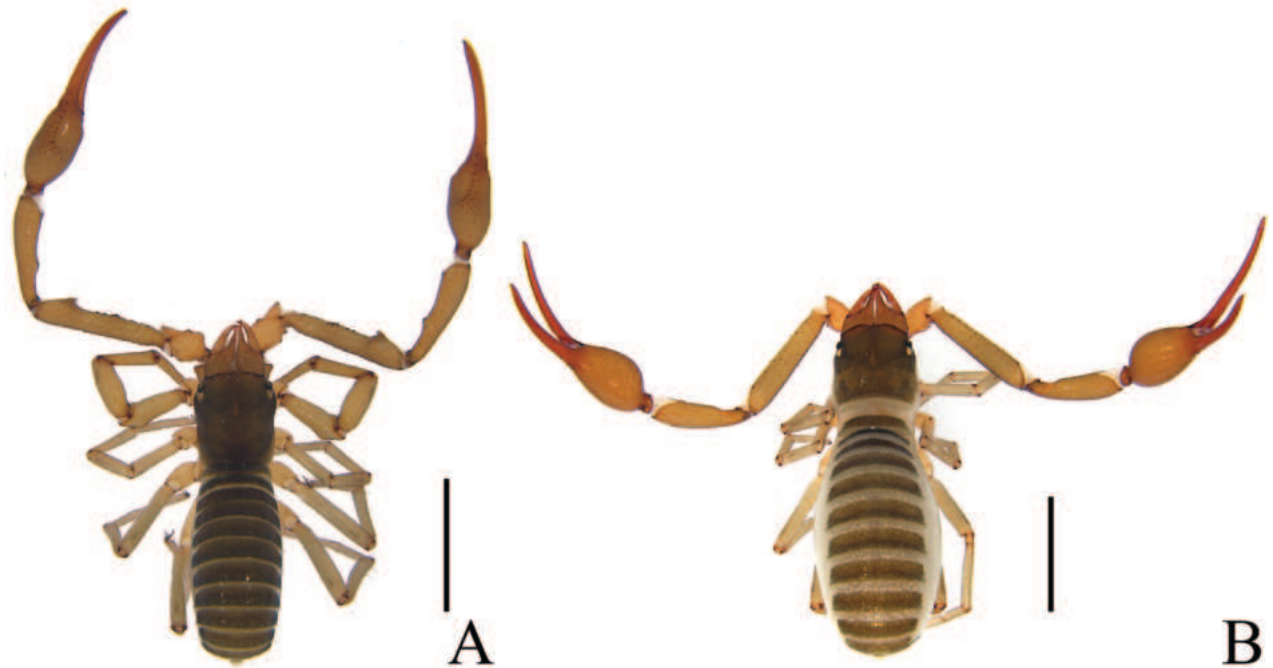


Figure 7. *Stenohya papillata* sp. nov. **A** holotype male (dorsal view) **B** paratype female (dorsal view). Scale bars: 2 mm.

Legs (Figs 9I, J, 10F, G). Leg I specialized, femur and patella enlarged, basitarsus and telotarsus semi-fused, the dividing line between the two limb segments visible. Leg IV generally typical, long, and sinewy. Leg I: trochanter 1.16–1.71, femur 2.56–3.28, patella 2.61–4.10, tibia 4.24–4.75, basitarsus 3.06–3.87, telotarsus 3.29–3.64 times longer than deep. Leg IV: trochanter 2.60–2.81, femur + patella 3.77–5.18, tibia 6.58–7.45, basitarsus 4.20–4.57, telotarsus 5.88–7.07 times longer than deep; tibia with two submedial tactile setae (TS = 0.68–0.74, 0.96–1.03), basitarsus with two tactile setae (TS = 0.09–0.11, 0.53–0.56), telotarsus with two tactile setae (TS = 0.14–0.17, 0.84–0.88); subterminal tarsal seta bifurcate (Fig. 9E). Arolium not divided, shorter than the slender and simple claws.

Adult female (paratype females) (Figs 7B, 8B): mostly same as males, except where noted.

Carapace (Figs 11A, 12A). Carapace 1.04–1.13 times longer than broad, with a total of 39–42 setae, including 5–6 near anterior margin and 8–9 near posterior margin; three lyrifissures near the eyes, two lyrifissures near posterior margin; carapace divided into three parts by two transverse, shallow grooves, the anterior part uplifted, the median part smooth, the posterior part uplifted, and with microgrooves.

Chelicera (Figs 11B, 12B). Fixed finger with 12–15 teeth; movable finger with 6–7 teeth; serrula exterior with 49–51 lamellae; serrula interior with 36–44 lamellae.

Pedipalps (Figs 11G, H, 12C, E). Apex of pedipalpal coxa with eight long setae. Femur with several tubercles on the prolateral position, as well as a few small tubercles placed lateral surface. Trochanter 1.89–2.09, femur 4.76–4.98, patella 3.10–3.55, chela with pedicel 3.89–4.27, chela without pedicel 3.86–4.09 times longer than broad, movable finger 1.56–1.72 times longer than hand without pedicel. Fixed chelal finger with 99–102 pointed teeth, movable finger with 90–94 teeth, 43–49 rounded teeth at base, and 45–47 pointed ones.

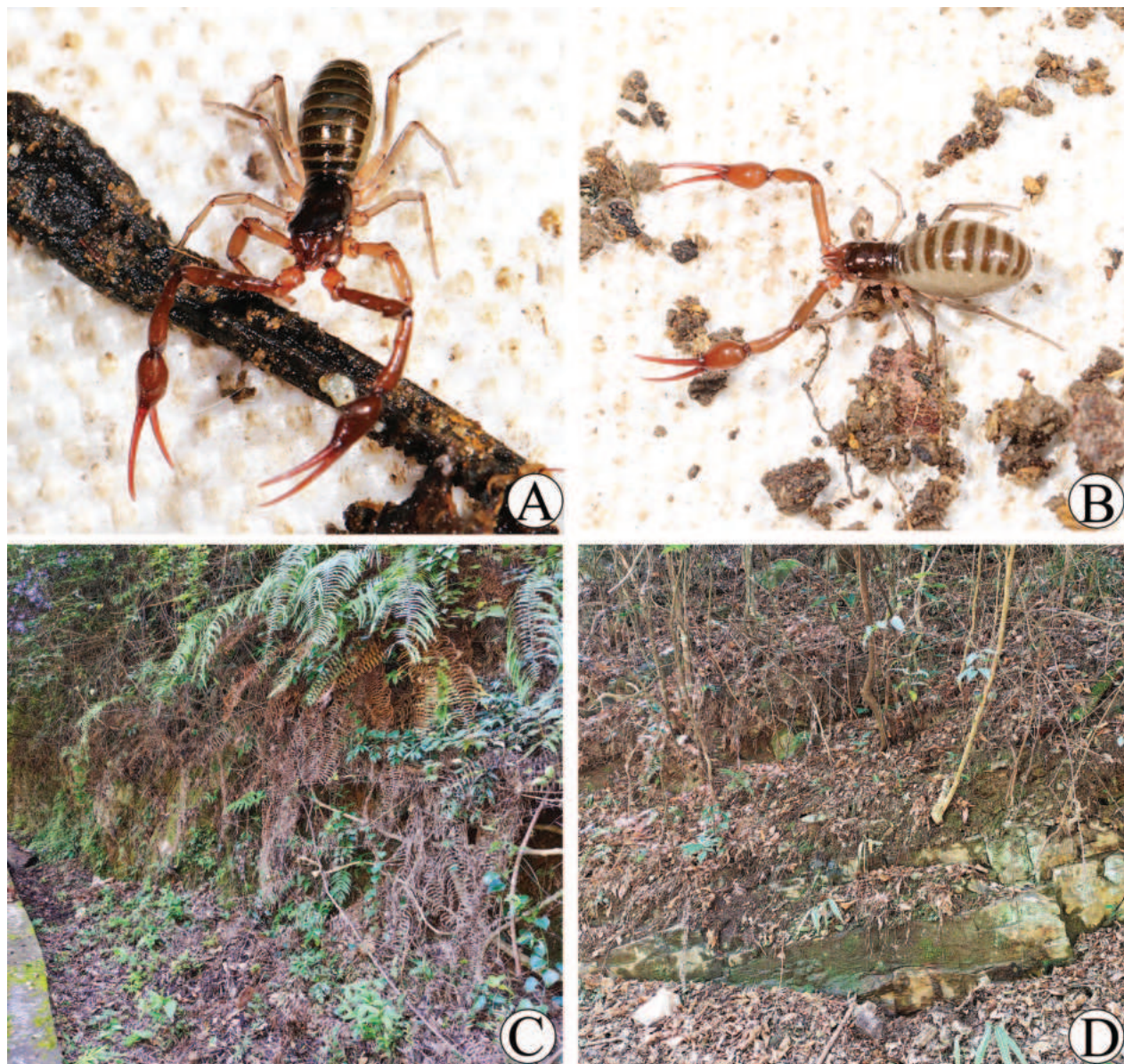


Figure 8. Type locality and habitus of *Stenohya papillata* sp. nov. **A** male habitus **B** female habitus **C, D** litter layer inhabited by habitus.

Abdomen. Tergal chaetotaxy (I–XI): 6: 7–8: 10–11: 12: 11: 11–13: 12: 11–12: 11–12: 12–13: 12, sternal chaetotaxy (IV–XI): 22–24: 20–22: 18–19: 17–19: 17–19: 15–18: 12: 4–5, sternites VI–VIII with 2–3 medial scattered glandular setae; genital area (Figs 11F, 12D): sternite II with total of 27–35 setae and two lyrifissures; sternite III with a row of 35–38 setae and two lyrifissures along posterior margin.

Legs (Figs 11I, J, 12F, G). Leg I: trochanter 1.18–1.74, femur 3.06–4.35, patella 2.96–3.57, tibia 4.61–5.31, basitarsus 3.57–4.33, telotarsus 4.14–4.69 times longer than deep. Leg IV: trochanter 3.03–3.24, femur + patella 3.93–5.05, tibia 5.88–7.71, basitarsus 4.13–5.00, telotarsus 5.88–9.00 times longer than deep; tibia with three submedial tactile setae (TS = 0.20–0.30, 0.69–0.77, 0.98–1.06), basitarsus with two tactile setae (TS = 0.14–0.15, 0.83–0.88), telotarsus with two tactile setae (TS = 0.25–0.32, 0.57–0.61).

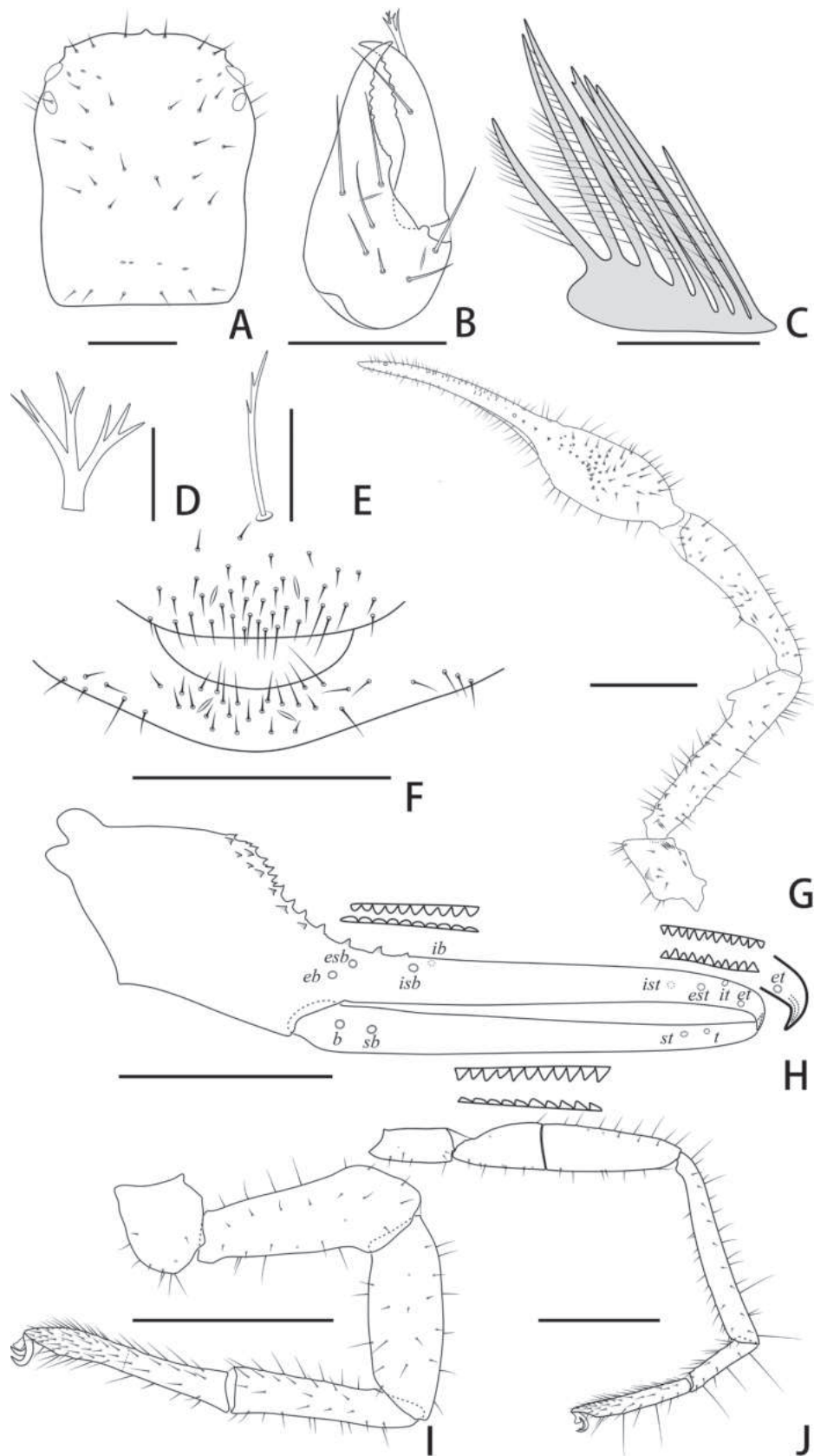


Figure 9. Holotype male of *Stenohya papillata* sp. nov. **A** carapace, dorsal view **B** right chelicera, dorsal view **C** rallum **D** galea **E** subterminal tarsal seta **F** chaetotaxy of genital area, ventral view **G** right pedipalp, dorsal view **H** right chela, lateral view, showing trichobothriotaxy, teeth and venom apparatus **I** right leg I, lateral view **J** right leg IV, lateral view. Scale bars: 0.5 mm (**A, B, F**); 0.1 mm (**C–E**); 1 mm (**G–J**).

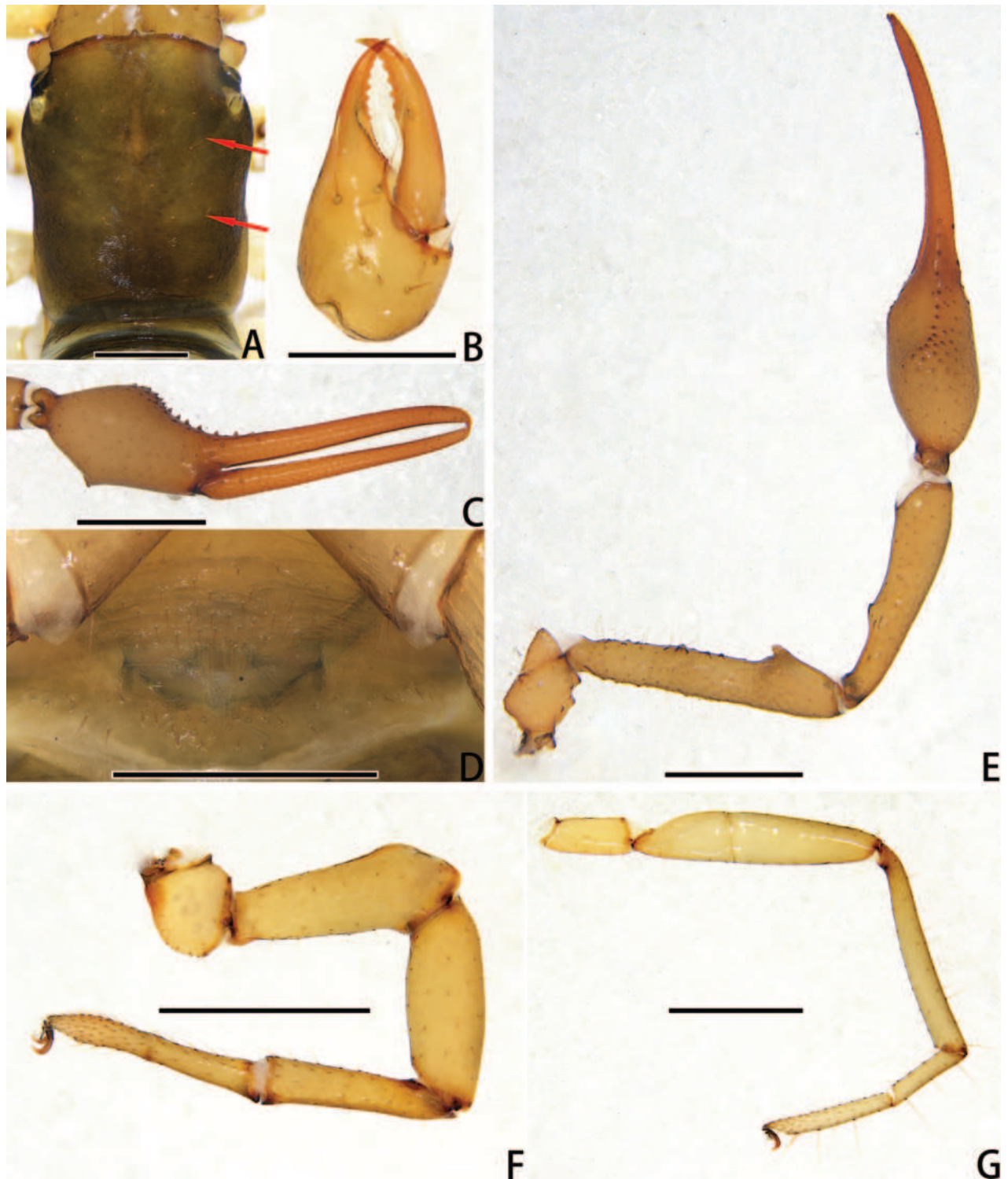


Figure 10. Holotype male of *Stenohya papillata* sp. nov. **A** carapace, dorsal view (red arrows showing two transverse grooves) **B** right chelicera, dorsal view **C** right chela, lateral view **D** genital area, ventral view **E** right pedipalp, dorsal view **F** right leg I, lateral view **G** right leg IV, dorsal view. Scale bars: 0.5 mm (**A**, **B**, **D**); 1 mm (**C**, **E–G**).

Measurements (in mm; length/breadth or, for legs, length/depth). Male (holotype and paratypes). Body length 4.00–4.53. Carapace 1.50–1.70/1.16–1.28. Pedipalpal trochanter 0.76–0.80/0.49–0.52, femur 2.02–2.06/0.41–0.46, patella 1.69–1.81/0.36–0.46, chela with pedicel 3.24–3.40/0.83–0.92, chela without pedicel 3.08–3.25/0.83–0.92, hand without pedicel length 1.13–1.30,

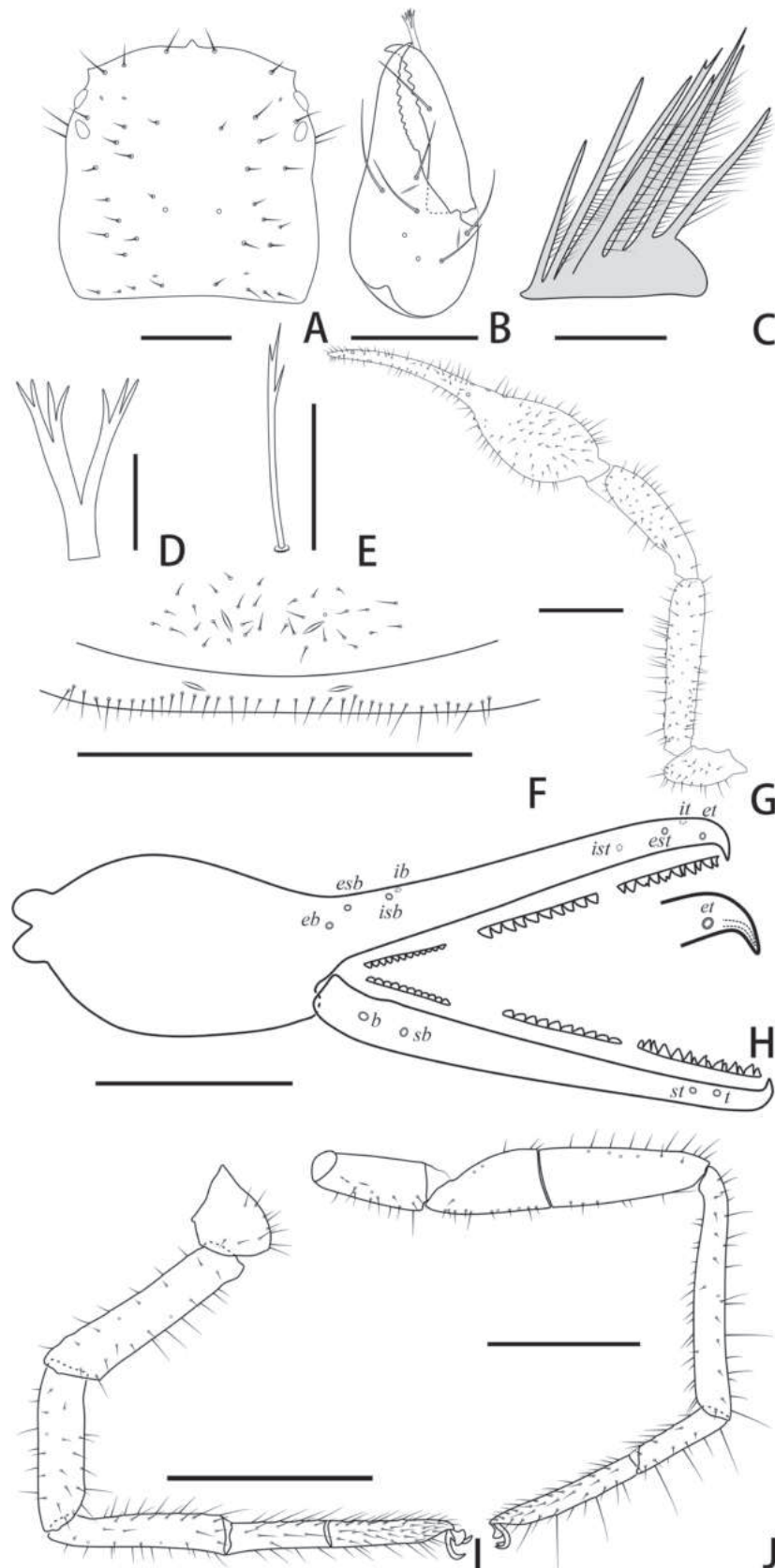


Figure 11. Paratype female of *Stenohya papillata* sp. nov. **A** carapace, dorsal view **B** right chelicera, dorsal view **C** rallum **D** galea **E** subterminal tarsal seta **F** chaetotaxy of genital area, ventral view **G** right pedipalp, dorsal view **H** right chela, lateral view, showing trichobothriotaxy, teeth and venom apparatus **I** left leg I, lateral view **J** right leg IV, lateral view. Scale bars: 0.5 mm (**A, B**); 0.1 mm (**C–E**); 1 mm (**F–J**).

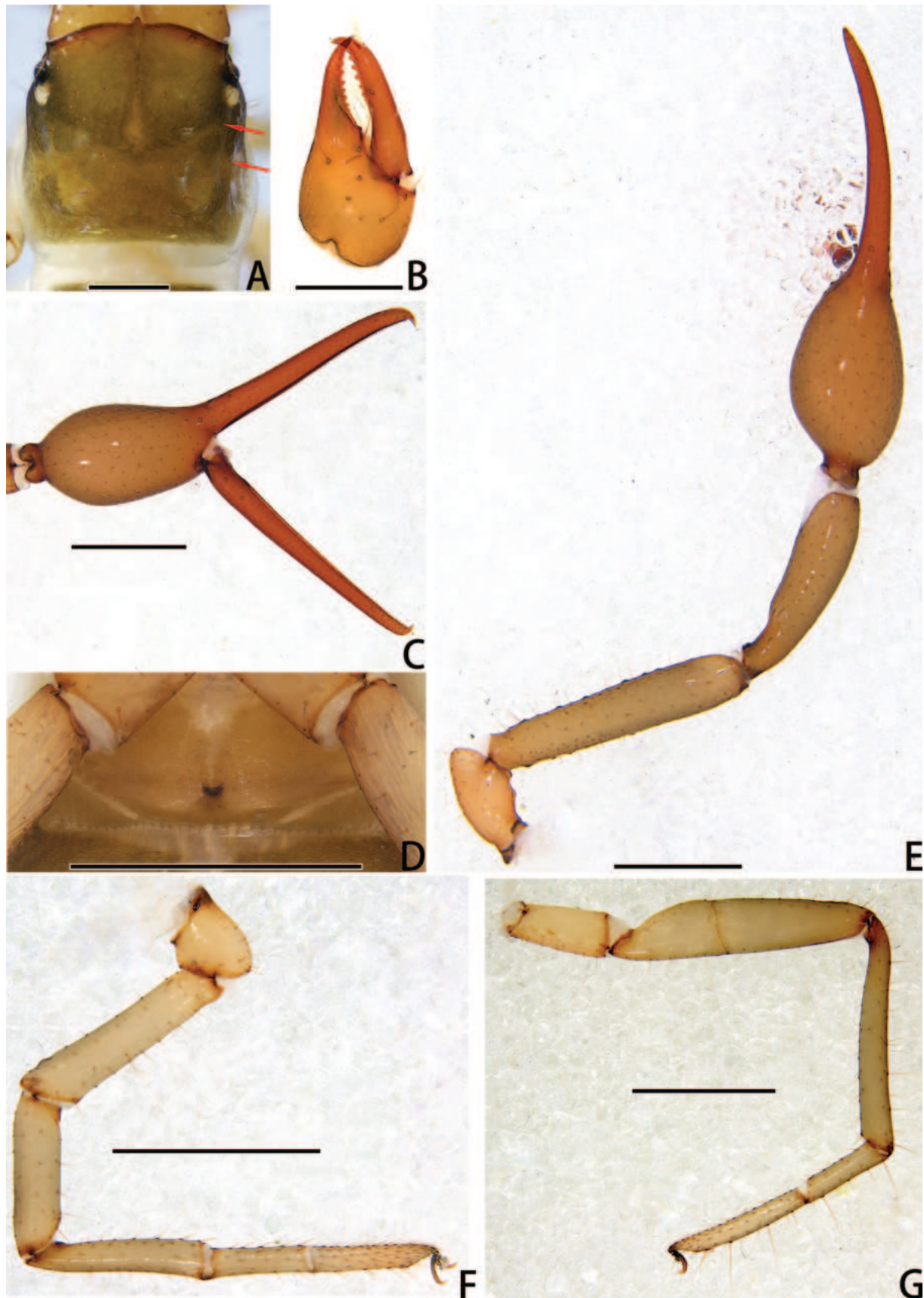


Figure 12. Paratype female of *Stenohya papillata* sp. nov. **A** carapace, dorsal view (red arrows showing two transverse grooves) **B** right chelicera, dorsal view **C** right chela, lateral view **D** genital area, ventral view **E** right pedipalp, dorsal view **F** left leg I, lateral view **G** right leg IV, lateral view. Scale bars: 0.5 mm (**A**, **B**); 1 mm (**C–G**).

movable finger length 2.08–2.23. Leg I: trochanter 0.50–0.59/0.31–0.43, femur 1.05–1.17/0.32–0.43, patella 0.86–1.09/0.21–0.39, tibia 0.87–0.95/0.20–0.21, basitarsus 0.49–0.58/0.15–0.17, telotarsus 0.46–0.51/0.14. Leg IV: trochanter 0.78–0.87/0.25–0.31, femur + patella 1.74–1.86/0.34–0.47, tibia 1.47–1.64/0.21–0.24, basitarsus 0.63–0.73/0.14–0.17, telotarsus 0.94–0.99/0.14–0.16.

Female (paratypes). Body length 3.77–6.12. Carapace 1.41–1.56/1.33–1.46. Pedipalpal trochanter 0.83–0.92/0.44–0.47, femur 2.00–2.14/0.42–0.43, patella 1.56–1.71/0.44–0.51, chela with pedicel 3.59–3.70/0.85–0.89, chela without pedicel 3.40–3.48/0.85–0.89, hand without pedicel length 1.36–1.40, movable finger length 2.18–2.34. Leg I: trochanter 0.45–0.49/0.27–0.38, femur 0.95–1.04/0.23–0.31, patella 0.77–0.82/0.23–0.26, tibia 0.81–0.85/0.16–0.18, basitarsus 0.50–0.52/0.12–0.14, telotarsus 0.58–0.61/0.13–0.14. Leg IV: trochanter 0.81–0.91/0.25–0.29, femur + patella 1.81–1.92/0.37–0.46, tibia 1.53–1.62/0.21–0.26, basitarsus 0.65–0.70/0.14–0.16, telotarsus 0.96–1.00/0.11–0.17.

Distribution. China (Hunan).

Remarks. Similar to *S. gibba* in having specialized leg I in male, this new species can be distinguished by the morphology of the pedipalpal chelal hand and leg I. The male of this new species has 30–33 dentate convex on the dorsal side, a papillary protuberance on the ventral side of chelal hand, and lacks the projection on the basitarsus and telotarsus of leg I, but the male *S. gibba* has 15–18 dentate convex, which arranged in a row on the dorsal side of chelal hand and a large columnar projection on the basitarsus and telotarsus in leg I. Female of this new species can be easily distinguished from the other *Stenohya* species in having 99–102 teeth on pedipalpal fixed chelal finger (124–129 in *S. arcuata*; 76 in *S. bomica*; 85–90 in *S. curvata*; 88–89 in *S. hainanensis*; 63–69 in *S. huangi*; 84 in *S. meiacantha*; 66–79 in *S. pengae*; 82–91 in *S. spinata*; 81–89 in *S. tengchongensis*), and pedipalpal femur 4.76–4.98 times longer than wide (4.23–4.45 in *S. arcuata*; 5.37 in *S. bicornuta*; 5.00–5.24 in *S. curvata*; 6.07–6.32 in *S. huangi*; 5.13 in *S. meiacantha*; 5.18–5.83 in *S. pengae*; 4.00–4.13 in *S. tengchongensis*), and pedipalpal chela with pedicel 3.89–4.27 times longer than wide (3.50–3.74 in *S. arcuata*; 4.19–4.37 in *S. curvata*; 4.67–4.98 in *S. gibba*; 3.56 in *S. meiacantha*) (Zhao et al. 2011; Zhao and Zhang 2011; Hu and Zhang 2012; Yang and Zhang 2013; Guo and Zhang 2016; Guo et al. 2019; Zhan et al. 2023).

***Stenohya guangmingensis* sp. nov.**

<https://zoobank.org/61EEA057-CB4E-48D9-A9BF-98FD1D9AE0C4>

Figs 13–18

Chinese name. 光明狭伪蝎

Type material. **Holotype** male (Ps.-MHBU-JX2023013101), China: Jiangxi Province, Jinggangshan City, Guangming Township, 868 County Road [26°26'04"N, 114°12'11"E], 305 m a.s.l., 31 January 2023, in leaf litter and under rocks (Fig. 14C, D), Xiangbo Guo, Jianzhou Sun, Tao Zheng & Songtao Shi leg. **Paratypes:** four males (Ps.-MHBU-JX2023013102–05), three females (Ps.-MHBU-JX2023013106–08), same data as for holotype.

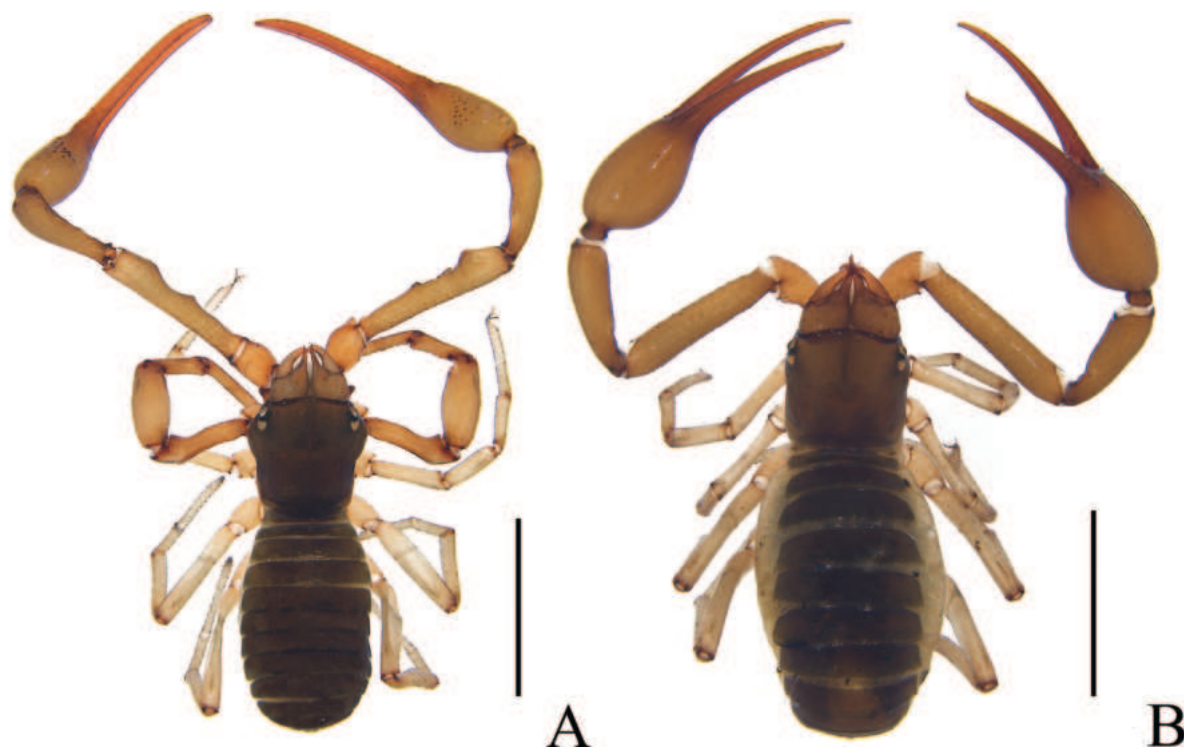


Figure 13. *Stenohya guangmingensis* sp. nov. **A** holotype male (dorsal view) **B** paratype female (dorsal view). Scale bars: 2 mm.

Etymology. The specific name refers to the type locality.

Diagnosis. Carapace with four well-developed eyes, epistome triangular (Figs 15A, 16A, 17A, 18A). Male pedipalpal femur with a large tubercle in the median area, two subdistal projections on the prolateral surface; patella smooth; chelal hand with 23 small, triangular, spinous apophyses on the dorsal side (Figs 15G, H, 16C, E). Male leg I femur with an inward depression at the distal part, patella enlarged (Figs 15I, 16F). Female carapace 1.02–1.10 times longer than broad; carapace with a total of 29–30 setae; apex of pedipalpal coxa with six long setae; pedipalpal patella 3.39–3.46; pedipalpal movable chelal finger with 92–94 teeth; pedipalpal fixed chelal finger with 95–98 teeth.

Description. Adult male (holotype and male paratypes) (Figs 13A, 14B).

Carapace (Figs 15A, 16A). Carapace 1.08–1.16 times longer than broad, with a total of 30–32 setae, including 5–6 near anterior margin and six near posterior margin; with six lyrifissures near the anterior eyes, four lyrifissures near posterior margin; epistome small, triangular, with rounded top; with four corneate eyes; the anterior half of the carapace uplifted and protruded to the sides, the front half significantly wider than the back part.

Chelicera (Figs 15B, 16B). Hand with seven setae and two lyrifissures; movable finger with one seta; fixed finger with 13–15 teeth; movable finger with 5–6 teeth; serrula exterior with 40–44 lamellae; serrula interior with 36–38 lamellae; galea developed, divided into three main branches, two main branches consisting of two forks each, and another with three forks (Fig. 15D); rallum consisting of eight blades, all with anteriorly directed spinules, the basal-most blade shortest (Fig. 15C).

Pedipalps (Figs 15G, H, 16C, E). Apex of pedipalpal coxa rounded, with 6–7 long setae. Femur with a tubercle in the median area, a big projection on the subdistal prolateral surface, as well as a hook-shaped process near the base of big projection (Figs 15G, 16E); patella smooth (Figs 15G, 16E); chelal hand

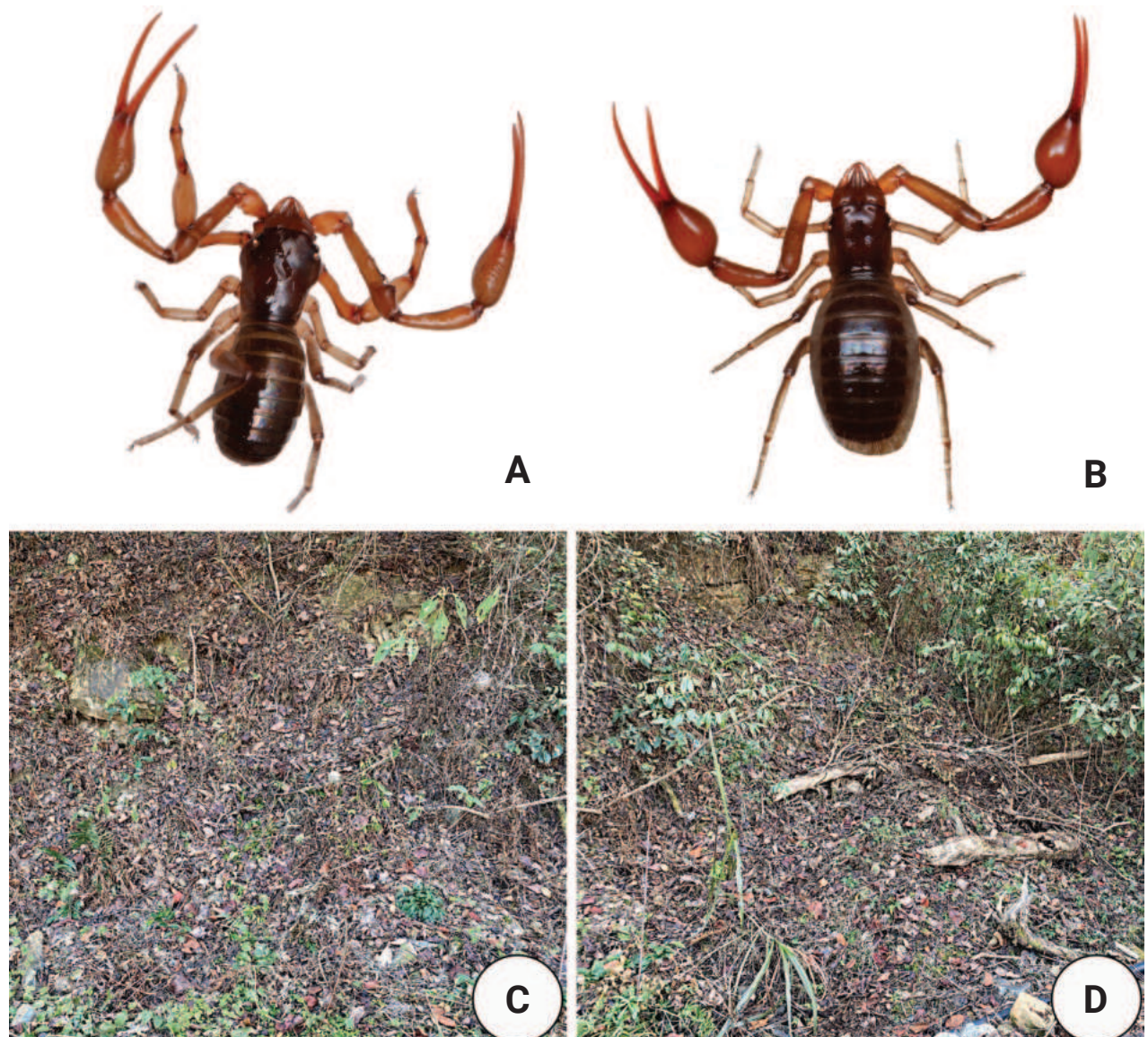


Figure 14. Type locality and habitus of *Stenohya guangmingensis* sp. nov. **A** male habitus **B** female habitus **C–D** litter layer inhabited by habitus.

with 17–19 small triangular, spinous apophyses at the dorsal side of distal half, each spinous apophysis with a seta at the base; on the posterior side, few small granular processes dispersedly located at the distal of the hand and near the base of fingers, and a few dentate bulges at the basal of the fixed finger; fixed chelal finger slightly curved upward at median to distal part (Figs 15H, 16C). Trochanter 1.52–1.83, femur 3.89–5.70, patella 3.53–4.05, chela with pedicel 4.67–4.98, chela without pedicel 4.50–4.80 times longer than broad, movable finger 1.74–2.02 times longer than hand without pedicel. Fixed chelal finger with eight, movable chelal finger with four trichobothria: *eb* and *esb* situated on the base of hand, grouped very closely with *ib* and *isb*; *est*, *et* and *it* grouped distally; *ist* situated midway between *isb* and *it*; *b* and *sb* situated closer to each other in basal half, *st* and *t* close to each other in distal half of movable finger. Venom apparatus present only in fixed chelal finger, venom duct short. Fixed chelal finger with 97–99 pointed teeth, movable finger with 91–95 teeth, 45–57 rounded teeth at base, and 38–46 pointed ones.

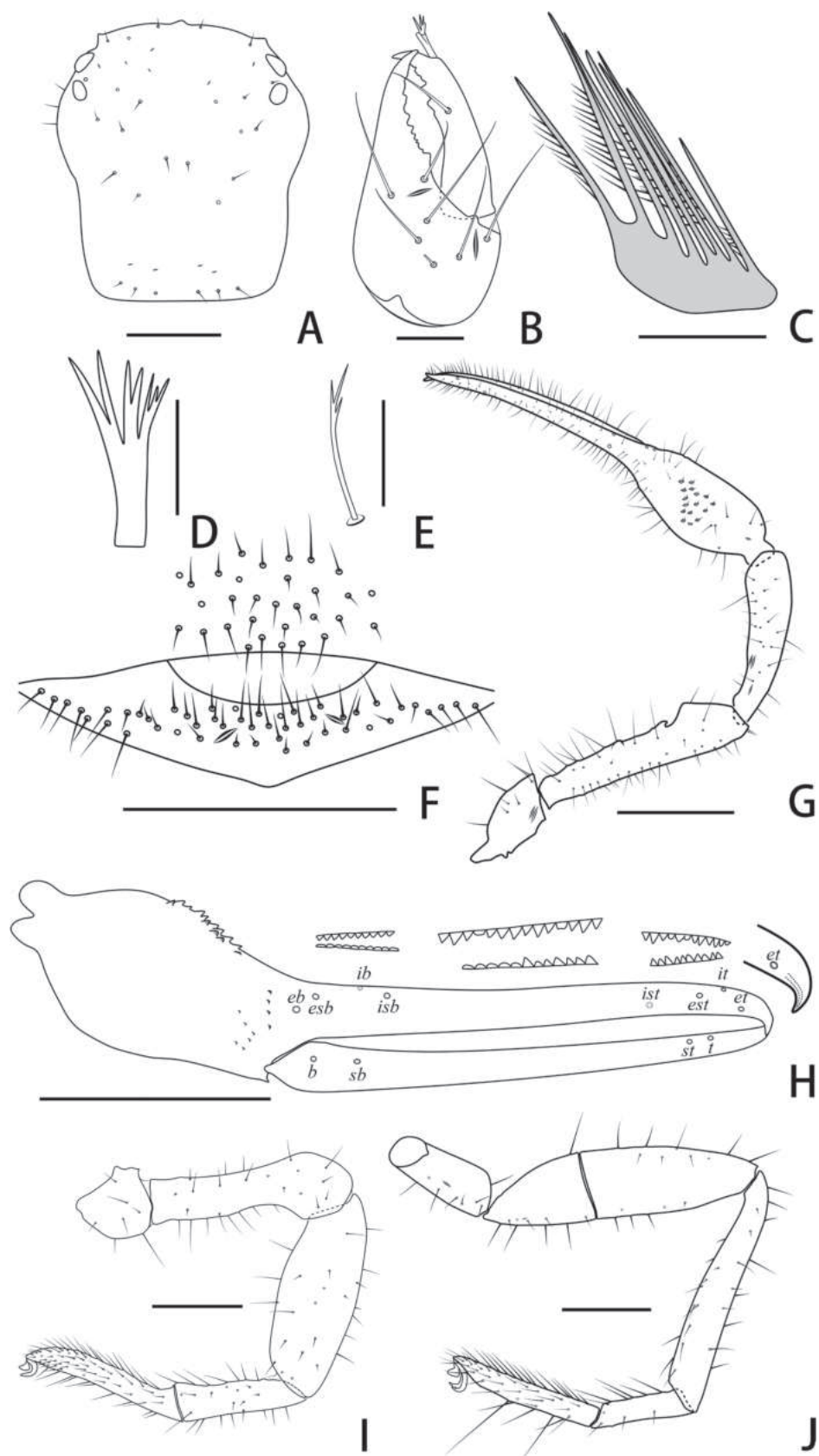


Figure 15. Holotype male of *Stenohya guangmingensis* sp. nov. **A** carapace, dorsal view **B** right chelicera, dorsal view **C** rallum **D** galea **E** subterminal tarsal seta **F** chaetotaxy of genital area, ventral view **G** right pedipalp, dorsal view **H** right chela, lateral view, showing trichobothriotaxy, teeth and venom apparatus **I** right leg I, lateral view **J** right leg IV, lateral view. Scale bars: 0.5 mm (**A, F, I, J**); 0.2 mm (**B**); 0.1 mm (**C–E**); 1 mm (**G, H**).

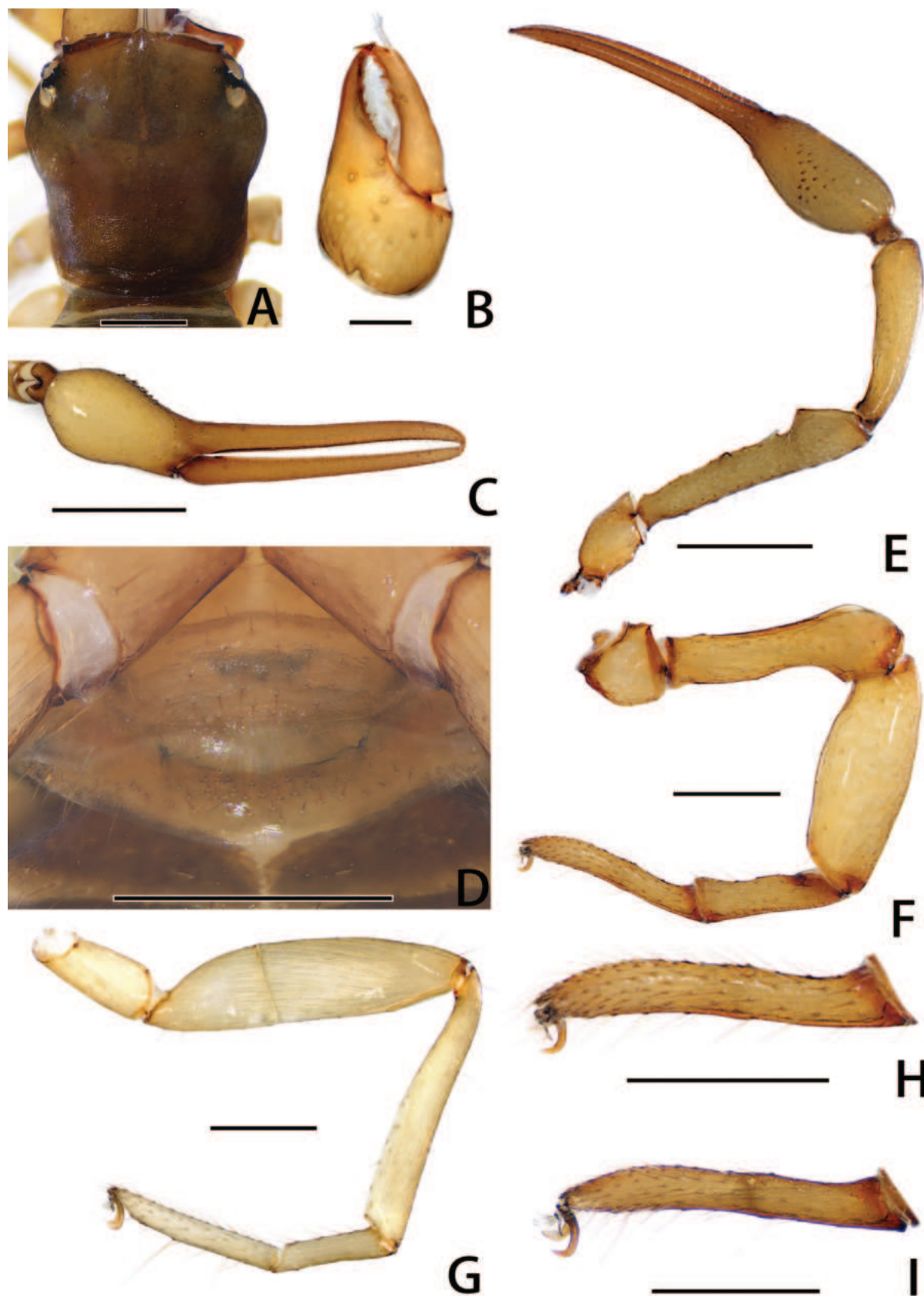


Figure 16. Holotype and paratype male of *Stenohya guangmingensis* sp. nov. **A–H** holotype male **I** paratype male **A** carapace, dorsal view **B** right chelicera, dorsal view **C** right chela, lateral view **D** genital area, ventral view **E** right pedipalp, dorsal view **F** right leg I, lateral view **G** right leg IV, lateral view **H** right leg I (basitarsus and telotarsus), lateral view **I** right leg I (basitarsus and telotarsus), lateral view (paratype). Scale bars: 0.5 mm (**A, D, F–I**); 0.2 mm (**B**); 1 mm (**C, E**).

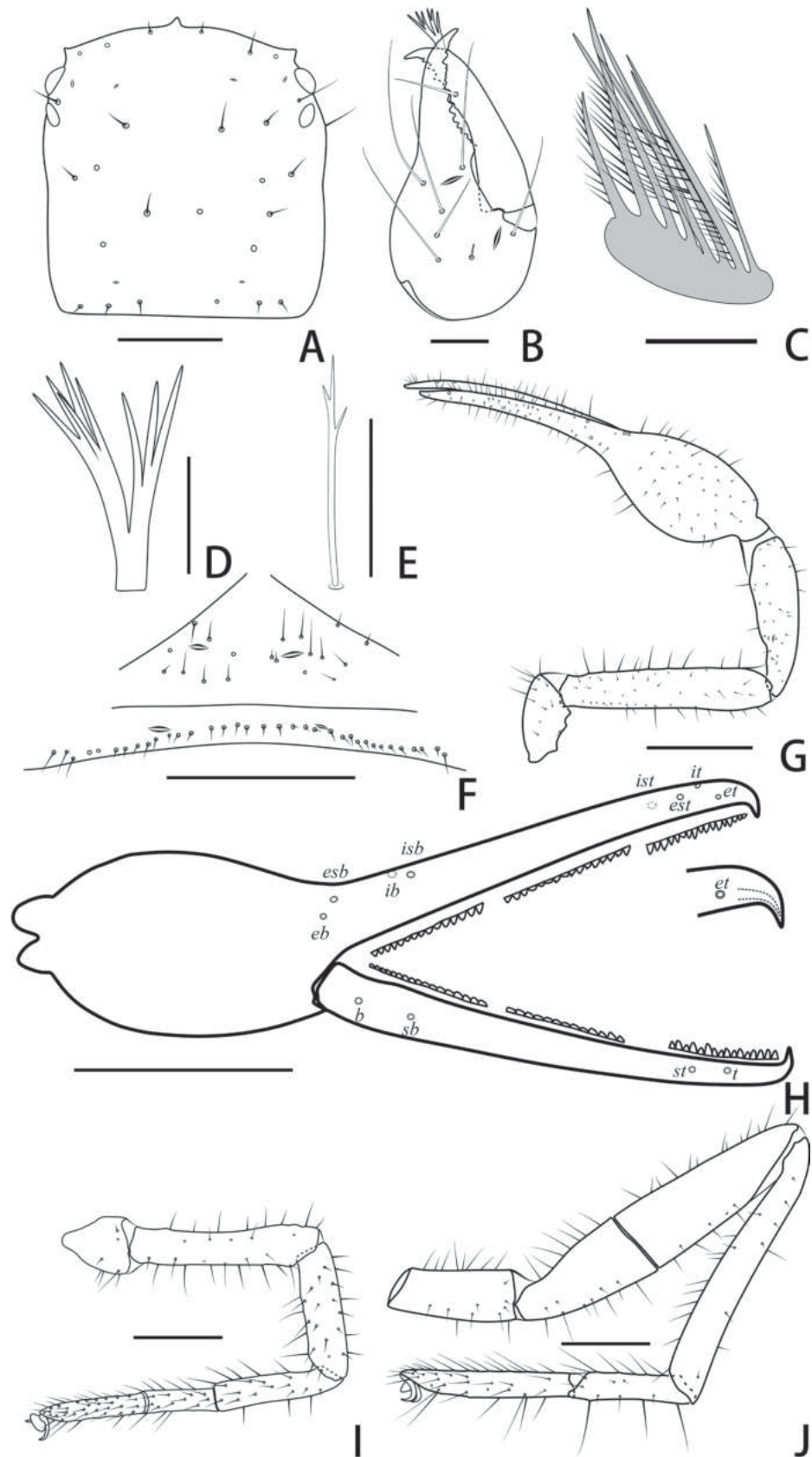


Figure 17. Paratype female of *Stenohya guangmingensis* sp. nov. **A** carapace, dorsal view **B** right chelicera, dorsal view **C** rallum **D** galea **E** subterminal tarsal seta **F** chaetotaxy of genital area, ventral view **G** right pedipalp, dorsal view **H** right chela, lateral view, showing trichobothriotaxy, teeth and venom apparatus **I** right leg I, lateral view **J** right leg IV, lateral view. Scale bars: 0.5 mm (**A, D, F–H**); 0.2 mm (**B**); 1 mm (**C, E**).

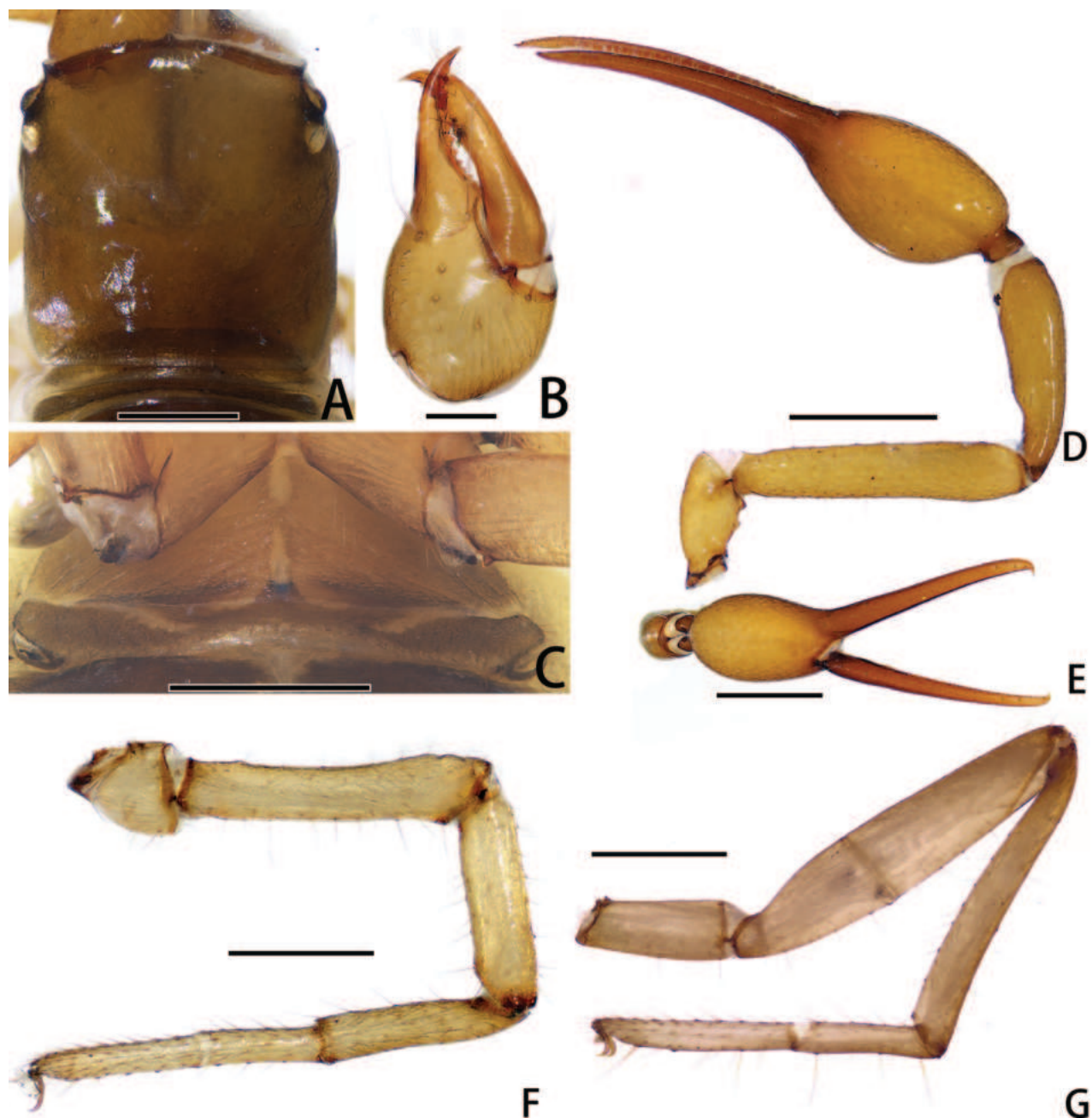


Figure 18. Paratype female of *Stenohya guangmingensis* sp. nov. **A** carapace, dorsal view **B** right chelicera, dorsal view **C** genital area, ventral view **D** right pedipalp, dorsal view **E** right chela, lateral view **F** right leg I, lateral view **G** right leg IV, lateral view. Scale bars: 0.5 mm (**A**, **C**, **F**, **G**); 0.2 mm (**B**); 1 mm (**D**, **E**).

Abdomen. Pleural membrane granulated. Tergites and sternites undivided, tergal chaetotaxy (I–XI): 4–5: 8–9: 9–11: 9–11: 10–11: 9–11: 9–12: 11–13: 11–12: 8–10: 8–10, sternal chaetotaxy (IV–XI): 23–26: 19–20: 15–19: 13–19: 15–16: 12–14: 10–12: 4–5, sternites VI–VIII with 9–13 medial scattered glandular setae, anal cone with two dorsal and two ventral setae. Genital area (Figs 15F, 16D): sternite II with total of 30–35 setae and two lyrifissures; sternite III with 46–56 setae.

Legs (Figs 15I, J, 16F–I). The femur with an inward depression at the distal of the leg I, leg I patella enlarged (Figs 15I, 16F), and fusing (Figs 15I, 16F, H) or semi-fusing (Fig. 16I) of the basitarsus and telotarsus, the dividing line between the basitarsus and telotarsus inconspicuous or slightly visible. Leg IV

generally typical, long, and sinewy (Figs 15J, 16G). Leg I: trochanter 1.05–1.16, femur 3.47–5.52, patella 2.53–2.90, tibia 3.45–4.29, basitarsus + telotarsus 6.64–6.80 times longer than deep. Leg IV: trochanter 2.36–2.78, femur + patella 4.08–4.88, tibia 6.80–7.56, basitarsus 4.23–4.85, telotarsus 6.62–8.40 times longer than deep; tibia with three submedial tactile setae (TS = 0.16, 0.61, 0.92), basitarsus with two tactile setae (TS = 0.14, 0.83–0.84), telotarsus with two tactile setae (TS = 0.24–0.30, 0.58–0.60); subterminal tarsal seta bifurcate (Fig. 15E). Arolium not divided, shorter than the slender and simple claws.

Adult female (paratype females) (Figs 13B, 14B): mostly same as males, except where noted.

Carapace (Figs 17A, 18A). Smooth and nearly rectangular, 1.02–1.10 times longer than broad, with a total of 27–31 setae, including 6–7 near anterior margin and 6–7 near posterior margin; with two pair lyrifissures near the anterior eyes, two lyrifissures near posterior margin.

Chelicera (Figs 17B, 18B). Fixed finger with 12–13 teeth; movable finger with seven teeth; serrula exterior with 42–45 lamellae; serrula interior with 35–37 lamellae; galea developed, divided into two main branches, one branch five, while the other three (Fig. 17D).

Pedipalps (Figs 17G, H, 18D, E). Apex of pedipalpal coxa with six long setae. Femur with some granular projections; trochanter 1.71–2.02; femur 4.90–5.39; patella 3.39–3.46; chela with pedicel 4.13–4.42; chela without pedicel 3.93–4.29 times longer than broad; movable finger 1.62–1.66 times longer than hand without pedicel. Fixed chelal finger with 95–98 pointed teeth, movable finger with 92–94 teeth, 47–48 rounded teeth at base, and 45–46 pointed ones.

Abdomen. Tergal chaetotaxy (I–XI): 4–5: 6–7: 8–9: 9–10: 10: 9: 9–10: 11: 9–12: 10–11: 7–10, sternal chaetotaxy (IV–XI): 24–26: 20–23: 16–17: 17–18: 15: 14: 12–13: 4–5, sternites VI–VIII with two medial scattered glandular setae; genital area (Figs 17F, 18C): sternite II with total of 19–23 setae and two lyrifissures; sternite III with a row of 35–37 setae and two lyrifissures along posterior margin.

Legs (Figs 17I, J, 18F, G). Leg I: trochanter 1.42–1.52, femur 4.78–5.95, patella 3.45–3.75, tibia 4.50–4.79, basitarsus 3.29–4.20, telotarsus 5.40–5.55 times longer than deep. Leg IV: trochanter 2.48–2.55, femur + patella 4.41–4.58, tibia 7.00–7.83, basitarsus 4.69–4.77, telotarsus 7.67–8.08 times longer than deep; tibia with two submedial tactile setae (TS = 0.20, 0.94), basitarsus with two tactile setae (TS = 0.13–0.15, 0.84–0.87), telotarsus with two tactile setae (TS = 0.23–0.26, 0.54–0.59); subterminal tarsal seta bifurcate (Fig. 17E).

Measurements (in mm; length/breadth or, for legs, length/depth). **Male** (holotype and paratypes). Body length 3.66–3.92. Carapace 1.48–1.55/1.31–1.43. Pedipalpal trochanter 0.64–0.75/0.41–0.43, femur 1.75–1.88/0.33–0.45, patella 1.34–1.50/0.37–0.38, chela with pedicel 3.27–3.30/0.66–0.70, chela without pedicel 3.15–3.17/0.66–0.70, hand without pedicel length 1.07–1.20, movable finger length 2.09–2.16. Leg I: trochanter 0.40–0.44/0.38, femur 1.11–1.18/0.21–0.32, patella 1.09–1.13/0.39–0.43, tibia 0.73–0.76/0.17–0.22, basitarsus + telotarsus 0.93–1.03/0.14–0.15. Leg IV: trochanter 0.59–0.71/0.23–0.26, femur + patella 1.55–1.66/0.34–0.38, tibia 1.36–1.44/0.18–0.20, basitarsus 0.55–0.63/0.12–0.13, telotarsus 0.84–0.90/0.10–0.13.

Female (paratypes). Body length 4.73–6.31. Carapace 1.34–1.43/1.30–1.32. Pedipalpal trochanter 0.70–0.85/0.41–0.42, femur 1.94–1.96/0.36–0.40, patella 1.42–1.49/0.41–0.44, chela with pedicel 3.35–3.47/0.76–0.84, chela

without pedicel 3.26–3.30/0.76–0.84, hand without pedicel length 1.25–1.32, movable finger length 2.07–2.14. Leg I: trochanter 0.37–0.38/0.25–0.26, femur 0.86–1.13/0.18–0.19, patella 0.69–0.75/0.20, tibia 0.67–0.72/0.14–0.16, basitarsus 0.42–0.46/0.10–0.14, telotarsus 0.54–0.61/0.10–0.11. Leg IV: trochanter 0.77–0.84/0.31–0.33, femur + patella 1.74–1.81/0.33–0.41, tibia 1.41–1.47/0.18–0.21, basitarsus 0.61–0.62/0.13, telotarsus 0.92–0.97/0.12.

Distribution. China (Jiangxi).

Remarks. The dividing line between basitarsus and telotarsus of the male leg I of this new species is usually indistinct in specimens examined, except for one paratype, which has this line slightly visible (Fig. 16l). There is no other distinct difference among these male specimens and, as a result, we consider this difference in the visibility of the dividing lines as intraspecific variation.

The males of *S. guangmingensis*, *S. gibba*, and *S. papillata* have a specialized leg I, but this new species can be separated by having a distal depression on leg I femur. Females of this new species can be distinguished from other *Stenohya* species by the following: carapace 1.02–1.10 times longer than broad (1.15–1.28 in *S. curvata*; 1.13 in *S. hainanensis*; 1.33–1.49 in *S. huangji*; 1.15–1.28 in *S. pengae*; 1.18–1.24 in *S. tengchongensis*), the presence of 27–31 setae on carapace (24 in *S. bicornuta* and *S. hainanensis*; 23 in *S. meiacantha* and *S. tengchongensis*; 39–42 in *S. papillata*); the presence of six long setae on apex of pedipalpal coxa (eight in *S. bicornuta* and *S. papillata*; 10 in *S. spinata*), the pedipalpal patella 3.39–3.46 times longer than broad (2.81–2.86 in *S. arcuata*; 4.70–5.31 in *S. huangji*; 2.68 in *S. meiacantha*; 3.83–3.93 in *S. pengae*; 3.53–3.62 in *S. spinata*; 2.63–2.67 in *S. tengchongensis*); the presence of 92–94 teeth on pedipalpal movable chelal finger (115–119 in *S. arcuata*; 68 in *S. bomica*; 46–51 in *S. huangji*; 76 in *S. meiacantha*; 79–87 in *S. gibba*; 45–55 in *S. pengae*; 76–78 in *S. spinata*); and the presence of 95–98 teeth on pedipalpal fixed chelal finger (124–129 in *S. arcuata*; 105 in *S. bicornuta*; 76 in *S. bomica*; 63–69 in *S. huangji*; 84 in *S. meiacantha*; 66–79 in *S. pengae*) (Zhao and Zhang 2011; Zhao et al. 2011; Hu and Zhang 2012; Yang and Zhang 2013; Guo and Zhang 2016; Guo et al. 2019; Zhan et al. 2023).

Discussion

In addition to sexually dimorphic pedipalp, the three new species described here have uniquely sexual dimorphic leg I; that is, the femur and patella are enlarged or have an inward depression, and the basitarsus and telotarsus are fused or semi-fused in males. In particular, the male of *S. gibba* has a large columnar projection on the basitarsus and telotarsus of leg I, which has not been reported in other *Stenohya* species. According to Zhan et al. (2023) the three potential functions of the sexually dimorphic pedipalp are controlling the female during mating, attracting a female during courtship, or serving as a weapon in male-to-male competition. Given the proximity of the pedipalp and leg I, the specialized leg I may interact with the pedipalp in some manner while conducting any of these three potential functions. The discovery of new species enriches our knowledge of the morphological diversity of *Stenohya* pseudoscorpions. The various sexually dimorphic structures imply that *Stenohya* species may have differing adaptive methods under sexual or natural selection.

Updated key to the genus *Stenohya* species from China (modified from Zhan et al. 2023)

- 1 Male leg I enlarged 2
- Male leg I not enlarged..... 4
- 2 Male basitarsus and telotarsus of leg I each with a large columnar projection on the lateral side..... ***S. gibba* sp. nov.**
- Male basitarsus and telotarsus of leg I without large projections..... 3
- 3 Male pedipalpal chelal hand with a papillary projection on the ventral face; femur of leg I straight..... ***S. papillata* sp. nov.**
- Male femur of leg I with an inward depression at the distal part.....
..... ***S. guangmingensis* sp. nov.**
- 4 Male pedipalpal femur and/or patella with projections on prolateral surfaces..... 5
- Male pedipalpal femur and patella without prolateral projections 7
- 5 Male pedipalpal femur and patella with strong long peg-like projections on prolateral surfaces ***S. spinata* Zhan, Feng & Zhang, 2023**
- Male pedipalpal patella normal, femur with tubercles on prolateral face... 6
- 6 Chelal hand with 14 tooth-shaped tubercles
..... ***S. dongtianensis* Li & Shi, 2023**
- Chelal hand with 42 tooth-shaped tubercles ***S. jiahensis* Li & Shi, 2023**
- 7 Male pedipalpal chelal hand with projection on prolateral surface 8
- Male pedipalpal chelal hand without prolateral projection..... 10
- 8 Prolateral projection of male chelal hand with 2 hornlike bulges
..... ***S. bicornuta* Guo, Zang & Zhang, 2019**
- Prolateral projection of male chela hand with pointed projection 9
- 9 Male pedipalpal femur with a depression at the base of prolateral face; movable finger basally curved in ventral view
..... ***S. curvata* Zhao, Zhang & Jia, 2011**
- Male pedipalpal with straight femur; movable finger straight or slightly procurved ***S. meiacantha* Yang & Zhang, 2013**
- 10 Male pedipalpal femur strongly procurved..... 11
- Male pedipalpal femur straight or slightly procurved 12
- 11 Male apex of pedipalpal coxa only with 4 long setae, short acicular seta absent ***S. arcuata* Guo, Zang & Zhang, 2019**
- Male apex of pedipalpal coxa with 3 long setae and 10–12 short acicular ones..... ***S. setulosa* Guo & Zhang, 2016**
- 12 Each of chelal fingers with more than 85 teeth..... 13
- Each of chelal fingers with less than 85 teeth..... 14
- 13 Male pedipalpal femur distally thickened, noticeably thicker than the basal section..... ***S. tengchongensis* Yang & Zhang, 2013**
- Male pedipalpal femur not distally thickened.....
..... ***S. hainanensis* Guo & Zhang, 2016**
- 14 Pedipalpal patella 4.0–6.0 times longer than broad..... 15
- Pedipalpal patella 2.5–3.0 times longer than broad.....
..... ***S. bomica* Zhao & Zhang, 2011**
- 15 Carapace with more than 30 setae 16
- Carapace with less than 30 setae ... ***S. xiningensis* Zhao, Zhang & Jia, 2011**

- 16 Movable chelal finger with less than 50 teeth; galea divided into 4 or 5 branches**S. *huangi* Hu & Zhang, 2012**
– Movable chelal finger with more than 50 teeth; galea divided into 6 branches**S. *pengae* Hu & Zhang, 2012**

Acknowledgements

We sincerely thank Jianzhou Sun, Tao Zheng, and Songtao Shi (Hebei University) for their help during the fieldwork. The manuscript benefited greatly from comments by Dr Xinping Wang (University of Florida, USA). We are grateful to subject editor Jana Christophoryová and copy editor Robert Forsyth and Polina Petrakieva, and two reviewers Dr Mark Harvey, and the anonymous reviewer for their helpful suggestions that substantially improved this manuscript.

Additional information

Conflict of interest

The authors have declared that no competing interests exist.

Ethical statement

No ethical statement was reported.

Funding

This research is supported by the Natural Science Foundation of Hebei Province (no. C2021201030), and the Advanced Talents Incubation Program of the Hebei University (grant 521100223004).

Author contributions

Writing-original draft: Jiaqi Zhao. Writing-review and editing: Jiaqi Zhao, Xiangbo Guo, Feng Zhang.

Author ORCIDs

Jiaqi Zhao  <https://orcid.org/0009-0001-4397-1697>

Xiangbo Guo  <https://orcid.org/0000-0002-7074-8642>

Feng Zhang  <https://orcid.org/0000-0002-3347-1031>

Data availability

All of the data that support the findings of this study are available in the main text.

References

- Beier M (1967) Pseudoscorpione vom kontinentalen Südost-Asien. *Pacific Insects* 9: 341–369.
- Chamberlin JC (1931) The arachnid order Chelonethida. *Stanford University Publications. Biological Sciences* 7 (1): 1–284.
- Guo XB, Zhang F (2016) Description of two new species of *Stenohya* Beier, 1967 (Pseudoscorpiones: Neobisiidae) from China. *Entomological News* 126(1): 1–11. <https://doi.org/10.3157/021.126.0102>

- Guo XB, Zang X, Zhang F (2019) Two new *Stenohya* species (Pseudoscorpiones: Neobisiidae) from the Gaoligong Mountains, Southwestern China. *Acta Zoologica Academiae Scientiarum Hungaricae* 65(2): 95–105. <https://doi.org/10.17109/AZH.65.2.95.2019>
- Harvey MS (1991) Notes on the genera *Parahya* Beier and *Stenohya* Beier (Pseudoscorpionida: Neobisiidae). *Bulletin - British Arachnological Society* 8(9): 288–292.
- Harvey MS (1992) The phylogeny and classification of the Pseudoscorpionida (Chelicerata: Arachnida). *Invertebrate Systematics* 6(6): 1373–1435. <https://doi.org/10.1071/IT9921373>
- Hu JF, Zhang F (2012) Description of two new *Stenohya* species from China (Pseudoscorpiones, Neobisiidae). *ZooKeys* 213: 79–91. <https://doi.org/10.3897/zookeys.213.2237>
- Judson MLI (2007) A new and endangered species of the pseudoscorpion genus *Lagynochthonius* from a cave in Vietnam, with notes on chelal morphology and the composition of the Tyrannochthoniini (Arachnida, Chelonethi, Chthoniidae). *Zootaxa* 1627(1): 53–68. <https://doi.org/10.11646/zootaxa.1627.1.4>
- Leclerc P, Mahnert V (1988) A new species of the genus *Levigatocreagris* Čurčić (Pseudoscorpiones: Neobisiidae) from Thailand, with remarkable sexual dimorphism. *Bulletin - British Arachnological Society* 7(9): 273–277.
- Li YC, Shi AM (2023) Two new species of the pseudoscorpion genus *Stenohya* (Pseudoscorpiones: Neobisiidae) from Guangxi Zhuang Autonomous Region, China. *Zootaxa* 5278(2): 387–395. <https://doi.org/10.11646/zootaxa.5278.2.11>
- Schawaller W (1987) Neue Pseudoskorpion-Funde aus dem Nepal-Himalaya, II (Arachnida: Pseudoscorpiones). *Senckenbergiana Biologica* 68: 199–221.
- WPC (2022) World Pseudoscorpiones Catalog. Natural History Museum Bern. <https://wac.nmbe.ch/order/pseudoscorpiones/3> [Accessed on 05.08.2024]
- Yang J, Zhang F (2013) Two new species of the genus *Stenohya* Beier from Yunnan, China (Pseudoscorpiones Neobisiidae). *Acta Zoologica Academiae Scientiarum Hungaricae* 59(2): 131–141.
- Zhan NN, Feng ZG, Guo XB, Zhang F (2023) Description of two *Stenohya* species from China (Pseudoscorpiones, Neobisiidae), with comments on the exaggerated sexual dimorphic pedipalp in this genus. *ZooKeys* 1172: 217–237. <https://doi.org/10.3897/zookeys.1172.104773>
- Zhao YW, Zhang F (2011) A new species of the genus *Stenohya* Beier, 1967 (Pseudoscorpiones: Neobisiidae) from China. *Journal of Hebei University Natural Science Edition* 31(3): 299–303. <https://doi.org/10.11646/zootaxa.2834.1.5>
- Zhao YW, Zhang F, Jia Y (2011) Two new species of the genus *Stenohya* Beier, 1967 (Pseudoscorpiones, Neobisiidae) from China. *Zootaxa* 2834: 57–64. <https://doi.org/10.11646/zootaxa.2834.1.5>

Three new species of dragon pseudoscorpions (Pseudoscorpiones, Pseudotyranochthoniidae) from China

Yanmeng Hou^{1,2}, Feng Zhang²

¹ College of Life Sciences, Capital Normal University, 105 Xisanhuanbeilu, Haidian District, Beijing 100048, China

² The Key Laboratory of Zoological Systematics and Application, Institute of Life Science and Green Development, College of Life sciences, Hebei University, Baoding, Hebei 071002, China

Corresponding author: Feng Zhang (dudu06042001@163.com)

Abstract

Three new pseudoscorpions in the family Pseudotyranochthoniidae are described from China: *Allochthonius hispidus* **sp. nov.** from Chongqing (Wushan County), *Spelaeochthonius huanglaoensis* **sp. nov.** from Beijing (Fangshan District), and *Spelaeochthonius tuoliangensis* **sp. nov.** from Hebei (Pingshan County). Detailed diagnoses and illustrations of all new species are provided.

Key words: *Allochthonius*, morphology, *Spelaeochthonius*, taxonomy

Introduction

The monophyletic pseudoscorpion family Pseudotyranochthoniidae Beier, 1932, originated in East Asia during the Middle Triassic (Harms et al. 2024) and is one of the earliest branches of pseudoscorpion families. The group is small-bodied, usually less than 3 mm, but the chelicerae are disproportionately large and resemble the jaws of the mythical dragon. Consequently, its group has earned the colloquial name dragon pseudoscorpions (Harms et al. 2024). Members of the family can be distinguished from all other pseudoscorpions in having trichobothria *ib* and *isb* located at the base of the fixed chelal finger and coxal spines present only on coxae I (Harms and Harvey 2013). Pseudotyranochthoniidae are distributed on all continents except Antarctica and inhabit leaf litter and caves (You et al. 2022; Gao et al. 2023). Niche modeling suggests that the distribution of pseudotyranochthoniids is determined by the interaction of constantly moderate temperatures and high moisture availability, a pattern that is globally repeated (Harms 2018; Harms et al. 2019). To date, this group comprises 80 described species in six genera. Throughout Asia, pseudotyranochthoniids are represented by three genera, *Allochthonius* Chamberlin, 1929, *Centrochthonius* Beier, 1931, and *Spelaeochthonius* Morikawa, 1954, and all extant species in these three genera are narrow-range endemics (Fig. 1; WPC 2024).

The monophyly of both *Allochthonius* and *Spelaeochthonius* receives high support (Harms et al. 2024). The genus *Allochthonius* comprises 34 species, with 14 species documented from China and the remainder distributed across Russia,



Academic editor: Fedor Konstantinov

Received: 29 August 2023

Accepted: 13 May 2024

Published: 4 June 2024

ZooBank: <https://zoobank.org/41A41142-ED13-4322-8B86-3681C2FAE4F3>

Citation: Hou Y, Zhang F (2024)

Three new species of dragon pseudoscorpions (Pseudoscorpiones, Pseudotyranochthoniidae) from China. ZooKeys 1204: 135–154. <https://doi.org/10.3897/zookeys.1204.111842>

Copyright: © Yanmeng Hou & Feng Zhang.
This is an open access article distributed under terms of the Creative Commons Attribution License (Attribution 4.0 International – CC BY 4.0).

Japan, and South Korea. It is diagnosed by the carapace frequently having 22–28 setae (but fewer in some cave-dwelling congeners; Sakayori 2000; Viana and Ferreira 2021; Gao et al. 2023), coxal spines present on a common protuberance, spray- or fan-shaped, and the intercoxal tubercle generally larger (Harvey and Harms 2022; Schwarze et al. 2022). About 35% (12 of 34) of the species in this genus lack eyes, with almost all of them being cave-dwelling, except for *A. brevitus* Hu & Zhang, 2012, which is the only epigeal species (Morikawa 1954, 1956, 1960; Hu and Zhang 2012; Zhang and Zhang 2014; Viana and Ferreira 2021; Gao et al. 2023).

The genus *Spelaeochthonius*, currently found only in East Asia, includes 11 described species. It can be distinguished from other pseudotyranochthoniid genera by the number of carapaceal setae (only 16), the number, shape, and arrangement of the coxal spines (never on a common protuberance and more than seven blades that are longer and distally pinnate or serrate), and the shape of the intercoxal tubercle (bisetose and generally smaller than that of *Allochthonius*) (Morikawa 1956; You et al. 2022). The genus consists exclusively of subterranean species with strongly troglitic habitus occurring in China (two species), South Korea (three species), and Japan (six species) (WPC 2024).

This study describes three new pseudotyranochthoniid species from both the surface and subterranean environments. Detailed diagnoses, descriptions, and illustrations are provided for each species. Two of these species are placed in *Spelaeochthonius*, while one is assigned to *Allochthonius*. Additionally, a distribution map of all Chinese pseudotyranochthoniid species is given.

Materials and methods

The specimens examined for this study are preserved in 75% alcohol and deposited in the Museum of Hebei University (**MHBU**), Baoding, China, and the Museum of Southwest University (**MSWU**), Chongqing, China. Photographs, drawings, and measurements were taken using a Leica M205A stereomicroscope equipped with a Leica DFC550 camera. Detailed examination was carried out under an Olympus BX53 upright microscope. Scanning electron microscopy (SEM) was done under high vacuum with a JEOL JSM-IT500 after critical-point drying and gold-palladium coating. The distribution map was made using ArcGIS v. 10.6 (Fig. 1). All images were edited and formatted using Inkscape v. 1.0.2.0 and Adobe Photoshop 2022.

Terminology and measurements follow Chamberlin (1931) with minor modifications to the terminology of trichobothria (Harvey 1992; Judson 2007) and chelicera (Judson 2007). The chela and legs were measured in lateral view and others were taken in dorsal view. All measurements are given in mm unless noted otherwise. Proportions and measurements of chelicerae, carapace and pedipalps correspond to length/breadth, and those of legs to length/depth. For abbreviations of trichobothria, see Chamberlin (1931).

Taxonomy

Family Pseudotyranochthoniidae Beier, 1932

Genus *Allochthonius* Chamberlin, 1929

Type species. *Chthonius opticus* Ellingsen, 1907, by original designation.

***Allochthonius hispidus* sp. nov.**

<https://zoobank.org/FB289038-20FB-46BD-8B36-07A04E1BF95B>

Figs 1–4

Chinese name. 多毛异伪蝎.

Type materials. **Holotype:** CHINA • ♂; Chongqing Municipality, Wushan County, Dangyang Town, Wushanya; 31°28.356'N, 109°59.172'E; 1740 m a.s.l.; 02 Oct. 2021; Luyu Wang leg. (Fig. 1); Ps.-MHBU-CQWLP-21-02-01. **Paratypes:** • 2♂1♀; same data as for holotype; Ps.-MHBU-CQWLP-21-02-02–04 • 2♂1♀; Wushan County, Dangyang Town, Qizhi Mountain; 31°28.109'N, 109°58.716'E; 1475 m a.s.l.; same collector and collection date as for holotype; Ps.-MHBU-CQWLP-21-03-01–03 • 1♂1♀; Wushan County, Dangyang Town, Congping Mountain; 31°23.786'N, 110°2.467'E; 2150 m a.s.l.; 03 Oct. 2021; same collector as for holotype; Ps.-MHBU-CQWLP-21-07-01 & 02 • 1♀; Wushan County, Dangyang Town, Congping Management Station; 31°23.786'N, 110°2.055'E; 1970 m a.s.l.; 03 Oct. 2021; same collector as for holotype; Ps.-MHBU-CQWLP-21-08-01 • 1♂1♀; Wushan County, Guanyang Town, Pingqian Management Station; 31°22.379'N, 109°56.287'E; 1832 m a.s.l.; 04 Oct. 2021; same collector as for holotype; Ps.-MSWU-CQWLP-21-10-01 & 02.

Diagnosis (♂♀). *Allochthonius hispidus* sp. nov. is most similar to another epigean blind species from China, *A. brevitus*, but differs from this species in having more carapaceal setae (22–24 (♂), 21 or 22 (♀) for *A. hispidus* vs 16 (♂♀) for *A. brevitus*), more cheliceral setae (♂) (10 or 11 vs seven), more numerous chelal fingers teeth (♂) (fixed finger with 26–29 vs 18–20 teeth, movable finger with 22 or 23 vs 17 or 18 teeth), and longer pedipalps (e.g. palpal femur 5.19 (♂), 5.13–5.61 (♀) × vs 4.33–4.73 (♂), 4.79–4.92 (♀) × longer than broad, length 1.09 (♂), 1.18–1.29 (♀) mm vs 0.52–0.57 (♂), 0.64–0.67 (♀) mm; chela length 1.59–1.60 (♂), 1.76–1.84 (♀) mm vs 0.80–0.84 (♂), 0.98–1.01 (♀) mm). It differs from the other blind species in China (*A. bainiensis* Gao, Hou & Zhang, 2023, *A. pandus* Gao, Hou & Zhang, 2023, and *A. xinqiaoensis* Gao, Hou & Zhang, 2023) in having more numerous carapaceal setae (♀) (the latter three with only 14 setae) and the presence of a pair of hirsute pedipalps. It also differs from all blind congeners from Japan (*A. yoshizawai* Viana & Ferreira, 2021, *A. ishikawai* Morikawa, 1954, and its subspecies) in having more cheliceral setae (♂) (10 or 11 vs at most seven) and more numerous fixed chelal finger teeth (♂) (26–29 vs at most 17).

Etymology. The specific name is derived from the Latin word *hispidus* (hirsute, hairy), which refers to the presence of abundant setae on the chela, palpal femur, and patella.

Description. **Adult males** (Figs 1, 2A, 3A–G, 4). **Colour:** generally pale yellow; chelicerae, pedipalps and tergites slightly darker; soft parts pale. **Cephalothorax** (Figs 3A, C, 4A, C): carapace subquadrate, 0.87–0.88× longer than broad, gently narrowed posteriorly; surface smooth but the posterior lateral parts with squamous sculpturing; without furrows but with five anterior lyrifissures and two posterior lyrifissures; no traces of eyes; epistome absent, space between median setae slightly recurved; with 22–24 setae arranged 12–14: 4: 2: 2: 2, most setae heavy, long and gently curved. Chaetotaxy of coxae: P 3, I 3–4, II 5–6, III 4–5, IV 5; manducatory process with two acuminate distal setae, anterior seta more than 1/2 length of medial seta; coxal spines present on coxa I only, consisting of a tubercle expanded terminally into a characteristic spray- or fan-shaped of

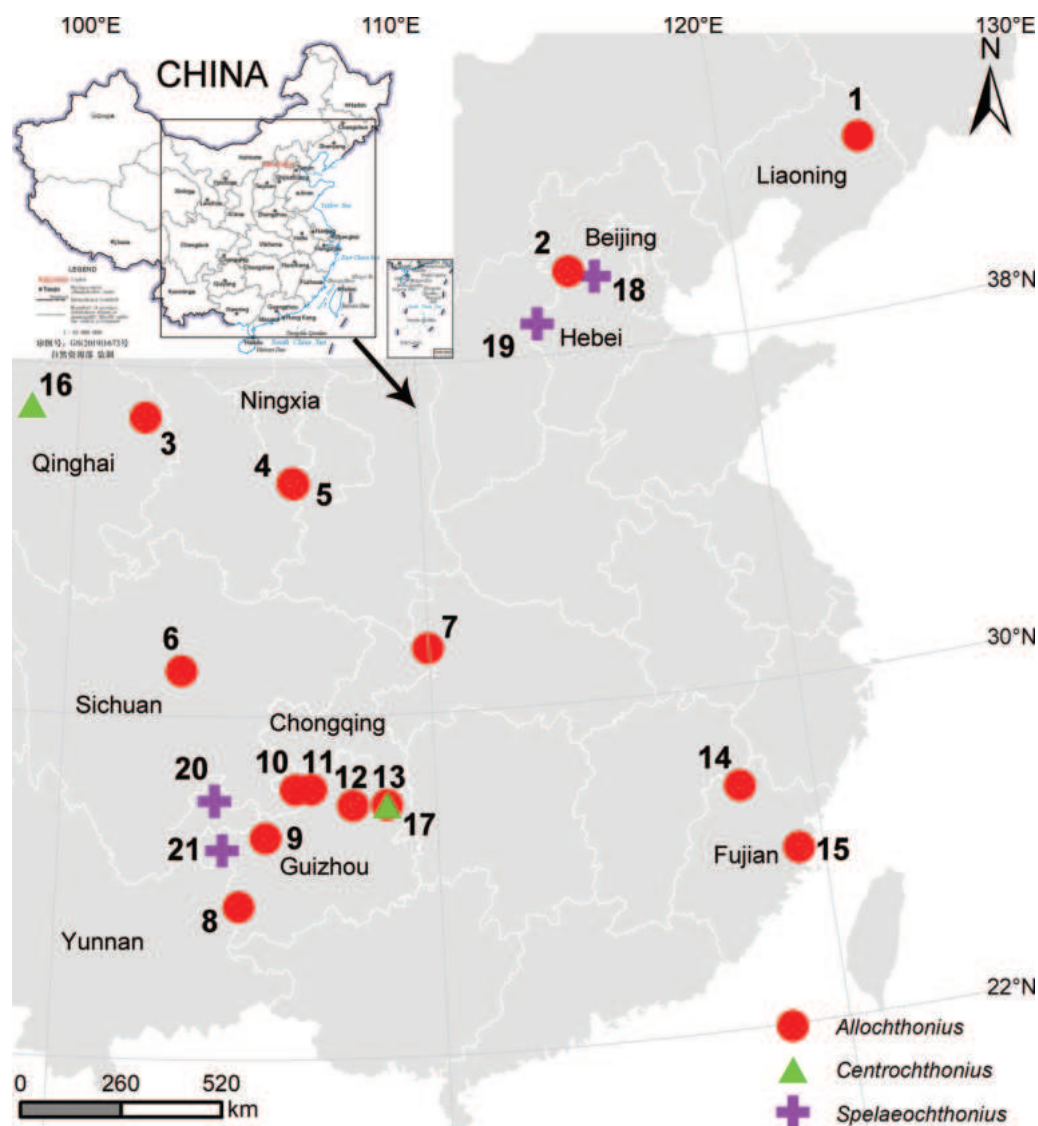


Figure 1. Distribution of all Pseudotyranchothoniidae species in China. **1** *Allochthonius liaoningensis* Hu & Zhang, 2012 **2** *A. exornatus* Gao & Zhang, 2013 **3** *A. wui* Hu & Zhang, 2011 **4** *A. jingyuanus* Zhang & Zhang, 2014 **5** *A. brevitus* **6** *A. sichuanensis* (Schawaller, 1995) **7** *A. hispidus* sp. nov. **8** *A. lini* Li, 2023 **9** *A. xuae* Li, 2023 **10** *A. bainiensis* **11** *A. pandus* **12** *A. xinqiaoensis* **13** *A. fanjingshan* Gao, Zhang & Zhang, 2016 **14** *A. trigonus* Hu & Zhang, 2011 **15** *A. fuscus* Hu & Zhang, 2011 **16** *Centrochthonius kozlovi* (Redikorzev, 1918) **17** *C. cheni* (Gao, Zhang & Zhang, 2016) **18** *Spelaeochthonius huan-glaensis* sp. nov. **19** *S. tuoliangensis* sp. nov. **20** *S. yinae* **21** *S. wulibeiensis*.

five elevate processes which extend apically, subequal in length (Figs 3C, 4C); a larger bisetose intercoxal tubercle present between coxae III and IV (Fig. 3C). **Chelicera** (Figs 3B, 4B, D): large, approximately as long as carapace, 2.52× longer than broad; nine or 10 setae and two lyrifissures (exterior condylar lyrifissure and exterior lyrifissure) present on hand, all setae acuminate, ventrobasal seta shorter than others; movable finger with one medial seta. Cheliceral palm with moderate hispid granulation on both ventral and dorsal sides. Both fingers with well-developed teeth, fixed finger with eight or nine acute teeth, distal one largest, plus five or six small basal teeth, 13–15 in total; movable finger with 15 or 16 retrorse contiguous teeth of equal length; galea absent. Serrula exterior with 20 or 21 blades and serrula interior with 12–14 blades. Rallum in two rows and composed of 11 finely pinnate blades (Fig. 4D). **Pedipalp** (Figs 3D–F, 4E–G):



Figure 2. *Allochthonius hispidus* sp. nov. **A** holotype male, habitus (dorsal view) **B** paratype female, habitus (dorsal view). Scale bars: 0.50 mm.

long and slender, trochanter 1.38–1.48, femur 5.19, patella 2.62–2.89, chela 4.82–5.16, hand 1.79–1.90× longer than broad; femur 1.98× longer than patella; movable chelal finger 1.73–1.76× longer than hand and 0.64–0.65× longer than chela. Setae generally long and acuminate; one distal lyrifissure present on patella (Figs 3E, 4F). Chelal palm robust and slightly constricted towards fingers. Fixed chelal finger and hand with eight trichobothria plus duplex trichobothrium (*dt*), movable chelal finger with four trichobothria, *ib*, *isb*, *eb*, *esb*, and *ist* clustered at the base of fixed finger, *ist* slightly distal to *esb*; *it* slightly distal to *est*, situated subdistally; *et* situated subdistally, very close to chelal teeth; *dt* situated distal to *et*, near the tip of fixed finger; *sb* situated closer to *b* than to *st* (Fig. 4E). Abundant setae present on palpal femur, patella, and chela. Sensilla absent. Both chelal fingers with a row of teeth, homodontate, spaced regularly along the margin, larger and well-spaced teeth present in the middle of the row, becoming smaller and closer distally and proximally: fixed chelal finger with 26–29 teeth, slightly retrorse and pointed; movable chelal finger with 22 or 23 teeth (slightly smaller than teeth on fixed chelal finger) and a tubercle between the seventh and eighth teeth (Figs 3D, 4E). Chelal fingers slightly curved in dorsal view (Figs 3F, 4G). **Opisthosoma**: generally typical, pleural membrane finely granulated. Tergites and sternites undivided; setae uniseriate and acuminate. Tergal chaetotaxy I–XII: 2: 6–8: 8–10: 10–11: 10–11: 11–12: 10–13: 13–14: 8: 6: TT: 0. Sternal chaetotaxy III–XII: 12–14: 15–17: 14–15: 12–15: 12–14: 13–14: 12: 8–9: 0: 2. Anterior genital operculum with eight or nine setae, genital opening pit-like, with seven or 10 marginal setae on each side, 26 in total, with a pair of lyrifissures present anterolateral and posterolateral to genital opening, respectively (Fig. 3G). **Legs** (Fig. 4H, I): generally typical, long, and

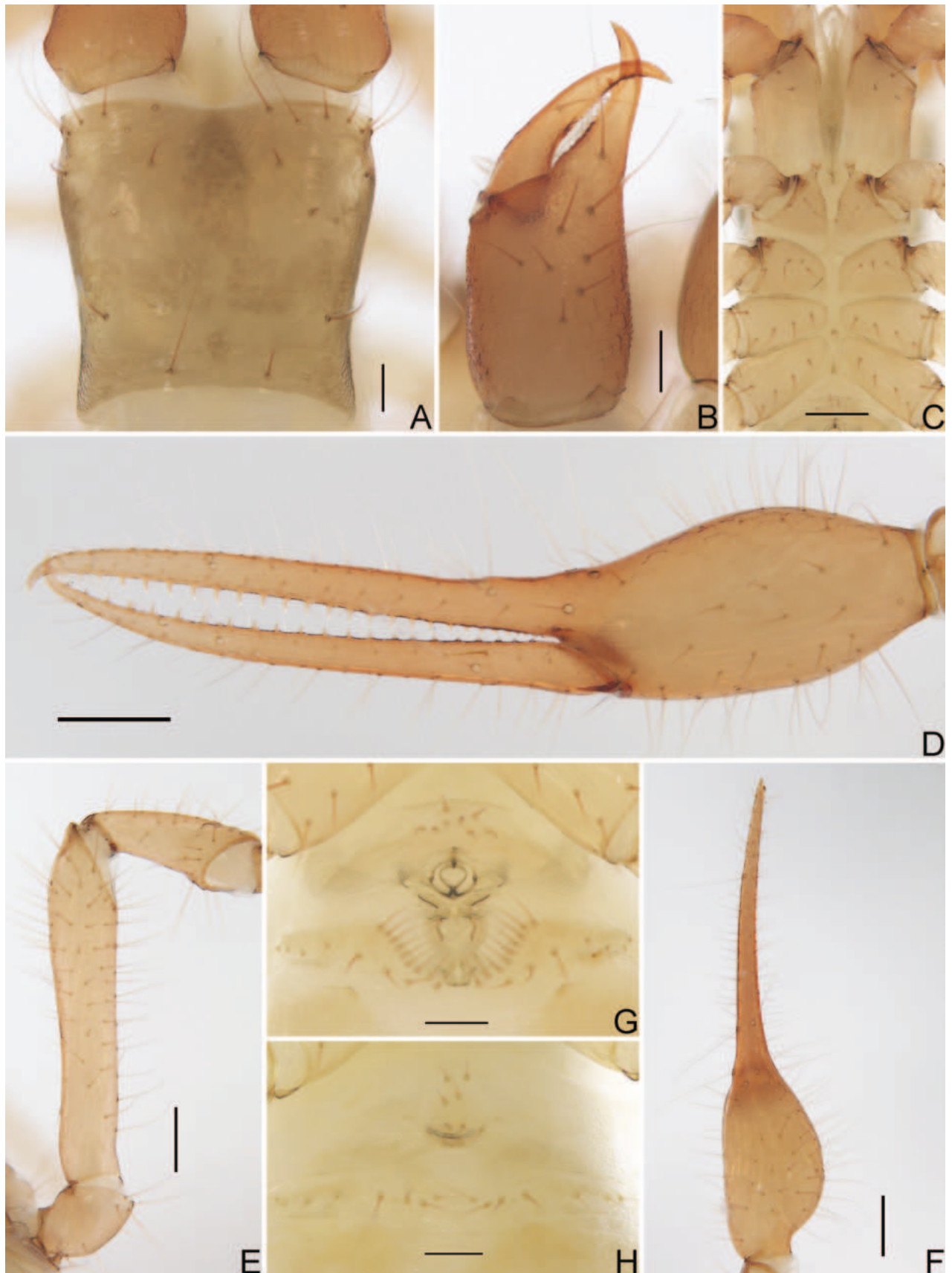


Figure 3. *Allochthonius hispidus* sp. nov. **A** carapace (dorsal view) **B** left chelicera (dorsal view) **C** coxae (ventral view) **D** left chela (lateral view) **E** left pedipalp (minus chela, dorsal view) **F** left chela (dorsal view) **G** male genital area (ventral view) **H** female genital area (ventral view). Scale bars: 0.20 mm (**C–F**); 0.10 mm (**A, B, G, H**).

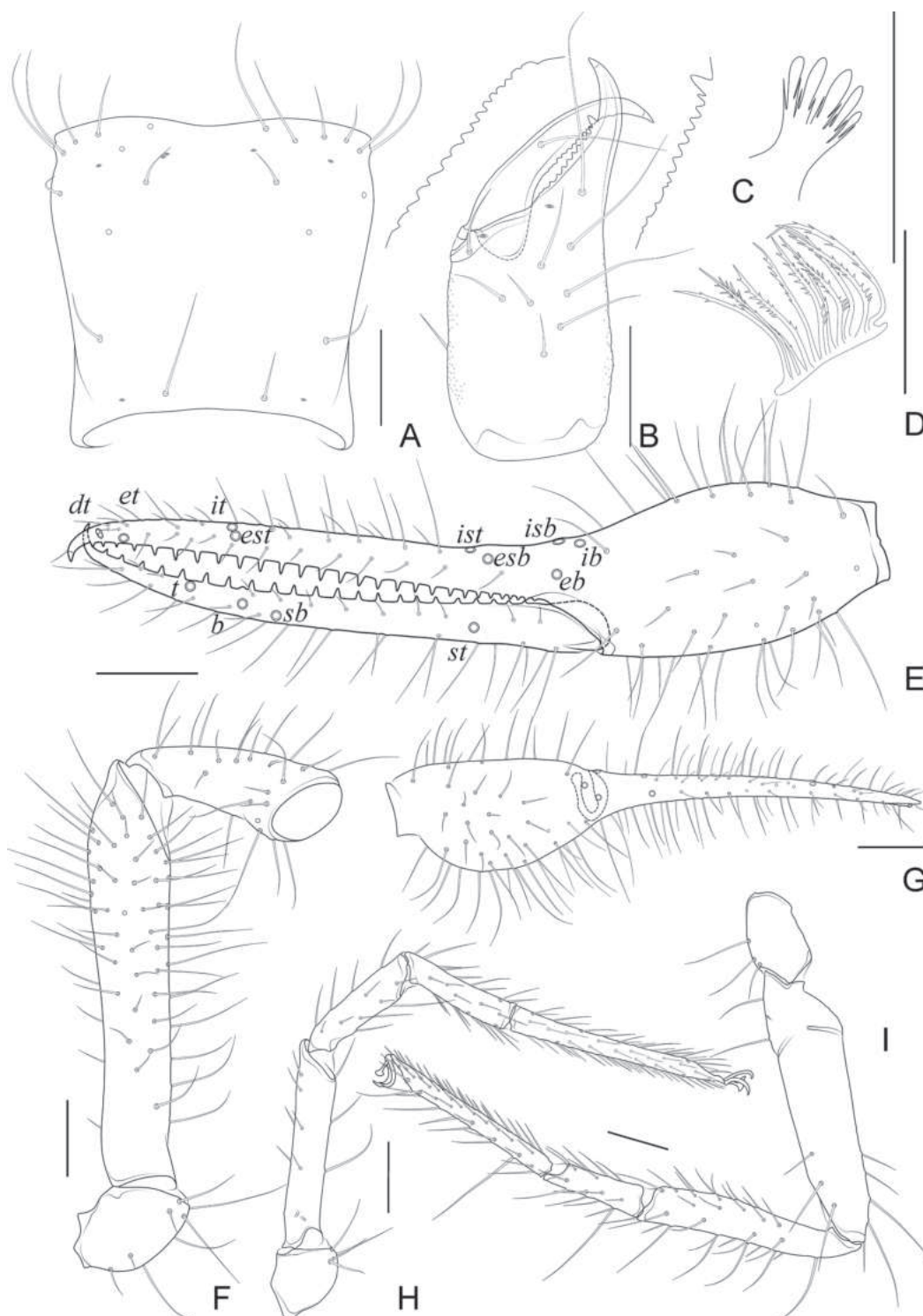


Figure 4. *Allochthonius hispidus* sp. nov., holotype male **A** carapace (dorsal view) **B** left chelicera (dorsal view), with details of teeth **C** coxal spines on coxae I (ventral view) **D** rallum **E** left chela (lateral view), with details of trichobothrial pattern **F** left pedipalp (minus chela, dorsal view) **G** left chela (dorsal view) **H** leg I (lateral view) **I** leg IV (lateral view). Scale bars: 0.20 mm.

slender. Fine granulation present on anterodorsal faces of femur IV and patella IV. Femur of leg I 1.45× longer than patella and with two lyrifissures at the base of femur; tarsus 2.00× longer than tibia. Femoropatella of leg IV 3.48–3.70× longer than deep and with one lyrifissure at the base of femur; tibia 5.25–5.67×

longer than deep; with basal tactile setae on both tarsal segments: basitarsus 3.44–3.56× longer than deep (TS = 0.25–0.32), telotarsus 8.86–9.14× longer than deep and 2.00× longer than basitarsus (TS = 0.17–0.21). Arolium slightly shorter than the claws, not divided; claws simple. **Dimensions of adult males** (length/breadth or, in the case of the legs, length/depth in mm): body length 2.72–2.78. Pedipalps: trochanter 0.29–0.31/0.21, femur 1.09/0.21, patella 0.55/0.19–0.21, chela 1.59–1.60/0.31–0.33, hand 0.59/0.31–0.33, movable finger length 1.02–1.04. Chelicera 0.68/0.27, movable finger length 0.36–0.38. Carapace 0.56–0.58/0.64–0.67. Leg I: trochanter 0.19–0.20/0.17–0.18, femur 0.55/0.11, patella 0.38/0.09–0.10, tibia 0.31–0.32/0.08, tarsus 0.62–0.64/0.06. Leg IV: trochanter 0.31–0.32/0.18–0.19, femoropatella 0.80–0.85/0.23, tibia 0.63–0.68/0.12, basitarsus 0.31–0.32/0.09, telotarsus 0.62–0.64/0.07.

Adult females (Figs 2B, 3H). Mostly same as males but a little larger (i.e. body length is about 1.08× that of males); cheliceral hand of one female with 11 setae; chaetotaxy of coxae: P 3, I 4, II 4–5, III 5, IV 5; tergal chaetotaxy I–XII: 2: 6: 6–8: 10: 10–11: 11–12: 12: 11–12: 8–9: 5: TT: 0; sternal chaetotaxy IV–XII: 15–17: 11–13: 13–14: 13–14: 13: 12–14: 9: 0: 2; anterior genital operculum with eight setae, posterior margin with 15 or 17 marginal setae, 23–25 in total; leg IV with a long tactile seta on both tarsal segments: basitarsus 3.33–3.50× longer than deep (TS = 0.37–0.40), telotarsus 9.57–11.00× longer than deep and 1.91–2.20× longer than basitarsus (TS = 0.20–0.21). Body length 2.44–2.97. Pedipalps: trochanter 0.32–0.37/0.22–0.24 (1.33–1.68×), femur 1.18–1.29/0.23 (5.13–5.61×), patella 0.59–0.60/0.22–0.24 (2.46–2.73×), chela 1.76–1.84/0.34–0.41 (4.49–5.18×), hand 0.64–0.68/0.34–0.41 (1.66–1.88×), movable chelal finger length 1.15–1.20. Chelicera 0.77–0.81/0.32–0.36 (2.25–2.41×), movable finger length 0.42–0.46. Carapace 0.58–0.64/0.72–0.83 (0.77–0.81×). Leg I: trochanter 0.23/0.19 (1.21×), femur 0.56–0.61/0.11–0.12 (4.67–5.55×), patella 0.38–0.39/0.10–0.11 (3.55–3.80×), tibia 0.35/0.07–0.08 (4.38–5.00×), tarsus 0.68–0.69/0.06–0.07 (9.71–11.50×). Leg IV: trochanter 0.33–0.35/0.20 (1.65–1.75×), femoropatella 0.85–0.90/0.25 (3.40–3.60×), tibia 0.68/0.13–0.14 (4.86–5.23×), basitarsus 0.30–0.35/0.09–0.10 (3.33–3.50×), telotarsus 0.66–0.67/0.06–0.07 (9.57–11.00×).

Distribution. China (Chongqing).

Genus *Spelaeochthonius* Morikawa, 1954

Type species. *Spelaeochthonius kubotai* Morikawa, 1954, by original designation.

Spelaeochthonius huanglaoensis sp. nov.

<https://zoobank.org/AFD5997B-116A-44E4-91B8-F682E488F620>

Figs 1, 5–8

Chinese name. 黄老穴伪蝎.

Type material. **Holotype:** CHINA • ♂; Beijing City, Fangshan District, Shidu Town, Wanglaopu Village, Huanglao Cave; 39°40.916'N, 115°39.041'E; 495 m a.s.l.; 19 Oct. 2021; Nana Zhan leg.; under a stone in the deep zone (Fig. 1); Ps.-MHBUBJFS-21-10-19-02-01. **Paratype:** • 1♀; same data as for holotype; Ps.-MHBUBJFS-21-10-19-02-02.



Figure 5. *Spelaeochthonius huanglaoensis* sp. nov. **A** holotype male, habitus (dorsal view) **B** paratype female, habitus (dorsal view). Scale bars: 0.50 mm.

Diagnosis (♂♀). *Spelaeochthonius huanglaoensis* sp. nov. is most similar to *S. wulibeiensis* Gao, Hou & Zhang, 2023, but differs from it in having shorter pedipalps (e.g. chela 7.94 (♂), 6.14 (♀) × vs 6.21–6.22 (♂), 5.68 (♀) × longer than broad, length 1.43 (♂), 1.72 (♀) mm vs 1.68–1.74 (♂), 1.76 (♀) mm), 1 additional cheliceral seta (seven vs six), and more numerous fixed chelal finger teeth (29 vs 22–24). It differs from *S. yinae* Li, 2023 in the number of setae on tergite II (four vs two), smaller body size (e.g. chela 7.94 (♂), 6.14 (♀) × vs 5.93 (♂), 6.30 (♀) × longer than broad, length 1.43 (♂), 1.72 (♀) mm vs 1.72 (♂), 1.89 (♀) mm), and more numerous fixed chelal finger teeth (♂) (29 vs 23).

Etymology. The species is named after its type locality, Huanglao Cave.

Description. Adult male (Figs 5A, 6A–E, 7). **Colour:** generally pale yellow; chelicerae, pedipalps and tergites slightly darker; soft parts pale. **Cephalothorax** (Figs 6A, C, 7A): carapace inverted-trapezoid, 1.04× longer than broad, gently narrowed posteriorly; surface mostly with fine reticulations; with four anterior lyrifissures and two posterior lyrifissures; no traces of eyes but eye region bulging and convex in dorsal view; epistome present and with some tiny spinules; with 16 setae arranged s4s: 4: 2: 2: 2, most setae heavy, long, and gently curved. Chaetotaxy of coxae: P 3, I 6, II 5, III 4–5, IV 4; manducatory process with two acuminate distal setae, anterior seta less than 1/2 length of medial seta (refer to female, Fig. 8C); coxal spines present on coxa I only, comprising a transverse, contiguous series of six or seven tridentate blades, which arise from a lightly sclerotized or translucent hillcock, the central ramus of each blade (except the basal one) sharply acumino-spatulate and extending beyond the lateral rami (refer to female, Fig. 8A); a small, bisetose intercoxal tubercle present between coxae III and IV (Fig. 6C). **Chelicera** (Figs 6B, 7B, C): large, approximately as long as carapace, 2.50× longer than broad; six setae and two lyrifissures (exterior condylar lyrifissure and exterior lyrifissure)

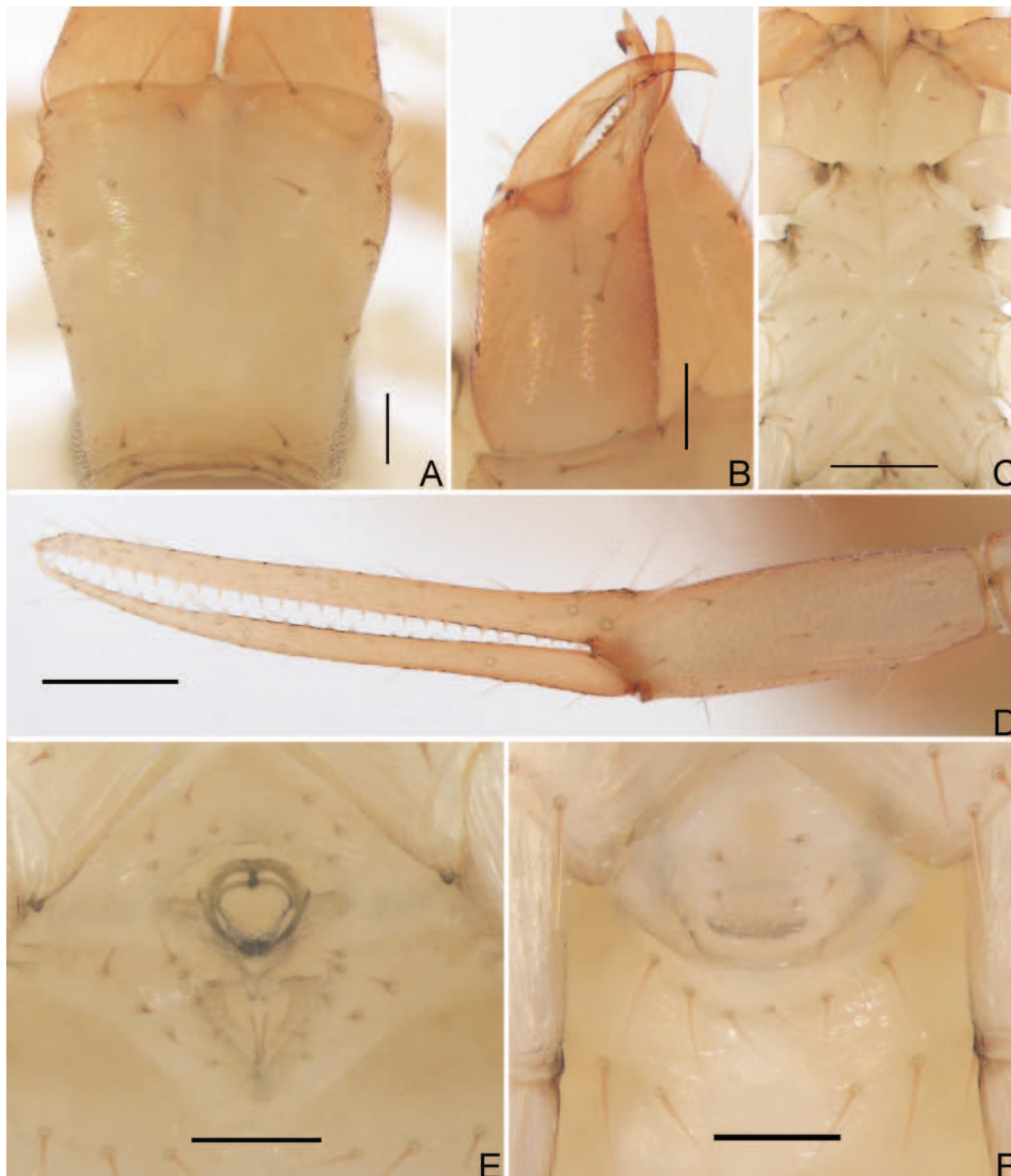


Figure 6. *Spelaeochthonius huanglaoensis* sp. nov. **A** carapace (dorsal view) **B** left chelicera (dorsal view) **C** coxae (ventral view) **D** left chela (lateral view) **E** male genital area (ventral view) **F** female genital area (ventral view). Scale bars: 0.20 mm (**C, D**); 0.10 mm (**A, B, E, F**).

present on hand, movable finger with one medial seta, all setae acuminate, ventrobasal seta shorter than others. Cheliceral palm with moderate hispid granulation on both ventral and dorsal sides. Both fingers with well-developed teeth, fixed finger with 14 acute teeth, distal one largest; movable finger with 11 retrorse contiguous teeth of equal length; galea absent. Serrula exterior with 19 blades

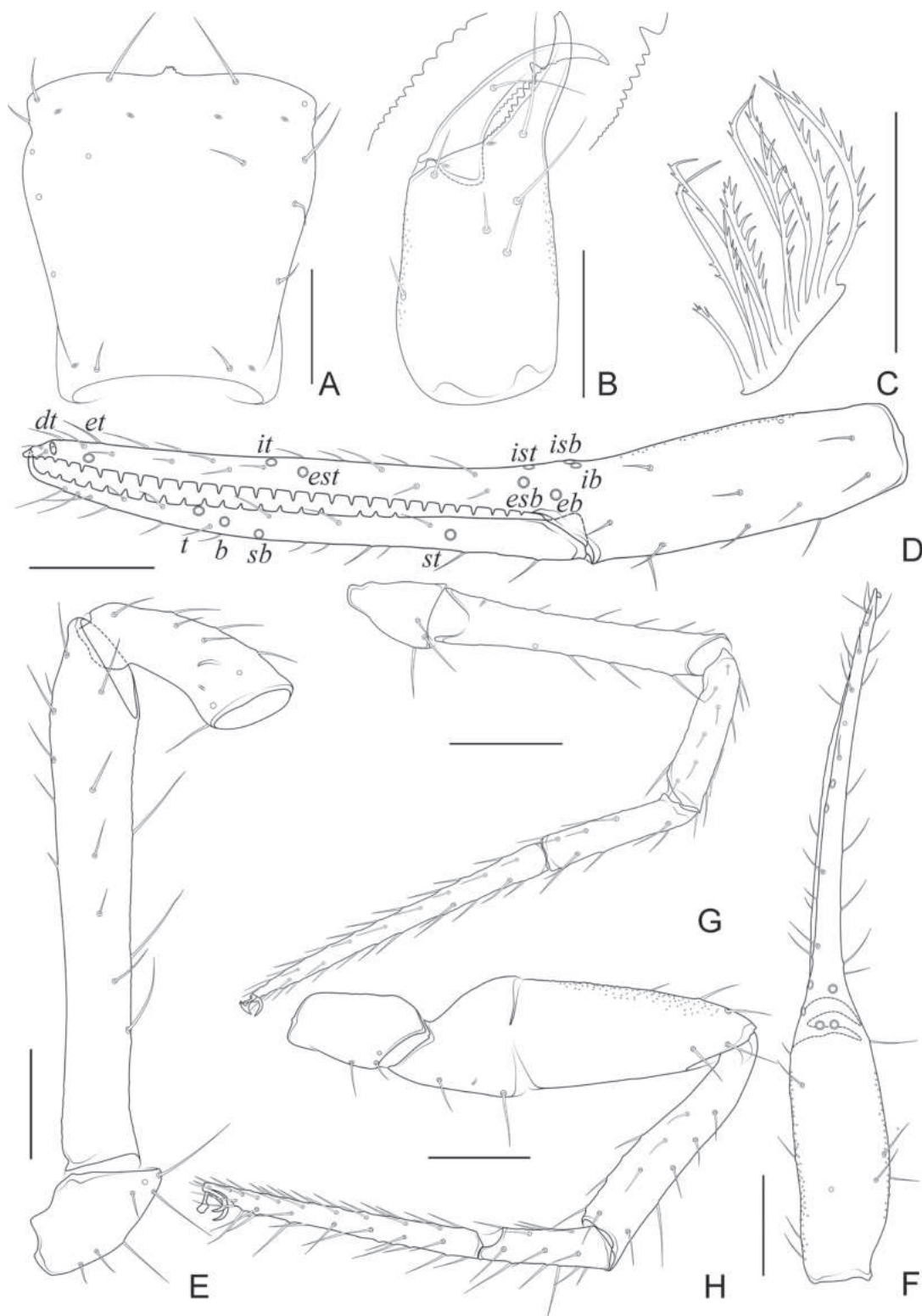


Figure 7. *Spelaeochthonius huanglaensis* sp. nov., holotype male **A** carapace (dorsal view) **B** left chelicera (dorsal view), with details of teeth **C** rallum **D** left chela (lateral view), with details of trichobothrial pattern **E** left pedipalp (minus chela, dorsal view) **F** left chela (dorsal view) **G** leg I (lateral view) **H** leg IV (lateral view). Scale bars: 0.20 mm.

(refer to female, Fig. 8B) and serrula interior with 15 blades. Rallum in two rows and composed of ten finely pinnate blades (11 blades in female), of which the basal-most blade shorter than the others (Figs 7C, 8D). **Pedipalp** (Figs 6D, 7D–F):

surfaces mostly with fine reticulations; long and slender, trochanter 1.87, femur 6.38, patella 2.69, chela 7.94, hand 3.00× longer than broad; femur 2.37× longer than patella; movable chelal finger 1.69× longer than hand and 0.64× longer than chela. Setae generally long and acuminate; one distal lyrifissure present on patella (Fig. 7E). Chelal palm slightly constricted towards fingers. Fixed chelal finger and hand with eight trichobothria plus duplex trichobothrium (*dt*), movable chelal finger with four trichobothria, *ib*, *isb*, *eb*, *esb*, and *ist* clustered at the base of fixed finger, *esb* slightly distal to *ist*; *it* slightly distal to *est*, situated subdistally and forming a pair; *et* situated subdistally, very close to chelal teeth; *dt* situated distal to *et*, near the tip of fixed finger; *sb* distinctly closer to *b* than to *st* (Fig. 7D). Microsetae (chemosensory setae) absent on hand and both palpal fingers. Sensilla absent. Both chelal fingers with a row of teeth, homodontate, spaced regularly along the margin, larger and well-spaced teeth present in the middle of the row, becoming smaller and closer distally and proximally: fixed chelal finger with 29 teeth, slightly retrorse and pointed; movable chelal finger with 19 teeth (slightly smaller than teeth on fixed chelal finger) (Figs 6D, 7D). Chelal fingers slightly curved in dorsal view (Fig. 7F). **Opisthosoma**: generally typical, ovate, pleural membrane finely granulated. Tergites and sternites undivided; setae uniseriate and acuminate. Tergal chaetotaxy I–XII: 2: 4: 4: 5: 7: 7: 7: 6: 5: 4: TT: 0. Sternal chaetotaxy III–XII: 9: 8: 10: 9: 10: 9: 7: 8: 0: 2. Anterior genital operculum with nine setae, genital opening pit-like, with seven marginal setae on each side, 23 in total (Fig. 6E). **Legs** (Fig. 7G, H): generally typical, long, and slender. Fine granulation present on anterodorsal faces of patella IV. Femur of leg I 1.73× longer than patella and with one lyrifissure at the base of femur; tarsus 2.24× longer than tibia. Femoropatella of leg IV 3.04× longer than deep and with one lyrifissure at the base of femur; tibia 5.80× longer than deep; with a long tactile seta on both tarsal segments: basitarsus 3.86× longer than deep (TS = 0.37), telotarsus 11.40× longer than deep and 2.11× longer than basitarsus (TS = 0.35). Arolium slightly shorter than the claws, not divided; claws simple. **Dimensions of adult male** (length/breadth or, in the case of the legs, length/depth in mm). Body length 1.80. Pedipalps: trochanter 0.28/0.15, femur 1.02/0.16, patella 0.43/0.16, chela 1.43/0.18, hand 0.54/0.18, movable finger length 0.91. Chelicera 0.55/0.22, movable finger length 0.28. Carapace 0.53/0.51. Leg I: trochanter 0.21/0.15, femur 0.52/0.09, patella 0.30/0.08, tibia 0.25/0.06, tarsus 0.56/0.05. Leg IV: trochanter 0.27/0.15, femoropatella 0.70/0.23, tibia 0.58/0.10, basitarsus 0.27/0.07, telotarsus 0.57/0.05.

Adult female (Figs 5B, 6F, 8). Mostly same as male; tergal chaetotaxy I–XII: 2: 4: 4: 5: 6: 6: 6: 6: 5: 4: TT: 0; sternal chaetotaxy IV–XII: 5: 6: 8: 8: 9: 9: 8: 0: 2; anterior genital operculum with five setae, posterior margin with six marginal setae, 11 in total; leg IV with a long tactile seta on both tarsal segments: basitarsus 3.44× longer than deep (TS = 0.35), telotarsus 9.86× longer than deep and 2.23× longer than basitarsus (TS = 0.36). Body length 1.86. Pedipalps: trochanter 0.35/0.19 (1.84×), femur 1.20/0.20 (6.00×), patella 0.52/0.21 (2.48×), chela 1.72/0.28 (6.14×), hand 0.62/0.28 (2.21×), movable chelal finger length 1.09. Chelicera 0.81/0.33 (2.45×), movable finger length 0.41. Carapace 0.69/0.74 (0.93×). Leg I: trochanter 0.22/0.14 (1.57×), femur 0.56/0.08 (7.00×), patella 0.37/0.08 (4.63×), tibia 0.32/0.07 (4.57×), tarsus 0.68/0.06 (11.33×). Leg IV: trochanter 0.31/0.18 (1.72×), femoropatella 0.82/0.28 (2.93×), tibia 0.68/0.11 (6.18×), basitarsus 0.31/0.09 (3.44×), telotarsus 0.69/0.07 (9.86×).

Distribution. China (Beijing).

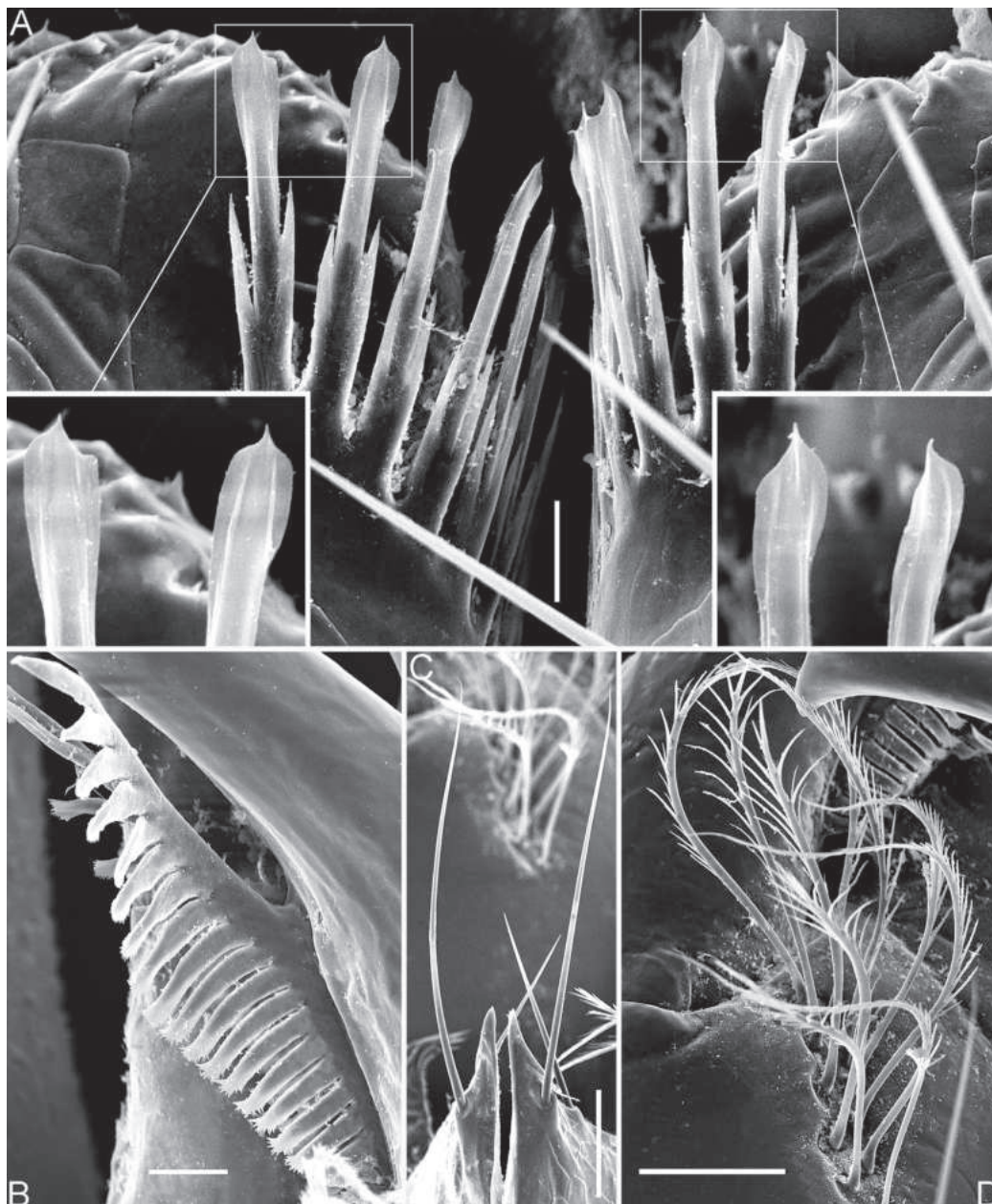


Figure 8. *Spelaeochthonius huanglaoensis* sp. nov. scanning electron micrographs, paratype female **A** coxal spines in overview, with details of tips **B** serrula exterior **C** manducatory process **D** rillum. Scale bars: 50 μm (**C**, **D**); 20 μm (**B**); 10 μm (**A**).

***Spelaeochthonius tuoliangensis* sp. nov.**

<https://zoobank.org/91BA3955-15FC-4214-B45D-2D27571EDCCA>

Figs 1, 9–11

Chinese name. 驼梁穴伪蝎.

Type material. **Holotype:** CHINA • ♀; Hebei Province, Shijiazhuang City, Pingshan County, Tuoliang National Nature Reserve; 38°43.233'N, 113°46.800'E; 1620 m a.s.l.; 13 May. 2018; Xiangbo Guo and Zhaoyi Li leg. (Fig. 1); Ps.-MHBU-HB2018.05.13-01-01. **Paratype:** • 1 ♀; same data as for holotype; Ps.-MHBU-HB2018.05.13-01-02.

Diagnosis (♀). *Spelaeochthonius tuoliangensis* sp. nov. can be separated from its congeners by its visible eyespots. It is most similar to *S. huanglaoensis* sp. nov.

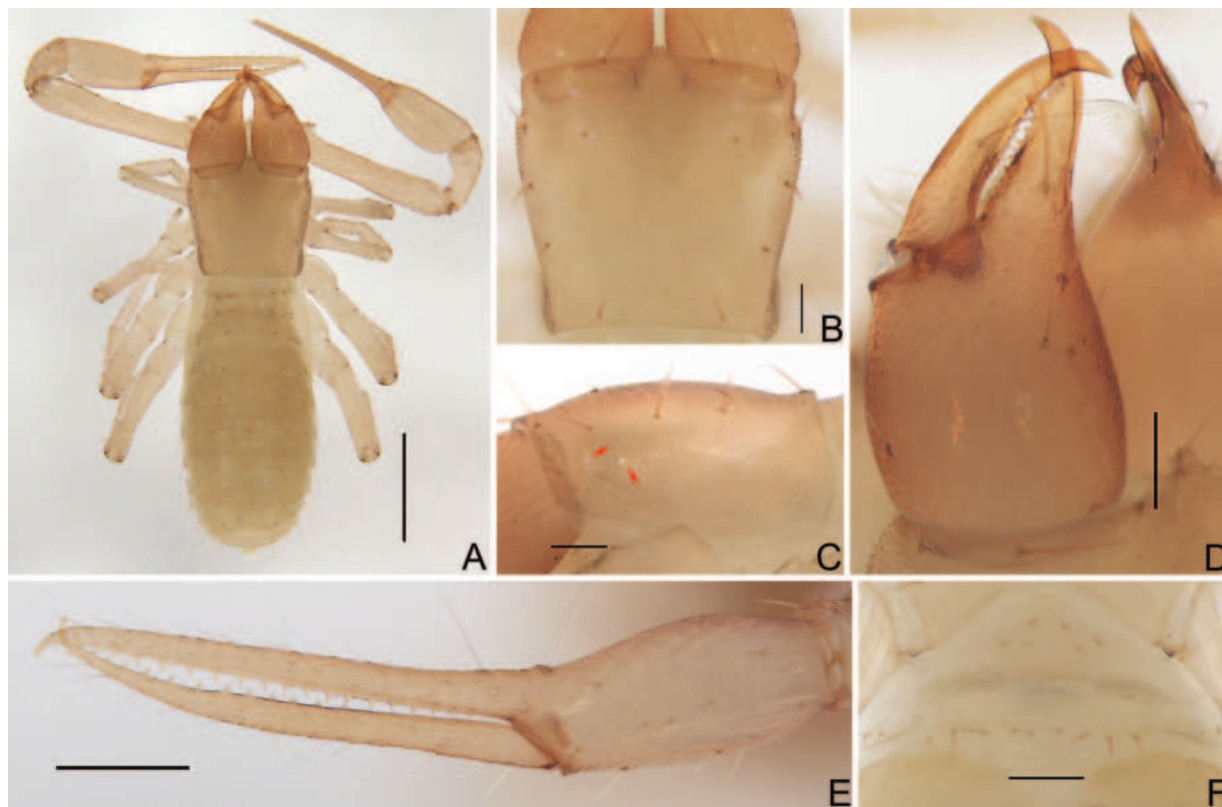


Figure 9. *Spelaeochthonius tuoliangensis* sp. nov., holotype female **A** habitus (dorsal view) **B** carapace (dorsal view) **C** carapace (lateral view), indicate eyespots (red arrows) **D** left chelicera (dorsal view) **E** left chela (lateral view) **F** female genital area (ventral view). Scale bars: 0.50 mm (**A**); 0.20 mm (**E**); 0.10 mm (**B–D, F**).

but differs from it in having shorter pedipalps (e.g. chela 5.48–5.71× vs 6.14× longer than broad, length 1.15–1.20 mm vs 1.72 mm; palpal femur 5.00–5.13× vs 6.00× longer than broad, length 0.77–0.80 mm vs 1.20 mm) and more setae on tergite I (4 vs 2). It differs from the two congeners from China, *S. wulibeiensis* and *S. yinae*, in having more setae on tergite I (four vs two) and shorter pedipalps (e.g. chela length 1.15–1.20 mm vs 1.76/1.89 mm; palpal femur 5.00–5.13× vs 6.40/7.26× longer than broad, length 0.77–0.80 mm vs 1.28/1.30 mm).

Etymology. This species is named after its type locality, Tuoliang National Nature Reserve.

Description. Adult females (male unknown) (Figs 9–11). **Colour:** generally pale yellow; chelicerae, pedipalps, and tergites slightly darker; soft parts pale. **Cephalothorax** (Figs 9B, C, 10A, 11A, B, D, E): carapace inverted-trapezoid, 0.98–1.02× longer than broad, gently narrowed posteriorly; surface mostly with fine reticulations, without furrows but with four anterior lyrifissures and two posterior lyrifissures; with two pairs of eyespots and eye region bulging and convex in dorsal view; epistome present and with some tiny spinules; with 16 setae arranged s4s: 4: 2: 2: 2, most setae heavy, long, and gently curved. Chaetotaxy of coxae: P 3, I 5, II 4, III 4, IV 4; manducatory process with two acuminate distal setae, anterior seta more than 1/2 length of medial seta (Fig. 11D); coxal spines present on coxa I only, comprising a transverse, contiguous series of seven or eight tridentate blades, which arise from a lightly sclerotized or translucent hillock, the central ramus of each blade (except the basal one) sharply acumino-spatulate and extending beyond the lateral rami (Fig. 11A, B); a small, bisetose intercoxal

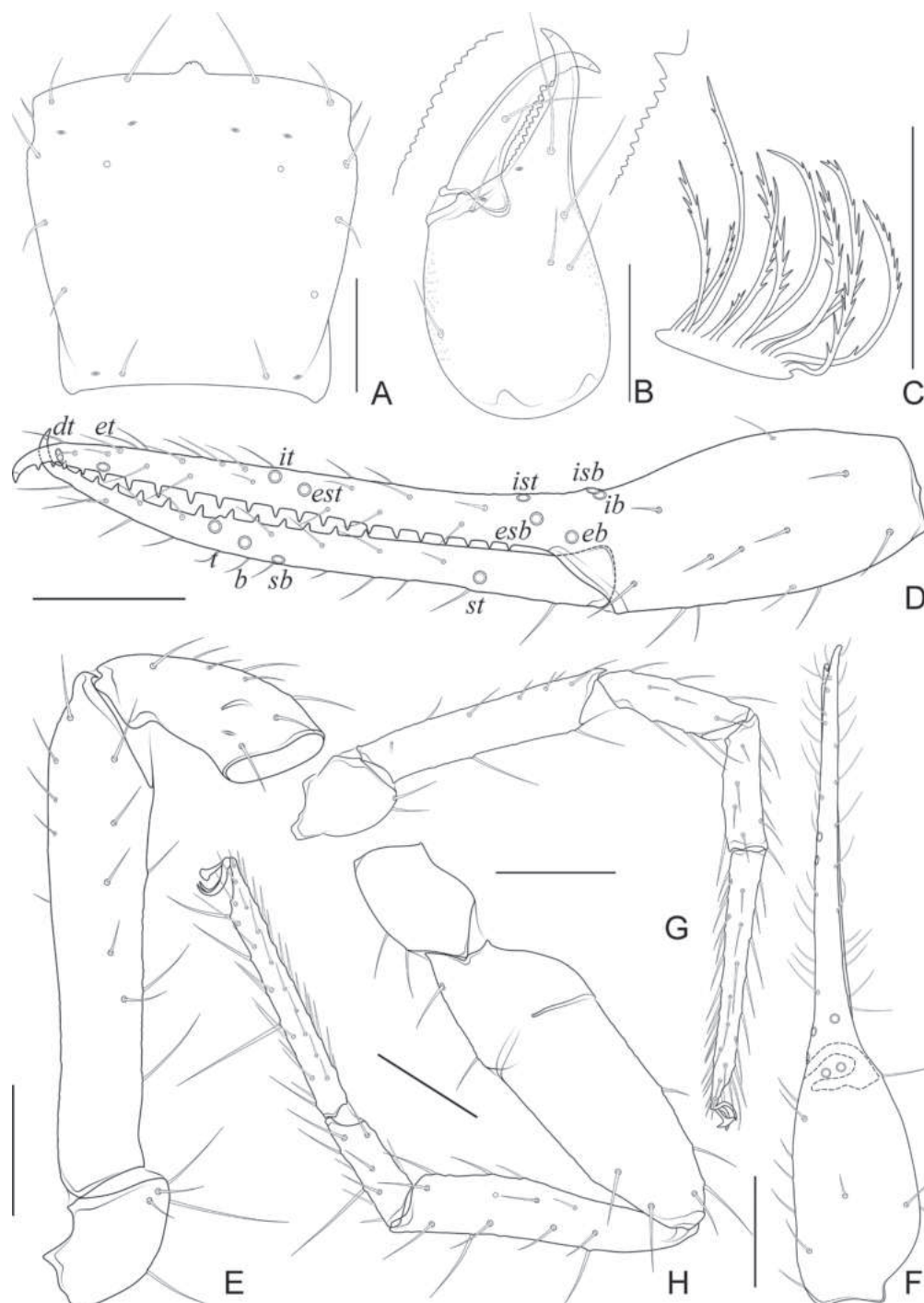


Figure 10. *Spelaeochthonius tuoliangensis* sp. nov., holotype female **A** carapace (dorsal view) **B** left chelicera (dorsal view), with details of teeth **C** rallum **D** left chela (lateral view), with details of trichobothrial pattern **E** left pedipalp (minus chela, dorsal view) **F** left chela (dorsal view) **G** leg I (lateral view) **H** leg IV (lateral view). Scale bars: 0.20 mm.

tubercle present between coxae III and IV (Fig. 11E). **Chelicera** (Figs 9D, 10B, C, 11C, F): large, approximately as long as carapace, 2.12–2.19× longer than broad; six setae and two lyrifissures (exterior condylar lyrifissure and exterior lyrifissure) present on hand, movable finger with one medial seta, all setae acuminate, ventrobasal seta shorter than others. Cheliceral palm with moderate hispid granulation on both ventral and dorsal sides. Both fingers with well-developed teeth, fixed finger with 12 or 13 acute teeth, distal one largest;

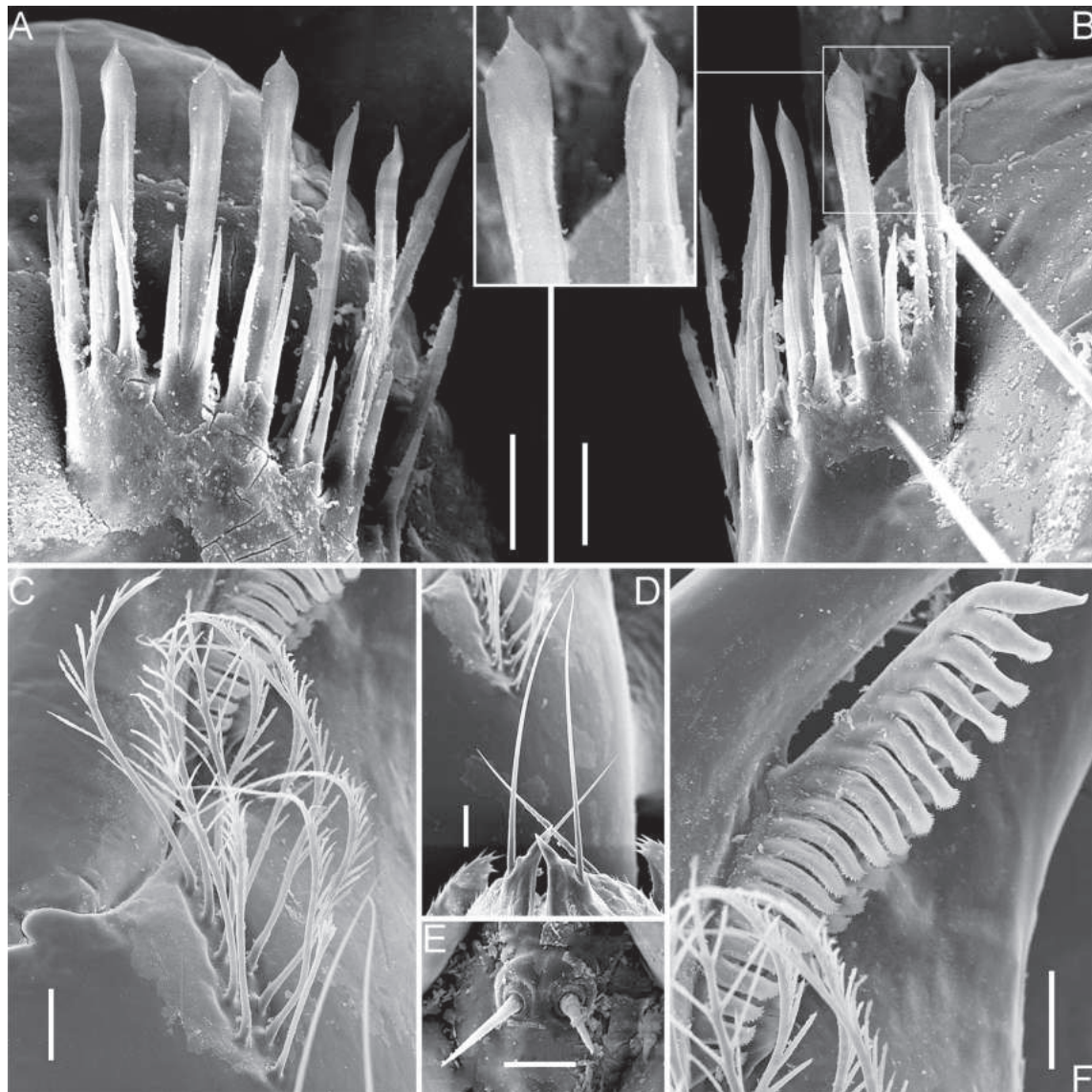


Figure 11. *Spelaeochthonius tuoliangensis* sp. nov. scanning electron micrographs, paratype female **A** left coxal spines **B** right coxal spines, with details of tips **C** rallum **D** manducatory process **E** intercoxal tubercle **F** serrula exterior. Scale bars: 20 μm (**C**, **D**, **F**); 10 μm (**A**, **B**, **E**).

movable finger with 14–16 retrorse contiguous teeth of equal length; galea absent. Serrula exterior with 19 blades and serrula interior with 15–17 blades (Fig. 11F). Rallum in two rows and composed of 11 finely pinnate blades (Figs 10C, 11C). **Pedipalp** (Figs 9E, 10D–F): surfaces mostly with fine reticulations; long and slender, trochanter 1.53–1.73, femur 5.00–5.13, patella 2.25–2.40, chela 5.48–5.71, hand 2.05–2.10 \times longer than broad; femur 2.14–2.22 \times longer than patella; movable chelal finger 1.70–1.77 \times longer than hand and 0.63–0.65 \times longer than chela. Setae generally long and acuminate; two distal lyrifissures present on patella (Fig. 10E). Chelal palm slightly constricted towards fingers. Fixed chelal finger and hand with eight trichobothria plus duplex trichobothrium (*dt*), movable chelal finger with four trichobothria, *ib*, *isb*, *eb*, *esb*, and *ist* clustered at the base of fixed finger, *ist* slightly distal to *esb*; *it* slightly distal to *est*, situated subdistally and forming a pair; *et* situated subdistally, very close to chelal teeth; *dt* situated distal to *et*, near the tip of fixed finger; *sb* distinctly closer to

b than to *st* (Fig. 10D). Microsetae (chemosensory setae) absent on hand and both palpal fingers. Sensilla absent. Both chelal fingers with a row of teeth, homodontate, spaced regularly along the margin, larger and well-spaced teeth present in the middle of the row, becoming smaller and closer distally and proximally: fixed chelal finger with 21 teeth, slightly retrorse and pointed; movable chelal finger with 13 teeth (slightly smaller than teeth on fixed chelal finger) (Figs 9E, 10D). Chelal fingers straight in dorsal view (Fig. 10F). **Opisthosoma:** generally typical, ovate, pleural membrane finely granulated. Tergites and sternites undivided; setae uniseriate and acuminate. Tergal chaetotaxy I–XII: 4: 5–6: 6: 6: 6: 7: 7: 5–6: 4: TT: 0. Sternal chaetotaxy IV–XII: 12–13: 11–12: 11–12: 9–10: 9–11: 8–9: 8–9: 0: 2. Anterior genital operculum with six setae plus 13 or 14 setae on posterior margin, 19 or 20 in total (Fig. 9F). **Legs** (Fig. 10G, H): generally typical, long, and slender. Fine granulation present on anterodorsal faces of femur IV and patella IV. Femur of leg I 1.58–1.71× longer than patella and with one lyrifissure at the base of femur; tarsus 2.09–2.27× longer than tibia. Femoropatella of leg IV 2.76–2.77× longer than deep; tibia 4.90–5.22× longer than deep; with a long tactile seta on both tarsal segments: basitarsus 3.00–3.14× longer than deep (TS = 0.32–0.38), telotarsus 9.20–9.60× longer than deep and 2.09–2.29× longer than basitarsus (TS = 0.35). Arolium slightly shorter than the claws, not divided; claws simple. **Dimensions of adult females** (length/breadth or, in the case of the legs, length/depth in mm). Body length 1.71–1.88. Pedipalps: trochanter 0.23–0.26/0.15, femur 0.77–0.80/0.15–0.16, patella 0.336/0.15–0.16, chela 1.15–1.20/0.21, hand 0.43–0.44/0.21, movable finger length 0.73–0.78. Chelicera 0.55–0.57/0.26, movable finger length 0.29. Carapace 0.57/0.56–0.58. Leg I: trochanter 0.16/0.13–0.14, femur 0.41/0.08–0.09, patella 0.24–0.26/0.07, tibia 0.22/0.06, tarsus 0.46–0.50/0.05. Leg IV: trochanter 0.25/0.14–0.15, femoropatella 0.58–0.61/0.21–0.22, tibia 0.47–0.49/0.09–0.10, basitarsus 0.21–0.22/0.07, telotarsus 0.46–0.48/0.05.

Distribution. China (Hebei).

Discussion

The morphology of the coxal spines is an important diagnostic feature that allows to distinguish the two Asian endemic genera: *Centrochthonius* and *Spelaeochthonius* (Harvey and Harms 2022; You et al. 2022). In general, *Centrochthonius* shows a unique arrangement of fewer than six coxal blades that are short, tripartite, and distally acute (Gao et al. 2016; Harvey and Harms 2022; Schwarze et al. 2022). In contrast, *Spelaeochthonius* is characterized by having more than seven coxal blades that are longer and distally plumose or terminate as a feathered tassel (Morikawa 1954; You et al. 2022). The two new species of *Spelaeochthonius* described in this study, along with the previously described *S. wulibeiensis*, exhibit typical characters of the genus *Spelaeochthonius*, although with atypical coxal spines that are longer and distally spatulate (Figs 8A, 11A, B; Gao et al. 2023). In addition, the diversity of coxal spine morphology within *Spelaeochthonius* is notable, as seen in *S. undecimclavatus* Morikawa, 1956, where the spines are club-shaped rather than distally plumose (Morikawa 1956). Therefore, it is appropriate to place these two new species in the genus *Spelaeochthonius*, and it may be assumed that the species exhibiting these atypical spines are endemic to China. These atypical spines are similar

to those found in the three North American species classified as “*Pseudotyranochthonius*” and forming a monophyletic sister group to *Spelaeochthonius* (Harms et al. 2024); these are all characterized by tripartite spines with spatulate tips. However, the intermediate rami of these atypical spines are notably elongated (Muchmore 1967; Benedict and Malcolm 1970).

All 11 currently known *Spelaeochthonius* species are exclusively found within caves and are completely blind (WPC 2024). *Spelaeochthonius tuoliangensis* sp. nov. represents the first epigeal species of this genus with small eye spots (Fig. 9C). While most China’s karst landforms are distributed in the southern subtropical regions, there are also a few karst caves located in temperate regions (Liu et al. 2020). Due to Pleistocene glaciation, caves served as refugia for troglobites, like *S. huanglaoensis* sp. nov., while their surface counterparts would have normally gone extinct under adverse climatic conditions (Holsinger 2000). *Spelaeochthonius tuoliangensis* sp. nov. may be the remnant of a former surface fauna of *Spelaeochthonius* that is now largely extinct in eastern Asia but remains highly diverse in subterranean habitats. The discovery of two new *Spelaeochthonius* species further extends the geographic range of the genus in East Asia. In contrast, the genus *Allochthonius*, which is also endemic to East Asia, is more widely distributed; the discovery of *Allochthonius* in Baltic amber from Europe (Schwarze et al. 2022) indicates a previously wider distribution of this genus. The larger population and perhaps greater adaptability of *Allochthonius* have allowed this genus to occupy a wider range of ecological niches.

The research on the family Pseudotyranochthoniidae is still in its infancy in China, with 21 species recorded thus far (Fig. 1; WPC 2024), mostly concentrated in Yunnan and Guizhou provinces of southwestern China. More investigations are needed in northern and central China to explore the geographic range of this family. However, our fieldwork has revealed that these small arachnids have very low abundance, are endemic to small areas (some are confined to a single cave), are vulnerable to environmental changes, and are easily overlooked. Therefore, it is extremely important to protect their habitat while investigating.

Acknowledgements

We are grateful to Dr Xiangbo Guo, Zhaoyi Li, Nana Zhan (Hebei University, Baoding, China) and Dr Luyu Wang (Southwest University, Chongqing, China) for their assistance in the field, to Mr Jianzhou Sun and Ms Mengjiao Xu (Hebei University, Baoding) for the high-resolution SEM images, to Dr Xinping Wang (University Florida, Gainesville, USA) for revising the language and to Dr Fedor Konstantinov, Dr Jason Dunlop, Dr Mark S. Harvey, Dr Robert Forsyth, and the anonymous reviewer for their helpful suggestions that greatly improved this paper.

Additional information

Conflict of interest

The authors have declared that no competing interests exist.

Ethical statement

No ethical statement was reported.

Funding

This work was supported by the National Natural Science Foundation of China (no. 31872198) and the Natural Science Foundation of Hebei Province (no. C2021201030).

Author contributions

Conceptualization: Feng Zhang, Yanmeng Hou. Species identification, illustrations and original draft writing: Yanmeng Hou. Review and editing: Feng Zhang, Yanmeng Hou.

Author ORCIDs

Yanmeng Hou  <https://orcid.org/0000-0003-0059-3419>

Feng Zhang  <https://orcid.org/0000-0002-3347-1031>

Data availability

All of the data that support the findings of this study are available in the main text.

References

- Beier M (1932) Pseudoscorpionidea I. Subord. Chthoniinea et Neobisiinea. Tierreich 57: [i–xx,] 1–258. <https://doi.org/10.1515/9783111435107>
- Benedict EM, Malcolm DR (1970) Some pseudotyranochthoniine false scorpions from western North America (Chelonethida: Chthoniidae). Journal of the New York Entomological Society 78: 38–51.
- Chamberlin JC (1929) On some false scorpions of the suborder Heterosphyronida (Arachnida - Chelonethida). Canadian Entomologist 61(7): 152–155. <https://doi.org/10.4039/Ent61152-7>
- Chamberlin JC (1931) The arachnid order Chelonethida. Stanford University Publications, University Series (Biological Science) 7(1): 1–284.
- Gao ZZ, Zhang YF, Zhang F (2016) Two new species of Pseudotyranochthoniidae, including the first species of *Pseudotyranochthonius* (Pseudoscorpiones) from China. Acta Zoologica Academiae Scientiarum Hungaricae 62(2): 117–131. <https://doi.org/10.17109/AZH.62.2.117.2016>
- Gao ZZ, Hou YM, Zhang F (2023) Four new species of cave-adapted pseudoscorpions (Pseudoscorpiones, Pseudotyranochthoniidae) from Guizhou, China. ZooKeys 1139: 33–69. <https://doi.org/10.3897/zookeys.1139.96639>
- Harms D (2018) The origins of diversity in ancient landscapes: Deep phylogeographic structuring in a pseudoscorpion (Pseudotyranochthoniidae: *Pseudotyranochthonius*) reflects Plio-Pleistocene climate fluctuations. Zoologischer Anzeiger 273: 112123. <https://doi.org/10.1016/j.jcz.2018.01.001>
- Harms D, Harvey MS (2013) Review of the cave-dwelling species of *Pseudotyranochthonius* Beier (Arachnida: Pseudoscorpiones: Pseudotyranochthoniidae) from mainland Australia, with description of two troglobitic species. Australian Journal of Entomology 52(2): 129–143. <https://doi.org/10.1111/aen.12009>
- Harms D, Roberts JD, Harvey MS (2019) Climate variability impacts on diversification processes in a biodiversity hotspot: A phylogeography of ancient pseudoscorpions in south-Western Australia. Zoological Journal of the Linnean Society 186(4): 934–949. <https://doi.org/10.1093/zoolinnean/zlz010>
- Harms D, Harvey MS, Roberts JD, Loria SF (2024) Tectonically driven climate change and the spread of temperate biomes: Insights from dragon pseudoscorpions

- (Pseudotyranochthoniidae), a globally distributed arachnid lineage. *Journal of Biogeography* 51(6): 1032–1048. <https://doi.org/10.1111/jbi.14801>
- Harvey MS (1992) The phylogeny and classification of the Pseudoscorpionida (Chelicerata: Arachnida). *Invertebrate Systematics* 6(6): 1373–1435. <https://doi.org/10.1071/IT9921373>
- Harvey MS, Harms D (2022) The pseudoscorpion genus *Centrochthonius* (Pseudoscorpiones: Pseudotyranochthoniidae) from central Asia and description of a new species from Nepal. *The Journal of Arachnology* 50(2): 158–174. <https://doi.org/10.1636/JoA-S-21-033>
- Holsinger JR (2000) Ecological derivation, colonization, and speciation. In: Wilkens H, Culver DC, Humphries WF (Eds) *Subterranean Ecosystems*. Elsevier, Amsterdam, 399–415.
- Hu JF, Zhang F (2012) Two new species of the genus *Allochthonius* Chamberlin from China (Pseudoscorpiones: Pseudotyranochthoniidae). *Entomologica Fennica* 22(4): 243–248. <https://doi.org/10.33338/ef.5003>
- Judson MLI (2007) A new and endangered species of the pseudoscorpion genus *Lagynochthonius* from a cave in Vietnam, with notes on chelal morphology and the composition of the Tyrannochthoniini (Arachnida, Chelonethi, Chthoniidae). *Zootaxa* 1627(1): 53–68. <https://doi.org/10.11646/zootaxa.1627.1.4>
- Liu K, Sun WJ, Wang SS, Sun Y (2020) Study on the characteristics of karst development in Beijing. *Carbonates and Evaporites* 35(2): 1–13. <https://doi.org/10.1007/s13146-020-00584-7>
- Morikawa K (1954) On some pseudoscorpions in Japanese lime-grottoes. *Memoirs of Ehime University* 2(2B): 79–87.
- Morikawa K (1956) Cave pseudoscorpions of Japan (I). *Memoirs of Ehime University* 2(2B): 271–282.
- Morikawa K (1960) Systematics studies of Japanese pseudoscorpions. *Memoirs of Ehime University* 2(2B): 85–172.
- Muchmore WB (1967) Pseudotyranochthoniine pseudoscorpions from the western United States. *Transactions of the American Microscopical Society* 86(2): 132–139. <https://doi.org/10.2307/3224679>
- Sakayori H (2000) A new species of the genus *Allochthonius* (Pseudoscorpion, Chthoniidae) from Mt. Kohshin, Tochigi Prefecture, Central Japan. *Edaphologia* 65: 13–18.
- Schwarze D, Harms D, Hammel J, Kotthoff U (2022) The first fossils of the most basal pseudoscorpion family (Arachnida: Pseudoscorpiones: Pseudotyranochthoniidae): evidence for major biogeographical shifts in the European paleofauna. *Palaontologische Zeitschrift* 96(1): 11–27. <https://doi.org/10.1007/s12542-021-00565-8>
- Viana ACM, Ferreira RL (2021) A new troglobitic species of *Allochthonius* (subgenus *Urochthonius*) (Pseudoscorpiones, Pseudotyranochthoniidae) from Japan. *Subterranean Biology* 37: 47–55. <https://doi.org/10.3897/subtbiol.37.58580>
- World Pseudoscorpiones Catalog (2024) World Pseudoscorpiones Catalog. Natural History Museum Bern. <https://wac.nmbe.ch/order/pseudoscorpiones/3> [Accessed on 16.04.2024]
- You JY, Yoo JS, Harvey MS, Harms D (2022) Some cryptic Korean karst creatures: revalidation of the pseudoscorpion genus *Spelaeochthonius* (Pseudoscorpiones: Pseudotyranochthoniidae) and description of two new species from Korea. *The Journal of Arachnology* 50(2): 135–157. <https://doi.org/10.1636/JoA-S-21-025>
- Zhang FB, Zhang F (2014) A new species of the genus *Allochthonius* (Pseudoscorpiones, Pseudotyranochthoniidae) from Liupan Mountains, China, with the description of the male of *Allochthonius brevitus*. *Acta Zoologica Academiae Scientiarum Hungaricae* 60: 45–56.

Review of the genus *Karschia* Walter, 1889 from Xizang, China (Solifugae, Karschiidae)

Wenlong Fan^{1,2}, Chao Zhang^{1,2}, Feng Zhang^{1,2}

¹ Key Laboratory of Zoological Systematics and Application, College of Life Sciences, Hebei University, Baoding, Hebei 071002, China

² Hebei Basic Science Center for Biotic Interaction, Hebei University, Baoding, Hebei 071002, China

Corresponding author: Feng Zhang (dudu06042001@163.com)

Abstract

The species of the genus *Karschia* Walter, 1889, collected from Xizang, China, were reviewed. A total of six species were recognized using morphological and molecular data, *Karschia* (*Karschia*) *tibetana* Hirst, 1907 is redescribed based on newly collected males and females, and five new species, *Karschia* (*Karschia*) *dingye* **sp. nov.**, *Karschia* (*Karschia*) *lhasa* **sp. nov.**, *Karschia* (*Karschia*) *zhui* **sp. nov.**, *Karschia* (*Karschia*) *shigatse* **sp. nov.**, and *Karschia* (*Karschia*) *namling* **sp. nov.**, are described.

Key words: Camel-spider, COI, taxonomy

Introduction

The family Karschiidae Kraepelin, 1899, comprising four genera and 45 species, is a small family within Solifugae, with a palearctic distribution in north Africa, the Middle East, and central Asia (WSC 2024). Among the four genera within Karschiidae, *Barrus* Simon, 1880, is a monotypic genus; *Barrussus* Roewer, 1928, comprises three species, *Eusimonia* Kraepelin, 1899, comprises 15 species; and *Karschia* Walter, 1899, comprises 26 species (WSC 2024).

The genus *Karschia* is divided into two subgenera: the nominative subgenus, *Karschia* Walter, 1889, found in North Africa, the Middle East, and central Asia, comprising 18 species; and the subgenus *Rhinokarschia* Birula, 1935, found in central Asia, comprising eight species. Five *Karschia* species have been recorded from China, one *Rhinokarschia* species, *Karschia* (*Rhinokarschia*) *rhinoceros* Birula, 1922 (♂♀, Xinjiang), and four *Karschia* species, *Karschia* (*Karschia*) *birulae* Roewer, 1934 (♂♀, Xinjiang), *Karschia* (*Karschia*) *tarimina* Roewer, 1933 (♀, Xinjiang), *Karschia* (*Karschia*) *tienschanica* Roewer, 1933 (♀, Xinjiang) and *Karschia* (*Karschia*) *tibetana* Hirst, 1907 (♂♀, Xizang) (Harvey 2003). Additionally, Lawrence (1954) described *Karschia* (*Karschia*) *nubigena*, collected by Dr. Noel Humphreys, a medical officer in the British Mount Everest expedition of 1936; the World Solifugae Catalog (WSC) and Harvey's catalog mention the type locality as Mount Everest, Nepal (Harvey 2003; WSC 2024), but the route followed by that expedition suggests it was more likely collected from the Xizang side (Ruttledge et al. 1936). Based on this, it is believed that *Karschia* (*Karschia*) *nubigena* also occurs in Xizang.



Academic editor: Paula Cushing

Received: 3 February 2024

Accepted: 7 May 2024

Published: 4 June 2024

ZooBank: <https://zoobank.org/02D0B0C3-219A-46F6-A433-D1D77CE5F312>

Citation: Fan W, Zhang C, Zhang F (2024) Review of the genus *Karschia* Walter, 1889 from Xizang, China (Solifugae, Karschiidae). ZooKeys 1204: 155–190. <https://doi.org/10.3897/zookeys.1204.120164>

Copyright: © Wenlong Fan et al.
This is an open access article distributed under terms of the Creative Commons Attribution License (Attribution 4.0 International – CC BY 4.0).

The genus *Karschia* sets itself apart from other genera within Karschiidae easily by possessing a rotatable, long, and rolled flagellum, often described as sessile (Birula 1922, 1938; Bird et al. 2015). This flagellum maintains a core resemblance to a plumose seta, typically adorned with a delicate fringe of setae, which Lawrence (1954) mistakenly referred to as “cilia”. The flagellum of *Karschia* is understood to comprise three components: a distinct stalk, a basal peg sharing similarities with the base of a whip-like flagellum, and an elongated filiform structure resembling a shaft, thus resembling a composite flagellum (Bird et al. 2015). Roewer (1934) described the flagellum of *Karschia* as an elongated double-walled tubular structure, originating from a seta that widened along its length. The margins of the flagellum rolled inward until they nearly formed a closed canal, suggesting a process of longitudinal in-furling. However, it is possible that the hypothesized double membrane was lost. Consequently, the flagellum of *Karschia* resembles a composite flagellum, with identifiable components such as a “stalk”, “base”, and “shaft”, though its sessile nature awaits further investigation (Bird et al. 2015).

The flagellar complex of *Karschia* comprises several structures: a long, typically coiled, filiform flagellum; plumose setae, located ventrally to the flagellum and modified to varying degrees, including broadening referred to as flagellar complex plumose (*fcp*) setae; and one or two acuminate subspiniform setae, usually swollen at the base and situated dorsoproximal to the flagellar attachment point, labeled as flagellar complex subspiniform (*fcs*) setae (Gromov 2004; Bird et al. 2015).

Males of *Karschia* lack spiniform setae on the anterior edge of the propeltidium (on both sides of the ocular tubercle) (Gromov 1998, 2004). Females of this genus exhibit differences, notably in the morphology of the more modified genital segment. The subgenus *Karschia* differs from the subgenus *Rhinokarschia* by the absence of a hornlike process on the fixed finger of the chelicerae in males (though a low crest may be present instead), and by the presence of transverse, oval, or triangular-shaped genital sternites in females, which cover the genital opening (Gromov 2004).

The systematics and phylogenetic relationships of *Karschia* remain poorly understood, as its congeners are relatively local and rare species (Gromov 2004). Species diagnoses in this genus are mainly based on male characters. Female descriptions are limited to body size and coloration, chelicerae dentition, and the shape and number of ctenidia on the fourth abdominal segment. The female genital segment has previously been considered of little or no taxonomic significance in species diagnosis (Roewer 1933; Birula 1938). This makes it difficult to identify female specimens. In order to address the issues related to female identification, Gromov (2004) proposed that for female diagnosis, the shape and size of the ctenidia on the fourth abdominal segment, as well as the shape, size, and relative arrangement of the sclerites of the genital segment are more reliable than others, i.e., the chelicerae dentition, the number of ctenidia on the fourth abdominal segment, the body size and coloration.

Xizang Autonomous Region, located in the southwestern part of the Qinghai-Xizang Plateau and known as the “Roof of the World,” has an average elevation exceeding 4,000 meters. The high altitude and unique geographical location form its distinctive climate and rich biodiversity, including many rare and endangered species. Xizang has become a hotspot and crucial area for global

biodiversity research in recent years. However, research on Solifugae in Xizang has been limited, with only four species previously reported: *Galeodes caspius* Birula, 1890, *Karschia tibetana* Hirst, 1907, *Karschia nubigena* Lawrence 1954, and *Triditarsus tibetanus* Roewer, 1933.

During our biodiversity survey, we revealed a widespread distribution of Solifugae in Xizang. During the process of identifying collected specimens, we observed a high level of diversity within the genus *Karschia* in Xizang through comparison with diagnoses, descriptions, and drawings in original literature of all known species. This research used morphological characters and molecular data to investigate the taxonomy of Solifugae in Xizang. To solve the problem of male and female combinations and to ensure the precision of our morphological identifications, we carried out genetic distance comparisons on suspected new species. For each species, both a male and a female specimen were chosen to extract genomic DNA and the COI gene was amplified. In conclusion, comparisons of morphological characteristics and molecular genetic distances have led us to conclude that there are seven species of *Karschia* distributed in Xizang.

From the study of the newly collected material, we provide a redescription of *Karschia (Karschia) tibetana* Hirst, 1907 based on males and females collected from the type locality, and the description of five new species: *Karschia (Karschia) dingye* sp. nov., *Karschia (Karschia) lhasa* sp. nov., *Karschia (Karschia) zhui* sp. nov., *Karschia (Karschia) shigatse* sp. nov., and *Karschia (Karschia) namling* sp. nov.

Materials and methods

The specimens were collected during the day by hand from under stones, and preserved in 75% and 95% alcohol, respectively. Photographs were taken using a Leica M205A stereomicroscope equipped with a DFC 550 CCD and an Olympus BX51 microscope equipped with a Kuy Nice CCD camera and were imported into Helicon Focus v. 7 for stacking. Plates and photographs were edited and retouched using Adobe Photoshop 2022. Drawings were made using the Inkscape software (v. 1.0.2.0). All measurements are in mm. Pedipalp measurements are shown as: total length (femur, tibia, metatarsus, tarsus); leg measurements are shown as: total length (femur, tibia, metatarsus, tarsus, claw). All specimens are deposited in the Museum of Hebei University (MHBUS), Baoding, China.

Descriptions follow the format of Birula (1938), with some modifications by Gromov (2004). The terminology used for identifying teeth and other structures in the chelicerae follows Bird et al. (2015). Identification of individual teeth used Bird et al.'s criteria (2015) for primary homology assessment of dentition. The term 'ctenidia' stands for long, single-tipped (non-bifid) and flexible setiform structures present on some opisthosomal sternites.

The QIAGEN DNeasy Blood & Tissue Kit (Qiagen Inc., Valencia, CA) was used to extract genomic DNA from the muscle tissues of the legs for one male and one female of each species. The PCR primer for a partial fragment of the mitochondrial cytochrome oxidase subunit (COI) gene is the universal primer for invertebrate DNA barcoding LCO1490 and HCO2198 (Folmer et al. 1994). All sequences were analyzed using BLAST and are deposited in GenBank (Table 1). Sequence alignment was performed in MAFFT v. 7.313. The p-distance of intra-specific nucleotide divergence was calculated in MEGA.11.0.

Table 1. Voucher specimen information.

	Species	Sex	GenBank accession number	Sequence length
1	<i>K. tibetana</i>	Male	PP587316	685
2	<i>K. tibetana</i>	female	PP594087	687
3	<i>K. zhui</i> sp. nov.	Male	PP600574	687
4	<i>K. zhui</i> sp. nov.	Female	PP600573	696
5	<i>K. shigatse</i> sp. nov.	Male	PP600575	687
6	<i>K. shigatse</i> sp. nov.	Female	PP600578	683
7	<i>K. dingye</i> sp. nov.	Male	PP600577	687
8	<i>K. dingye</i> sp. nov.	Female	PP600576	670
9	<i>K. namling</i> sp. nov.	Male	PP600579	687
10	<i>K. namling</i> sp. nov.	Female	PP600580	688
11	<i>K. lhasa</i> sp. nov.	Male	PP600581	683
12	<i>K. lhasa</i> sp. nov.	Female	PP600582	682

Abbreviations as follows: **A/CP** is the sum of the lengths of pedipalp, leg I, and leg IV divided by the sum of the lengths of chelicera and propeltidium, indicating the length of appendages in relation to body size. Long-legged species have larger A/CP ratios. **CL/CH**, chelicera length/height, large CL/CH ratios suggest a narrow cheliceral morphology, while a more robust morphology is represented by a smaller ratio. **CL**, chelicera length; **CH**, chelicera height; **fcp** (modified *pvd*), flagellar complex plumose setae; **fcs**, flagellar complex sub-spiniform to spiniform setae; **FD**, fixed finger, distal tooth; **FM**, fixed finger, medial tooth; **FP**, fixed finger, proximal tooth; **FSD**, fixed finger, subdistal tooth/teeth; **FSM**, fixed finger, submedial tooth/teeth; **pdp**, prodorsal proximal setae; **PF**, profundal teeth; **PFM**, profundal medial tooth/teeth; **PFP**, profundal proximal tooth/teeth; **PFSP**, profundal subproximal tooth/teeth; **PH**, Propeltidium height; **PL**, Propeltidium length; **pvd**, proventral distal setae; **pvsd**, proventral subdistal setae; **MM**, movable finger, medial tooth; **MP**, movable finger, proximal tooth; **MSM**, movable finger, submedial tooth/teeth; **MSP**, movable finger, subproximal tooth/teeth; **MST**, movable finger, subterminal tooth/teeth; **RF**, retrofondal teeth; **RFA**, retrofondal apical tooth/teeth; **RFM**, retrofondal medial tooth/teeth; **RFP**, retrofondal proximal tooth/teeth; **RFSM**, retrofondal submedial tooth/teeth; **RFSP**, retrofondal subproximal tooth/teeth; **rif**, retrolateral finger setae; **sme**, socket margin elevation.

Results of genetic analyses

In this study, genomic DNA was extracted from one male and one female of each species, and genetic distances were analyzed. The intraspecific genetic distance ranged from 0% to 2.20%, while the interspecific genetic distance varied from 8.08% (between *K. shigatse* sp. nov. (female) and *K. dingye* sp. nov. (male)) to 12.92% (*K. shigatse* sp. nov. (male) and *K. lhasa* sp. nov. (male)) (Table 2). The average genetic distance ranged from 0% to 7.92% within *Galeodes caspius* Birula, 1890 (Maddahi et. al 2016). Therefore, based on significant morphological differences and genetic distance, we conclude that the six species in this study can be distinguished effectively.

Table 2. Genetic distance among the six species.

	<i>K. tibetana</i>	<i>K. tibetana</i>	<i>K. zhui</i>	<i>K. zhui</i>	<i>K. shigatse</i>	<i>K. shigatse</i>	<i>K. dingye</i>	<i>K. dingye</i>	<i>K. namling</i>	<i>K. namling</i>	<i>K. lhasa</i>	<i>K. lhasa</i>
<i>K. tibetana</i>												
<i>K. tibetana</i>	0.88%											
<i>K. zhui</i>	11.45%	11.16%										
<i>K. zhui</i>	11.31%	11.01%	0.15%									
<i>K. shigatse</i>	10.57%	10.28%	10.87%	10.72%								
<i>K. shigatse</i>	11.16%	10.57%	10.57%	10.57%	2.20%							
<i>K. dingye</i>	12.79%	12.50%	9.71%	9.85%	8.53%	8.09%						
<i>K. dingye</i>	12.99%	12.69%	9.82%	9.97%	8.61%	8.16%	0.30%					
<i>K. namling</i>	8.52%	8.22%	11.31%	11.45%	11.60%	11.60%	11.91%	12.39%				
<i>K. namling</i>	8.52%	8.22%	11.31%	11.45%	11.60%	11.60%	11.91%	12.39%	0%			
<i>K. lhasa</i>	12.33%	12.04%	11.60%	11.75%	12.92%	12.33%	10.59%	10.88%	12.78%	12.78%		
<i>K. lhasa</i>	12.33%	12.04%	11.60%	11.75%	12.92%	12.33%	10.59%	10.88%	12.78%	12.78%	0%	

Taxonomy

Family Karschiidae Kraepelin, 1899

Genus *Karschia* Walter, 1889

Karschia (Karschia) tibetana Hirst, 1907

Figs 1, 3A–D, 6A, B, 8A–D, 11A, 12A, 13A–D, 16A, B, 17A, 18A, 19A, C, Tables 1, 2

Karschia tibetana: Hirst, 1907a: 322–324, figs 1, 2; Hirst, 1912: 233–234; Birula, 1922: 197; Roewer, 1932: n/a, figs 110c, 143a, 143a; Roewer, 1933: 298, figs 221a, 222a, 223o; Zilch, 1946: 123.

Karschia (Karschia) tibetana Hirst: Harvey, 2003: 286.

Type material. *Holotype* ♂, CHINA: Xizang, Shigatse Prefecture, Gyangze County, stored at NHMUK (of Natural History Museum, United Kingdom), not examined. **Paratypes:** 6♂♂, 9♀♀, CHINA: Xizang, Gyangze, Kamba-Dzong, Tinki, Shekar, Kyishong, stored at SMF (Naturmuseum und Forschungsinstitut Senckenberg, Frankfurt am Main), not examined.

Materials examined. 4♂♂ (MHBU-Sol-XZ2014080601–04), 3♀♀ (MHBU-Sol-XZ2014080605–08), CHINA: Xizang, Shigatse Prefecture, Gyangze County, Enzha Village, 6.VIII.2014, leg. Chao Zhang; 1♂ (MHBU-Sol-XZ2018070901), CHINA: Xizang, Shigatse Prefecture, Gyangze County, Ralung Town, 28.8176°N, 90.0369°E, 4451 m elev., 9.VII.2018, leg. Yannan Mu.

Diagnosis. *K. tibetana* differs from all *Karschia* species except *K. nubigena*, *K. dingye* sp. nov., *K. lhasa* sp. nov., *K. zhui* sp. nov., *K. shigatse* sp. nov. and *K. namling* sp. nov. by male cheliceral movable finger with MSM teeth. *K. tibetana* differs from *K. nubigena* by having fringed flagellum (Fig. 11A) and male ctenidia in sternite IV cylindrical and not wide at bottom (Fig. 19C), from *K. dingye* sp. nov., *K. lhasa* sp. nov. and *K. zhui* sp. nov. by pedipalpal metatarsus without or with only a few papillae (Fig. 16B), and from *K. shigatse* sp. nov. and *K. namling* sp. nov. by flagellum without lateral apophysis and long *fcp* (Fig. 11A). The female genital operculum is easily recognizable in all known species; it is long, subtriangular, and with no clear demarcation between the plates, with the rear edge being lightly chitinized (Fig. 17A).

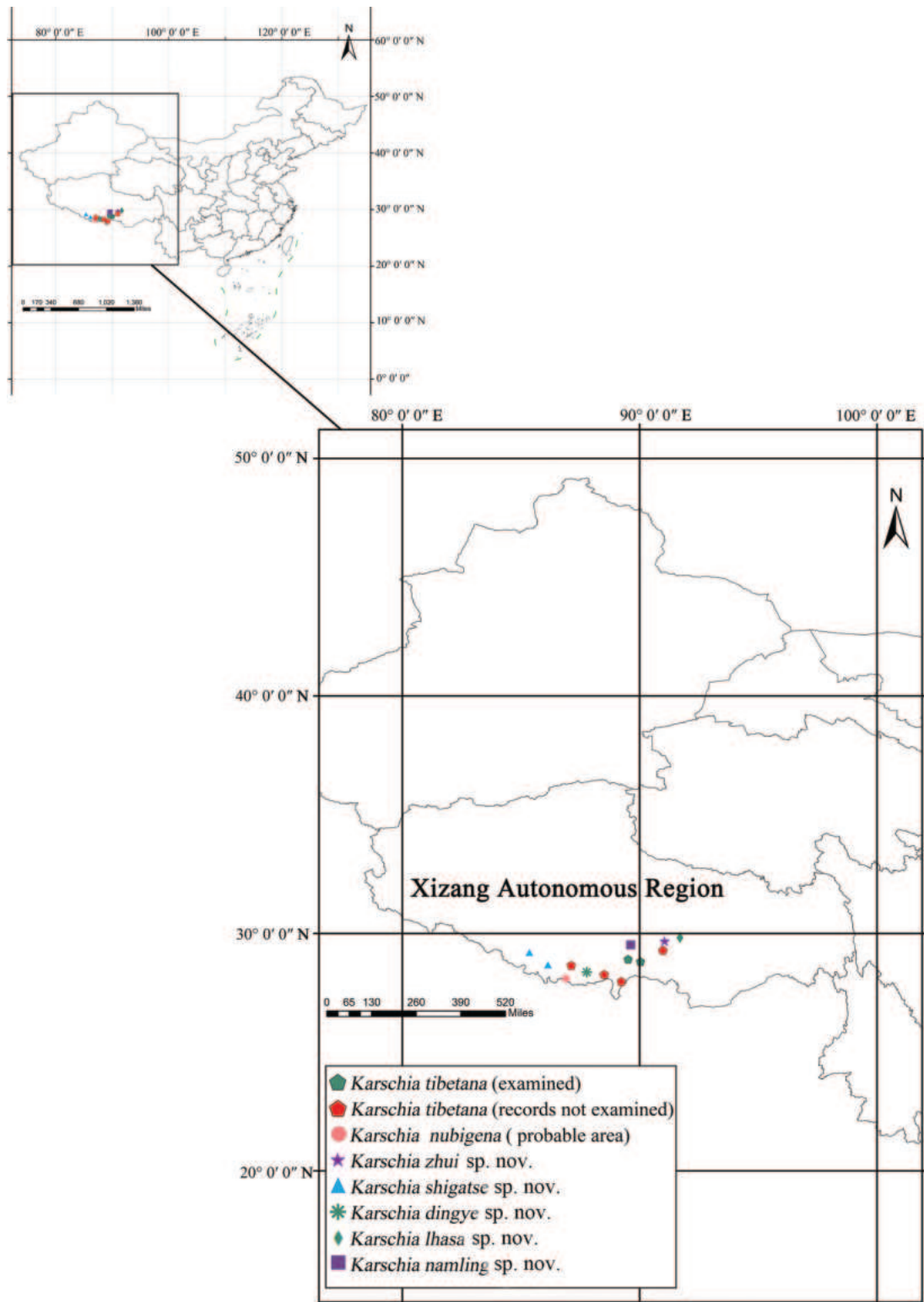


Figure 1. Map plotting known locality records.

Redescription. Male (MHBU-Sol-XZ2014080601).

Measurements. Total body length 17.86, CL 4.61, CH 1.64, PL 2.14, PW 2.72, A/CP 8.28, CL/CH 2.81. Pedipalp 18.77 (5.34, 6.13, 3.81, 0.96), Leg I 14.70 (3.33, 3.68, 2.70, 1.30, 0.09), Leg II 11.49 (2.12, 2.81, 2.00, 0.85, 0.93), Leg III 15.07 (3.51, 3.91, 2.18, 0.55, 0.88), Leg IV 22.366 (5.07, 5.76, 3.60, 1.30, 1.28).

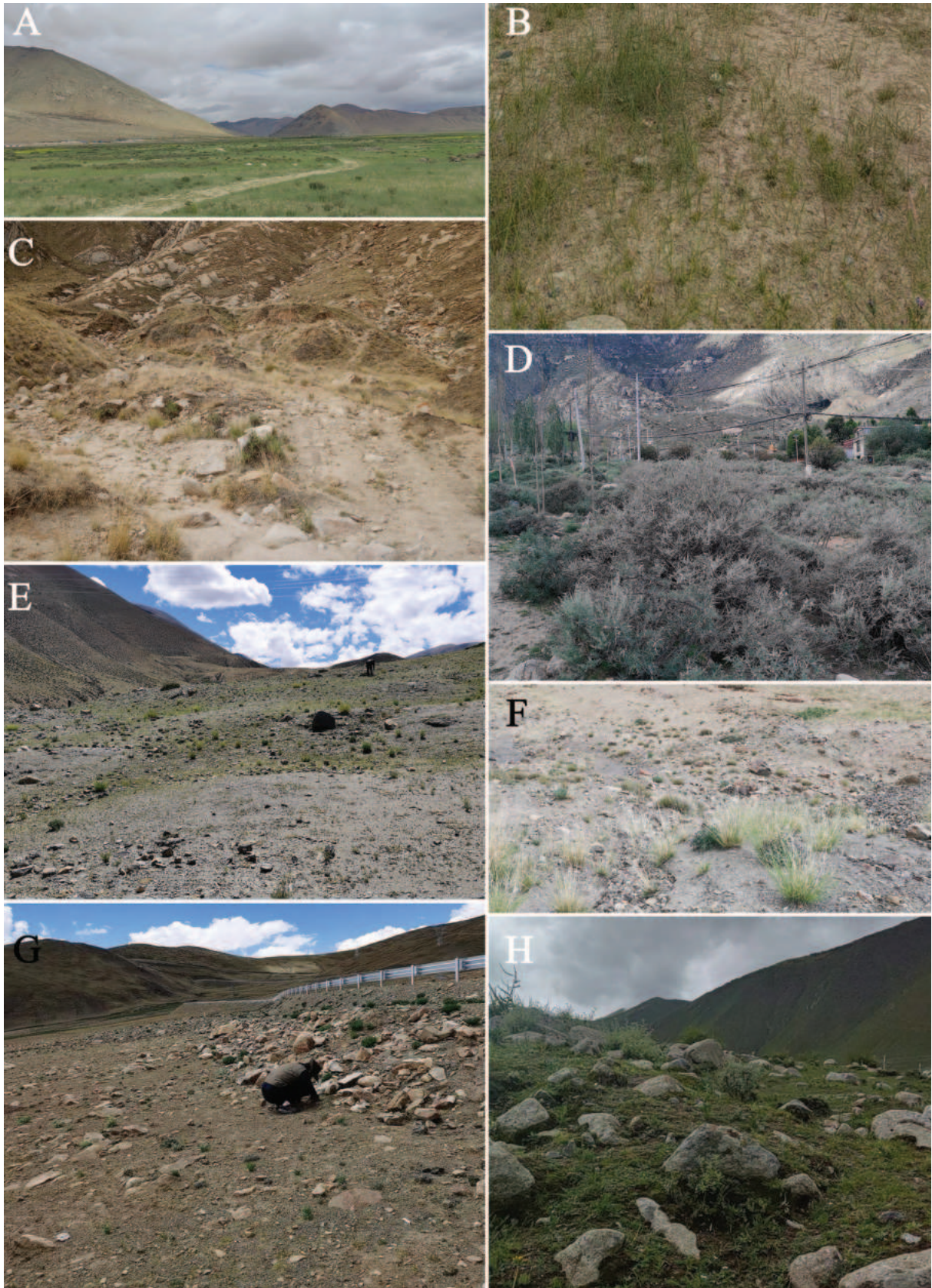


Figure 2. Habitat where *K. dingye* sp. nov. (**A, B**), *K. lhasa* sp. nov. (**C**), *K. shigatse* sp. nov. (**E–G**) and *K. namling* sp. nov. (**H**) have been found. **A, B** Xizang, Dingye County, Gyankar Town **C** Xizang, Lhasa City, Maizhokunggar County **D** Xizang, Lhasa City, Drepung Monastery **E, F** Xizang, Nyalam County, Mainqu Town **G** Xizang, Gyirong County, Zheba Town **H** Xizang, Namling County, Nubma Town.

Coloration. In 75% ethanol-preserved specimens (Fig. 3A, B). The general background deep yellow. Opisthosoma gray-yellow, with black tergites and pale black sternites. Propeltidium tinged pale brown. Ocular tubercle black. Mesopeltidium and metapeltidium with special black stripes. Chelicerae with manus predominantly yellowish with some black areas, and a retrolateral view of chelicerae with three black longitudinal stripes. Pedipalps and legs yellow, legs III and legs IV tinged with pale brown on distal regions of femora and proximal parts of tibiae. Proximal regions of the pedipalpal femur, tibia, metatarsus, and tarsus tinged with brown. Malleoli yellow.

Propeltidium. Wider than long, with dense pubescence of thin, short, anteriorly directed setae. Anterior, posterior, and lateral edges with several long, curved spiniform setae perpendicular to the surface of the propeltidium. Ocular tubercle with two short and two long middle distal spiniform setae, one long middle spiniform setae, two short spiniform setae, and numerous shorter, thinner, proximal setae (Fig. 6A).

Chelicerae. Fixed finger primary teeth graded as $FP \approx FD < FM$. Profondal teeth series with three tiny teeth; retrofondal teeth series with seven teeth. Dental formulation of fixed finger: $FD-(2)-FM-(2)-FP-(7RF)$ (3PF). Movable finger MP tooth about the same size as MM. Movable finger dental formula: $MM-(2)-MP$, with two MSM teeth and two MSP (Figs 8A, 13A). Flagellum coiled, fringed and sessile, without lateral apophysis. The flagellar complex includes two long *fcp* and two short, thick *fcs* (Figs 8B, 11A, 13B). Retro-lateral and dorsal surfaces of the manus with large, bifurcated tip setae and short simple tip bristle-like setae; retrolateral and dorsal surfaces of the fixed finger with simple tip setae of different sizes. Retrolateral setose area reaching the FSM teeth; prolateral surface with an array of setal types (Figs 8A, B, 13A, B).

Opisthosoma. The entire surface covered with almost adpressed setae, and numerous long, curved, bifurcate setae. Sternite III with two posterior paramedian groups of ctenidia, being gradually larger to posterior (Fig. 19A); sternite IV with a row of 19 long and thin cylindrical ctenidia (Fig. 19C).

Pedipalps. Entirely covered with short setae and long, thick setae. Tarsus with ten ventral spines; metatarsus with six ventral spines not arranged in pairs and without papillae (Figs 16A, B).

Legs. Entirely covered with long, thick, setae and short setae. Leg I with no spines and two small claws. Tibiae II, III, and IV with a pair of distal spines ventrally, and tibiae II and III with a single dorsal spine. Metatarsus II and III with a series of three dorsal spines, a pair of distal spines ventrally, and some paired short, thick, spine-shaped bristles over their entire ventral surface; metatarsus IV also with these paired bristles over its entire ventral surface and two distal spines ventrally.

Female (MHBU-Sol-XZZ2014080605).

Measurements. Total body length 20.14, CL 7.35, CH 2.93, PL 4.15, PW 2.91, A/CP 4.66, CL/CH 2.50. Pedipalp 17.34 (3.82, 5.25, 4.04, 1.15), Leg I 14.62 (3.04, 4.00, 2.17, 1.22, 0.15), Leg II 11.93 (2.00, 2.70, 1.72, 0.84, 0.98), Leg III 14.97 (2.66, 3.36, 2.40, 0.75, 1.04), Leg IV 21.55 (4.16, 6.06, 3.44, 1.49, 1.10).

Coloration. In 75% ethanol-preserved specimens (Fig. 3C, D). Coloration as in the males.

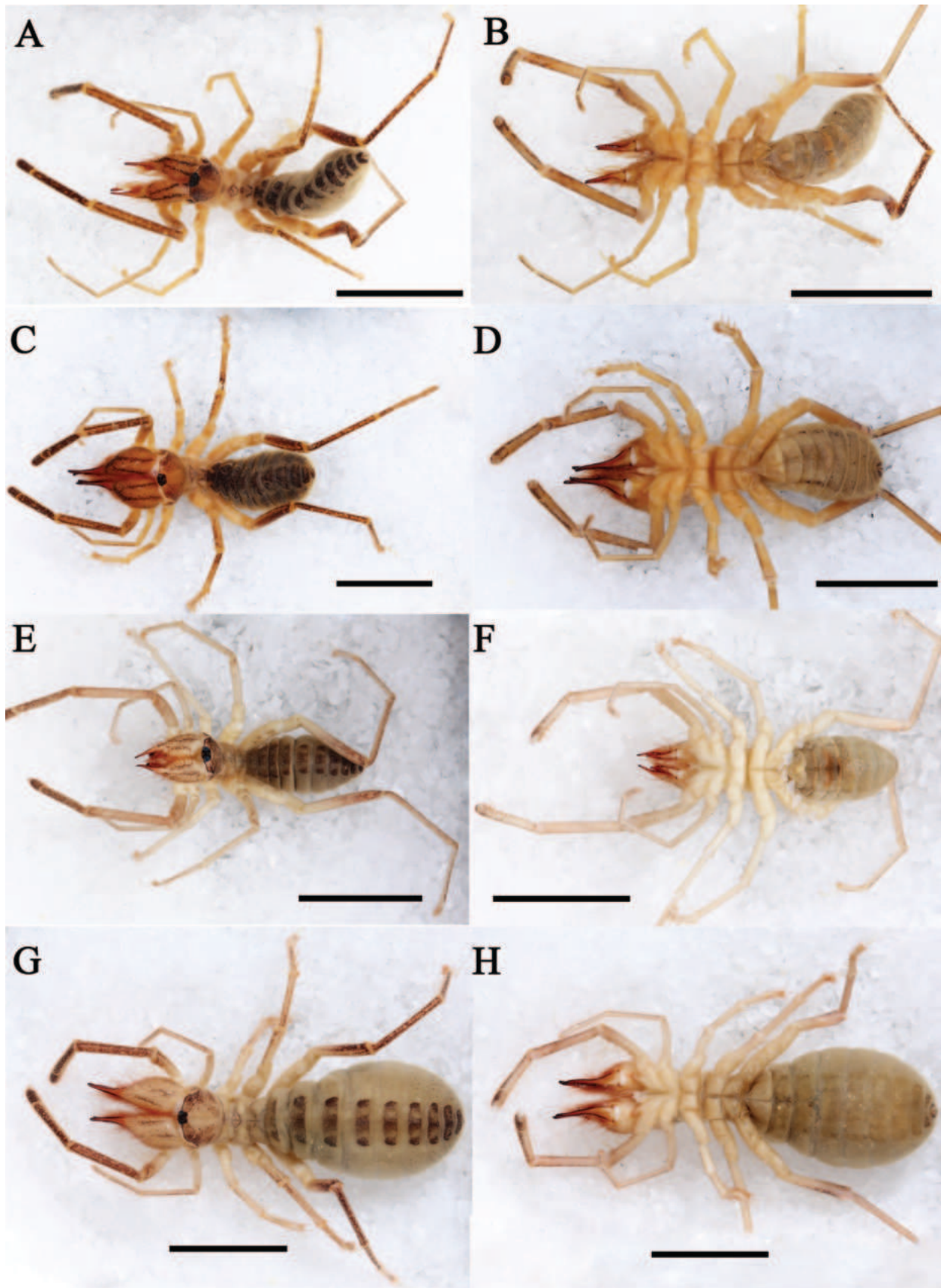


Figure 3. Habitus A–D *K. tibetana*, habitus, male (A, B) and female (C, D) E–H *K. dingye* sp. nov. habitus, male (E, F) and female (G, H). Scale bars: 8 mm.

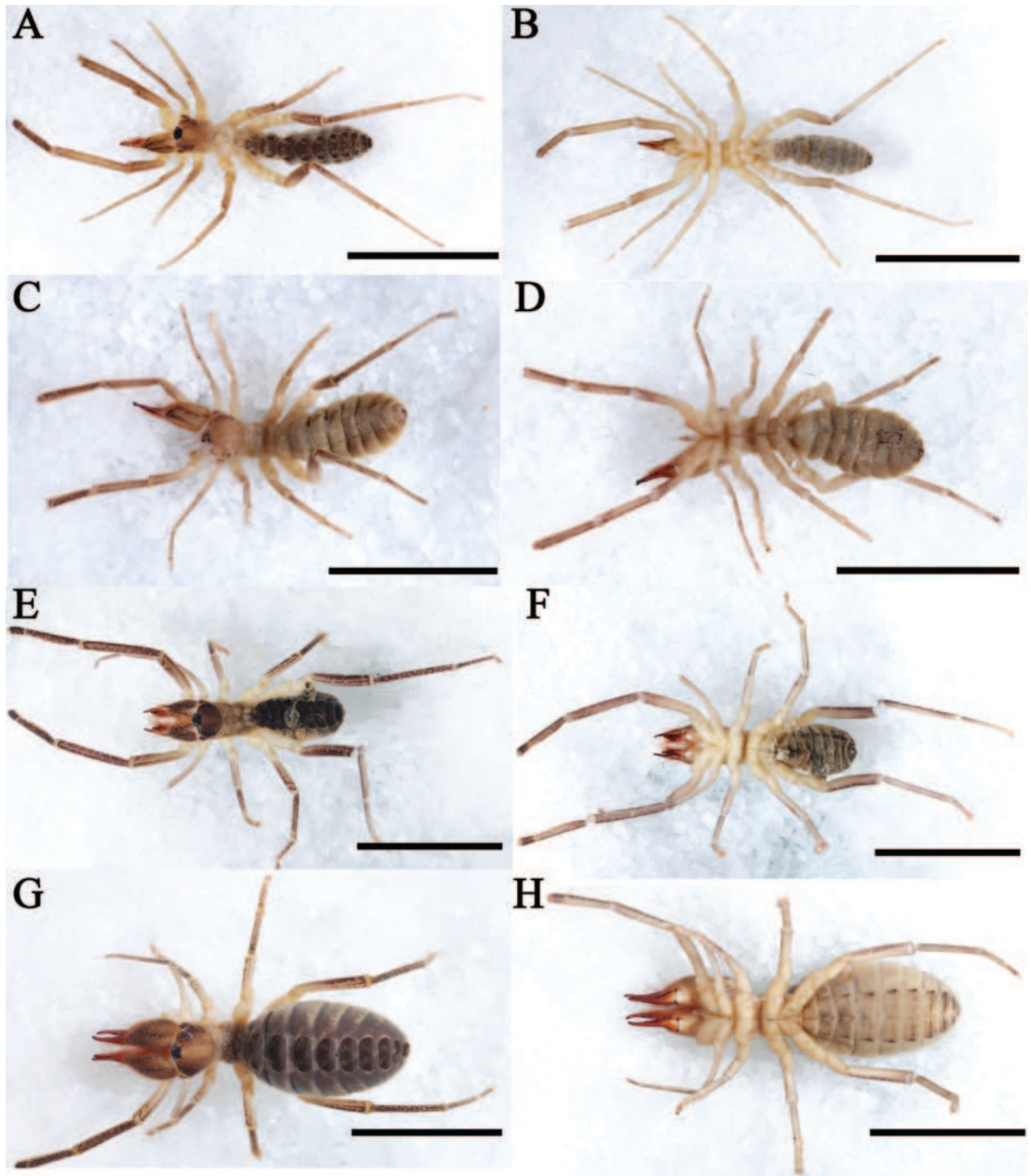


Figure 4. Habitus A–D *K. lhasa* sp. nov., habitus, male (A, B) and female (C, D) E–H *K. zhui* sp. nov., habitus, male (E, F) and female (G, H). Scale bars: 10 mm.

Propeltidium. Much longer than wide with a dense pubescence of thinner, short, anteriorly directed setae. Anterior, posterior, and lateral edges with several long, curved spiniform setae that are perpendicular to the surface of the propeltidium. Ocular tubercle with some long setae and numerous shorter, thinner setae (Fig. 6B).

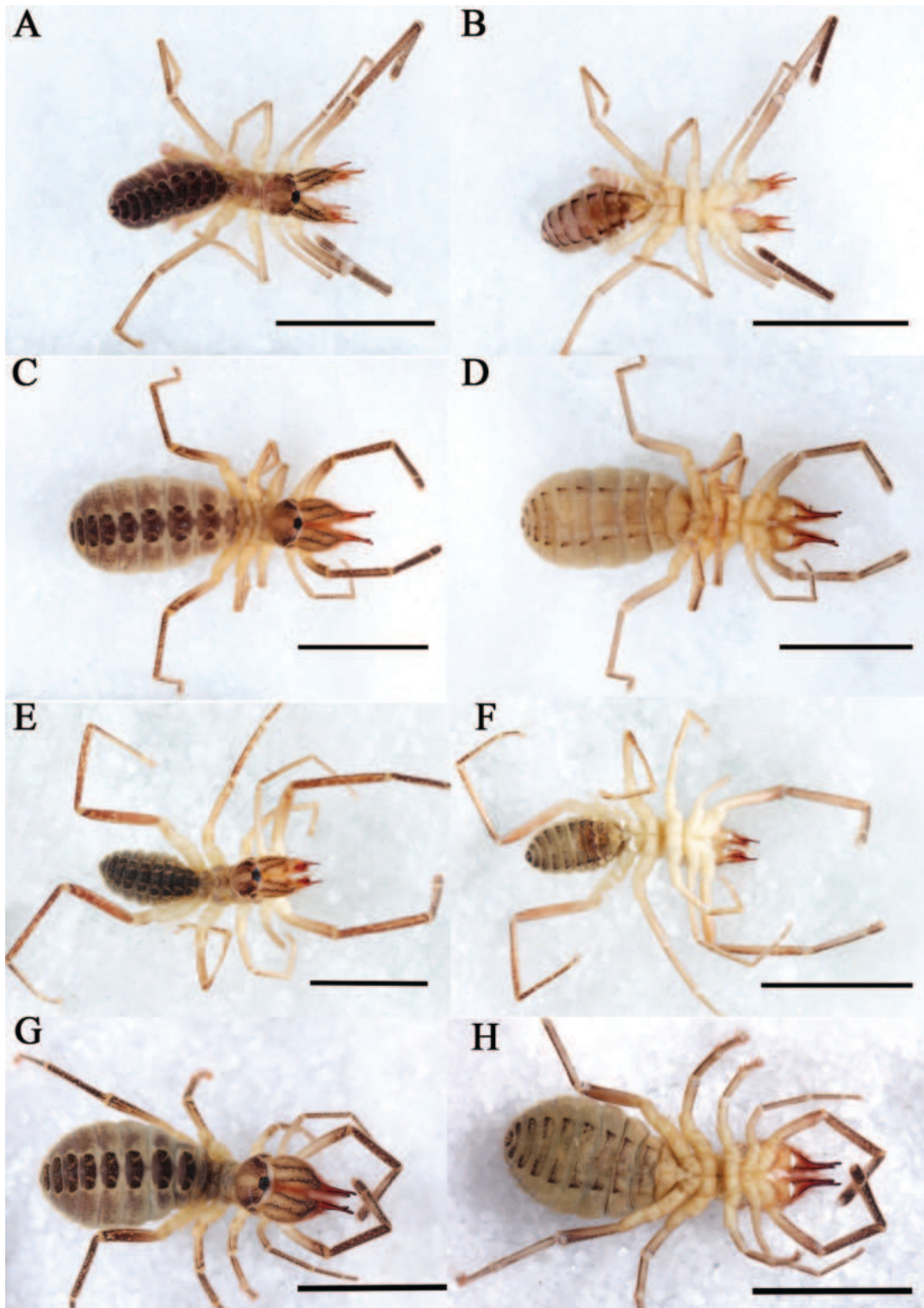


Figure 5. Habitus A–D *K. shigatse* sp. nov., habitus, male (A, B) and female (C, D) E–H *K. namling* sp. nov., habitus, male (E, F) and female (G, H). Scale bars: 10 mm.

Chelicerae. Dental formulation of fixed finger: FD-(2)-FM-(2)-FP-(7RF) (5PF). Dental formulation of movable finger: MM-(2)-MP, with four MST and four MSP. Fondal teeth graded as II, III, IV, I, tiny V, tiny VI, tiny VII retrolaterally; II, I, III, tiny IV, tiny V prolaterally (Figs 8C, D, 12A, 13C, D).

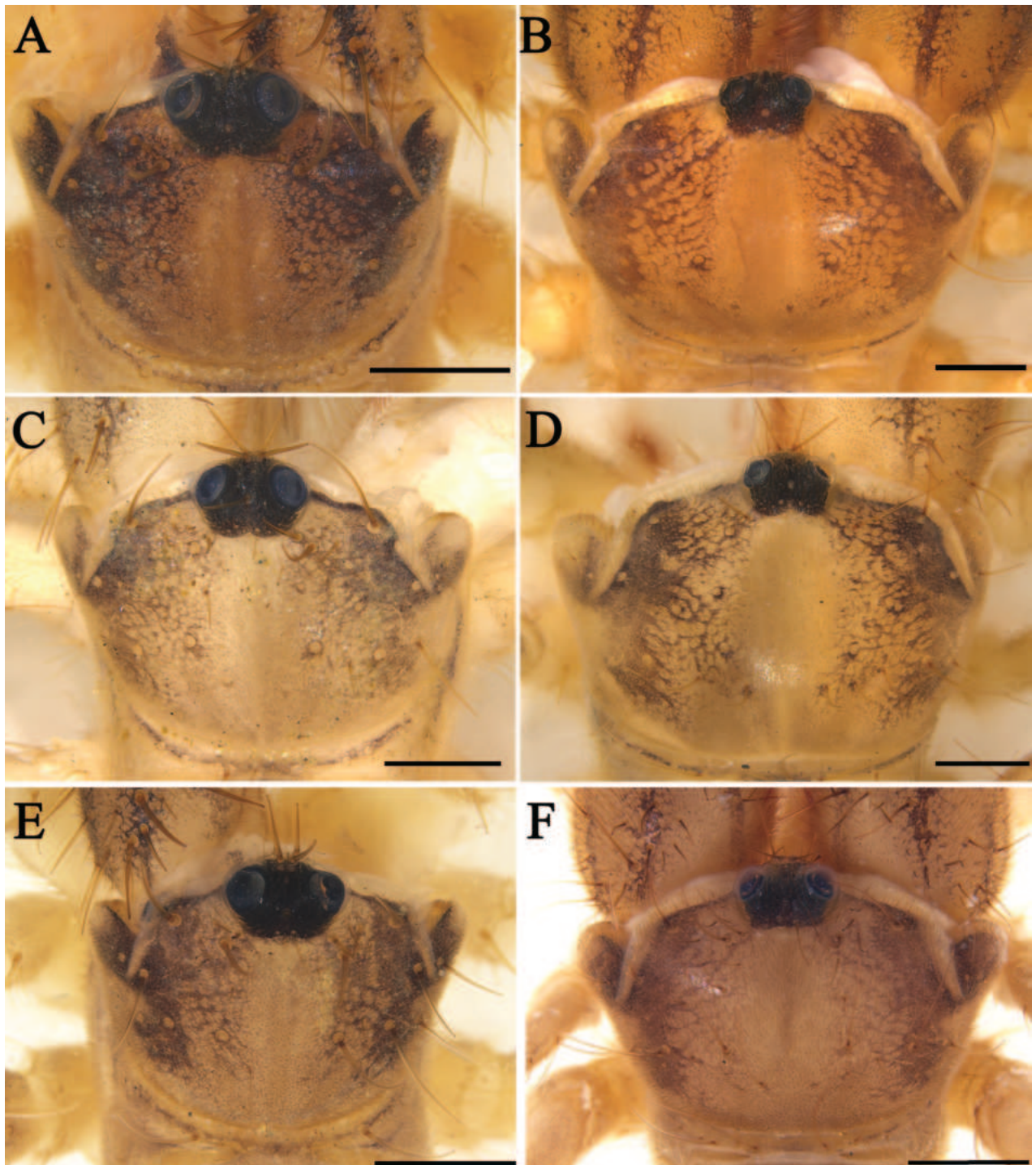


Figure 6. Propeltidium **A** *K. tibetana*, male **B** *K. tibetana*, female **C** *K. dingye* sp. nov., holotype male **D** *K. dingye* sp. nov., paratype female **E** *K. lhasa* sp. nov., holotype male **F** *K. lhasa* sp. nov., paratype female. Scale bars: 1 mm.

Opisthosoma. The entire surface covered with almost adpressed setae and numerous long, curved, bifurcate setae. Genital operculum long subtriangular and bottom widened (with lightly chitinized folds) between and behind them (Fig. 17A). Sternite IV with eight ctenidia on each side, for a total of 16 longer acicular ctenidia extending 1/2 length of the succeeding sternite (Fig. 18A).

Pedipalps. Entirely covered with short setae and long, thick setae, without spines.

Legs. As in the males.

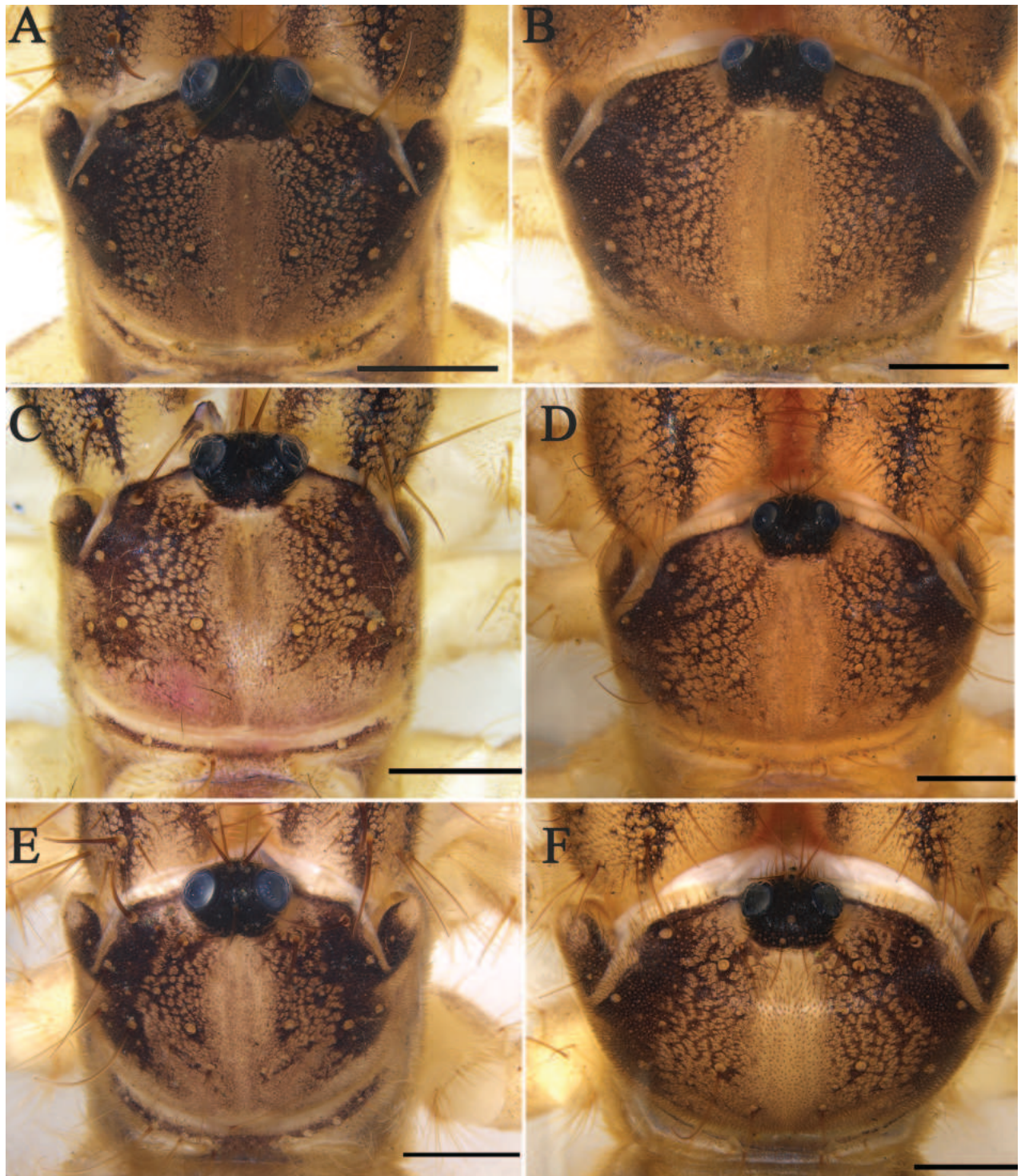


Figure 7. Propeltidium **A.** *K. zhui* sp. nov., holotype male **B.** *K. zhui* sp. nov., paratype female **C.** *K. shigatse* sp. nov., holotype male **D.** *K. shigatse* sp. nov., paratype female **E.** *K. namling* sp. nov., holotype male **F.** *K. namling* sp. nov., paratype female. Scale bars: 1 mm.

Variability. Males. Total length 16.17–20.35. Body coloration pale yellow to tan. Chelicerae with manus yellowish to brown. Pedipalps without or with only a few papillae. The number of cheliceral fixed finger fondal teeth 9–11 (profondal teeth 3–4; retrofondal teeth 6–7). The number of ctenidia on sternite IV 18–20. Pedipalp tarsus with 9–11 spines, metatarsus with 5–7 spines. Females.

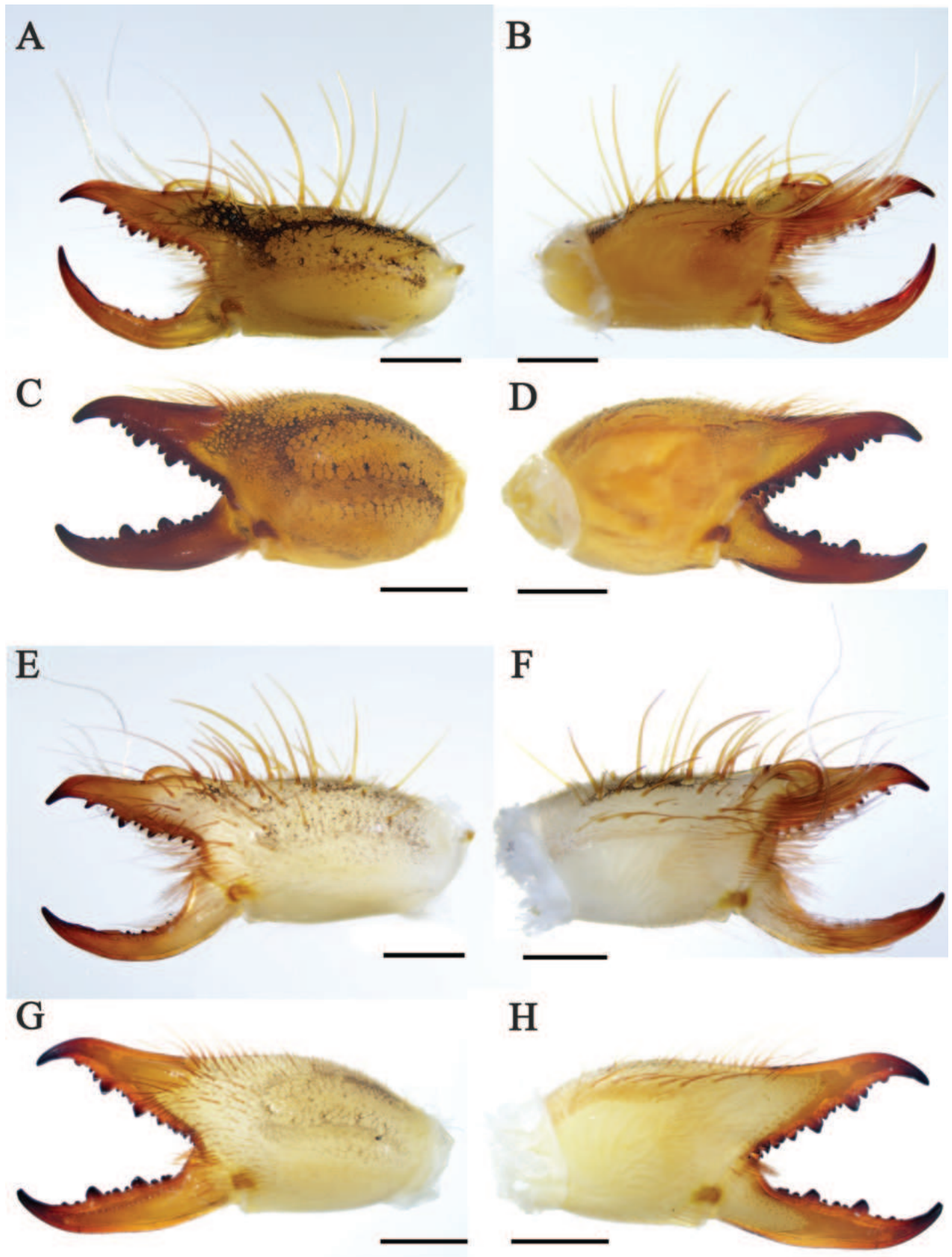


Figure 8. Retrolateral (left) and prolateral (right) cheliceral views **A, B** *K. tibetana*, male **C, D** *K. tibetana*, female **E, F** *K. dingye* sp. nov., holotype male **G, H** *K. dingye* sp. nov., paratype female. Scale bars: 1.0 mm (**A, B; E–H**); 2.0 mm (**C, D**).

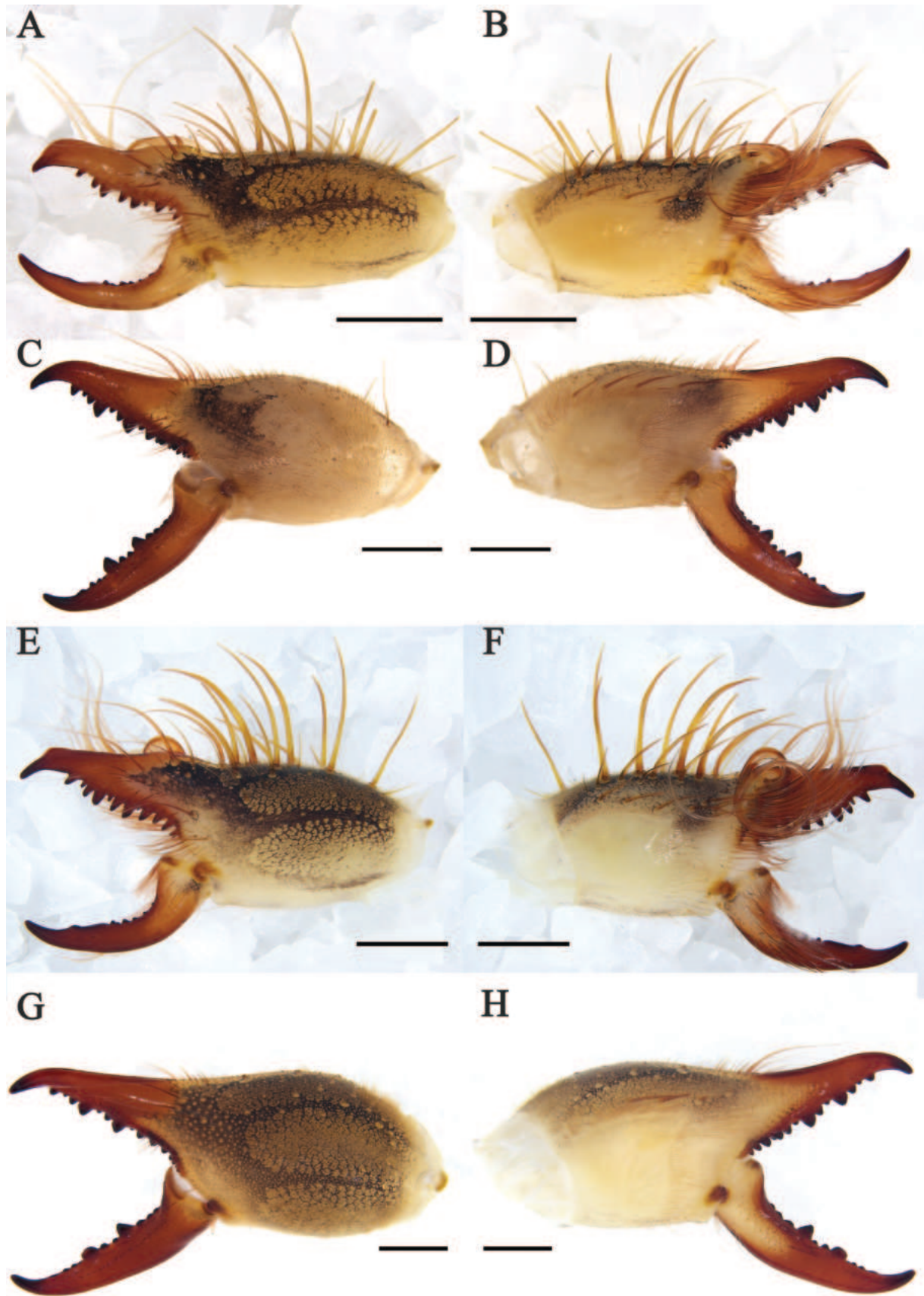


Figure 9. Retrolateral (left) and prolateral (right) cheliceral views **A, B** *K. lhasa* sp. nov., holotype male **C, D** *K. lhasa* sp. nov., paratype female **E, F** *K. zhui* sp. nov., holotype male **G, H** *K. zhui* sp. nov., paratype female. Scale bars: 1.0 mm.

Total length 19.53–22.36. Variability of body coloration as in males. The number of cheliceral fixed finger fonal teeth 10–13 (profondal teeth 4–5; retrofonda teeth 6–8). MST 3–4, MSP 4–5. The number of ctenidia on sternite IV 16–18.

Distribution and Habitat. China (Xizang). Habitat: high altitude meadow and semi-desert meadow.

Remark. In the original description, *K. tibetana* flagellum was described as smooth with small lateral apophysis (Hirst 1907). However, upon re-examination by Hirst (1912), it was found that the flagellum did not have a small lateral apophysis. Roewer (1933) reexamined the holotype and confirmed that the flagellum is fringed, not smooth. Based on my examination of specimens collected from the type locality, the flagellum of *K. tibetana* is fringed, and without small lateral apophysis. Based on the comparison of genetic distances, with a genetic distance of 0.88% (Table 2) between male and female collected from same locations, we believe that they are same species.

***Karschia (Karschia) dingye* sp. nov.**

<https://zoobank.org/CFF26FE4-7DF2-48B8-B670-5C202CE715D2>

Figs 1, 3E–H, 6C, D, 8E–H, 11B, 12B, 13E–H, 16C, D, 17B, 18B, 19B, D, Tables 1, 2

Type material. Holotype ♂ (MHBU-Sol-XZ2023072701), CHINA: Xizang, Shigatse Prefecture, Dingye County, Gyankar Town, 28.3702°N, 87.7732°E, ca 4200 m elev., 27.VII.2023, leg. Yanmeng Hou, Zhiyong Yang. **Paratypes:** 25♂♂ (MHBU-Sol-XZ2023072702–27), 15♀♀ (MHBU-Sol-XZ2023072728–43), with same data as holotype.

Etymology. Noun in apposition taken from Dingye County where this species was collected.

Diagnosis. *Karschia dingye* sp. nov. differs from *K. nubigena* by having fringed flagellum (Fig. 11B), and pedipalpal metatarsus with papillae (Fig. 16D), differs from *K. tibetana* by flagellar complex plumose (*fcp*) setae short (Fig. 11B), from *K. lhasa* sp. nov. and *K. zhui* sp. nov. by cheliceral fixed finger mucron without dorsal crest (Figs 8F, 13F), and from *K. shigatse* sp. nov. and *K. namling* sp. nov. by flagellum without lateral apophysis (Fig. 11B). The female genital operculum is easily recognizable across all known species, its bottom is slightly widened, giving it a trapezoidal appearance (Fig. 17B).

Description. Male. Holotype (MHBU-Sol-XZ2023072701).

Measurements. Total body length 17.58, CL 4.96, CH 1.77, PL 2.11, PW 3.28, A/CP 7.86, CL/CH 2.80. Pedipalp 17.70 (3.68, 5.95, 4.07, 1.51), Leg I 14.65 (3.67, 3.66, 2.72, 1.48, 0.15), Leg II 11.13 (2.74, 2.73, 2.25, 1.03, 0.76), Leg III 14.58 (3.78, 3.77, 2.87, 1.04, 1.16), Leg IV 23.25 (5.45, 6.41, 4.42, 1.38, 1.23).

Coloration. In 95% ethanol-preserved specimens (Fig. 3E, F). The general background brown-yellow. Opisthosoma pale yellow, with black tergites and pale black sternites. Propeltidium tinged with pale brown. Ocular tubercle black. Mesopeltidium and metapeltidium with special black stripes. Chelicerae with manus predominantly yellowish, with some black areas, and a retrolateral view of chelicerae with three black longitudinal stripes (paler than *K. tibetana*). Pedipalps and legs pale yellow, legs III and legs IV tinged with pale brown on distal regions of femora and proximal parts of tibiae. Proximal regions of the pedipalpal femur, tibia, metatarsus, and tarsus tinged with brown. Malleoli white.

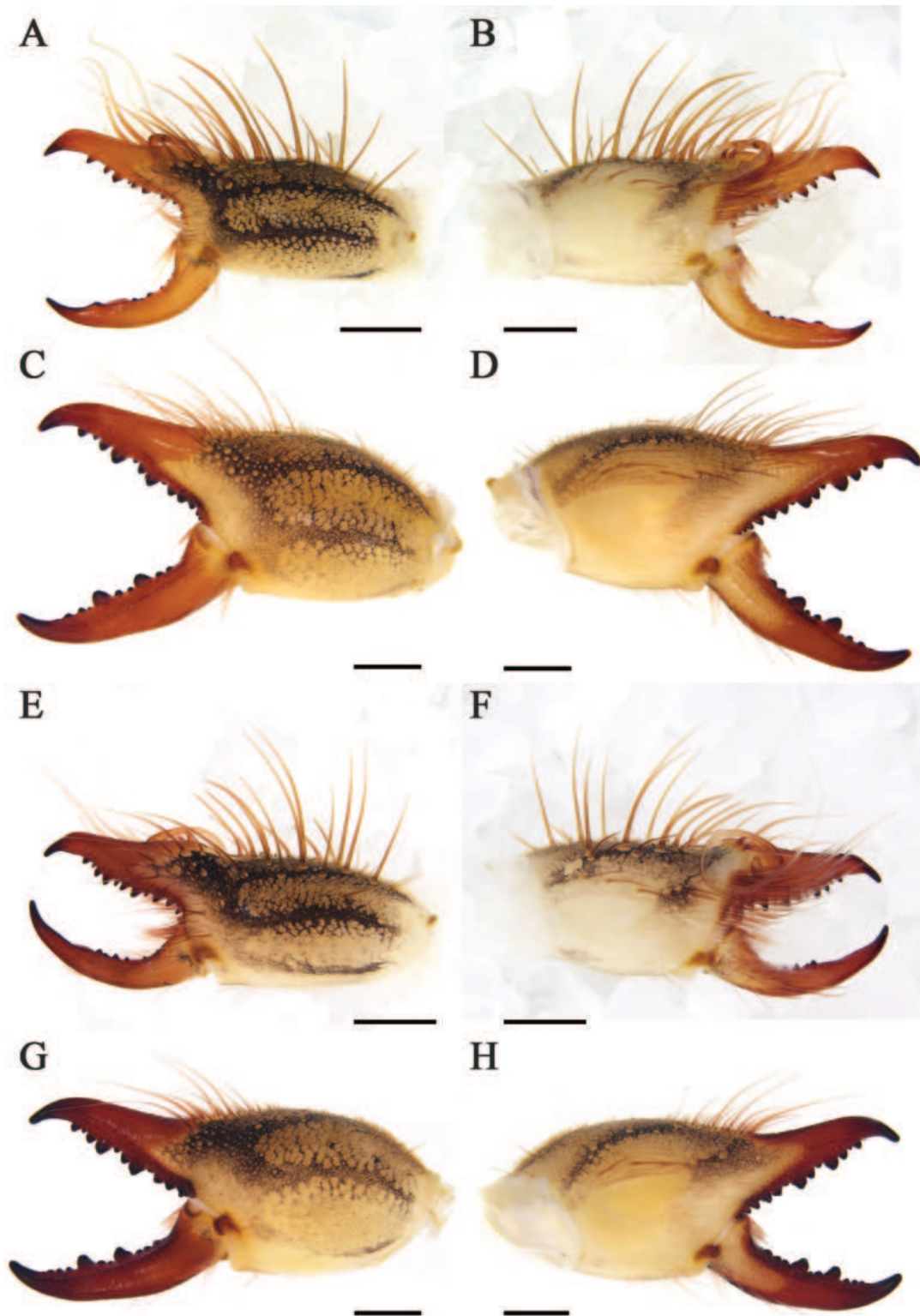


Figure 10. Retrolateral (left) and proteral (right) cheliceral views **A, B** *K. shigatse* sp. nov., holotype male **C, D** *K. shigatse* sp. nov., paratype female **E, F** *K. namling* sp. nov., holotype male **G, H** *K. namling* sp. nov., paratype female. Scale bars: 1.0 mm.

***Propeltidium*.** Much wider than long with dense pubescence of thin, short, anteriorly directed setae. Anterior, posterior, and lateral edges with several long, curved spiniform setae, perpendicular to the surface of the propeltidium. Ocular tubercle with one short and four long middle distal spiniform setae which

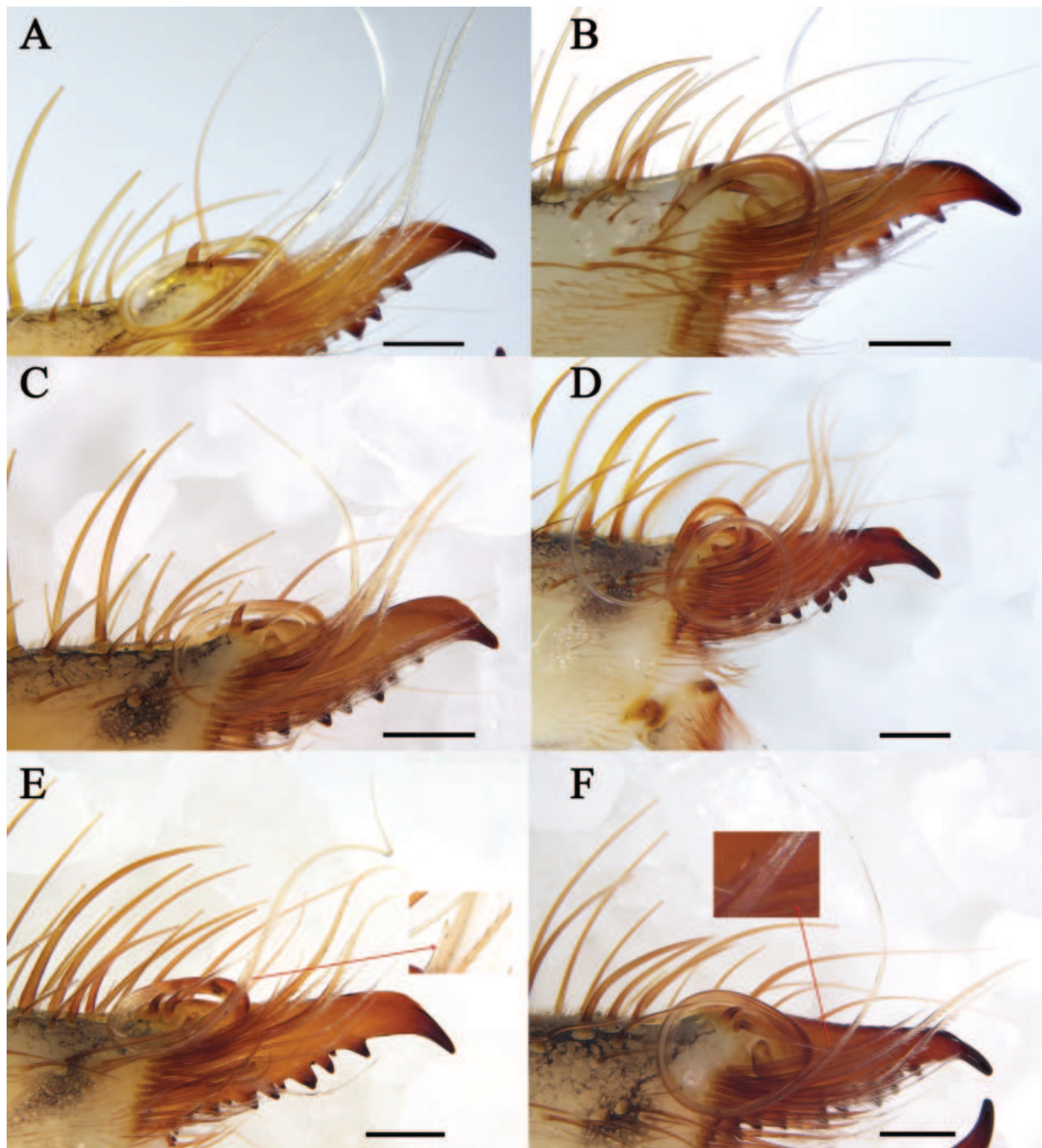


Figure 11. Flagellum **A** *K. tibetana* **B** *K. dingye* sp. nov. **C** *K. lhasa* sp. nov. **D** *K. zhui* sp. nov. **E** *K. shigatse* sp. nov. **F** *K. namling* sp. nov. Scale bars: 0.5 mm.

are arranged symmetrically on both sides of the short spiniform setae, one long middle spiniform setae, two short spiniform setae, and numerous shorter, thinner proximal setae (Fig. 6C).

Chelicerae. Fixed finger primary teeth graded as $FD < FP < FM$. Profondal teeth series with four tiny teeth; retrofondal teeth series with six teeth. Dental formulation of fixed finger: $FD-(3)-FM-(2)-FP-(6RF)$ (4PF). Fixed finger mucron moderately long, without dorsal crest. Movable finger MP tooth about the same size as MM. Dental formulation of movable finger: $MM-(2)-MP$, with two MSM

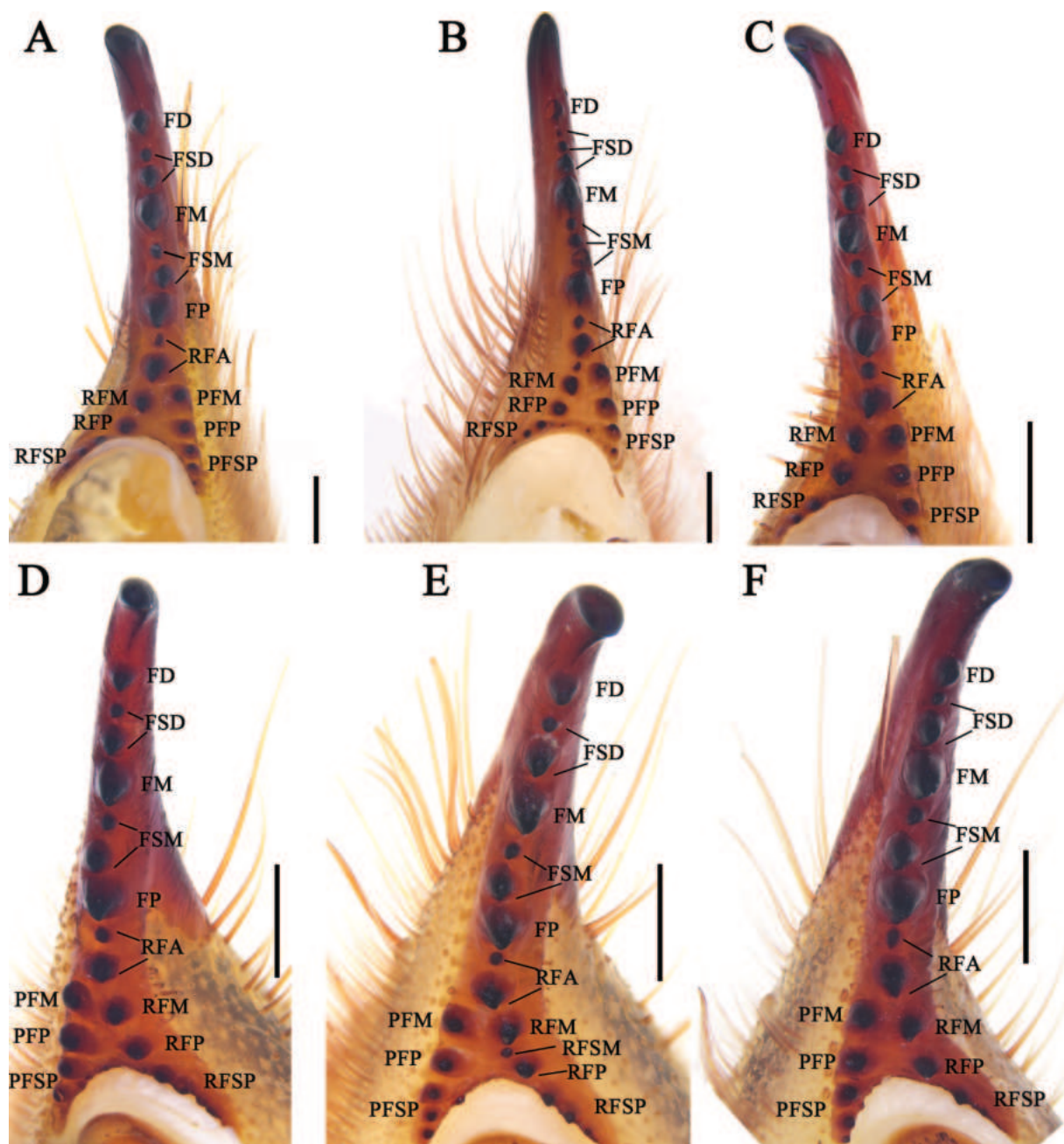


Figure 12. Female fixed finger ventral views **A** *K. tibetana* **B** *K. dingye* sp. nov. **C** *K. lhasa* sp. nov. **D** *K. zhui* sp. nov. **E** *K. shigatse* sp. nov. **F** *K. namling* sp. nov. Abbreviations: FD, fixed finger, distal tooth; FSD, fixed finger, subdistal tooth/teeth; FM, fixed finger, medial tooth; FSM, fixed finger, submedial tooth/teeth; FP, fixed finger, proximal tooth; RFA, retrofondal apical tooth/teeth; RFM, retrofondal medial tooth; RFSM, retrofondal submedial tooth/teeth; RFP, retrofondal proximal tooth; RFSP, retrofondal subproximal tooth/teeth; PFM, profondal medial tooth; PFP, profondal proximal tooth; PFSP, profondal subproximal tooth. Scale bars: 0.5 mm.

and three MSP (Figs 8E, 13E). Flagellum, fringed without lateral apophysis, and basal peg expand. The flagellar complex includes two short *fcp* and two short, thick *fcs* (Figs 8F, 11B, 13F). Retrolateral and dorsal surfaces of the manus with large, bifurcated tip setae and short simple tip bristle-like setae; retrolateral and dorsal surfaces of the fixed finger with simple tip setae of different sizes. Retrolateral setose area reaching the FSM teeth; prolateral surface with an array of setal types (Figs 8E, F, 13E, F).

Opisthosoma. The entire surface covered with almost adpressed setae and numerous long, curved, bifurcate setae. Sternite III with two posterior paramedian groups of ctenidia, being gradually larger to posterior. (Fig. 19B); Sternite IV with 17 short peg-like ctenidia extending 1/4 the length of the succeeding sternite (Fig. 19D).

Pedipalps. Entirely covered with short setae and long, thick setae. Tarsus with eleven short, sturdy ventral spines; metatarsus with nine ventral spines not arranged in pairs and with thin papillae (Fig. 16C, D).

Legs. Entirely covered with long, thick setae and short setae. Leg I with no spines and two small claws. Tibias II, III, and IV with a pair of distal spines ventrally. Tibias II and III with a single dorsal spine; metatarsi II and III with a series of three dorsal spines, a pair of distal spines ventrally, and some paired short, thick, spine-shaped bristles over their entire ventral surface. Metatarsus IV also with these paired bristles over its entire ventral surface and two distal spines ventrally.

Female. Paratype (MHBU-Sol-XZ2023072701).

Measurements. Total body length 25.64, CL 7.18, CH 2.75, PL 3.23, PW 4.25, A/CP 4.72, CL/CH 2.61, Palp 17.61 (4.16, 4.97, 3.70, 1.24), Leg I 9.84 (2.52, 3.60, 2.57, 1.18, 0.12), Leg II 10.21 (1.48, 2.49, 1.56, 0.83, 0.70), Leg III 12.80 (2.13, 2.87, 2.51, 0.94, 0.10), Leg IV 21.68 (4.06, 5.77, 3.96, 1.13, 1.19).

Coloration. In 95% ethanol-preserved specimens (Fig. 3G, H). Coloration as in the males.

Propeltidium. Much wider than long with a dense pubescence of thin, short, anteriorly directed setae. Anterior, posterior, and lateral edges with several long, curved spiniform setae that perpendicular to the surface of the propeltidium. Ocular tubercle with four middle distal spiniform setae, covered with some long setae and numerous shorter, thinner setae (Fig. 6D).

Chelicerae. Dental formulation of fixed finger: FD-(3)-FM-(3)-FP-(7RF) (4PF). Dental formulation of movable finger: MM-(3)-MP, with three MST (front one tiny) and two MSP. Fondal teeth graded as II, IV, V, tiny I, tiny III, tiny VI, tiny VII retrolaterally; I, II, III, tiny IV prolaterally (Figs 8G, H, 12B, 13G, H).

Opisthosoma. The entire surface covered with almost adpressed setae and numerous long, curved, bifurcate setae. The bottom of the genital operculum slightly widened, resembling a trapezoid (Fig. 17B). Sternite IV with 19 short spine-like ctenidia extending from the edge of sternite IV (Fig. 18B).

Pedipalps. Entirely covered with short setae and long, thick setae and without spines.

Legs. As in the males.

Variability. Males. Total length 14.25–18.76. Body coloration pale yellow to tan. Chelicerae with manus yellowish to brown. The number of cheliceral fixed finger fondal teeth 9–11 (profondal teeth 3–4; retrofondal teeth 6–7). The number of ctenidia on sternite IV 16–18. Pedipalp tarsus with 10–12 spines, metatarsus with 8–10 spines. Females. Total length 20.13–27.68. Variability of body coloration as in males. The number of cheliceral fixed finger fondal teeth 9–12 (profondal teeth 3–5; retrofondal teeth 6–7). MST 2–3, MSP 1–2. The number of ctenidia on sternite IV 17–21. Additionally, we found that all specimen with 3FSD.

Distribution and habitat. China (Xizang). Habitat: meadow (Fig. 2A, B).

Remark. Based on the comparison of genetic distances, with a genetic distance of 0.30% (Table 2) between male and female collected from same locations, we believe that they are same species.

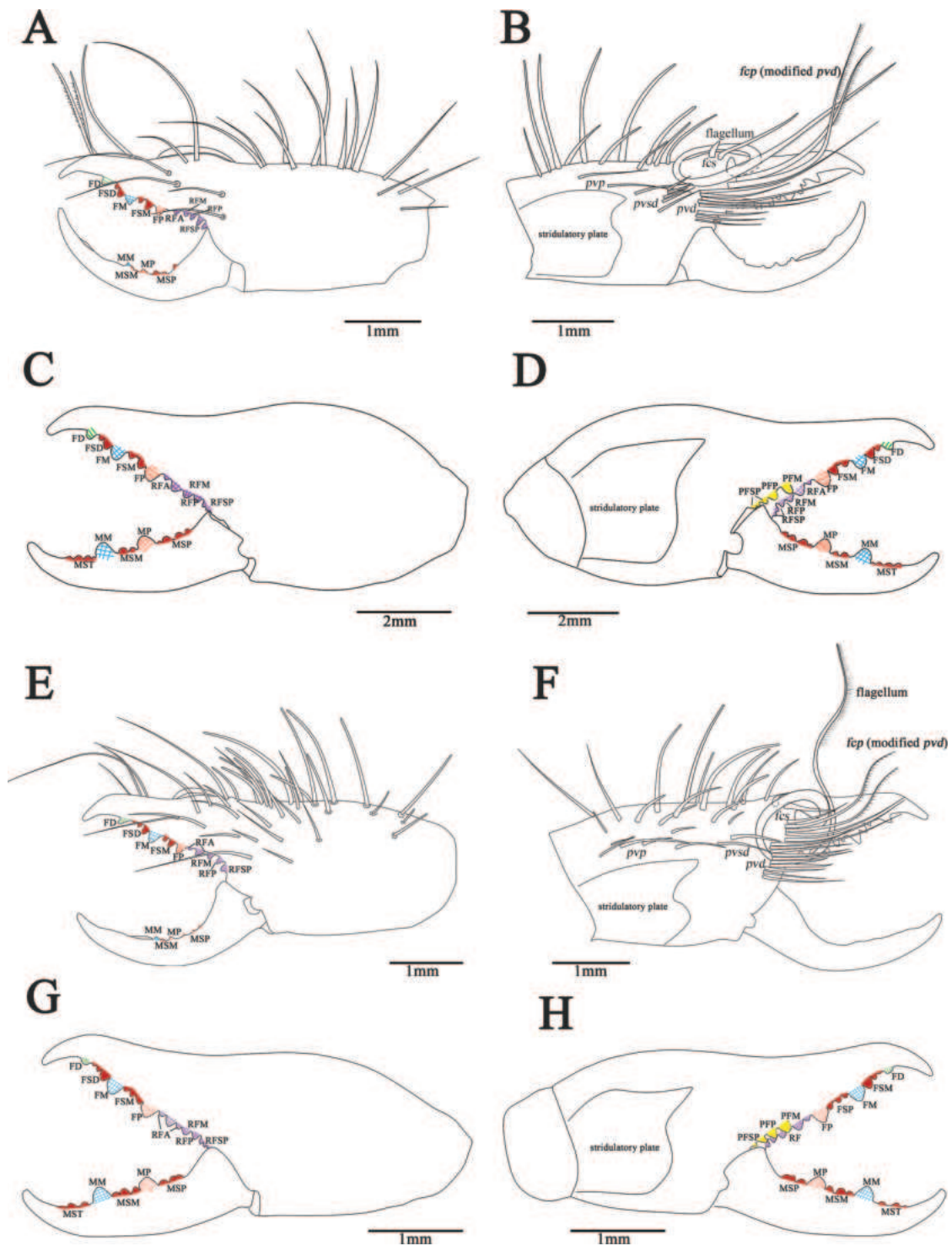


Figure 13. Retrolateral (left) and proteral (right) cheliceral views **A, B** *K. tibetana*, male **C, D** *K. tibetana*, female **E, F** *K. dingye* sp. nov., holotype male **G, H** *K. dingye* sp. nov., paratype female. Abbreviations: FD, fixed finger, distal tooth; FSD, fixed finger, subdistal tooth/teeth; FM, fixed finger, medial tooth; FSM, fixed finger, submedial tooth/teeth; FP, fixed finger, proximal tooth; RF, retrofondal teeth; RFA, retrofondal apical tooth/teeth; RFM, retrofondal medial tooth; RFP, retrofondal proximal tooth; RFSP, retrofondal subproximal tooth/teeth; PF, profundal teeth; PFM, profundal medial tooth; PFP, profundal proximal tooth; PFSP, profundal subproximal tooth; MSP, movable finger, subproximal tooth/teeth; MP, movable finger, proximal tooth; MSM, movable finger, submedial tooth/teeth; MM, movable finger, medial tooth; MST, movable finger, subterminal teeth; *pvd*, proventral distal setae; *fcp* (modified *pvd*), flagellar complex plumose setae; *pdp*, prodorsal proximal setae; *fcs*, flagellar complex subspiniform to spiniform setae; *pvsd*, proventral subdistal setae; *pvd*, proventral distal setae. Scale bars: 1.0 mm (**A, B; E–H**); 2.0 mm (**C, D**).

Karschia (Karschia) lhasa sp. nov.

<https://zoobank.org/5F281BD9-03EC-49E6-9A95-1E6E1A096FEF>

Figs 1, 4A–D, 6E, F, 9A–D, 11C, 12C, 14A–D, 16E, F, 17C, 18C, 19E, G, Tables 1, 2

Type material. *Holotype* ♂ (MHBU-Sol-XZ2018070501), CHINA: Xizang, Lhasa City, Maizhokunggar County, 29.8268°N, 91.6991°E, ca 3800 m elev., 5. VIII.2018, leg. Yannan Mu. *Paratypes*: 1♂ (MHBU-Sol-XZ2018070502), 1♀ (MHBU-Sol-XZ2018070503), with same data as holotype.

Etymology. Noun in apposition taken from Lhasa City where this species was collected.

Diagnosis. *Karschia lhasa sp. nov.* differs from all *Karschia* species except *K. zhui sp. nov.* by cheliceral fixed finger mucron having dorsal crest (Fig. 11C). *K. lhasa sp. nov.* differs from *K. zhui sp. nov.* by cheliceral fixed finger mucron crescent-shaped dorsal crest broader (Fig. 11C), and pedipalp having more spines and thick papillae (Fig. 16H). The female genital operculum is easily recognizable when compared to that of other species; it has a clear demarcation between the plates. and resembles a fan-shaped structure. (Fig. 17C).

Description. **Male** Holotype (MHBU-Sol-XZ2018070501).

Measurements. Total body length 16.60, CL 4.03, CH 1.26, PL 2.01, PW 2.59, A/CP 7.57, CL/CH 3.19. Pedipalp 15.64 (3.12, 4.69, 2.46, 1.04), Leg I 10.06 (2.18, 2.78, 2.00, 0.97, 0.18), Leg II 9.28 (1.37, 2.16, 1.69, 0.74, 0.45), Leg III 12.95 (2.13, 3.13, 2.49, 0.71, 0.78), Leg IV 19.99 (4.76, 5.35, 3.75, 1.29, 1.28).

Coloration. In 75% ethanol-preserved specimens (Fig. 4A, B). The general background pale yellow. Opisthosoma grey-yellow, with black tergites and pale black sternites. Propeltidium tinged pale brown. Ocular tubercle black. Mesopeltidium and metapeltidium with special black stripes. Chelicerae with manus predominantly brown-yellow, with some black areas, and a retrolateral view of chelicerae with three black longitudinal stripes. Pedipalps and legs yellow, legs III and legs IV tinged with pale brown on distal regions of femora and proximal parts of tibiae. Proximal regions of the pedipalpal femur, tibia, metatarsus, and tarsus tinged with brown. Malleoli yellow.

Propeltidium. Slightly wider than long with a dense pubescence of thin, short, anteriorly directed setae. Anterior, posterior, and lateral edges with several long, curved spiniform setae that perpendicular to the surface of the propeltidium. Ocular tubercle with one short and four long middle distal spiniform setae, one long median spiniform setae, two shorter posterior spiniform setae, and numerous short, thin posterior setae (Fig. 6E).

Chelicerae. Fixed finger primary teeth graded as $FD < FP \approx FM$. Profondal teeth series with three or four tiny teeth; retrofondal teeth series with six teeth. Dental formulation of fixed finger: $FD-(2)-FM-(1)-FP-(6RF)$ (3PF). Fixed finger mucron with wider and crescent-shaped dorsal crest. Movable finger MP tooth about the same size as MM. Dental formulation of movable finger: $MM-(2)-MP$, with one tiny MSM and four MSP (Figs 9A, B, 14A, B). Flagellum coiled, fringed and sessile, without lateral apophysis. The flagellar complex includes two medium length *fcp* and two short, thick *fcs* (Figs 9B, 11C, 14B). Retrolateral and dorsal surfaces of the manus with large, bifurcated tip setae and short, simple tip bristle-like setae; retrolateral and dorsal surfaces of the fixed finger with simple tip setae of different sizes. Retrolateral setose area reaching the FSM teeth; prolateral surface with an array of setal types (Figs 9A, B, 14A, B).

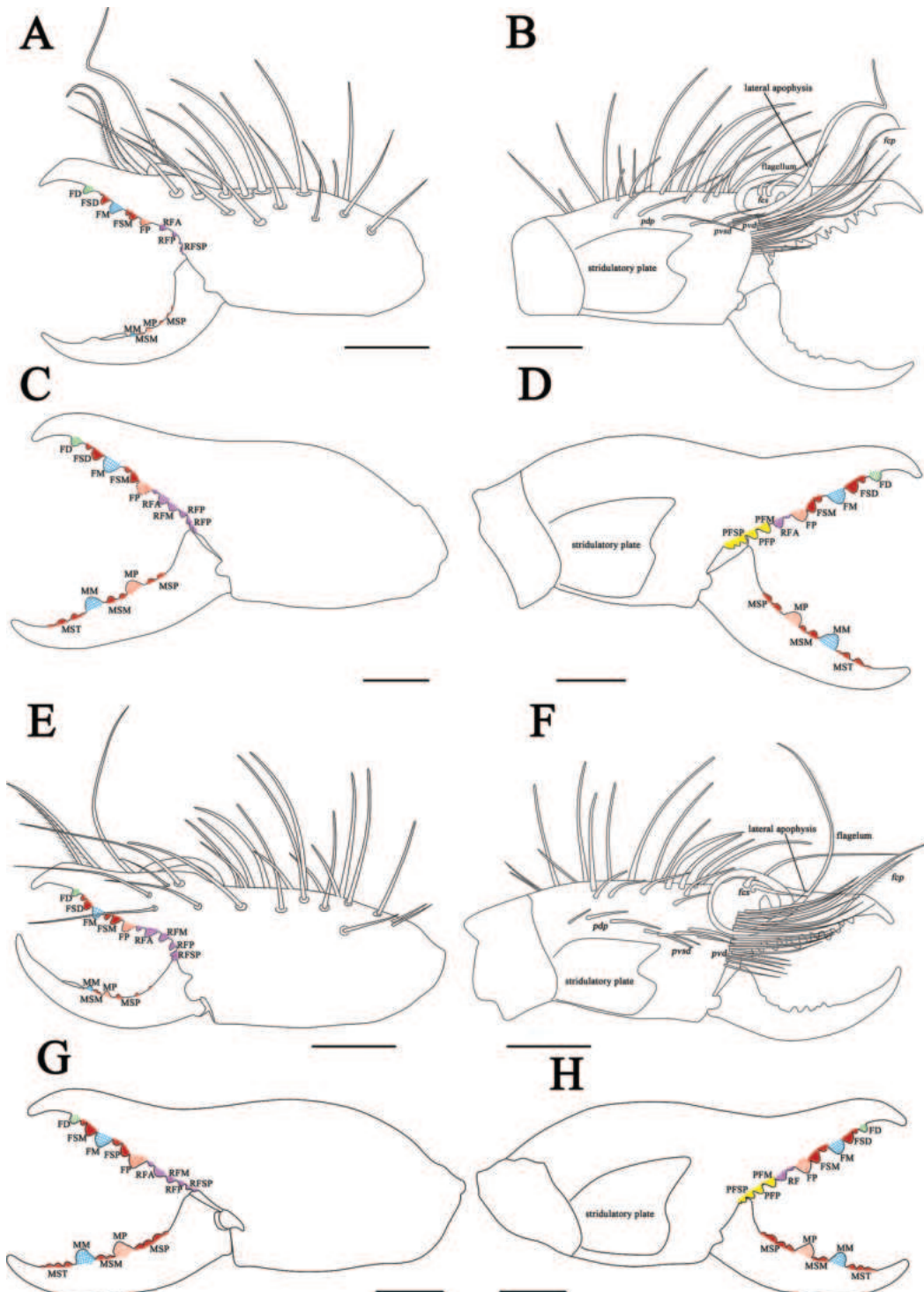


Figure 15. Retrolateral (left) and proteral (right) cheliceral views **A, B** *K. shigatse* sp. nov., holotype male **C, D** *K. shigatse* sp. nov., paratype female **E, F** *K. namling* sp. nov., holotype male **G, H** *K. namling* sp. nov., paratype female. Abbreviations: FD, fixed finger, distal tooth; FSD, fixed finger, subdistal tooth/teeth; FM, fixed finger, medial tooth; FSM, fixed finger, submedial tooth/teeth; FP, fixed finger, proximal tooth; RF, retrofondal teeth; RFA, retrofondal apical tooth/teeth; RFM, retrofondal medial tooth; RFP, retrofondal proximal tooth; RFSP, retrofondal subproximal tooth/teeth; PF, profondal teeth; PFM, profondal medial tooth; PFP, profondal proximal tooth; PFSP, profondal subproximal tooth; MSP, movable finger, subproximal tooth/teeth; MP, movable finger, proximal tooth; MSM, movable finger, submedial tooth/teeth; MM, movable finger, medial tooth; MST, movable finger, subterminal teeth; *pvd*, proventral distal setae; *fcp* (modified *pvd*), flagellar complex plumose setae; *pdp*, prodo rsal proximal setae; *fcs*, flagellar complex subspiniform to spiniform setae; *pvsd*, proventral subdistal setae; *pvd*, proventral distal setae. Scale bars: 1.0 mm.

Opisthosoma. The entire surface covered with almost adpressed setae and numerous long, curved, bifurcate setae. Sternite III with short, thin ctenidia: 14+15 (on the right and left side, respectively) (Fig. 19E); Sternite IV with 13 short peg-like ctenidia, the length of which almost 1/3 the width of the succeeding sternite (Fig. 19G).

Pedipalps. Totally covered with short setae and long, thick setae. Tarsus not swollen with five sturdy ventral spines; metatarsus with eight ventral spines not arranged in pairs and with thick papillae (Fig. 16E, F).

Legs. Totally covered with long, thick setae and short setae. Leg I with no spines and two small claws. Tibias II, III, and IV with a pair of distal spines ventrally. Tibias II and III with a single dorsal spine. Metatarsi II and III with a series of three dorsal spines, a pair of distal spines ventrally, and some paired short, thick, spine-shaped bristles over their entire ventral surface; metatarsus IV also with these paired bristles over its entire ventral surface and two distal spines ventrally.

Female. Paratype (MHBU-Sol-XZ2018070503).

Measurements. Total body length 16.69, CL 5.10, CH 1.76, PL 2.45, PW 3.53, A/CP 4.60, CL/CH 2.90. Pedipalp 12.55 (3.13, 3.52, 2.73, 1.05), Leg I 8.15 (1.60, 2.32, 1.70, 0.93, 0.14), Leg II 7.66 (1.05, 1.53, 1.38, 0.98, 0.61), Leg III 7.74 (0.81, 1.71, 2.23, 0.98), Leg IV 14.06 (1.96, 4.25, 2.23, 0.74, 0.78).

Coloration. In 75% ethanol-preserved specimens (Fig. 4C, D). Coloration as in the males. *Propeltidium.* Much wider than long with a dense pubescence of thin, short, anteriorly directed setae. Anterior, posterior, and lateral edges with several long, curved spiniform setae that perpendicular to the surface of the propeltidium. Ocular tubercle with four middle distal spiniform setae, two middle spiniform setae, and two posterior spiniform setae (Fig. 6F).

Chelicerae. Dental formulation of fixed finger: FD-(2)-FM-(2)-FP-(6RF) (4PF). Dental formulation of movable finger: MM-(2)-MP, with four MST and five MSP. Fondal teeth graded as II, III, IV, I, V, VI retrolaterally; I, II, III, IV prolaterally (Figs 9C, D, 12C, 14C, D).

Opisthosoma. The entire surface covered with almost adpressed setae and numerous long, curved, bifurcate setae. The bottom of the genital operculum slightly widened, resembling a fan-shaped structure (with chitinized folds) between and behind it (Fig. 17C). Sternite IV with 13 long needle-like ctenidia extending 3/4 the length of the succeeding sternite (Fig. 18C).

Pedipalps. Totally covered with short setae and long, thick setae without spines.

Legs. As in the males.

Variability. Males. Total length 15.52–16.60. The number of cheliceral fixed finger fondal teeth 9–10 (profondal teeth 3–4). The number of ctenidia on sternite III 28–32 and on sternite IV 13–14. Pedipalp tarsus with 5–6 spines, metatarsus with 8–10 spines.

Distribution and habitat. China (Xizang). Habitat: wild grassy slope (Fig. 2C).

Remark. Based on the comparison of genetic distances, with a genetic distance of 0% (Table 2) between male and female collected from same locations, we believe that they are same species.

***Karschia (Karschia) zhui* sp. nov.**

<https://zoobank.org/CC55BE2C-C5C7-4B7D-A4A8-8019022A4339>

Figs 1, 4E–H, 7A, B, 9E–H, 11D, 12D, 14E–H, 16G, H, 17D, 18D, 19F, H, Tables 1, 2

Type material. *Holotype* ♂ (MHBU-Sol-XZ2022070401), CHINA: Xizang, Lhasa City, Drepung Monastery, 29.6697°N, 91.0548°E, 3672.7 m elev., 4.VII.2022, leg. Wenlong Fan. *Paratype*: 1 ♀ (MHBU-Sol-XZ2023070501), CHINA: Xizang, Lhasa City, Drepung Monastery, 29.6758°N, 91.0490°E, 3903 m elev., 5.VII.2023, leg. Quanyu Ji.

Etymology. Patronym honors Prof. Ming-Sheng Zhu (Hebei University), who significantly contributed to arachnological studies in China.

Diagnosis. *Karschia zhui* sp. nov. differs from all *Karschia* species except *K. lhasa* sp. nov. by cheliceral fixed finger mucron having dorsal crest (Figs 9F, 11D). *K. zhui* sp. nov. differs from *K. lhasa* sp. nov. by cheliceral fixed finger mucron dorsal crest small crescent-shaped (Figs 9F, 11D), and pedipalp having less spines and thin papillae (Fig. 16H). Female genital operculum like *K. tibetana*, but can be diagnosed by the lower edge, which is somewhat convex, not flat (Fig. 17D).

Description. Male. Holotype (MHBU-Sol-XZ2022070401).

Measurements. Total body length 14.10, CL 4.33, CH 1.61, PL 2.11, PW 2.96, A/CP 7.50, CL/CH 2.69. Pedipalp 16.39 (3.83, 5.41, 3.66, 1.33), Leg I 11.95 (3.06, 3.32, 2.41, 0.97, 0.14), Leg II 10.08 (1.73, 2.33, 1.77, 0.63, 0.67), Leg III 12.31 (2.57, 3.11, 1.56, 0.52, 0.61), Leg IV 19.95 (3.88, 5.36, 2.94, 1.19, 0.98).

Coloration. In 95% ethanol-preserved specimens (Fig. 4E, F). The general background pale yellow. Opisthosoma brow yellow, with black tergites and pale black sternites. Propeltidium black tinged with pale brown. Ocular tubercle black. Mesopeltidium and metapeltidium with special black stripes. Chelicerae with manus predominantly yellowish, with some black areas, and a retrolateral view of chelicerae with three black longitudinal stripes. Pedipalps and legs pale brown-yellow, legs III and legs IV tinged with pale brown on distal regions of femora and proximal parts of tibiae. Proximal regions of the pedipalpal femur, tibia, metatarsus, and tarsus tinged with brown. Malleoli white.

Propeltidium. Wider than long with a dense pubescence of thin, short, anteriorly directed setae. Anterior, posterior, and lateral edges with several long, curved spiniform setae that perpendicular to the surface of the propeltidium. Ocular tubercle with four middle distal spiniform setae, one middle spiniform setae, and two proximal spiniform setae (Fig. 7A).

Chelicerae. Fixed finger primary teeth graded as $FP < FM \approx FD$. Profondal teeth series with four or five tiny teeth; retrofondal teeth series with six teeth. Dental formulation of fixed finger: FD-(2)-FM-(2)-FP-(6RF) (4PF). Fixed finger mucron with crescent-shaped dorsal crest smaller than *K. lhasa*. Movable finger MP tooth about the same size as MM. Dental formulation of movable finger: MM-(1)-MP, with one tiny MSM and three MSP (Figs 9E, 14E). Flagellum coiled, fringed and sessile, without lateral apophysis. The flagellar complex includes two medium length *fcp* and two short, thick *fcs*. (Figs 9E, 11D, 14F). Retrolateral and dorsal surfaces of the manus with large, bifurcated tip setae and short, simple tip bristle-like setae; retrolateral and dorsal surfaces of the fixed finger with simple tip setae of different sizes. Retrolateral setose area reaching the FSM teeth; prolateral surface with an array of setal types (Figs 9E, F, 14E, F).

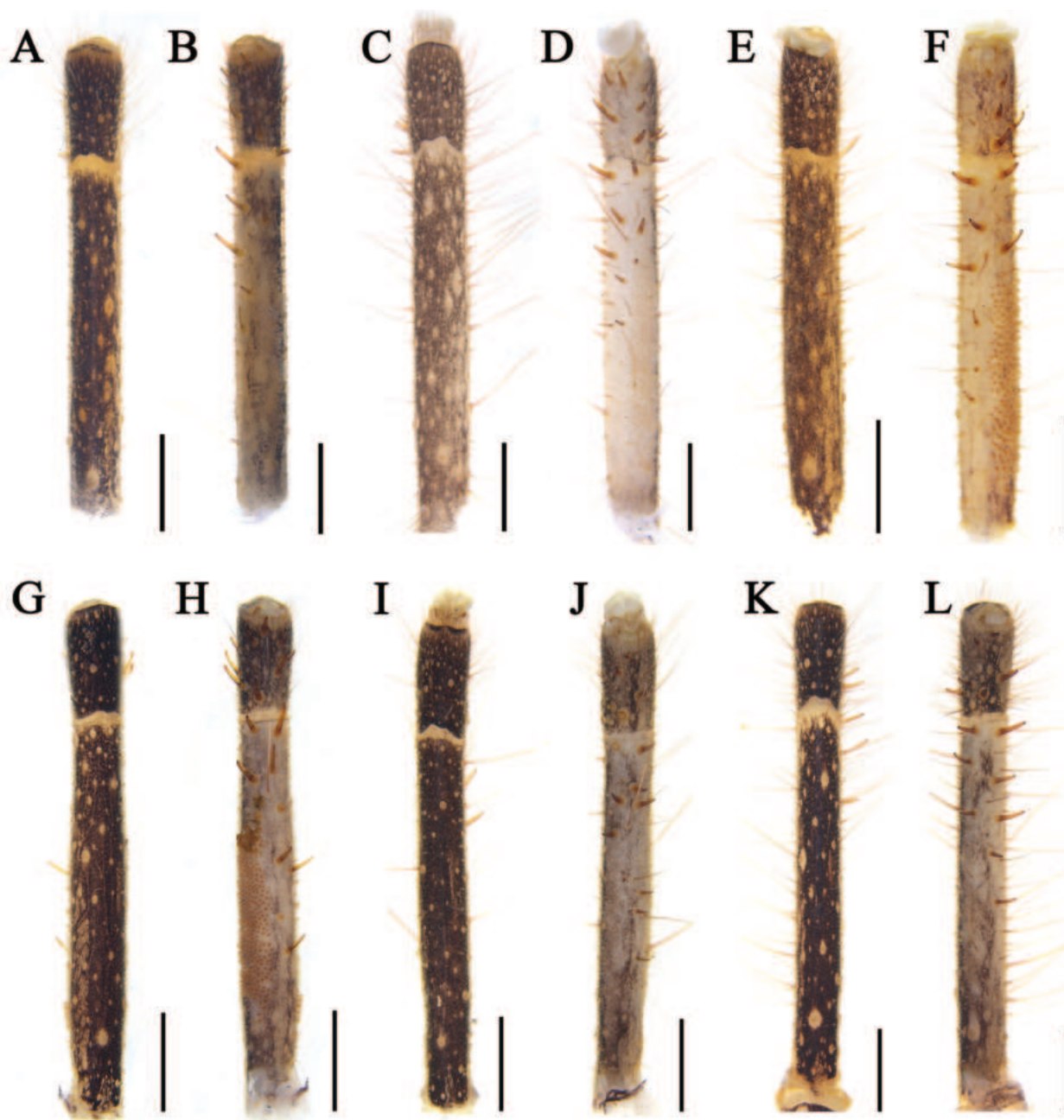


Figure 16. Male pedipalp A, B *K. tibetana* C, D *K. dingye* sp. nov. E, F *I. hasa* sp. nov. G, H *K. zhui* sp. nov. I, J *K. shigatse* sp. nov. K, L *K. namling* sp. nov. Scale bars: 1.0 mm.

Opisthosoma. The entire surface covered with almost adpressed setae and numerous long, curved, bifurcate setae. Sternite III with a row of disordered ctenidia (Fig. 19F). Sternite IV with 16 long peg-like ctenidia, the length of which almost equal to 1/2 the width of the succeeding sternite (Fig. 19H).

Pedipalps. Totally covered with short setae and long, thick setae. Tarsus with nine sturdy ventral spines; metatarsus with 11 ventral spines not arranged in pairs and with thick papillae (Fig. 16G, H).

Legs. Totally covered with long, thick setae and short setae. Leg I with no spines and two small claws. Tibias II, III, and IV with a pair of distal spines ventrally. Tibias II and III with a single dorsal spine; metatarsi II and III with a series of three dorsal spines, a pair of distal spines ventrally, and some paired short, thick,

spine-shaped bristles over their entire ventral surface. Metatarsus IV also with these paired bristles over its entire ventral surface and two distal spines ventrally.

Female. Paratype (MHBU-Sol-XZ2023070501).

Measurements. Total body length 21.52, CL 6.81, CH 2.50, PL 2.94, PW 4.27, A/CP 4.47, CL/CH 2.72. Pedipalp 13.39 (2.74, 4.28, 3.31, 1.11), Leg IV 11.35 (1.98, 3.13, 2.21, 1.09, 0.11), Leg II 10.29 (1.53, 2.13, 1.62, 0.87, 0.79), Leg III 12.78 (1.69, 2.70, 2.06, 0.62, 0.96), Leg IV 18.81 (4.41, 4.29, 2.25, 1.05, 1.19).

Coloration. In 75% ethanol-preserved specimens (Fig. 4G, H). Coloration as in the males.

Propeltidium. Much wider than long with a dense pubescence of thin, short, anteriorly directed setae. Anterior, posterior, and lateral edges with several long, curved spiniform setae that stand perpendicular to the surface of the propeltidium. Ocular tubercle with four middle distal spiniform setae, one middle spiniform setae, and two proximal spiniform setae (Fig. 7B).

Chelicerae. Dental formulation of fixed finger: FD-(2)-FM-(2)-FP-(8RF) (4PF). Dental formulation of movable finger: MM-(2)-MP, with four MST and three MSP. Fondal teeth graded as II, III, IV, I, V, VI, tiny VII, tiny VIII retrolaterally; II, I, III, tiny IV prolaterally (Figs 9G, H, 12D, 14G, H).

Opisthosoma. The entire surface covered with almost adpressed setae and numerous long, curved, bifurcate setae. The bottom of the genital operculum slightly widened, resembling a triangular-shape (with chitinized folds) between and behind them (Fig. 17D). Sternite IV with 13 long needle-like ctenidia extending one-third the length of the succeeding sternite (Fig. 18D).

Pedipalps. Totally covered with short and long setae, thick setae and without spines.

Legs. As in the males.

Distribution and habitat. China (Xizang). Habitat: shrubbery (Fig. 2D).

Remark. Based on the comparison of genetic distances, with a genetic distance of 0.15% (Table 2) between the male and female collected from the same location, we believe that they are same species.

Karschia (Karschia) shigatse sp. nov.

<https://zoobank.org/A84E6F7D-8AC8-45D1-A756-F0172B2C3289>

Figs 1, 5A–D, 7C, D, 10A–D, 11E, 12E, 15A–D, 16I, J, 17E, 18E, 19I, K, Tables 1, 2

Type material. Holotype ♂ (MHBU-Sol-XZ2022071501), CHINA: Xizang, Shigatse Prefecture, Nyalam County, Mainqu Town, 28.6773°N, 86.1395°E, 4552.71 m elev., 15.VII.2022, leg. Wenlong Fan. **Paratype:** 1 ♀ (MHBU-Sol-XZ2023072101), CHINA: Xizang, Shigatse Prefecture Gyirong County, Zheba Town, 29.1976°N, 85.3571°E, 4605.8 m elev., 21.VII.2023, leg. Xiangbo Guo.

Etymology. Noun in apposition taken from Shigatse Prefecture where this species was collected.

Diagnosis. *Karschia shigatse* sp. nov. differs from *K. nubigena* by having fringed flagellum (Fig. 11E), from *K. tibetana*, *K. dingye* sp. nov., *K. lhasa* sp. nov. and *K. zhui* sp. nov. by flagellum with lateral apophysis (Fig. 11E), and from *K. namling* sp. nov. by wide cheliceral fixed finger mucron, and lateral apophysis of flagellum larger (Fig. 11E). Female differs from other species by genital operculum equilateral subtriangular and with no clear demarcation between the plates. (Fig. 17E).

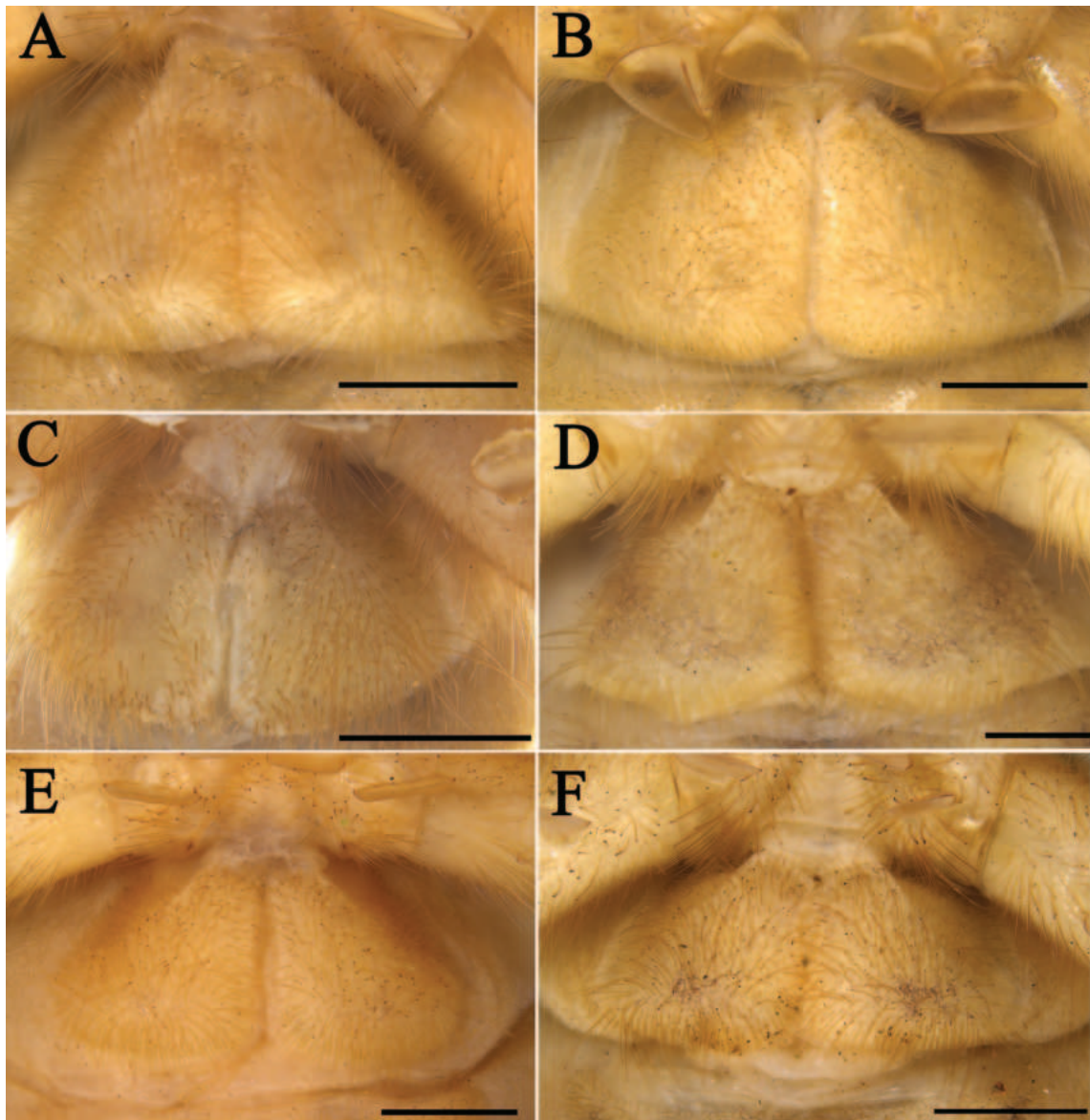


Figure 17. Genital operculum of female **A** *K. tibetana* **B** *K. dingye* sp. nov. **C** *K. lhasa* sp. nov. **D** *K. zhui* sp. nov. **E** *K. shigatse* sp. nov. **F** *K. namling* sp. nov. Scale bars: 1.0 mm.

Description. Male. Holotype (MHBU-Sol-XZ2022071501).

Measurements. Total body length 15.52, CL 4.88, CH 1.56, PL 2.26, PW 2.74, A/CP 7.24, CL/CH 3.14. Pedipalp 19.38 (5.35, 5.62, 4.12, 1.26), Leg I 13.51 (3.17, 3.90, 2.23, 1.02, 0.19), Leg II 10.95 (2.66, 2.33, 1.37, 0.92, 0.70), Leg III 16.87 (3.62, 4.59, 3.02, 0.54, 0.87), Leg IV 18.77 (4.71, 6.49, 4.71, 1.57, 1.31).

Coloration. In 95% ethanol-preserved specimens (Fig. 5A, B). The general background pale yellowish. The opisthosoma slightly darker, with black tergites and yellow around the black sternites. Propeltidium pale tan and tinged with pale brown. Ocular tubercle black. Mesopeltidium and metapeltidium with special black stripes. Chelicerae with manus predominantly yellowish, with some black areas, and a retrolateral view of chelicerae with three black longitudinal stripes. Pedipalps and legs pale yellow, legs III and legs IV tinged with pale brown on distal regions of femora and proximal parts of tibiae. Proximal regions of the pedipalpal femur, tibia, metatarsus, and tarsus tinged with brown. Malleoli yellow.

Propeltidium. Wider than long with a dense pubescence of thin, short, anteriorly directed setae. Anterior, posterior, and lateral edges with several long, curved spiniform setae that perpendicular to the surface of the propeltidium. Ocular tubercle with two middle distal spiniform setae and one middle spiniform setae (Fig. 7C). **Chelicerae.** Fixed finger primary teeth graded as $FP < FD < FM$. Profondal teeth series with three tiny teeth; retrofondal teeth series with seven teeth. Dental formulation of fixed finger: $FD-(2)-FM-(2)-FP-(7RF)$ (3PF). Fixed finger mucron without dorsal crest. Movable finger MP tooth about the same size as MM. Dental formulation of movable finger: $MM-(2)-MP$, with two tiny MSM and three MSP (Figs 10A, 15A). Flagellum coiled, fringed and sessile, with lateral apophysis. The flagellar complex includes two medium length *fcp* and two short, thick *fcs* (Figs 10B, 11E, 15B). Retrolateral and dorsal surfaces of the manus with large, bifurcated tip setae and short, simple tip bristle-like setae; retrolateral and dorsal surfaces of the fixed finger with simple tip setae of different sizes. Retrolateral setose area reaching the FSM teeth; prolateral surface with an array of setal types (Figs 10A, B, 15A, B).

Opisthosoma. Entire surface covered almost addressed setae, and numerous long, curved, bifurcate setae. Sternite III with 21 pine needle-like ctenidia (Fig. 19I). Sternite IV with 15 long peg-like ctenidia, the length of which almost equal to half the width of the succeeding sternite (Fig. 19K).

Pedipalps. Totally covered with short setae and long, thick setae. Tarsus with eight sturdy ventral spines; metatarsus with 10 ventral spines not arranged in pairs and with thin papillae (Fig. 16I, J).

Legs. Totally covered with long, thick setae and short setae. Leg I with no spines and two small claws. Tibias II, III, and IV with a pair of distal spines ventrally. Tibias II and III with a single dorsal spine; metatarsi II and III with a series of three dorsal spines, a pair of distal spines ventrally, and some paired short, thick, spine-shaped bristles over their entire ventral surface. Metatarsus IV also with these paired bristles over its entire ventral surface and two distal spines ventrally.

Female. Paratype (MHBU-Sol-XZ2023072101).

Measurements. Total body length 24.17, CL 6.84, CH 2.47, PL 2.63, PW 3.73, A/CP 4.97, CL/CH 2.77. Pedipalp 16.57 (4.08, 4.48, 3.50, 1.24), Leg I 12.72 (3.69, 3.37, 2.04, 0.97, 0.19), Leg II 10.86 (1.86, 2.41, 1.91, 0.75, 0.61), Leg III 13.77 (2.44, 3.29, 2.24, 0.72, 0.83), Leg IV 17.75 (4.07, 4.08, 2.61, 1.44, 0.78).

Coloration. In 75% ethanol-preserved specimens (Fig. 5C, D). Coloration as in the males.

Propeltidium. Much wider than long with a dense pubescence of thin, short, anteriorly directed setae. Anterior, posterior, and lateral edges with several long, curved spiniform setae that perpendicular to the surface of the propeltidium. Ocular tubercle with four middle distal spiniform setae and three middle spiniform setae arranged in a triangle shape (Fig. 7E).

Chelicerae. Dental formulation of fixed finger: $FD-(2)-FM-(2)-FP-(8RF)$ (5PF). Dental formulation of movable finger: $MM-(2)-MP$, with four MST and two MSP. Fondal teeth graded as II, III, V, VI, VII, I, IV, tiny VIII retrolaterally; I, II, III, IV, V prolaterally (Figs 10C, D, 12E, 15C, D).

Opisthosoma. The entire surface covered with almost addressed setae and numerous long, curved, bifurcate setae. Genital operculum equilateral subtriangular and with no clear demarcation between the plates. The rear edge of the genital sternite not chitinized (Fig. 17E). Sternite IV with 17 long needle-like ctenidia extending a half of the length of the succeeding sternite (Fig. 18E).

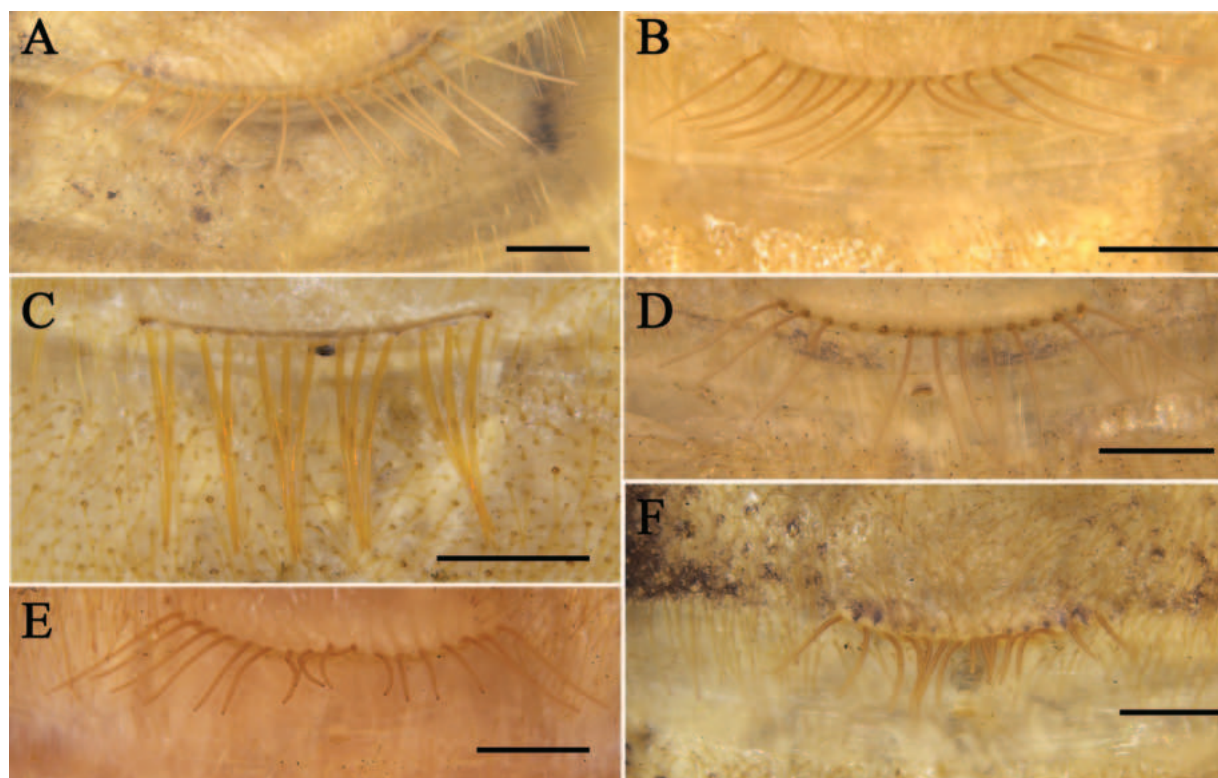


Figure 18. Ctenidia on sternite IV of female **A** *K. tibetana* **B** *K. dingye* sp. nov. **C** *K. lhasa* sp. nov. **D** *K. zhui* sp. nov. **E** *K. shigatse* sp. nov. **F** *K. namling* sp. nov. Scale bars: 0.5 mm.

Pedipalps. Totally covered with short setae and long, thick setae and without spines.

Legs. As in the males.

Distribution and habitat. China (Xizang). Habitat: desert grassland (Fig. 2E–G).

Remark. Based on the comparison of genetic distances, with a genetic distance of 2.20% (Table 2) between male and female collected from different near locations, we believe that they are same species.

***Karschia (Karschia) namling* sp. nov.**

<https://zoobank.org/D73D6B1F-73C4-4D8A-8802-AF0C93B46AE6>

Figs 1, 2H, 5E–H, 7E, F, 10E–H, 11F, 12F, 15E–H, 16K, L, 17F, 18E, 19J, L, Tables 1, 2

Type material. **Holotype** ♂ (MHBU-Sol-XZ2023073001), CHINA: Xizang, Namling County, Nubma Town, 29.5172°N, 89.6237°E, 4016.27 m elev., 30. VIII.2023, leg. Yanmeng Hou, Zhiyong Yang. **Paratypes:** 1♂ (MHBU-Sol-XZ2023073002), 4♀♀ (MHBU-Sol-XZ2023073003–07), same data as holotype.

Etymology. Noun in apposition taken from Namling County, where this species was collected.

Diagnosis. *K. namling* sp. nov. differs from *K. nubigena* by have fringed flagellum (Fig. 11F), differs from *K. tibetana*, *K. dingye* sp. nov., *K. lhasa* sp. nov. and *K. zhui* sp. nov. by flagellum with lateral apophysis (Fig. 11F), and from *Karschia shigatse* sp. nov. by less wide cheliceral fixed finger mucron, flagellum with small lateral apophysis (Fig. 11F). Female differs from other species by its genital operculum triangular (Fig. 17F) and ctenidia on sternite IV very short (Fig. 18F).

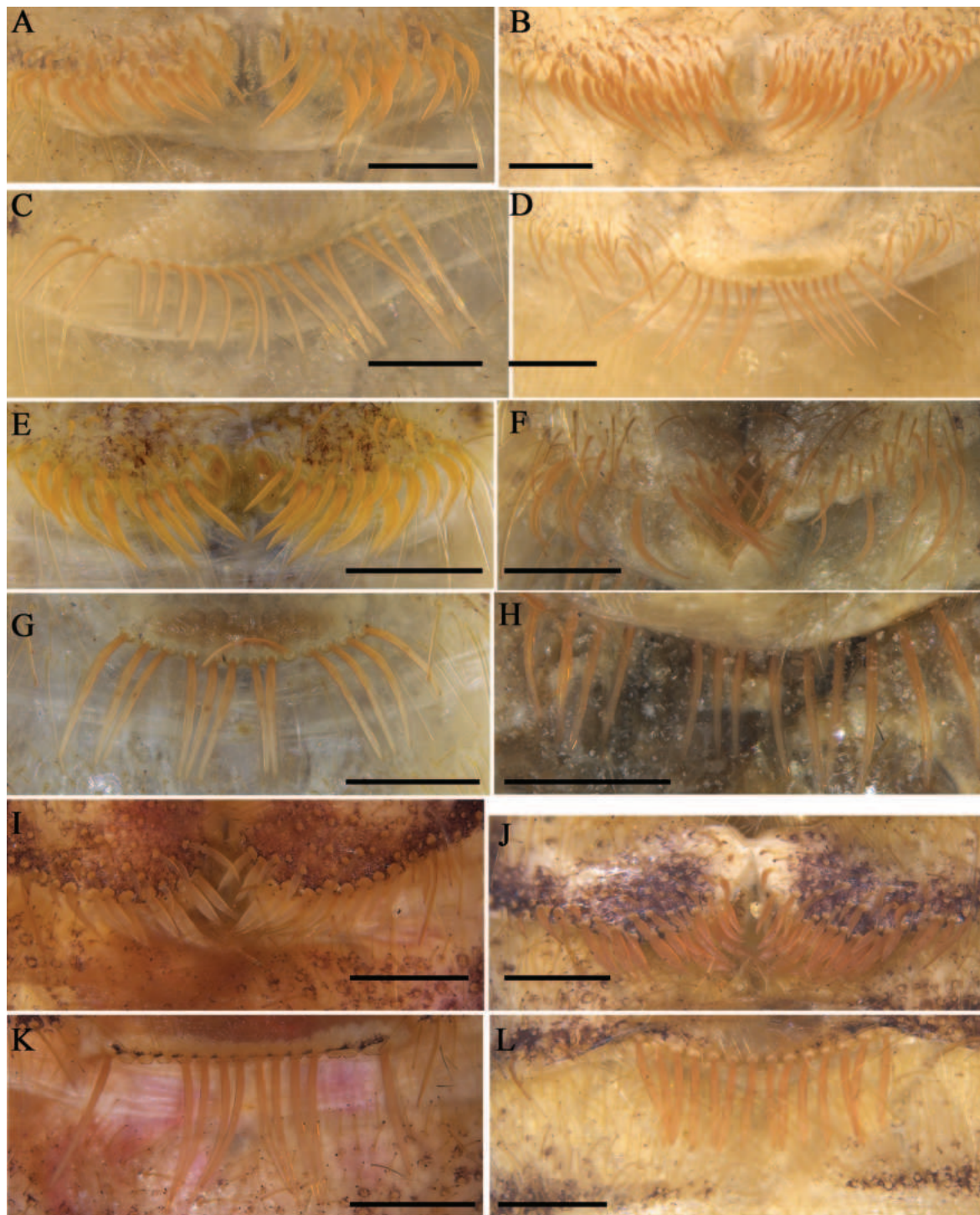


Figure 19. Ctenidia on sternite III (A, B, E, F, I, J) and sternite IV (C, D, G, H, K, L) of male **A, C** *K. tibetana* **B, D** *K. dingye* sp. nov. **E, G** *K. lhasa* sp. nov. **F, H** *K. zhui* sp. nov. **I, K** *K. shigatse* sp. nov. **J, L** *K. namling* sp. nov. Scale bars: 0.5 mm.

Description. Male. Holotype (MHBU-Sol-XZ2023073001).

Measurements. Total body length 16.61, CL 4.68, CH 1.58, PL 2.35, PW 3.04, A/CP 8.66, CL/CH 2.97. Pedipalp 22.21 (6.51, 6.56, 4.60, 1.50), Leg I 14.99 (3.56, 3.93, 2.59, 1.36, 0.12), Leg II 11.46 (2.52, 2.65, 1.46, 1.17, 0.19), Leg III 16.72 (3.45, 4.39, 2.86, 0.92, 0.92), Leg IV 23.73 (4.81, 6.47, 3.54, 1.42, 1.43).

Coloration. In 95% ethanol-preserved specimens (Fig. 5E, F). The general background pale yellowish. Opisthosoma slightly darker, with black tergites and yellow

around the black sternites. Propeltidium pale tan and tinged with pale brown. Ocular tubercle black. Mesopeltidium and metapeltidium with special black stripes. Chelicerae with manus predominantly brown yellowish, with some black areas, and a retrolateral view of chelicerae with three black longitudinal stripes. Pedipalps and legs pale yellow, legs III and legs IV tinged with pale brown on distal regions of femora and proximal parts of tibiae. Proximal regions of the pedipalpal femur, tibia, metatarsus, and tarsus were tinged with brown. Malleoli white.

Propeltidium. Wider than long with a dense pubescence of thin, short, anteriorly directed setae. Anterior, posterior, and lateral edges with several long, curved spiniform setae that stand perpendicular to the surface of the propeltidium. Ocular tubercle with four middle distal spiniform setae, one middle spiniform setae, and one proximal spiniform setae. (Fig. 7E).

Chelicerae. Fixed finger primary teeth graded as $FD < FM \approx FP$. Profondal teeth series with three tiny teeth; retrofondal teeth series with six teeth. Dental formulation of fixed finger: $FD-(2)-FM-(2)-FP-(6RF)$ (3PF). Fixed finger mucron without dorsal crest. Movable finger MP tooth about the same size as MM. Dental formulation of movable finger: $MM-(2)-MP$, with two tiny MSM and three MSP (Figs 10E, 15E). Flagellum coiled, fringed and sessile, with a small lateral apophysis. The flagellar complex includes two short *fcp* and two short, thick *fcs* (Figs 10F, 11F, 15F). Retrolateral and dorsal surfaces of the manus with large, bifurcated tip setae and short, simple tip bristle-like setae; retrolateral and dorsal surfaces of the fixed finger with simple tip setae of different sizes. Retrolateral setose area reaching the FSM teeth; prolateral surface with an array of setal types (Figs 10E, F, 15E, F).

Opisthosoma. The entire surface covered with almost adpressed setae and numerous long, curved, bifurcate setae. Sternite III with numbers short and cylindrical ctenidia (Fig. 19J). Sternite IV with 14 long peg-like ctenidia, the length of which almost 1/3 the width of the succeeding sternite (Fig. 19L).

Pedipalps. Totally covered with short setae and long, thick setae. Tarsus with six sturdy ventral spines; metatarsus with eight ventral spines not arranged in pairs and with thick papillae (Fig. 16K, L).

Legs. Totally covered with long, thick setae and short setae. Leg I with no spines and two small claws. Tibias II, III, and IV with a pair of distal spines ventrally. Tibias II and III with a single dorsal spine; metatarsi II and III with a series of three dorsal spines, a pair of distal spines ventrally, and some paired short, thick, spine-shaped bristles over their entire ventral surface. Metatarsus IV also with these paired bristles over its entire ventral surface and two distal spines ventrally.

Female. Paratype. (MHBU-Sol-XZ2023073003).

Measurements. Total body length 21.28, CL 6.77, CH 2.53, PL 2.76, PW 4.39, A/CP 4.6, CL/CH 2.67. Pedipalp 16.16 (4.70, 4.40, 3.63, 1.25), Leg I 9.872 (2.18, 2.89, 1.66, 0.98, 0.19), Leg II 10.49 (1.93, 2.21, 1.80, 0.84, 0.66), Leg III 11.56 (2.04, 2.96, 1.44, 0.43, 0.50), Leg IV 17.90 (4.06, 4.74, 2.06, 0.49, 0.99).

Coloration. In 75% ethanol-preserved specimens (Fig. 5G, H). Coloration as in the males.

Propeltidium. Much wider than long with a dense pubescence of thin, short, anteriorly directed setae. Anterior, posterior, and lateral edges with several long, curved spiniform setae that perpendicular to the surface of the propeltidium. Ocular tubercle with four middle distal spiniform setae and three middle spiniform setae arranged in a triangle shape (Fig. 7F).

Chelicerae. Dental formulation of fixed finger: FD-(2)-FM-(2)-FP-(6RF) (5PF). Dental formulation of movable finger: MM-(2)-MP, with four MST and four MSP. Fondal teeth graded as II, III, IV, V, I, tiny VI retrolaterally; I, II, III, IV, tiny V prolaterally (Figs 10G, H, 12F, 15G, H).

Opisthosoma. The entire surface covered with almost adpressed setae and numerous long, curved, bifurcate setae. Genital operculum triangular in shape with no clear demarcation between the plates., and the rear edge of the genital sternite not chitinized (Fig. 17F). Sternite IV with 14 short needle-like ctenidia extending 1/3 the length of the succeeding sternite (Fig. 18E).

Pedipalps. Totally covered with short setae and long, thick setae.

Legs. As in the males.

Variability. Female. Total length 20.13–23.67. Body coloration pale yellow to yellow. The number of cheliceral fixed finger fondal teeth 10–12 (profondal teeth 4–6; retrofondal teeth 6–7). MST 3–5, MSP 3–4. The number of ctenidia on sternite IV 14–16.

Distribution and habitat. China (Xizang). Habitat: grassland (Fig. 2H).

Remark. Based on the comparison of genetic distances, with a genetic distance of 0% (Table 2) between male and female collected from same locations, we believe that they are same species.

Discussion

The cytochrome c oxidase subunit I (COI) gene has been extensively employed in taxonomic and differentiation studies of Arachnida species. Analysis of COI sequences enables researchers to deepen their understanding of genetic variances among various species, thus facilitating more precise delineation and differentiation (Maddahi et. al. 2016).

The rich diversity of *Karschia* in Xizang can be ascribed to its distinctive geographical environment and climate conditions. With an average elevation surpassing 4000 meters, Xizang features vast high-altitude lakes and intricate geographical terrain, which hinder species dispersal, resulting in geographic isolation. Furthermore, we documented the highest Solifugae record (*K. shigatse* sp. nov.) in the Old World, complete with precise geographic coordinates, at an elevation of 4605.8 meters.

After examining various taxonomic characteristics of solifuge species and comparative specimens in this research, we think cheliceral teeth possess some taxonomic value, particularly regarding the relative size between the primary teeth of the median teeth series, which remains constant: the fondal series typically exhibit variability, and the numbers of secondary teeth generally have poor taxonomic value unless a specific type of tooth is entirely missing. Body size and coloration are subject to variation, with the opisthosoma being relatively soft and its size susceptible to change based on the nutritional state of the specimen; coloration can fluctuate with environmental changes, indicating that these traits have limited taxonomic value. The numbers of ctenidia on the sternite and spines of the male pedipalp also display variation, albeit to a lesser extent, making them suitable as additional diagnostic characters; however, the shape and size of ctenidia on the sternite are relatively constant, rendering them reliable taxonomic characteristics. The study confirms the significance of the female genital operculum in classification, as the

shape, size, and relative arrangement of the genital operculum remain consistent among female individuals of the same species; the flagellar complex of the male serves as reliable diagnostic characteristics, particularly regarding the degree of modification of the *fc*p (flagellar complex process plumose setae), the shape and number of *fc*s (flagellar complex subspiniform to spiniform setae), and the lateral apophysis.

Reevaluating the taxonomy of numerous Karschiidae species is indeed crucial and urgent. Historically, their classification and diagnostic criteria have heavily leaned on the cheliceral teeth traits of only a limited number of female specimens (Birula 1922, 1938; Roewer 1933, 1934). However, this approach may not fully capture the diversity and variation present within these species. Therefore, a more comprehensive assessment that considers a broader range of taxonomic characters, including those mentioned earlier such as the shape and numbers of ctenidia on the sternite and the shape and size of the genital operculum in females, is necessary. By incorporating these additional diagnostic characteristics, we can better elucidate the taxonomy and improve our understanding of the intricate relationships among *Karschia* species.

Acknowledgments

We are grateful to the subject editor Dr. Paula Cushing, reviewer Dr. Hernán Augusto Iuri, and one anonymous reviewer for providing significant comments on the manuscript. Thanks to Chao Zhang, Xiangbo Guo, Yannan Mu, Yanmeng Hou, Zhiyong Yang, and Quanyu Ji (Hebei University) for collecting these specimens during the fieldwork.

Additional information

Conflict of interest

The authors have declared that no competing interests exist.

Ethical statement

No ethical statement was reported.

Funding

This work was supported by the Survey of Wildlife Resources in Key Areas of Tibet (ZL202203601).

Author contributions

Wenlong Fan wrote the first draft, while Feng Zhang and Chao Zhang reviewed and revised the article.

Author ORCIDs

Wenlong Fan  <https://orcid.org/0009-0004-6854-6330>

Chao Zhang  <https://orcid.org/0000-0003-1702-1206>

Feng Zhang  <https://orcid.org/0000-0002-3347-1031>

Data availability

All of the data that support the findings of this study are available in the main text.

References

- Bird TL, Wharton R, Prendini L (2015) Cheliceral morphology in Solifugae (Arachnida): Primary homology, terminology and character survey. *Bulletin of the American Museum of Natural History* 394: 1–355. <https://doi.org/10.1206/916.1>
- Birula A (1922) Revisio analytica specierum asiaticarum generis *Karschia* Walter (Arachnoidea, Solifugae). *Annuaire du Musée Zoologique de l'Académie Impériale des Sciences de St.-Pétersbourg (Petrograd)* 23: 197–201.
- Birula A (1938) Arachnides, Ordo Solifuga. In: *Faune de l'URSS L'Académie des Sciences de l'URSS, Moscow, Leningrad* 1(3): i–vii: 1–173.
- Folmer O, Black M, Hoeh W, Lutz R, Vrijenhoek R (1994) DNA primers for amplification of mitochondrial cytochrome c oxidase subunit I from diverse metazoan invertebrates. *Molecular Marine Biology and Biotechnology* 3: 294–299.
- Gromov AV (1998) Solpugids (Arachnida: Solifugae) of Turkmenistan. *Arthropoda Selecta* 7: 179–188.
- Gromov AV (2004) Four new species of the genus *Karschia* Walter, 1889 (Arachnida: Solifugae: Karschiidae) from Central Asia. *European Arachnology 2003. Arthropoda Selecta* 1(Special Issue): 83–92.
- Harvey MS (2003) Catalogue of the smaller arachnid orders of the world: Amblypygi, Uropygi, Schizomida, Palpigradi, Ricinulei and Solifugae. CSIRO Publishing, Melbourne, 376 pp. <https://doi.org/10.1071/9780643090071>
- Hirst S (1907) On a new species of *Karschia* from Xizang. *Annals & Magazine of Natural History* 19(7): 322–324. <https://doi.org/10.1080/00222930709487271>
- Hirst S (1912) Descriptions of new arachnids of the orders Solifugae and Pedipalpi. *Annals & Magazine of Natural History* 9(8): 229–237. <https://doi.org/10.1080/00222931208693125>
- Lawrence RF (1954) Some Solifugae in the collection of the British Museum (Natural History). *Proceedings of the Zoological Society of London* 124(1): 111–124. <https://doi.org/10.1111/j.1096-3642.1954.tb01483.x>
- Maddahi HM, Khazanehdari M, Aliabadian M, Kami HG, Mirshamsi A, Mirshamsi O (2016) Mitochondrial DNA phylogeny of camel spiders (Arachnida: Solifugae) from Iran. *Mitochondrial DNA. Part A, DNA Mapping, Sequencing, and Analysis* 28(6): 909–919. <https://doi.org/10.1080/24701394.2016.1209194>
- Roewer CF (1932) Solifugae, Palpigradi. In: *Bronn's Klassen und Ordnungen des Tierreichs. 5: Arthropoda. IV: Arachnoidea* Akademische Verlagsgesellschaft M.B.H., Leipzig 5(IV)(4) (2–3): 1–160.
- Roewer CF (1933) Solifugae, Palpigradi. In: *Bronn's Klassen und Ordnungen des Tierreichs. 5: Arthropoda. IV: Arachnoidea* Akademische Verlagsgesellschaft M.B.H., Leipzig 5(IV)(4) (2–3): 161–480.
- Roewer CF (1934) Solifugae, Palpigradi. In: *Bronn's Klassen und Ordnungen des Tierreichs. 5: Arthropoda. IV: Arachnoidea* Akademische Verlagsgesellschaft M.B.H., Leipzig 5(IV)(4) (2–3): 161–480.
- Ruttledge H, Morris CJ, Smijth Windham WR, Smythe FS, Humphreys N, Warren CB (1936) The Mount Everest Expedition of 1936. *The Geographical Journal* 88(6): 491–519. <https://doi.org/10.2307/1787082>
- World Solifugae Catalog (2024). World Solifugae Catalog. Natural History Museum Bern. <http://wac.nmbe.ch> [accessed on 6 May 2024]
- Zilch A (1946) Katalog der Solifugen (Arach.) des Senckenberg-Museums. *Senckenbergiana* 27: 119–154.

Melanastera sinica He & Burckhardt, sp. nov., a new psylloid species (Hemiptera, Psylloidea, Liviidae) from China developing on *Grewia* sp. (Malvaceae)

Zhixin He¹, Daniel Burckhardt², Xinyu Luo¹, Rongzhen Xu¹, Wanzhi Cai¹, Fan Song¹

¹ Department of Entomology & MOA Key Lab of Pest Monitoring and Green Management, College of Plant Protection, China Agricultural University, Beijing, 100193, China

² Naturhistorisches Museum, Augustinergasse 2, 4001 Basel, Switzerland

Corresponding author: Fan Song (fansong@cau.edu.cn)

Abstract

Melanastera sinica He & Burckhardt, **sp. nov.**, a new psylloid species developing on *Grewia* sp., is described from Hainan, China. It is the first *Melanastera* species reported from Asia and China, and the second species from the Old World. While New World species of *Melanastera* are mostly associated with the plant families Melastomataceae and Annonaceae, the two Old World species develop on the malvaceous *Grewia*, a host otherwise used in psylloids by two *Haplaphalara* species. The new species is described, diagnosed and illustrated, and its host plant and biogeographic ranges are discussed.

Key words: Jumping plant lice, Liviinae, Oriental Region, Paurocephalini, Sternorrhyncha, taxonomy



Academic editor: Igor Malenovský

Received: 22 March 2024

Accepted: 8 May 2024

Published: 6 June 2024

ZooBank: <https://zoobank.org/34FB4522-549E-48D1-9E88-B9165112E9CC>

Citation: He Z, Burckhardt D, Luo X, Xu R, Cai W, Song F (2024) *Melanastera sinica* He & Burckhardt, sp. nov., a new psylloid species (Hemiptera, Psylloidea, Liviidae) from China developing on *Grewia* sp. (Malvaceae). ZooKeys 1204: 191–198. <https://doi.org/10.3897/zookeys.1204.123740>

Copyright: © Zhixin He et al.

This is an open access article distributed under terms of the Creative Commons Attribution License (Attribution 4.0 International – CC BY 4.0).

Introduction

Jumping plant lice or psylloids constitute the superfamily Psylloidea, with slightly over 4000 species worldwide (Burckhardt et al. 2023). They are characterised by narrow host ranges mostly associated with eudicots and magnoliids, while hosts from the monocots and conifers are rare. In addition, related psylloid species tend to develop on related hosts (Hodkinson and Bird 2000; Burckhardt 2005a, 2005b; Burckhardt et al. 2014; Ouvrard et al. 2015). Ouvrard et al. (2015) conducted an analysis of the host patterns of psylloids worldwide and found that psylloid hosts are not evenly distributed across angiosperms. Instead, they identified particular plant taxa that are preferred hosts for psylloids. The Malvaceae is such a family, ranking as the 9th most important host taxon while it constitutes only the 12th largest plant family worldwide. Apart from a single species of Triozidae, *Bactericera lavaterae* (Van Duzee, 1924) (Burckhardt and Lauterer 1997), Malvaceae hosts all the members of the subfamily Carsidarinae (Carsidaridae) (Hollis 1987) and many species of the tribe Paurocephalini (Liviidae, Liviinae) (Burckhardt et al. 2023). Of the Paurocephalini, all of the seven recognised genera include members associated with Malvaceae. All species of *Klyveria* and *Woldaia*, and many species of *Diclidophlebia*, *Haplaphalara* and *Liella* develop on

Malvaceae, while only a few species of *Melanastera* and *Paurocephala* are associated with this family (Burckhardt et al. 2023; Serbina et al. in press).

Recently, an undescribed *Melanastera* species was discovered on the malvaceous genus *Grewia* in China. *Melanastera* currently comprises more than 60 extant species in the New World, many of which develop on Melastomataceae and Annonaceae (Burckhardt et al. 2023; Serbina et al. in press). In the Old World, the genus is represented only by a single Afrotropical species, also associated with *Grewia* (Burckhardt et al. 2023).

Here, we describe *Melanastera sinica* He & Burckhardt, sp. nov., which represents the first record of the genus from China and Asia. Morphological information and illustrations are provided for adults and fifth instar immatures.

Material and methods

Material was examined from the Entomological Museum of the China Agricultural University, Beijing, China (CAU) and the Naturhistorisches Museum, Basel, Switzerland (NHMB).

The morphological terminology accords with Burckhardt et al. (2023) and Serbina et al. (in press). For examining morphological structures under the compound microscope, the whole insect was cleared in a hot potassium hydroxide (KOH) solution for ten minutes, washed in distilled water and then mounted on a slide in glycerine. Measurements were taken from slide-mounted specimens. Photos were taken with a Nikon SMZ18 microscope (Tokyo, Japan) attached to a Cannon 7D camera (Tokyo, Japan). Helicon Focus version 5.3 (Helicon Soft Ltd., Kharkiv, Ukraine) was used for image stacking. Line drawings were made using an Olympus BX41 microscope. Photoshop 2020 (Adobe Systems Inc., USA) was used to edit photos including adjustments of background colour and cropping without modifying any characters of specimens. The concept of host plants adopted here is that of Burckhardt et al. (2014). The nomenclature of plants accords with POWO (2024).

Taxonomy

Melanastera sinica He & Burckhardt, sp. nov.

<https://zoobank.org/6F961330-7600-4B39-9885-BBC1F01FF45F>

Figs 1–3

Type locality. CHINA, Hainan: Ledong County, Jianfengling, Mingfenggu, 18°74'24"N, 108°84'81"E.

Type material. Holotype: CHINA • ♂; Hainan, Ledong County, Jianfengling, Mingfenggu; 18°74'24"N, 108°84'81"E; 24 Apr. 2016; X.-Y. Luo leg.; on *Grewia* cf. *chuniana*; CAU, dry mounted. **Paratypes:** CHINA • 2 ♂, 7 ♀, 12 immatures; same data as holotype; CAU, NHMB, dry and slide mounted, and in 95% ethanol.

Diagnosis. Adult. Body yellowish brown with small dark brown dots; forewing with each a broad medial and subapical light brown band and small, dark brown irregular spots. Metatibia with 3+4 grouped apical metatibial spurs separated by five unsclerotised bristle-like setae anteriorly. Forewing oval, widest in apical third; pterostigma long, strongly widening to middle; surface spinules present in all cells, covering membrane up to the veins; irregularly spaced to form



Figure 1. Habitus of adults of *Melanastera sinica* He & Burckhardt, sp. nov. **A** dorsal view **B** lateral view. Scale bars: 1.0 mm.

groups of 5–6 spinules. Male proctiger weakly expanded posteriorly. Paramere, in lateral view, subrectangular with antero-apical sclerotised tooth. Aedeagus two-segmented; distal segment lacking ventral process. Female proctiger with relatively straight dorsal margin; apex obliquely truncate. Circumanal ring cruciform. – Fifth instar immature. Antenna 10-segmented. Forewing pad with 5 marginal subacute sectasetae. Tarsal arolium narrowly lamellar, widening to apex which is rounded; about twice as long as claws. Caudal plate with anterior margin distant from anterior margin of extra pore fields; with 2 lateral sectasetae on either side near fore margin, and three pointed sectasetae on either side of circumanal ring dorsally.

Description. Adult. Colouration. Body (Fig. 1A, B) yellowish brown. Head and thorax covered with sparse small brown dots. Antenna yellow to yellowish brown, with apices of segments IV–IX and entire segment X dark brown to black. Femora with brown spots. Forewing yellowish with light brown pattern consisting of each a broad medial and subapical band and small, brown irregular spots, veins pale yellow.

Structure. Head, in lateral view (Fig. 1B), inclined at 45° from longitudinal body axis; in dorsal view (Fig. 1A), about as wide as mesoscutum. Vertex (Fig. 2A) subrectangular, about half as long as wide; surface with fine microsculpture and microscopical setae; median suture developed; posterior margin weakly concave. Genae weakly rounded, with each a pair of long setae on either side of frons (Fig. 2A). Frons relatively large, triangular. Eyes hemispherical. Antenna (Fig. 2B) 1.7–1.8 times as long as head width, with a single, large subapical rhinarium on each of segments IV, VI, VIII and IX; relative length of flagellar segments as 1.0: 0.5: 0.5: 0.5: 0.6: 0.6: 0.5: 0.4; relative length of segment 10 and terminal setae as 1.0: 1.3: 1.1. Clypeus flattened, in ventral view almost triangular. Thorax distinctly arched, with fine microsculpture; mesoscutellum swollen; metapostnotum with small subacute, laterally compressed tooth. Metacoxa with relatively short horn-shaped, blunt meracanthus; metatibia 1.0 times as long as head width, slender, weakly expanded apically; with 3+4 grouped apical metatibial spurs separated by five unsclerotised bristle-like setae anteriorly. Forewing (Fig. 2C) 2.7–3.1 times as long as head width, 1.6–1.8 times as long as wide, oval, widest in apical third; wing apex in the middle of cell r_2 ; veins densely clothed in conspicuous setae; vein C+Sc straight in basal two thirds, strongly bent in apical third; pterostigma long, strongly widening to middle; vein Rs relatively straight in

the middle, curved in a 30° angle to costal margin apically; vein M weakly, irregularly curved; veins M_{1+2} and M_{3+4} slightly shorter than M; vein Cu shorter than M+Cu; vein Cu_{1a} evenly curved; vein Cu_{1b} straight, slightly shorter than Cu; surface spinules present in all cells, covering membrane up to the veins, along veins slightly finer; irregularly spaced to form groups of 5–6 spinules. Hindwing (Fig. 2D) slightly shorter than forewing, with indistinctly grouped costal setae. Visible abdominal tergites III–V with a tubercular bump in the middle in both sexes.

Terminalia (Fig. 2E–G). Male proctiger (Fig. 2E) 1.2–1.3 times as long as head width, broad with posterior margin produced; in lateral view, widest in basal third. Subgenital plate (Fig. 2E) subglobular, weakly irregularly curved dorsally. Paramere (Fig. 2E, F), in lateral view, subrectangular with antero-apical, partly sclerotised tooth-like process; posterior margin weakly sinuate; outer and inner face covered in long setae in apical half, denser on inner face and along apical and posterior margins. Aedeagus (Fig. 2E) two-segmented; distal segment, in lateral view, tubular and slightly angular postero-apically, lacking ventral process; sclerotised end tube of ductus ejaculatorius moderately long, relatively straight. – Female terminalia (Fig. 2G) cuneate, moderately long. Proctiger 0.4 times as long as head width; in lateral view, dorsal margin, distal to circumanal ring, almost straight; with a transverse row of long setae in the middle and a lateral longitudinal row of long setae on either side in apical third; apex, in lateral view, obliquely truncate, apex slightly upturned. Circumanal ring 0.4 times as long as proctiger; in dorsal view, cruciform. Subgenital plate 0.6 times as long as proctiger; irregularly narrowing to pointed apex, in lateral view; beset with long setae in apical two thirds.

Measurements (in mm; 3 ♂, 2 ♀). Total body length measured from anterior margin of vertex to tip of folded forewing ♂ 2.31–2.52, ♀ 2.42–2.68; antennal length ♂ 1.23–1.31, ♀ 1.24–1.34; metatibia length ♂ 0.70–0.73, ♀ 0.72–0.74; forewing length ♂ 1.87–2.12, ♀ 1.96–2.26; proctiger length ♂ 0.15–0.16 ♀ 0.26–0.28; paramere length 0.12–0.13; length of distal segment of aedeagus 0.13–0.14.

Fifth instar immature (Fig. 3). Body (Fig. 3C) 1.1–1.2 times as long as wide; sparsely covered in microscopic setae. Antenna (Fig. 3A) 10-segmented with a subapical rhinarium on each of segments IV, VI, VIII and IX, and following numbers of subacute sectasetae: 1 (0), 2 (2), 3 (0), 4 (2), 5 (0), 6 (2), 7 (1), 8 (1), 9 (0), 10 (0). Legs moderately long with 4–5 subacute sectasetae on tibiotarsi; tarsal arolium (Fig. 3B) narrowly lamellar, widening to apex which is rounded; about twice as long as claws. Forewing pad 0.7 times as long as antenna, bearing 5 moderately large marginal subacute sectasetae (Fig. 3C); hindwing pad with 2 marginal subacute sectasetae. Caudal plate (Fig. 3C–E) with anterior margin distant from outer band of extra pore fields, inner band of pores less distinct than outer band; with 2 sectasetae on either side laterally, and three pointed sectasetae on either side of circumanal ring dorsally.

Measurements (in mm; 2 immatures). Body length 0.98–1.01; antennal length 0.52–0.54; length of forewing pad 0.35–0.37; length of tarsal arolium 0.03–0.04; length of claws 0.01–0.02.

Etymology. From the Latin adjective *sinicus* = Chinese, referring to the unexpected discovery of this mostly American genus in China.

Distribution. China: Hainan.

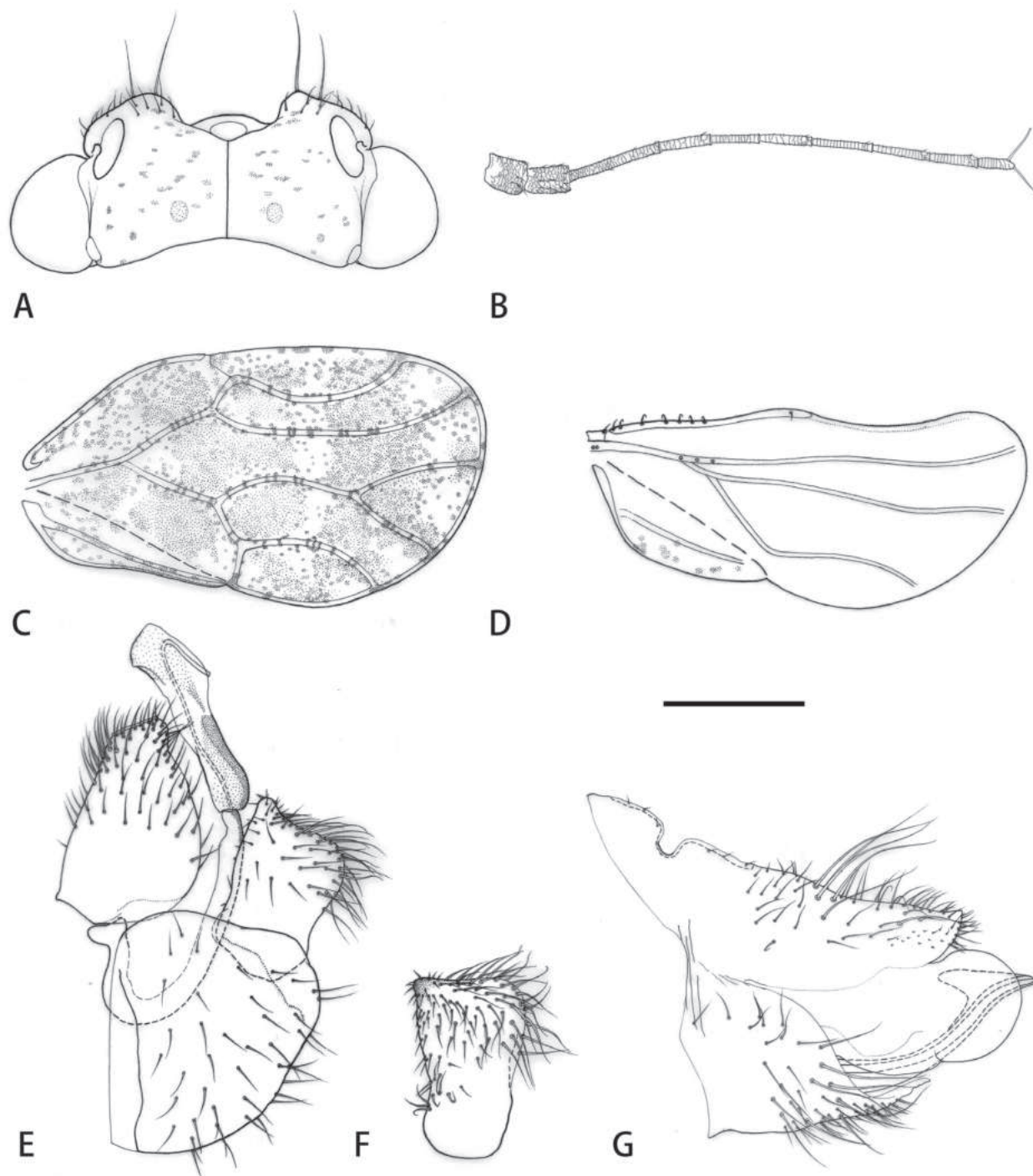


Figure 2. *Melanastera sinica* He & Burckhardt, sp. nov., adult **A** head **B** antenna **C** forewing **D** hindwing **E** male terminalia **F** inner face of paramere **G** female terminalia. Scale bars: 0.25 mm (**A**); 0.3 mm (**B**); 0.5 mm (**C**, **D**); 0.1 mm (**E–G**).

Host plant. *Grewia* cf. *chuniana* Burret (Malvaceae).

Comments. Serbina et al. (in press) defined several species groups within *Melanastera* mostly on the basis of morphological characters of adults. *Melanastera sinica* is a member of the *curtisetosa*-group for the absence of a ventral process on the distal segment of the aedeagus. The *curtisetosa*-group is composed of four species from Brazil associated with Asteraceae (confirmed or likely hosts) and *M. pilosa* (Burckhardt et al. 2006) from Kenya and Tanzania,

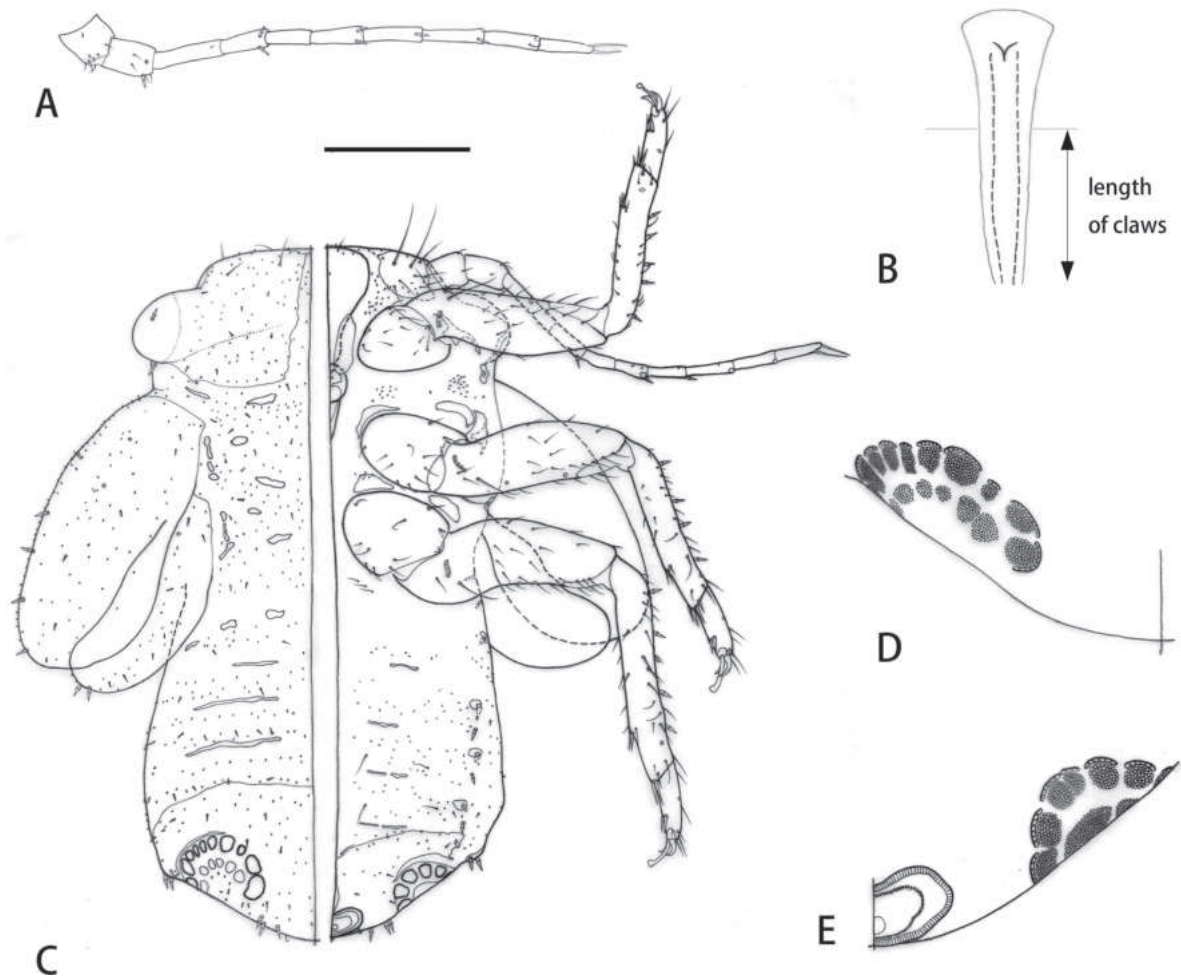


Figure 3. *Melanastera sinica* He & Burckhardt, sp. nov., fifth instar immature **A** antenna **B** tarsal arolium **C** habitus (left: dorsal side, right: ventral side) **D** detail of extra pore fields (dorsal side) **E** detail of extra pore fields and circumanal ring (ventral side). Scale bars: 0.15 mm (**A**); 0.03 mm (**B**); 0.2 mm (**C**); 0.01 mm (**D, E**).

developing on *Grewia bicolor* Juss. (Malvaceae) (confirmed). *Melanastera sinica* differs from the four Brazilian species in the forewing with a much more expanded dark pattern, which is slightly expanding towards the apex (versus parallel-sided) and bears a broad (versus narrow) pterostigma, in the broad subrectangular paramere (versus narrow, lamellar), the 10-segmented antenna in the last instar immature (versus 9-segmented), and the host association with Malvaceae (versus Asteraceae). From the African *M. pilosa* with which it shares the expanded dark forewing pattern, the 10-segmented antenna in the last instar immature and the host genus *Grewia*, it differs in the broader paramere, the absence of long setae on the body and forewing, the broad (versus narrow) pterostigma, the broader paramere (versus narrower), and the apically broader and obliquely truncate (versus slender and subacute) female proctiger (Burckhardt et al. 2006).

Discussion and conclusions

Burckhardt et al. (2023) suggested that, within Liviinae, new species are more likely to be discovered among the tropical Paurocephalini rather than among

its sister group, the predominantly north-temperate *Liviini*. The discovery of *Melanastera sinica* in tropical Hainan supports this notion. *Melanastera* is primarily found in the Neotropical region (Serbina et al. in press), with only a single species known from the Old World so far, viz. *M. pilosa* (Burckhardt et al. 2006). *Melanastera sinica* represents the second species from the Old World and the first from Asia. The presence of an expanded dark pattern on the forewing in the adults and 10-segmented antennae in the last instar immatures, shared by the two Old World species, suggests a putative sister group relationship of *M. pilosa* and *M. sinica*. The two species also share the malvaceous *Grewia* as the host, representing a family absent among the hosts of the New World *Melanastera* species.

Grewia includes 277 species in Africa, Asia and Australia (POWO 2024). Among psylloids, another two species use *Grewia* as the host: *Haplaphalara grewiae* (Kandasamy, 1986) and *H. menoni* (Mathur, 1975), two species of Purocephalini from India (Burckhardt et al. 2023). Targeted surveys of *Grewia* species in China will show, if additional, currently unknown psylloids are associated with this genus.

Acknowledgements

We thank Liliya Serbina (Berlin) and Igor Malenovský (Brno) for constructive comments on a previous manuscript draft.

Additional information

Conflict of interest

The authors have declared that no competing interests exist.

Ethical statement

No ethical statement was reported.

Funding

This work was supported by the National Natural Science Foundation of China (Nos. 32170474, 32120103006), the Young Elite Scientist Sponsorship Program by CAST (YESS20200106) and the 2115 Talent Development Program of the China Agricultural University.

Author contributions

Conceptualization: ZH, DB. Resources (field work): XL. Investigation (laboratory work): ZH, XL, RX. Formal analysis: ZH, DB. Data curation: ZH. Writing – Original draft, Review and Editing: ZH, DB. Supervision: DB, WC, FS. Funding acquisition: WC, FS.

Author ORCIDs

Zhixin He  <https://orcid.org/0000-0002-9148-8157>

Daniel Burckhardt  <https://orcid.org/0000-0001-8368-5268>

Xinyu Luo  <https://orcid.org/0009-0001-0412-353X>

Rongzhen Xu  <https://orcid.org/0009-0003-1831-2328>

Wanzhi Cai  <https://orcid.org/0000-0002-8620-0446>

Fan Song  <https://orcid.org/0000-0002-2900-4174>

Data availability

All of the data that support the findings of this study are available in the main text.

References

- Burckhardt D (2005a) *Ehrendorferiana*, a new genus of Neotropical jumping plant lice (Insecta: Hemiptera: Psylloidea) associated with conifers (Cupressaceae). *Organisms, Diversity & Evolution* 5(4): 317–319. <https://doi.org/10.1016/j.ode.2005.08.001>
- Burckhardt D (2005b) Biology, ecology, and evolution of gall-inducing psyllids (Hemiptera: Psylloidea). In: Raman A, Schaefer CW, Withers TM (Eds) *Biology, Ecology, and Evolution of Gall-inducing Arthropods*. Science Publishers, Enfield, 143–157.
- Burckhardt D, Lauterer P (1997) A taxonomic reassessment of the trioqid genus *Bactericera* (Hemiptera: Psylloidea). *Journal of Natural History* 31(1): 99–153. <https://doi.org/10.1080/00222939700770081>
- Burckhardt D, Aléné DC, Ouvrard D, Tamesse JL, Messi J (2006) Afrotropical members of the jumping plant-lice genus *Diclidophlebia* (Hemiptera, Psylloidea). *Invertebrate Systematics* 20(3): 367–393. <https://doi.org/10.1071/IS05039>
- Burckhardt D, Ouvrard D, Queiroz DL, Percy D (2014) Psyllid host-plants (Hemiptera: Psylloidea): resolving a semantic problem. *The Florida Entomologist* 97(1): 242–246. <https://doi.org/10.1653/024.097.0132>
- Burckhardt D, Serbina LŠ, Malenovský L, Queiroz DL, Aléné CD, Cho G, Percy DM (2023) Phylogeny and classification of jumping plant lice of the subfamily Liviinae (Hemiptera: Psylloidea: Liviidae) based on molecular and morphological data. *Zoological Journal of the Linnean Society*, zlad128. <https://doi.org/10.1093/zoolinnean/zlad128>
- Hodkinson ID, Bird J (2000) Sedge and rush-feeding psyllids of the subfamily Liviinae (Insecta: Hemiptera: Psylloidea): a review. *Zoological Journal of the Linnean Society* 128(1): 1–49. <https://doi.org/10.1111/j.1096-3642.2000.tb00648.x>
- Hollis D (1987) A review of the Malvales-feeding psyllid family Carsidaridae (Homoptera). *Bulletin of the British Museum (Natural History). Entomology* 56(2): 87–127.
- Ouvrard D, Chalise P, Percy DM (2015) Host-plant leaps versus host-plant shuffle: A global survey reveals contrasting patterns in an oligophagous insect group (Hemiptera, Psylloidea). *Systematics and Biodiversity* 13(5): 434–454. <https://doi.org/10.1080/14772000.2015.1046969>
- POWO (2024) Plants of the World Online. <http://www.plantsoftheworldonline.org/> [Accessed 1 March 2024]
- Serbina LŠ, Malenovský I, Queiroz DL, Burckhardt D (in press) Jumping plant-lice of the tribe Paurocephalini (Hemiptera: Psylloidea: Liviidae) in Brazil. *Zootaxa*. [Submitted in September 2023]

Taxonomic revision of the Southeast Asian brook barb genus *Poropuntius* Smith, 1931 (Teleostei, Cyprinidae) with description of a new species from Vietnam

Huy Duc Hoang^{1,2}, Hung Manh Pham^{1,2}, Ngan Trong Tran^{1,2}, Jean-Dominique Durand³, Ling Wu^{4,5}, John Pfeiffer⁶, Xiao-Yong Chen^{4,5}, Lawrence M. Page⁷

1 Department of Ecology and Evolutionary Biology, University of Science, Ho Chi Minh City, Vietnam

2 Vietnam National University, Ho Chi Minh City, Vietnam

3 IRD, MARBEC (University of Montpellier, CNRS, Ifremer, IRD), Montpellier, France

4 Southeast Asia Wildlife Biodiversity Research Group, Kunming Institute of Zoology, the Chinese Academy of Sciences, Kunming, Yunnan 650223, China

5 Southeast Asia Biodiversity Research Institute, Chinese Academy of Science, Yezin, Nay Pyi Taw 05282, Myanmar

6 Department of Invertebrate Zoology, National Museum of Natural History, Smithsonian Institution, 10th and Constitution Avenue NW, Washington, DC 20560, USA

7 Florida Museum of Natural History, University of Florida, 1659 Museum Road, Gainesville, FL 32611, USA

Corresponding author: Huy Duc Hoang (hdhuy@hcmus.edu.vn)



Academic editor: Yahui Zhao

Received: 14 February 2024

Accepted: 4 May 2024

Published: 6 June 2024

ZooBank: <https://zoobank.org/1AFB6FE4-6EDB-41CB-A283-4308077F903F>

Citation: Hoang HD, Pham HM, Tran NT, Durand J-D, Wu L, Pfeiffer J, Chen X-Y, Page LM (2024) Taxonomic revision of the Southeast Asian brook barb genus *Poropuntius* Smith, 1931 (Teleostei, Cyprinidae) with description of a new species from Vietnam. ZooKeys 1204: 199–222. <https://doi.org/10.3897/zookeys.1204.120873>

Copyright: © Huy Duc Hoang et al.
This is an open access article distributed under terms of the Creative Commons Attribution License (Attribution 4.0 International – CC BY 4.0).

Abstract

Molecular data from samples encompassing 22 nominal species of *Poropuntius* indicate that the species-level diversity in the genus has been vastly overestimated, likely due to inadequate taxon and geographic sampling and reliance on morphological characters that vary intra-specifically. The latter includes discrete mouth morphologies related to alternate feeding strategies (ecomorphs) within populations. One new species is described, *Poropuntius anlaensis* Hoàng, Phạm & Trần, **sp. nov.**, and 17 synonyms of six valid species names of *Poropuntius*, *P. krempfi*, *P. alloiopterus*, *P. huangchuchieni*, *P. laoensis*, *P. kontumensis*, and *P. deauratus*, are recognised. Additional taxonomic changes in this widespread and generally poorly known genus are likely as more molecular and morphological data become available.

Key words: Cypriniformes, molecular systematics, phylogeny, *Poropuntius anlaensis* sp. nov.

Introduction

Thirty-three names currently are recognised as valid for species of *Poropuntius* (Fricke et al. 2023) with distribution of the genus ranging from the Irrawaddy River basin in Myanmar to the Mekong and Red River basins in Yunnan, China and south through Vietnam, Laos, Cambodia, Thailand, and peninsular Malaysia to Sumatra, Indonesia. The greatest diversity occurs in the Mekong basin of Yunnan and Vietnam, and only one species is known from peninsular Malaysia and one from Sumatra (Fricke et al. 2023).

Poropuntius has been characterised as usually having 8½ branched dorsal rays, large serrae on the posterior edge of the last simple dorsal ray, and tubercles covering the tip of the snout and occurring on the lacrimal bones (Rainboth 1996;

Roberts 1998). Tubercles occur on both sexes and, at least in most species, on juveniles as well as adults (Roberts 1998). In addition, most species have rostral and maxillary barbels, a black to dusky submarginal stripe on the upper and lower caudal-fin lobes, and a well-developed keratinised edge on the lower jaw.

Considerable confusion surrounds the taxonomy of *Poropuntius*, with most species having been diagnosed using morphological characters that tend to be highly plastic and comparisons made to few congeners. Wu et al. (2013) and Muhammad-Rasul et al. (2018) investigated molecular diversity of *Poropuntius* and, although they targeted only a few species and small geographic areas, their results suggested some morphological hypotheses concerning species delimitations are incorrect, and larger molecular studies are needed to improve our understanding of species diversity in *Poropuntius*. Recent fieldwork throughout much of the distribution of *Poropuntius*, especially in species-rich Vietnam, has provided material for a broader study of molecular variation in the genus. Results of that study, reported herein, suggest that several species names, including nominal species of *Acrossocheilus* and *Hypsibarbus* in Vietnam, are synonyms of previously described species. A newly discovered species from Vietnam is described using morphological and molecular characteristics.

Materials and methods

Field sampling

Tissues were taken from selected specimens collected in the field or purchased in local markets throughout much of the range of *Poropuntius* (Fig. 1) and stored in 95% ethanol for molecular analysis. Specimens were then fixed in 10% formalin, subsequently transferred to 70% ethanol, and deposited at the University of Science, Ho Chi Minh City, Vietnam (**UNS**), Florida Museum of Natural History, Florida, USA (**UF**), and Kunming Institute of Zoology, Yunnan, China (**KIZ**). Samples newly obtained for this study included those from the same drainages as type localities for all nominal species in the molecular analysis except *P. krempfi* (Pellegrin & Chevey, 1934) for which samples were from near the type locality in the Red River drainage (Suppl. material 1: table S1). Multiple samples and localities were included, when possible, for widespread species. Sampling sites were assigned to freshwater ecoregions following Abell et al. (2008) and Hoang et al. (2021a, 2021b).

Molecular analysis

Molecular sequence data were newly generated or taken from GenBank for the following currently recognised species of *Poropuntius* (Fricke et al. 2023): *P. alloiopleurus* (Vaillant, 1893), *P. aluoiensis* (Nguyen, 1997), *P. angustus* Kottelat, 2000, *P. bantamensis* (Rendahl, 1920), *P. bolovenensis* Roberts, 1998, *P. burtoni* (Mukerji, 1933), *P. carinatus* (Wu & Lin, 1977), *P. deauratus* (Valenciennes, 1842), *P. genyognathus* Roberts, 1998, *P. hampaloides* (Vinciguerra, 1890), *P. hathe* Roberts, 1998, *P. heterolepidotus* Roberts, 1998, *P. huangchuchieni* (Tchang, 1962), *P. kontumensis* (Chevey, 1934), *P. krempfi* (Pellegrin & Chevey, 1934), *P. laoensis* (Günther, 1868), *P. melanogrammus* Roberts, 1998, *P. normani* Smith, 1931, *P. opisthopterus* (Wu, 1977), *P. rhomboides* (Wu & Lin, 1977), *P. schanicus*

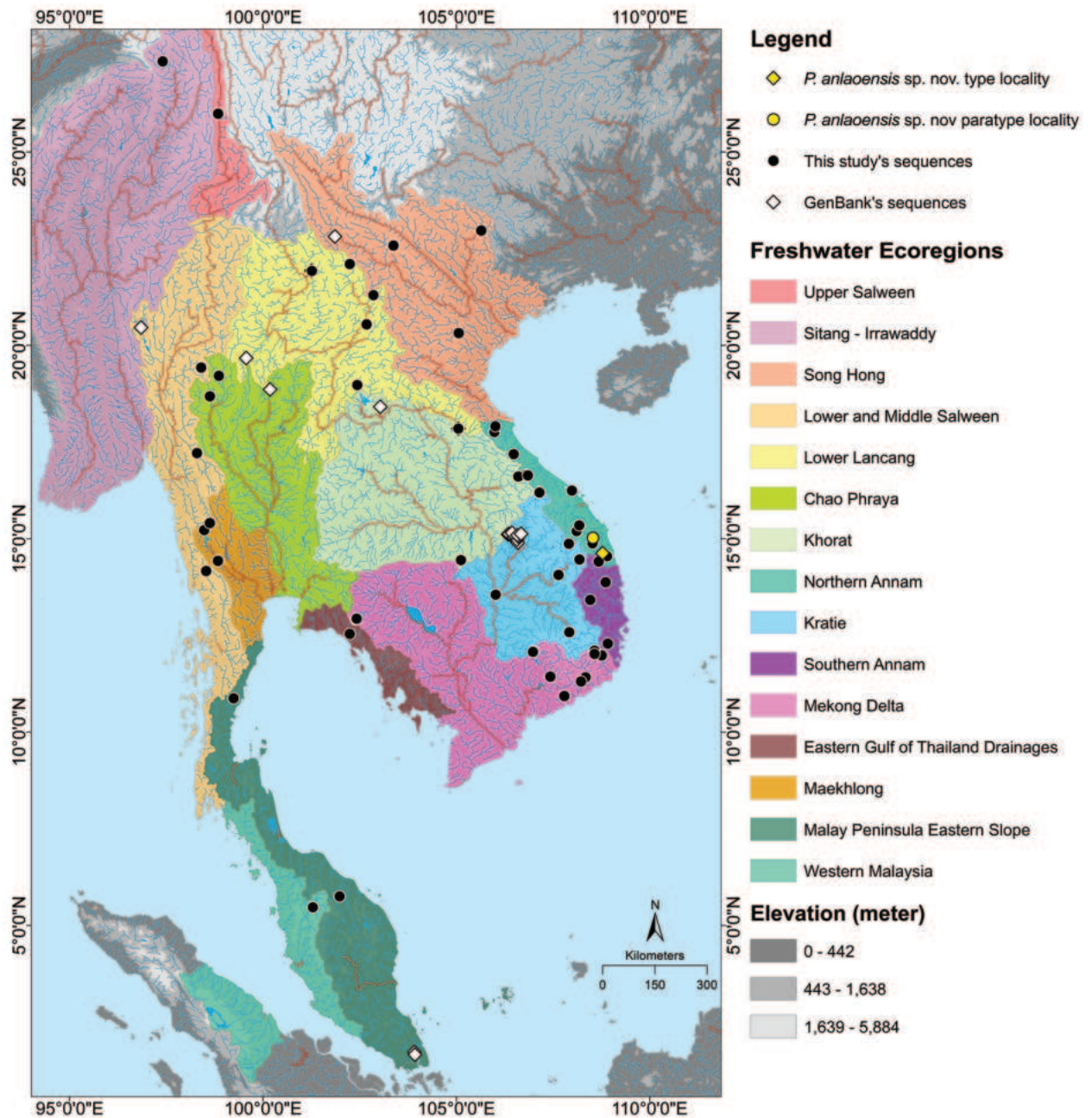


Figure 1. Sampling sites of *Poropuntius* in this study in 15 freshwater ecoregions shown in various colours.

(Boulenger, 1893), and *P. yalyensis* (Nguyen, 2001). Sequence data also were included for the following species considered to be related to *Poropuntius* and for which taxonomic ambiguity exists (Wu et al. 2013; Yang et al. 2015; Kang et al. 2016; Zheng et al. 2016; Muhammad-Rasul et al. 2018): *Poropuntius baolacensis* (Nguyen, 2001), *P. brevispinus* (Nguyễn & Đoàn, 1969), *Acrossocheilus xamensis* Kottelat, 2000, *A. macrophthalmus* (Nguyen, 2001), *Hypsibarbus anamensis* (Pellegrin & Chevey, 1936), and *H. macrosquamatus* (Mai, 1978). *Hypsibarbus wetmorei* was used at the outgroup species based on recent studies of cyprinid higher-level relationships (Yang et al. 2015; Stout et al. 2016; Wang et al. 2016). Given taxonomic ambiguities, it is important to identify methods used to identify specimens newly acquired by the authors for this study.

Specimens of *Acrossocheilus baolacensis* Nguyen, in Nguyễn and Ngô 2001 (recently as *Poropuntius baolacensis*) was described from Vietnam, Cao Bang Province, Nho Que, Bao Lac, Song Hong ecoregion. Near-topotypic material (UNS 2018-1410) was collected in the Gâm River of the Song Hong ecoregion and identified through comparison with the description in Nguyễn and Ngô (2001: 385–387).

Acrossocheilus macrophthalmus Nguyễn & Ngô, 2001 was described from Vietnam, Hòa Bình, Song Hong ecoregion, Black River. Near-topotypic material (UNS 2018-1310) was collected in the Gâm River of the Song Hong ecoregion and identified through comparison with the description in Nguyễn and Ngô (2001).

Acrossocheilus xamensis Kottelat, 2000 was described from Laos, Houaphan Province, Houay Tangoua, Nậm Xám. Near-topotypic material (UNS 2019-1506) was collected from Vietnam, Thanh Hóa, Quan Hóa, Lò River, Song Hong ecoregion, in the same drainage as the type locality. The identification followed Kottelat (2000: 38–39).

Acrossocheilus yalyensis Nguyen, in Nguyễn and Ngô 2001 (recently as *Poropuntius yalyensis*) was described from Vietnam, Kon Tum Province, Sesan River. Topotypic material (UNS 2019-1201) was collected from the Sesan River, Kon Tum, Dak Poko - Dak Pek, in the Kratie-Stung Treng ecoregion and identified through comparison with the description in Nguyễn and Ngô (2001: 393–395).

Barbodes huangchuchieni rhomboides Wu & Lin (in Wu et al. 1977: 248; recently as *Poropuntius rhomboides*) was described from China, Yunnan Province, Yunnanjiang (upper Red River). Near-topotypic material (UNS 2018-3010, UNS 2018-1111) was collected in the upper Red River in Vietnam, Lào Cai, Bản Hồ, Nậm Cùn, and identified through comparison with the description in Wu et al. (1977).

Barbus alloiopterus Vaillant, 1893 (now *Poropuntius alloiopterus*) was described from Vietnam, Đà River, Song Hong ecoregion. Topotypic material (UNS 2018-3010) was collected from the Đà River and identified through comparison with the description in Kottelat (2001: 35–36).

Barbus (Puntius) annamensis Pellegrin & Chevey, 1936 (recently as *Hypsiibarbus annamensis*) was described from Vietnam, Annam, Quảng Nam, Hàn Giang. Topotypic material (UNS 2018-2702) and near-topotypic material (UNS 2018-2402, UNS 2018-0704) from the northern Annam ecoregion was identified following Rainboth (1996: 55–58).

Barbus bantamensis Rendahl, 1920 (recently as *Poropuntius bantamensis*) was described from Thailand, Chiang Mai Province, Ban Tam. Topotypic material was collected in Thailand, Chiang Mai Province, Ping River drainage in the Chao Phraya ecoregion (UF 183366, UF 243217, UF 177816) and identified through comparison with the description in Rendahl (1920: 1–3).

Lissochilus aluoiensis Nguyen, 1997 (recently as *Poropuntius aluoiensis*) was described from Vietnam, Thua Thien Hue Province, A Luoi, A Sap at Nham, Se Kong basin. Topotypic material (UNS 2018-0304) was collected from the A Sap River of the upper Sekong drainage and identified through comparison with the description in Nguyen (1997: 1–4).

Lissochilus brevispinus Nguyễn & Đoàn, 1969 (recently as *Poropuntius brevispinus*) was described from Vietnam, Hoa Binh Province, Suối Rút. Material (UNS 2018-1310, UNS 2018-1010) was collected from Hà Giang, Lô River, in the Song Hong ecoregion and identified through comparison with the description Nguyễn and Ngô (2001: 387–388).

Lissochilus macrosquamatus Mai, 1978 (recently as *Hypsibarbus macrosquamatus*) was described from Vietnam, Song Hong ecoregion. Near-topotypic material (UNS 2018-1204, UNS 2018-1604) was collected in the Long Đại River, Quảng Bình of the northern Annam ecoregion and identified through comparison with the description in Mai (1978: 99–100).

Poropuntius angustus Kottelat, 2000 was described from Laos, Louangphabang Province: Houay Houn, Ban Houay Lek. Topotypic material (UNS 2018-07-11) was collected from the Nam Núa, Lower Lancang ecoregion, in the upper reach of Nam Ou, the type locality, and identified through comparison with the description in Kottelat (2000: 46).

Poropuntius bolovenensis Roberts, 1998 was described from Laos, Champasak Province, Bolavens, Plateau, Sekong basin, Xe Nam Noi. Topotypic material was collected from Xe Nam Noi and Xe Pian in the Kratie-Stung Treng ecoregion and identified through comparisons with descriptions in Roberts (1998: 124–127) and Kang et al. (2016).

Poropuntius krempfi (Pellegrin & Chevey, 1934) was collected in the Gâm River of the Song Hong ecoregion. Identification of our specimens (UNS 2018-1410) was based on comparison with material from the Red River of Song Hong, northern Vietnam, the type locality.

Poropuntius normani Smith, 1931 was described from Thailand, Chantaburi Province, Pliew Waterfall. Topotypic material (UF 235973) and near-topotypic material (UF 170368, 188709, 235982) was collected from Chantaburi Province, in the Eastern Gulf of Thailand Drainages ecoregion and identified through comparisons with descriptions in Smith (1931: 15) and Muhammad-Rasul et al. (2018: 327–342).

No genetic data are available for the following species, and no opinions are offered on their validity: *Poropuntius chondrorhynchus* (Fowler, 1934), *P. chonglingchungi* (Tchang, 1938), *P. cogginii* (Chaudhuri, 1911), *P. exiguus* (Wu & Lin, 1977), *P. faucis* (Smith, 1945), *P. fuxianhuensis* (Wang, Zhuang & Gao, 1982), *P. margarianus* (Anderson, 1879), *P. shanensis* (Hora & Mukerji, 1934), *P. speleops* (Roberts, 1991), and *P. tawarensis* (Weber & de Beaufort, 1916).

DNA extraction and amplification

DNA was extracted from fin clips stored in 95–99% ethanol using the DNeasy Blood & Tissue Kit (Qiagen, Valencia, CA, USA) and following the protocol suggested by the manufacturer. Two mitochondrial genes, cytochrome oxidase subunit I (COI) and cytochrome b (*Cytb*), were amplified using polymerase chain reaction (PCR). Primers and PCR conditions followed Ward et al. (2005) for COI and Durand et al. (2012) for *Cytb*. PCR products were visualised on 1–2% agarose gels, and the most intense products were selected for purifying and Sanger sequencing by 1ST BASE (<https://base-asia.com/>).

Phylogenetic analyses

Chromas 2.6.6 (<http://technelysium.com.au/>) was used to inspect the sequence chromatograms and assemble them into contigs, and MUSCLE in MEGA 7 (Edgar 2004; Kumar et al. 2016) was used to align the consensus sequences for each gene. Alignments were inspected by eye for accuracy, and

sequences were trimmed at the 3' and 5' ends to minimise missing characters. The final data matrix consisted of 568 bp for COI and 872 bp for *Cytb* used in the separated analyses. Uncorrected pairwise sequence divergence was estimated using the substitution model of Kimura 2-parameters, bootstraps 1000 implemented in MEGA 7 (Kumar et al. 2016). All sequences generated for this study were deposited in GenBank (Suppl. material 1: table S1). For each independent dataset of COI and *Cytb*, phylogenetic inferences based on Maximum Likelihood (ML) were made using IQ-TREE (Nguyen et al. 2015) through the IQ-TREE web server (Trifinopoulos et al. 2016, <http://www.iqtree.org/>). Optimal partitioning models for the ML inference were selected by ModelFinder (Chernomor et al. 2016; Kalyaanamoorthy et al. 2017) in IQ-TREE, using the minimum BIC score. Partition analysis suggested best fit models for ML inference: TN+F+I+G4 (BIC = 6531.319, lnL = - 2650.474) for COI and HKY+F+I+G4 (BIC = 6910.503, lnL = - 3065.931) for *Cytb*. Ultrafast bootstrap (BS) analysis for 1000 iterations (Bui et al. 2013) was carried out to determine statistical support for the nodes in ML. The trees obtained from ML were visualised using Figtree v. 1.4.3 (<http://tree.bio.ed.ac.uk/software/figtree>).

List of abbreviations

BD	body depth;	DNA	Deoxyribonucleic Acid;
BIC	Bayesian information criterion;	HL	head length;
BS	bootstrap;	LCP	length of caudal peduncle;
COI	Cytochrome c oxidase sub-unit 1;	ML	Maximum Likelihood;
<i>Cytb</i>	Cytochrome <i>b</i> ;	PCR	Polymerase Chain Reaction;
DCP	depth of caudal peduncle;	SL	standard length.

Results

The ML trees for the COI and *Cytb* sequences are shown in Fig. 2. The COI topology is consistent with recognition of 16 species (Fig. 2A), all represented by more than one sequence with $\geq 83\%$ bootstrap support, including one undescribed species.

The *Cytb* sequences were used to examine the results of the study of *P. huangchuchieni* in southwest China by Wu et al. (2013) with a greater *Cytb* dataset (Fig. 2B). The five major lineages identified by Wu et al. (2013) are reassigned. The LX lineage of Wu et al. (2013) from the Song Hong aligned with *P. krempfi* in our sequences, the SW of the Upper Salween with *P. opisthopterus*, the RL of the Song Hong with *P. alloiopterus*, the MK-A of the Lower Lancang with *P. huangchuchieni*, and the MK-B of the Lower Lancang with *P. laoensis*. The greatest similarity in the *Cytb* sequences was 98% (± 0.00), found between *P. laoensis*, which occurs in the Lower Lancang, Kratie – Stung Treng, northern Annam, Chao Phraya, and Middle & Lower Salween ecoregions, and *P. huangchuchieni* in the Lower Lancang (Table 1). The COI data for *P. huangchuchieni* (Fig. 2A) aligned with the reassignments based on the *Cytb* data and are not discussed further.

Seven of the 16 species recognised with COI data (Fig. 2A) include representatives of other nominal species now to be recognised as synonyms. One, the

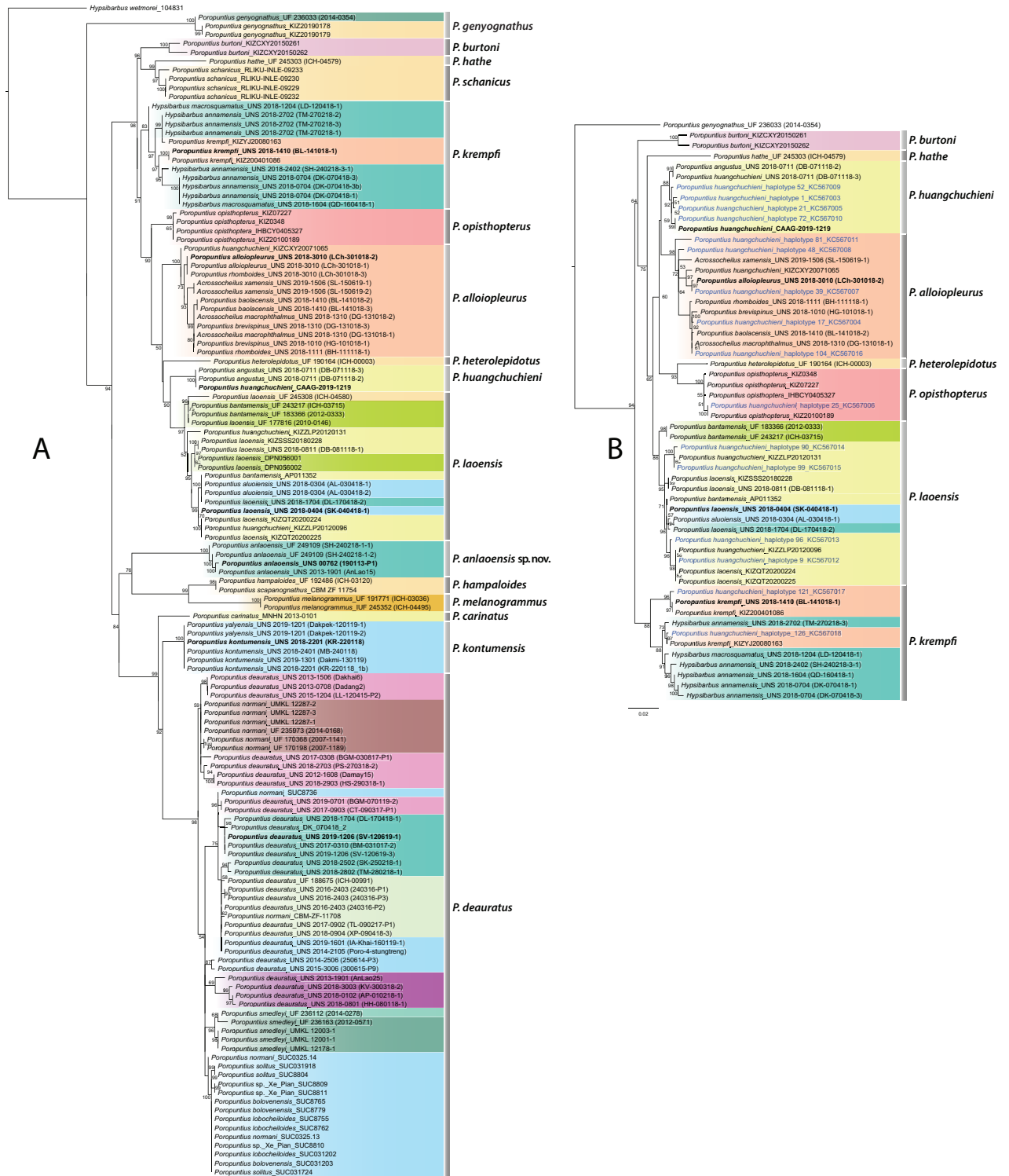


Figure 2. Maximum-likelihood tree based on (A) COI and (B) Cytb mitochondrial gene sequences for species of *Poropuntius*. Numbers on branches are ML bootstrap values (values > 50% shown). Bold sample labels are sequences from type localities. Blue sample labels in the Cytb tree are sequences from Wu et al. (2013). Colours of clades correspond to the freshwater ecoregions in Fig. 1.

P. kremphi clade includes 12 specimens of three nominal species currently assigned to two genera: *P. kremphi*, *Hypsibarbus annamensis*, and *H. macrosquamatus*. The newly collected specimens of all three nominal taxa were collected

Table 1. Cytochrome *b* genetic distances between species in the phylogenetic analysis with *P. genyognathus* as the out-group using the Kimura 2-parameter model, standard error estimates shown above the diagonal with bootstraps 1000.

	1	2	3	4	5	6	7	8	9
1. <i>P. genyognathus</i>		0.01	0.01	0.01	0.01	0.01	0.01	0.01	0.01
2. <i>P. burtoni</i>	0.09		0.01	0.01	0.01	0.01	0.01	0.01	0.01
3. <i>P. hathe</i>	0.10	0.06		0.01	0.01	0.01	0.01	0.01	0.01
4. <i>P. huangchuchieni</i>	0.08	0.05	0.05		0.00	0.01	0.01	0.00	0.01
5. <i>P. alloiopterus</i>	0.08	0.06	0.05	0.03		0.01	0.01	0.01	0.01
6. <i>P. heterolepidotus</i>	0.09	0.06	0.06	0.03	0.04		0.01	0.01	0.01
7. <i>P. opisthopterus</i>	0.09	0.06	0.06	0.04	0.04	0.03		0.01	0.01
8. <i>P. laoensis</i>	0.08	0.05	0.05	0.02	0.03	0.04	0.04		0.01
9. <i>P. krempfi</i>	0.08	0.05	0.06	0.04	0.05	0.05	0.04	0.04	

from their type localities in the Song Hong and northern Annam ecoregions and are embedded with *P. krempfi* specimens from the Song Hong with a mean similarity of 98.8% (± 0.29) (Fig. 2A). This clade received 83% bootstrap support. *Hypsibarbus annamensis*, and *H. macrosquamatus* are synonyms of *P. krempfi*. The *P. krempfi* lineage in the Song Hong ecoregion has a COI sequence similarity of 97% (± 1.00) with *P. alloiopterus* from the Song Hong, *P. opisthopterus* from the Upper Salween, *P. burtoni* from the Sittang - Irrawaddy, and *P. schanicus* from the Inle Lake, Myanmar (Table 2).

The *P. alloiopterus* clade (Fig. 2A, B) consists of 13 specimens of six nominal species (plus specimens labelled *P. huangchuchieni* in Wu et al. (2013) and Zheng et al. (2016)), currently in two genera: *P. alloiopterus*, *P. baolacensis*, *P. brevispinus*, *P. rhomboides*, *Acrossocheilus macrophthalmus*, and *A. xamensis* collected in the Song Hong and northern Annam ecoregions from their type drainages (Fig. 2A). The newly collected specimens are embedded with *P. alloiopterus* specimens from the Song Hong and show a mean similarity of 99.5% (± 0.20). This clade receives 100% bootstrap support. Thus, we conclude that *P. baolacensis*, *P. brevispinus*, *P. rhomboides*, *A. macrophthalmus* and *A. xamensis* are synonyms of *P. alloiopterus*. The *P. alloiopterus* lineage observed in the Song Hong ecoregion has a COI sequence similarity of 97% (± 1.00) with *P. krempfi* from the Song Hong, *P. huangchuchieni* and *P. laoensis* from the Lower Lancang, and *P. opisthopterus* from the Upper Salween (Table 2).

The *P. huangchuchieni* clade consists of three specimens of two nominal species, *P. huangchuchieni* and *P. angustus* collected from their type drainages in the Lower Lancang ecoregion. These specimens have a mean similarity of 100% (± 0.00) (Fig. 2A). *Poropuntius angustus* is a synonym of *P. huangchuchieni*. The *P. huangchuchieni* lineage in the Lower Lancang ecoregion has a COI sequence similarity of 97% (± 1.00) with *P. laoensis* from the Lower Lancang, *P. alloiopterus* from the Song Hong, and *P. opisthopterus* from the Upper Salween (Table 2).

The *P. laoensis* clade consists of 17 specimens of three nominal species, *P. laoensis*, *P. aluoensis*, and *P. bantamensis* collected in the Lower Lancang, Kratie – Stung Treng, northern Annam, Chao Phraya, and Middle & Lower Salween ecoregions including from their type localities. The newly collected specimens are embedded with *P. laoensis* specimens from the Kratie – Stung Treng

Table 2. COI genetic distances between species in the phylogenetic analysis with *Hypsibarbus wetmorei* as the outgroup using the Kimura 2-parameter model, standard error estimates shown above the diagonal with bootstraps 1000.

	1	2	3	4	5	6	7	8	9	10	11	12	13	14	15	16	17
1. <i>H. wetmorei</i>		0.02	0.01	0.02	0.01	0.01	0.02	0.02	0.02	0.02	0.01	0.02	0.02	0.02	0.02	0.02	0.02
2. <i>P. genyognathus</i>	0.10		0.01	0.01	0.01	0.01	0.01	0.01	0.02	0.01	0.01	0.01	0.02	0.02	0.01	0.01	0.02
3. <i>P. burtoni</i>	0.08	0.08		0.01	0.01	0.01	0.01	0.01	0.01	0.01	0.01	0.01	0.01	0.01	0.01	0.01	0.01
4. <i>P. hathe</i>	0.10	0.09	0.04		0.01	0.01	0.01	0.01	0.01	0.01	0.01	0.01	0.01	0.01	0.01	0.01	0.01
5. <i>P. schanicus</i>	0.09	0.07	0.03	0.03		0.01	0.01	0.01	0.01	0.01	0.01	0.01	0.01	0.01	0.01	0.01	0.01
6. <i>P. krempfi</i>	0.09	0.08	0.03	0.05	0.03		0.01	0.01	0.01	0.01	0.01	0.01	0.01	0.01	0.01	0.01	0.01
7. <i>P. opisthopterus</i>	0.10	0.09	0.04	0.05	0.03	0.03		0.01	0.01	0.01	0.01	0.01	0.01	0.01	0.01	0.01	0.01
8. <i>P. alloioleurus</i>	0.11	0.08	0.04	0.05	0.04	0.03	0.03		0.01	0.01	0.01	0.01	0.01	0.02	0.01	0.01	0.01
9. <i>P. heterolepidotus</i>	0.12	0.10	0.04	0.06	0.05	0.04	0.03	0.04		0.01	0.01	0.01	0.01	0.02	0.01	0.01	0.01
10. <i>P. huangchuchieni</i>	0.10	0.07	0.05	0.06	0.05	0.04	0.03	0.03	0.04		0.01	0.01	0.01	0.01	0.01	0.01	0.01
11. <i>P. laoensis</i>	0.09	0.07	0.04	0.05	0.04	0.04	0.03	0.03	0.04	0.03		0.01	0.01	0.01	0.01	0.01	0.01
12. <i>P. anlaoensis</i> sp. nov.	0.12	0.09	0.08	0.09	0.07	0.08	0.08	0.09	0.08	0.09	0.08		0.01	0.01	0.01	0.01	0.01
13. <i>P. hampaloides</i>	0.12	0.10	0.07	0.09	0.07	0.07	0.07	0.08	0.07	0.07	0.07	0.07		0.01	0.01	0.01	0.01
14. <i>P. melanogrammus</i>	0.12	0.10	0.09	0.09	0.08	0.08	0.09	0.10	0.10	0.08	0.08	0.09	0.05		0.02	0.02	0.01
15. <i>P. carinatus</i>	0.11	0.07	0.06	0.08	0.06	0.06	0.06	0.05	0.07	0.05	0.05	0.07	0.09	0.10		0.01	0.01
16. <i>P. kontumensis</i>	0.11	0.09	0.06	0.08	0.05	0.06	0.05	0.06	0.07	0.05	0.05	0.06	0.08	0.09	0.03		0.01
17. <i>P. deauratus</i>	0.11	0.10	0.07	0.08	0.06	0.07	0.06	0.07	0.08	0.07	0.07	0.07	0.08	0.09	0.04	0.04	

and show a mean similarity of 99.1% (± 0.23) (Fig. 2A). This clade receives 97% bootstrap support. *Poropuntius aluoiensis* and *P. bantamensis* are synonyms of *P. laoensis*. The *P. laoensis* lineage observed in the Lower Lancang, Kratie – Stung Treng, northern Annam, Chao Phraya, and Middle & Lower Salween ecoregions has a COI sequence similarity of 97% (± 1.00) with *P. huangchuchieni* from the Lower Lancang, *P. alloioleurus* from the Song Hong, and *P. opisthopterus* from the Upper Salween (Table 2).

The *P. anlaoensis* sp. nov. lineage consists of four specimens of a new species of *Poropuntius*. This lineage from the Annam ecoregion has its greatest COI sequence similarity of 94% (± 1.00) with *P. kontumensis* from the Kratie – Stung Treng (Table 2).

The *P. kontumensis* clade consists of six specimens of two nominal species, *P. kontumensis* and *P. yalyensis*, collected in the Kratie – Stung Treng ecoregion from their type localities. The newly collected specimens are embedded with *P. kontumensis* specimens from the type locality and have a similarity of 100% (± 0.00) (Fig. 2A). *Poropuntius yalyensis* is a synonym of *P. kontumensis*. The *P. kontumensis* lineage from the Kratie – Stung Treng ecoregion is most similar to *P. carinatus* from the Lower Lancang with a COI sequence similarity of 97% (± 1.00) (Table 2).

The *P. deauratus* clade consists of 57 specimens of six nominal species, *P. normani*, *P. deauratus*, *P. bolovenensis*, *P. lobocheiloides*, *P. smedleyi*, and *P. solitus*, collected the eastern Gulf of Thailand drainages, Malay Peninsula, Mekong Delta, Kratie – Stung Treng, Khorat Plateau, and Annam ecoregions, including from their type localities. These specimens are embedded with *P. deauratus* specimens from the Annam ecoregion and have a mean similarity of 98.7% (± 0.25). This

clade receives 98% bootstrap support. *Poropuntius normani*, *P. bolovenensis*, *P. lobocheiloides*, *P. smedleyi*, and *P. solitus* are synonyms of *P. deauratus*. The *P. deauratus* lineage in the Eastern Gulf of Thailand drainages, Malay Peninsula, Mekong Delta, Kratie – Stung Treng, Khorat Plateau, and Annam ecoregions has a COI sequence similarity of 96% (± 1.00) with *P. carinatus* from the Lower Lancang and *P. kontumensis* from the Kratie – Stung Treng ecoregion (Table 2).

Taxonomic conclusions

Based on molecular data, 17 nominal species of *Poropuntius*, *Hypsibarbus*, and *Acrossocheilus* are reduced to synonyms of the six valid species of *Poropuntius* listed below. Also considered a junior synonym of *P. deauratus* is *P. conster-nans*, referred to as a variant of *P. bolovenensis* by Kottelat (2013) in an environmental assessment of a hydroelectric power project in the Bolaven Plateau, Laos and relegated to the synonymy of *P. deauratus* by Kang et al. (2016).

Morphological and molecular data also provide evidence that newly collected specimens from the Annam ecoregion represent a new species of *Poropuntius*, described below. Synonyms listed are only those addressed in this study.

Taxonomic account

Cypriniformes

Cyprinidae Rafinesque, 1815

Poropuntini Menon, 1999

Poropuntius Smith, 1931

Poropuntius krempfi (Pellegrin & Chevey, 1934)

Barbus (*Lissochilichthys*) *krempfi* Pellegrin & Chevey, 1934: 339. Type locality: Vietnam, Tonkin, Ngoi-Thia River at Nghia Lô, tributary of Red River upstream of Yên Bay. Holotype: MNHN 1934-0262.

Barbus (*Puntius*) *annamensis* Pellegrin & Chevey, 1936: 225, fig. 3. Type locality: Vietnam, Annam, Quảng Nam, Hàn Giang. Holotype: MNHN 1935-0337.

Lissochilus macrosquamatus Mai, 1978: 99, fig. 42. Type locality: northern Vietnam. Syntypes: DVZUT.

Notes. Specimens of *Poropuntius krempfi* (Fig. 3A, B) were recovered in a clade including topotypic material of *Barbus annamensis* and *Lissochilus macrosquamatus*. The clade was sister to a large clade including *P. alloiopterus*, *P. heterolepidotus*, *P. huangchuchieni*, *P. laoensis*, and *P. opisthopterus* (Fig. 2A).

Specimens of *P. krempfi* from northern Annam (MNHN 1935:0337, MNHN 1969:42) were assigned by Rainboth (1996) to *Hypsibarbus annamensis* presumably due to the presence of a few tiny tubercles on the tip of the snout, but this trait is not useful for separating all species of the two genera. Some of our 41 specimens of *P. krempfi* have tiny tubercles on the tip of the snout. Rainboth (1996) noted that this species was unusual in being the only species of *Hypsibarbus* on the coastal side of the Annam Cordillera and in having a much longer dorsal spine with 26–28 serrations, compared to 20 or fewer in other species in the Mekong River drainage.

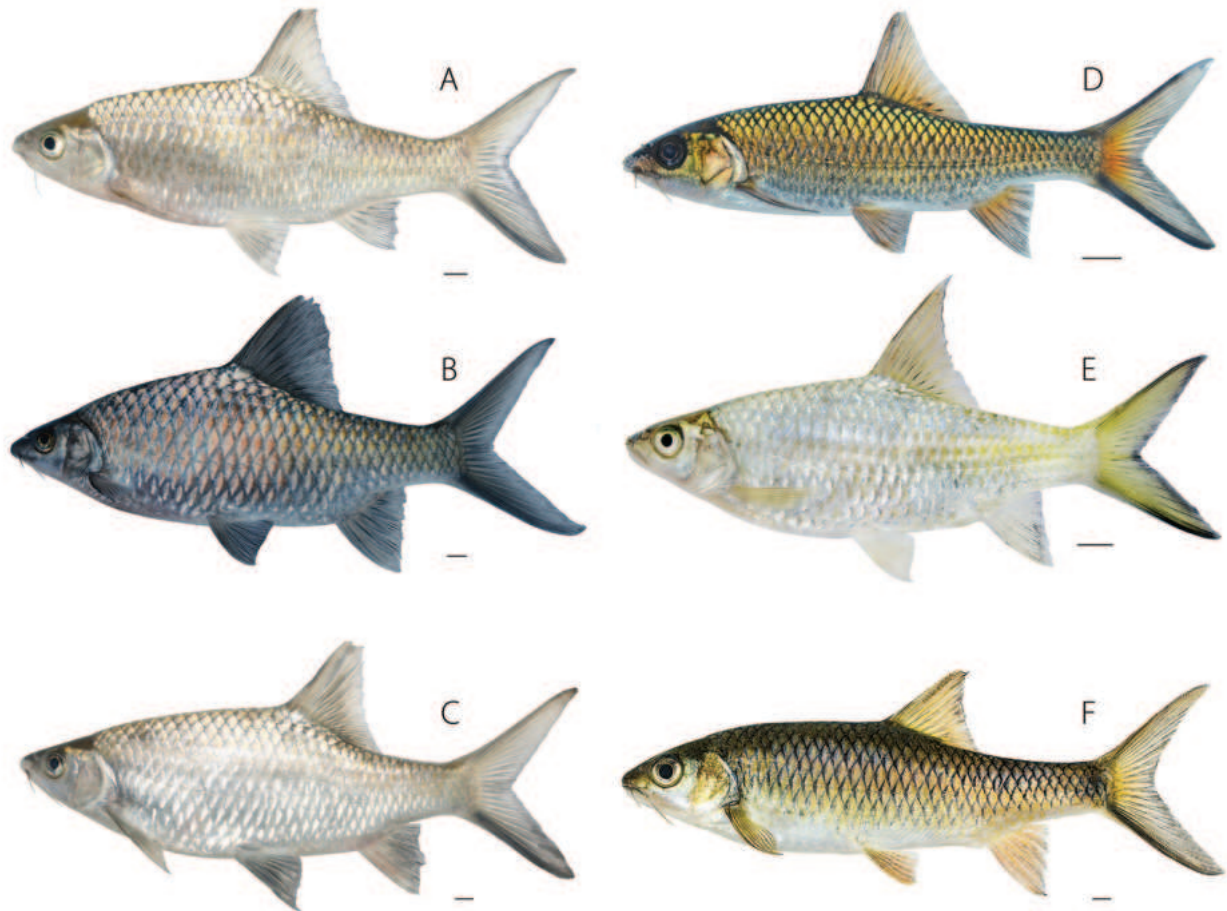


Figure 3. Species of *Poropuntius*. *Poropuntius krempfi* from **A** Song Hong ecoregion, UNS 2018-1410 **B** northern Annam, UNS 2018-2702; *P. alloiopleurus* from **C** Song Hong, UNS 2018-3010; *P. laoensis* from **D** upper Sekong's tributary, UNS 2018-0404 **E** upper Sekong's pool, UNS 2018-0304; *P. huangchuchieni* from **F** Lower Lancang, UNS 2018-0711. All photographed in life. Scale bars: 10 mm.

Hypsibarbus macrosquamatus from Song Hong, northern Vietnam (type: DVZUT) described by Mai (1978) and treated as *Acrossocheilus macrosquamatus* by Nguyễn and Ngô (2001) resembles our *P. krempfi* specimens from northern Annam with a lateral-line scale count of 29–33.

Distribution. *Poropuntius krempfi* is found in the Song Hong and northern Annam ecoregions.

***Poropuntius alloiopleurus* (Vaillant, 1893)**

Barbus alloiopleurus Vaillant, 1893: 201. Type locality: Vietnam, Tonkin, Black River. Holotype: MNHN 1892-0261.

Barbodes (*Barbodes*) *huangchuchieni rhomboides* Wu & Lin, in Wu et al. 1977: 248, pl. 7–8. Type locality: China, Yunnan, Yuanjiang River. Syntypes (15): KIZ 645614-15, 645617-19, 645622, 645624, 6440093, 6440392, 6440461, 6440564, 6450172, 6450191, 6450207, 6450322.

Poropuntius baolacensis (Nguyen, in Nguyễn and Ngô 2001): 387, fig. 189. Type locality: Vietnam, Cao Bang Province, Nho Que, Bao Lac [22°56'60"N, 105°40'00"E], Song Hong River drainage. Holotype: VNCNTTS H.01.72.13.01.

Poropuntius brevispinus (Nguyễn & Đoàn, 1969):12, fig. 7. Type locality: Vietnam, Hoa Binh Province, Suoi Rut stream. Syntypes (3): NCNTTSI H.01.72.10.01-03.

Acrossocheilus macrophthalmus Nguyen, in Nguyễn and Ngô 2001: 390, fig. 191. Type locality: Vietnam, Hoa Binh Province, Da Bac District, Da River at Thac Bo. Holotype: NCNTTSI H.01.72.14.01.

Acrossocheilus xamensis Kottelat, 2000: 38, fig. 1. Type locality: Laos, Houaphan Province, Houay Tangoua, small stream entering Nam Xam in Ban Houay Tangoua, 20°09'24"N, 104°32'50"E. Holotype: ZRC 45297.

Notes. Specimens of *Poropuntius alloiopterus* (Fig. 3C) were recovered in a clade including topotypic material of *Acrossocheilus macrophthalmus*, *A. xamensis*, *Barbodes huangchuchieni rhomboides*, *Poropuntius baolacensis*, and *P. brevispinus* and was sister to a clade including *P. heterolepidotus*, *P. huangchuchieni*, and *P. laoensis* (Fig. 2A).

Kottelat (2000) noted that *Acrossocheilus xamensis* resembles *Poropuntius* but lacks the branched lateral-line canals diagnostic of *Poropuntius*. Our 12 specimens of *P. alloiopterus* are missing branched lateral-line canals; branched canals are variable within *Poropuntius* and do not distinguish *Poropuntius* from *Acrossocheilus*. A paratype of *A. xamensis* exhibits the typical caudal-fin characteristic of *Poropuntius*, a dark marginal stripe along the lower lobe (Kottelat 2000, fig. 1).

According to Nguyễn (2001), *A. macrophthalmus* resembles *P. alloiopterus* but has an eye diameter longer than the snout. Our 12 specimens of *P. alloiopterus* have eye diameters that are shorter or longer than the snout.

Nguyễn and Ngô (2001) distinguished *P. baolacensis* from *P. brevispinus* in having 28–30 vs 18–22 serrae along the posterior margin of the last simple dorsal-fin ray. Our 12 specimens of *P. alloiopterus* have 20–29 serrae on the last dorsal-fin ray, partially overlapping the serrae counts given to distinguish *P. baolacensis* and *P. brevispinus*.

Distribution. *Poropuntius alloiopterus* is found in the Song Hong ecoregion.

***Poropuntius huangchuchieni* (Tchang, 1962)**

Barbus huangchuchieni Tchang, 1962: 96, fig. 1. Type locality: China, Yunnan, Hsi-Shuan- Pan-Na [Xishuangbanna]; Syntypes: ASIZB [now NZMC] 39256(1), 39865(1).

Poropuntius angustus Kottelat, 2000: 46, fig. 14. Type locality: Laos, Louangphabang Province, Houay Houn, ca. 3 km upstream of Ban Houay Lek, approx. 20°32'32"N, 102°40'51"E. Holotype: ZRC 45308.

Notes. In the original description of *P. angustus*, Kottelat (2000) made no specific mention of *P. huangchuchieni*. Topotypic material (UNS 2018-07-11, Fig. 3F) from the Nam Núa, Lower Lancang ecoregion, in the upper reach of Nam Ou, the type locality of *P. angustus*, was genetically identical to that of *P. huangchuchieni* from the Lancang Jiang in Yunnan.

Distribution. *Poropuntius huangchuchieni* is found in the Lower Lancang ecoregion.

***Poropuntius laoensis* (Günther, 1868)**

Barbus laoensis Günther, 1868: 115. Type locality: Laos Moutains, Cochinchina. Holotype: BMNH 1862.7.28.15.

Poropuntius bantamensis (Rendahl, 1920): 1, fig. 1. Type locality: Thailand, Ban Tam, east of Doi Chieng Dao, pond fed by a subterranean stream. Holotype: NRM 10969.

Poropuntius aluoiensis (Nguyen, 1997): 1, fig. 1. Type locality: Vietnam, Thua Thien Hue Province, A Luoi District, A Sap stream at Nham, Sekong basin, 16°15'32"N, 107°13'31"E. Holotype: HNUE V1.1.21.

Notes. Our seven specimens of *P. laoensis* specimens (Fig. 3D, E) were collected in the upper Xekong drainage of Central Vietnam, the type locality, i.e., in the Lao Mountains of Cochin-China, now Central Vietnam. Topotypic material of *P. bantamensis* and *P. aluoiensis* resembled *P. laoensis* in having the proximal half of the caudal fin orange and the distal half bright yellow, and bold black submarginal stripes on the caudal fin.

Distribution. *Poropuntius laoensis* occurs in the Lower Salween, Chao Phraya, Lower Lancang, northern Annam, and Kratie-Stung Treng ecoregions.

***Poropuntius kontumensis* (Chevey, 1934)**

Cyclocheilichthys kontumensis Chevey, 1934: 32, fig. 1. Type locality: Vietnam, Annam, Pleiku Province, Kontum Lake [Mekong River drainage]. Types unknown.

Acrossocheilus yalyensis Nguyễn, in Nguyễn and Ngô 2001: 393, fig. 193. Type locality: Vietnam, Kon Tum Province, Sông Sesan [river]. Holotype: NCNTTSI H.01.72.15.01.

Notes. The five specimens of *Poropuntius kontumensis* (Fig. 4A) and *Acrossocheilus yalyensis* were collected in the Kratie – Stung Treng ecoregion from their type localities and were genetically identical.

Distribution. *Poropuntius kontumensis* occurs in the Kratie-Stung Treng ecoregion.

***Poropuntius deauratus* (Valenciennes, in Cuvier & Valenciennes, 1842)**

Barbus deauratus Valenciennes, in Cuvier and Valenciennes 1842: 188. Type locality: Vietnam, Cochinchina [South of Hué; Kottelat 2000: 45]. Holotype: MNHN 2727.

Poropuntius normani Smith, 1931: 15. Type locality: Thailand, Chantaburi Province, Nam Tok Pliu, Kao Sabap, near Chantaburi. Holotype: USNM 90297.

Poropuntius smedleyi de Beaufort, 1933: 44. Type locality: Malaysia, Johor. Syntypes: ZRC [1, missing], ZMA 101.007 [Nijssen et al. 1993: 214].

Poropuntius bolovenensis Roberts, 1998: 124, fig. 5. Type locality: Laos, Champasak Province, Bolavens Plateau, Sekong basin, Xe Nam Noi, 300 m

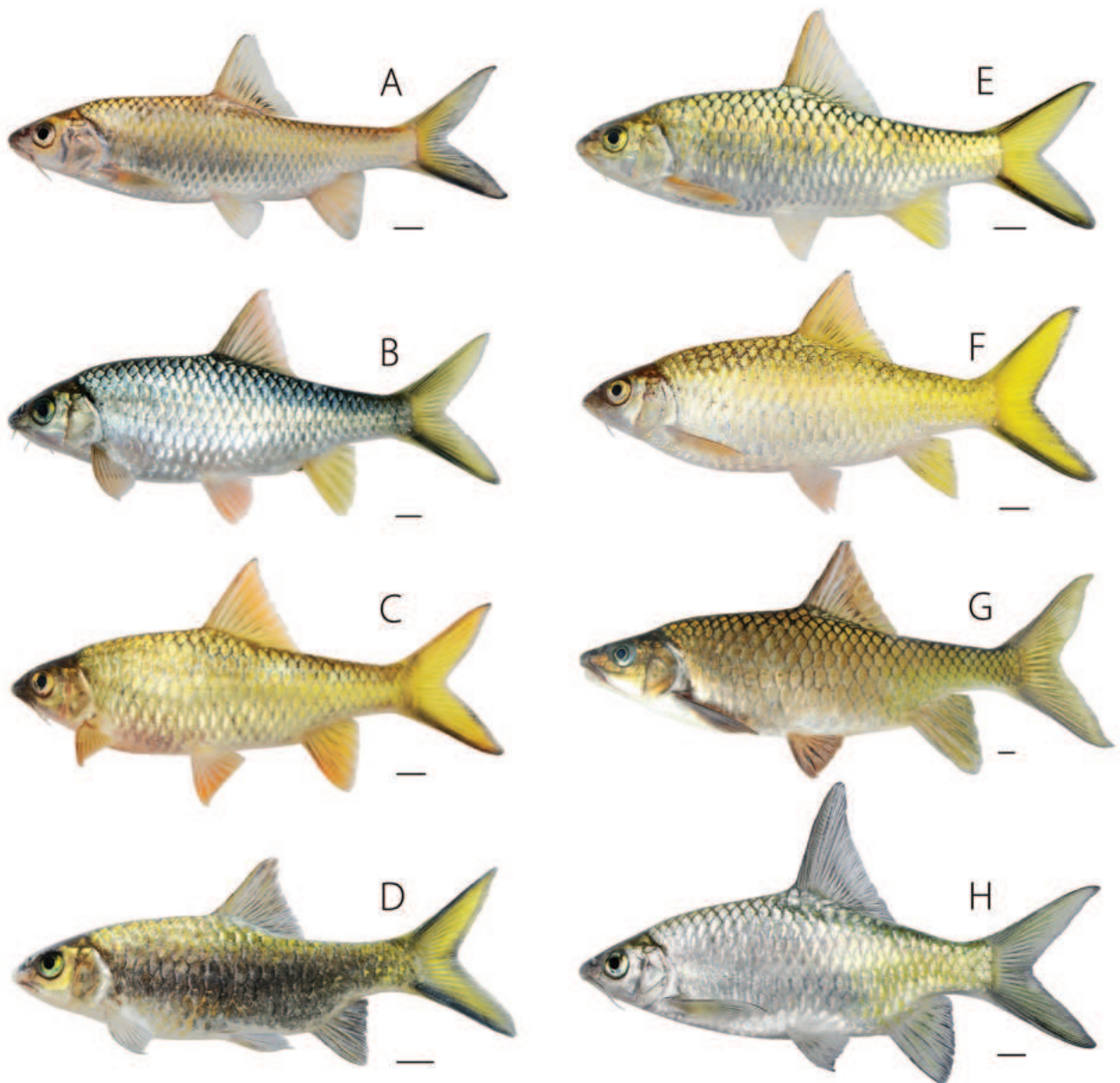


Figure 4. *Poropuntius kontumensis* and *P. deauratus*. *Poropuntius kontumensis* from **A** Kratie–Stung Treng ecoregion (the Sesan drainage), UNS 2018-2201; *P. deauratus* from **B** northern Annam, UNS 2017-0310 **C** northern Annam, UNS 2018-2502 **D** southern Annam, UNS 2018-0801 **E** Mekong Delta (the Đòng Nai drainage) UNS 2017-1612 **F** Khorat Plateau (Sepon drainage), UNS 2018-0904 **G** upper Srepok drainage, UNS 2015-2301 **H** lower Srepok drainage’s pool, UNS 2015-3006. All photographed in life. Scales bars: 10 mm.

downstream from primary dam site of Xe Nam Noi–Xe Pian hydropower scheme. Lectotype: CAS 94251 [designated by Kottelat 2000: 46].

Poropuntius lobocheiloides Kottelat, 2000: 48. Type locality: Laos, Champasak Province, Bolavens Plateau, Xe Nam Noi 300 m downstream from primary dam site for Xe Nam Noi–Xe Pian hydropower scheme, Bolavens Plateau, Sekong watershed. Holotype: CAS 94257.

Poropuntius solitus Kottelat, 2000: 48, fig. 15. Type locality: Laos, Champasak Province, Bolavens Plateau, Huay Makchan-Gnai (Xe Nam Noy basin), south of Ban Taot at turnoff to Xe Nam Noy Project, on road from Pakse to Attapu, 15°04'14"N, 106°32'33"E. Holotype: ZRC 45310.

Poropuntius consternans Kottelat, 2000: 48. Type locality: Laos, Champasak Province, Bolavens Plateau, Sekong drainage, Xe Nam Noi, 300 m downstream from primary dam site of Xe Nam Noi–Xe Pian hydropower scheme, Bolavens Plateau, Sekong watershed. Holotype: CAS 94255.

Notes. The *P. deauratus* clade contained 56 specimens of six nominal species, *P. normani*, *P. deauratus*, *P. bolovenensis*, *P. lobocheiloides*, *P. smedleyi*, and *P. solitus*, collected from a wide area including the Eastern Gulf of Thailand drainages, Malay Peninsula, Mekong Delta, Kratie – Stung Treng, Khorat Plateau, and Annam ecoregions, including type localities.

Molecular data from specimens originally identified as *P. bolovenensis*, *P. lobocheiloides*, and *P. solitus* (GenBank: Song et al. 2017) are from specimens identified morphologically by Kang et al. (2016), who also discussed variation in these forms and in *P. consternans*. Kang et al. (2016) considered all to be *P. bolovenensis*. Our results agree with the conspecificity demonstrated by Kang et al. (2016) but place *P. bolovenensis* in the synonymy of *P. deauratus*. Roberts (1998) had correctly treated *P. consternans* and *P. lobocheiloides*, later named by Kottelat (2000), as ecomorphs of *P. bolovenensis*. Our five specimens of *P. normani* were collected in the same small area as the type locality.

Poropuntius deauratus occurs over a large geographic area and shows considerable variation in shape and color (Fig. 4B–H) as well as in the structural traits related to feeding morphology.

Distribution. *Poropuntius deauratus* is found in the Western Malaysia, Malay Peninsula Eastern Slope, Eastern Gulf of Thailand, Mekong Delta, Kratie-Stung Treng, Khorat, northern Annam, and southern Annam ecoregions.

***Poropuntius anlaensis* Hoàng, Phạm & Trần, sp. nov.**

<https://zoobank.org/17935DFC-446B-4F5C-AF44-4719D31BAD3C>

Material examined. Holotype: UNS00762, 139.46 mm SL, female; An Lão drainage, Bình Định Province, VIETNAM (14°40'30.6"N, 108°54'13.4"E, 547 m), 19 January 2013, Hoàng Đức Huy, Phạm Mạnh Hùng and Trần Trọng Ngân (Fig. 5). **Paratypes:** An Lão drainage, Bình Định Province, VIETNAM (14°40'30.6"N, 108°54'13.4"E): UNS 2013-19-01, 5 specimens, 104–139 mm SL, 19 January 2013; Re River, Sơn Hà, Quảng Ngãi Province, Vietnam (15°01'03.9"N, 108°31'55.0"E): UF 249109, 5 specimens, 99–150 mm SL, 24 February 2018.

Diagnosis. *Poropuntius anlaensis* is the only species of the genus found on the coastal side of the Annamite Cordillera and nowhere else. It differs from all other species of *Poropuntius* genetically (Fig. 2A), and by having distal margin of dorsal fin distinctly concave (vs straight to slightly concave). It most closely resembles *P. deauratus* but has 29–31 (vs 25–28) lateral-line scales, snout distinctly pointed (vs slightly pointed), and caudal fin light yellow with bold black submarginal stripes (vs bright lemon yellow to dusky with bold to faint black submarginal stripes). *Poropuntius anlaensis* differs from *P. genyognathus*, *P. ham-paloides*, and *P. melanogrammus* in having barbels (vs no barbels); from *P. heterolepidotus* and *P. hathe* in having scales on posterior half of body not markedly smaller (vs markedly smaller) than those on anterior half; from *P. alloioleurus*, *P. burtoni*, *P. carinatus*, *P. huangchuchieni*, *P. kontumensis*, *P. krempfi*, *P. laensis*,

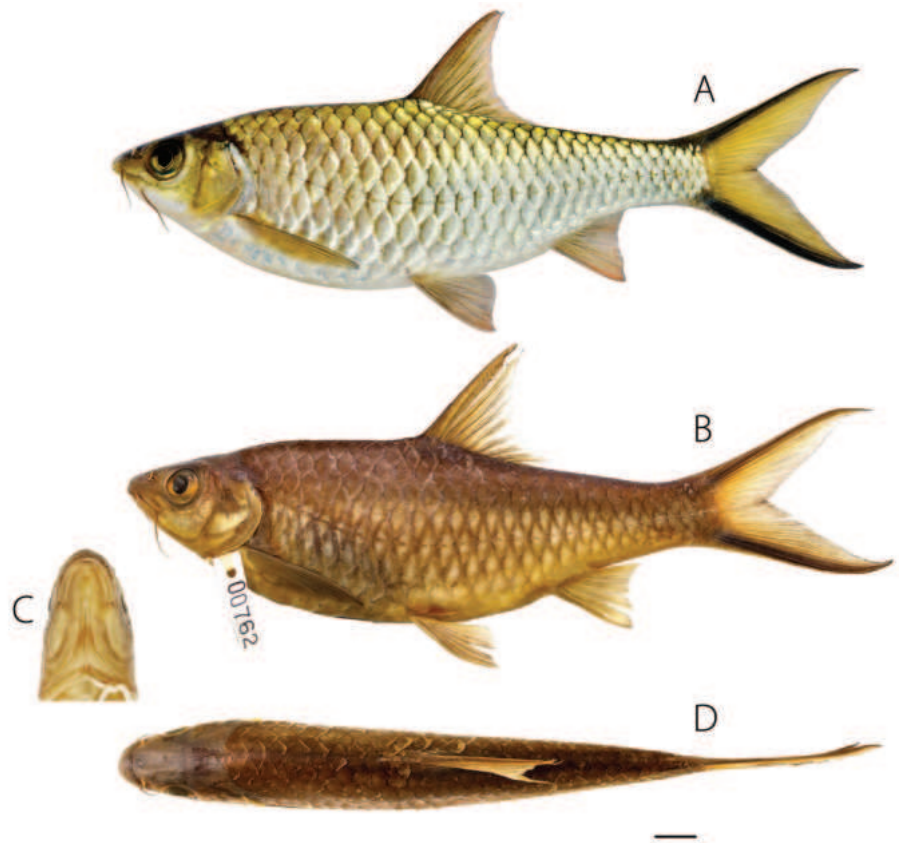


Figure 5. *Poropuntius anlaensis* **A** adult holotype (UNS00762, 139.46 mm SL) in life **B** in preservative **C** ventral view of head **D** dorsal view. Scale bars: 10 mm.

P. opisthoptera, and *P. schanicus* in having 29–31 (vs > 32) lateral-line scales and bold black submarginal stripes (vs no bold black stripes) on caudal fin.

Description. General appearance in Fig. 5; meristic and morphometric data of 11 specimens in Table 3. Head conical, longer than deep, depth 1.2–1.4 × in HL. Snout pointed. Tubercles tiny and few on tip of the snout, many irregular transverse rows of small tubercles reaching front of eyes in male. Mouth subterminal and oblique, extending posteriorly in length slightly longer than eye diameter and broadly horseshoe-shaped (Fig. 5C). Rostral barbel shorter than maxillary barbel, both longer than eye diameter.

Body moderately deep and compressed, depth approximately 2.8–3.3 × in SL. Dorsal body profile convex, slightly convexity from nape with narrow dorsum almost straight in front of dorsal origin to dorsal fin. Base dorsal fin decreasing in height nearly straight dorsal margin of the body, extending from dorsal-fin origin to narrowest part of the caudal peduncle. Ventral profile rounded, rising through anal-fin insertion to caudal-fin base. Caudal peduncle slender, moderately shallow and long, 1.6–2.1 × longer than deep. Anus immediately in front of anal fin. Lateral line complete, 29–31 scales; 10–12 predorsal scales; 5/1/3 scales in transverse row anterior to pelvic-fin origin. Lateral-line tubes extending at least halfway across each scale, with accessory pore on ventral branch on nearly every lateral-line scale. Dorsal iv-8.5, pectoral i-15, pelvic i-8, and anal iii-5.5.

Dorsal fin high and sharply pointed at apex, last unbranched ray longest, followed by first branched ray which is considerably shorter. Last unbranched ray ossified with 18–20 serrae. Posterior extensions of serrae forms straight

Table 3. Morphometric and meristic characters of *Poropuntius anlaensis* sp. nov., n = 11 including holotype.

	<i>Poropuntius anlaensis</i>		
	Holotype UNS00762	Range	Mean ± SD / mode
SL (mm)	139.46	99.2–150.9	118.6 ± 16.4
Morphometrics			
% SL			
Total length	127.6	124.8–129.3	127.1 ± 1.4
Fork length	108.1	107.2–109.7	108.3 ± 0.6
Body depth	31.4	29.9–35.7	31.6 ± 1.5
Body width	13.5	13.5–16.3	14.8 ± 0.7
Head length	24.4	22.4–25.7	24.4 ± 1.2
Caudal peduncle length	22.5	18–23.9	21.1 ± 1.6
Caudal peduncle depth	10.9	10.9–13.4	11.9 ± 0.7
Dorsal-fin base length	15.6	15.6–18.8	16.2 ± 0.9
Dorsal-fin length	25.8	21.4–29.7	25.3 ± 2.1
Anal-fin base length	8.9	8.4–10.5	9.3 ± 0.6
Anal-fin length	16.2	14.8–21.3	16.5 ± 1.8
Pectoral-fin length	22.1	20.2–22.6	21.4 ± 0.8
Pelvic-fin length	18.7	16.8–20.9	18.8 ± 1.1
Predorsal length	48.8	44.5–49.4	48.1 ± 1.2
Prepectoral length	21.3	19.8–23.7	21.6 ± 1
Preanal length	72.2	69.7–75.2	72.5 ± 1.6
Prepelvic length	48.0	46.5–50.8	48.6 ± 1.4
Pelvic-fin base to anal-fin base	22.0	18.8–22.8	21.1 ± 1.1
Pectoral-fin base to pelvic-fin base	25.5	21.3–26.2	23.4 ± 1.6
% HL			
Head depth at nape	84.3	44.5–84.3	76.6 ± 10.7
Head width	56.7	54.8–63.7	58.3 ± 2.5
Snout length	30.8	26.3–35.8	29.5 ± 2.6
Interorbital width	35	32.9–41.9	37.9 ± 2.7
Eye diameter	23.5	23.5–27.3	25.9 ± 1.1
Mouth width	30.8	25.4–33.2	29.6 ± 2.5
Rostral barbel length	38.2	23.1–38.2	30.4 ± 4
Maxillary barbel length	31.4	23.3–39	33.4 ± 4.3
Counts			
Dorsal-fin spines and rays	iv,8.5	iv,8.5	
Anal-fin spines and rays	iii,5.5	iii,5.5	
Pectoral-fin spines and rays	i,15	i,11–16	mode = i,15
Pelvic-fin spines and rays	i,8	i,8	
Lateral-line scales	29	29–31	mode = 30
Transverse scales rows above lateral-line	5.5	5.5	
Transverse scales rows below lateral-line	3.5	3.5	
Circumferential scale rows	20	20–22	mode = 22
Circumpeduncular scale rows	14	14	
Predorsal scales	11	10–12	mode = 10
Scales from end of anal-fin base to caudal-fin origin	8	7–9	mode = 7
Serrae on last simple dorsal-fin ray	24	16–27	mode = 24

line, with base line curved posteriorly. More distal denticles curved along their lengths. Distal margin of fin strongly concave, with posteriormost ray equalling length of third branched ray. Dorsal-fin origin approximately opposite pelvic-fin origin. Dorsal-fin base longer than anal-fin base.

Pectoral fin long, extending to third scale row before pelvic-fin origin.

Pelvic fin not extending to base of last unbranched anal ray. Distal margin concave near tip with falcate apex. Axillary scale present at base of pelvic fin.

Anal fin moderate, distal margin straight when fin is erect.

Caudal fin deeply forked with outer rays nearly 4 × length of middle rays. Upper and lower lobes nearly equal in length with straight distal margin on each lobe.

Colour in life. Head dark greenish golden on top, greenish golden around orbit and on opercula, white on lower jaw. Body primarily silvery but greenish golden on dorsally to lateral line, scale bases with melanophores. All fins except caudal hyaline with pinkish orange tinge on branched rays; fins more darkly pigmented in adults. Caudal fin yellow with bold black submarginal stripes (Fig. 5A).

Colour in preservative. Body including head dark brown on back. Opercula dark at base. Lower half of body light brown. Scale margins lined with brown, forming network. All fins brown to dark brown (Fig. 5B).

Etymology. Specific epithet is in reference to the type locality, the An Lão drainage.

Suggested common name. Cá hồng nhau An Lão (Vietnamese), Anlao brook barb (English).

Distribution. *Poropuntius anlaoensis* is restricted to the southern Annam ecoregion and is possibly endemic to the coastal side of the Annamite Cordillera.

Key to species of *Poropuntius*

- 1 No barbels; black on distal half of dorsal fin **2**
- Maxillary barbels present; black, if present, confined to margin of fin **3**
- 2 Bold black midlateral stripe on body ***P. melanogrammus***
- No black midlateral stripe on body ***P. hampaloides***
- 3 No rostral barbels; maxillary barbels very small (nubs) ***P. genyognathus***
- Rostral and maxillary barbels present **4**
- 4 Scales on posterior half of body markedly smaller than those on anterior **5**
- Scales on posterior half of body not markedly smaller than those on anterior **6**
- 5 Lateral-line scales 39–40; no black submarginal stripes on caudal fin ***P. heterolepidotus***
- Lateral-line scales 33–35; bold black submarginal stripes on caudal fin ***P. hathe***
- 6 Lateral-line scales 35–46; branched lateral-line canals almost absent ***P. alloiopterus***
- Lateral-line scales ≤ 40; branched lateral-line canals present **7**
- 7 No black submarginal stripes on caudal fin **8**
- Black submarginal stripes on caudal fin **10**
- 8 Lateral-line scales 29–31; barbels short and thin, rostral barbel not extending to anterior margin of eye ***P. schanicus***
- Lateral-line scales > 35; barbels well developed, rostral barbel extending to anterior margin of eye **9**

9	Predorsal scales 12–14.....	<i>P. burtoni</i>
–	Predorsal scales 15–16.....	<i>P. opisthoptera</i>
10	Lateral-line scales < 32 or > 32 with caudal fin bright yellow to dusky greenish yellow	11
–	Lateral-line scales > 32 without caudal fin colour as above.....	12
11	Head longer than deep; distal margin of dorsal fin distinctly concave.....	<i>P. anlaoensis</i>
–	Head shorter than deep; distal margin of dorsal fin straight....	<i>P. deauratus</i>
12	Bold black marginal stripes on caudal fin; green-gold to silver scales; orange to orangish yellow caudal fin.....	<i>P. laoensis</i>
–	Dusky grey or brown marginal stripes on caudal fin.....	13
13	Dorsal fin height \geq body depth at dorsal-fin origin	<i>P. carinatus</i>
–	Dorsal fin height < body depth at dorsal-fin origin	14
14	Caudal fin dusky, grey to black.....	<i>P. kremphi</i>
–	Caudal fin orange to yellow-orange at base or very pale yellow	15
15	Silver scales on body; Lower Lancang ecoregion	<i>P. huangchuchieni</i>
–	Orange-bronze scales on body; Kratie-Stung Treng ecoregion	<i>P. kontumensis</i>

Discussion

The objective of this study was to test, using molecular data, the species diversity of *Poropuntius*, especially that of Vietnam in which 15 species names have been recognised recently as valid. As noted above, most species of *Poropuntius* have been described using only morphological data, and recent investigations using molecular data suggested that some morphological hypotheses were incorrect. Our data indicate that 17 names assigned to species are synonyms.

Several factors led to the inflation of species names for *Poropuntius*. These include limited efforts overall in collecting and classifying cyprinid fishes, especially in northern Vietnam, limited access to type specimens in European museums, limited availability of publications (often in foreign languages – although now this is being alleviated by online access), inadequate descriptions containing limited information, and failure to appreciate morphological variation related to trophic diversification within species. Finally, a substantial portion of the cyprinid diversity of northern Vietnam is shared with that of southern China, but researchers in the two countries have not had access to specimens from both countries or to original descriptions in other languages. Consequently, studies were limited to in-country fauna, and species in each country were treated as endemic to that country.

Ecomorphological variation in *Poropuntius* was described and figured by Roberts (1998: figs 6, 8), and Kang et al. (2016) interpreted *P. bolovenensis*, *P. lobocheiloides*, and *P. solitus* as ecomorphs of *P. bolovenensis*. The often-extreme intraspecific phenotypic variation in the shape of the mouth and lips, and in the development of the horny sheath on the lower jaw, has led to taxonomic confusion in *Poropuntius*. Ecophenotypic variation is expressed especially clearly in species occupying pools isolated by barriers such as waterfalls in streams on plateaus at high elevations (e.g., on the Bolaven, Kontum, and Langbiang Plateaus) and in drainages leading to the Gulf of Tonkin (in the Song Hong and Annam ecoregions). Species not exhibiting such extreme polymorphism

may nevertheless carry information in their genomes necessary to generate an array of potentially taxonomically confusing, continuous variation as well as more disjunct phenotypes. For example, the position of the dorsal fin, often used in taxonomic diagnoses, varies from more anteriorly to more posteriorly positioned in *Poropuntius*, as seen in *P. alloiopleurus*, *P. huangchuchieni*, and *P. laoensis* (Wu et al. 2013; this study). Specimens of *Poropuntius* from flowing water habitats are characterised by a more elongated body and a relatively long caudal peduncle, while those from pools have a deeper body and larger unpaired fins (Figs 3A, B, D, E, 4G, H). Similar patterns have been described in other cyprinids, e.g., *Rasbora paviana* and *Lobocheilos rhabdoura*, with populations inhabiting fast-flowing streams having more slender bodies than those inhabiting slower-flowing habitats (Stolbunov et al. 2011; Ciccotto and Page 2016).

During a decade of field work on Southeast Asian freshwater fishes, the first author and colleagues have collected samples of *P. deauratus*, *P. krempfi*, *P. alloiopleurus*, and *P. laoensis* revealing marked intraspecific phenotypic variation. These samples include those from river basins in which few or no fish collections have been made or reported upon previously, and which fill in gaps in the distributions of these species. Pronounced variation among adult individuals in these species has been observed in body depth, dorsal-fin spine length, ossification and serration of the last simple dorsal-fin ray, body colour, and caudal fin colour. For example, in the wide-ranging *P. deauratus*, the typical colour in life is a silvery to light green gold body with bright yellow on the posterior half of the body and a bright lemon-yellow caudal fin with bold black submarginal stripes. However, colour in this species may be much more subtle with the body uniformly dusky to dark and the fins dusky (Fig. 4B, H).

Conclusions

This study has revealed that scientific names have been applied erroneously to populations of *P. krempfi*, *P. alloiopleurus*, *P. huangchuchieni*, *P. laoensis*, *P. kontumensis*, and *P. deauratus*. Errors in the taxonomy of *Poropuntius* have resulted primarily from inadequate sampling and reliance on characters that vary intraspecifically. Additional samples from unsampled or poorly sampled populations allowed the use of molecular data to test previous species hypotheses. More sampling and use of molecular as well as morphological data on species of *Poropuntius* that could not be included in this study are likely to require additional taxonomic changes.

Acknowledgements

Võ Thị Bích Thảo assisted with lab work. Anonymous peer reviewers scrutinised and commented on the manuscript. For all of this assistance we are most grateful.

Additional information

Conflict of interest

The authors have declared that no competing interests exist.

Ethical statement

No ethical statement was reported.

Funding

This research is funded by Vietnam National University HoChiMinh City (VNU-HCM) under grant number GEN2019-18-01, the Rufford Foundation, the “Fondation Total” (fondation.total.com) through the “DECODIV” project and the U.S. National Science Foundation through a Rules of Life award (uROL) (NSF 1839915) and a Planetary Biodiversity Inventory award (NSF-DEB 0315963). Institutional records were searched through iDigBio, funded by the NSF Advancing Digitization of Biodiversity Collections program (NSF-EF 1115210, NSF-DBI 1547229).

Author contributions

DHH worked on conceptualisation and wrote the manuscript; DHH, J-DD, X-YC, and LMP got funds for this research; MHP, J-DD, WL, and JP worked on molecular analysis; DHH, NTT, MHP, LMP, WL and X-YC collected specimens; J-DD, LMP and JP revised the manuscript.

Author ORCIDs

Huy Duc Hoang  <https://orcid.org/0000-0001-6528-193X>

Hung Manh Pham  <https://orcid.org/0000-0003-3186-818X>

Ngan Trong Tran  <https://orcid.org/0000-0001-7254-2835>

Jean-Dominique Durand  <https://orcid.org/0000-0002-0261-0377>

Wu Ling  <https://orcid.org/0009-0001-5700-1616>

John Pfeiffer  <https://orcid.org/0000-0001-5368-0589>

Xiao-Yong Chen  <https://orcid.org/0000-0002-0924-5560>

Lawrence M. Page  <https://orcid.org/0000-0002-8823-0729>

Data availability

Voucher specimens are available as described in the text and sequence data are posted on GenBank.

References

- Abell R, Thieme ML, Revenga C, Bryer M, Kottelat M, Bogutskaya N, Coad B, Mandrak N, Balderas SC, Bussing W, Stiassny MLJ, Skelton P, Allen GR, Unmack P, Naseka A, Ng R, Sindorf N, Robertson J, Armijo E, Higgins JV, Heibel TJ, Wikramanayake E, Olson D, López HL, Reis RE, Lundberg JG, Sabaj Pérez MH, Petry P (2008) Freshwater Ecoregions of the World: A New Map of Biogeographic Units for Freshwater Biodiversity Conservation. *Bioscience* 58(5): 403–414. <https://doi.org/10.1641/B580507>
- Bui QM, Nguyen MAT, von Haeseler A (2013) Ultrafast approximation for phylogenetic bootstrap. *Molecular Biology and Evolution* 30(5): 1188–1195. <https://doi.org/10.1093/molbev/mst024>
- Chernomor O, Von Haeseler A, Bui QM (2016) Terrace Aware Data Structure for Phylogenomic Inference from Supermatrices. *Systematic Biology* 65(6): 997–1008. <https://doi.org/10.1093/sysbio/syw037>
- Ciccotto PJ, Page LM (2016) From 12 to One Species: Variation in *Lobocheilos rhabdoura* (Fowler, 1934) (Cyprinidae: Labeonini). *Copeia* 104(4): 879–889. <https://doi.org/10.1643/CI-16-433>

- Durand JD, Shen KN, Chen WJ, Jamandre BW, Blel H, Diop K, Nirchio M, Garcia de León FJ, Whitfield AK, Chang CW, Borsa P (2012) Systematics of the grey mullets (Teleostei: Mugiliformes: Mugilidae): molecular phylogenetic evidence challenges two centuries of morphology-based taxonomy. *Molecular Phylogenetics and Evolution* 64(1): 73–92. <https://doi.org/10.1016/j.ympev.2012.03.006>
- Edgar RC (2004) MUSCLE: Multiple sequence alignment with high accuracy and high throughput. *Nucleic Acids Research* 32(5): 1792–1797. <https://doi.org/10.1093/nar/gkh340>
- Fricke R, Eschmeyer WN, van der Laan R (2023) Eschmeyer's Catalog of Fishes: Genera, Species, References. <http://researcharchive.calacademy.org/research/ichthyology/catalog/fishcatmain.asp> [accessed 23 February 2023]
- Hoang DH, Pham MH, Nguyen DT, Tran TN, Vo VP (2021a) Geographic Distribution of Indigenous Inland Fishes in Central Coast rivers, Northern Annam. *Technology Journal of Agriculture & Rural Development* 10/2021: 14–30.
- Hoang HD, Pham HM, Tran NT, Nguyen DT, Vo VP (2021b) Geographic Distribution of Indigenous Inland Fishes in Central Coast rivers, Southern Annam. *Geographic Distribution of Indigenous Inland Fishes* 10/2021: 31–46.
- Kalyaanamoorthy S, Bui QM, Wong TKF, Von Haeseler A, Jermini LS (2017) ModelFinder: Fast model selection for accurate phylogenetic estimates. *Nature Methods* 14(6): 587–589. <https://doi.org/10.1038/nmeth.4285>
- Kang D-W, Thamavongseng P, Lee HY, Choi S-H (2016) Fish Fauna in the Bolaven Plateau and Trophic Polymorphism of *Poropuntius bolovenensis* in Laos. *Korean Journal of Environment and Ecology* 30(3): 369–375. <https://doi.org/10.13047/KJEE.2016.30.3.369>
- Kottelat M (2000) Diagnoses of a new genus and 64 new species of fishes from Laos (Teleostei: Cyprinidae, Balitoridae, Bagridae, Syngnathidae, Chaudhuriidae and Tetraodontidae). *Journal of South Asian Natural History* 5: 37–82.
- Kottelat M (2001) *Fishes of Laos*. WHT Publications (Pte) Ltd, Sri Lanka.
- Kottelat M (2013) Xe-Pian Xe-Namnoy Hydroelectric Power Project Environmental Impact Assessment (EIA).
- Kumar S, Stecher G, Tamura K (2016) MEGA7: Molecular Evolutionary Genetics Analysis Version 7.0 for Bigger Datasets. *Molecular Biology and Evolution* 33(7): 1870–1874. <https://doi.org/10.1093/molbev/msw054>
- Mai DY (1978) *Identification of Freshwater Fishes of Northern Viet Nam*. Science & Technics Publishing House [In Vietnamese], Ha Noi, 339 pp.
- Muhammad-Rasul AH, Ramli R, Low VLUN, Ahmad A, Grudpan C, Koolkalya S, Khaironizam MDZ (2018) Taxonomic revision of the genus *Poropuntius* (teleostei: Cyprinidae) in Peninsular Malaysia. *Zootaxa* 4472(2): 327–342. <https://doi.org/10.11646/zootaxa.4472.2.6>
- Nguyen HD (1997) Cá sao, một loài mới thuộc giống *Lissochilus* Weber et de Beaufort, 1916 (Osteichthyes, Cyprinidae, Barbinae) được tìm thấy ở Việt Nam. *Journal of Biology* 19: 1–4.
- Nguyễn HV, Ngô VS (2001) *Freshwater Fishes of Vietnam*. Vol. 1. Family Cyprinidae. Agriculture Publish House, Ha Noi, 622 pp.
- Nguyen LT, Schmidt HA, Von Haeseler A, Minh BQ (2015) IQ-TREE: A fast and effective stochastic algorithm for estimating maximum-likelihood phylogenies. *Molecular Biology and Evolution* 32(1): 268–274. <https://doi.org/10.1093/molbev/msu300>
- Nijssen H, van Tuijl L, Isbrücker IJH (1993) Revised catalogue of the type specimens of recent fishes in the Institute of Taxonomic Zoology (Zoologisch Museum), University

- of Amsterdam, the Netherlands. Bulletin Zoölogisch Museum Universiteit van Amsterdam 13(18): 211–260.
- Rainboth WJ (1996) The taxonomy, systematics and zoogeography of *Hypsibarbus*, a new genus of large barbs (Pices, Cyprinidae) from the rivers of southeastern Asia. University of California publications in zoology, California, USA, 129 pp.
- Rendahl H (1920) Eine neue *Barbus*-Art aus Siam. Arkiv för Zoologi 12: 1–3. <https://doi.org/10.5962/bhl.part.791>
- Roberts TR (1998) Review of the tropical Asian cyprinid fish genus *Poropuntius*, with descriptions of new species and trophic morphs. The Natural History Bulletin of the Siam Society 46: 105–135.
- Smith HM (1931) Descriptions of new genera and species of Siamese fishes. Proceedings of the United States National Museum. <https://doi.org/10.5479/si.00963801.79-2873.1>
- Song X, Tang W, Zhang Y (2017) Freshwater fish fauna and zoogeographical divisions in the Wuyi-Xianxialing Mountains of eastern China. Shengwu Duoyangxing 25(12): 1331–1338. <https://doi.org/10.17520/biods.2017207>
- Stolbunov IA, Nguyen THT, Pavlov DS (2011) Morphological and behavioral variation of *Rasbora paviei* (Cyprinidae, Cypriniformes) from lotic and limnic habitats (Central Vietnam). Journal of Ichthyology 51(4): 352–357. <https://doi.org/10.1134/S003294521102010X>
- Stout CC, Tan M, Lemmon AR, Lemmon EM, Armbruster JW (2016) Resolving Cypriniformes relationships using an anchored enrichment approach. BMC Evolutionary Biology 16(1): 1–13. <https://doi.org/10.1186/s12862-016-0819-5>
- Trifinopoulos J, Nguyen L-T, von Haeseler A, Bui QM (2016) W-IQ-TREE: A fast online phylogenetic tool for maximum likelihood analysis. Nucleic Acids Research 44(W1): W232–W235. <https://doi.org/10.1093/nar/gkw256>
- Wang X, Gan X, Li J, Chen Y, He S (2016) Cyprininae phylogeny revealed independent origins of the Tibetan Plateau endemic polyploid cyprinids and their diversifications related to the Neogene uplift of the plateau. Science China. Life Sciences 59(11): 1149–1165. <https://doi.org/10.1007/s11427-016-0007-7>
- Ward RD, Zemlak TS, Innes BH, Last PR, Hebert PDN (2005) DNA barcoding Australia's fish species. Philosophical Transactions of the Royal Society of London. Series B, Biological Sciences 360(1462): 1847–1857. <https://doi.org/10.1098/rstb.2005.1716>
- Wu HW, Lin RD, Chen JX, Chen XL, He MQ (1977) Barbinae. In: Wu HW (Ed.) The cyprinid fishes of China. People's Press, Shanghai, 229–394.
- Wu X, Luo J, Huang S, Chen Z, Xiao H, Zhang Y (2013) Molecular phylogeography and evolutionary history of *Poropuntius huangchuchieni* (Cyprinidae) in Southwest China. PLoS One 8(11): e79975. <https://doi.org/10.1371/journal.pone.0079975>
- Yang L, Sado T, Vincent Hirt M, Pasco-Viel E, Arunachalam M, Li J, Wang X, Freyhof J, Saitoh K, Simons AM, Miya M, He S, Mayden RL (2015) Phylogeny and polyploidy: Resolving the classification of cyprinine fishes (Teleostei: Cypriniformes). Molecular Phylogenetics and Evolution 85: 97–116. <https://doi.org/10.1016/j.ympev.2015.01.014>
- Zheng LP, Yang JX, Chen XY (2016) Molecular phylogeny and systematics of the Barbinae (Teleostei: Cyprinidae) in China inferred from mitochondrial DNA sequences. Biochemical Systematics and Ecology 68: 250–259. <https://doi.org/10.1016/j.bse.2016.07.012>

Supplementary material 1

Samples included in the molecular analysis, with GenBank accession numbers

Authors: Huy Duc Hoang, Hung Manh Pham, Ngan Trong Tran, Jean-Dominique Durand, Wu Ling, John Pfeiffer, Xiao-Yong Chen, Lawrence M. Page

Data type: xlsx

Explanation note: **table S1**. Samples included in the molecular analysis, with GenBank accession numbers for Cytochrome oxidase c subunit 1 (COI) and Cytochrome *b* (Cytb) sequence data.

Copyright notice: This dataset is made available under the Open Database License (<http://opendatacommons.org/licenses/odbl/1.0/>). The Open Database License (ODbL) is a license agreement intended to allow users to freely share, modify, and use this Dataset while maintaining this same freedom for others, provided that the original source and author(s) are credited.

Link: <https://doi.org/10.3897/zookeys.1204.120873.suppl1>

A new species of the genus *Yoldiella* (Bivalvia, Protobranchia, Yoldiidae) from Haima Cold Seep, South China Sea, China

Qi Gao^{1,2}, Yan Tang², Junlong Zhang^{2,3,4}

¹ School of Life Sciences, Qingdao Agricultural University, Qingdao 266109, China

² Laboratory of Marine Organism Taxonomy and Phylogeny, Qingdao Key Laboratory of Marine Biodiversity and Conservation, Institute of Oceanology, Chinese Academy of Sciences, Qingdao 266071, China

³ Marine Biological Museum, Chinese Academy of Sciences, Qingdao 266071, China

⁴ University of Chinese Academy of Sciences, Beijing 100049, China

Corresponding author: Junlong Zhang (zhangjl@qdio.ac.cn)

Abstract

In present study, a previously unidentified but frequently encountered species of deep-sea protobranch, *Yoldiella haimaensis* **sp. nov.**, is described new to science from the Haima Cold Seep on the northwestern slope of the South China Sea. A morphological analysis confirmed that this species belongs to a previously undescribed species of the genus *Yoldiella* A.E. Verrill & K.J. Bush, 1897. It differs morphologically from other known species within the genus in its shell shape, degree of inflation, beaks, and number of hinge teeth. Furthermore, we sequenced three gene segments of *Y. haimaensis* **sp. nov.**, comprising a nuclear ribosomal gene (18S rRNA), a nuclear protein-coding gene (histone H3), and a mitochondrial gene (cytochrome c oxidase subunit I, COI). Our phylogenetic analysis performed on the superfamily Nuculanoidea and family Yoldiidae indicates that the genus *Yoldiella* is non-monophyletic, and the widely recognized families within the superfamily Nuculanoidea are also not monophyletic. Our results provide molecular insights into the Protobranchia and highlight the necessity for further samples and data to revise the classification of families and genera within the superfamily using an integrative approach that combines morphological analysis and molecular data.

Key words: Anatomy, chemosynthetic ecosystems, deep-sea, molecular analysis, morphology



Academic editor: Andrew Davinack

Received: 17 February 2024

Accepted: 8 May 2024

Published: 6 June 2024

ZooBank: <https://zoobank.org/26E3E1D9-8571-454A-A8B6-773C92BFF30F>

Citation: Gao Q, Tang Y, Zhang J (2024) A new species of the genus *Yoldiella* (Bivalvia, Protobranchia, Yoldiidae) from Haima Cold Seep, South China Sea, China. ZooKeys 1204: 223–240. <https://doi.org/10.3897/zookeys.1204.121088>

Copyright: © Qi Gao et al.

This is an open access article distributed under terms of the Creative Commons Attribution License (Attribution 4.0 International – CC BY 4.0).

Introduction

Protobranchia, with a significant evolutionary history dating back to the Cambrian, represents an ancestral and basal group of Bivalvia. The protobranchs are primarily found in the subtidal zone, especially in the deep sea, and are generally deposit feeders that bury themselves in the soft sediment (Allen 1978). They have limited presence in the intertidal zone. So, it is difficult to collect specimens of this group (Xu 1999). The highly conserved and distinctive morphology and anatomy, including gill structure, hinge conformation, shell microstructure, as well as the pericalymma larval development, small in size and lifestyle of the group make it a difficult but fascinating taxon of Bivalvia

(Zardus 2002). The simplicity in the form of protobranch bivalves veils the complexity of their phylogeny. The monophyly of Protobranchia has been discussed intensively and become a subject of controversy due to the extensive use of molecular methods (Smith et al. 2011; Sharma et al. 2012; Bieler et al. 2014; González et al. 2015; Combosch et al. 2017; Lemer et al. 2019). Phylogenetic analyses using four nuclear genes (Sharma et al. 2012) and an exemplar-based approach combining Sanger-based sequences and an extensive morphological data matrix (Bieler et al. 2014), as well as the phylogenomic analysis using genomes and transcriptomes (González et al. 2015), recovered the monophyly of Protobranchia. However, the subsequent analysis by Combosch et al. (2017), which utilized five genes and included more taxa, supported the polyphyly of Protobranchia. The latest research has divided Protobranchia into three orders and five superfamilies: Nuculanoidea and Sareptoidea in Nuculanida, Solemyoidea and Manzanelloidea in Solemyida, and Nuculoidea in the order Nuculida (Sharma et al. 2013; Sato et al. 2020). The reconstruction of the phylogeny has indicated that eight families (i.e. Nuculanidae, Bathyspinulidae, Malletiidae, Neilonellidae, Phaseolidae, Siliculidae, Tindariidae, and Yoldiidae) within the superfamily Nuculanoidea are all non-monophyletic (Sato et al. 2020). Shell microstructure of protobranchs play a crucial role in their classification at the superfamily level. Moreover, subtle differences in shell microstructure can aid in distinguishing similar species (Sato et al. 2020). Extensive research has revealed a multitude of unknown or cryptic protobranch species awaiting description and classification under the integrative taxonomy framework (e.g. Neulinger et al. 2006; Zardus et al. 2006). Additional samples and data are required to revise the families and genera within the superfamily Nuculanoidea through a combination of morphological diagnosis and molecular analysis.

Cold seeps are natural phenomena widely distributed across the globe. On the seafloor of these areas, the hydrocarbon-rich fluids and gases leak from cracks and enter the water column through sediment, forming a distinctive habitat (Dong et al. 2021). In March 2015, a newly active cold seep was discovered using the *Haima* remotely operated vehicle (ROV) on the northwestern slope of the South China Sea (SCS) (Zhao et al. 2020). Dong et al. (2021) documented 34 epibenthic macrofauna species collected from Haima Cold Seep with 24 species being identified. Yao et al. (2022) identified 12 macrobenthic species from five phyla and 12 families in the Haima Cold Seep, including two species first found in this location. Seven phyla, 14 classes, and 65 species were identified by He et al. (2023) in this cold seep. To date, more than 80 species of macrobenthic organisms have been collected from the Haima cold seeps (Wang et al. 2022).

This study presents the description of a new *Yoldiella* species, *Y. haimaensis* sp. nov., from the Haima Cold Seep in the SCS. This species had been identified as *Malletia* sp. or *Yoldiella* sp. (Dong et al. 2021; Ke et al. 2022; He et al. 2023). Additionally, we provide the sequences of three gene segments of the new species, including a nuclear ribosomal gene (18S rRNA), a nuclear protein-coding gene (histone H3), and a mitochondrial gene (cytochrome c oxidase subunit 1, COI). A phylogenetic analysis was conducted on the superfamily Nuculanoidea and family Yoldiidae, providing molecular data for the study of Protobranchia and enhancing understanding of macrobenthos at the Haima Cold Seep.

Materials and methods

Specimen collection and identification

The specimens were collected on July 4–12, 2022 from the Haima Cold Seep at a water depth of 1390 m in the SCS (16°43'N, 110°28'E) (Fig. 1) using the ROV and TV Grab of Research Vessel *Kexue*. All specimens were fixed in 100% ethanol and deposited at the Marine Biological Museum (MBM), Chinese Academy of Sciences, Qingdao, China.

DNA extraction, amplification, and sequencing

Two specimens with tissues were randomly selected from the specimens collected. DNA was extracted from the muscle tissues using the TIANamp Marine Animals DNA Kit. Three gene fragments were amplified, including a nuclear ribosomal gene (18S rRNA), a nuclear protein-coding gene (histone H3), and a mitochondrial gene (cytochrome c oxidase subunit 1, COI), which were subsequently utilized for phylogenetic analyses. The PCR program for the mitochondrial genes was as follows: initial denaturation for 180 s at 94 °C, followed by 35 cycles of denaturation for 30 s at 94 °C, annealing for 45 s at 46 °C and elongation for 60 s at 72 °C. The final elongation step was conducted for 10 min at 72 °C. The PCR conditions for the 18S rRNA and H3 genes were performed the same as above, with the only difference being in the annealing step. The annealing temperature for H3 was 55 °C,

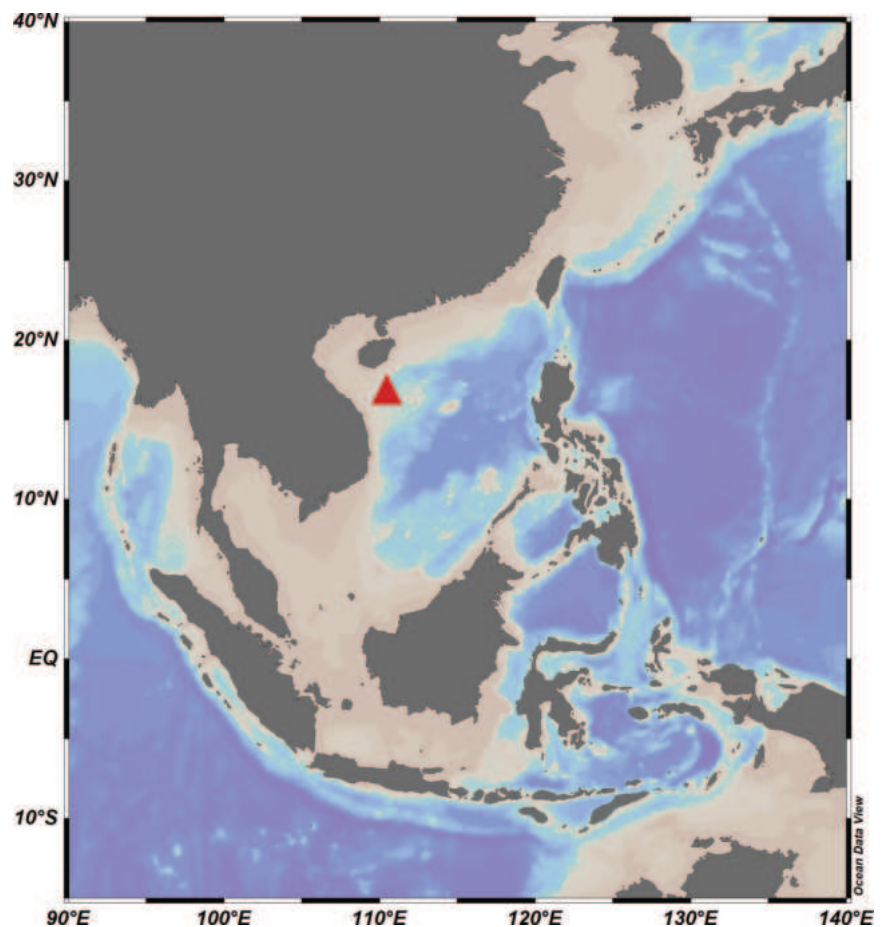


Figure 1. Map of samples site (triangle) of *Yoldiella haimaensis* sp. nov.

and the annealing step for 18S rRNA was performed in a touch-down manner (Don et al. 1991) with an initial annealing temperature of 70 °C followed by a reduction of 1 °C per cycle until 65 °C. The primer sequences are listed in Suppl. material 1.

The PCR products were separated by electrophoresis using 1.0% agarose gels, purified, and then sent for sequencing to Sangon Biotech Co. Ltd.

Phylogenetic analyses

The sequences newly acquired in this study and obtained from NCBI are listed in Suppl. materials 2, 3. All sequences were aligned using MAFFT v. 7 software (Kato and Standley 2013) based on the amino acid sequences and employing the Auto and G-INS-I algorithms. Subsequently, the aligned sequences in each dataset were manually trimmed to the same length. Ambiguously aligned sites in the ribosomal gene were removed using GBLOCKS v. 0.91b (Castresana 2000) with the least stringent settings. Because of the limited molecular data of Protobranchia, different combined gene datasets were used for phylogenetic analyses of the family Yoldiidae and superfamily Nuculanoidea. The final dataset for Yoldiidae phylogenetic trees comprised 1059 bp of 18S rRNA (88% of 1192 bp before Gblock), and 594 bp of COI. The final dataset for Nuculanoidea phylogenetic trees included 1101 bp of 18S rRNA (81% of 1352 bp before Gblock), 588 bp of COI, and 305 bp of H3. The COI, 18S rRNA, and H3 gene sequences from the same individuals were concatenated using SequenceMatrix software (Vaidya et al. 2011) to form a combined gene dataset. The Maximum likelihood (ML) and Bayesian inference (BI) analysis based on concatenated datasets of COI and 18S rRNA were used for phylogenetic analyses. The ML tree was conducted using IQ-TREE v. 2.2.0-Linux (Nguyen et al. 2015). The most suitable evolution model was found by ModelFinder (Kalyaanamoorthy et al. 2017) and adopted automatically to infer the ML tree. Bootstrap supports (BS) were calculated with 1,000 replicates to assess branch supports. Gene partition models chosen for IQ-TREE were 18S rRNA, K2P+I; COI, TIM+F+I+G4; and combined gene, TIM3+F+I+G4. jModelTest v. 2.1.10 (Darriba et al. 2012) was used to evaluate the best-fitting nucleotide substitution model and derive the optimal model of the Bayesian phylogenetic tree. According to the Akaike information criterion (AIC), the best model for each isolated gene was 18S rRNA, HKY+I; COI, GTR+I+G; and combined gene, HKY+I+G. A Bayesian-inference (BI) analysis was performed using MrBayes v. 3.2.6 (Sharma et al. 2013) and the best model of each dataset. The posterior probability (PP) was estimated using four chains running 1 million generations and sampled every 100 generations. The first 25% of sampled trees were discarded as burn-in. The results of ML and BI trees were visualized and rendered using Figtree v. 1.4.4 (<http://tree.bio.ed.ac.uk/software/figtree/>).

Species delimitation

A variety of species delimitation methods were employed to determine that the species described here is not conspecific with another, already known species of Yoldiidae. COI data were analyzed using the program Automated Barcode Gap Discovery (ABGD; Puillandre et al. 2012) and Assemble Species by Automatic Partitioning (ASAP; Puillandre et al. 2021), a method to build species partitions from single-locus sequence alignments. Single gene trees were ana-

lyzed by applying the Bayesian implementation of the Poisson Tree Processes model (bPTP; Zhang et al. 2013) at the web server of the Heidelberg Institute for Theoretical Studies, Germany (<http://species.h-its.org/>).

Results

Systematics

Subclass Protobranchia Pelseneer, 1889

Order Nuculanida J.G. Carter, D.C. Campbell & M.R. Campbell, 2000

Superfamily Nuculanoidea H. Adams & A. Adams, 1858 (1854)

Family Yoldiidae Dall, 1908

Genus *Yoldiella* A.E. Verrill & K.J. Bush, 1897

Type species. *Yoldiella lucida* (Lovén, 1846) (International Commission on Zoological Nomenclature 1985: Opinion 1306) by original designation (Recent, North Atlantic).

***Yoldiella haimaensis* sp. nov.**

<https://zoobank.org/CCA23CFC-0081-4096-BD4C-98ACEB76DD8F>

Figs 2–4

Malletia sp.: Dong et al. 2021: 4, fig. 5b; Ke et al. 2022: 4, fig. 2h.

Yoldiella sp.: He et al. 2023: 6, fig. 2Q.

Type specimens. Holotype: MBM 229041: length 7.5 mm, width 3.2, height 5.1 mm. Paratypes: MBM 229042: length 7.4 mm, width 3.3 mm, height 5.0 mm; MBM 229043: length 6.5 mm, width 2.6 mm, height 4.4 mm; MBM229044: length 6.3 mm, width 2.5 mm, height 4.1 mm; MBM229045: length 7.6 mm, width 3.0 mm, height 4.9 mm.

Type locality. Haima Cold Seep (depth 1390 m, 16°43.00'N, 110°28.00'E), off southern Hainan Island, South China Sea.

Diagnosis. *Yoldiella haimaensis* sp. nov. differs morphologically from other known species within the genus in shell shape, degree of inflation, beaks, and number of hinge teeth. Diagnostic characteristics: shell small, ovate, inflated medially. Posterior end slight produced. Resilifer triangular, projecting. Beak rather lower than other species, suborthogyrate, and easily worn. Hinge plate narrow; posterior hinge plate smaller than anterior one, with taxodont teeth in two series; 17–19 anterior and 15–16 posterior teeth on hinge plate.

Description. Shell small, elongate, ovate in outline, moderately inflated, opaque, fragile, 2.2–8.2 mm long, W/L about 0.40; H/L about 0.66, usually subequivalve, inequilateral. Shell surface smooth, with numerous very fine, regular, and nearly isometric growth lines, without radial stria. Periostracum light brown and flaky. Umbo slightly posterior to middle, low, large, obscure, opisthogyrate, and easily worn. Antero-dorsal margin convex; anterior end broadly rounded, merging smoothly to ventral margin. Ventral margin slightly convex, with very shallow sinus at postero-ventral corner. Postero-dorsal margin oblique and

then convex, descending to blunt posterior margin. Posterior end slight produced. Escutcheon and lunule obscure. ligament amphidetic, thin, short.

Internal surface porcelaneous white. Hinge plate moderately broad, narrow below umbo, moderately long, and rather strong, with two chevron-shaped columns and moderately sized taxodont lateral teeth, about 17–19 anterior teeth, about 15–16 posterior teeth, interrupted by a triangular, projecting resilifer, and not extend beyond the inner limit of adductor muscles. Angle of about 140° between anterior and posterior hinge plates. Posterior hinge plate usually smaller than anterior. Resilium oblique and often obscure in dry preserved specimens. Adductor scar obscure to evident; triangular anterior adductor scar larger than droplet-shaped posterior adductor scar. Pallial sinus obsolete; pallial line usually entire.

Mantle large, thin, and opaque; anterior adductor crescent-shaped, twice or three times size of posterior. Ctenidium structure simple and lamellar, at posterior side parallel to the postero-dorsal shell margin. Labial palp size moderate, consisting of flat, paired lamellae on each side, with appendages of elongated palp proboscis. Foot muscular and large, with a regular series of nearly rectangular protrusions at margins, partially covered by labial palp. Siphons combined posteriorly.

Etymology. The species epithet "*haimaensis*" is Latin and means "from Haima", which refers to the name of the cold seep where the specimens were collected.

Distribution. Currently known only from the Haima Cold Seep on the north-western slope of the South China Sea.

Remarks. *Yoldiella haimaensis* sp. nov. differs morphologically from other known species of *Yoldiella* in its shell shape, degree of inflation, beak characteristics, and number of hinge teeth. Its beaks are lower than those of other species, suborthogyrate, and prone to wearing easily. This new species resembles the type species of *Yoldiella*, *Y. lucida*. However, *Y. haimaensis* sp. nov.

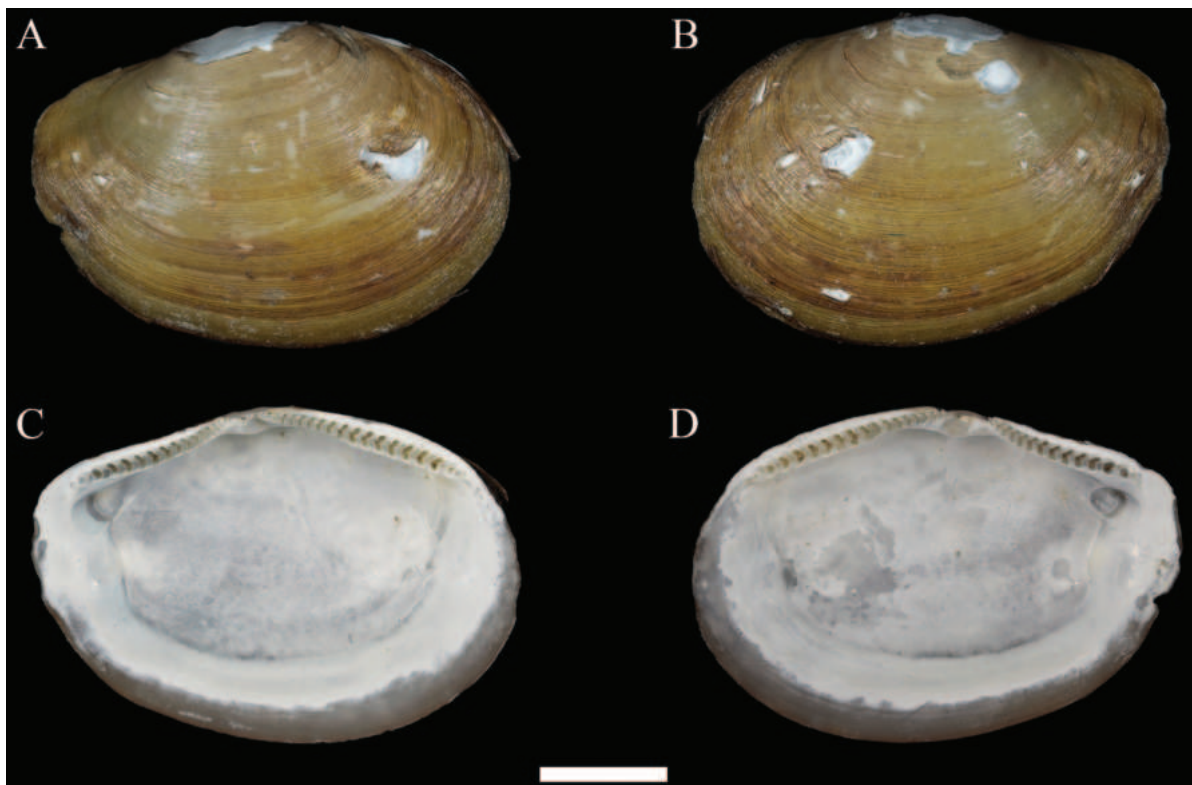


Figure 2. *Yoldiella haimaensis* sp. nov. A–D holotype, MBM229041. Scale bar: 2 mm (all at the same scale).

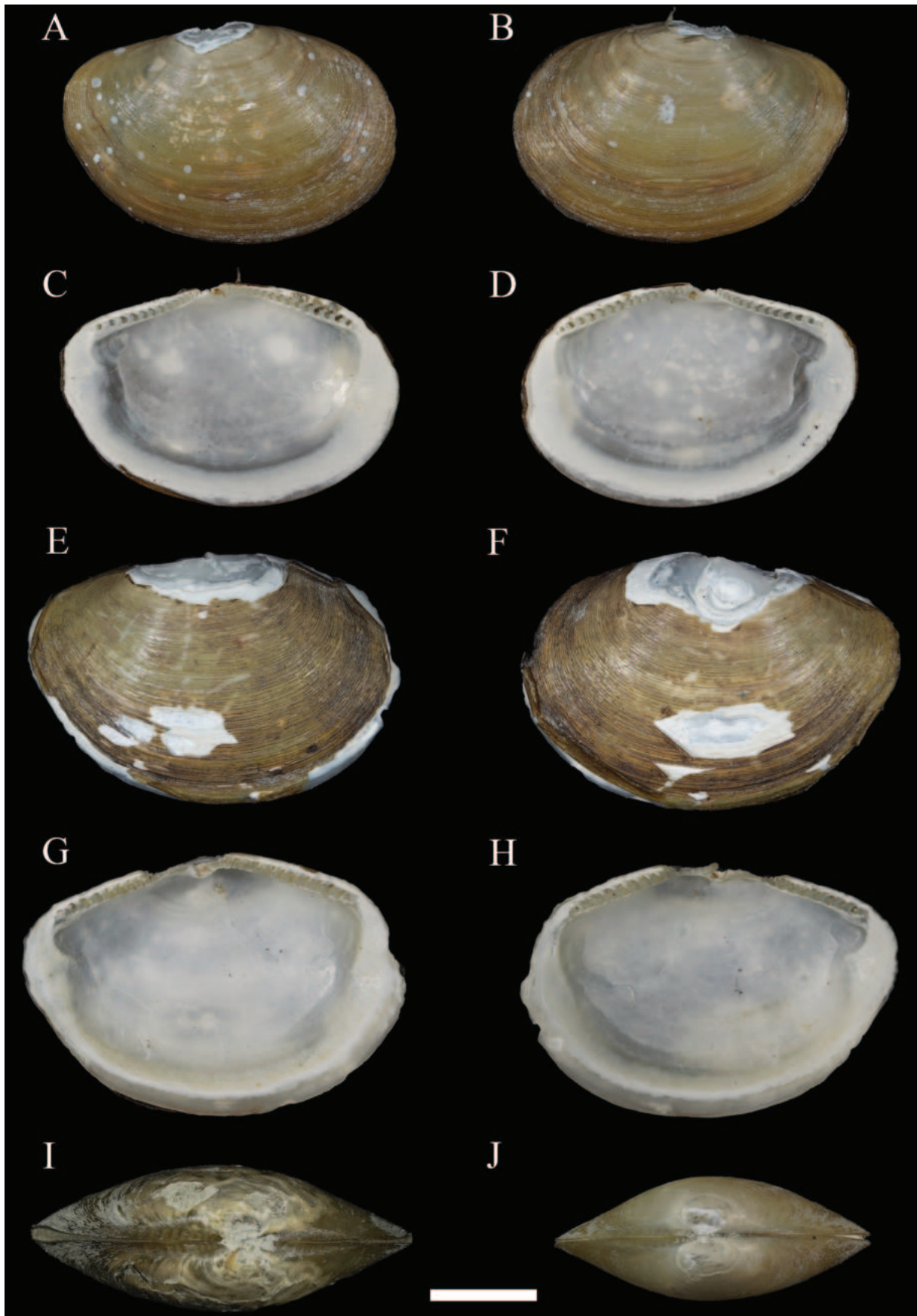


Figure 3. *Yoldiella haimaensis* sp. nov. **A–D** paratype 1, MBM229042 **E–H** paratype 2, MBM229043 **I** paratype 3, MBM229044 **J** paratype 4 MBM229045. Scale bar: 2 mm (all at the same scale).

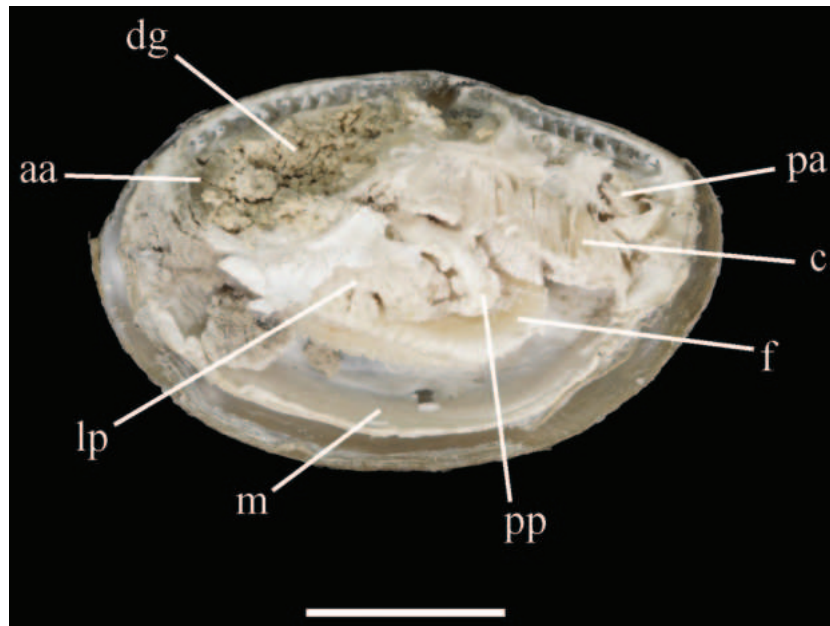


Figure 4. Anatomy features of *Yoldiella haimaensis* sp. nov. **aa**, anterior adductor; **c**, ctenidium; **f**, foot; **lp**, labial palp; **m**, mantle; **pa**, posterior adductor; **pp**, Palp proboscis; **dg**, digestive gland. Scale bar: 2 mm.

differs from *Y. lucida* in having lower, suborthogyrate beaks that wear easily and a slightly rounded posterior end. *Yoldiella haimaensis* sp. nov. has more teeth (17–19 anterior teeth, 15–16 posterior teeth) than *Y. lucida* (8 teeth on each end), with more anterior teeth than posterior teeth. Another species closely resembling *Y. haimaensis* sp. nov. in outline is *Yoldiella sagamiana* T. Okutani & K. Fujikura, 2022 from Sagami Bay, but *Y. sagamiana* has a larger W/L ratio and fewer teeth (15 anterior teeth, 10 posterior teeth) than the new species, and *Y. sagamiana* also has more pointed beaks and finer commarginal cords and lines. The outline of the new species is similar to *Yoldiella biguttata* Allen, H. L. Sanders & F. Hannah, 1995 from the Guyana Basin, but *Y. biguttata* has the more prominent umbo and the anterior and posterior series are either equal or with the anterior series having one additional tooth (5–6 in the largest specimen).

Species delimitation

Our species delimitation using the ABGD, ASAP, and bPTP methods show slightly different results, but they all support that our two samples are the same new species, and distinct from others in the family Yoldiidae (Fig. 5). ABGD and bPTP delineated the data into 19 species, while ASAP delineated the data into 12 species. ASAP grouped *Yoldiella nana* (M. Sars, 1865), *Yoldiella frigida* (Torrell, 1859), *Yoldiella inconspicua* A.E. Verrill & K.J. Bush, 1898, and *Yoldiella orcia* (Dall, 1916) into one species; ASAP and bPTP grouped *Yoldiella philippiana* (Nyst, 1845) and *Yoldiella propinqua* (Leche, 1878), which clustered together, into one species; ABGD and bPTP grouped *Yoldia* sp. and *Yoldia scissurata* Dall, 1897 into one species; ABGD grouped *Yoldia notabilis* Yokoyama, 1922 and *Yoldia johanni* Dall, 1925 into one species; bPTP delineated two species for the two individuals of *Y. notabilis*; ASAP grouped *Yoldia hyperborea* (A. Gould, 1841), *Yoldia* sp., *Y. scissurata*, *Y. notabilis*, and *Y. johanni* into one species; ABGD delineated two species for the seven individuals of *Portlandia arctica* (Gray, 1824).

Y. inconspicua and *Y. orcia*. In addition, the COI analysis revealed that species of the genus *Yoldia* Møller, 1842 were nested among species of *Yoldiella*. Conversely, in the phylogenetic analysis constructed using 18S rRNA, *Yoldia* clustered as a distinct branch. The phylogenetic status of *Y. haimaensis* sp. nov. was different owing to the incongruent results of separate molecular analyses. The phylogenetic analysis based on COI showed that the new species was positioned at the base of the clade including species of *Yoldia* (Fig. 5), while it was at the basal position of the clade containing all *Yoldiella*, *Yoldia*, and *Megayoldia* species in the 18S rRNA phylogenetic tree with low support values (Fig. 6).

Phylogenetic analysis constructed using a combined gene dataset (COI+18S+H3) did not improve resolution as more taxa were added within the superfamily Nuculanoidea (Suppl. materials 4, 5). The BI and ML analyses recovered different topologies, and most nodes at high levels received very low support values. Furthermore, the results indicate that the family Yoldiidae is non-monophyletic, and that none of the widely recognized families (Nuculaniidae, Neilonellidae, Malletiidae, Siliculidae, Phaseolidae, Tindariidae, and Bathyspinulidae) form monophyletic groups in this reconstruction.

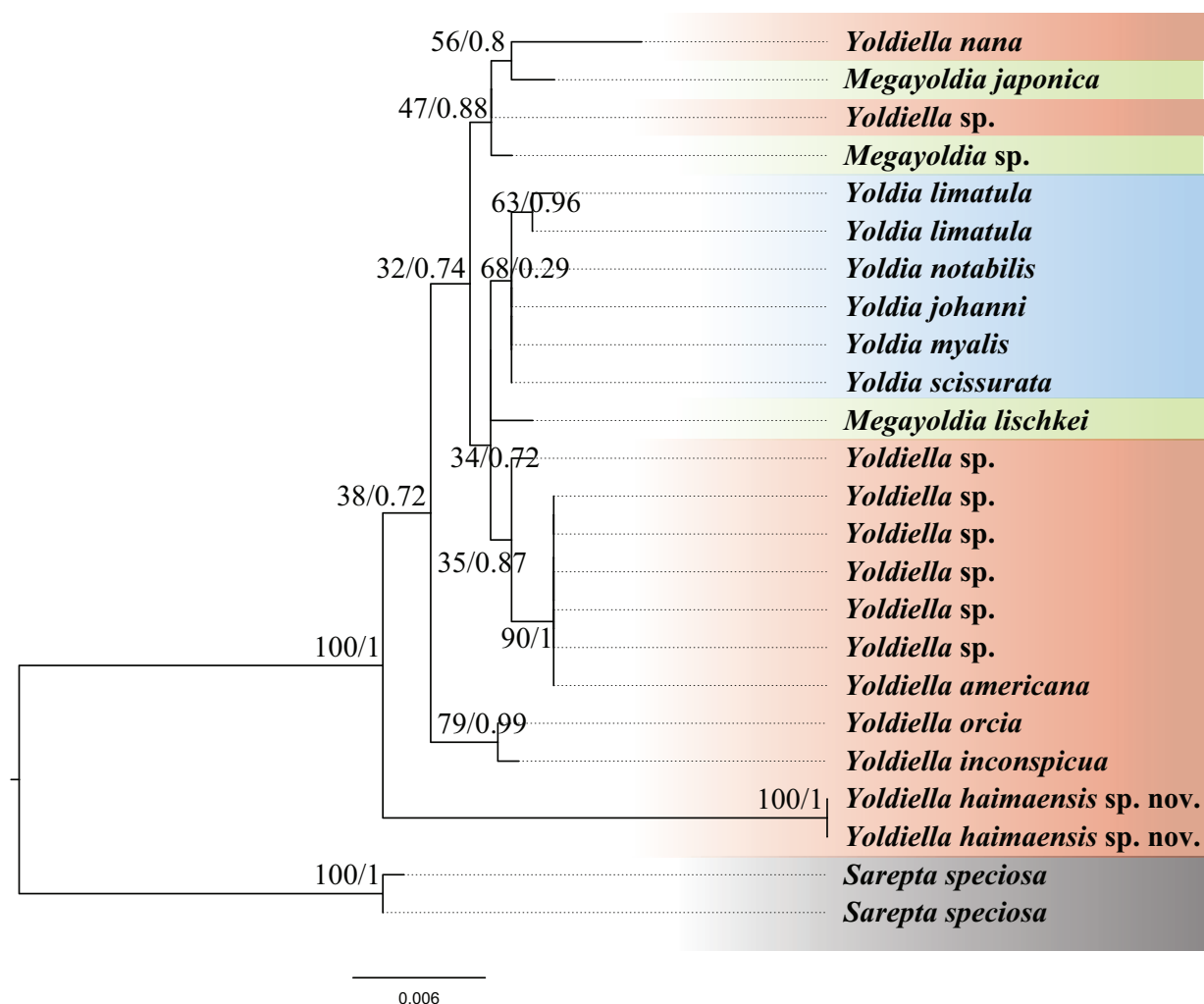


Figure 6. Phylogenetic tree inferred by Bayesian inference (BI) and maximum likelihood (ML) based on 18S rRNA gene. Numbers adjacent to nodes refer to ML bootstrap scores and BI posterior probability (left, and right, respectively).

Discussion

The genus *Yoldiella* is believed to be ubiquitous in all the world's oceans, with a particularly high abundance in deep waters (Benaim and Absalão 2011a). Environmental differences are likely to have a significant impact on the weight of their shell and the rate of their growth (Reed et al. 2013). However, their small size and offshore habitat contribute to their rarity in collections. Prior to this study, no species of this genus had been identified in the South China Sea. The discovery of *Y. haimaensis* sp. nov. bridges this geographical gap. In fact, this new species has been encountered more than once during the investigation and research on cold-seep fauna in the South China Sea, but in these studies, it has been misidentified as *Malletia* sp. or as *Yoldiella* not to species (Dong et al. 2021; Ke et al. 2022; He et al. 2023). The detailed description of *Y. haimaensis* sp. nov. contributes to the understanding of macrobenthos in the Haima Cold Seep.

Yoldiella is a difficult taxon to define because the morphological differences within this genus are mostly subtle and there are many closely related species. This genus was established by Verrill and Bush (1897), and it is usually characterized by ovate or wedge-shaped shells, which always have a slight postero-ventral sinuosity. The internal cartilage is often relatively large and occupies a simple notch. The external ligament is weak, and the pallial sinus is usually indistinct. Since then, its classification and composition have been controversial. Allen and Hannah (1986) and Allen et al. (1995) redefined the genus *Yoldiella* considering shell shape, hinge morphology, musculature, and the extent and course taken by the hindgut, which have been widely accepted by researchers. The redescription of *Yoldiella* by Coan and Valentich Scott (2012) limited it to forms having an elongate, amphidetic ligament with an internal section, an obscure or absent escutcheon and lunule, and a small pallial sinus.

It is widely acknowledged that soft-tissue analysis plays a crucial role in contemporary malacology. However, there is a significant lack of detailed morphological descriptions for this taxon. Yonge and Calman (1939) presented a comprehensive summary of the anatomical characteristics of Protobranchia. Purchon (1956) surveyed the structure and function of the stomach throughout the Protobranchia to establish evidence for phylogenetic relationships between the families and orders within the subclass. Xu (1999) highlighted a significant distinction in the anatomical features of Protobranchia compared to other bivalves, emphasizing the muscular nature of their feet for crawling. The ctenidium assumes a lamellar shape primarily for respiratory purposes, while the well-developed labial palp functions as a distinct feeding organ. Okutani and Fujiwara (2005) illustrated the soft part of *Yoldiella kaikonis* Okutani & Fujiwara, 2005. Reed et al. (2014) described and deliberated on the gonad morphology and oocyte size of four species of *Yoldiella*. Yonge and Calman (1939) and Allen et al. (1995) provided detailed accounts of the anatomical characteristics of *Y. lucida*, the type species of *Yoldiella*, noting that the organs in this species are more compactly arranged due to its relatively shorter shell, which exhibits a greatly abbreviated posterior rostrum. The labial palps are moderately large and extended, with well-developed, long, and muscular palp proboscides. The foot is relatively larger, as are the ctenidia, the filaments of which are broader and deeper. The shell and anatomical features of the new species align with the aforementioned characteristics of *Y. lucida*.

The genus *Yoldiella* may encompass species from other genera due to its small size and the potential for confusion with immature specimens. La Perna (2004) observed that, based on the traditional description at the time, *Yoldiella* was regarded as a provisional “pigeon-hole”, where numerous species were temporarily allocated in a kind of waiting list, rather than a natural group. It was proposed that within this genus, some clusters of morphologically similar species could be recognized, with the morphological differences among these clusters suggesting distinct systematic ranks. Benaim and Absalão (2011a) followed this conjecture by analyzing the morphological characteristics of some Atlantic species using empty shell specimens and proposed three distinct clusters, grouping together *Y. nana*, *Y. inconspicua*, and *Y. americana* Allen, H.L. Sanders & F. Hannah, 1995. However, in our molecular phylogenetic analysis of these three species, they did not cluster in a single branch. The feasibility of this hypothesis requires validation through the combination of anatomy, morphometry, molecular data, and other methods. In addition, hinge plate features are considered a significant diagnostic feature in descriptions of *Yoldiella* species, especially the width of the posterior hinge plate (Benaim and Absalão 2011b; Benaim et al. 2011). Further meticulous examination of all taxa is essential before achieving confidence in the accuracy of classification.

Based on anatomical and morphological characteristics, Protobranchia has traditionally been regarded as a monophyletic group (Pelseneer 1889; Xu 1999), but the widespread application of molecular methods in phylogenetic analysis has not provided support for the monophyly of the Protobranchia (Combosch et al. 2017). Recent studies have supported the monophyly of Protobranchia and five superfamilies (Nuculoidea, Manzanelloidea, Solemyoidea, Sareptoidea, and Nuculanoidea) (Smith et al. 2011; Sharma et al. 2012; Bieler et al. 2014; González et al. 2015; Lemer et al. 2019; Sato et al. 2020). Notably, the monophyly of lower taxa (family and below) is still uncertain, particularly within the superfamily Nuculanoidea. In this study, all currently recognized families were found to be non-monophyletic, which is consistent with previous research findings (Sharma et al. 2013; Sato et al. 2020). In addition, the limited support for the majority of nodes within the Nuculanoidea has resulted in largely ambiguous internal relationships. This phenomenon may be the result of a combination of factors, possibly the lack of genetic information, deficient taxon sampling, or both, or even the possibility that this taxon may have undergone rapid radiation (Lemer et al. 2019).

Phylogenetic analysis of the Yoldiidae revealed differences between the evolutionary relationships inferred from the COI and the 18S rRNA genes. Specifically, the phylogenetic tree based on COI gene shows that *Yoldia* is polyphyletic, in which species were interspersed among other genera rather than forming a distinct clade. In contrast, the phylogenetic tree derived from the 18S rRNA gene shows that *Yoldia* is a monophyletic group within a single clade. Such incongruities may be attributed to variations in the evolutionary rates of the two genes. The genetic markers employed in this study, such as COI and H3, exhibit rapid evolutionary rates, particularly at the third codon position, which are almost certainly saturated when applied across multiple taxonomic families. In addition, Mallatt et al. (2010) explored the metazoan tree using almost complete rRNA genes (18S and 28S), which suggested that non-monophyly of Mollusca in analyses based on 18S rRNA might be explained by these non-ho-

mologous forms, and indeed paraphyly/polyphyly of Mollusca has been found in many studies of metazoan phylogeny based on 18S rRNA. In addition, Mallatt et al. (2010) investigated the metazoan phylogenetic tree by analyzing nearly complete 18S rRNA genes. Their findings did not support the monophyly of Mollusca, indicating that the non-monophyly of Mollusca in 18S rRNA-based analyses could be attributed to non-homologous forms. Indeed, the paraphyly/polyphyly of Mollusca has been observed in numerous studies on metazoan phylogeny utilizing 18S rRNA (e.g. Winnepenninckx et al. 1996; Mallatt et al. 2010, 2012). Based on the findings derived from the analysis of 18S rRNA, the potential scenario cannot be ruled out. Consequently, great care needed to be taken in the application of 18S rRNA for phylogenetics to avoid the incorporation of non-homologous variants of 18S rRNA in the assessments.

There may be more problems with traditional identification that relies solely on anatomy and morphology. Challenges persist due to the difficulty in obtaining protobranch samples, resulting in relatively limited molecular data with insufficient resolution. As shown in our phylogenetic analysis, the bootstrap values are low which may be unreliable. Nonetheless, this work represented a minor step forward and demonstrated the complexity of the taxonomic classification system within this taxon and made it clear that a greater coverage of taxa and more informative genetic markers (not limited to a single gene, but based on high-throughput sequencing technologies for massive orthologous genes from transcriptomes or even genomes) will provide great potential for improving the resolution of phylogenetic classification in this group in the future.

Additional information

Conflict of interest

The authors have declared that no competing interests exist.

Ethical statement

No ethical statement was reported.

Funding

This work was supported by the National Key Research and Development Program of China (2021YFE0193700), Qingdao New Energy Shandong Laboratory Open Project (QNESL OP202306), the Science and Technology Innovation Project of Laoshan Laboratory (LSKJ202203100), the Strategic Priority Research Program of the Chinese Academy of Sciences (XDB42000000), and the Taishan Scholars Program (tsqn202306280).

Author contributions

Junlong Zhang: research conceptualization, funding provision, writing, and editing; Qi Gao: morphological study, molecular experiments, methodology, data analysis and interpretation, original draft writing. Yan Tang: methodology, data analysis and interpretation, writing. All authors contributed critically to the drafts and gave final approval for publication.

Author ORCIDs

Yan Tang  <https://orcid.org/0000-0003-0564-7279>

Junlong Zhang  <https://orcid.org/0000-0003-3831-4673>

Data availability

All of the data that support the findings of this study are available in the main text or Supplementary Information.

References

- Adams H, Adams A (1858) The Genera of Recent Mollusca, Arranged According to Their Organization. Van Voorst, London, 661. <https://doi.org/10.5962/bhl.title.4772>
- Allen JA (1978) Evolution of the deep sea protobranch bivalves. Philosophical Transactions of the Royal Society of London. Series B, Biological Sciences 284: 387–401. <https://doi.org/10.1098/rstb.1978.0076>
- Allen JA, Hannah FJ (1986) A reclassification of the Recent genera of the subclass Protobranchia Mollusca Bivalvia. Journal of Conchology 324: 225–249.
- Allen JA, Sanders HL, Hannah F (1995) Studies on the deep-sea Protobranchia (Bivalvia); the subfamily Yoldiellinae. Bulletin of the Natural History Museum Zoology Series 61: 11–90.
- Benaim NP, Absalão RS (2011a) Deep sea *Yoldiella* (Pelecypoda: Protobranchia: Yoldiidae) from Campos Basin, Rio de Janeiro, Brazil. Journal of the Marine Biological Association of the United Kingdom 91(2): 513–529. <https://doi.org/10.1017/S0025315410001372>
- Benaim NP, Absalão RS (2011b) Discriminating among similar deep-sea *Yoldiella* (Pelecypoda: Protobranchia) species with a morphometric approach. Journal of the Marine Biological Association of the United Kingdom 91(8): 1665–1672. <https://doi.org/10.1017/S0025315411000063>
- Benaim NP, Viegas D, Absalão RS (2011) How features of the hinge plate aid in discriminating among three *Yoldiella* (Pelecypoda, Protobranchia) species from the Campos Basin, Brazil. Zootaxa 2883(1): 39–51. <https://doi.org/10.11646/zootaxa.2883.1.3>
- Bieler R, Mikkelsen PM, Collins TM, Glover EA, González VL, Graf DL, Harper EM, Healy J, Kawauchi GY, Sharma PP, Staubach S, Strong EE, Taylor JD, Tëmkin I, Zardus JD, Clark S, Guzmán A, McIntyre E, Sharp P, Giribet G (2014) Investigating the bivalve tree of life—An exemplar-based approach combining molecular and novel morphological characters. Invertebrate Systematics 28(1): 32. <https://doi.org/10.1071/IS13010>
- Castresana J (2000) Selection of conserved blocks from multiple alignments for their use in phylogenetic analysis. Molecular Biology and Evolution 17(4): 540–552. <https://doi.org/10.1093/oxfordjournals.molbev.a026334>
- Coan EV, Valentich Scott P (2012) Bivalve Seashells of Tropical West America: Marine Bivalve Mollusks from Baja California to Northern Perú (Part I). Santa Barbara Museum of Natural History, Santa Barbara, 598 pp.
- Combosch DJ, Collins TM, Glover EA, Graf DL, Harper EM, Healy JM, Kawauchi GY, Lemer S, McIntyre E, Strong EE, Taylor JD, Zardus JD, Mikkelsen PM, Giribet G, Bieler R (2017) A family-level Tree of Life for bivalves based on a Sanger-sequencing approach. Molecular Phylogenetics and Evolution 107: 191–208. <https://doi.org/10.1016/j.ympev.2016.11.003>
- Dall WH (1908) Reports on the dredging operations off the west coast of Central America to the Galapagos, to the west coast of Mexico, and in the Gulf of California, in charge of Alexander Agassiz, carried on by the U.S. Fish Commission steamer “Albatross,” during 1891, Lieut.-Commander Z.L. Tanner, U.S.N., commanding. XXXVII. Reports on the scientific results of the expedition to the eastern tropical Pacific, in charge of Alexander Agassiz, by the U.S. Fish Commission steamer “Albatross”, from October, 1904 to March, 1905, Lieut.-Commander L.M. Garrett, U.S.N., commanding. XIV. The Mollusca and Brachiopoda. Bulletin of the Museum of Comparative Zoology 43(6): 205–487, [pls 1–22].

- Darriba D, Taboada GL, Doallo R, Posada D (2012) jModelTest 2: More models, new heuristics and parallel computing. *Nature Methods* 9(8): 772–772. <https://doi.org/10.1038/nmeth.2109>
- Don RH, Cox PT, Wainwright BJ, Baker K, Mattick JS (1991) ‘Touchdown’ PCR to circumvent spurious priming during gene amplification. *Nucleic Acids Research* 19(14): 4008–4008. <https://doi.org/10.1093/nar/19.14.4008>
- Dong D, Li X, Yang M, Gong L, Li Y, Sui J, Gan Z, Kou Q, Xiao N, Zhang J (2021) Report of epibenthic macrofauna found from Haima cold seeps and adjacent deep-sea habitats, South China Sea. *Marine Life Science & Technology* 3(1): 1–12. <https://doi.org/10.1007/s42995-020-00073-9>
- González VL, Andrade SCS, Bieler R, Collins TM, Dunn CW, Mikkelsen PM, Taylor JD, Giribet G (2015) A phylogenetic backbone for Bivalvia: An RNA-seq approach. *Proceedings of the Royal Society B: Biological Sciences* 282(1801): 20142332. <https://doi.org/10.1098/rspb.2014.2332>
- He X, Xu T, Chen C, Liu X, Li Y-X, Zhong Z, Gu X, Lin Y-T, Lan Y, Yan G, Sun Y, Qiu J-W, Qian P-Y, Sun J (2023) Same (sea) bed different dreams: Biological community structure of the Haima seep reveals distinct biogeographic affinities. *The Innovation Geoscience* 1(2): 100019. <https://doi.org/10.59717/j.xinn-geo.2023.100019>
- International Commission on Zoological Nomenclature (1985) Opinion 1306. *Ledella bushae* Warén, 1978 is the type species of *Ledella* Verrill & Bush, 1897 (Mollusca, Bivalvia). *Bulletin of Zoological Nomenclature* 42: 146–147.
- Kalyaanamoorthy S, Minh BQ, Wong TKF, Von Haeseler A, Jermiin LS (2017) ModelFinder: Fast model selection for accurate phylogenetic estimates. *Nature Methods* 14(6): 587–589. <https://doi.org/10.1038/nmeth.4285>
- Katoh K, Standley DM (2013) MAFFT Multiple Sequence Alignment Software version 7: Improvements in performance and usability. *Molecular Biology and Evolution* 30(4): 772–780. <https://doi.org/10.1093/molbev/mst010>
- Ke Z, Li R, Chen Y, Chen D, Chen Z, Lian X, Tan Y (2022) A preliminary study of macrofaunal communities and their carbon and nitrogen stable isotopes in the Haima cold seeps, South China Sea. *Deep-sea Research. Part I, Oceanographic Research Papers* 184: 103774. <https://doi.org/10.1016/j.dsr.2022.103774>
- La Perna R (2004) The identity of *Yoldia micrometrica* Seguenza, 1877 and three new deep-sea protobranchs from the Mediterranean (Bivalvia). *Journal of Natural History* 38(8): 1045–1057. <https://doi.org/10.1080/0022293021000056936>
- Lemer S, Bieler R, Giribet G (2019) Resolving the relationships of clams and cockles: Dense transcriptome sampling drastically improves the bivalve tree of life. *Proceedings. Biological Sciences* 286(1896): 20182684. <https://doi.org/10.1098/rspb.2018.2684>
- Lovén SL (1846) Index Molluscorum litora Scandinaviae occidentalia habitantium. *Kongliga Vetenskaps Akademiens Förhandlingar* 1846: 134–160, 182–204.
- Mallatt J, Craig CW, Yoder MJ (2010) Nearly complete rRNA genes assembled from across the metazoan animals: Effects of more taxa, a structure-based alignment, and paired-sites evolutionary models on phylogeny reconstruction. *Molecular Phylogenetics and Evolution* 55(1): 1–17. <https://doi.org/10.1016/j.ympev.2009.09.028>
- Mallatt J, Craig CW, Yoder MJ (2012) Nearly complete rRNA genes from 371 Animalia: Updated structure-based alignment and detailed phylogenetic analysis. *Molecular Phylogenetics and Evolution* 64(3): 603–617. <https://doi.org/10.1016/j.ympev.2012.05.016>
- Neulinger S, Sahling H, Süling J, Imhoff J (2006) Presence of two phylogenetically distinct groups in the deep-sea mussel *Acharax* (Mollusca: Bivalvia: Solemyidae). *Marine Ecology Progress Series* 312: 161–168. <https://doi.org/10.3354/meps312161>

- Nguyen L-T, Schmidt HA, Von Haeseler A, Minh BQ (2015) IQ-TREE: A fast and effective stochastic algorithm for estimating maximum-likelihood phylogenies. *Molecular Biology and Evolution* 32(1): 268–274. <https://doi.org/10.1093/molbev/msu300>
- Okutani T, Fujikura K (2022) A new tiny protobranch bivalve from Sagami Bay, Japan. *Venus (Tokyo)* 80: 87–90. https://doi.org/10.18941/venus.80.3-4_87
- Okutani T, Fujiwara Y (2005) Four protobranch bivalves collected by the ROV Kaiko from hadal depths in the Japan Trench. *Venus (Tokyo)* 63(3–4): 87–94.
- Pelseneer P (1889) Sur la classification phylogenetique de pelecypods. *Bulletin Scientifique de la France et de la Belgique (série 3)* 20 (1–4): 27–52.
- Puillandre N, Lambert A, Brouillet S, Achaz G (2012) ABGD, Automatic Barcode Gap Discovery for primary species delimitation. *Molecular Ecology* 21(8): 1864–1877. <https://doi.org/10.1111/j.1365-294X.2011.05239.x>
- Puillandre N, Brouillet S, Achaz G (2021) ASAP: Assemble Species by Automatic Partitioning. *Molecular Ecology Resources* 21(2): 609–620. <https://doi.org/10.1111/1755-0998.13281>
- Purchon RD (1956) The stomach in the Protobranchia and Septibranchia. *Journal of Zoology* 127: 511–525. <https://doi.org/10.1111/j.1096-3642.1956.tb00485.x>
- Reed AJ, Morris JP, Linse K, Thatje S (2013) Plasticity in shell morphology and growth among deep-sea protobranch bivalves of the genus *Yoldiella* (Yoldiidae) from contrasting Southern Ocean regions. *Deep-sea Research. Part I, Oceanographic Research Papers* 81: 14–24. <https://doi.org/10.1016/j.dsr.2013.07.006>
- Reed AJ, Morris JP, Linse K, Thatje S (2014) Reproductive morphology of the deep-sea protobranch bivalves *Yoldiella ecaudata*, *Yoldiella sabrina*, and *Yoldiella valettei* (Yoldiidae) from the Southern Ocean. *Polar Biology* 37(10): 1383–1392. <https://doi.org/10.1007/s00300-014-1528-4>
- Sato K, Kano Y, Setiamarga DHE, Watanabe HK, Sasaki T (2020) Molecular phylogeny of protobranch bivalves and systematic implications of their shell microstructure. *Zoologica Scripta* 49(4): 458–472. <https://doi.org/10.1111/zsc.12419>
- Sharma PP, González VL, Kawauchi GY, Andrade SCS, Guzmán A, Collins TM, Glover EA, Harper EM, Healy JM, Mikkelsen PM, Taylor JD, Bieler R, Giribet G (2012) Phylogenetic analysis of four nuclear protein-encoding genes largely corroborates the traditional classification of Bivalvia (Mollusca). *Molecular Phylogenetics and Evolution* 65(1): 64–74. <https://doi.org/10.1016/j.ympev.2012.05.025>
- Sharma PP, Zardus JD, Boyle EE, González VL, Jennings RM, McIntyre E, Wheeler WC, Etter RJ, Giribet G (2013) Into the deep: A phylogenetic approach to the bivalve subclass Protobranchia. *Molecular Phylogenetics and Evolution* 69(1): 188–204. <https://doi.org/10.1016/j.ympev.2013.05.018>
- Smith SA, Wilson NG, Goetz FE, Feehery C, Andrade SCS, Rouse GW, Giribet G, Dunn CW (2011) Resolving the evolutionary relationships of molluscs with phylogenomic tools. *Nature* 480(7377): 364–367. <https://doi.org/10.1038/nature10526>
- Vaidya G, Lohman DJ, Meier R (2011) SequenceMatrix: Concatenation software for the fast assembly of multi-gene datasets with character set and codon information. *Cladistics* 27(2): 171–180. <https://doi.org/10.1111/j.1096-0031.2010.00329.x>
- Verrill AE, Bush KJ (1897) Revision of the genera of Ledidae and Nuculidae of the Atlantic Coast of the United States. *American Journal of Science* 3(13): 51–63. <https://doi.org/10.2475/ajs.s4-3.13.51>
- Wang H, Liu H, Wang X, Zhang J, Sirenko BI, Liu C, Dong D, Li X (2022) Stirring the deep, disentangling the complexity: Report on the third species of *Thermochiton* (Mollusca: Polyplacophora) From Haima Cold Seeps. *Frontiers in Marine Science* 9: 889022. <https://doi.org/10.3389/fmars.2022.889022>

- Winnepenninckx B, Backeljau T, De Wachter R (1996) Investigation of molluscan phylogeny on the basis of 18S rRNA sequences. *Molecular Biology and Evolution* 13(10): 1306–1317. <https://doi.org/10.1093/oxfordjournals.molbev.a025577>
- Xu F (1999) *Fauna Sinica. Phylum Mollusca. Class Bivalvia. Subclasses Protobranchia and Anomalodesmata*. Science Press, Beijing, 244 pp.
- Yao G, Zhang H, Xiong P, Jia H, Shi Y, He M (2022) Community characteristics and genetic diversity of macrobenthos in Haima Cold Seep. *Frontiers in Marine Science* 9: 920327. <https://doi.org/10.3389/fmars.2022.920327>
- Yonge M, Calman WT (1939) The protobranchiate mollusca; a functional interpretation of their structure and evolution. *Philosophical Transactions of the Royal Society of London. Series B, Biological Sciences* 230(566): 79–148. <https://doi.org/10.1098/rstb.1939.0005>
- Zardus JD (2002) Protobranch bivalves. *Advances in Marine Biology* 42: 1–65. [https://doi.org/10.1016/S0065-2881\(02\)42012-3](https://doi.org/10.1016/S0065-2881(02)42012-3)
- Zardus JD, Etter RJ, Chase MR, Rex MA, Boyle EE (2006) Bathymetric and geographic population structure in the pan-Atlantic deep-sea bivalve *Deminucula atacellana* (Schenck, 1939). *Molecular Ecology* 15(3): 639–651. <https://doi.org/10.1111/j.1365-294X.2005.02832.x>
- Zhang J, Kapli P, Pavlidis P, Stamatakis A (2013) A general species delimitation method with applications to phylogenetic placements. *Bioinformatics* 29(22): 2869–2876. <https://doi.org/10.1093/bioinformatics/btt499>
- Zhao J, Liang Q, Wei J, Tao J, Yang S, Liang J, Lu J, Wang J, Fang Y, Gong Y, He X (2020) Seafloor geology and geochemistry characteristic of methane seepage of the “Haima” cold seep, northwestern slope of the South China Sea. *Geochimica* 49: 108–118.

Supplementary material 1

Primers used in this study

Authors: Qi Gao , Yan Tang , Junlong Zhang

Data type: xlsx

Copyright notice: This dataset is made available under the Open Database License (<http://opendatacommons.org/licenses/odbl/1.0/>). The Open Database License (ODbL) is a license agreement intended to allow users to freely share, modify, and use this Dataset while maintaining this same freedom for others, provided that the original source and author(s) are credited.

Link: <https://doi.org/10.3897/zookeys.1204.121088.suppl1>

Supplementary material 2

The sequences of COI, 18S and H3 genes used for phylogenetic analyses of the superfamily Nuculanoidea

Authors: Qi Gao , Yan Tang , Junlong Zhang

Data type: xlsx

Copyright notice: This dataset is made available under the Open Database License (<http://opendatacommons.org/licenses/odbl/1.0/>). The Open Database License (ODbL) is a license agreement intended to allow users to freely share, modify, and use this Dataset while maintaining this same freedom for others, provided that the original source and author(s) are credited.

Link: <https://doi.org/10.3897/zookeys.1204.121088.suppl2>

Supplementary material 3

The sequences of COI and 18S genes used for phylogenetic analyses of the family Yoldiidae

Authors: Qi Gao , Yan Tang , Junlong Zhang

Data type: xlsx

Copyright notice: This dataset is made available under the Open Database License (<http://opendatacommons.org/licenses/odbl/1.0/>). The Open Database License (ODbL) is a license agreement intended to allow users to freely share, modify, and use this Dataset while maintaining this same freedom for others, provided that the original source and author(s) are credited.

Link: <https://doi.org/10.3897/zookeys.1204.121088.suppl3>

Supplementary material 4

Phylogenetic tree inferred by Bayesian inference (BI) based on combined gene dataset (COI+18S+H3)

Authors: Qi Gao , Yan Tang , Junlong Zhang

Data type: pdf

Copyright notice: This dataset is made available under the Open Database License (<http://opendatacommons.org/licenses/odbl/1.0/>). The Open Database License (ODbL) is a license agreement intended to allow users to freely share, modify, and use this Dataset while maintaining this same freedom for others, provided that the original source and author(s) are credited.

Link: <https://doi.org/10.3897/zookeys.1204.121088.suppl4>

Supplementary material 5

Phylogenetic tree inferred by Maximum likelihood (ML) based on combined gene dataset (COI+18S +H3)

Authors: Qi Gao , Yan Tang , Junlong Zhang

Data type: pdf

Copyright notice: This dataset is made available under the Open Database License (<http://opendatacommons.org/licenses/odbl/1.0/>). The Open Database License (ODbL) is a license agreement intended to allow users to freely share, modify, and use this Dataset while maintaining this same freedom for others, provided that the original source and author(s) are credited.

Link: <https://doi.org/10.3897/zookeys.1204.121088.suppl5>

Phylogenetic analysis reveals a new net-winged beetle genus of Eurrhacini (Coleoptera, Lycidae) from the Pacific slopes of Central America and Ecuador

Elynton Alves Nascimento¹, Milada Bocakova²

1 Departamento de Engenharia Ambiental, Universidade Estadual do Centro-Oeste, Rua Professora Maria Roza Zanon de Almeida, s/n, Engenheiro Gutierrez, Irati-PR, CEP 84505-677, Brazil

2 Department of Biology, Faculty of Education, Palacky University, Purkrabska 2, CZ-77140 Olomouc, Czech Republic

Corresponding author: Milada Bocakova (milada.bocakova@upol.cz)

Abstract

The first phylogenetic inference of Calopterini and Eurrhacini focused on *Calocladon* and related taxa was carried out. A data matrix composed of 46 species and 51 morphological characters was assembled and analyzed using parsimony and model-based approaches. Eurrhacini were recovered monophyletic. Furthermore, phylogenetic analyses highly supported the *Calocladon* clade including also *Atlanticolycus*, *Cladocalon*, and *Gorhamium* **gen. nov.** as its sister clade. Our trees consistently recovered monophyly of the new genus with two new species: *Gorhamium bidentatum* **sp. nov.** (Panama, Baru Volcano) and *G. unidentatum* **sp. nov.** from the Pacific slopes of Ecuador. A revised key to the genera of Eurrhacini is given and illustrations of distinguishing characters are provided. Phylogenetic relationships of Eurrhacini and character evolution are discussed.

Key words: Lycinae, Neotropical Region, new genus, new species



Academic editor: Vinicius S. Ferreira

Received: 30 October 2023

Accepted: 18 March 2024

Published: 6 June 2024

ZooBank: <https://zoobank.org/F5134CC6-A83C-48B6-A1EA-235E6858D5CB>

Citation: Nascimento EA, Bocakova M (2024) Phylogenetic analysis reveals a new net-winged beetle genus of Eurrhacini (Coleoptera, Lycidae) from the Pacific slopes of Central America and Ecuador. ZooKeys 1204: 241–259. <https://doi.org/10.3897/zookeys.1204.114932>

Copyright: © E. A. Nascimento & M. Bocakova. This is an open access article distributed under terms of the Creative Commons Attribution License (Attribution 4.0 International – CC BY 4.0).

Introduction

The Eurrhacini is a Neotropical lineage of Lycidae, which until recently was part of the tribe Calopterini in the broader sense (Bocakova 2003, 2005). However, the inclusion of Eurrhacini in Calopterini was challenged by the first molecular analysis of Lycidae (Bocak et al. 2008) which showed that *Eurrhacus* Waterhouse, 1879 is sister to the Oriental *Conderis*. Consequently, Eurrhacini was excluded from Calopterini (Bocak and Bocakova 2008) and elevated to the tribal rank. Nevertheless, inferring the Eurrhacini sister group is convoluted because DNA analyses proposed several candidates. Recent molecular trees on large data sets (Masek et al. 2018) recovered the Eurrhacini sister is either American Thonalmini or Oriental Lycoprogenthini, thus indicating that Calopterini and Eurrhacini are not sister lineages.

The placement of Eurrhacini in the Calopterini was based on their resemblance, as the two groups often have similar coloration. Eurrhacini, however, are characterized by a very long male terminal sternum, which is twice as long as that of the Calopterini, and a distorted phallus and phallobase. When

established (Bocakova 2005), Eurrhacini included six genera. Of these, *Calocladon* Gorham, 1881 has a markedly elongated pronotum, *Lycoplateros* Pic, 1922 is characteristic by a conspicuous protuberance on the posterior margin of the pronotum, and *Haplobothris* Bourgeois, 1879 is easily distinguishable by the absence of secondary elytral costae. The remaining three genera (*Eurrhacus*, *Emplectus* Erichson, 1847, and *Neolinoptes* Nascimento & Bocakova, 2017) are less distinctive externally, but easily separated by the shape of the male genitalia.

Likewise, species of the recently discovered *Cladocalon* Nascimento & Bocakova, 2022, *Currhaeus* Nascimento, Bressan & Bocakova, 2020, and *Atlanticolycus* Nascimento & Bocakova, 2023 were originally placed in *Calocladon*, as they are similar to *Calocladon* and *Emplectus* (Nascimento et al. 2020; Nascimento and Bocakova 2022). However, showing great male genitalia disparity, they were assigned to generic rank. Recently, an examination of H. S. Gorham's types from Panama and further research on material from Ecuador have revealed another previously hidden generic lineage described below. Here we elucidate phylogenetic relationships of the group and its placement within Eurrhacini by analyzing morphological data.

Materials and methods

The morphological matrix is based on that of Bocakova (2005), updated by Nascimento et al. (2020) and Ferreira et al. (2023). The dataset was expanded by the inclusion of two recently proposed Eurrhacini genera (*Atlanticolycus*, *Cladocalon*) and the new one described here (altogether six newly coded species). Our final matrix (Table 1) is composed of 46 species and 51 characters (Suppl. material 1), including five outgroup taxa. Of these, ten characters were coded to multistates, 41 characters as binary. Eight additional characters (#44–51) were newly defined, other characters required the inclusion of new character states, or minor redefinition. Unknown and inapplicable characters were coded by a question mark "?", or a dash "-", respectively.

Phylogenetic analyses were conducted using maximum parsimony (MP), Bayesian (BA), and maximum likelihood (ML) criteria. MP analyses were performed in TNT 1.5 (Goloboff et al. 2008; Goloboff and Catalano 2016) using traditional search with characters treated as unordered. MP trees were evaluated by tree length (TL), consistency (CI), and retention indices (RI), and summarized in strict and majority rule consensus trees. Initial fundamental analyses with equal weights were followed by searches with implied weighted schemes (Goloboff 1993) with concavity constant $k = 3–25$. Standard bootstrapping (Bootstrap support, BS) and symmetric resampling (SR) with 1000 replicates were applied to the unweighted dataset to assess the branch support. Furthermore, Bremer support values (BrS; Bremer 1994) were calculated in TNT for the clades of the unweighted MP tree. Character optimizations were mapped on the strict consensus tree using unambiguous changes, accelerated (ACCTRAN) and delayed (DELTRAN) transformations in WinClada (Nixon 2002).

Maximum likelihood (ML) searches were applied under IQ-Tree 2 software (Minh et al. 2020) with branch support estimated by ultrafast bootstrapping (UF-Boot) using 1000 replicates. The best-fit model was selected by ModelFinder (Kalyaanamoorthy et al. 2017) according to Bayesian information criterion

diameter is equal to the interocular distance; in small eyes the eye diameter is less than the interocular distance; in large eyes the eye diameter is greater than the interocular distance. Nine longitudinal elytral costae are distinguished in four strong primary costae and five less elevated alternate secondary costae. Costae and intercostal intervals are numbered from the suture as in other Coleoptera. Dissection of genitalia was made after boiling in 10% KOH solution and followed previous studies (Nascimento and Bocakova 2017). Relative measurements were taken using an ocular micrometer, and dimension measurements (in millimeters) and scale bar insertions were processed by the camera software. Digital photographs were taken using an attached Canon EOS 1100D camera and stacked by QuickPhoto Camera 3.0 microscope software using a Deep Focus 3.3 module. Images were further edited in GIMP 2.10.22 and Adobe Photoshop CS3.

The syntypes of *Calocladon chiriquense* Gorham, 1884 were borrowed from The Natural History Museum (**NHMUK**) in London, U.K., while other material is deposited in the collection of Palacky University Olomouc (**UPOL**), Czech Republic.

Results

Phylogenetic analyses

Different analytical approaches resulted in congruent patterns of major lineages. Our ML tree (Fig. 1) applying the best-fit MK+FQ+ASC+G4 model recovered two distinct clades: Calopterini (UFBoot = 51) and Eurrhacini (UFBoot = 78), although the ultrafast bootstrap support values were low. Inferred internal relationships within Calopterini revealed Caloptera receiving low support (UFBoot = 77), while the Acroleptina were paraphyletic. Basal relationships of Eurrhacini showed a pectinate pattern. The *Calocladon* clade was recovered (UFBoot = 88, Fig. 1), including *Gorhamium* gen. nov. as sister to *Cladocalon*, whereas *Calocladon* was sister to *Atlanticolycus*.

Bayesian analyses of the dataset resulted in trees with low posterior probabilities for Eurrhacini (PP = 0.51), while Calopterini were unsupported (PP = 0.29, Suppl. material 2). The subtribe Caloptera obtained low support (PP = 0.52) and Acroleptina were again found paraphyletic forming two clades. Within the Eurrhacini, the *Calocladon* clade received moderate support (PP = 0.93), whereas support for the crown clade *Gorhamium* gen. nov. + *Cladocalon* was low (PP = 0.61).

Initial unweighted MP analyses resulted in 23 shortest trees (TL = 131, CI = 49.62, RI = 80.7), the strict consensus of which recovered monophyly of Eurrhacini (Suppl. materials 3–5). However, most Calopterini formed a basal multifurcation and the tribe was present only on the majority rule consensus tree (91%, Suppl. material 6). MP analyses found some Bremer support for both Calopterini and Eurrhacini (BrS = 1, Suppl. material 7), while bootstrapping and symmetric resampling showed the clades unsupported (Calopterini - BS = 6, SR = 10; Eurrhacini - BS = 1, SR = 2; Suppl. materials 8, 9). Subsequent implied weighting schemes always resulted in a single identical topology (Suppl. material 10) regardless of the concavity constant applied (k = 3–25). The implied weighted trees showed the Eurrhacini, while Calopterini were broken into the subtribes of Caloptera and Acroleptina.

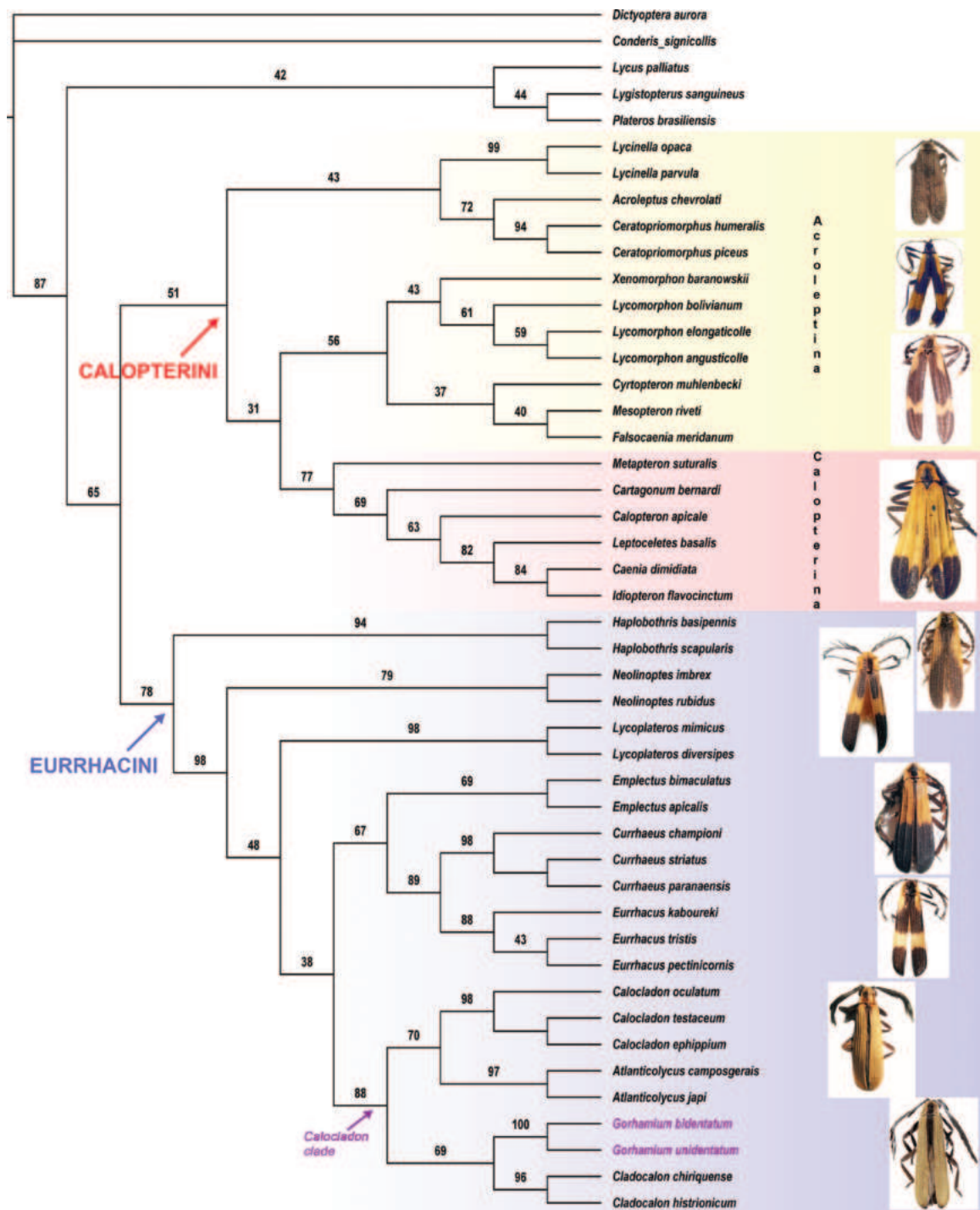


Figure 1. Maximum likelihood phylogeny of Calopterini and Eurrhacini inferred from the morphological data-set using IQ-Tree 2 and the best-fit MK+FQ+ASC+G4 model selected by ModelFinder. Node labels represent ultrafast bootstrap support values.

Phylogenetic relationships within the tribe Eurrhacini revealed the genus *Haplobothris* as the most basal branch in all analyses. The remaining Eurrhacini was strongly supported (UFBoot = 98, PP = 0.98, BrS = 4). MP trees further indicated a bifurcation of *Calocladon* and *Eurrhacus* clades (Suppl. materials 3, 10). While the *Calocladon* clade was supported in all analyses (UFBoot = 88, PP = 0.93, BrS = 3), the latter was paraphyletic in ML and BA trees (Fig. 1, Suppl.

material 2). Similarly, relationships within the *Calocladon* clade showed high Bremer support for *Cladocalon* + *Gorhamium* gen. nov. (BrS = 14), whereas the clade received low support in ML and BA trees (UFBoot = 69, pp = 0.6). Our MP analyses also found *Calocladon* + *Atlanticolycus* clade well supported (BrS = 3), but the group received low support in ML analyses (UFBoot = 70) and was broken in Bayesian trees.

Taxonomy

Gorhamium gen. nov.

<https://zoobank.org/C31BE6D3-296C-45B1-B685-AD85CB34EA65>

Type species. *Gorhamium bidentatum* sp. nov. (by present designation).

Diagnosis. *Gorhamium* gen. nov. can be distinguished from other Eurrhacini by the combination of the following characters: a) elytra (Fig. 2A–C) with nine longitudinal costae (4 costae in *Haplobothris*); b) pronotum (Fig. 3A, B) wider than long (elongated in *Calocladon*); c) median areola on pronotum slenderly lenticular (slightly wider in *Cladocalon* and *Atlanticolycus*); d) male antennomere 3–10 flabellate (Fig. 4B, C); e) aedeagus with each paramere projected ventrobasally into a slender, medially curved process (d_1 , Fig. 6C), sometimes joining at midline forming an annular bridge (d_3 , Fig. 6G) (also present in *Calocladon*, *Cladocalon*, and *Atlanticolycus*). Among unique features of *Gorhamium* gen. nov. belong: a) base of phallus pointed anchored-shaped (inverted mushroom-shaped), with arcuate arms and a pointed tip (a_1 , Fig. 6E, F), while the base of phallus of *Cladocalon* and *Atlanticolycus* is flat, or rounded (a_2 , Fig. 6A); b) median portion of phallus extending ventrally into oval opening (b, Fig. 6C); c) dorsal edge of phallus hooked (c, Fig. 6D, G); d) internal sac membranous with minute spines distally (e, Fig. 6D, G); e) parameres shorter than 2/3 of phallus (while the parameres are almost as long as phallus in *Atlanticolycus*); f) base of parameres semicircular in cross-section (flattened/ribbon-like in *Cladocalon*); g) apex of parameres denticulate, provided with one or two coarse teeth; h) female genitalia with valvifers as long as coxites and styli combined (Fig. 6H).

Description. Body length: 5.5–6.4 mm, width across the humeri: 1.2 mm. Head partly covered by pronotum from above. Labrum small, mandibles slender, arcuate (Fig. 4A). Maxillary palps 4-segmented, gradually widened distally, palpomere 1 (=P1) at least 3× shorter than P2, P2 longest of all, ~ 2× longer than P4, P3 1.5× shorter than P4, terminal palpomere securiform, apex obliquely rounded (Fig. 4A). Terminal palpomere of labial palps securiform. Pronotum somewhat trapezoidal, with anterior margin produced forward, posterior margin 1.4× wider than median length; lateral margins divergent posterad, with anterior 2/3 almost straight, convergent anteriorly, posterior angles acute; posterior margin bisinuate, medioposterior process almost triangular (Fig. 3A, B); median longitudinal carina on pronotum bifurcating in anterior third, forming very slender, lenticular areola. Scutellum square, apex minutely emarginate medially (Fig. 3A). Elytra subparallel-sided, slender, 4× longer than humeral width (Fig. 2A–C). Each elytron with nine longitudinal costae (4 primary costae and 5 less elevated secondary costae), primary costae 2 and 4 strongly elevated; intercostal intervals with a row of irregular reticulate cells, secondary costae 3 and 4 absent posteriorly. Anterior thoracic spiracles small, tubulate. Legs compressed, tro-

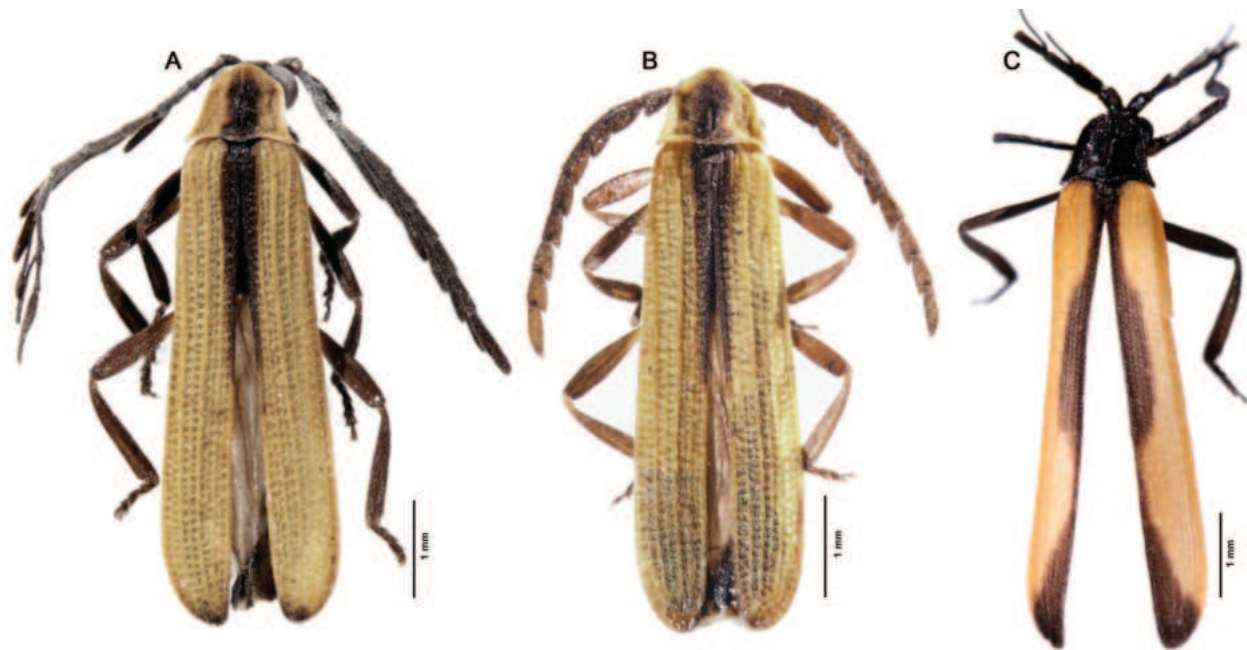


Figure 2. Habitus, dorsal view **A, B** *Gorhamium bidentatum* sp. nov. **A** male **B** female **C** *Gorhamium unidentatum* sp. nov., male.

chanters almost triangular (Fig. 4A), as long as third of femur, tibiae straight, their spurs small, covered by pubescence, tarsomeres 1–4 lobed.

Male. Eyes medium-sized to large, eye diameter 1.3–1.7× longer than interocular distance. Antennae reaching beyond elytral midlength, antennomeres 3–10 flabellate, antennal branches flattened, antennomere 1 (=A1) stout, A2 small, transverse, A3 slightly (1.15–1.3×) shorter than A4, A4–A10 subequal in length. Lamellae arise basally, lamella of A3 slightly longer than antennomere body, remaining lamellae considerably longer. Abdominal sternum VIII widely emarginated distally (Fig. 5C, F), emargination shallow, as deep as $\frac{1}{4}$ of sternum length. Sternum IX elongate, 3.5× longer than wide (Fig. 5A, E), widest in distal quarter, proximal half narrow with lateral margins convergent. Phallus with ventromedial oval opening (b, Fig. 6C, G), base of phallus pointed anchored-shaped, or inverted mushroom-shaped (a, Fig. 6E, F); distal portion of phallus rod-like, apex clavate, dorsal margin hooked (c, Fig. 6D, G); internal sac membranous with minute spines distally (e, Fig. 6G), sometimes also medially. Parameres at most as long as $\frac{2}{3}$ of phallus, base of parameres almost semicircular in cross-section; each paramere projected basally in a thin ventral, medially arched, process (d, Fig. 6C), sometimes joining medially in a ring-like bridge (d₃, Fig. 6G); parameral apex denticulate, provided with one or two coarse teeth. Phallobase slightly asymmetrical, distorted, moderately arched ventrally.

Female. Eyes small, interocular distance 1.3× longer than eye diameter, antennae serrate (Fig. 2B). Terminal sternum (IX) simple (Fig. 5D), spiculum gastrale rudimentary, triangular. Ovipositor with valvifers 1.3× longer than coxites (Fig. 6H).

Etymology. The genus is named in honor of H. S. Gorham, the author of chapters on Malacodermata in *Biologia-Centrali Americana* (Gorham 1880, 1881, 1884), where he described many genera and species of Eurrhacini and Calopterini. The gender is neuter.

Distribution. Panama, Ecuador.

***Gorhamium bidentatum* sp. nov.**

<https://zoobank.org/C1E7CBDC-5EBC-457E-BB8D-5B51E6ACE0F6>

Figs 2A, B, 3A, 4A, B, 5A–D, 6C–E, H

Type material. Holotype • male, “PANAMA, V. de Chiriqui, 25–4000 ft. Champion”, secondary labels - B.C.A. Col. III. (2). *Calocladon chiriquense*, SYNTYPE - blue-edged circle (BMNH). [Volcan de Chiriqui is now referred to as Volcán Barú].

Paratypes • PANAMA, same data as for holotype, 1 male, 3 females (BMNH); • “PANAMA, V. de Chiriqui, 2-3000 ft. Champion”, secondary labels - same data as for holotype, SYNTYPE - blue-edged circle, 1 female (BMNH); • “PANAMA, V. de Chiriqui, 4000–6000 ft. Champion, secondary labels - same data as for holotype, SYNTYPE - blue-edged circle, 3 males (BMNH).

Diagnosis. Pronotum and elytra largely yellow, only median longitudinal stripe on pronotum, basal half of elytral suture, and elytral apex black. Phallus rod-like apically, ventromedial opening oval, widest medially. Parameres shorter than half of phallus, their ventrobasal projects separated (d_1 , Fig. 6C), apex of parameres bidentate, internal sac largely membranous, micro spurs barely visible.

Description. Body length: 5.1–6 mm, width across the humeri: 1.1–1.2 mm. Body dark brown, only anterior pronotal margin, broad sides of pronotum, trochanters, bases of femora, scutellum, and most of elytra yellow (Fig. 2A, B). Sutural stripe in basal half of elytra and apical 1/30 of elytra black. Head largely covered by pronotum. Elytra 4–4.8× longer than humeral width (Fig. 2A). Primary costae 2 and 4 and basal quarter of primary costa 3 more elevated. Reticulate cells irregular, secondary costae 3 and 4 present only basally.

Male. Eyes large, hemispherically prominent, eye diameter 1.5–1.7× longer than interocular distance. Antennae with antennomere 3 (=A3) 1.15× shorter than A4, A4–A10 subequal in length; antennal branches flattened, lamella of A3 1.7× longer than antennomere length, remaining lamellae considerably longer, ~ 2.4× longer than antennomere length (Fig. 4B). Abdominal sternum VIII with a broad, shallow emargination distally (up to 1/5 of sternum length), its proximal margin minutely



Figure 3. Pronotum **A** *Gorhamium bidentatum* sp. nov., male **B** *Gorhamium unidentatum* sp. nov., male.

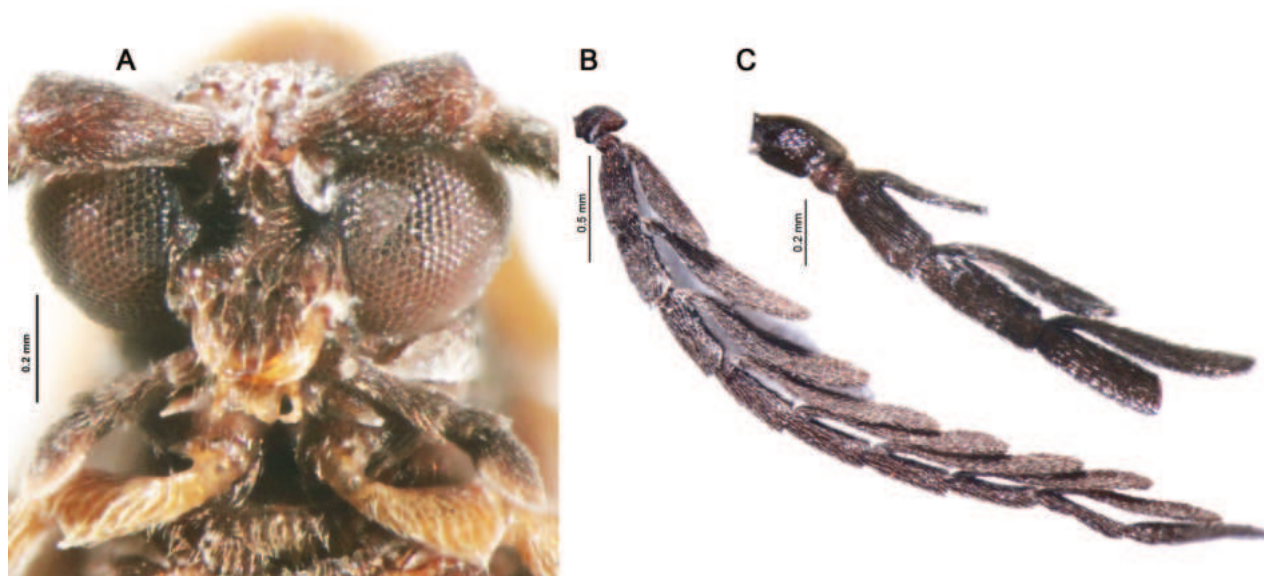


Figure 4. A head ventrally B, C antenna dorsally A, B *Gorhamium bidentatum* sp. nov., male C *Gorhamium unidentatum* sp. nov., male.

emarginated up to 1/10 of sternum length (Fig. 5C). Tergum X small, only 1.3× longer than preceding sternum IX on the sides (Fig. 5B). Phallus rod-like in distal 1/3, slightly widened apically, with a dorsal hook in median portion (c, Fig. 6D) and large ventral opening widest medially (b, Fig. 6C). Parameres moderately shorter than half of phallus, each with two coarse teeth apically, ventrobasal parameral protrusions slender, medially separated by 1/3 of phallic width (Fig. 6C).

Female. Eyes small, eye diameter 1.3× shorter than interocular distance. Antennae serrate (Fig. 2B). Terminal sternum with spiculum gastrale rudimentary, triangular to slightly pointed (Fig. 5D). Ovipositor elongate (Fig. 6H), valvifers rod-like, 1.4× longer than coxites, basally coalescent. Coxites medially distant, their base and apex closer, styli as long as half of coxites.

Etymology. Named after the shape of apical portion of parameres.

Distribution. Panama.

***Gorhamium unidentatum* sp. nov.**

<https://zoobank.org/8CEF51B9-4C36-4654-BEB4-B3BFA4F63DC3>

Figs 2C, 3B, 4C, 5E–H, 6F, G

Type material. Holotype • male, “ECUADOR, 50 km SW Quito, San Francisco de las Pampas, Otonga res., 1500 m, 0°25’S, 79°00’W, 5–6.Dec 2010, Bolm lgt.” (UPOL).

Diagnosis. Pronotum black. Elytra bicolor orange-black with suture, longitudinal median oval spot, and triangular apical spot black. Phallus ball-shaped apically, ventromedial opening widest in basal third. Apex of each paramere fitted with a sharp laterally projected tooth, internal sac with a series of diminutive teeth (e, Fig. 6G).

Description. Body length: 6.4 mm, width across the humeri: 1.2 mm. Body black, only elytral sidebars orange (with whole suture, longitudinal median oval spot and triangular spot in apical quarter black, remaining sidebars orange (Fig. 2C). Head mostly hidden by pronotum in dorsal view. Elytra slender, 4.5×

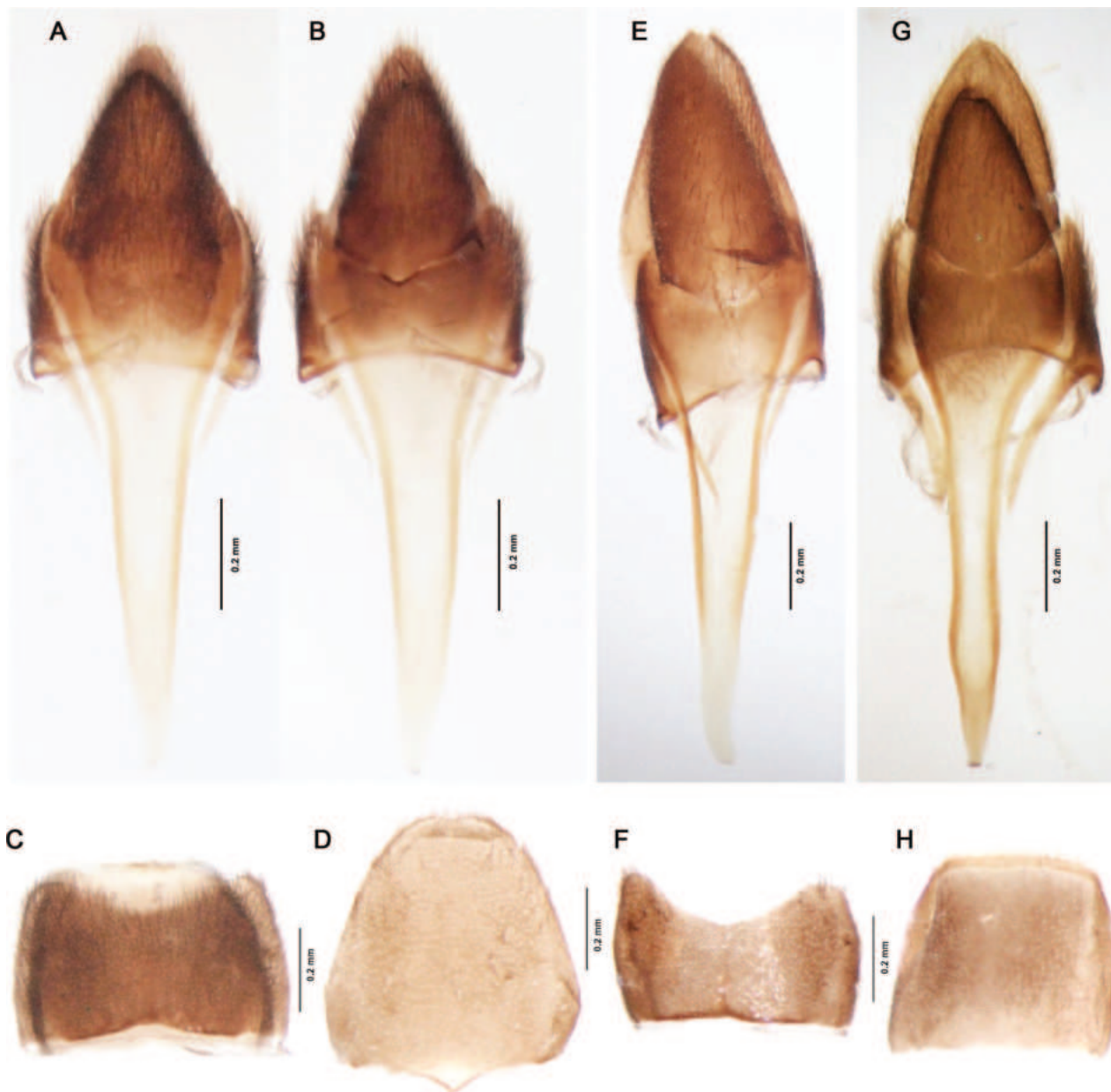


Figure 5. Terminal abdominal segments **A–D** *Gorhamium bidentatum* sp. nov. **E–H** *Gorhamium unidentatum* sp. nov., male **G** *Cladocalon chiriquense* (Gorham, 1884) **A, B, E, G** male terminalia (sternum IX and tergum IX–X), **A** – ventral view; **B, E, G** – dorsal view **C** Male sternum and tergum VIII, ventral view **D** female terminal sternum, ventral view. **F**, Male sternum VIII, ventral view **H** Male tergum VIII, dorsal view.

longer than humeral width (Fig. 2C); primary costae 2 and 4 and basal 1/5 of primary costa 3 elevated; reticulate cells oval, strongly irregular, secondary costae 3 and 4 diminishing apically.

Male. Eyes medium-sized, interocular distance 1.3× longer than eye diameter (Fig. 3B). Antennae with antennomere 3 (= A3) 1.3× shorter than A4, A4–A10 subequal in length; antennal branches flattened, considerably lengthening medially, A3 lamella 1.2× longer than antennomere A3 length, A4 lamella 1.35× longer than A4 length, A5 lamella 1.5× longer than A5 length (Fig. 4C). Abdominal sternum VIII widely emarginated in distal third (Fig. 5F), its proximal margin almost straight. Tergum X elongate, 1.7× longer than sternum IX on the sides



Figure 6. A–G, Male genitalia A, B *Cladocalon chiriquense* (Gorham, 1884) C–E *Gorhamium bidentatum* sp. nov. F–H *Gorhamium unidentatum* sp. nov. H female genitalia of *Gorhamium bidentatum* sp. nov., ventral view. A, C, F ventral view B, D, G lateral view E ventrolateral view. Abbreviations: a1 – pointed anchor-shaped base of phallus, a2 – flat anchor-shaped base of phallus, b – phallic ventral opening, c – dorsal dent, d1 – arcuate ventrobasal parameral process, d2 – flattened ventrobasal parameral process, d3 – a ring-like ventral bridge (ventrobasal processes medially fused), e – internal sac.

(Fig. 5E). Phallus bent ventrally in distal 1/3, constricted subapically, apex ball-shaped; ventromedial opening widest in basal quarter (b, Fig. 6G); dorsal hook shifted in distal quarter (c, Fig. 6G). Parameres as long as 2/3 of phallus, with a single, laterally projected, apical tooth; ventrobasal parameral protrusions slender, joined medially in a ring-like bridge (d₃, Fig. 6G).

Female. Unknown.

Etymology. The specific name refers to the single sharp tooth at the apex of each paramere.

Distribution. Ecuador.

Key to genera of Eurrhacini

- 1 Each elytron with only 4 longitudinal costae, secondary costae absent..... **Haplobothris Bourgeois, 1879**
- Each elytron with 9 longitudinal costae, alternate costae strong, more elevated..... **2**
- 2 Pronotum with a median longitudinal carina, areola absent, or at most slot-like **3**
- Pronotum with longitudinal carinae forming median longitudinal areola **4**
- 3 Median longitudinal areola on pronotum absent, posterior pronotal margin with prominent medioposterior protrusion covering whole scutellum, male antennae flabellate..... **Lycoplateros Pic, 1922**
- Median longitudinal areola on pronotum slot-like, basal margin of pronotum almost straight in median portion, scutellum visible, male antennae serrate **Neolinoptes Nascimento & Bocakova, 2017**
- 4 Aedeagus trilobate, parameres often shortened, but separate from the phallus, basal portion of each paramere with an arcuate ventral protrusion, usually joining medially in a ring-like bridge (character 45, state 1) **7**
- Aedeagus unilobed, parameres either absent, or strongly shortened and coalescent with phallus, sometimes with remnants of sutures dorsally **5**
- 5 Male genitalia with phallobase not fused to phallus and parameres, terminal maxillary palpomere enlarged, 1.8× longer than palpomere 2 (P2); parameres entirely integrated into the widened basal 1/10–1/3 of tubular phallus, posterior trochanters spinose **Eurrhacus Waterhouse, 1879**
- Male genitalia with phallobase fused to phallus and parameres (if present), terminal maxillary palpomere small, 1.3–1.6× shorter than P2 **6**
- 6 Phallus and phallobase ventrally coalescent to parameres, basal 3/5 of phallus with integrated parameres conical, parameres dorsally visible, slightly folded. Terminal maxillary palpomere 1.3× shorter than P2, posterior trochanters triangular **Emplectus Erichson, 1847**
- Parameres absent, phallus S-shaped, basally fused to median portion of phallobase, terminal maxillary palpomere 1.6× shorter than P2 **Currhaeus Nascimento, Bressan & Bocakova, 2020**
- 7 Pronotum ~ 1.3× longer than wide; apical half of phallus strongly curved ventrally, parameres short, as long as 1/3 of phallus; base of phallus sharply triangular (character 47, state 1), integrated to dorsobasal portion of parameres; phallobase elongate, as long as 2/3 of phallus..... **Calocladon Gorham, 1881**
- Pronotum wider than long, base of phallus anchor-shaped (inverted mushroom-shaped) (Fig. 6A–G) **8**

- 8 Primary costa 3 usually joined to primary costa 2 in distal 1/3–1/4 of elytra. Parameres almost as long as phallus, laterally compressed, connected basally by a strong annular ventral bridge, apex rounded..... ***Atlanticolycus* Nascimento & Bocakova, 2023**
- Primary costa 3 almost fully developed, not joining to primary costa 2. Parameres shorter than the phallus by at least a quarter of the length, distal half flattened, with ventrobasal projects either strongly flattened (Fig. 6A, B), or slender (d_1 , Fig. 6C), sometimes fused forming ventral bridge (d_3 , Fig. 6G) **9**
- 9 Parameres flattened, ribbon-like, L-shaped in lateral view, apex with basally-oriented hooks, ventrobasal parameral projects flattened, sometimes constituting a ventral bridge, base of phallus more or less flat anchor-shaped (inverted mushroom-shaped)..... ***Cladocalon* Nascimento & Bocakova, 2022**
- Parameres basally semicircular in cross-section, apex of parameres with 1 or 2 laterodistal teeth. Ventrobasal parameral projects, or ventral bridge very slender, base of phallus pointed anchor-shaped, or inverted mushroom-shaped (character 47, state 1)..... ***Gorhamium* gen. nov.**

Discussion

The Calopterini

Support for a monophyletic origin of Calopterini and the subtribe Calopterina has been confirmed by previous (Bocakova 2005; Nascimento et al. 2020; Ferreira et al. 2023) and our current (this study) morphology-based analyses. However, the formerly recovered Acroleptina, comprising all neotenic calopterins, is now predominantly paraphyletic (Table 2) and split into two lineages.

The Eurrhacini

Consistent with our results, previous analyses supported the Eurrhacini and showed *Haplobothris* as the deepest branch. The initial trees (Bocakova 2005; Nascimento et al. 2020) further implied an early separation of *Calocladon*. However, after the inclusion of *Xenomorphon*, an enigmatic anelytrous beetle male (Ferreira et al. 2023), *Calocladon* was recovered as a crown group being sister to *Lycoplateros*, although support values were low. By contrast, our results (Fig. 1) have indicated the *Calocladon* clade is sister to *Emplectus* + *Eurrhacus* + *Currhaeus* clade, whereas *Lycoplateros* is recovered as one of early Eurrhacini branches.

The *Calocladon* clade

Our updated dataset is the first to include the recently described *Atlanticolycus* (Brazil), *Cladocalon* (Mexico, Guatemala, and Panama), and *Gorhamium* gen. nov. (Panama, Ecuador) proposed here. The analyses show *Calocladon* and the three closely related genera constitute a highly supported clade (UFBoot = 88, pp = 0.93).

Members of the *Calocladon* clade share two unambiguous synapomorphies (Suppl. materials 3–5), particularly the convergent ventrobasal projections on the parameres that often fuse medially into a ventral bridge (character 45, state 1; Fig. 6G, d_3). The character is present in all genera, although the length and thickness of these projections varies. While *Calocladon* and *Atlanticolycus*

Table 2. Support for major Calopterini and Eurrhacini lineages (Bocakova 2005; Bocak and Bocakova 2008; this study). Branch support values are based on ultrafast bootstrapping (UFBoot) for maximum likelihood (ML) and posterior probabilities (PP) for Bayesian analyses (BA). For maximum parsimony (MP) analyses, clade percentages on the majority-rule consensus tree (MRCT), standard bootstrapping (BS) and symmetric resampling (SR) values are given. Abbreviations: P – paraphyletic or polyphyletic; NW – no weights, IW – implied weights.

Tree search procedures	ML	BA	MP	MP	MP	MP
			NW	NW	NW	IW
	UFBoot	PP	MRCT	BS	SR	MRCT
Calopterini + Eurrhacini	65	38	100	22	24	100
Calopterini	51	29	91	6	10	P
Calopterina	77	52	P	10	16	100
Acroleptina	P	P	100	P	P	100
Eurrhacini	78	51	100	1	2	100
<i>Calocladon</i> clade	88	93	100	49	55	100
<i>Eurrhacus</i> clade	P	P	100	P	P	100

have the strongly developed ventral bridge of the parameres, the ventrobasal parameral projects are often shorter and less pronounced in the *Cladocalon* + *Gorhamium* clade. The second unambiguous synapomorphy of the *Calocladon* clade is the strong, sharply triangular, or inverted mushroom-shaped base of phallus (character 47, state 1). Furthermore, *Cladocalon* has the characteristic L-shaped parameres. The feature is also present in *Gorhamium unidentatum* sp. nov. (Fig. 6G), while it is only indicated in *G. bidentatum* sp. nov. (Fig. 6C, D). Genera *Cladocalon*, *Atlanticolycus*, and *Gorhamium* gen. nov. also share several external characters as flabellate antennae in males, transversely trapezoidal pronotum with lenticular median areola (areola absent, replaced by median longitudinal carina in *Lycoplateros* and *Neolinoptes*), and each elytron with nine longitudinal costae (i.e., secondary less elevated alternate costae present). Conversely, secondary costae are absent in *Haplobothris* (each elytron with only four longitudinal costae). While in *Eurrhacus* and *Lycoplateros* primary costae 1 and 3 are strongly elevated, the genera of the *Calocladon* clade have primary costae 1 and 3 only slightly thicker compared to primary costae 2 and 4. These features are also shared by *Calocladon*, except for its characteristic elongated pronotum and considerably more slender median areola.

Acknowledgements

We would like to thank M. Geiser (The Natural History Museum, London) who has kindly searched and loaned us H. S. Gorham's syntypes. We are also indebted to V. S. Ferreira for sending preliminary photographs of syntypes from the NHMUK.

Additional information

Conflict of interest

The authors have declared that no competing interests exist.

Ethical statement

No ethical statement was reported.

Funding

This study was supported by a GFD_PdF_2023_06 grant from Palacky University Olomouc (Czech Republic).

Author contributions

Both authors contributed to this work.

Author ORCIDs

Elynton Alves Nascimento  <https://orcid.org/0000-0002-9071-2823>

Milada Bocakova  <https://orcid.org/0000-0002-2507-0887>

Data availability

All of the data that support the findings of this study are available in the main text or Supplementary Information.

References

- Bocak L, Bocakova M (2008) Phylogeny and classification of the family Lycidae (Insecta: Coleoptera). *Annales Zoologici* 58(4): 695–720. <https://doi.org/10.3161/000345408X396639>
- Bocak L, Bocakova M, Hunt T, Vogler AP (2008) Multiple ancient origins of neoteny in Lycidae (Coleoptera): Consequences for ecology and macroevolution. *Proceedings. Biological Sciences* 275(1646): 2015–2023. <https://doi.org/10.1098/rspb.2008.0476>
- Bocakova M (2003) Revision of the Tribe Calopterini (Coleoptera, Lycidae). *Studies on Neotropical Fauna and Environment* 38(3): 270–234. <https://doi.org/10.1076/snfe.38.3.207.28169>
- Bocakova M (2005) Phylogeny and classification of the tribe Calopterini (Coleoptera, Lycidae). *Insect Systematics & Evolution* 35(4): 437–447. <https://doi.org/10.1163/187631204788912472>
- Bremer K (1994) Branch support and tree stability. *Cladistics* 10(3): 295–304. <https://doi.org/10.1111/j.1096-0031.1994.tb00179.x>
- Ferreira VS, Barbosa FF, Bocakova M, Solodovnikov A (2023) An extraordinary case of elytra loss in Coleoptera (Elateroidea: Lycidae): discovery and placement of the first anelytrous adult male beetle. *Zoological Journal of the Linnean Society* 199(2): 553–566. <https://doi.org/10.1093/zoolinnean/zlad026>
- Goloboff PA (1993) Estimating character weights during tree search. *Cladistics* 9(1): 83–91. <https://doi.org/10.1111/j.1096-0031.1993.tb00209.x>
- Goloboff PA, Catalano SA (2016) TNT version 1.5, including a full implementation of phylogenetic morphometrics. *Cladistics* 32(3): 221–238. <https://doi.org/10.1111/cla.12160>
- Goloboff PA, Farris JS, Nixon K (2008) TNT: A free program for phylogenetic analysis. *Cladistics* 24(5): 774–786. <https://doi.org/10.1111/j.1096-0031.2008.00217.x>
- Gorham HS (1880) Malacodermata. Fam. Lycidae. *Biologia Centrali-Americana. Coleoptera* 3: 1–24.
- Gorham HS (1881) Malacodermata. Fam. Lycidae. *Biologia Centrali-Americana. Coleoptera* 3: 25–29.
- Gorham HS (1884) Malacodermata. Supplement. Fam. Lycidae. *Biologia Centrali-Americana. Coleoptera* 3: 225–272.

- Kalyaanamoorthy S, Minh BQ, Wong TKF, von Haeseler A, Jermini LS (2017) ModelFinder: Fast model selection for accurate phylogenetic estimates. *Nature Methods* 14(6): 587–589. <https://doi.org/10.1038/nmeth.4285>
- Lewis PO (2001) A Likelihood Approach to Estimating Phylogeny from Discrete Morphological Character Data. *Systematic Biology* 50(6): 913–925. <https://doi.org/10.1080/106351501753462876>
- Masek M, Motyka M, Kusy D, Bocek M, Li Y, Bocak L (2018) Molecular Phylogeny, Diversity and Zoogeography of Net-Winged Beetles (Coleoptera: Lycidae). *Insects* 9(4): 154. <https://doi.org/10.3390/insects9040154>
- Minh BQ, Schmidt HA, Chernomor O, Schrempf D, Woodhams MD, von Haeseler A, Lanfear R (2020) IQ-TREE 2: New models and efficient methods for phylogenetic inference in the Genomic Era. *Molecular Biology and Evolution* 37(5): 1530–1534. <https://doi.org/10.1093/molbev/msaa015>
- Nascimento EA, Bocakova M (2017) A revision of neotropical genus *Eurrhacus* (Coleoptera: Lycidae). *Annales Zoologici* 67(4): 689–697. <https://doi.org/10.3161/00034541ANZ2017.67.4.006>
- Nascimento EA, Bocakova M (2022) *Cladocalon*, a new genus of net-winged beetles from Central America and Mexico (Coleoptera: Lycidae). *Zootaxa* 5124(5): 577–584. <https://doi.org/10.11646/zootaxa.5124.5.6>
- Nascimento EA, Bocakova M (2023) A new genus of Eurrhacini from the Brazilian Atlantic Forest (Coleoptera: Lycidae: Lycinae). *Zootaxa* 5383(2): 242–250. <https://doi.org/10.11646/zootaxa.5383.2.8>
- Nascimento EA, Bressan TD, Bocakova M (2020) *Currhaeus*, a new genus of net-winged beetles and phylogenetic analysis of Eurrhacini (Coleoptera: Lycidae: Lycinae). *Zootaxa* 4869(3): 387–403. <https://doi.org/10.11646/zootaxa.4869.3.5>
- Nixon KC (2002) WinClada ver. 1.0000. Published by the author, Ithaca, NY, USA.
- Ronquist F, Teslenko M, van der Mark P, Ayres DL, Darling A, Höhna S, Larget B, Liu L, Suchard MA, Huelsenbeck JP (2012) MrBayes 3.2: Efficient Bayesian phylogenetic inference and model choice across a large model space. *Systematic Biology* 61(3): 539–542. <https://doi.org/10.1093/sysbio/sys029>

Supplementary material 1

List of morphological characters

Authors: Elynton Alves do Nascimento, Milada Bocakova

Data type: docx

Explanation note: List of morphological characters (adapted from Bocakova 2005; Nascimento et al. 2020; Ferreira et al. 2023). Characters 6 and 42 were edited. Characters 12, 17, 21, and 30 include new character states. Characters 44–51 were newly added.

Copyright notice: This dataset is made available under the Open Database License (<http://opendatacommons.org/licenses/odbl/1.0/>). The Open Database License (ODbL) is a license agreement intended to allow users to freely share, modify, and use this Dataset while maintaining this same freedom for others, provided that the original source and author(s) are credited.

Link: <https://doi.org/10.3897/zookeys.1204.114932.suppl1>

Supplementary material 2

Bayesian phylogeny of Calopterini and Eurrhacini

Authors: Elynton Alves Nascimento, Milada Bocakova

Data type: tif

Explanation note: Bayesian phylogeny of Calopterini and Eurrhacini inferred from morphological data, node labels represent posterior probabilities.

Copyright notice: This dataset is made available under the Open Database License (<http://opendatacommons.org/licenses/odbl/1.0/>). The Open Database License (ODbL) is a license agreement intended to allow users to freely share, modify, and use this Dataset while maintaining this same freedom for others, provided that the original source and author(s) are credited.

Link: <https://doi.org/10.3897/zookeys.1204.114932.suppl2>

Supplementary material 3

Strict consensus of 23 parsimony trees of Calopterini and Eurrhacini using equal weights

Authors: Elynton Alves Nascimento, Milada Bocakova

Data type: tif

Explanation note: Unambiguous character changes mapped on branches in WinClada, black circles represent nonhomoplasious changes, white circles homoplasious changes. Circles are labelled with small character numbers above and character states below.

Copyright notice: This dataset is made available under the Open Database License (<http://opendatacommons.org/licenses/odbl/1.0/>). The Open Database License (ODbL) is a license agreement intended to allow users to freely share, modify, and use this Dataset while maintaining this same freedom for others, provided that the original source and author(s) are credited.

Link: <https://doi.org/10.3897/zookeys.1204.114932.suppl3>

Supplementary material 4

Strict consensus of 23 unweighted parsimony trees, fast optimization using ACCTRAN

Authors: Elynton Alves Nascimento, Milada Bocakova

Data type: tif

Explanation note: Fast optimization using accelerated (ACCTRAN) transformations mapped on branches in WinClada, black circles represent non-homoplasious changes, white circles homoplasious changes. Circles are labelled with small character numbers above and character states below.

Copyright notice: This dataset is made available under the Open Database License (<http://opendatacommons.org/licenses/odbl/1.0/>). The Open Database License (ODbL) is a license agreement intended to allow users to freely share, modify, and use this Dataset while maintaining this same freedom for others, provided that the original source and author(s) are credited.

Link: <https://doi.org/10.3897/zookeys.1204.114932.suppl4>

Supplementary material 5

Strict consensus of 23 unweighted parsimony trees, fast optimization using DELTRAN

Authors: Elynton Alves Nascimento, Milada Bocakova

Data type: tif

Explanation note: Slow optimization using delayed (DELTRAN) transformations mapped on branches in WinClada, black circles represent nonhomoplasious changes, white circles homoplasious changes. Circles are labelled with small character numbers above and character states below.

Copyright notice: This dataset is made available under the Open Database License (<http://opendatacommons.org/licenses/odbl/1.0/>). The Open Database License (ODbL) is a license agreement intended to allow users to freely share, modify, and use this Dataset while maintaining this same freedom for others, provided that the original source and author(s) are credited.

Link: <https://doi.org/10.3897/zookeys.1204.114932.suppl5>

Supplementary material 6

The majority-rule consensus of the 23 MP trees from the initial equal weights parsimony analysis of Calopterini and Eurrhacini

Authors: Elynton Alves Nascimento, Milada Bocakova

Data type: tif

Copyright notice: This dataset is made available under the Open Database License (<http://opendatacommons.org/licenses/odbl/1.0/>). The Open Database License (ODbL) is a license agreement intended to allow users to freely share, modify, and use this Dataset while maintaining this same freedom for others, provided that the original source and author(s) are credited.

Link: <https://doi.org/10.3897/zookeys.1204.114932.suppl6>

Supplementary material 7

Bremer support values mapped on the strict consensus of 23 parsimony unweighted trees of Calopterini and Eurrhacini

Authors: Elynton Alves Nascimento, Milada Bocakova

Data type: tif

Copyright notice: This dataset is made available under the Open Database License (<http://opendatacommons.org/licenses/odbl/1.0/>). The Open Database License (ODbL) is a license agreement intended to allow users to freely share, modify, and use this Dataset while maintaining this same freedom for others, provided that the original source and author(s) are credited.

Link: <https://doi.org/10.3897/zookeys.1204.114932.suppl7>

Supplementary material 8

Branch support using standard bootstrapping applied on the unweighted Calopterini-Eurrhacini dataset

Authors: Elynton Alves Nascimento, Milada Bocakova

Data type: tif

Copyright notice: This dataset is made available under the Open Database License (<http://opendatacommons.org/licenses/odbl/1.0/>). The Open Database License (ODbL) is a license agreement intended to allow users to freely share, modify, and use this Dataset while maintaining this same freedom for others, provided that the original source and author(s) are credited.

Link: <https://doi.org/10.3897/zookeys.1204.114932.suppl8>

Supplementary material 9

Branch support using symmetric resampling applied on the unweighted Calopterini-Eurrhacini dataset

Authors: Elynton Alves Nascimento, Milada Bocakova

Data type: tif

Copyright notice: This dataset is made available under the Open Database License (<http://opendatacommons.org/licenses/odbl/1.0/>). The Open Database License (ODbL) is a license agreement intended to allow users to freely share, modify, and use this Dataset while maintaining this same freedom for others, provided that the original source and author(s) are credited.

Link: <https://doi.org/10.3897/zookeys.1204.114932.suppl9>

Supplementary material 10

The single implied weighted parsimony tree using TNT and the concavity constant in the range $k = 3-25$

Authors: Elynton Alves Nascimento, Milada Bocakova

Data type: tif

Copyright notice: This dataset is made available under the Open Database License (<http://opendatacommons.org/licenses/odbl/1.0/>). The Open Database License (ODbL) is a license agreement intended to allow users to freely share, modify, and use this Dataset while maintaining this same freedom for others, provided that the original source and author(s) are credited.

Link: <https://doi.org/10.3897/zookeys.1204.114932.suppl10>

Review of the genus *Paradelius* De Saeger, 1942 of East Asia (Hymenoptera, Braconidae, Cheloninae, Adeliini) with the description of a new species from South Korea

Sergey A. Belokobylskij¹, Deokseo Ku², Xue-xin Chen³

1 Zoological Institute, Russian Academy of Sciences, St Petersburg 199034, Russia

2 The Science Museum of Natural Enemies, Geochang 50147, Republic of Korea

3 Institute of Insect Sciences, College of Agriculture and Biotechnology, Zhejiang University, Hangzhou 310058, China

Corresponding author: Sergey A. Belokobylskij (doryctes@gmail.com)

Abstract

The East Palaearctic species of the adeliine genus *Paradelius* De Saeger, 1942 are reviewed. The genus *Sculptomyriola* Belokobylskij, 1988 is synonymised with *Paradelius* and treated as its subgenus. The following species are transferred to subgenus *Paradelius* (*Sculptomyriola*): *P.* (*Sc.*) *extremiorientalis* (Belokobylskij, 1988), **comb. nov.**; *P.* (*Sc.*) *ghilarovi* (Belokobylskij, 1988), **comb. nov.**; *P.* (*Sc.*) *neotropicalis* Shimbori & Shaw, 2019; *P.* (*Sc.*) *nigrus* Whitfield, 1988; *P.* (*Sc.*) *rubrus* Whitfield, 1988; *P.* (*Sc.*) *sinevi* (Belokobylskij, 1998), **comb. nov.** A new species *Paradelius* (*Sculptomyriola*) *koreanus* **sp. nov.** from Korean Peninsula is described. The genus *Sinadelius* He & Chen, 2000 is synonymised with *Paradelius* De Saeger and also treated as its subgenus. The species *Sinadelius guangxiensis* He & Chen, 2000 and *S. nigricans* He & Chen, 2000 are transferred to *Paradelius* (*Sinadelius*) (**comb. nov.**). A key for determination of the World known *Paradelius* species from three its subgenera, *Paradelius* s.str., *Sculptomyriola* Belokobylskij and *Sinadelius* He & Chen, and illustrated redescriptions of the type of genus and its Asian species are provided.

Key words: Ichneumonoidea, new species, new synonyms, parasitoids, redescriptions, *Sculptomyriola*, *Sinadelius*



Academic editor: Kees van Achterberg

Received: 25 March 2024

Accepted: 22 April 2024

Published: 7 June 2024

ZooBank: <https://zoobank.org/D398FB26-DB4A-4FA1-B8FC-117BDDECC197>

Citation: Belokobylskij SA, Ku D, Chen X-xin (2024) Review of the genus *Paradelius* De Saeger, 1942 of East Asia (Hymenoptera, Braconidae, Cheloninae, Adeliini) with the description of a new species from South Korea. ZooKeys 1204: 261–299. <https://doi.org/10.3897/zookeys.1204.123909>

Copyright: © Sergey A. Belokobylskij et al.
This is an open access article distributed under terms of the Creative Commons Attribution License (Attribution 4.0 International – CC BY 4.0).

Introduction

The members of the braconid wasps of the small tribe Adeliini have been considered as a separate subfamily in the Braconidae microgasteroid complex for a long time (Čapek 1970; Tobias 1986; Belokobylskij 1988, 1998; Quicke and van Achterberg 1990; van Achterberg 1993; Whitfield 1997; Shi et al. 2005). However, the following morphological and especially molecular phylogenetic analyses of the Braconidae subfamilies (Whitfield and Mason 1994; Downton and Austin 1998; Kittel et al. 2016) have shown that this taxonomic group is nested within the subfamily Cheloninae, and subsequently it has been treated only as a chelonine tribe (Chen and van Achterberg 2019; Shimbori et al. 2019; Jasso-Martínez et al. 2022).

This subfamily (and later tribe) was long time considered to consist of four genera: *Adelius* Haliday, 1833 (with its synonyms *Acaelius* Haliday, 1834, *Acoelius* Haliday, 1835, *Anomopterus* Rohwer, 1914, *Myriola* Shestakov, 1932, and *Pleiomerus* Wesmael, 1837), *Paradelius* De Saeger, 1942, *Sculptomyriola* Belokobylskij, 1988, and *Sinadelius* He & Chen, 2000 (Yu et al. 2016; Shimbori et al. 2019). The members of this taxonomic group are relatively rarely presented in the scientific collection (perhaps except for *Adelius*), although the adeliine wasps have an almost worldwide distribution.

Adeliine species are known as solitary koinobiont larval or perhaps egg-larval endoparasitoids of mainly leaf-mining moths from predominantly the families Nepticulidae, but also were reared from the species of the families Coleophoridae, Gracillariidae, Lyonetiidae, Tischeriidae and Tortricidae (Yu et al. 2016; Shimbori et al. 2019).

In this article, the description of a new species, two generic synonyms, five new combinations, and redescriptions of the *Paradelius* type species and seven East Asian species are provided, and a key to all adeliine genera and *Paradelius* species is compiled.

Materials and methods

The braconid specimens were examined with an Olympus SZ51 stereomicroscope. Photographs were obtained using a Canon EOS 70D digital camera mounted on an Olympus SZX10 microscope (Zoological Institute RAS, St Petersburg). The photographs of Chinese species were made by a digital microscope (KEYENCE VHX-2000, Osaka, Japan) (Zhejiang University, Hangzhou). Image stacking was performed using Helicon Focus 8.0. The figures were produced using the Adobe Photoshop CS6 and CC2018 programs. In the keys, additional features useful for separating species are listed after the dash (-).

The terminology used for morphological features, sculpture, and body measurements follow Belokobylskij and Maetô (2009). Wing venation nomenclature also follows Belokobylskij and Maetô (2009), with the terminology of van Achterberg (1993) shown in parentheses.

Abbreviations are indicated for the type material as **HT**, holotype and **PT**, paratype. Abbreviations of specimen depositories and collections are as follows:

- AMTB** African Museum, Tervuren, Belgium;
- NIBR** National Institute of Biological Resources, Incheon, Republic of Korea;
- SMNE** the Science Museum of Natural Enemies, Geochang, Republic of Korea;
- ZISP** the Zoological Institute of the Russian Academy of Sciences, St Petersburg, Russia;
- ZJUH** Parasitoid Hymenoptera Collection of the Institute of Insect Sciences, Zhejiang University, Hangzhou, China.

Taxonomy

Class Insecta Linnaeus, 1758

Order Hymenoptera Linnaeus, 1758

Family Braconidae Nees, 1811

Subfamily Cheloninae Foerster, 1863

Tribe Adeliini Viereck, 1918

Key to the World genera of the tribe Adeliini

- 1 All metasomal tergites smooth, only rarely first tergite shortly rugose-striate in basomedial excavation; sutures between first and second and second and third tergites absent or very weak, present as track.....
..... ***Adelius* Haliday, 1833**
- First metasomal tergite entirely, second tergite entirely or at least basally, and often third tergites in basal 0.3–0.8 rugose-reticulate and sometimes partly with striation; sutures between first and second and often also between second and third tergites present, distinct, rather wide and crenulate or rugose, but sometimes partially hidden by irregular sculpture (Figs 11, 2F, 3F, 5G, 6G, 7G, 9D, 10F, 11G).....***Paradelius* De Saeger, 1942 (*Sculptomyriola* Belokobylskij, 1988, syn. nov.; *Sinadelius* He & Chen, 2000, syn. nov.)**

Genus *Paradelius* De Saeger, 1942

Paradelius De Saeger, 1942: 313; Belokobylskij 1988: 148; Whitfield 1988: 313; He et al. 2000: 682; Yu et al. 2016; Shimbori et al. 2019: 190.

Sculptomyriola Belokobylskij, 1988: 145 (type species: *S. extremiorientalis* Belokobylskij, 1988) (syn. nov.); He et al. 2000: 681; Yu et al. 2016; Shimbori et al. 2019: 154.

Sinadelius He & Chen in He et al. 2000: 681 (type species: *S. guangxiensis* He & Chen, 2000) (syn. nov.); Yu et al. 2016; Shimbori et al. 2019: 154.

Type species. *Paradelius ghesquierei* De Saeger, 1942, for primary designation and monotypy.

Notes. A careful restudy of the type species of the genus *Paradelius* De Saeger, with the redescribed *P. ghesquierei* De Saeger, as well as the descriptions of all known taxa of this and related genera (Belokobylskij 1988; Whitfield 1988; He et al. 2000; Shimbori et al. 2019) and available material for most Asian *Paradelius* species have shown that the characters suggested for the separation of *Sculptomyriola* from *Paradelius* (mainly fore wing venation, sculpture of metasoma, and condition of prepectal carina) are distinctly variable, not taxonomically stable and as result, not available for use as generic features. The infrageneric variation of the adeliine fore wing venation was already noted in the genus *Adelius* Haliday on the examples of the species originally described in the synonymised genus *Myriola* Shestakov, 1932 (Muesebeck and Walkley 1951; Yu et al. 2016). Additionally, only laterally developed prepectal carina (which is reduced below) in the type species of *Paradelius* De Saeger, *P. ghesquierei* De Saeger, as well as in *P. chinensis* He & Chen, 2000, are variable, weakly visible (often because of distinct sculpture surrounding this carina) or reduced in other species former belonged to *Sculptomyriola*. As a result of this study, *Sculptomyriola* Belokobylskij, 1988 is synonymised under *Paradelius* De Saeger, 1942 (syn. nov.), but we keep this name as a subgeneric subdivision including the larger part of previously described species of *Paradelius*.

The different levels of sculpture covering the first three metasomal tergites found in the *Paradelius* and *Sinadelius* species studied (and even in some

Adelius) as well as its variation in the sculpture distribution surface, also allow the name *Sinadelius* He & Chen, 2000 to be synonymised with *Paradelius* De Saeger, 1942 (syn. nov.). However, this name with three known eastern Asian species should be kept as a subgeneric subdivision of *Paradelius* because the members of *Sinadelius* have kept sculpture basically only on the whole first and basal part of second tergites (by the way, the second tergite is incompletely sculptured also in the type of the genus, *P. ghesquierei* De Saeger), and with only weakly designated second suture.

Redescription of the genus. Head transverse (dorsal view). Occipital carina distinct and complete, joined below with hypostomal carina. Vertex densely reticulate-punctate, sometimes additionally with irregular transverse striae. Ocelli relatively small, arranged in triangle with base 1.1–1.3× its sides. Eye large, covered by dense and long or short setae. Frons weakly concave, sometimes with medial longitudinal carina. Clypeal suture deep and complete. Clypeus weakly or distinctly convex in lower margin. Malar suture distinct and complete. Antenna relatively short, thickened, setiform or filiform. Scape long and wide, 2.0–2.5× longer than maximum width; pedicel short. Flagellar segments in apical quarter of antenna longitudinal or subsquare to transverse. Mesosoma relatively short and high. Mesoscutum densely and distinctly punctate, high and curvedly elevated above pronotum. Notauli absent. Prescutellar depression short or very short and distinctly crenulate. Prepectal carina variable, present laterally at least weakly or completely absent, always absent ventrally. Precoxal sulcus distinct, narrow or wide, long, distinctly sinuate, entirely crenulate or rugulose. Mesopleuron mainly smooth. Propodeum usually with areas delineated by distinct carinae, partly or widely smooth or entirely rugose. Fore wing with large pterostigma. Radial vein (r + 3-SR) with one (r) or two (r + 3-SR) abscissae, with its distal 0.5–0.7 transparent; vein arising from pterostigma separately from first radiomedial vein (2-SR) or joined and from one point of pterostigma, sometimes first radiomedial vein (2-SR) arising from short first abscissa of radial vein (r) closely to pterostigma. Discoidal (discal) cell large, anteriorly usually sessile on parastigma, but sometimes shortly petiolate near parastigma. Recurrent vein (m-cu) usually postfurcal to first radiomedial vein (2-SR), only rarely subinterstitial or very weakly antefurcal. Mediocubital vein (M+CU1) distinctly curved towards longitudinal anal vein (1-1A). Brachial (subdiscal) cell widely open distally; most part of second abscissa of longitudinal anal (2-1A) and brachial (CU1b) veins absent. In hind wing, radial (marginal) cell without additional transverse vein (r). First abscissa of mediocubital vein (M+CU) distinctly longer than its second abscissa (1-M). Nervellus (cu-a) desclerotised and transparent. Hind coxa enlarged; hind femur wide. Hind tibia clavate, distinctly or strongly widened distally; long inner tibial spur not shorter than half of basitarsus. First and second segments of hind tarsus sometimes with distinct transparent keels below. Claw small and distinctly or weakly curved. Metasoma at least weakly depressed dorsoventrally, with immovably fused from first to third tergites, not formed complete coarse carapace and its posterior metasomal tergites usually distinctly protruding behind third tergite. First tergite without or with small dorsope, without dorsal carinae. Both sutures (between first and second, second and third tergites)

present, rather deep or shallow, relatively narrow and densely sculptured. First and second tergites entirely or also third tergite at least in basal third or half densely striate-rugulose. Ovipositor short.

Composition. *Paradelius (Paradelius) chinensis* He & Chen, 2000, *P. (P.) ghesquierei* De Saeger, 1942; *P. (Sculptomyriola) extremiorientalis* (Belokobylskij, 1988), comb. nov., *P. (Sc.) ghilarovi* (Belokobylskij, 1988), comb. nov., *P. (Sc.) koreanus* Belokobylskij & Ku, sp. nov., *P. (Sc.) neotropicalis* Shimbori & Shaw, 2019, *P. (Sc.) nigrus* Whitfield, 1988, *P. (Sc.) rubrus* Whitfield, 1988, *P. (Sc.) sinevi* (Belokobylskij, 1998), comb. nov.; *P. (Sinadelius) guangxiensis* (He & Chen, 2000), comb. nov., *P. (S.) nigricans* (He & Chen, 2000), comb. nov., *P. (S.) ussuriensis* Belokobylskij, 1988.

Hosts. Solitary koinobiont endoparasitoids of leaf-mining moths, *Stigmella* sp. and *Stigmella variella* (Braun, 1910) (Nepticulidae), as well as *Enarmonia* sp. (Tortricidae) (Lepidoptera) (Yu et al. 2016; Shimbori et al. 2019).

A host record for *P. ghesquierei*, *Enarmonia* sp. (Tortricidae) (De Saeger 1942), has not been confirmed later and might be erroneous (Shimbori et al. 2019).

Distribution. East Palaearctic (Russia: Far East; China: Liaoning; Korean Peninsula), Oriental (China: Zhejiang, Guangxi); Afrotropics (D.R. Congo); Nearctic (USA); Neotropics (Costa Rica).

Key to the World species of the genus *Paradelius* De Saeger

- 1 Prepectal carina present laterally and rather distinctly visible. – Propodeum mainly smooth between carinae of areas (Figs 1H, 2F). Third metasomal tergite entirely smooth (Figs 1I, 2F). (Subgenus *Paradelius* s. str.) **2**
- Prepectal carina laterally usually absent or very weakly visible..... **3**
- 2 Recurrent vein (m-cu) of fore wing postfurcal to first radiomedial vein (3-SR) (Figs 1K, 4C). Head behind eyes weakly convex in anterior half and roundly narrowed in posterior half; transverse diameter of eye almost twice longer than temple (dorsal view) (Fig. 1D). Second metasomal tergite rugose-striate in basal 0.8, smooth posteriorly. – D.R. Congo..... **P. (P.) ghesquierei** De Saeger, 1942
- Recurrent vein (m-cu) of fore wing very weakly antifurcal to first radiomedial vein (3-SR) (Figs 2H, 4A). Head behind eyes entirely distinctly roundly narrowed; transverse diameter of eye ~ 4.5× longer than temple (dorsal view) (Fig. 2C). Second metasomal tergite entirely striate with rugosity. – China (Zhejiang) **P. (P.) chinensis** He & Chen, 2000
- 3 First (between first and second tergites) and second (between second and third tergites) sutures distinct and relatively wide. First and second tergites entirely, and often third tergite in basal 0.3–0.8 rugose-reticulate or striate with reticulation (Figs 1I, 2F, 3F, 5G, 6G, 7G). Antenna 20-segmented (Subgenus *Sculptomyriola* Belokobylskij, 1988)..... **4**
- Only first suture (between first and second tergites) distinct and relatively wide; second suture very fine. First tergite entirely and second tergite only basally rugose-reticulate (Figs 9D, 10F, 11G). Antenna 22–23-segmented (Subgenus *Sinadelius* He & Chen, 2000)..... **11**
- 4 Radial vein (r) of fore wing only with single abscissa; first radiomedial vein (2-SR) arising from pterostigma usually distant from radial vein (r),

- or rarely from one point with radial vein (r) (Fig. 4). Medial vein (1-SR+M) of fore wing arising from basal vein (1-M) relatively far from parastigma; discoidal (discal) cell distinctly petiolate or subpetiolate anteriorly (Figs 3H, 4C) **5**
- Radial vein of fore wing with two abscissae (r and 3-SR), first abscissa (r) short; first radiomedial vein (2-SR) arising from radial vein (r) (Fig. 8). Medial vein (1-SR+M) of fore wing arising from parastigma; discoidal (discal) cell sessile anteriorly (Fig. 8)..... **6**
- 5** First radiomedial vein (2-SR) arising from pterostigma from one point with radial vein (r). Sclerotised basal part of metacarp (1-R1) 0.4–0.5× as long as pterostigma (Figs 3H, 4C). Tenth–twentieth antennal segments subsquare (Fig. 3D). Body usually entirely black, rarely head partly reddish brown (Fig. 3A). – Russia (south of Far East), Korean Peninsula (See also couplet 8)..... ***P. (Sc.) extremiorientalis* (Belokobylskij, 1988), comb. nov.**
- First radiomedial vein (2-SR) arising from pterostigma distant from radial vein (r). Sclerotised basal part of metacarp (1-R1) 0.2–0.3× as long as pterostigma. Tenth–twentieth antennal segments weakly elongate. Body entirely or at least partly reddish brown, pale reddish brown or yellowish brown. – USA (California, Wyoming)..... ***P. (Sc.) rubrus* Whitfield, 1988**
- 6** Body completely brownish yellow (Fig. 6A). Third metasomal tergites mainly smooth, only finely rugulose in narrow basomedial part (Fig. 6G). Small, body length 1.5 mm. – Medial segments of antenna weakly transverse or subsquare (Fig. 6D). Propodeum with long and inversely-pentagonal areola delineated by strong and complete carinae (Fig. 6G). First and second metasomal sutures rather weak (Fig. 6G). – Korean Peninsula ***P. (Sc.) koreanus* sp. nov.**
- Body completely dark brown or black, only sometimes with reddish brown areas on head and anterior parts of mesosoma (Figs 5A, 7A). Third metasomal tergites mainly rugose-reticulate and sometimes with additional striation, smooth only in distal 0.2–0.5 (Figs 5G, 7G). Large, body length 2.1–2.7 mm..... **7**
- 7** Antennae distinctly shorter than body, in female length of segments behind middle of antenna distinctly less than their width, these segments transverse (Fig. 5D). Penultimate segment of female antenna 0.75–0.85× as long as wide (Fig. 5D). Body only partly black, most part of head, prothorax, mesoscutum in anterior 0.3–0.5 and part or all mesopleuron reddish brown (Fig. 5A). – Russia (south of Far East), Korean Peninsula ***P. (Sc.) ghilarovi* (Belokobylskij, 1988), comb. nov.**
- Antennae almost equal to or longer than body, in female length of segments behind middle of antenna not less than their width, these segments subsquare or elongated (Fig. 7D). Penultimate segment of female antenna 1.3–1.5× longer than wide (Fig. 7D) (unknown in *P. nigra* and *P. neotropicalis*). Body completely black (Fig. 7A), very rarely head partly (dark) reddish brown **8**
- 8** Medial vein (1-SR+M) of fore wing arising from basal vein (1-M) relatively far from parastigma; discoidal (discal) cell distinctly petiolate anteriorly (Figs 3H, 4B). Sclerotised basal part of metacarp (1-R1) 0.4–0.5× as long as pterostigma (Figs 3H, 4B). – Tenth–twentieth antennal segments

- subsquare (Fig. 3D). (See also couplet 5)
 ***P. (Sc.) extremiorientalis* (Belokobylskij, 1988), comb. nov.**
- Medial vein (1-SR+M) of fore wing arising from parastigma; discoidal (discal) cell sessile anteriorly (Figs 7H, 8C). Sclerotised basal part of metacarp (1-R1) 0.2–0.3× as long as pterostigma (Figs 7H, 8C) **9**
 - 9 Sutures between first and second and second and third tergites distinct and relatively wide (Fig. 3FG). Propodeum smooth within carinae of areas. – USA (Texas) ***P. (Sc.) nigrus* Whitfield, 1988**
 - Sutures between first and second and second and third tergites rather weak and poorly visible, covered by additional sculpture (Fig. 7G). Propodeum rugose-reticulate within distinct carinae of areas (Fig. 7G) **10**
 - 10 Fore wing entirely hyaline (Figs 7H, 8C). Antenna basally pale reddish brown (Fig. 7D). All legs mainly pale reddish brown or yellowish brown (Fig. 7A). Third metasomal tergite rugose-reticulate in basal 0.7–0.8 (Fig. 7G). – Russia (south of Far East) ***P. (Sc.) sinevi* (Belokobylskij, 1998), comb. nov.**
 - Fore wing medially distinctly and widely infusate. Antenna basally dark reddish brown to black. All legs mainly dark reddish brown to black. Third metasomal tergite longitudinally striate in basal 0.8–0.9. – Costa Rica
 ***P. (Sc.) neotropicalis* Shimbori & Shaw, 2019**
 - 11 Body mainly yellowish brown (Fig. 9A). Transverse diameter of eye ~ 2.5× larger than length of temple (dorsal view) (Fig. 9C). First metasomal tergite behind spiracular tubercles subparallel-sided (Fig. 9D). – China (Guangxi) ***P. (S.) guangxiensis* (He & Chen, 2000), comb. nov.**
 - Body mainly black or dark brown, however metasoma often reddish brown (Figs 10A, 11A). Transverse diameter of eye 1.2–1.5× larger than length of temple (dorsal view) (Figs 10C, 11C). First metasomal tergite behind spiracular tubercles narrowed towards its apex (Figs 10F, 11G) **12**
 - 12 First metasomal tergite behind spiracular tubercles distinctly narrowed towards its apex (Fig. 11G). Second suture poorly visible (Fig. 11G). – Russia (Primorskiy Territory) ***P. (S.) ussuriensis* Belokobylskij, 1988**
 - First metasomal tergite behind spiracular tubercles weakly narrowed towards its apex (Fig. 10F). Second suture distinct (Fig. 10F). – China (Liaoning) ***P. (S.) nigricans* (He & Chen, 2000), comb. nov.**

Subgenus *Paradelius* s. str.

Figs 1, 2

***Paradelius (Paradelius) ghesquierei* De Saeger, 1942**

Figs 1, 4A

Paradelius ghesquierei De Saeger 1942: 314; Belokobylskij 1988: 148; Whitfield 1988: 313; Yu et al. 2016.

Material examined. D.R. OF CONGO: “Holotypus *P. ghesquierei* D.S. ♂ [Sic!]” (red), “Musée du Congo, 3728, Rutshuru, II – 1937, J. Ghesquière”, “♀”, “R. dét. X. 4690”, “H. De Saeger det. 1942: *Paradelius Ghesquierei*. Holotype ♀”, 1 female (HT) (AMTB).

Description. Female. Body length 2.0 mm; fore wing length 1.8 mm.



Figure 1. *Paradelius (Paradelius) ghesquierei* De Saeger, 1942 (female, holotype) **A** habitus, dorsal view **B** habitus, lateral view **C** head, front view **D** head, dorsal view **E** head, lateral view **F** antenna, basal segments **G** mesosoma, lateral view **H** mesosoma, dorsal view **I** metasoma, dorsal view **J** hind leg **K** wings.

Head. Head almost twice wider than its medial length (dorsal view), 1.2× wider than mesoscutum. Occiput distinctly evenly concave. Head behind eyes weakly convex in anterior half and roundly narrowed in posterior half; transverse diameter of eye almost twice larger than length of temple (dorsal view). Ocelli arranged in equilateral triangle. POL 1.3× Od, 0.4× OOL. Eye 1.3× as high as broad. Malar space almost equal to basal width of mandible, 0.2× height of eye. Face convex, width of face 1.3× its median height, 0.9× height of eye. Tentorial pits small, distance between pits 1.25× distance from pit to eye. Clypeus high and weakly convex, its width 1.8× median height, 0.8× width of face; its lower margin convex medially. Head strongly roundly narrowed below eyes (front view).

Antenna. Antenna partly missing apically, 20-segmented (according to original description), weakly thickened, all preserved submedial segments elongated, but 10th segment shorter and wide. Scape 2.2× longer than wide. First flagellar segment 3.8× longer than its apical width, 1.5× longer than second segment. Tenth antennal segment 1.3× as long as its width.

Mesosoma. Mesosoma 1.4× longer than maximum height. Mesoscutum highly and curvedly elevated above pronotum (lateral view), 1.6× wider than its medial length (dorsal view). Prescutellar depression (scutellar sulcus) short and shallow, with numerous distinct carinae. Scutellum 1.1× longer than anterior width. Prepectal carina present laterally and absent ventrally. Precoxal sulcus distinct, long, oblique, sinuate, extending below almost throughout all mesopleuron, crenulate.

Wings. Fore wing 3.2× longer than maximum width. Pterostigma 2.7× longer than its maximum width. Radial vein (r) arising from distal 0.2 of pterostigma and far from point of arising of first radiomedial vein (2-SR). Present only single abscissa of radial vein (r), which distinctly curved, almost entirely desclerotised and reaching as track distal margin of wing. Radial (marginal) cell shortened, 2.5× longer than its maximum width. Metacarp (1-R1) sclerotised at most basal part, its sclerotised part 1.2× longer than pterostigma. First radiomedial vein (2-SR) mainly distinctly sclerotised, almost 5.0× longer than recurrent vein (m-cu). Recurrent vein (m-cu) subinterstitial to first radiomedial vein (2-SR), posteriorly weakly convergent with basal vein (1-M). Discoidal (discal) cell widely sessile anteriorly, 1.2× longer than its maximum width. Nervulus (cu-a) subperpendicular to longitudinal anal vein (1-1A), weakly postfurcal, distance between basal vein (1-M) and nervulus (cu-a) 0.25× nervulus (cu-a) length. Hind wing 3.3× longer than maximum width. First abscissa of mediocubital vein (M+CU) almost 2.0× longer than second abscissa (1-M).

Legs. Hind coxa long, ~ 2.0× longer than maximum width, 1.5× longer than propodeum (lateral view). Hind femur 3.2× longer than maximum width. Hind tibia claviform, 3.9× longer than maximum width, only weakly narrower than hind femur; longest inner tibial spur 0.6× length of hind basitarsus. Hind tarsus as long as hind tibia, its basitarsus 0.7× as long as second–fifth segments combined, 2.5× longer than second segment, 3.3× longer than fifth segments (without pretarsus).

Metasoma. Metasoma almost as long as mesosoma. First to third tergites distinctly sclerotised, with distinct, narrow, curved, complete and crenulate first and second sutures; following tergites relatively weak sclerotised. Medial length of first tergite 0.6× its apical width, as long as second tergite. Second tergite 2.5× longer than third tergite. Length of first to third tergites combined 0.8× their maximum width. Third tergite almost straight on posterior margin. Ovipositor sheaths narrow, rather short, ~ 0.5× as long as first–third tergites combined.

Sculpture. Head densely areolate-punctate, clypeus weakly and sparsely punctate, smooth between punctures. Mesoscutum densely and distinctly punctate; scutellum mainly smooth. Mesopleuron mainly smooth, only partly with fine and sparse punctation; metapleuron smooth. Propodeum with areas distinctly delineated by carinae, with large and inversely-pentagonal areola, elongated anterolateral and transverse posterolateral areas, petiolate area short, subsquare; propodeum mainly rugulose between carinae. First tergite entirely and second tergite mostly (in basal 0.8) distinctly and densely rugose-striate, first tergite basally only rugose; third and following tergites smooth.

Colour. Body mainly reddish brown to dark reddish brown partly, first to third tergites yellowish brown. Antenna pale brown, brownish yellow in basal third. Palpi pale yellow. Legs mainly yellow, distally brownish yellow. Fore wing subhyaline basally and apically, with faintly infuscate band under pterostigma. Pterostigma and parastigma dark brown, most veins yellow.

Male. Unknown.

Distribution. Democratic Republic of Congo.

Host. Undetermined species of *Enarmonia* Hübner, 1825 (Lepidoptera: Tortricidae) on *Zehneria scabra* (Linn. f.) Sond (Cucurbitaceae) (De Saeger, 1942).

***Paradelius (Paradelius) chinensis* He & Chen, 2000**

Figs 2, 4B

Paradelius chinensis He & Chen in He et al. 2000: 682; Yu et al. 2016.

Material examined. CHINA: Zhejiang Province, Qingyuan, Mt. Baishanzu, 30.IX.1993 (Wu Hong col.), No. 941501, 1 female (HT) (ZJUH).

Redescription. Female. Body length 1.8 mm; fore wing length 1.6 mm.

Head. Head 1.9× wider than its medial length (dorsal view), 1.1× wider than mesoscutum. Occiput weakly evenly concave. Head behind eyes distinctly roundly narrowed; transverse diameter of eye ~ 4.5× larger than length of temple in dorsal view or ~ 2.0× in lateral view. Ocelli arranged in triangle with base 1.2× its sides. POL 1.4× Od, 0.5× OOL. Eye 1.7× as high as broad. Malar space almost equal to basal width of mandible, 0.15× height of eye. Face weakly convex, width of face ~ 1.2× its median height. Tentorial pits small, distance between pits 1.4× distance from pit to eye. Clypeus high and weakly convex, its width 2.5× median height, 0.8× width of face; its lower margin medially almost straight. Head strongly roundly narrowed below eyes (front view).

Antenna. Antenna 20-segmented, thickened, weakly setiform, submedial and apical segments elongate. Scape 2.1× longer than wide. First flagellar segment 3.7× longer than its apical width, 1.6× longer than second segment. Tenth segment elongate, 1.6× longer than wide.

Mesosoma. Mesosoma 1.4× longer than maximum height. Mesoscutum highly and curvedly elevated above pronotum (lateral view), 1.7× as wide as its medial length (dorsal view). Prescutellar depression (scutellar sulcus) short and shallow, with numerous distinct carinae. Scutellum 0.8× as long as anterior width. Prepectal carina present laterally and absent ventrally. Precoxal sulcus distinct, long, oblique, sinuate, extending below almost throughout all mesopleuron, crenulate-rugose.

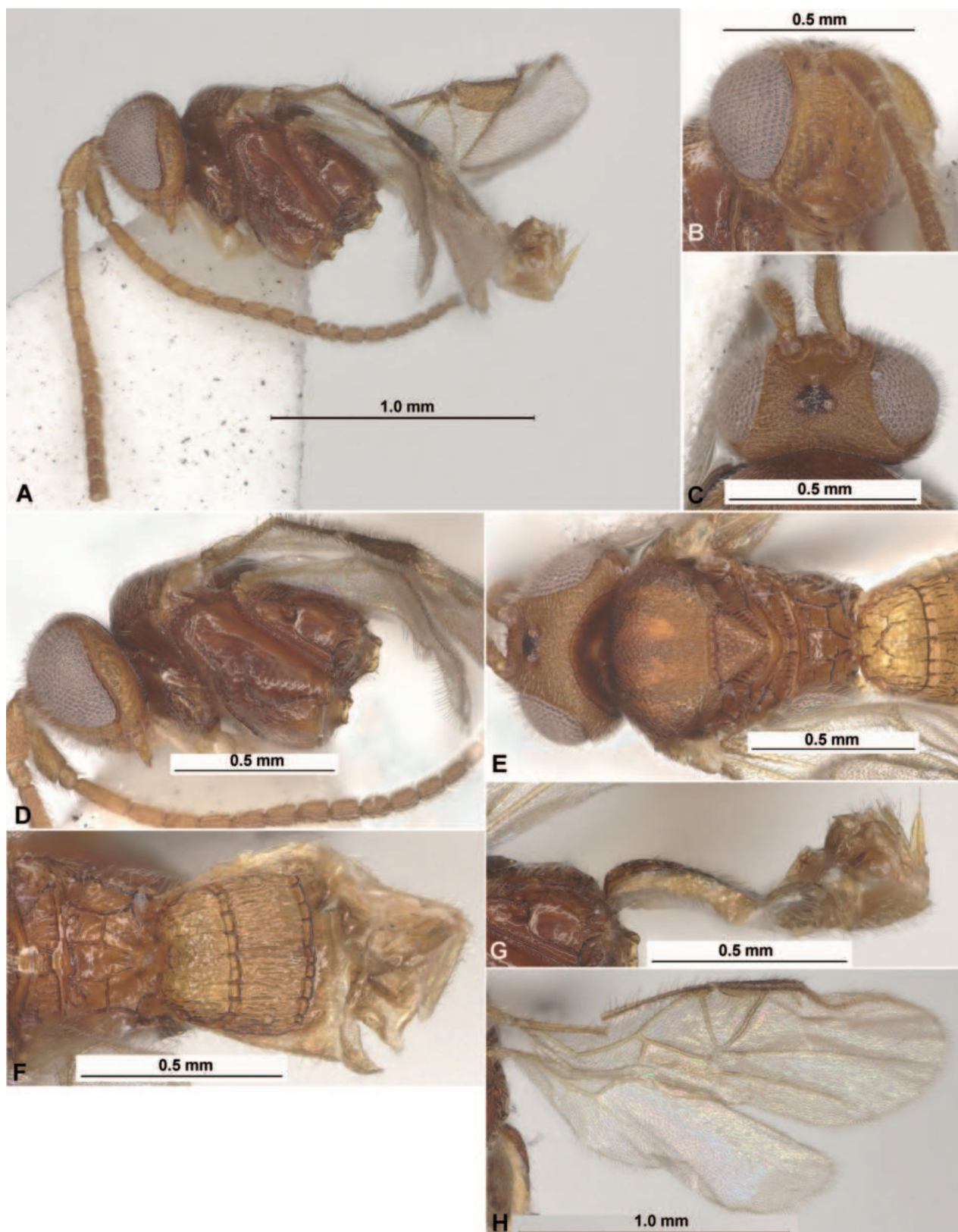


Figure 2. *Paradelius (Paradelius) chinensis* He & Chen, 2000 (female, holotype) **A** habitus, lateral view **B** head, latero-frontal view **C** head, dorsal view **D** head and mesosoma, lateral view **E** head, mesosoma and base of metasoma, dorsal view **F** propodeum and metasoma, dorsal view **G** propodeum and metasoma, lateral view **H** wings.

Wings. Fore wing damaged and distinctly dented anteriorly, $\sim 3.0\times$ longer than maximum width. Radial vein (r) arising almost from distal 0.3 of pterostigma and far from first radiomedial vein (2-SR). Present only single abscissa of radial vein (r), this vein distinctly curved, mainly desclerotised and reaching as track distal margin of wing. Radial (marginal) cell shortened. Metacarp (1-R1) sclerotised at basal part, its sclerotised part $\sim 0.6\times$ as long as pterostigma. First radiomedial vein (2-SR) distinctly sclerotised, $\sim 6.0\times$ longer than recurrent vein (m-cu). Recurrent vein (m-cu) very weakly antefurcal to first radiomedial vein (2-SR), posteriorly weakly divergent with basal vein (1-M). Discoidal (discal) cell broadly sessile anteriorly, $1.4\times$ longer than its maximum width. Nervulus (cu-a) perpendicular to longitudinal anal vein (1-1A), postfurcal, distance between basal vein (1-M) and nervulus (cu-a) $0.5\times$ nervulus (cu-a) length. Hind wing $\sim 3.0\times$ longer than maximum width. First abscissa of mediocubital vein (M+CU) $\sim 2.7\times$ longer than second abscissa (1-M).

Legs. Legs entirely missing.

Metasoma. Metasoma $1.1\times$ longer than mesosoma. First to third tergites sclerotised, with distinct, relatively wide, sparsely crenulate and weakly curved first and second sutures; following tergites relatively weakly sclerotised. Medial length of first tergite $0.6\times$ its apical width, approximately as long as second tergite. Second tergite almost $2.0\times$ longer than short third tergite. Length of first to third tergites combined $1.15\times$ their maximum width. Third tergite weakly curved in posterior margin. Ovipositor sheath narrow and short, $\sim 0.25\times$ as long as first–third tergites combined.

Sculpture. Vertex densely and small areolate-punctate; frons areolate-punctate, but almost smooth medially; face transverse striate with reticulation between striae, only rugulose-reticulate medially, clypeus rather weakly and sparsely punctate, smooth between punctures. Mesoscutum densely punctate, with dense striation in medio-posterior one–third; scutellum rather densely and distinctly punctate, smooth between punctures. Mesopleuron smooth in long posterior area, mainly punctate with reticulation in anterior lower two–thirds; metapleuron mainly smooth, reticulate-areolate marginally. Propodeum mainly widely smooth, with areas distinctly delineated by high carinae, with wide and inversely-pentagonal areola (wide anteriorly and narrow posteriorly), anterolateral areas subsquare, posterolateral areas transverse-curved. First and second tergites entirely and sparsely striate, with dense rugosity between striae. Third and following tergites smooth.

Colour. Body mainly pale reddish brown, mesosoma reddish brown. Antenna yellowish brown. Palpi pale yellow. Fore coxa pale brown. Fore wing entirely faintly infusate, without dark band under pterostigma. Pterostigma and parastigma brown; most veins brown.

Male. Unknown.

Distribution. China (Zhejiang).

Subgenus *Sculptomyriola* Belokobylskij, 1988

Figs 3, 5–8

Description of subgenus. Vertex densely and coarsely reticulate-rugulose. Ocelli arranged in weakly obtuse or subequilateral triangle. Eye covered by dense and relatively long setae. Antenna long, thickened and setiform. Flagellar



Figure 3. *Paradelius (Sculptomyriola) extremiorientalis* (Belokobylskij, 1988), comb. nov. (female, holotype) A habitus, dorsal view B head, front view C head, dorsal view D antenna E mesosoma, dorsal view F propodeum and metasoma, dorsal view G head and mesosoma, lateral view H wings I hind leg.

segments longitudinal, subsquare or weakly transverse in apical half of antenna. Mesoscutum densely and distinctly punctate. Prescutellar depression short and densely crenulate. Prepectal carina laterally weakly present or completely absent. Precoxal sulcus distinct, long, relatively narrow, sinuate, entirely crenulate or rugulose. Propodeum widely rugulose-reticulate, rarely also with areas delineated by carinae at least posteriorly. Fore wing with large pterostigma. Radial vein ($r + 3\text{-SR}$) with one (r) or two ($r + 3\text{-SR}$) abscissae, arising from posterior 0.3 of pterostigma separately or joined with first radiomedial vein (2-SR). Discoidal (discal) cell anteriorly usually sessile on parastigma, but sometimes shortly petiolate. Recurrent vein ($m\text{-cu}$) usually postfurcal to first radiomedial vein (2-SR), only rarely subinterstitial or very weakly antefurcal. Hind femur wide; hind tibia distinctly clavate. First tergite of metasoma distinctly widened towards apex. Both first metasomal sutures present, rather deep and relatively distinct, densely sculptured. First and second tergites entirely and also third tergite at least in basal third or half densely striate-rugulose. Ovipositor short.

***Paradelius (Sculptomyriola) extremiorientalis* (Belokobylskij, 1988), comb. nov.**
Figs 3, 4C

Sculptomyriola extremiorientalis Belokobylskij, 1988: 145; 1998: 554; Ku et al. 2001: 15; Yu et al. 2016.

Material examined. RUSSIA. PRIMORSKIY TERRITORY: "Primorskiy Territory, [Partizansk District], env. Sergeevka, Belokobylskij [col.], forest, 21.VII.1979", "Holotypus *Sculptomyriola extremiorientalis* Belokobylsk.[ij]", 1 female (HT) (ZISP); 'Kedrovaya Pad' Nature Reserve, 12.VIII.1976 (Berezantsev), 1 male (PT); 30 km S of Slavyanka, at light, 2, 3 & 5.VIII.1985 (S. Belokobylskij), 5 females (PTs); same locality, forest, clearings, 5.VIII.1985 (S. Belokobylskij), 2 females (PTs); 25 km S of Slavyanka, Vityaz', at light, 2.VIII.1982 (I. Kerzhner), 3 females; Vladivostok, Sedanka, forest, 31.VII.1984 (S. Belokobylskij), 1 female (PT); 10 km S of Partizansk, forest, 18.VII.1979 (S. Belokobylskij), 1 female (PT); 15 km SE of Partizansk, oak-forest, 22.VII.1984 (S. Belokobylskij), 10 females, 2 males (PTs); 10 km SE of Partizansk, oak-forest, 22.VII.1984 (S. Belokobylskij), 2 females; Lazovskiy Nature Reserve, 10 km SW of Sokolchi, rocks, mixed forest, 23.VII.1993 (S. Belokobylskij), 1 female, 1 male; 20 km N of Rudnaya Pristan', oak-forest, 18.VII.1979 (S. Belokobylskij), 1 female (PT); 20 km SE of Ussuriysk, at light, 31.VII & 1–4.VIII.1991 (S. Belokobylskij), 4 females, 1 male; same locality, forest, clearings, 1 & 5.VIII.1991 (S. Belokobylskij), 3 females; 20 km E of Ussuriysk, at light, 26.VII.1999 (S. Sinev), 1 female; 25 km E of Spassk-Dal'niy, forest, 12.VII.1991 (S. Belokobylskij), 1 female; 20 km SE of Spassk-Dal'niy, Evseevka, forest, 18.VII.1991 (S. Belokobylskij), 1 female; 20 km NNW of Spassk-Dal'niy, Novosel'skoe, meadow, bush, 19.VII.1998 (S. Belokobylskij), 1 female; Spassk-Dal'niy, forest, 13.VII.1991 (S. Belokobylskij), 1 female. KURIL ISLANDS: Shikotan I., 5–7 km S of Krabozavodsk, 17.VIII.1973 (D. Kasparyan), 1 male (PT) (All in ZISP).

SOUTH KOREA. Gyeonggi-do, Mt. Chungnyeong, at light, 3.VII–16.VIII.1999 (D. Ku), 1 female (SMNE); Gyeongsangnam-do, Geochang-gun, Sinwon-myeon, Waryong-ri, Malaise Trap, 18.VI–2.VII.2022 (D. Ku, J. Lee, H. Jeong), 1 female (SMNE); Gyeongsangnam-do, Goseong-gun, Hail-myeon, Suyang-ri,

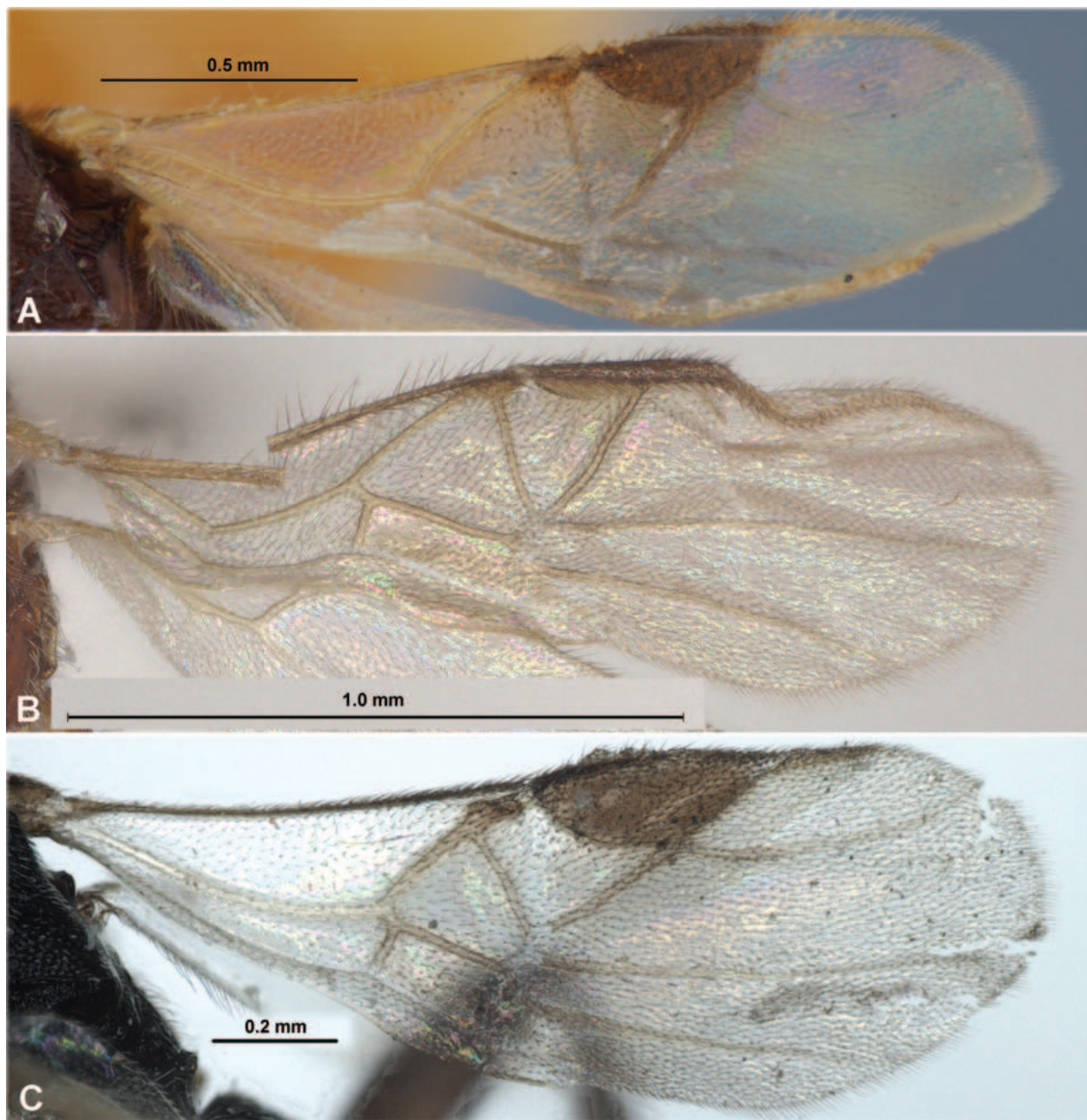


Figure 4. Fore wings. **A** *Paradelius (Paradelius) ghesquierei* De Saeger **B** *P. (P.) chinensis* He & Chen **C** *P. (Sculptomyrriola) extremiorientalis* (Belokobylskij).

34°58'34.8"N, 128°12'08.3"E, 23.VI.2023 (S. Belokobylskij), 1 male (ZISP); Gyeongsangnam-do, Sancheong-gun, 30 km NNW of Jinju, forest, bush, 800 m, 29.VI.2002 (S. Belokobylskij), 1 female (ZISP).

Description. Female. Body length 2.0–2.6 mm; fore wing length 1.7–2.0 mm.

Head. Head 2.0–2.2× wider than its medial length (dorsal view), approximately as wide as mesoscutum. Occiput distinctly evenly concave. Head behind eyes weakly convex to roundly narrowed; transverse diameter of eye 1.2–1.4× larger than length of temple (dorsal view). Ocelli arranged in triangle with base 1.2–1.3× its sides. POL 2.0–2.5× Od, 0.6–0.7× OOL. Eye 1.5–1.6× as high as broad. Malar space 1.0–1.2× basal width of mandible, 0.2–0.3× height

of eye. Face convex, width of face 1.6–1.7× its median height, 1.1–1.3× height of eye. Tentorial pits small, distance between pits 1.1–1.3× distance from pit to eye. Clypeus high and weakly convex, its width 1.5–1.7× median height, ~ 0.6× width of face. Head strongly roundly narrowed below eyes (front view).

Antenna. Antenna 20-segmented, thickened, setiform, its apical segments elongate, but medial ones often subsquare. Scape 2.2–2.6× longer than wide. First flagellar segment 2.6–2.8× longer than its apical width, 1.1–1.2× longer than second segment. Tenth–twentieth segments subsquare. Penultimate segment 1.1–1.5× longer than its width, 0.7–0.8× as long as obtuse apical segment.

Mesosoma. Mesosoma 1.5–1.7× longer than maximum height. Mesoscutum highly and curvedly elevated above pronotum (lateral view), 1.4–1.5× as wide as its medial length (dorsal view). Prescutellar depression (scutellar sulcus) shallow, with distinct numerous carinae. Scutellum 0.7–0.8× as long as anterior width. Prepectal carina widely absent, sometimes only weakly or very weakly visible laterally. Precoxal sulcus distinct, oblique, extending below almost throughout all lower part of mesopleuron, rugulose.

Wings. Fore wing 2.6–2.8× longer than maximum width. Pterostigma 2.5–2.7× longer than its maximum width. Radial vein (r) arising from distal 0.4 of pterostigma. First radiomedial vein (2-SR) arising from pterostigma from one point with radial vein (r) or (more usually) weakly distant from it. Present two abscissae of radial vein (r and 3-SR) with very short first radial abscissa (r) and long second abscissa (3-SR), but sometimes present only single abscissa of radial vein (r); second abscissa (3-SR) weakly curved, sclerotised in basal 0.2–0.3 and desclerotised on remaining part, reaching as track distal margin of wing. Radial (marginal) cell shortened, 2.5–4.0× longer than its maximum width. Metacarp (1-R1) sclerotised in basal half, its sclerotised part 0.4–0.5× as long as pterostigma. First radiomedial vein (2-SR) mainly distinctly sclerotised, 4.0–6.0× longer than recurrent vein (m-cu). Recurrent vein (m-cu) distinctly postfurcal to first radiomedial vein (2-SR), posteriorly subparallel with basal vein (1-M). Discoidal (discal) cell shortly petiolate anteriorly 1.3–1.4× longer than its maximum width. Nervulus (cu-a) subperpendicular to longitudinal anal vein (1-1A), weakly postfurcal, distance between basal vein (1-M) and nervulus (cu-a) ~ 0.3× nervulus (cu-a) length. Hind wing 3.2–3.4× longer than maximum width. First abscissa of mediocubital vein (M+CU) 2.0–2.5× longer than second abscissa (1-M).

Legs. Hind coxa long, 1.7–1.8× longer than maximum width, 1.4–1.5× longer than propodeum (lateral view). Hind femur 3.1–3.5× longer than maximum width. Hind tibia claviform, 4.5–5.2× longer than maximum width, 0.7–0.8× as wide as hind femur; longest inner tibial spur ~ 0.5× hind basitarsus length. Hind tarsus as long as hind tibia, its basitarsus 0.8–0.9× as long as second–fifth segments combined, 2.5–3.0× longer than second segment, 3.3–3.5× longer than fifth segment (without pretarsus).

Metasoma. Metasoma 0.8–0.9× as long as mesosoma. All tergites (especially first to third ones) distinctly sclerotised. First suture shallow, poorly visible, strongly curved; second suture distinct, narrow, weakly curved. Medial length of first tergite 0.6–0.7× its apical width, 1.2–1.4× longer than second tergite. Second tergite 1.2–1.5× longer than third tergite. Length of first to third tergites combined 1.1–1.2× their maximum width. Third tergite weakly evenly curved on posterior margin. Ovipositor sheaths short, weakly thickened, 0.2–0.3× as long as first–third tergites combined.

Sculpture. Head densely and small areolate-punctate, vertex sometimes with fine transverse striae posteriorly, frons punctate-shagreened; face densely punctate-reticulate and upper with transverse striation upper, clypeus weakly and sparsely punctate, shagreened between punctures. Mesoscutum and scutellum densely and distinctly punctate. Mesopleuron anteriorly and below sparse punctate and finely shagreened, almost smooth in posterior upper half; metapleuron transversely striate with sparse punctation anteriorly, rugose-reticulate posteriorly. Propodeum submedially with coarse curved transverse keel; often areas distinctly delineated by carinae, with narrow and inversely-pentagonal areola, but sometimes anterior carinae of areola indistinct and areola indistinctly delineated; anterolateral areas elongated, petiolate area short; propodeum usually entirely densely rugulose in basal half, but sometimes almost smooth in posterior half. First and second tergites entirely and third tergite in basal 0.5–0.7 distinctly and densely striate with dense rugosity or densely areolate-rugose; posterior half of third and following tergites densely and finely shagreened to smooth.

Colour. Body mainly black, only sometimes head partly dark reddish brown. Antenna black, few basal segments dark reddish brown. Palpi yellow, usually infusate basally. Fore and middle legs yellowish brown or reddish brown, partly paler; hind leg reddish brown to dark reddish brown, partly black. Fore wing faintly infusate, without dark band under pterostigma or only with wide darkening. Pterostigma and parastigma dark brown, most veins brown, metacarp (1-R1) pale brown.

Male. Body length 1.9–2.3 mm; fore wing length 1.8–2.0 mm. Antenna 20-segmented, evenly setiform, distinctly longer than body. First flagellar segment 2.2–2.4× longer than its apical width, 1.1–1.2× longer than second segment. Penultimate segment ~2.0× longer than its width. Discoidal (discal) cell of fore wing distinctly petiolate. First tergite only weakly longer than second tergite. Second tergite 1.3–1.7× longer than third tergite. Length of first to third tergites combined 1.1–1.3× their maximum width. Head often dark reddish brown to black, sometimes face reddish brown. Hind femur mainly (dark) reddish brown or pale brown. Fore wing hyaline or subhyaline. Pterostigma and parastigma brown, most veins hyaline and transparent. Otherwise similar to female.

Distribution. Russia (Primorskiy Territory, Sakhalin Province: Kuril Islands), Korean Peninsula.

***Paradelius (Sculptomyriola) ghilarovi* (Belokobylskij, 1988), comb. nov.**

Figs 5, 8A

Sculptomyriola ghilarovi Belokobylskij, 1988: 147; 1998: 556; Ku et al. 2001: 15; Yu et al. 2016.

Material examined. RUSSIA. PRIMORSKIY TERRITORY: “Primorskiy Territory, 20 km SE of Ussuriysk, Gornotayozhnoe, at light, Budris [col.], 3.IX.1983”, “Holotypus *Sculptomyriola ghilarovi* Belokobylskij”, 1 female (HT) (ZISP); 20 km E of Ussuriysk, GTS, at light, 3, 5 & 6.IX.1983 (E. Budris), 5 females (PTs); 20 km E of Ussuriysk, GTS, at light, 27.VIII.1984 (S. Sinev), 2 females (PTs) (All in ZISP).

SOUTH KOREA. Gyeongsangbuk-do, Mt. Baekam, Guryeong, at light, 10–11.VIII.1999 (D. Ku), 1 female (SMNE).



Figure 5. *Paradelius (Sculptomyriola) ghilarevi* (Belokobylskij, 1988), comb. nov. (female, holotype) **A** habitus, dorsal view **B** head, front view **C** head, dorsal view **D** antenna **E** head and mesosoma, lateral view **F** head and mesosoma, dorsal view **G** propodeum and metasoma, dorsal view **H** wings **I** hind leg.

Description. Female. Body length 2.1–2.5 mm; fore wing length 1.9–2.0 mm.

Head. Head 2.0–2.3× wider than its medial length (dorsal view), 0.9–1.0× as wide as mesoscutum. Occiput distinctly evenly concave. Head behind eyes distinctly roundly narrowed; transverse diameter of eye 1.5–1.8× larger than length of temple (dorsal view). Ocelli arranged in triangle with base 1.3–1.5× its sides. POL 2.3–2.6× Od, 0.9–1.1× OOL. Eye 1.5–1.6× as high as broad. Malar space 0.8–1.1× basal width of mandible, 0.2–0.3× height of eye. Face convex, its width 1.5–1.7× median height, almost equal to height of eye. Tentorial pits small, distance between pits almost equal to distance from pit to eye. Clypeus high and weakly convex, its width ~ 2.0× median height, 0.6–0.7× width of face; its ventral margin straight medially. Head strongly roundly narrowed below eyes (front view).

Antenna. Antenna 20-segmented, thickened, setiform, apical segments started from ninth transverse and wide in beginning and subsquare or almost rounded subapically (three–four segments). Scape 2.0–2.3× longer than wide. First flagellar segment 2.4–2.7× longer than its apical width, 1.2–1.4× longer than second segment. Tenth segment 0.6× as long as maximum width. Penultimate segment subround, as long as its width, 0.6–0.7× as long as obtuse apical segment.

Mesosoma. Mesosoma 1.5–1.6× longer than maximum height. Mesoscutum highly and curvedly elevated above pronotum (lateral view), 1.3–1.4× as wide as its medial length (dorsal view). Prescutellar depression (scutellar sulcus) shallow, with numerous distinct carinae. Scutellum 0.9× as long as anterior width. Prepectal carina almost entirely absent, sometimes very weakly visible laterally. Precoxal sulcus distinct, oblique, extending below almost throughout all lower part of mesopleuron, rugulose-crenulate.

Wings. Fore wing 2.4–2.5× longer than maximum width. Pterostigma 2.5–2.7× longer than its maximum width. Radial vein (r) arising from distal 0.4 of pterostigma; first radiomedial vein (2-SR) arising from radial vein (r) weakly distant from pterostigma. Present short first (r) and long second (3-SR) abscissae of radial vein, second abscissa (3-SR) curved anteriorly and almost straight posteriorly, sclerotised in basal 0.2–0.3 and desclerotised on remaining part, reaching as track distal margin of wing. Radial (marginal) cell weakly shortened, 2.7–2.8× longer than its maximum width. Sclerotised basal part of metacarp (1-R1) short, ~ 0.2× as long as pterostigma. First radiomedial vein (2-SR) mainly distinctly sclerotised and pigmented, 5.0–7.0× longer than recurrent vein (m-cu). Recurrent vein (m-cu) weakly postfurcal to first radiomedial vein (2-SR), posteriorly weakly convergent distally with basal vein (1-M). Discoidal (discal) cell broadly sessile anteriorly, ~ 1.3× longer than its maximum width. Nervulus (cu-a) long, subperpendicular to longitudinal anal vein (1-1A), weakly postfurcal, distance between basal vein (1-M) and nervulus (cu-a) 0.2–0.3× nervulus (cu-a) length. Hind wing 3.0–3.6× longer than maximum width. First abscissa of mediocubital vein (M+CU) ~ 2.5× longer than second abscissa (1-M).

Legs. Hind coxa short and high, 1.4–1.5× longer than maximum width, 1.5–1.7× longer than propodeum (lateral view). Hind femur 2.7–3.1× longer than its maximum width. Hind tibia distinctly claviform, ~ 4.5× longer than maximum width, ~ 0.7× as wide as hind femur; longest inner tibial spur ~ 0.5× hind basitarsus length. Hind tarsus 0.9–1.0× as long as hind tibia, its basitarsus 0.8–0.9× as long as second–fifth segments combined, 2.6–2.8× longer than second segment, 3.0–3.3× longer than fifth segments (without pretarsus).

Metasoma. Metasoma 0.8–0.9× as long as mesosoma. All tergites (especially first to third ones) distinctly sclerotised; first and second sutures distinct, narrow and crenulate, first suture strongly curved, second one weakly curved. Medial length of first tergite 0.6–0.7× its apical width, 1.3–1.4× longer than second tergite. Second tergite ~ 1.3× longer than third tergite. Length of first to third tergites combined 1.1–1.2× their maximum width. Third tergite almost straight on posterior margin. Ovipositor sheaths short, weakly thickened, 0.2–0.3× as long as first–third tergites combined.

Sculpture. Head densely and small areolate-punctate with additional small granulation, frons and face densely transversely curvedly striae with dense reticulation between striae, clypeus distinctly densely punctate and smooth between punctures. Mesoscutum and scutellum densely and distinctly punctate-areolate. Mesopleuron entirely or widely and rather sparsely punctate, smooth between punctulae, sometimes entirely smooth in posterior upper half; metapleuron entirely rugose-areolate. Propodeum medially with coarse transverse curved keel; areas rather distinctly or relatively finely delineated by carinae, with rather wide and inversely-pentagonal areola, anterolateral areas relatively wide, petiolate area short and trapezoid; propodeum entirely or almost entirely densely rugulose-reticulate. First and second tergites entirely and third tergite in basal 0.8–0.9 distinctly and densely curvedly striate with rugosity; following tergites densely and very finely shagreened to smooth.

Colour. Head mainly pale reddish brown, darkened only dorsally on vertex. Mesosoma dorsally mainly black, but pale reddish brown in anterior one–fifth and on large medial area of mesopleuron or almost entirely laterally. Metasoma entirely black. Antenna brownish yellow to pale reddish brown in basal 0.5–0.7, dark brown or black in apical 0.3–0.5. Palpi pale yellow, but distinctly infuscate basally. Legs mainly pale reddish brown to partly reddish brown, sometimes hind tibia and always hind tarsus infuscate; all tibia yellow or pale yellow basally. Fore wing partly faintly infuscate, hyaline in basal one–third, with rather distinct and wide dark spot medially (under pterostigma and along basal (1-M) vein). Pterostigma and parastigma dark brown; most veins brown, but veins in basal one third and apically pale, hyaline.

Male. Unknown.

Distribution. Russia (Primorskiy Territory), Korean Peninsula.

***Paradelius (Sculptomyriola) koreanus* Belokobylskij & Ku, sp. nov.**

<https://zoobank.org/A6D53983-6522-47C5-8B7F-4DA041E9B399>

Figs 6, 8B

Type material. *Holotype*, female, South Korea, Gyeongsangnam-do, Jinju-si, Gajwa-dong, Light trap, 2–3.VIII.2000 (Tae-Ho An) (NIBR).

Description. Female. Body length 1.5 mm; fore wing length 1.4 mm.

Head. Head almost twice wider than its medial length (dorsal view), 1.1× wider than mesoscutum. Occiput distinctly evenly concave. Head behind eyes weakly convex in anterior half and roundly narrowed in posterior half; transverse diameter of eye twice larger than length of temple. Ocelli arranged in triangle with base 1.25× its sides. POL 1.5× Od, 0.8× OOL. Eye 1.5× as high as broad. Malar space 0.6× basal width of mandible, 0.15× height of eye.

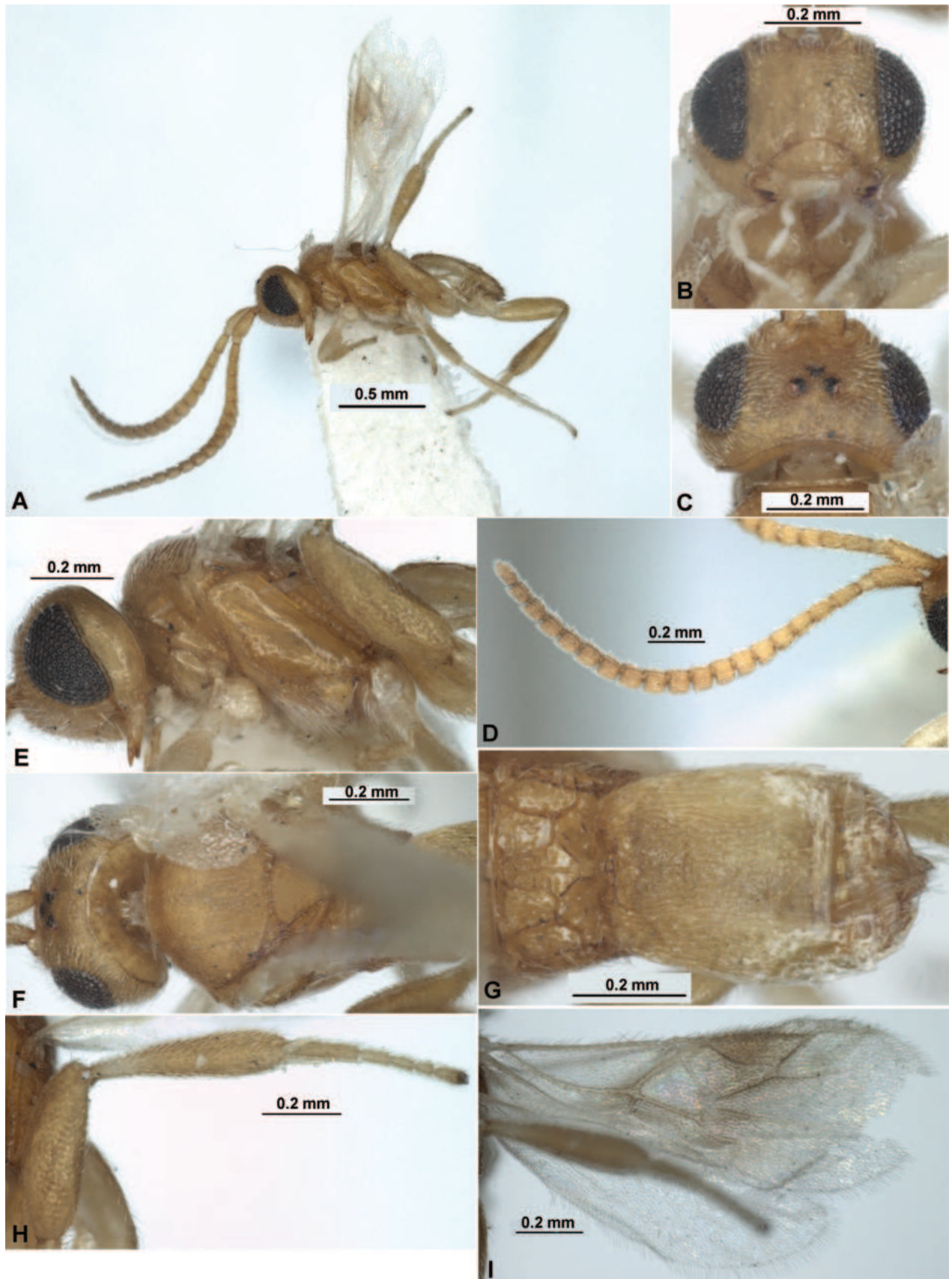


Figure 6. *Paradelius (Sculptomyriola) koreanus* Belokobylskij & Ku, sp. nov. (female, holotype) **A** habitus, lateral view **B** head, front view **C** head, dorsal view **D** antenna **E** head and mesosoma, lateral view **F** head and mesosoma, dorsal view **G** propodeum and metasoma, dorsal view **H** hind leg **I** wings.

Face convex, width of face 1.3× its median height, almost equal to height of eye. Tentorial pits small, distance between pits 1.3× distance from pit to eye. Clypeal suture distinct and narrow. Clypeus wide and weakly convex, its width 2.4× median height, 0.7× width of face; almost straight on lower margin medially. Head distinctly roundly narrowed below eyes (front view). Occipital carina dorsally complete, but weak.

Antenna. Antenna 20-segmented, 1.3× longer than body, rather thick, sub-medial segments short and wide. Scape 2.0× longer than wide. First flagellar segment almost twice longer than its apical width, 1.3× longer than second segment; seven to 15th segments subsquare or weakly transverse, 1.0–1.2× as wide as their length. Penultimate segment 1.2× longer than its width, 0.7× as long as apical segment.

Mesosoma. Mesosoma 1.5× longer than maximum height. Mesoscutum highly and roundly elevated above pronotum (lateral view), 1.3× as wide as medial length (dorsal view). Prescutellar depression (scutellar sulcus) very narrow and shallow, with distinct numerous carinae. Scutellum 0.8× as long as its anterior width. Prepectal carina weakly present laterally and widely absent ventrally. Precoxal sulcus distinctly impressed, long and curved, extending below almost throughout mesopleuron, crenulate.

Wings. Fore wing 2.8× longer than maximum width. Pterostigma 3.4× longer than its maximum width. Radial vein (r) arising from distal 0.3 of pterostigma. First radial vein (r) present, short, subvertical, 0.3× as long as width of pterostigma. Second radial vein (3-SR) sclerotised in basal half and unsclerotised in apical half, reaching as track distal margin of wing. Radial (marginal) cell distinctly shortened, almost 3.0× longer than its maximum width. Metacarp (1-R1) unsclerotised distally, its sclerotised basal part ~ 0.5× as long as pterostigma. First radiomedial vein (2-SR) distinctly sclerotised, 7.2× longer than first radial abscissa (r), 4.5× longer than recurrent vein (m-cu). Recurrent vein (m-cu) postfurcal to first radiomedial vein (2-SR), posteriorly subparallel with basal vein (1-M) and 0.25× as long as basal vein (1-M). Discoidal (discal) cell narrowly sessile anteriorly, 1.4× longer than its maximum width. Nervulus (cu-a) weakly postfurcal, subperpendicular and oblique to longitudinal anal vein (1-1A), distance between basal vein (1-M) and nervulus (cu-a) 0.2× nervulus (cu-a) length. Hind wing 3.2× longer than maximum width. First abscissa of mediocubital vein (M+CU) 2.0× longer than second abscissa (1-M).

Legs. Hind coxa long and rather low, 1.8× longer than maximum width, 1.6× longer than propodeum (lateral view). Hind femur thickened and short, 3.0× longer than maximum width. Hind tibia distinctly claviform, strongly thickened apically, 4.2× longer than maximum width, 0.8× as wide as hind femur; its longest inner spur 0.7× hind basitarsus length. Hind tarsus 0.9× as long as hind tibia. Basitarsus of hind leg 0.6× as long as second–fifth segments combined, 2.5× longer than second segment, ~3.0× longer than fifth segments (without pretarsus).

Metasoma. Metasoma 0.9× as long as mesosoma. All tergites distinctly sclerotised; first and second sutures rather distinct, almost complete, narrow and curved. Medial length of first tergite ~ 0.4× its apical width, almost as long as second tergite. Second tergite 1.6× longer than third tergite. Length of first to third tergites combined 1.2× their maximum width. Third tergite weakly curved on posterior margin. Hypopygium setose, reaching apex of metasoma. Ovipositor sheaths very short not projected behind tip of metasoma, ~ 0.2× as long as first–third tergites combined.

Sculpture. Head densely areolate-rugulose with additional dense granulation; face densely punctate, with transverse striation in upper half, clypeus weakly and sparsely punctate. Mesoscutum and scutellum densely foveolate with fine additional granulation. Mesopleuron anteriorly and below finely foveolate-punctate, almost smooth upper and posteriorly; metapleuron rugose-striate, but almost smooth medially. Propodeum entirely distinctly reticulate-carinate, with strong and complete carinae separated long and inversely-pentagonal areola, elongated anterolateral and subround distolateral areas, with short and subsquare petiolate area. First and second tergites entirely distinctly and densely rugose-striate, first tergite medially widely and densely rugose; third tergite mainly smooth, only finely rugulose in narrow basomedial part.

Colour. Body entirely brownish yellow, only antenna very faintly infusate apically. Palpi pale yellow. Legs basally yellow, brownish yellow on remaining part. Fore wing subhyaline basally and apically, with distinctly infusate and wide band medially. Pterostigma pale brown, yellow in apical one-third.

Male. Unknown.

Comparative diagnosis. *Paradelius (Sculptomyriola) koreanus* sp. nov. distinctly differs from all eastern Palaearctic species of this genus with sessile anteriorly discoidal (discal) cell of fore wing (Belokobylskij, 1988, 1998) by almost completely brownish yellow coloration of the body, only medially sculptured third metasomal tergite and the short and weakly transverse or subsquare medial segments of antenna.

Etymology. This species is named after the Korean Peninsula, where new species was collected.

Distribution. Korean Peninsula.

***Paradelius (Sculptomyriola) sinevi* (Belokobylskij, 1998), comb. nov.**

Figs 7, 8C

Sculptomyriola sinevi Belokobylskij, 1998: 555; Yu et al. 2016.

Material examined. RUSSIA. PRIMORSKIY TERRITORY: "Primorskiy Territory, 20 km SE of Ussuriysk, at light, 31.VII.1991, Belokobylskij [col.]", "Holotype *Sculptomyriola sinevi* Belokobylskij", 1 female (HT) (ZISP); 7 km S of Zanadvorovka, at light, 13.VIII.1984 (S. Sinev), 1 male (PT); 'Kedrovaya Pad' Nature Reserve, cordon of Sukhaya Rechka, 6.VIII.1988 (E. Budris), 1 male (PT); 'Kedrovaya Pad' Nature Reserve, at light, 7.VIII.1988 (E. Budris), 1 female (PT); 10 km SE of Partizansk, bush on slopes of hill, 11.VII.1996 (S. Belokobylskij), 1 male (PT); 20 km SE of Ussuriysk, at light, 27.VIII.1984 (S. Sinev), 1 female (PT); 20 km SE of Ussuriysk, Gornotayozhnoe, at light, 26.VII.1999 (S. Sinev), 1 female; 30 km E of Spassk-Dal'niy, forest, 27.VIII.1992 (S. Belokobylskij), 1 female (PT) (All in ZISP).

Description. Female. Body length 2.2–2.4 mm; fore wing length 1.8–1.9 mm.

Head. Head 1.7–1.9× wider than its medial length (dorsal view), 0.9–1.0× as wide as mesoscutum. Occiput distinctly evenly concave. Head behind eyes distinctly roundly narrowed; transverse diameter of eye 1.3–1.4× larger than length of temple (dorsal view). Ocelli arranged in triangle with base 1.5–1.6× its sides. POL ~ 2.5× Od, 0.8–1.0× OOL. Eye 1.4–1.6× as high as broad. Malar space 1.1–1.3× basal width of mandible, 0.30–0.35× height of eye. Face weakly convex, width of

face $\sim 1.5\times$ its median height, $1.1\text{--}1.3\times$ height of eye. Tentorial pits small, distance between pits almost equal to distance from pit to eye. Clypeus high and weakly convex, its width $\sim 2.0\times$ median height, $0.7\times$ width of face; ventral margin of clypeus weakly curved. Head strongly roundly narrowed below eyes (front view).

Antenna. Antenna 20-segmented, thickened medially, weakly narrowed basally and apically, subfiliform, medial segments started from eighth to 17th weakly elongated or sometimes subsquare. Scape $2.0\text{--}2.2\times$ longer than wide. First flagellar segment $2.6\text{--}2.7\times$ longer than its apical width, $\sim 1.3\times$ longer than second segment. Tenth segment $1.20\text{--}1.25\times$ longer than its maximum width. Penultimate segment $1.2\text{--}1.3\times$ longer than its width, $0.7\text{--}0.8\times$ as long as obtuse apical segment.

Mesosoma. Mesosoma $1.5\text{--}1.6\times$ longer than maximum height. Mesoscutum highly and curvedly elevated above pronotum (lateral view), $1.3\text{--}1.5\times$ as wide as its medial length (dorsal view). Prescutellar depression (scutellar sulcus) shallow, with numerous distinct carinae. Scutellum $0.9\times$ as long as anterior width. Prepectal carina widely absent, rarely only weakly visible laterally. Precoxal sulcus distinct, wide, strongly curved, extending below almost throughout all lower part of mesopleuron, rugulose-crenulate.

Wings. Fore wing $2.3\text{--}2.6\times$ longer than maximum width. Pterostigma $2.3\text{--}2.5\times$ longer than its maximum width. Radial vein (r) arising from distal $0.40\text{--}0.45$ of pterostigma, radiomedial vein (2-SR) arising from radial vein (r) weakly separated from pterostigma. Present short first (r) and second (3-SR) abscissa of radial vein, second abscissa (3-SR) entirely evenly curved, weakly sclerotised in basal 0.25 and desclerotised on remaining part, reaching as track distal margin of wing. Radial (marginal) cell shortened, $\sim 3.0\times$ longer than its maximum width. Metacarp (1-R1) short, pigmented, its sclerotised basal part $0.3\times$ as long as pterostigma. First radiomedial vein (2-SR) mainly distinctly sclerotised and pigmented, $6.5\text{--}7.5\times$ longer than short recurrent vein (m-cu). Recurrent vein (m-cu) distinctly postfurcal to first radiomedial vein (2-SR), approximately as long as second medial abscissa (2-SR+M), posteriorly subparallel with basal vein (1-M). Discoidal (discal) cell narrowly sessile anteriorly, $1.3\text{--}1.4\times$ longer than its maximum width. Nervulus (cu-a) oblique to longitudinal anal vein (1-1A), postfurcal, distance between basal vein (1-M) and nervulus (cu-a) $\sim 0.4\times$ nervulus (cu-a) length. Hind wing $3.3\text{--}3.5\times$ longer than maximum width. First abscissa of mediocubital vein (M+CU) $2.0\text{--}2.5\times$ longer than second abscissa (1-M).

Legs. Hind coxa long and high, $1.5\text{--}1.6\times$ longer than maximum width, $1.1\text{--}1.2\times$ longer than propodeum (lateral view). Hind femur $3.0\text{--}3.4\times$ longer than maximum width. Hind tibia distinctly claviform, $4.2\text{--}4.4\times$ longer than maximum width, $0.8\times$ as wide as hind femur; longest inner tibial spur $0.6\times$ hind basitarsus length. Hind tarsus $0.9\times$ as long as hind tibia, its basitarsus $0.8\times$ as long as second–fifth segments combined, $2.3\text{--}2.7\times$ longer than second segment, $3.0\text{--}3.7\times$ longer than fifth segments (without pretarsus).

Metasoma. Metasoma $0.8\text{--}0.9\times$ as long as mesosoma. All tergites (especially first to third ones) distinctly sclerotised; first and second sutures distinct, but narrow, first suture strongly curved, second one weakly curved. Medial length of first tergite $0.5\times$ its apical width, $1.0\text{--}1.2\times$ as long as second tergite. Second tergite $1.1\text{--}1.4\times$ longer than third tergite. Length of first to third tergites combined $1.0\text{--}1.1\times$ their maximum width. Third tergite weakly evenly curved on posterior margin. Ovipositor sheaths weakly thickened, short, $0.3\text{--}0.4\times$ as long as first–third tergites combined.

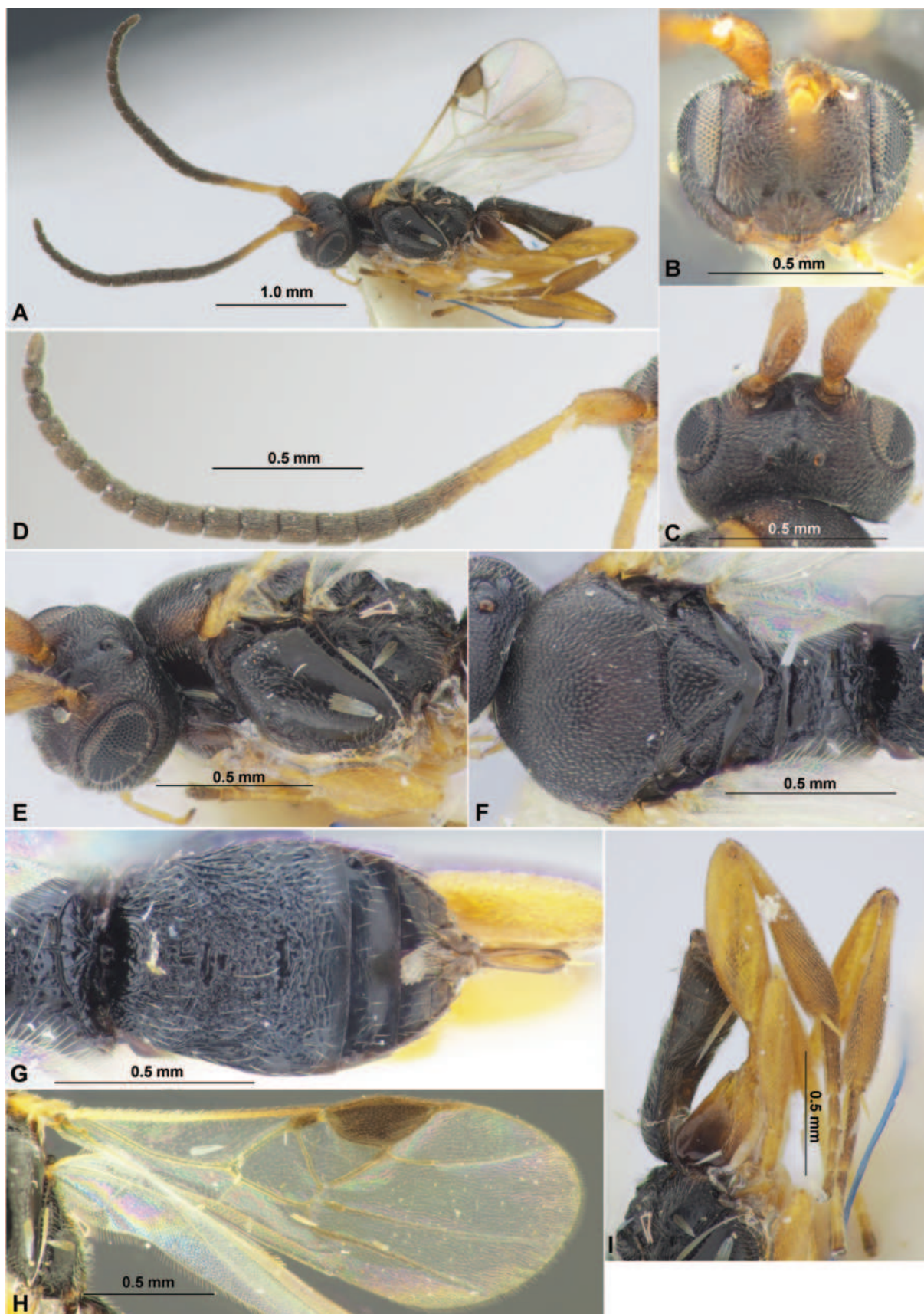


Figure 7. *Paradelius (Sculptomyriola) sinevi* (Belokobylskij, 1998), comb. nov. (female, holotype) **A** habitus, lateral view **B** head, front view **C** head, dorsal view **D** antenna **E** head and mesosoma, lateral view **F** mesosoma, dorsal view **G** propodeum and metasoma, dorsal view **H** wings **I** hind leg.

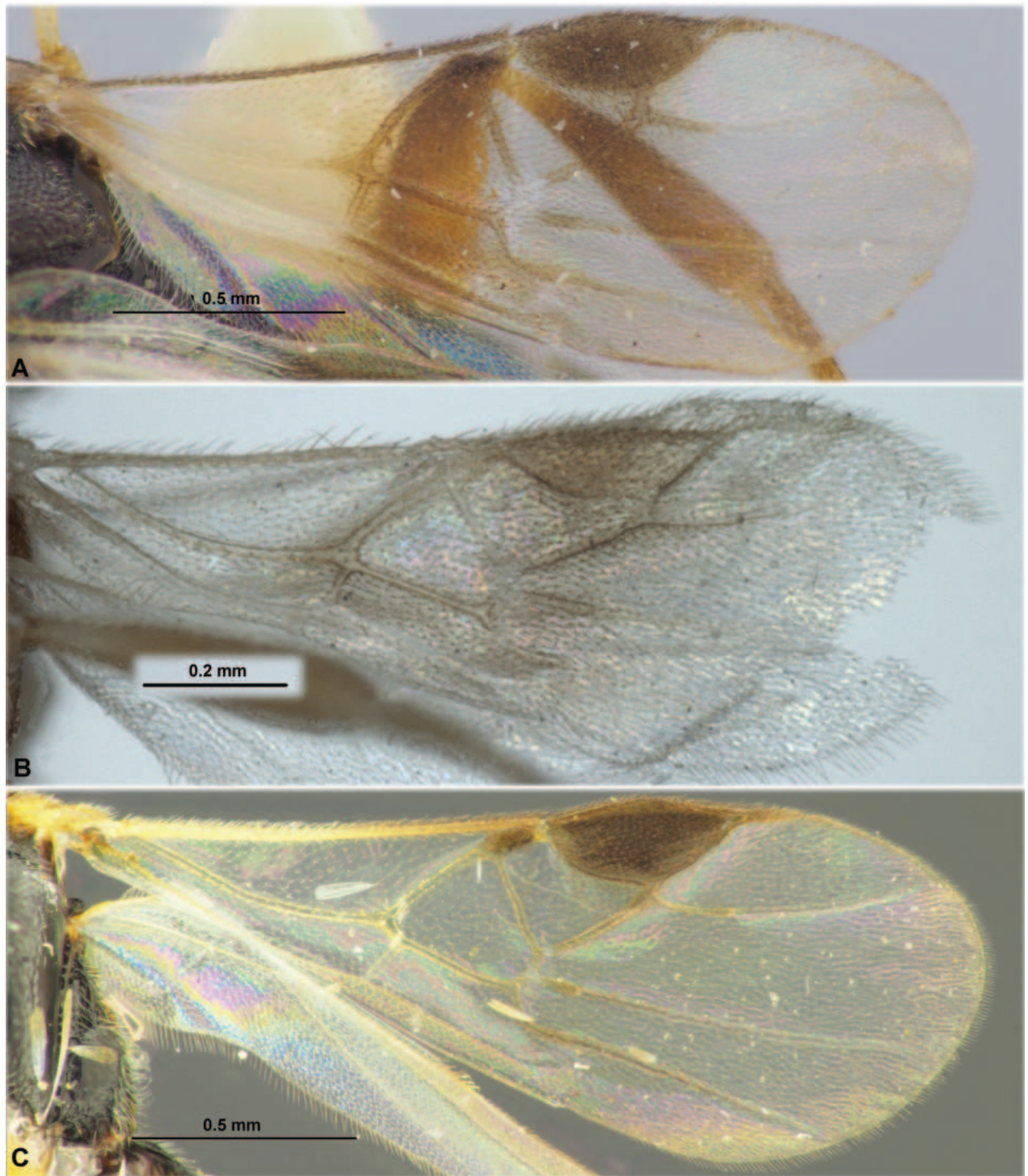


Figure 8. Fore wings. **A** *Paradelius (Sculptomyriola) ghilarovi* (Belokobylskij) **B** *P. (Sc.) koreanus* sp. nov. **C** *P. (Sc.) sinevi* (Belokobylskij).

Sculpture. Head densely and small areolate-punctate, partly arranged in transverse curved lines, frons densely reticulate in upper half and striate in lower half; face densely curvedly transverse striate and with dense additional punctation, clypeus with sparse punctation, smooth between punctures. Mesoscutum and scutellum very densely and distinctly punctate, sometimes partly with small areolae. Mesopleuron mainly smooth in posterior upper half and

in narrow area upper precoxal sulcus, distinctly and rather sparse punctate with reticulation in anterior lower half; metapleuron rugose-areolate with striation, usually with two small, subround and almost smooth areas. Propodeum submedially with coarse transverse and curved keel; areas not clearly delineated by carinae, areola and anterolateral areas absent; propodeum almost entirely densely rugulose-reticulate. First and second tergites entirely and third tergite in basal 0.7–0.8 (at least laterally) distinctly and densely rugose-reticulate, sometimes third tergite medially in basal 0.7 with transverse curved striae; apical part of third tergite and following tergites smooth.

Colour. Body black, rarely head dark reddish brown. Antenna yellow or brownish yellow in basal 0.3, black in apical 0.7, scape pale reddish brown. Palpi pale brown or yellow. Legs pale reddish brown, fore and middle legs paler, hind coxa in basal half, hind tibia mostly or widely and hind tarsus almost entirely reddish brown to dark reddish brown; tibial spurs yellow. Fore wing hyaline or very faintly infuscate, without dark bands. Pterostigma and parastigma dark brown, pterostigma sometimes faintly paler basally and apically; most veins pale brown or yellow.

Male. Body length 2.3–2.5 mm; fore wing length 1.9–2.0 mm. Antenna 20-segmented, less thickened, evenly setiform, longer than body, its basal one-third or half pale reddish brown to dark reddish brown. First flagellar segment 2.2–2.3× longer than its apical width, 1.10–1.15× longer than second segment; tenth segment 1.5–2.0× longer than its maximum width; penultimate segment 2.2–2.3× longer than its width. Mesopleuron widely smooth or sparsely to very sparsely punctate. First tergite 1.2–1.5× as long as second tergite. Third tergite rugulose-reticulate only in basal 0.2–0.3; following tergites usually weakly shagreened. Hind leg mainly reddish brown to dark reddish brown, almost black partly. Fore wing entirely hyaline; most veins subhyaline or pale. Otherwise similar to female.

Distribution. Russia (Primorskiy Territory).

Subgenus *Sinadelius* He & Chen, 2000

Figs 9–12

Description of subgenus. Vertex densely reticulate-punctate. Ocelli arranged in obtuse triangle. Eye covered by dense and long setae. Antenna long, thickened (especially medially) and setiform. Flagellar segments always longitudinal in apical half of antenna. Mesoscutum densely and distinctly punctate. Prescutellar depression short and crenulate. Prepectal carina laterally absent. Precoxal sulcus distinct, relatively wide, entirely crenulate or rugulose. Propodeum almost entirely rugulose-reticulate, often with areas delineated by carinae. Fore wing with large pterostigma. Radial vein (r) always with one abscissa, arising from pterostigma distinctly distant from first radiomedial vein (2-SR). Discoidal (discal) cell anteriorly always sessile. Recurrent vein (m-cu) weakly postfurcal or interstitial to first radiomedial vein (2-SR). Hind femur wide; hind tibia distinctly clavate. First tergite of metasoma subparallel or weakly narrowed towards apex behind distinct spiracular tubercles, entirely rugose-reticulate. Suture between first and second tergites present, usually distinct, densely crenulate. Second and following tergites smooth, only second one shortly rugulose basally; suture between second and third tergites very weak, shallow and smooth (as trace). Ovipositor short.

***Paradelius (Sinadelius) guangxiensis* (He & Chen, 2000), comb. nov.**

Figs 9, 12A

Sinadelius guangxiensis He & Chen in He et al. 2000: 682; Yu et al. 2016.

Material examined. CHINA: Guangxi, Longzhou, Nonggang, 20.V. 1985 (He Junhua col.), No. 824419, 1 female (HT) (ZJUH); same label as in holotype, 1 female (PT) (ZJUH).

Description. Female. Body length 1.8 mm; fore wing length 1.8 mm.

Head. Head 1.9× wider than its medial length (dorsal view), 1.2× wider than mesoscutum. Occiput weakly concave. Head behind eyes distinctly evenly roundly narrowed; transverse diameter of eye ~ 2.5× larger than length of temple (dorsal view). Ocelli arranged in triangle with base 1.5× its sides. POL ~ 2.0× Od, 0.9× OOL. Eye large, 1.5× as high as broad. Malar space ~0.5× basal width of mandible, 0.1× height of eye. Face weakly convex, width of face 1.2× its median height, 0.9× height of eye. Tentorial pits distinct, distance between pits 1.3× distance from pit to eye. Clypeus rather high and convex, its width 2.2× median height, 0.8× width of face; its ventral margin almost straight medially. Head distinctly roundly narrowed below eyes (front view).

Antenna. Antenna 22-segmented, weakly thickened, weakly setiform, with elongated medial segments. Scape ~ 2.0× longer than wide. First flagellar segment 3.3× longer than its apical width, 1.8× longer than second segment.

Mesosoma. Mesosoma 1.7× longer than maximum height. Mesoscutum highly and convex-curvedly elevated above pronotum (lateral view), ~ 2.0× as wide as its medial length (dorsal view). Prescutellar depression (scutellar sulcus) shallow, straight, with distinct numerous carinae. Scutellum almost as long as anterior width. Prepectal carina not visible laterally. Precoxal sulcus distinct, narrow, short, oblique, crenulate.

Wings. Fore wing ~ 3.0× longer than maximum width. Pterostigma ~ 2.0× longer than its maximum width. Radial vein (r) arising from distal 0.2 of pterostigma; radiomedial vein (2-SR) arising almost from middle of pterostigma and strongly separated from radial vein (r). Present only single and evenly curved abscissa of radial vein (r), which finely sclerotised in basal 0.25 and desclerotised on remaining part, reaching as track distal margin of wing. Radial (marginal) cell weakly shortened, 3.0× longer than its maximum width. Sclerotised part of metacarp (1-R1) relatively long, faintly pigmented, 0.6× as long as pterostigma. First radiomedial vein (2-SR) weakly curved, sclerotised and brown, ~ 4.3× longer than recurrent vein (m-cu). Recurrent vein (m-cu) weakly postfurcal to first radiomedial vein (2-SR), posteriorly subparallel posteriorly with basal vein (1-M). Discoidal (discal) cell broadly sessile anteriorly, 1.4× longer than its maximum width. Nervulus (cu-a) perpendicular to longitudinal anal vein (1-1A), postfurcal, distance between basal vein (1-M) and nervulus (cu-a) 0.6× nervulus (cu-a) length. Hind wing ~ 3.6× longer than maximum width. First abscissa of mediocubital vein (M+CU) 1.8× longer than second abscissa (1-M).

Legs. Hind femur ~ 3.5× longer than maximum width. Hind tibia claviform, distinctly widened distally. 4.8× longer than maximum width, 0.8× as wide as hind femur. Hind tarsus ~ 0.9× as long as hind tibia, its basitarsus 0.8× as long as second–fifth segments combined. Second segment of hind tarsus 0.35× as long as basitarsus.

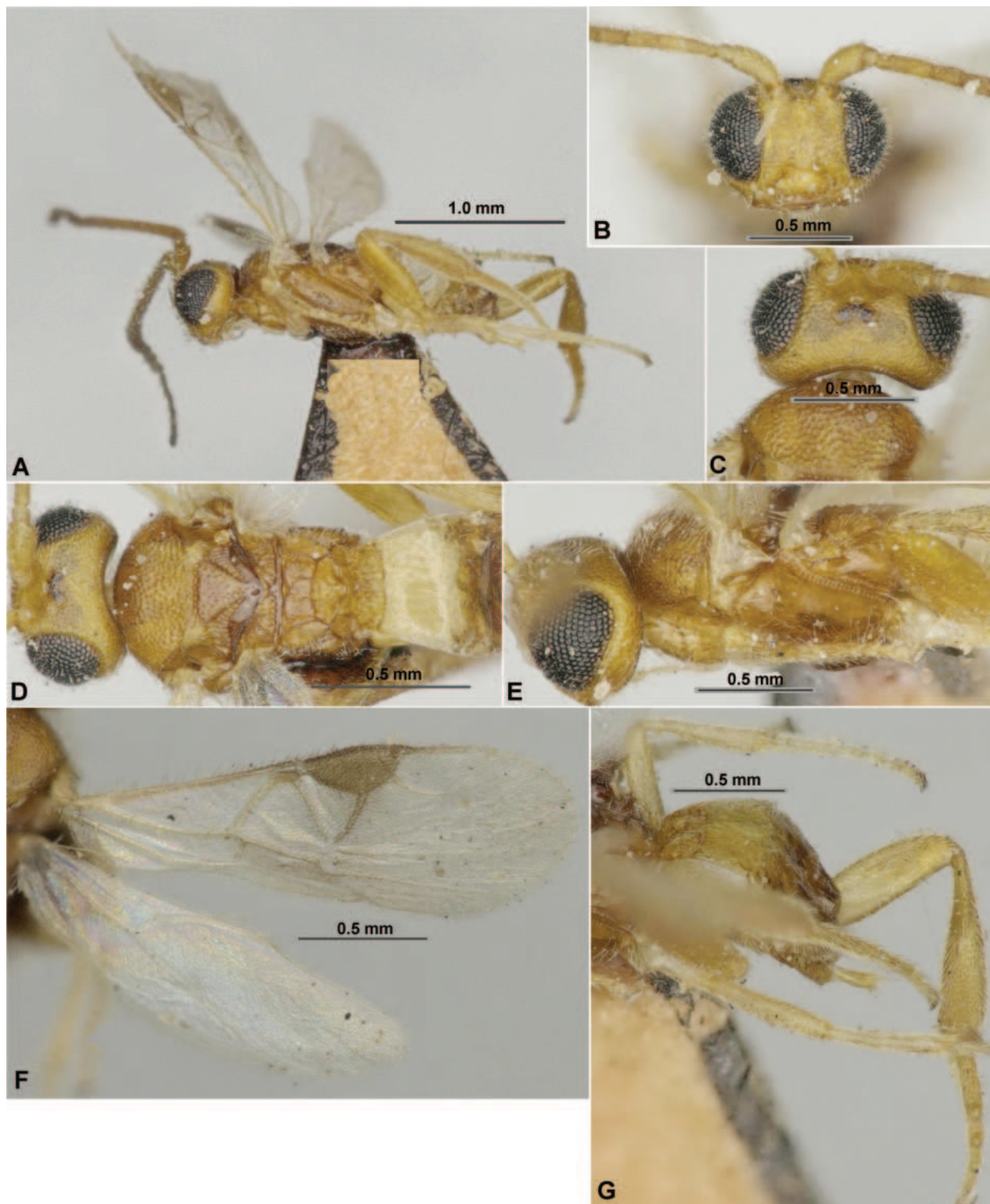


Figure 9. *Paradelius (Sinadelius) guangxiensis* (He & Chen, 2000), comb. nov. (female, holotype) **A** habitus, lateral view **B** head and base of antenna, front view **C** head, dorsal view **D** head, mesosoma and base of metasoma, dorsal view **E** head and mesosoma, lateral view **F** wings **G** metasoma and hind leg, lateral view.

Metasoma. Metasoma approximately as long as mesosoma. All tergites rather distinctly sclerotised. First tergite with weak and thick spiracular tubercles, strongly widened from base to spiracular tubercles situated submedially on tergite, then almost subparallel-sided towards posterior margin of tergite. First suture

distinct, rather deep, weakly curved, densely crenulate. Medial length of first tergite 0.5× its maximum width at level of spiracles, 0.6× as long as second tergite. Second suture present, but very fine and almost straight. Second tergite 1.4× longer than third tergite. Length of first to third tergites combined 0.9× their maximum width. Third tergite almost straight on posterior margin. Ovipositor sheaths weakly thickened, short, 0.4× as long as first–third tergites combined.

Sculpture. Vertex densely and small punctate-reticulate; face distinctly transverse striate, with reticulation between striae, laterally below partly almost smooth; clypeus finely rugulose to smooth. Mesoscutum entirely densely punctate, smooth between punctulae, without very dense punctation in its medioposterior area. Scutellum widely smooth and with small sparse punctulae. Mesopleuron almost entirely smooth. Propodeum with distinct and strongly curved submedial transverse keel, without areola, with wide and narrow petiolate area posteriorly; anterolateral areas distinctly delineated by carinae, almost smooth and with punctation, weakly reticulate marginally; propodeum mainly sparsely and rather finely rugose-reticulate. First tergite entirely distinctly rugose-reticulate. Second tergite entirely smooth. Remaining tergites smooth.

Colour. Body pale reddish brown or yellowish brown; second and basal one-third of third tergites pale yellow. Antenna mainly pale reddish brown, infuscate towards apex. Palpi yellow. Legs mainly yellow or pale brown, hind tibia and tarsus faintly darkened. Wing mainly subhyaline, with infuscation below pterostigma. Pterostigma and parastigma brown, most veins pale brown, first radiomedial vein (2-SR) brown.

Male. Unknown.

Distribution. China (Guangxi Autonomous Region).

***Paradelius (Sinadelius) nigricans* (He & Chen, 2000), comb. nov.**

Figs 10, 12B

Sinadelius nigricans He & Chen in He et al. 2000: 682; Yu et al. 2016.

Material examined. CHINA: Liaoning, Shenyang, Dongling, 21.VI.1994 (Lou Juxian col.), No. 947731, 1 male (HT) (ZJUH).

Description. Male. Body length 2.4 mm; fore wing length 2.1 mm.

Head. Head 1.7× wider than its medial length (dorsal view), 1.1× wider than mesoscutum. Occiput weakly concave. Head behind eyes evenly roundly narrowed; transverse diameter of eye 1.5× larger than length of temple (dorsal view). Ocelli arranged in triangle with base 1.2× its sides. POL 2.5× Od, 0.8× OOL. Eye 1.3× as high as broad. Malar space ~ 0.7× basal width of mandible, 0.2× height of eye. Face weakly convex, width of face 1.5× its median height, ~ 1.1× height of eye. Tentorial pits distinct, distance between pits 1.4× distance from pit to eye. Clypeus rather low and distinctly convex, its width 2.3× median height, 0.7× width of face; its ventral margin almost straight. Head distinctly roundly narrowed below eyes (front view).

Antenna. Antenna 22-segmented, weakly thickened, weakly setiform, with medial segments elongated. Scape ~ 2.0× longer than wide. First flagellar segment 3.3× longer than its apical width, 1.5× longer than second segment. Tenth segment ~ 2.0× longer than its maximum width. Subapical segment 1.6× longer than its width.

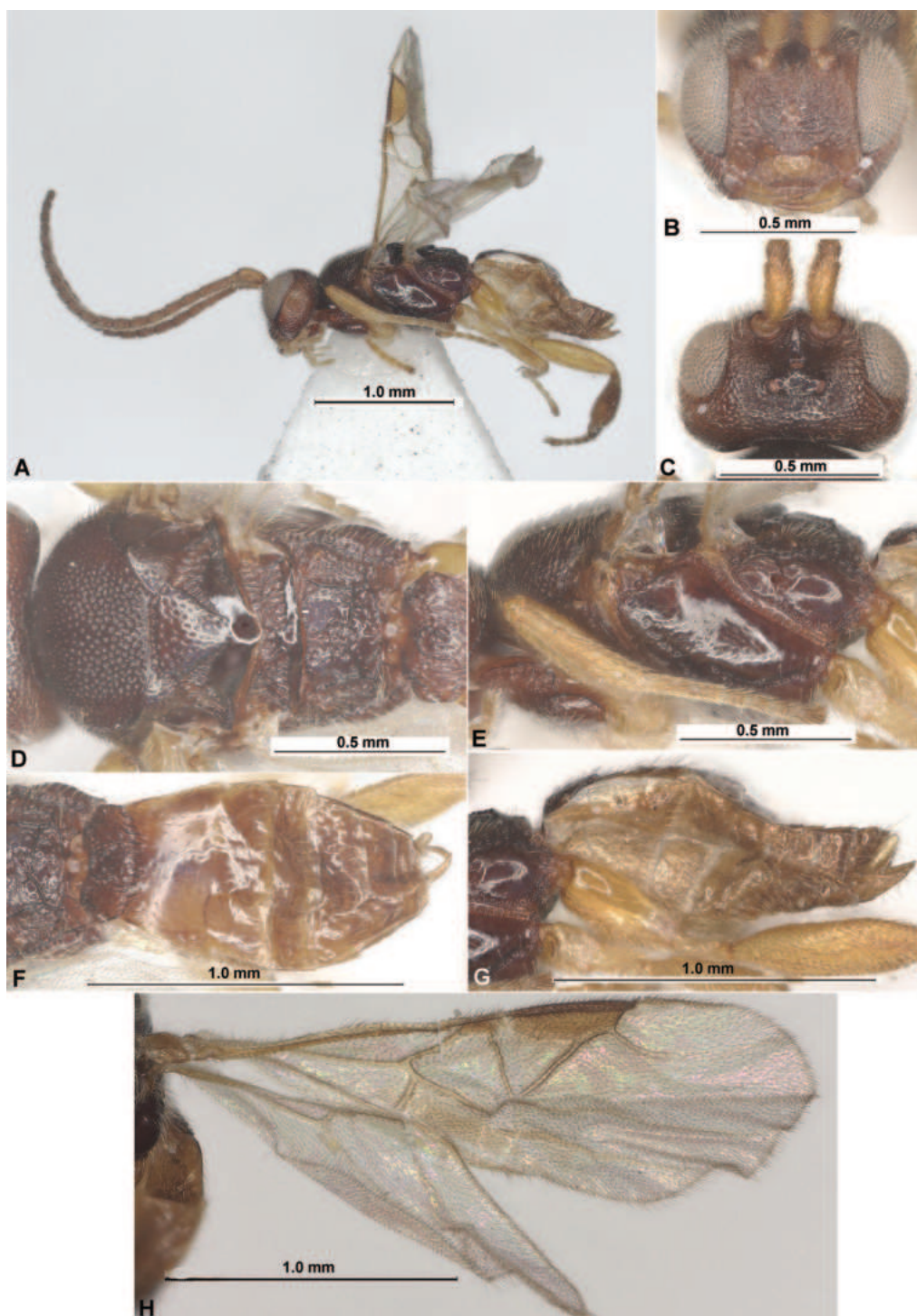


Figure 10. *Paradelius (Sinadelius) nigricans* (He & Chen, 2000), comb. nov. (male, holotype) **A** habitus, lateral view **B** head, front view **C** head, dorsal view **D** mesosoma, dorsal view **E** mesosoma, lateral view **F** propodeum and metasoma, dorsal view **G** propodeum and metasoma, lateral view **H** wings.

Mesosoma. Mesosoma 1.7× longer than maximum height. Mesoscutum highly and convex-curvedly elevated above pronotum (lateral view), 2.0× as wide as its medial length (dorsal view). Prescutellar depression (scutellar sulcus) shallow, straight, with distinct numerous carinae. Scutellum 1.1× as long as anterior width. Prepectal carina almost not visible laterally. Precoxal sulcus distinct, narrow, long, curved, distinctly crenulate.

Wings. Fore wing ~ 3.0× longer than maximum width. Pterostigma 3.2× longer than its maximum width. Radial vein (r) arising from distal 0.2 of pterostigma; radiomedial vein (2-SR) arising weakly behind middle of pterostigma and strongly separated from radial vein (r). Present only single and evenly curved abscissa of radial vein (r), which distinctly sclerotised in basal 0.25 and desclerotised on remaining part, reaching as track distal margin of wing. Radial (marginal) cell shortened, 3.2× longer than its maximum width. Sclerotised part of metacarp (1-R1) relatively long, faintly pigmented, 0.7× as long as pterostigma. First radiomedial vein (2-SR) sclerotised and brown, 4.5× longer than short recurrent vein (m-cu). Recurrent vein (m-cu) subinterstitial to first radiomedial vein (2-SR), approximately as long as sclerotised part of second medial abscissa (2-SR+M), posteriorly divergent with basal vein (1-M). Discoidal (discal) cell broadly sessile anteriorly, 1.5× longer than its maximum width. Nervulus (cu-a) perpendicular to longitudinal anal vein (1-1A), postfurcal, distance between basal vein (1-M) and nervulus (cu-a) 0.4× nervulus (cu-a) length. Hind wing ~ 4.0× longer than maximum width. First abscissa of mediocubital vein (M+CU) ~ 2.0× longer than second abscissa (1-M).

Legs. Hind coxa long, ~ 2.0× longer than maximum width. Hind femur 3.7× longer than maximum width. Hind tibia claviform, distinctly widened distally.

Metasoma. Metasoma approximately as long as mesosoma. All tergites distinctly sclerotised. First tergite with distinct and thick spiracular tubercles, strongly widened from base to spiracular tubercles situated almost in middle of tergite, then weakly narrowed towards posterior margin of tergite. First suture distinct, rather wide, curved, densely crenulate. Medial length of first tergite 0.4× its maximum width at level of spiracles, 0.7× as long as second tergite. Second suture present, but very fine and almost straight. Second tergite 1.3× longer than third tergite. Length of first to third tergites combined approximately equal to their maximum width. Third tergite straight on posterior margin.

Sculpture. Vertex densely and small punctate-reticulate, frons with additional granulation; face densely rugose-reticulate, below laterally almost smooth; clypeus finely rugulose to smooth in upper half and rugose-reticulate in lower half. Mesoscutum entirely densely punctate and smooth between punctulae, without very dense punctation in its medioposterior area. Scutellum widely smooth and with small sparse punctulae. Mesopleuron almost entirely smooth, with fine and sparse punctulae upper precoxal sulcus; metapleuron mainly smooth, narrowly areolate-rugose along its margins. Propodeum with fine submedial transverse keel, with narrow subtriangular areola delineated by carinae, and with wide and narrow petiolate area posteriorly; anterolateral areas distinctly delineated by carinae, almost smooth medially and reticulate marginally; propodeum mainly rugose-reticulate. First tergite entirely coarsely rugose-reticulate, with transverse subbasal carina. Second tergite mainly smooth, only rugose in basal 0.1. Remaining tergites entirely smooth.

Colour. Head reddish brown; mesosoma mainly dark reddish brown to black; metasoma reddish brown or faintly paler, its first tergite almost black. Antenna mainly dark brown, scape reddish brown. Palpi pale brown. Legs mainly yellow or pale brown, hind tibia and tarsus almost entirely dark reddish brown. Wing entirely infusate, without dark bands. Pterostigma and parastigma brown, most veins of fore wing brown to pale brown.

Female. Unknown.

Distribution. China (Liaoning Province).

***Paradelius (Sinadelius) ussuriensis* Belokobylskij, 1988**

Figs 11, 12C

Paradelius ussuriensis Belokobylskij, 1988: 148; 1998: 556; Yu et al. 2016.

Material examined. RUSSIA. PRIMORSKIY TERRITORY: "Primorskiy Territory, 15 km S of Partizansk, forest, 16 VII 1979, Belokobylskij [col.]", "Holotype *Paradelius ussuriensis* Belokobylskij", 1 male (HT); Vladivostok, Sanatornaya, forest, 26.VII.1984 (S. Belokobylskij), 1 male (PT); 10 km S of Partizansk, forest, 19.VII.1979 (S. Belokobylskij), 1 male (PT); same locality, bushes, slopes, 11.VII.1996 (S. Belokobylskij), 2 males; 15 km S of Partizansk, forest, 17.VII.1979 (S. Belokobylskij), 1 male (PT); 10 km NW of Partizansk, forest, 13.VII.1979 (S. Belokobylskij), 1 male (PT); Lazovskiy Nature Reserve, 10 km SW of Sokolchi, 22 & 24.VII.1993 (S. Belokobylskij), 1 male; Spassk-Dal'niy, clearing, 13 & 17.VII.1991 (S. Belokobylskij), 1 female, 1 male; 20 km SE of Spassk-Dal'niy, forest, edge, 13 & 17.VII.1995 (S. Belokobylskij), 1 female, 1 male; 50 km N of Ol'ga, mixed forest, 30.VIII.1979 (S. Belokobylskij), 1 male (PT) (All in ZISP).

Description. Female. Body length 2.4–2.5 mm; fore wing length 2.0–2.1 mm.

Head. Head 1.8–2.0× wider than its medial length (dorsal view), 1.1–1.2× wider than mesoscutum. Occiput distinctly concave. Head behind eyes weakly convex in anterior half and roundly narrowed in posterior half; transverse diameter of eye 1.2–1.4× larger than length of temple (dorsal view). Ocelli arranged in triangle with base 1.3–1.5× its sides. POL 2.3–2.5× Od, 0.6–0.8× OOL. Eye 1.4–1.5× as high as broad. Malar space 0.6–0.8× basal width of mandible, 0.15–0.20× height of eye. Face almost flat, width of face 1.4–1.5× its median height, ~ 1.2× height of eye. Tentorial pits distinct, distance between pits 1.2–1.5× distance from pit to eye. Clypeus high and distinctly convex, its width 2.0–2.1× median height, 0.6–0.7× width of face; its ventral margin almost straight. Head distinctly roundly narrowed below eyes (front view).

Antenna. Antenna more than 20-segmented (missing apically), weakly thickened, weakly setiform, all its segments elongated. Scape 2.1–2.2× longer than wide. First flagellar segment 3.0–3.3× longer than its apical width, 1.3–1.6× longer than second segment. Tenth segment ~ 1.3× longer than its maximum width.

Mesosoma. Mesosoma 1.4–1.5× longer than maximum height. Mesoscutum highly and convex-curvedly elevated above pronotum (lateral view), 1.5–1.7× as wide as its medial length (dorsal view). Prescutellar depression (scutellar sulcus) shallow, with distinct numerous carinae. Scutellum almost as long as anterior width. Prepectal carina not visible laterally. Precoxal sulcus distinct, narrow, short, curved, situated in middle of mesopleuron, rugose-reticulate.

Wings. Fore wing 2.4–2.6× longer than maximum width. Pterostigma 2.1–2.3× longer than its maximum width. Radial vein (r) arising from distal 0.1–0.2 of pterostigma. Radiomedial vein (2-SR) arising almost from or weakly behind middle of pterostigma and strongly separated from radial vein (r). Present only single and evenly curved abscissa of radial vein (r), which weakly sclerotised in basal 0.2–0.3 and desclerotised on remaining part, reaching as track distal margin of wing. Radial (marginal) cell shortened, 2.8–3.0× longer than its maximum width. Sclerotised part of metacarp (1-R1) relatively short, faintly pigmented, 0.5–0.6× as long as pterostigma. First radiomedial vein (2-SR) sclerotised, 3.6–4.5× longer than recurrent vein (m-cu). Recurrent vein (m-cu) postfurcal

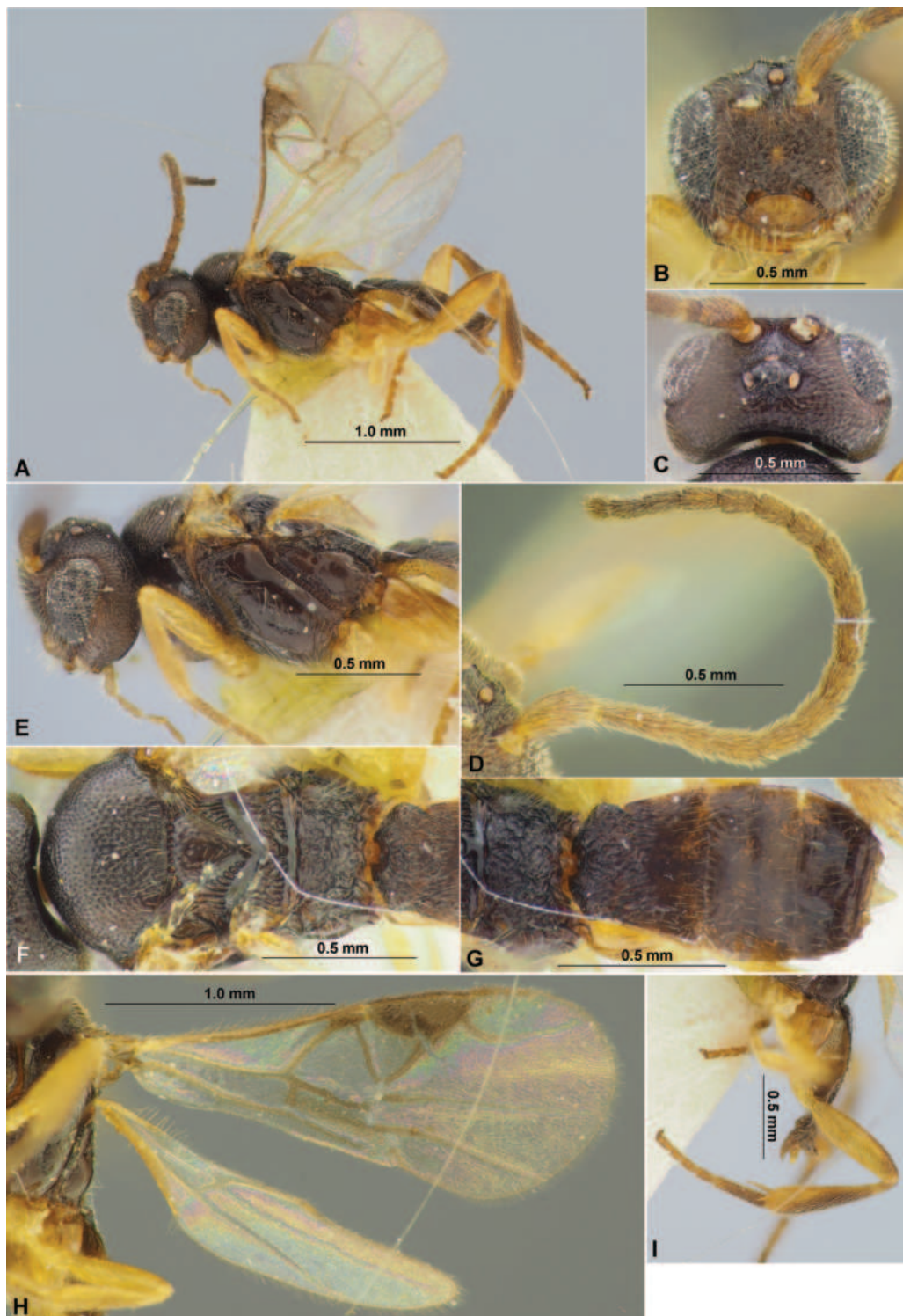


Figure 11. *Paradelius (Sinadelius) ussuriensis* Belokobylskij, 1988 (male, holotype) **A** habitus, lateral view **B** head, front view **C** head, dorsal view **D** antenna **E** head and mesosoma, lateral view **F** mesosoma and base of metasoma, dorsal view **G** propodeum and metasoma, dorsal view **H** wings **I** hind leg.

to first radiomedial vein (2-SR), approximately as long as sclerotised part of second medial abscissa (2-SR+M), posteriorly subparallel with basal vein (1-M). Discoidal (discal) cell broadly sessile anteriorly, 1.1–1.2× longer than its maximum width. Nervulus (cu-a) subperpendicular to longitudinal anal vein (1-1A), postfurcal, distance between basal vein (1-M) and nervulus (cu-a) 0.4–0.7×



Figure 12. Fore wings. **A** *Paradelius* (*Sinadelius*) *guangxiensis* (He & Chen) **B** *P.* (*S.*) *nigricans* (He & Chen) **C** *P.* (*S.*) *ussuriensis* Belokobylskij.

nervulus (cu-a) length. Hind wing 3.3× longer than maximum width. First abscissa of mediocubital vein (M+CU) ~ 2.0× longer than second abscissa (1-M).

Legs. Hind coxa long and high, 1.5–1.7× longer than maximum width. Hind femur 3.3–3.5× longer than maximum width. Hind tibia claviform, 4.6–5.3× longer than maximum width, 0.7–0.8× as wide as hind femur; longest inner tibial spur 0.5–0.7× hind basitarsus length. Hind tarsus approximately as long as hind tibia, its basitarsus 0.6–0.7× as long as second–fifth segments combined. Second segment of hind tarsus 0.4× as long as basitarsus, 1.1× longer than fifth segments (without pretarsus).

Metasoma. Metasoma approximately as long as mesosoma. All tergites distinctly sclerotised. First tergite with distinct and thick spiracular tubercles, strongly widened from base to spiracular tubercles in middle of tergite, then rather distinctly narrowed towards posterior margin of tergite. First suture rather distinct, narrow, curved, crenulate. Medial length of first tergite 0.5–0.7× its maximum width at level of spiracles, 0.7–0.8× as long as second tergite. Second suture present, but very fine and almost straight. Second tergite 1.1–1.3× longer than third tergite. Length of first–third tergites combined ~ 1.1× their maximum width. Third tergite straight in posterior margin. Ovipositor sheaths thickened, short, 0.3–0.4× as long as first–third tergites combined.

Sculpture. Head densely rugose-reticulate with punctation partly, vertex additionally with transverse striation laterally; clypeus entirely in dense punctation and smooth between punctures. Mesoscutum mainly rather densely punctate and smooth between punctulae, very densely punctate in subcircular area in its medioposterior half. Scutellum widely smooth with sparse punctulae. Mesopleuron almost entirely smooth, sometimes partly with sparse punctation; metapleuron mainly smooth, narrow areolate-rugose along its margins. Propodeum without or with fine submedial transverse keel, without or with wide areola delineated by carinae, widely densely rugulose-reticulate. First tergite entirely coarsely rugose-reticulate, with transverse subbasal carina. Second tergite mainly smooth, rugose-striate in basal 0.2–0.5. Remaining tergites entirely smooth.

Colour. Body dark reddish brown to black, sometimes head anteriorly and around eye reddish brown, rarely metasoma laterally and ventrally reddish brown to pale reddish brown at least partly. Antenna mainly dark reddish brown, black in apical half, scape reddish brown. Palpi pale brown or pale reddish brown, darkened basally. Legs mainly yellow, hind tibia dorsally and hind tarsus reddish brown to dark reddish brown; hind tibial spurs pale brown. Wing faintly infuscate, without dark bands. Pterostigma and parastigma dark brown, most veins brown to pale brown.

Male. Body length 2.4–2.6 mm; fore wing length 2.1–2.2 mm. Transverse diameter of eye 1.2–1.3× larger than length of temple (dorsal view). Antenna 22–23-segmented, subsetiform, all segments elongated. Tenth segment 1.8–1.9× longer than its maximum width. Penultimate segment 1.8–2.2× longer than its width, 0.8–0.9× as long as apical segment. Propodeum without submedial transverse keel and without areas delineated by carinae. Hind femur 3.4–3.7× longer than maximum width. Hind tibia distinctly claviform, 4.5–4.8× longer than maximum width, ~ 0.9× as wide as hind femur. Medial length of first tergite 0.6–0.7× its maximum width at level of spiracles, approximately as long as second tergite. Second tergite 1.3–1.5× longer than third tergite. Otherwise similar to female.

Distribution. Russia (Primorskiy Territory).

Discussion

The members of the tribe Adeliini are morphologically distinctly different from the other taxa of actual chelonine tribes: worldwide distributed Chelonini Foerster, 1863 and Phanerotomini Baker, 1926 (including Pseudophanerotomini Zettel, 1990), and Afrotropical Odontospaeropygini Zettel, 1990 (Zettel 1990; Yu et al. 2016; Kittel et al. 2016). One of the important diagnostic characters is located in the adeliine fore wing venation. Venation of the tribe Adeliini is very specialised,

highly reduced, and includes several high-level valuable taxonomic characters, such as the second radiomedial vein (r-m) and second radiomedial (submarginal) cell are absent; the radial (marginal) cell distally is widely open; the radial (r) and first radiomedial (2-SR) veins are often separately arising from the pterostigma; the apical parts of the radial (r), medial (2-M), second longitudinal anal (2-1A), third cubital (3-CU1) and parallel (CU1a) veins are strongly reduced; the first transverse anal (2A) and brachial (CU1b) veins are completely absent and, as a result, the brachial (subdiscal) cell is widely open distally. In turn, in the members of the other three chelonine tribes, including the Phanerotomini molecularly the most related to Adeliini (Kittel et al. 2016), all discussed veins of the fore wing are present and distinctly sclerotised, and the cells are closed.

The structures of the metasoma are also seriously different between adeliines and other chelonines. In the members of the actual chelonine groups, the three immovably fused, heavily sclerotised and coarsely sculptured basal metasomal tergites are predominantly strongly enlarged and cover all following posterior segments; also a third tergite is often apically curved down and in some cases (many Chelonini) additionally below continued forwards. On the other side, all members of Adeliini have less sclerotised and often entirely or mainly smooth from first to third tergites, which are not covered the protruding far posterior segments; the third tergite never curved down posteriorly. The previously expressed opinion (Dowton and Austin 1998) about the plesiomorphic state of the carapace-like metasoma in the actual chelonines and derived (apomorphic) its condition in Adeliini is very questionable, because the evolutionary transformation of such complicated structure of actual chelonine metasoma to much simple adeliine metasoma state is not easy to explain and justify. On the other hand, the characteristic for these taxonomic groups immovably fused the first to third tergites are also met in several genera from other Braconidae subfamilies (namely, Braconinae, Doryctinae, Rogadinae, Hormiinae, Telengaiinae, Acampsohelconinae, Brachistinae, etc.) (van Achterberg 1993), which showed the possibility of the parallel evolution of this character state in the different braconid phylogenetic lines and subfamilies.

Thus, discussed upper strong morphological differences are not allowed to definitely unite the members of adeliines with the representatives of the actual chelonines. Currently, the association of these groups inside the subfamily Cheloninae is supported mainly at the molecular level (Kittel et al. 2016). Nevertheless, a new molecular data based on the more number of genes will be very useful for the additional analyses of the phylogenetic relationship of these morphologically strongly different taxonomic groups.

Acknowledgements

The authors are very thankful to Prof. Cornelis van Achterberg (Leiden, the Netherland), Dr Angélica Penteado-Dias (São Paulo, Brazil), and an anonymous reviewer for their useful suggestions and comments on this manuscript.

Additional information

Conflict of interest

The authors have declared that no competing interests exist.

Ethical statement

No ethical statement was reported.

Funding

This work was funded in part by the Russian State Research Project No 122031100272-3 for SAB, and was supported by a grant from the National Institute of Biological Resources (NIBR), funded by the Ministry of Environment (MOE) of the Republic of Korea (project number: NIBR202402202) for DSK, and the Key International Joint Research Program of National Natural Science Foundation of China (31920103005) for XXC.

Author contributions

Conceptualisation: SAB, DK. Data curation: SAB. Investigation: SAB, DK, XXC. Methodology: SAB, DK, XXC. Writing - original draft: SAB. Writing - review and editing: DK, XXC.

Author ORCIDs

Sergey A. Belokobylskij  <https://orcid.org/0000-0002-3646-3459>

Deokseo Ku  <https://orcid.org/0000-0002-6274-6479>

Xue-xin Chen  <https://orcid.org/0000-0002-9109-8853>

Data availability

All of the data that support the findings of this study are available in the main text.

References

- Belokobylskij SA (1988) Subfamily Adeliinae (Hymenoptera, Braconidae) in the Far East of the USSR. *Proceeding of the All-Union Entomological Society* 70: 144–152. [In Russian]
- Belokobylskij SA (1998) Subfam. Adeliinae (Acaeliinae). In: Lehr PA (Ed.) *Key to the insects of the Russian Far East*. Vol. 4. Neuropteroidea, Mecoptera, Hymenoptera. Pt 3. Dal'nauka, Vladivostok: 553–558. [In Russian]
- Belokobylskij SA, Maetô K (2009) Doryctinae (Hymenoptera, Braconidae) of Japan. *Fauna mundi*. Vol. 1. Warszawska Drukarnia Naukowa, Warszawa, 806 pp.
- Čapek M (1970) A new classification of the Braconidae (Hymenoptera) based on the cephalic structures of the final instar larva and biological evidence. *Canadian Entomologist* 102(7): 846–875. <https://doi.org/10.4039/Ent102846-7>
- Chen XX, van Achterberg C (2019) Systematics, phylogeny, and evolution of braconid wasps: 30 years of progress. *Annual Review of Entomology* 64(1): 335–358. <https://doi.org/10.1146/annurev-ento-011118-111856>
- De Saeger H (1942) *Paradelius* genre nouveau de Microgastrinae (Hymenoptera: Braconidae). *Revue de Zoologie et de Botanique Africaines* 36: 313–316.
- Downton M, Austin AD (1998) A phylogenetic relationships among the microgastroid wasps (Hymenoptera: Braconidae): combined analysis of 16S and 28S rDNA genes and morphological data. *Molecular Phylogenetics and Evolution* 10(3): 354–366. <https://doi.org/10.1006/mpev.1998.0533>
- He JH, Chen XX, Ma Y (2000) Hymenoptera, Braconidae. *Fauna Sinica. Insecta*, Vol. 18. Science Press, Beijing, 757 pp.
- Jasso-Martínez JM, Santos BF, Zaldívar-Riverón A, Fernández-Triana JL, Sharanowski BJ, Richter R, Dettman JR, Blaimer BB, Brady SG, Kula RR (2022) Phylogenomics of braconid wasps (Hymenoptera, Braconidae) sheds light on classification and the

- evolution of parasitoid life history traits. *Molecular Phylogenetics and Evolution* 173: 107452. <https://doi.org/10.1016/j.ympev.2022.107452>
- Kittel RN, Austin AD, Klopstein S (2016) Molecular and morphological phylogenetics of chelonine parasitoid wasps (Hymenoptera: Braconidae), with a critical assessment of divergence time estimations. *Molecular Phylogenetics and Evolution* 101: 224–241. <https://doi.org/10.1016/j.ympev.2016.05.016>
- Ku DS, Belokobylskij SA, Cha JY (2001) Hymenoptera (Braconidae). *Economic Insects of Korea* 16. *Insecta Koreana*. Supplement 23, 283 pp.
- Muesebeck CFW, Walkley LM (1951) Family Braconidae. In: Muesebeck CFW, Krombein KV, Townes HK (Eds) *Hymenoptera of America North of Mexico*. Synoptic catalog. U.S. Department, Agriculture Monograph 2: 90–184.
- Quicke DLJ, van Achterberg C (1990) Phylogeny of the subfamilies of the family Braconidae (Hymenoptera: Ichneumonoidea). *Zoologische Verhandlungen* 258: 1–95.
- Shi M, Chen XX, van Achterberg C (2005) Phylogenetic relationships among the Braconidae (Hymenoptera: Ichneumonoidea) inferred from partial 16S rDNA, 28S rDNA D2, 18S rDNA gene sequences and morphological characters. *Molecular Phylogenetics and Evolution* 37(1): 104–116. <https://doi.org/10.1016/j.ympev.2005.03.035>
- Shimbori EM, Bortoni MA, Shaw SR, Souza-Gessner CDS, Cerântola Pde CM, Penteado-Dias AM (2019) Revision of the New World genera *Adelius* Haliday and *Paradelius* de Saeger (Hymenoptera: Braconidae: Cheloninae: Adeliini). *Zootaxa* 4571(2): 151–200. <https://doi.org/10.11646/zootaxa.4571.2.1>
- Tobias VI 1986. Subfam. Acaeliinae (Adeliinae). In: Medvedev GS (Ed.) *Key to the insects of the USSR European part*. Vol. 3. Hymenoptera. Pt 4. Nauka, Leningrad: 336–337. [In Russian]
- van Achterberg C (1993) Illustrated key to the subfamilies of the Braconidae (Hymenoptera: Ichneumonoidea). *Zoologische Verhandlungen* 283: 1–189.
- Whitfield JB (1988) Two new species of *Paradelius* (Hymenoptera: Braconidae) for North America with biological notes. *The Pan-Pacific Entomologist* 64(4): 313–319.
- Whitfield JB (1997) Adeliinae. In: Wharton RA, Marsh PM, Sharkey MJ (Eds) *Manual of the New World genera of the family Braconidae* (Hymenoptera). International Society of Hymenopterists. Special Publication No. 1: 65–68.
- Whitfield JB, Mason WRM (1994) Mendesellinae, a new subfamily of braconid wasps (Hymenoptera, Braconidae) with a review of relationships within the microgastroid assemblage. *Systematic Entomology* 19(1): 61–76. <https://doi.org/10.1111/j.1365-3113.1994.tb00579.x>
- Yu DS, van Achterberg C, Horstmann K (2016) *Taxapad 2016. Ichneumonoidea 2015*. Nepean, Ottawa, Ontario. [Database on flash-drive]
- Zettel H (1990) Eine Revision der Gattungen der Cheloninae (Hymenoptera, Braconidae) mit Beschreibungen neuer Gattungen und Arten. *Annalen des Naturhistorischen Museums in Wien* 91B: 147–196.

Three new species of jumping spiders (Araneae, Salticidae) from Hunan, China

Song-Lin Li¹, Ping Liu¹, Xian-Jin Peng¹

¹ College of Life Sciences, Hunan Normal University, Changsha, Hunan 410081, China

Corresponding authors: Ping Liu (pingzi129@126.com); Xian-Jin Peng (xjpeng@126.com)

Abstract

Three new species of the genera *Thiania* C. L. Koch, 1846 and *Yaginumaella* Prószyński, 1979 are described and named as *T. bamian* sp. nov. (♂♀), *T. flacata* sp. nov. (♀) and *Y. curvata* sp. nov. (♂♀), from Hunan Province, China. Detailed descriptions, photos of somatic features and copulatory organs, as well as a distribution map are provided. Nucleotide data for the barcoding gene, cytochrome c oxidase subunit I (COI) of *T. bamian* sp. nov. (♂♀) and *Y. curvata* sp. nov. (♀) are provided.

Key words: Bamian Mountain, barcoding gene, COI, taxonomy

Introduction

Thiania C. L. Koch, 1846 is a well-known genus of the tribe Euophryini. It currently comprises 25 species mainly distributed in Asia, of which eight species are known from China (WSC 2024). Species belonging to *Thiania* can be recognized by the rectangular flattened carapace and robust leg I (Prószyński 2009).

Yaginumaella Prószyński, 1979 is currently placed in the tribe Plexippini according to molecular analysis (Maddison 2015). There are 21 species recorded from China (Zhu et al. 2005; Peng et al. 2008; Shao et al. 2014; Liu et al. 2016; Li et al. 2018; Peng 2020; Wang et al. 2023; Wang et al. 2024).

While examining specimens collected from Bamian Mountain, two new species of *Thiania* and one new species of *Yaginumaella* were recognized and are described here.

Materials and methods

Specimens are stored in 100% ethanol. Vulvae were cleaned with trypsin solution before examination and photography. Left male palps were dissected and used for description and color photos. Specimens were examined and measured with a Leica M205C stereomicroscope. Photos were taken with a digital camera Kuy Nice E3IS PM mounted on an Olympus BX53. Compound focus-stacked images were generated using Helicon Focus v. 7.6.1 and then adjusted in Adobe Photoshop 2020. The map was created by ArcMap v. 10.8. All measurements are given in millimeters (mm). Leg measurements are given



Academic editor: Zhiyuan Yao

Received: 12 March 2024

Accepted: 17 May 2024

Published: 7 June 2024

ZooBank: <https://zoobank.org/E05D5A85-37DF-468C-B92D-EF5B5C8936C0>

Citation: Li S-L, Liu P, Peng X-J (2024) Three new species of jumping spiders (Araneae, Salticidae) from Hunan, China. ZooKeys 1204: 301–312. <https://doi.org/10.3897/zookeys.1204.122887>

Copyright: © Song-Lin Li et al.
This is an open access article distributed under terms of the Creative Commons Attribution License (Attribution 4.0 International – CC BY 4.0).

in the following order: total length (femur, patella + tibia, metatarsus, tarsus). Genomic DNA was extracted from four legs of each specimen using an Animal Genomic DNA Isolation Kit (Tiangen Biotech, Beijing, China), and the universal primer pair LCO1490/HCO2198 was used for amplification of the COI gene (Folmer et al. 1994). The PCR products were sent to Tsingke Biotechnology Co., Ltd (Changsha, China) for purification and sequencing. The obtained sequences were aligned using Geneious Prime v. 9.0.2. The COI GenBank accession numbers of *T. bamian* sp. nov. (♂♀) and *Y. curvata* sp. nov. (♀) are also provided.

Specimens are deposited in the College of Life Sciences, Hunan Normal University (HUNNU) in Changsha, China. Abbreviations used are as follows: **AER** anterior eye row, **ALE** anterior lateral eye, **AME** anterior median eye, **CD** copulatory duct, **CO** copulatory opening, **E** embolus, **ED** embolic disc, **EFL** length of eye field, **EW** epigynal window, **FD** fertilization duct, **TL** tegular lobe, **MOA** median ocular area, **P** pocket, **PER** posterior eye row, **PLE** posterior lateral eye, **PME** posterior median eye, **RTA** retrolateral tibial apophysis, **S** spermatheca, **SD** sperm duct.

Taxonomy

Family Salticidae Blackwall, 1841

Genus *Thiania* C. L. Koch, 1846

Type species. *Thiania pulcherrima* C. L. Koch, 1846.

Thiania bamian sp. nov.

<https://zoobank.org/77A1258A-56A1-4564-81D8-3BE0D8DEB134>

Figs 1, 2, 6

Type material. **Holotype** ♂ (HNU-BMS-1905), CHINA, Hunan Prov., Chenzhou City, Guidong Co., Bamian Mountain National Nature Reserve, 25.975210°N, 113.702865°E, 1081 m, 18 Sept. 2019, Cheng Wang, Bo Lü and Xuan-Wei Zhou leg.; **paratypes**: 1 ♀ (HNU-BMS-1903), CHINA, Hunan Prov., Chenzhou City, Guidong Co., Bamian Mountain National Nature Reserve, 26.001944°N, 113.710675°E, 1678 m, 16 Sept. 2019, Cheng Wang, Bo Lü and Xuan-Wei Zhou leg.; 1 ♀ (HNU-BMS-2201), CHINA, Hunan Prov., Chenzhou City, Guidong Co., Bamian Mountain National Nature Reserve, 25.978498°N, 113.713744°E, 1025 m, 18 Aug. 2022, Song-Lin Li, Peng Yong, Li-Fen Li, Yu-Chen Zhou, Zi-Yue Liu leg.

Etymology. The specific epithet is derived from the type locality Bamian Mountain National Nature Reserve, noun.

Diagnosis. The male of this new species is similar to that of *Thiania longapophysis* Yu & Zhang, 2022 (Yu and Zhang 2022: figs 7A–D, 8A, B) in the shape of palpal bulb, sperm duct and embolus, but can be distinguished by: 1) the angle between RTA and cymbium (Fig. 1A) smaller than that angle in *T. longapophysis* (fig. 8A); and 2) the distal end of RTA bar-shaped (Fig. 1A), while barb-shaped in *T. longapophysis* (fig. 8A). The female of this new species is similar to that of *Thiania luteobrachialis* Schenkel, 1963 (Peng 2020: fig. 352a–c) in the

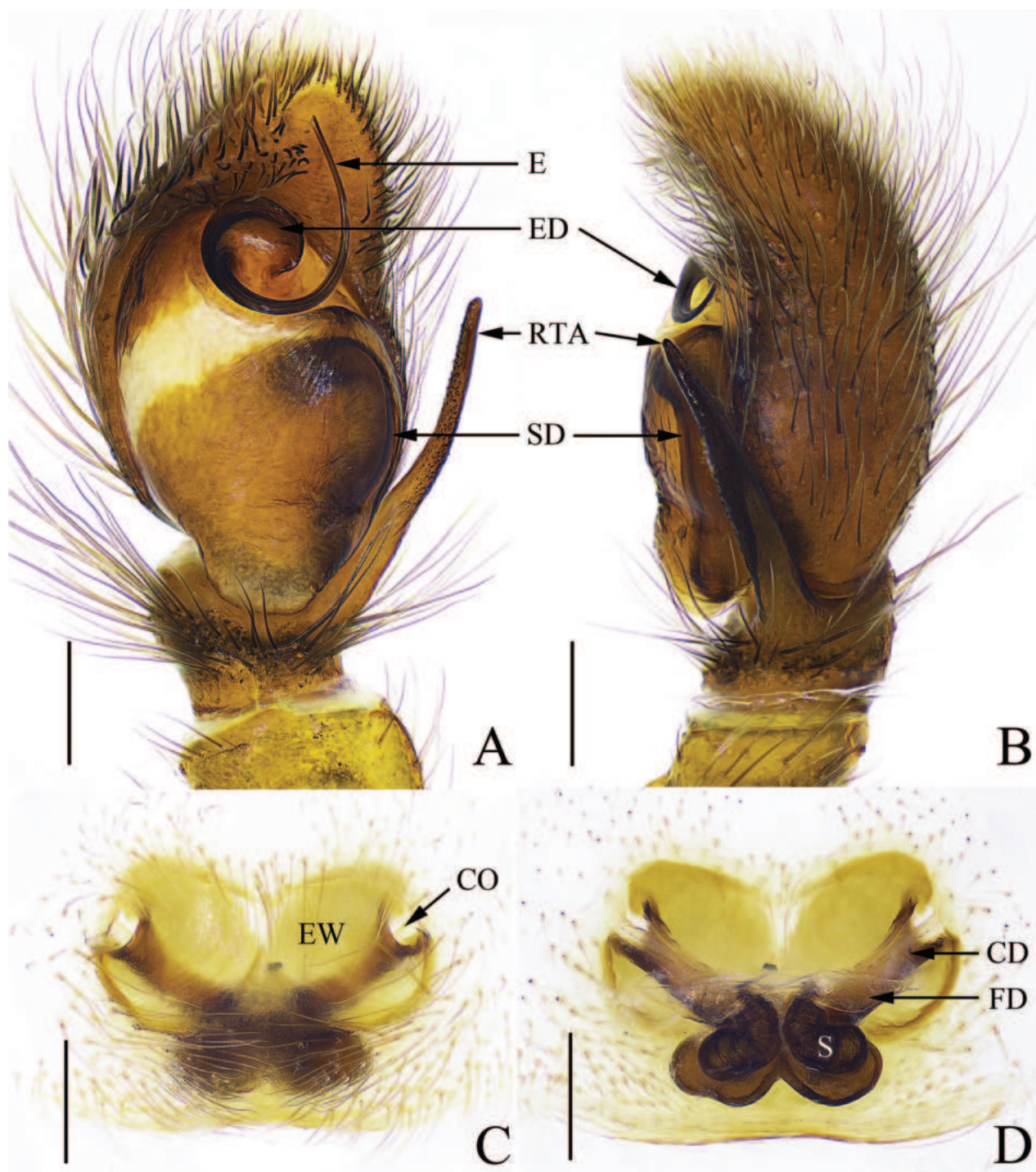


Figure 1. *Thiania bamian* sp. nov. **A** left palp, ventral view **B** ditto, retrolateral view **C** epigyne, ventral view **D** vulva, dorsal view. Scale bars: 0.2 mm.

shape of the epigynal window and the location of copulatory openings, but can be distinguished by the following characters: 1) proximal portion of copulatory ducts straight and V-shaped (Fig. 1D), while curved and U-shaped in *T. luteobranchialis* (fig. 352c); and 2) spermathecae overlapping with copulatory ducts (Fig. 1D), while not overlapping with copulatory ducts in *T. luteobranchialis* (fig. 352c).

Description. Male (holotype) (Fig. 2A, B). Total length 6.02; carapace 2.39 long, 2.03 wide; abdomen 3.45 long, 1.73 wide. Clypeus 0.24 high. Carapace



Figure 2. *Thiania bamian* sp. nov. **A** male holotype, habitus, dorsal view **B** ditto, ventral view **C** female paratype, habitus, dorsal view **D** ditto, ventral view. Scale bars: 1 mm.

dark brown, eye field covered with white setae. Fovea longitudinal, radial grooves distinct, cervical grooves indistinct. Eye sizes and interdistances: AME 0.50, ALE 0.29, PME 0.04, PLE 0.15, AER 1.64, PER 1.48, EFL 1.14. Chelicerae dark brown, promargin with one bicuspid tooth, retromargin with one tooth. Endites and labium brown, distal end pale yellow, with dark setae. Sternum yellow brown. Leg pale yellow to brown. Measurements of legs: I 7.27 (2.01, 3.03, 1.51, 0.72), II 5.04 (1.65, 1.76, 1.03, 0.60, 5.04), III 4.91 (1.52, 1.68, 1.22, 0.49), IV 4.82 (1.42, 1.80, 1.07, 0.53). Leg formula: 1234. Abdomen dorsum brown, with lighter edges; venter light yellow, with a wide light brown longitudinal band in the center.

Palp (Fig. 1A, B). Embolus long and thin, embolic disc distinct; retrolateral tibial apophysis long and thin, distal portion covered with many small granules, terminal end reached the antero-median portion of palpal bulb in retrolateral view; sperm duct obvious.

Female (paratype) (Fig. 2C, D). Total length 5.49; carapace 2.58 long, 2.11 wide; abdomen 2.86 long, 1.51 wide. Clypeus 0.32 high. Carapace yellow brown, with dark eye file and margins. Eye sizes and interdistances: AME 0.44, ALE 0.25, PME 0.05, PLE 0.20, AER 1.56, PER 1.52, EFL 1.14. Leg pale yellow to brown. Measurements of legs: I 5.47 (1.59, 2.29, 0.95, 0.64), II 4.44 (1.40, 1.72, 0.78, 0.54), III 4.51 (1.43, 1.60, 1.02, 0.46), IV 4.71 (1.42, 1.77, 1.09, 0.43). Leg formula: 1432. Abdomen dorsum brown, edges darker and with white hair, median portion with one pair of dark patches, posterior portion with four dark triangular patterns; venter pale yellow, median portion with one pair of gray longitudinal lines. Color paler than that in male.

Epigyne (Fig. 1C, D). Epigynal window circular. Copulatory openings oval, located on both sides of the epigynal window. Copulatory ducts with straight original portion and coiled terminal portion. Spermathecae shoe-shaped, slightly narrower than the copulatory ducts and overlapping with terminal portion of copulatory ducts.

Distribution. Known only from the type locality (Fig. 6).

GenBank accession number. Holotype (HNU-BMS-1905): PP786559; paratype ((HNU-BMS-2201): PP786560.

***Thiania flacata* sp. nov.**

<https://zoobank.org/A4578588-C911-4797-A06E-2CD405B48E63>

Figs 3, 6

Type material. **Holotype** ♀ (HNU-BMS-1905), CHINA, Hunan Prov., Chenzhou City, Guidong Co., Bamian Mountain National Nature Reserve, 25.975210°N, 113.702865°E, 1081 m, 18 Sept. 2019, Cheng Wang, Bo Lü and Xuan-Wei Zhou leg.

Etymology. The specific epithet is derived from the Latin "*falcata*" (falx-shaped), referring to the falx-shaped copulatory ducts, adjective.

Diagnosis. This new species can be distinguished from any other congeneric species by the vaulted copulatory openings.

Description. Female (holotype) (Fig. 3A, B). Total length 6.04; carapace 2.58 long, 2.24 wide; abdomen 3.37 long, 1.52 wide. Clypeus 0.12 high. Carapace yellow brown, with brown eye file and margins. Fovea longitudinal, radial and cervical grooves distinct. Eye sizes and interdistances: AME 0.51, ALE 0.27,

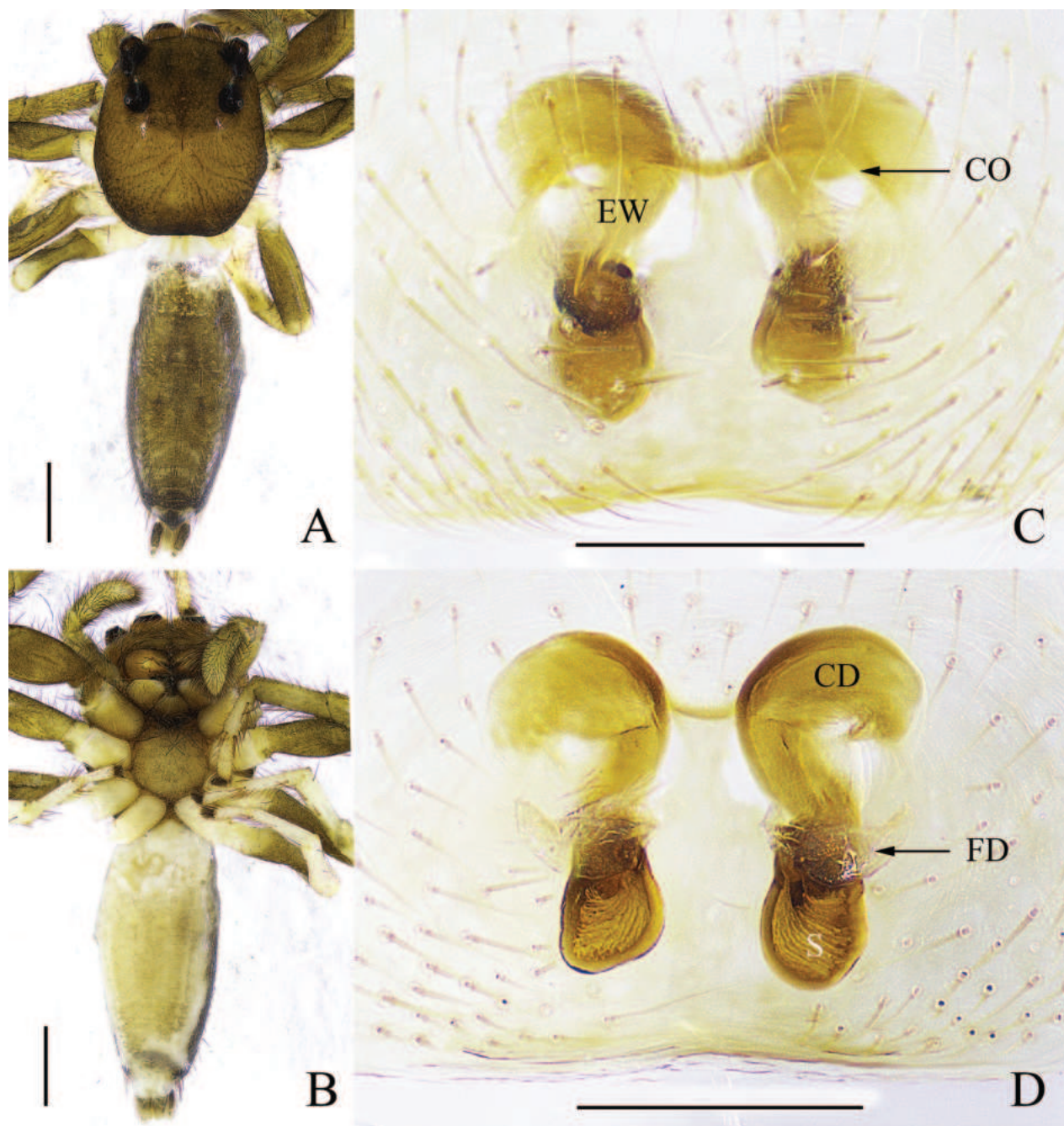


Figure 3. *Thiania flacata* sp. nov. **A** female paratype, habitus, dorsal view **B** ditto, ventral view **C** epigyne, ventral view **D** vulva, dorsal view. Scale bars: 1 mm (**A**, **B**); 0.2 mm (**C**, **D**).

PME 0.06, PLE 0.14, AER 1.62, PER 1.50, EFL 1.07. Chelicerae yellow brown, promargin with two teeth, retromargin with one tooth. Endites and labium yellow brown, distal end pale yellow with dark setae. Sternum yellow brown. Leg pale yellow to brown. Measurements of legs: I 6.33 (1.65, 2.65, 1.35, 0.68), II 4.58 (1.33, 1.83, 0.77, 0.65), III 4.61 (1.38, 1.67, 1.08, 0.48), IV 4.61 (1.40, 1.79, 0.99, 0.43). Leg formula: 1342. Abdomen dorsum brown, median portion with one pair of dark patches, posterior portion with three transverse light herringbone patterns, edges with white setae; venter light yellow, with a wide light brown longitudinal band in the center.

Epigyne (Fig. 3C, D). Epigynal window located medially on epigyne. Copulatory openings vaulted, located at the upper margin of the epigynal window. Copulatory ducts falx-shaped, original portion thicker. Spermathecae oval, slightly wider than the copulatory ducts.

Male. Unknown.

Distribution. Known only from the type locality (Fig. 6).

Genus *Yaginumaella* Prószyński, 1979

Type species. *Yaginumaella striatipes* Grube, 1861.

Remarks. The genus *Yaginumaella* is currently placed in the Plexippini tribe according to molecular analysis, together with the genus *Ptocasius* (Maddison 2015). *Yaginumaella* closely resembles *Ptocasius* (Logunov and Jäger 2015), especially in females (Li et al. 2018). However, there are clear differences in the type species of *Yaginumaella* and *Ptocasius* (Prószyński 2017). Patoleta et al. (2020), transferred 37 species of *Yaginumaella* to the genus *Ptocasius* only based on the similarity of genitalic structures. But, based on the characteristics shown in literature illustrations of species, these two genera can be distinguished by the following characters: 1) carapace with light longitudinal stripes in *Yaginumaella*, while usually with transverse stripes in *Ptocasius*; and 2) palpal bulb enlarged, with tegular lobe in *Yaginumaella*, while oblate, without tegular lobe in *Ptocasius* (Li et al. 2018). Therefore, according to the above characteristics, *Y. curvata* sp. nov. is described as a member of the genus *Yaginumaella*. In addition, based on the close collecting locations and genital characteristics of males and females, we tentatively identify them as the same species.

Yaginumaella curvata sp. nov.

<https://zoobank.org/C54A80DD-0FBE-42A5-9382-6BD123C9F2B5>

Figs 4, 5, 6

Type material. **Holotype** ♂ (HNU-BMS-1901), CHINA, Hunan Prov., Chenzhou City, Guidong Co., Bamian Mountain National Nature Reserve, 25.975914°N, 113.708825°E, 1001 m, 15 Sept. 2019, Cheng Wang, Bo Lü and Xuan-Wei Zhou leg.; **paratypes:** ♀ (HNU-BMS-2202), CHINA, Hunan Prov., Chenzhou City, Guidong Co., Bamian Mountain National Nature Reserve, 25.975568°N, 113.705383°E, 1143 m, 19 Aug. 2022, Song-Lin Li, Peng Yong, Li-Fen Li, Yu-Chen Zhou, Zi-Yue Liu leg.; 2♀ (HNU-BMS-2205), CHINA, Hunan Prov., Chenzhou City, Guidong Co., Bamian Mountain National Nature Reserve, 25.986542°N, 113.705841°E, 1250 m, 22 Aug. 2022, Song-Lin Li, Peng Yong, Li-Fen Li, Yu-Chen Zhou, Zi-Yue Liu leg.

Etymology. The specific epithet is derived from the Latin “*curvata*” (curved), referring to the curved retrolateral tibial apophysis, adjective.

Diagnosis. The male of this new species is similar to that of *Yaginumaella bulbosa* Peng, Tang & Li, 2008 (Peng et al. 2008: figs 26–28) in habitus and the curved RTA, but can be distinguished by: 1) cymbium longer than wide (Fig. 4A), while wider than long in *Y. bulbosa* (fig. 27); 2) length of RTA is about 1/3 of the palpal bulb (Fig. 4B), while about 1/2 of the palpal bulb in *Y. bulbosa* (fig.

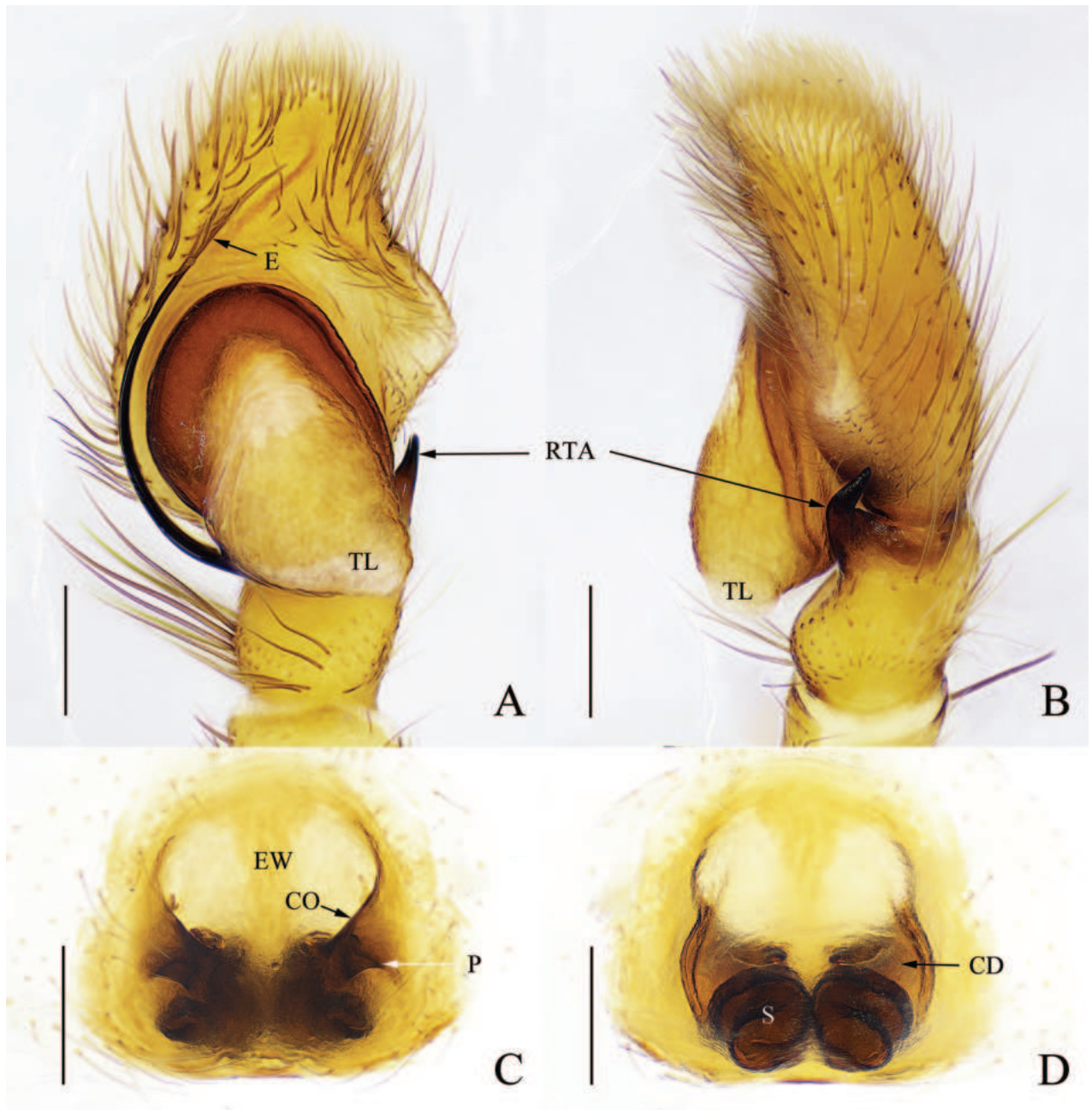


Figure 4. *Yaginumaella curvata* sp. nov. **A** left palp, ventral view **B** ditto, retrolateral view **C** epigyne, ventral view **D** vulva, dorsal view. Scale bars: 0.2 mm.

28); 3) RTA only extended to the basal 1/6 position of cymbium in retrolateral view (Fig. 4B), while to the basal 1/2 position of cymbium in retrolateral view in *Y. bulbosa* (fig. 28); and 4) embolus originates at about 7:00 o'clock position (Fig. 4A), while originates at about 9:00 o'clock position in *Y. bulbosa* (fig. 27). The female of this new species is similar to that of *Yaginumaella lushiensis* Zhang & Zhu, 2007 (Zhu and Zhang 2011: fig. 384A, D, E) in the short and stout copulatory ducts and the shape of spermathecae, but can be distinguished by the following characters: 1) distance of copulatory openings as wide as the

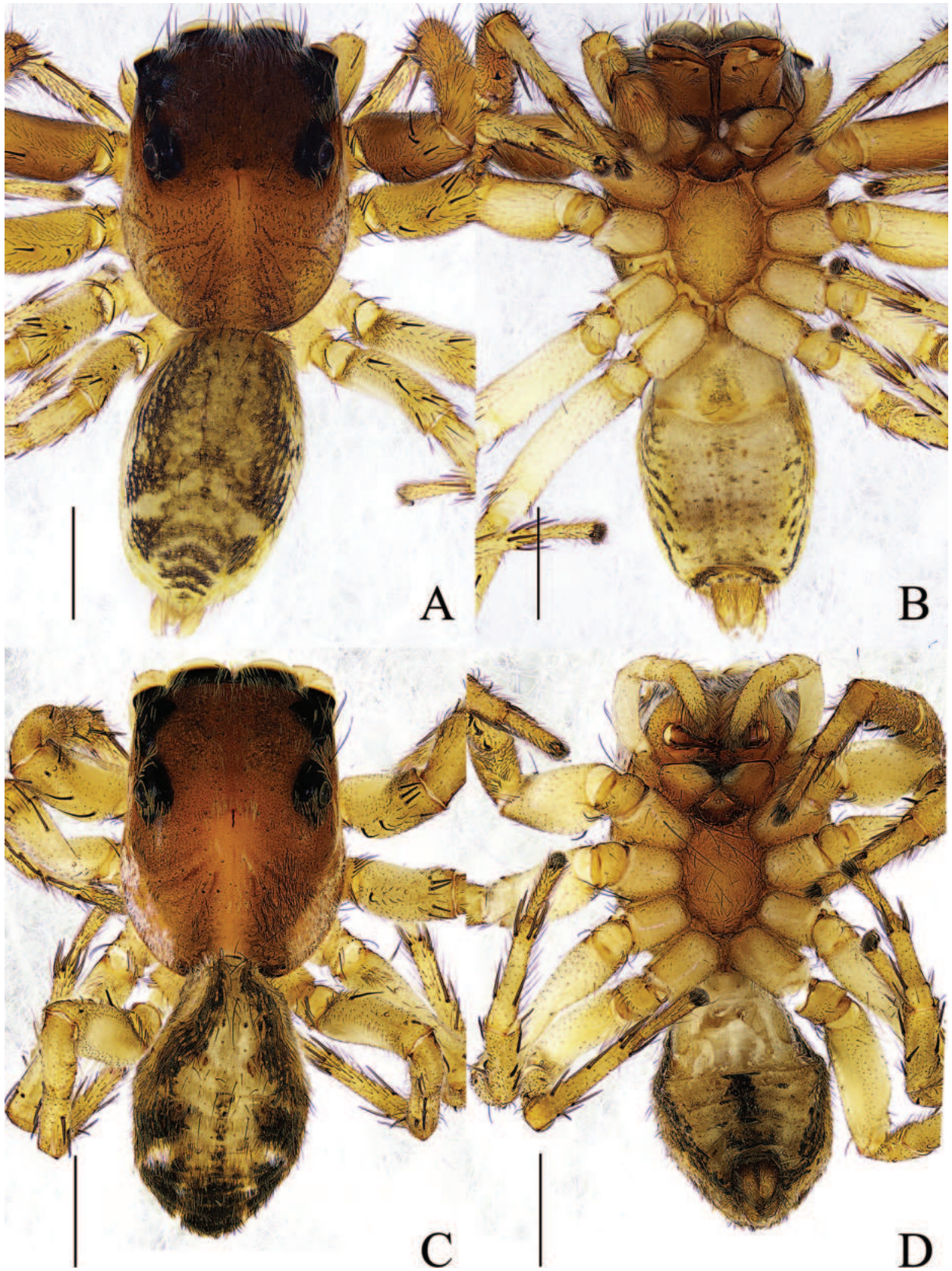


Figure 5. *Yaginumaella curvata* sp. nov. A male holotype, habitus, dorsal view B ditto, ventral view C female paratype, habitus, dorsal view D ditto, ventral view. Scale bars: 1 mm.

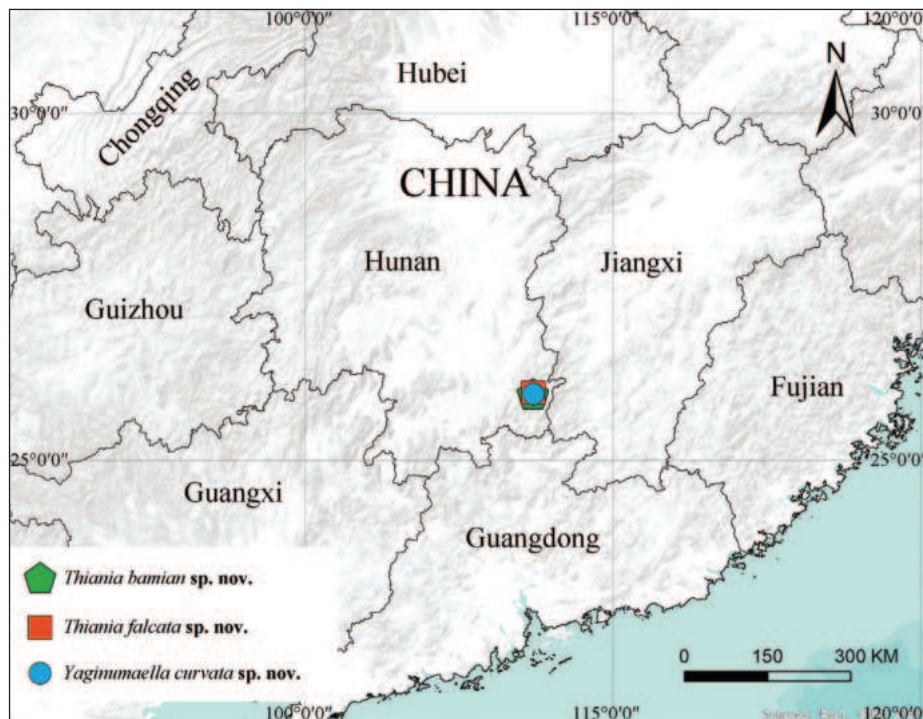


Figure 6. Collection localities of *Thiania bamian* sp. nov., *Thiania falcata* sp. nov. and *Yaginumaella curvata* sp. nov.

vulva (Fig. 4C), while about 1/3 width of the vulva in *Y. lushiensis* (fig. 384D); 2) epigynal pockets located at the median portion of epigyne (Fig. 4C), while located on the anterior portion in *Y. lushiensis* (fig. 384D); and 3) fertilisation duct about transverse (Fig. 4D), while oblique in *Y. lushiensis* (fig. 384E).

Description. Male (holotype) (Fig. 5A, B). Total length 5.14; carapace 2.60 long, 2.06 wide; abdomen 2.52 long, 1.59 wide. Carapace brown, with three longitudinal yellow stripes on the median and lateral margins, eye field and lateral margins covered with white setae. Fovea longitudinal, cervical and radial grooves distinct. Eye sizes and interdistances: AME 0.49, ALE 0.28, PME 0.08, PLE 0.21, AER 1.75, PER 1.65, EFL 0.78. Chelicerae light brown, promargin with two teeth, and retromargin with one tooth. Endites and labium light brown, distal end pale yellow. Sternum pale yellow. Legs yellow except for femora, patellae and tibiae of leg I brown. Measurements of legs: I 5.99 (1.76, 2.38, 1.17, 0.68), II 4.89 (1.59, 1.91, 0.67, 0.72), III 5.39 (1.70, 1.94, 1.14, 0.61), IV 5.50 (1.76, 1.79, 1.32, 0.63). Leg formula: 1432. Abdomen oval, dorsum with sparse long black hair, anterior margin black, the posterior median with two gray heringbone patterns and four chevrons; venter light yellow, with black maculation.

Palp (Fig. 4A, B). Embolus long and thin, originates at about 7:00 o'clock position; tegular lobe folds to retrolateral side; retrolateral tibial apophysis curved towards dorsal side at right angle from the middle.

Female. (paratype) (Fig. 5C, D). Total length 4.94; carapace 2.74 long, 2.04 wide; abdomen 2.54 long, 1.63 wide. Eye sizes and interdistances: AME 0.41, ALE 0.27, PME 0.11, PLE 0.23, AER 1.81, PER 1.79, EFL 0.72. Chelicerae promargin with two teeth, retromargin with one tooth. Legs pale yellow. Measurements of legs: I 4.79 (1.63, 1.80, 0.76, 0.60), II 4.44 (1.71, 1.49, 0.69, 0.55), III 5.49 (1.82, 1.94, 1.08, 0.65), IV 5.23 (1.63, 1.87, 1.03, 0.70). Leg

formula: 3412. Abdomen oval, dorsum black, with symmetric lighter yellowish central area, posterior portion covered with dense black and white long hairs; venter light yellow, with three longitudinal black stripes. Color darker than that in male.

Epigyne (Fig. 4C, D). Epigynal window oval, located at anterior portion of epigyne. Copulatory openings slit-shaped, located at the lower lateral margin of the epigynal window. Copulatory ducts short and stout. Spermathecae tubular and intertwined.

Distribution. Known only from the type locality (Fig. 6).

GenBank accession number. Paratype ((HNU-BMS-2205): PP786561).

Acknowledgements

We are grateful to Zhi-Yuan Yao and two reviewers for their high quality and constructive reviews. We also thank Dr Christopher Glasby for reviewing the English of the manuscript, and Cheng Wang, Bo Lü, Xuan-Wei Zhou, Peng Yong, Li-Fen Li, Yu-Chen Zhou and Zi-Yue Liu for collecting the specimens.

Additional information

Conflict of interest

The authors have declared that no competing interests exist.

Ethical statement

No ethical statement was reported.

Funding

This research was sponsored by the Scientific Research Projects of Hunan Education Department (no. 21B0055).

Author contributions

All authors have contributed equally.

Author ORCIDs

Song-Lin Li  <https://orcid.org/0000-0002-1127-0781>

Ping Liu  <https://orcid.org/0000-0002-4959-2735>

Xian-Jin Peng  <https://orcid.org/0000-0002-2614-3910>

Data availability

All of the data that support the findings of this study are available in the main text.

References

- Folmer O, Black M, Hoeh W, Lutz R, Vrijenhoek R (1994) DNA primers for amplification of mitochondrial cytochrome c oxidase subunit I from diverse metazoan invertebrates. *Molecular Marine Biology and Biotechnology* 3: 294–299.
- Li DQ, Wang C, Irfan M, Peng XJ (2018) Two new species of *Yaginumaella* (Araneae, Salticidae) from Wuling Mountain, China. *European Journal of Taxonomy* 488(488): 1–10. <https://doi.org/10.5852/ejt.2018.488>

- Liu W, Yang SF, Peng XJ (2016) Two new species of *Yaginumaella*, Prószyński 1976 from Yunnan, China (Araneae, Salticidae). *ZooKeys* 620: 57–66. <https://doi.org/10.3897/zookeys.620.7895>
- Logunov DV, Jäger P (2015) Spiders from Vietnam (Arachnida: Aranei): new species and records. *Russian Entomological Journal* 24(4): 343–363. <https://doi.org/10.15298/rusentj.24.4.09>
- Maddison WP (2015) A phylogenetic classification of jumping spiders (Araneae: Salticidae). *The Journal of Arachnology* 43(3): 231–292. <https://doi.org/10.1636/ arac-43-03-231-292>
- Patoleta BM, Gardzińska J, Żabka M (2020) Salticidae (Arachnida, Araneae) of Thailand: New species and records of *Epeus* Peckham & Peckham, 1886 and *Ptocasius* Simon, 1885. *PeerJ* 8(e9352): 1–23. <https://doi.org/10.7717/peerj.9352>
- Peng XJ (2020) *Fauna Sinica, Invertebrata* 53, Arachnida: Araneae: Salticidae. Science Press, Beijing, 612 pp.
- Peng XJ, Tang G, Li SQ (2008) Eight new species of salticids from China (Araneae, Salticidae). *Acta Zootaxonomica Sinica* 33: 248–259.
- Prószyński J (2009) Redescriptions of 16 species of Oriental Salticidae (Araneae) described by F. Karsch, E. Keyserling and C.L. Koch, with remarks on some related species. *Arthropoda Selecta* 18: 153–168.
- Prószyński J (2017) Pragmatic classification of the world's Salticidae (Araneae). *Ecologica Montenegrina* 12: 1–133. <https://doi.org/10.37828/em.2017.12.1>
- Shao XB, Li CG, Yang ZZ (2014) Two new species of the genus *Yaginumaella* (Araneae: Salticidae) from Yunnan, China. *Journal of Chuxiong Normal University* 29(4): 21–24.
- Wang C, Mi XQ, Wang WH, Gan JH, Irfan M, Zhong Y, Peng XJ (2023) Notes on twenty-nine species of jumping spiders from South China (Araneae: Salticidae). *European Journal of Taxonomy* 902: 1–91. <https://doi.org/10.5852/ejt.2023.902.2319>
- Wang C, Mi XQ, Li SQ (2024) Eleven species of jumping spiders from Sichuan, Xizang, and Yunnan, China (Araneae, Salticidae). *ZooKeys* 1192: 141–178. <https://doi.org/10.3897/zookeys.1192.114589>
- WSC (2024) World Spider Catalog. Version 25.0. Natural History Museum Bern. <http://wsc.nmbe.ch> [Accessed on 6 March 2024]
- Yu Y, Zhang JX (2022) Four new species of euophryine jumping spiders from China (Araneae: Salticidae: Euophryini). *Acta Arachnologica Sinica* 31(1): 1–10.
- Zhu MS, Zhang BS (2011) *Spider Fauna of Henan: Arachnida: Araneae*. Science Press, Beijing, 558 pp.
- Zhu MS, Zhang JX, Zhang ZS, Chen HM (2005) Arachnida: Araneae. In: Yang MF, Jin DC (Eds) *Insects from Dashahe Nature Reserve of Guizhou*. Guizhou People's Publishing House, Guiyang, 490–555 pp.

Five new species of the genus *Stigmus* Panzer (Hymenoptera, Crabronidae) from China, with a key to all Chinese species

Jinghong Li¹, Qiang Li¹, Li Ma¹

¹ Department of Entomology, College of Plant Protection, Yunnan Agricultural University, Kunming, Yunnan, 650201, China
Corresponding authors: Qiang Li (liqiangkm@126.com); Li Ma (maliwasps@aliyun.com)

Abstract

Five new species of the genus *Stigmus* Panzer, 1804 are described and illustrated from Yunnan and Shaanxi provinces of China: *S. carinannulatus* Li & Ma, **sp. nov.**, *S. clypeglabratus* Li & Ma, **sp. nov.**, *S. flagellipilaris* Li & Ma, **sp. nov.**, *S. rigidensus* Li & Ma, **sp. nov.**, and *S. sulciconspicus* Li & Ma, **sp. nov.** In addition, *S. solskyi* Morawitz, 1864 is recorded in China for the first time. An illustrated key to known and new species of the genus *Stigmus* Panzer from China is provided.

Key words: Digger wasps, identification key, new record, Pemphredoninae, taxonomy

Introduction

The genus *Stigmus* Panzer was erected by Panzer with *Stigmus pendulus* Panzer, 1804 as its type species. The classification system used in this study follows Melo (1999). *Stigmus* belongs to the Hymenoptera: Crabronidae: Pemphredoninae: Pemphredonini: Stigmina. All members of this genus are predatory towards aphids that are found on woody plants except that some species of *Rhopalosiphum* and *Aphis* that occur on herbaceous plants (Tsuneki 1954; Krombein 1958). The overwhelming majority of species within *Stigmus* nest in wood in some form. Reported nesting sites include in twigs, dead trees, or structural lumber of abandoned borings by other insects, principally beetle larvae, in borings made by themselves in the pith of twigs or stems, and in abandoned galls of other insects (Smith 1923; Tsuneki 1970; Krombein 1973). The nests usually consist of a linear series of cells separated by partitions of small pieces of pith of the wood substrate (Krombein 1955).

The main diagnostic characteristics of the subtribe Stigmina include forewing with two or fewer discoidal cells and one recurrent vein and a large stigma; forewing with elongate marginal cell, closed apically, larger than stigma; in dorsal view, petiole length significantly longer than its width. *Stigmus* can be easily distinguished from the similar genus *Carinostigmus* based on the following identifying characteristics: vertex with micropore field; hindwing submedian cell normal size; occipital carina usually incomplete, not ending to midventral line, suddenly ending at posterior ridge of stomal hollow; interantennal tubercle degenerative; petiole with carinae. *Carinostigmus* has the following characters:



Academic editor: Thorleif Dörfel
Received: 24 March 2024
Accepted: 6 May 2024
Published: 10 June 2024

ZooBank: <https://zoobank.org/B1FBD39B-E01A-4B0C-AA01-36DC49A609A4>

Citation: Li J, Li Q, Ma L (2024) Five new species of the genus *Stigmus* Panzer (Hymenoptera, Crabronidae) from China, with a key to all Chinese species. ZooKeys 1204: 313–336. <https://doi.org/10.3897/zookeys.1204.123831>

Copyright: © Jinghong Li et al.
This is an open access article distributed under terms of the Creative Commons Attribution License (Attribution 4.0 International – CC BY 4.0).

vertex without micropore field; hindwing submedian cell degenerative; occipital carina complete, ending to midventral line; interantennal tubercle distinct; petiole usually smooth (Krombein 1973, 1984; Bohart and Menke 1976; Budrys 1987; Fynnmore 1995).

The genus currently consists of 30 species and four subspecies worldwide, distributed across four major zoogeographic regions, in which the majority of species occurred in the Nearctic region (10 species and 2 subspecies) and the Palearctic region (10 species); additionally, six species and two subspecies occurred in the Oriental region, while the Neotropical region has a relatively low distribution with only two species. One species occurs in the Palearctic and Oriental regions, and one species in the Nearctic and Neotropical regions. Currently, eight species and two subspecies have been recorded in China, among them, four species and two subspecies are distributed in the Oriental region, while three species are distributed in the Palearctic; additionally, there is one species that is found in both the Palearctic and Oriental regions of China (Morawitz 1864; Packard 1867; Kohl 1892; Rohwer 1911; Tsuneki 1954, 1971; Krombein 1973; Kolesnikov 1977; Allen 1987; Budrys 1987, 1995; Uffen 1997, 1998; Jones 2001; Amarante 2002; Terayama 2012; Ratzlaff 2016; Mokrousov 2017; Pulawski 2024).

In the current study, five new species of *Stigmus* from China are described and illustrated as *S. carinannulatus* Li & Ma, sp. nov., *S. clypeglabratus* Li & Ma, sp. nov., *S. flagellipilaris* Li & Ma, sp. nov., *S. rugidensus* Li & Ma, sp. nov., and *S. sulciconspicus* Li & Ma, sp. nov., and one newly recorded species from Yunnan Province of China is reported. Additionally, an illustrated identification key to the Chinese *Stigmus* is provided.

Materials and methods

The specimens examined in this study are deposited in the Insect Collections of Yunnan Agricultural University, Kunming, Yunnan, China (YNAU). Specimens were observed with the help of an Olympus stereomicroscope (SZ Series) with an ocular micrometer. The photographs were taken with VHX-5000 and edited by using Adobe Photoshop 8.0. For the terminology we mainly followed Tsuneki (1954), Bohart and Menke (1976) and Bashir et al. (2019). The abbreviations and definitions utilized in the text are as follows:

opaque area	small area located between the ocellar triangle area and eye, close to the eye;
triangular area	area enclosed by scrobal suture, omaulus and hypersternaulus;
BL	body length;
HLD	head length in dorsal view, the distance from frons to occipital margin, medially;
HLF	head length in frontal view, the distance from vertex to clypeal margin, medially;
HW	head width in dorsal view, maximum;
EW	eye width in lateral view, maximum;
Ewd	eye width in frontal view, maximum;
TW	gena width in lateral view, maximum;
EL	eye length in lateral view, maximum;

POD	postocellar distance, distance between inner margins of hind ocelli, dorsally;
OOD	ocellocular distance, distance between outer margin of hind ocellus and nearest inner orbit, dorsally;
 OCD	ocello-occipital distance, distance between posterior margin of hind ocellus and occipital margin, dorsally;
PW	petiole width, maximum, dorsally;
PL	petiole length, dorsally;
WTI	width of metasomal tergum I, maximum, dorsally;
LTI	length of gastral tergum I, maximum, dorsally;
HFL	length of hind femur, maximum;
HTL	length of hind tibia, maximum.

Taxonomy

Genus *Stigmus* Panzer, 1804

Type species. *Stigmus pendulus* Panzer, 1804.

Key to the species of *Stigmus* from China, including males and females

Females of *S. flagellipilaris* Li & Ma, sp. nov., *S. capoblongus* Bashir & Ma and males of *S. fronticoncavus* Bashir & Ma, *S. sulciconspicus* Li & Ma, sp. nov., and *S. interruptus* Bashir & Ma are unknown. PR and OR represent Palearctic and Oriental Regions, respectively.

- 1 Clypeus deeply impressed, not produced (OR) ***S. fronticoncavus* Bashir & Ma**
- Clypeus flat or slightly convex, slightly (Fig. 1A) or strongly produced **2**
- 2 Triangular area with sturdy reticulation (Fig. 6D) or striations **3**
- Triangular area smooth and shiny (Fig. 1E) **4**
- 3 Scutellum coriaceous, without longitudinal impressed line medially (Fig. 6C); mesopleuron episcrobal area and triangular area with sturdy reticulation (Fig. 6D); in male, clypeus with dense, silvery, short setae, free margin of clypeus strongly produced and nearly truncate medially (Fig. 6H) (PR).
..... ***S. solskyi* Morawitz**
- Scutellum shiny, with single, slender longitudinal line medially; mesopleuron episcrobal area with dense, longitudinal striations, and triangular area with distinct striations anteriorly, smooth and shiny posteriorly; in male, clypeus without setae, free margin of clypeus slightly produced and with two triangular teeth medially (OR) ***S. shirozui alishanus* Tsuneki**
- 4 Ventral surface of petiole shiny, without rugae (OR) ***S. kansitakuanus* Tsuneki**
- Ventral surface of petiole with a few strong, longitudinal rugae medially and posteriorly **5**
- 5 Scrobal suture inconspicuous, lacking (Fig. 1E) or only with single weak rugae (Fig. 3E), not crenate **6**
- Scrobal suture narrow or broad, weakly or distinctly crenate (Fig. 4D) **9**

- 6 Hindwing media diverging before cu-a (Fig. 7A) (OR).....7
- Hindwing media diverging beyond cu-a8
- 7 Occipital carina complete, ending to midventral line (Fig. 1C); scutum with conspicuous, longitudinal striations, posterior area with dense, slender, short, longitudinal rugae (Fig. 1D); posterior area of mesopleuron with sparse, short longitudinal rugae, and episcrobal area smooth, without striations (Fig. 1E)..... **S. carinannulatus Li & Ma, sp. nov.**
- Occipital carina incomplete, not ending to midventral line, suddenly ended at posterior ridge of stomal hollow (Fig. 3B); scutum without striations or rugae (Fig. 3D); posterior area of mesopleuron smooth, without rugae, and episcrobal area with dense, slender, longitudinal striations (Fig. 3E)..... **S. flagellipilaris Li & Ma, sp. nov.**
- 8 Opaque area larger than hind ocellus (Fig. 5B); pronotal collar with complete, transverse carina anteriorly (Fig. 5C); dorsal surface of petiole with sturdy, irregular rugae anteriorly and medially, and several sturdy, longitudinal rugae posteriorly (Fig. 5F) (OR).....**S. sulciconspicus Li & Ma, sp. nov.**
- Opaque area smaller than hind ocellus; pronotal collar with incomplete, transverse carina anteriorly, narrowly emarginated in middle; dorsal surface of petiole with two strong longitudinal carinae, and irregular, strong rugae anteriorly and medially (PR) **S. denticorneus Bashir & Ma**
- 9 Hindwing media diverging before cu-a (Fig. 7A) (OR).....10
- Hindwing media diverging beyond cu-a 13
- 10 Pronotal collar with complete lateral rugae; lateral surface of propodeum with dense, sturdy or slender, oblique, longitudinal rugae anteriorly and medially 11
- Pronotal collar with incomplete lateral rugae, only distinct in posterior area (Fig. 3C); lateral surface of propodeum smooth, without rugae anteriorly and medially (Fig. 3D) 12
- 11 Ventral gena shiny, with dense, large punctures mixed with several irregular rugae laterally; inner orbital furrow broadened, with slender rugae; scutum shiny, with sparse, midsize to large punctures **S. lobomelanicus Bashir & Ma**
- Ventral gena smooth, impunctate and without rugae; inner orbital furrow lacking; scutum moderately matt, with sparse, tiny punctures, posterior area with several sturdy, short, longitudinal rugae **S. murotai (Tsuneki)**
- 12 Vertex with sparse, large punctures (Fig. 4B); occipital carina narrow, coarsely crenulate dorsally, and somewhat broadened, distinctly crenulate ventrally; pronotal lobe black (Fig. 4D); scutum shiny, with sparse, large punctures (Fig. 4C); in female, pygidial area moderately matt, basal area with several midsize punctures (Fig. 4G) **S. rugidensus Li & Ma, sp. nov.**
- Vertex with sparse, fine punctures (Fig. 2B); occipital carina much narrowed, not crenulate; pronotal lobe yellowish (Fig. 2D); scutum moderately matt, with sparse, tiny punctures (Fig. 2C); in female, pygidial area shiny, without punctures (Fig. 2G) **S. clypeglabratus Li & Ma, sp. nov.**
- 13 Lateral surface of propodeum smooth, without rugae anteriorly and medially; posterior area of mesopleuron with sparse, short, longitudinal rugae (PR)..... **S. capoblongus Bashir & Ma**
- Lateral surface of propodeum with dense, slender or sturdy, oblique, longitudinal rugae; posterior area of mesopleuron smooth, without rugae (OR) ... 14

- 14 Vertex with several midsize punctures; anterior area of pronotal collar with incomplete, transverse carina, narrowly emarginated in middle; scutum with sparse, large punctures, anterior and posterior areas with dense, longitudinal striations..... ***S. interruptus* Bashir & Ma**
- Vertex without puncture; anterior area of pronotal collar with complete, transverse carina; scutum with sparse, tiny punctures, without striations..... **15**
- 15 Hypersternaulus narrowed, not crenate; posterior surface of propodeum with shallow and somewhat narrow median groove; PL/PW ~ 5; in female, pygidial area impunctate, with dense, weak, longitudinal striations.....
.....***S. convergens ami* Tsuneki**
- Hypersternaulus broadened, distinctly crenate; posterior surface of propodeum without conspicuous groove; PL/PW ~ 3; in female, pygidial area with two lines of large punctures medially, without striations
.....***S. japonicus* Tsuneki**

Species accounts

***Stigmus carinannulatus* Li & Ma, sp. nov.**

<https://zoobank.org/CBECB838-47C0-4C4F-AA4B-ED9E9681ECDC>

Figs 1A–N, 7A, B

Type material. Holotype: CHINA • ♀; Yunnan, Tengchong City; 25°1'N, 92°28'E; 11.VIII.2011; coll. Jujian Chen; sweep net (YNAU). **Paratypes:** CHINA • 20♂♂; Yunnan, Kunming City, Yunnan Agricultural University; 25°7'N, 102°44'E; 12.IV.2023 (5♂♂), 12.VI.2023 (9♂♂), 19.VIII.2023 (6♂♂); 1910 m elev.; coll. Jinghong Li; sweep net (YNAU); CHINA • 1♂; Yunnan, Baoshan City, Longyang District, Lujiang Country, Pumanshao Village; 24°56'N, 98°47'E; 21.VII.2006; 1951 m elev.; coll. Zhongshi Zhou; sweep net (YNAU).

Diagnosis. The new species can be easily separated from the similar species *S. denticorneus* Bashir & Ma, 2019 by the following characters: hindwing media diverging before cu-a; occipital carina complete, ending to midventral line; anterior area of pronotal collar with complete, transverse carina; scutum with several, large punctures, anterior area with distinct, longitudinal striations, posterior area with dense, fine, short, longitudinal rugae; posterior area of mesopleuron with sparse, short, longitudinal rugae, episcrobal area smooth, without striation. *Stigmus denticorneus* has the following characters: hindwing media diverging beyond cu-a; occipital carina incomplete, not ending to midventral line, suddenly ended at posterior ridge of stomal hollow; anterior area of pronotal collar with incomplete, transverse carina, narrowly emarginated in middle; anterior area of scutum with dense, large punctures, remainder with sparse, midsize to large punctures; posterior area of mesopleuron smooth, without rugae, episcrobal area with dense, longitudinal striations.

Description. Female. Measurements. ♀, BL: 4.6 mm; HW: HLD: HLF = 78: 54: 59; HW: EWd: EW: TW: EL = 78: 23: 22: 28: 51; POD: OOD: OCD = 8: 14: 15; length of scape: length of pedicel: length of flagellomere I: width of flagellomere I: length of flagellomere II: width of flagellomere II = 21: 9: 8: 5: 8: 5; PL: PW: LTI: WTI: HFL: HTL = 36: 11: 40: 46: 48: 55. ♂, BL: 3.5–4.6 mm; HW: HLD: HLF = 53: 31: 42; HW: EWd: EW: TW: EL = 53: 15: 20: 12: 36; POD: OOD: OCD = 5.5: 10: 11; length of scape: length of pedicel: length of flagellomere I: width of

flagellomere I: length of flagellomere II: width of flagellomere II = 13: 5: 5: 3: 5: 3; PL: PW: LTI: WTI: HFL: HTL = 24: 5: 25: 26: 33: 57.

Color pattern. Body black; clypeus with reddish brown to dark brown band subapically; mandible fulvous except reddish brown apically; labrum dark brown; palpi, scape, pedicel, tegula and pronotal lobe fulvous; flagellomeres I–V beneath fulvous, above brown, remainder dark brown; forewing veins brown; fore and mid legs: fulvous except coxa largely and femur medially dark brown; hind leg: trochanter, basal 1/4 of tibia and tarsus fulvous, remainder dark brown; gastral sterna IV–VI fulvous to dark brown; setae on clypeus and mandible sparse and golden.

Head. Mandible tridentate apically, median tooth large (Fig. 1A). Labrum with two distinct cornuted teeth apically. Clypeus shiny, nearly flat, with sparse, midsize punctures; free margin of clypeus slightly produced and with two distinct triangular teeth medially, slightly reflected, area between two teeth deeply emarginated (Fig. 1A). Scapal hollow moderately matt, coriaceous, somewhat shallow and defined, provided with one vestigial minute tubercle medially, not spined (Fig. 1A). Frontal furrow very fine and weakly impressed, inconspicuously (Fig. 1A). Median and upper frons shiny, with sparse, fine punctures, gently convex (Fig. 1A). Ocellar triangle area flat, shiny, impunctate, area near eyes with dense, short, impressed lines, opaque area smaller than hind ocellus (Fig. 1B). Vertex shiny, impunctate (Fig. 1B). Gena shiny, smooth and impunctate (Fig. 1C). Head from above with temples rarely convergent posteriorly, subquadrate (Fig. 1B). Occipital carina complete, ending to midventral line, dorsal area much narrowed, not crenulate, ventral area gently broadened, coarsely crenate (Fig. 1C); inner and outer orbital furrows lacking (Fig. 1A).

Mesosoma. Pronotal collar with strong, transverse carina anteriorly, and with incomplete lateral rugae, only distinct in posterior area, without antero-lateral corner (Fig. 1D). Scutum moderately matt, with several large punctures, anterior area with dense, conspicuous, longitudinal striations, posterior area with dense, fine, short, longitudinal rugae (Fig. 1D); admedian line weakly impressed, extending to 1/2 of scutum length; notaulus deeply grooved and crenulate, reaching 2/5 of scutum length; parapsidal line distinct (Fig. 1D). Scutellum shiny, with sparse, fine punctures, without medial longitudinal line (Fig. 1D). Metanotum weakly coriaceous (Fig. 1D). Mesopleuron shiny, posterior area with several slender, short, longitudinal rugae, episcrobal area shiny and smooth (Fig. 1E); omaulus and hypersternaulus broadened, distinctly crenate, scrobal suture complete and inconspicuous, just with single longitudinal rugae (Fig. 1E). Propodeal enclosure triangular medially, with three sturdy longitudinal median rugae, and several transvers rugae, with sparse sturdy, oblique, longitudinal rugae laterally (Fig. 1F); posterior surface of propodeum with sparse irregular rugae, without conspicuous median groove (Fig. 1F); lateral surface of propodeum with dense, oblique, longitudinal rugae anteriorly and medially, and irregular reticulation posteriorly (Fig. 1E).

Legs. Outer surface of hind tibia with three long, slender, fulvous to dark brown spines.

Wings. Forewing venation typical for genus *Stigmus*, hindwing media diverging before cu-a.

Metasoma. Dorsal surface of petiole subquadrate, moderately convex and widened toward apex slightly, and with two sturdy, longitudinal, median carinae,

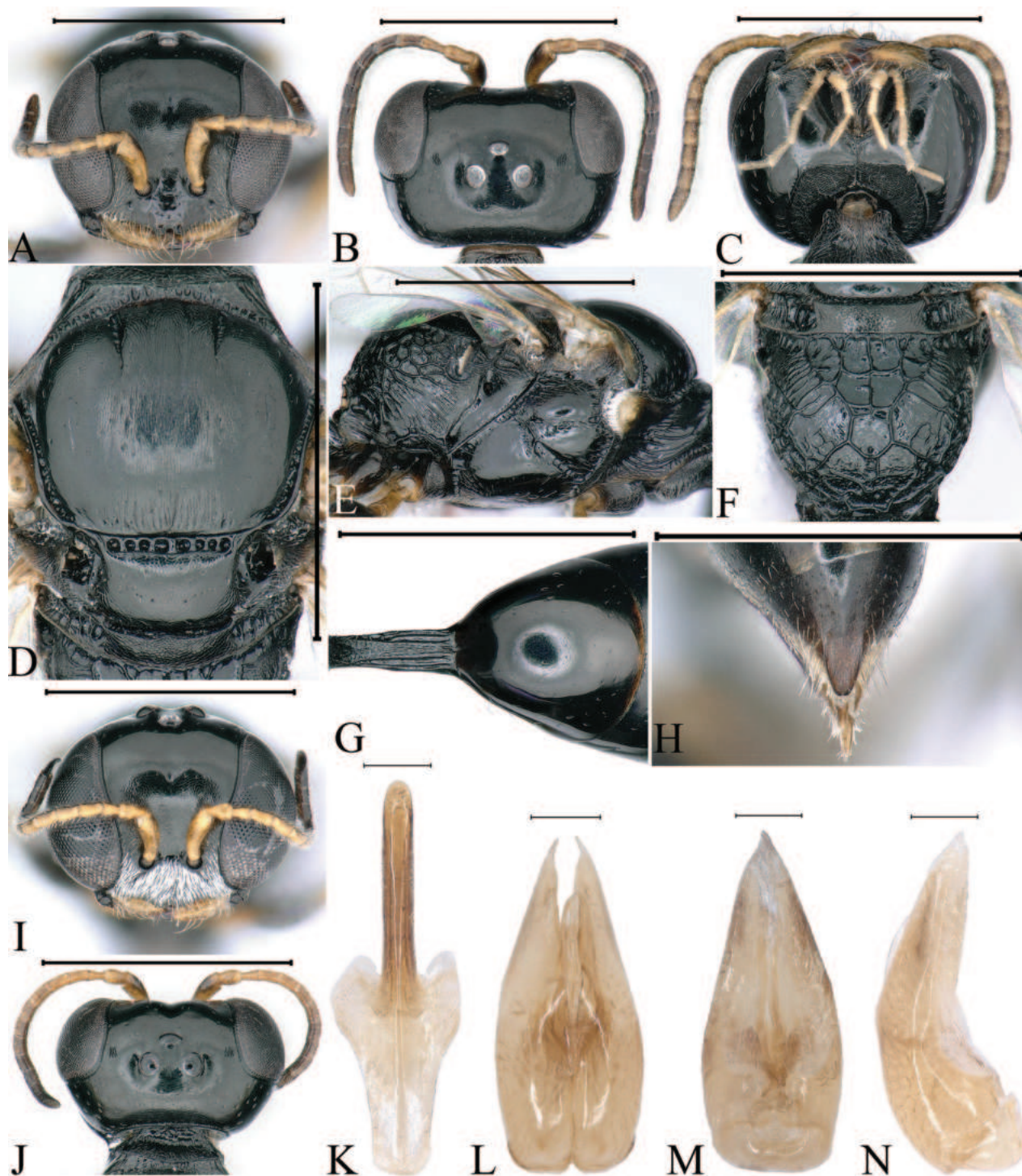


Figure 1. *Stigmus carinannulatus* Li & Ma, sp. nov. (A–H female I–N male) A, I head, frontal view B, J head, dorsal view C head, ventral view D collar, scutum, scutellum and metanotum, dorsal view E thorax, lateral view F propodeum, dorsal view G petiole, dorsal view H pygidial plate, dorsal view K gastral tergum VIII, ventral view L male genitalia, dorsal view M male genitalia, ventral view N male genitalia, lateral view. Scale bars: 1 mm (A–J); 0.1 mm (K–N).

area between carinae with dense, fine, irregular rugae, median and posterior areas with two sturdy, longitudinal, lateral rugae on each side (Fig. 1G). Lateral surface of petiole with three strong, longitudinal rugae medially and posteriorly (Fig. 7A). Ventral surface of petiole with a few strong, short, longitudinal rugae posteriorly. Gastral terga shiny, impunctate, gastral sternum VI with sparse, fine

punctures apically (Fig. 1H). Pygidial area moderately matt, broadly triangular, apex truncate, with longitudinal micro-striations (Fig. 1H).

Male. Same as female except tegula dark brown; setae on clypeus dense, silvery, short (Fig. 1I); mandible bidentate apically (Fig. 1I); free margin of clypeus slightly produced, nearly truncate medially, and with shallow emargination (Fig. 1I); head from above with temples somewhat roundly convergent posteriorly; dorsal area of occipital carina much narrowed, coarsely crenulate, and ventral area somewhat broadened, distinctly crenate (Fig. 1J); flagellomeres without tyloids, setae normal; gastral sterna impunctate (Fig. 1J).

Distribution. China (Yunnan).

Etymology. The name, *carinannulatus*, is derived from the Latin *carin-* (= carina) and the Latin word *annulatus* (= annular), referring to the complete occipital carina.

***Stigmus clypeglabratus* Li & Ma, sp. nov.**

<https://zoobank.org/A5CB1E7E-541A-4D20-ABB4-E62DBDE9ABA6>

Figs 2A–M, 7C, D

Type material. Holotype: CHINA • ♀; Shaanxi, Hanzhong City, Liuba County, Zibai Mountain; 33°40'N, 106°43'E; 3.VIII.2004; 1632 m elev.; coll. Min Shi; sweep net (YNAU). **Paratypes:** 3♂♂, same data as for holotype, except coll. Min Shi, Qiong Wu (YNAU).

Diagnosis. Differs from *S. japonicus* Tsuneki, 1954 by hindwing media diverging before cu-a; lateral surface of propodeum smooth and shiny anteriorly and medially; pronotal collar with incomplete lateral rugae, just distinct in posterior area; gena impunctate dorsally; opaque area larger than hind ocellus; in male, clypeus smooth and impunctate, and with several setae on free margin, yellowish and short; in female, pygidial area smooth, impunctate. *Stigmus japonicus* has the following characters: hindwing media diverging beyond cu-a; lateral surface of propodeum with dense, slender or sturdy, oblique, longitudinal rugae anteriorly and medially; pronotal collar without lateral rugae; gena with sparse, midsize punctures dorsally; opaque area smaller than hind ocellus; in male, clypeus with dense, tiny punctures, setae on clypeus dense, silvery, and short; in female, pygidial area with two lines of large punctures medially.

Description. Female. Measurements. ♀, BL: 4.2 mm; HW: HLD: HLF = 61: 36: 47; HW: EWd: EW: TW: EL = 61: 16: 21: 16: 39; POD: OOD: OCD = 5: 11: 16; length of scape: length of pedicel: length of flagellomere I: width of flagellomere I: length of flagellomere II: width of flagellomere II = 18: 6: 6: 3: 7: 3.5; PL: PW: LTI: WTI: HFL: HTL = 26: 8: 32: 35: 35: 40. ♂, BL: 3–3.8 mm; HW: HLD: HLF = 63: 32: 48; HW: EWd: EW: TW: EL = 63: 19: 23: 13: 41; POD: OOD: OCD = 6.5: 11: 14; length of scape: length of pedicel: length of flagellomere I: width of flagellomere I: length of flagellomere II: width of flagellomere II = 16: 7: 5: 3: 6: 3; PL: PW: LTI: WTI: HFL: HTL = 26: 8: 29: 34: 34: 40.

Color pattern. Body black; clypeus with reddish brown band subapically; mandible yellowish except reddish brown apically; labrum and dorsal scape fulvous; palpi and ventral scape ivory; pedicel, pronotal lobe, tegula and forewing veins yellowish; flagellomeres beneath and I-II above fulvous, remainder reddish brown; fore and mid legs: yellowish to fulvous except outer margin of femur somewhat brown, coxa dark brown largely; hind leg: coxa apically,

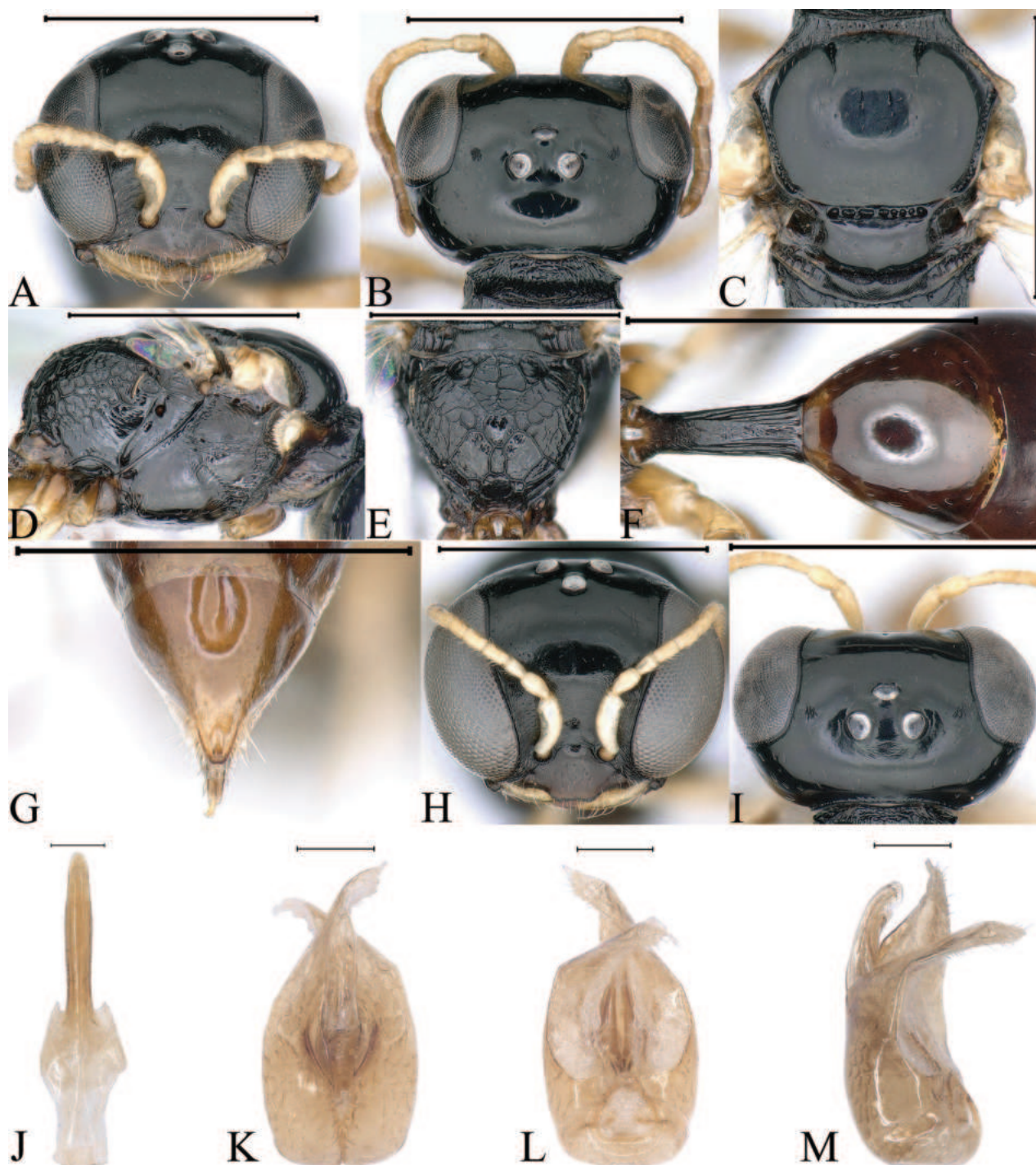


Figure 2. *Stigmus clypeglabratus* Li & Ma, sp. nov. (A–G female H–M male) A, H head, frontal view B, I head, dorsal view C collar, scutum, scutellum and metanotum, dorsal view D thorax, lateral view E propodeum, dorsal view F petiole, dorsal view G pygidial plate, dorsal view J gastral tergum VIII, ventral view K male genitalia, dorsal view L male genitalia, ventral view M male genitalia, lateral view. Scale bars: 1 mm (A–I); 0.1 mm (J–M).

trochanter, basal 1/2 of tibia, tarsi yellowish to fulvous, remainder dark brown; gaster dark brown, gastral sterna IV–VI bright yellow largely; setae on clypeal margin and mandible sparse, golden and long.

Head. Mandible tridentate apically, median tooth large. Labrum with two distinct triangular teeth apically (Fig. 2A). Clypeus smooth, shiny, flat; free margin of clypeus slightly produced and with two triangular teeth medially, slightly

reflected, area between two teeth with shallow emargination (Fig. 2A). Scapal hollow shiny, shallow, and broad, not clearly defined, provided with one vestigial minute tubercle medially; frontal furrow vestigial; median and upper frons shiny, with sparse, tiny punctures (Fig. 2A). Ocellar triangle area flat, shiny, impunctate, area near eyes with dense, short, impressed lines, opaque area smaller than hind ocellus (Fig. 2B). Vertex shiny, with sparse, tiny punctures (Fig. 2B). Gena shiny, impunctate. Head from above with temples rarely convergent posteriorly, subquadrate (Fig. 2B). Occipital carina incomplete, not ending to midventral line, suddenly ended at posterior ridge of stomal hollow, not dentate, occipital carina much narrowed, not crenulate. Inner and outer orbital furrows lacking (Fig. 2A).

Mesosoma. Pronotal collar with strong, transverse carina anteriorly, and with incomplete lateral rugae, only distinct in posterior area, without antero-lateral corner (Fig. 2C). Scutum moderately matt, with sparse, tiny punctures; admedian line distinctly impressed, extending to 2/5 scutum length; notaulus deeply grooved and crenulate, reaching quarter of scutum length; parapsidal line weakly impressed (Fig. 2C). Scutellum shiny, with sparse, fine punctures, and median longitudinal line weakly impressed (Fig. 2C). Metanotum weakly coriaceous (Fig. 2C). Mesopleuron smooth and shiny, posterior area smooth without rugae, episcrobal area with dense, slender, longitudinal rugae posteriorly; scrobal suture, omaulus and hypersternaulus broadened, slightly crenate, scrobal suture complete (Fig. 2D). Propodeal enclosure triangular medially, and with three sturdy, longitudinal rugae and sparse, irregular, transvers rugae, lateral area with irregular, short rugae; posterior surface of propodeum with sturdy reticulation, and without conspicuous median groove (Fig. 2E); lateral surface of propodeum smooth and shiny anteriorly and medially, and with irregular reticulation posteriorly (Fig. 2D).

Legs. Outer surface of hind tibia with three long, slender, fulvous to dark brown spines.

Wings. Forewing venation typical for genus *Stigmus*, hindwing media diverging before cu-a.

Metasoma. Dorsal surface of petiole subquadrate, gently convex and widened toward apex slightly, and with two sturdy oblique, longitudinal carinae forming V-shaped medially, area between V-shaped carinae with irregular rugae, medial and posterior areas with a few sturdy, longitudinal rugae on each side (Fig. 2F); lateral surface of petiole with several strong, longitudinal rugae medially and posteriorly (Fig. 7C); ventral surface of petiole with four strong, short, longitudinal rugae posteriorly. Gastral terga shiny, impunctate, gastral sternum VI moderately matt, and with dense fine punctures (Fig. 2G). Pygidial area smooth and shiny, broadly triangular (Fig. 2G).

Male. Almost same as female except mandible fulvous basally and medially; fore and mid legs yellowish to fulvous; hind femur dark brown largely, remainder yellowish; mandible bidentate apically; clypeus moderately convex, clypeal margin broadly produced, and nearly truncate medially (Fig. 2H); head from above with temples gradually convergent posteriorly (Fig. 2I); occipital carina narrowed, distinctly crenulate dorsally, and ventral area somewhat broadened, coarsely crenate (Fig. 2I); flagellomeres without tyloids, setae normal (Fig. 2I).

Distribution. China (Shaanxi).

Etymology. The name, *clypeglabratus*, is derived from the Latin *clype-* (= clypeus) and the Latin word *glabratus* (= smooth), referring to the smooth and impunctate clypeus.

***Stigmus flagellipilaris* Li & Ma, sp. nov.**

<https://zoobank.org/9DD287CF-D292-49D8-88E2-2FE6D9BB599B>

Figs 3A–K, 8A

Type material. Holotype: CHINA • ♂; Yunnan, Tengchong city, Shabadi Village; 25°23'N, 98°42'E; 2–18.IV.2020; 1739 m elev.; coll. Lang Yi; Malaise trap (YNAU). **Paratypes:** CHINA • 1♂; Yunnan, Baoshan city, Longyang District, Lujiang County, Pumanshao Village; 24°56'N, 98°47'E; 21.VII.2006; 1951 m elev.; coll. Zhongshi Zhou; sweep net (YNAU); CHINA • 1♂; Yunnan, Wenshan City, Maguan County, Wazishan Village; 22°51'N, 104°23'E; 13.VIII.2017; 1722 m elev.; coll. Li Ma; sweep net (YNAU).

Diagnosis. Differs from *S. japonicus* by hindwing media diverging before cu-a; scrobal suture inconspicuous, just single weak rugae; opaque area smaller than hind ocellus; median and upper frons with several large punctures; vertex shiny, and with sparse, fine punctures. *Stigmus japonicus* has the following characters: hindwing media diverging beyond cu-a; scrobal suture broadened, distinctly crenate; opaque area larger than hind ocellus; medial and upper frons with sparse, fine punctures; vertex moderately matt, with sparse, midsize punctures.

Description. Male. Measurements. ♂, BL: 3.2–4.3 mm; HW: HLD: HLF = 69: 44: 54; HW: EWd: EW: TW: EL = 69: 20: 19: 23: 43; POD: OOD: OCD = 8: 12: 12; length of scape: length of pedicel: length of flagellomere I: width of flagellomere I: length of flagellomere II: width of flagellomere II = 16: 6: 7: 4: 7: 4; PL: PW: LTI: WTI: HFL: HTL = 33: 7: 34: 32: 39: 50.

Color pattern. Body black; mandible yellowish except reddish brown apically; labrum, scape, pedicel and pronotal lobe fulvous; palpi yellowish; flagellomeres reddish brown except I–IV beneath fulvous; tegula brown; forewing veins fulvous to brown; fore and mid legs: trochanter, base and apex of femur, tibia largely, tarsi yellowish, remainder dark brown; hind leg: coxa apically, trochanter, base and apex of femur, tibia largely, tarsi yellowish, remainder dark brown; setae on clypeus and lateral upper frons silvery; mandible with sparse golden setae.

Head. Mandible bidentate apically (Fig. 3A). Labrum subquadrate (Fig. 3A). Clypeus nearly flat, with dense, tiny punctures; free margin of clypeus slightly produced and nearly truncate medially, with shallow emargination (Fig. 3A). Scapal hollow matt, distinctly coriaceous, somewhat shallow, provided with one vestigial minute tubercle medially; frontal furrow weakly impressed; medial and upper frons shiny, with several large punctures, slightly convex (Fig. 3A). Ocellar triangle area flat, shiny, impunctate, area near eyes with dense, short, impressed lines, opaque area smaller than hind ocellus (Fig. 3C). Vertex shiny, with sparse, fine punctures (Fig. 3C). Gena shiny, with sparse, midsize to large punctures dorsally; ventral gena shiny, smooth, impunctate (Fig. 3B). Head from above with temples gradually convergent posteriorly (Fig. 3C). Occipital carina incomplete, not ending to midventral line, suddenly ended at posterior ridge of stomal hollow, dorsal area much narrowed, not crenulate, ventral area gently broadened, distinctly crenate (Fig. 3B). Inner and outer orbital furrows lacking (Fig. 3A, B). Flagellomeres without tyloids, with longish and dense setae (Fig. 3A).

Mesosoma. Pronotal collar with strong, transverse carina anteriorly, and with incomplete lateral rugae, only distinct in posterior area, without antero-lateral corner (Fig. 3D). Scutum moderately matt, with several inconspicuous, large punctures; admedian line distinctly impressed, extending to 2/5 scutum length;

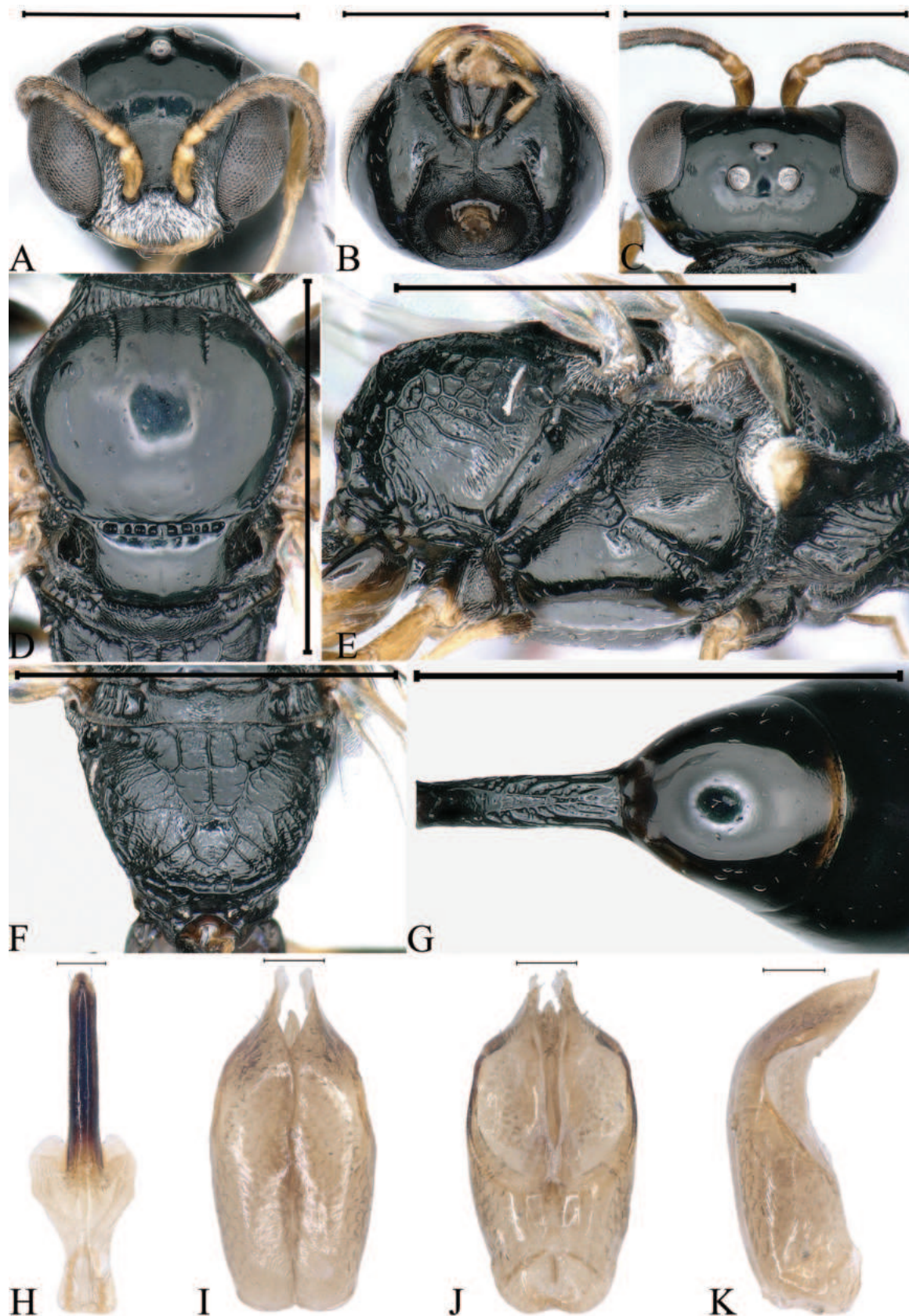


Figure 3. *Stigmus flagellipilaris* Li & Ma, sp. nov. (male) **A** head, frontal view **B** head, ventral view **C** head, dorsal view **D** collar, scutum, scutellum and metanotum, dorsal view **E** thorax, lateral view **F** propodeum, dorsal view **G** petiole, dorsal view **H** gastral tergum VIII, ventral view **I** male genitalia, dorsal view **J** male genitalia, ventral view **K** male genitalia, lateral view. Scale bars: 1 mm (**A–G**); 0.1 mm (**H–K**).

notaulus deeply grooved and crenulate, reaching 1/3 of scutum length; parapsidal line distinctly impressed (Fig. 3D). Scutellum matt, with sparse, midsize punctures, and median, longitudinal line weakly impressed (Fig. 3D). Metanotum distinctly coriaceous (Fig. 3D). Mesopleuron moderately matt, with fine sculptures and several large punctures, posterior area smooth, without rugae, episcrobal area with dense, slender, longitudinal striations; omaulus and hypersternaulus broadened, distinctly crenate, scrobal suture inconspicuous, just with several single rugae (Fig. 3E). Propodeal enclosure triangular medially, with three sturdy, longitudinal rugae and sparse, strong, transverse rugae, lateral area with irregular rugae mixed with a few, sturdy, oblique, longitudinal rugae; posterior surface of propodeum without distinct median groove, with sparse, strong, transverse rugae, remainder with sturdy reticulation (Fig. 3F); lateral surface of propodeum with contiguous, slender or sturdy, oblique, longitudinal rugae anteriorly and medially, and irregular reticulation posteriorly (Fig. 3E).

Legs. Outer surface of hind tibia with three long, slender, fulvous to dark brown spines.

Wings. Forewing venation typical for genus *Stigmus*, hindwing media diverging before cu-a.

Metasoma. Dorsal surface of petiole subquadrate, moderately convex and widened toward apex slightly, and with two sturdy oblique, longitudinal carinae forming V-shaped medially, area between carina gently convex, and with a few sturdy, oblique, longitudinal rugae on each side (Fig. 3G); lateral surface of petiole with several strong, longitudinal rugae (Fig. 8A); ventral surface of petiole with a few sturdy, short, longitudinal rugae posteriorly.

Female. Unknown.

Distribution. China (Yunnan).

Etymology. The specific name, *flagelli*, is derived from the Latin *flagell-* (= flagellum) and the Latin word *pilaris* (= crinal), referring to the flagella without tyloids, and with long setae and dense pilosity.

***Stigmus rugidensus* Li & Ma, sp. nov.**

<https://zoobank.org/B9DD920D-D1B6-46C6-A777-64CF2F1FB196>

Figs 4A–M, 7E, F

Type material. Holotype: CHINA • ♀; Yunnan, Kunming City, Yunnan Agricultural University; 25°7'N, 102°44'E; 12.VI.2023; 1910 m elev.; coll. Jinghong Li; sweep net (YNAU). **Paratypes:** CHINA • 1♂; Yunnan, Kunming City, Shimudi ecological park; 25°5'N, 102°50'E; 22.V.2023; 2210 m elev.; coll. Zhizhi Liu; sweep net (YNAU).

Diagnosis. Differs from *S. japonicus* by hindwing media diverging before cu-a; lateral surface of propodeum smooth and shiny anteriorly and medially, and with sparse, oblique, longitudinal rugae posteriorly; pronotal lobe black; mesopleuron with sparse, midsize punctures, episcrobal area finely coriaceous. *Stigmus japonicus* has the following characters: hindwing media diverging beyond cu-a; lateral surface of propodeum with dense, slender or sturdy, oblique longitudinal rugae anteriorly and medially, and irregular reticulation posteriorly; pronotal lobe ivory; mesopleuron impunctate, episcrobal area with contiguous, longitudinal rugae.

Description. Female. Measurements. ♀, BL: 5 mm; HW: HLD: HLF = 75: 57: 57; HW: EWd: EW: TW: EL = 75: 18: 22: 28: 52; POD: OOD: OCD = 9: 13: 17; length

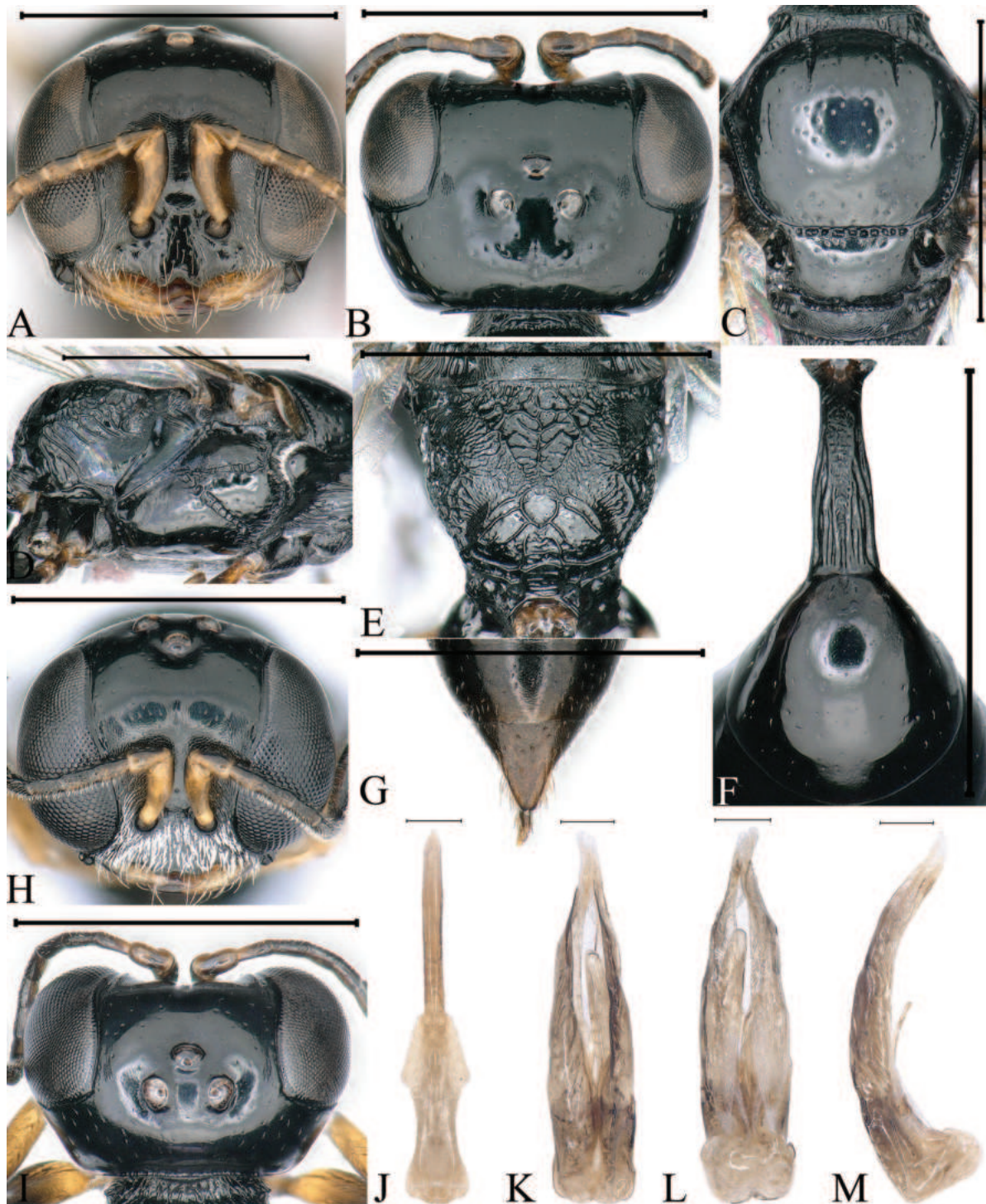


Figure 4. *Stigmus rugidensus* Li & Ma, sp. nov. (A–G female H–M male) **A, H** head, frontal view **B, I** head, dorsal view **C** collar, scutum, scutellum and metanotum, dorsal view **D** thorax, lateral view **E** propodeum, dorsal view **F** petiole, dorsal view **G** pygidial plate, dorsal view **J** gastral tergum VIII, ventral view **K** male genitalia, dorsal view **L** male genitalia, ventral view **M** male genitalia, lateral view. Scale bars: 1 mm (A–I); 0.1 mm (J–M).

of scape: length of pedicel: length of flagellomere I: width of flagellomere I: length of flagellomere II: width of flagellomere II = 24: 10: 10: 6: 10: 5; PL: PW: LTI: WTI: HFL: HTL = 38: 10: 40: 40: 41: 40. ♂, BL: 3.8 mm; HW: HLD: HLF = 70: 45: 47: 55; HW: EWd: EW: TW: EL = 70: 22: 22: 20: 46; POD: OOD: OCD = 8: 12: 14; length of scape: length of pedicel: length of flagellomere I: width of

flagellomere I: length of flagellomere II: width of flagellomere II = 17: 10: 5: 5: 10: 5; PL: PW: LTI: WTI: HFL: HTL = 35: 10: 34: 25: 40: 49.

Color pattern. Body black; mandible brown except dark brown apically; labrum dark brown; palpi yellowish; scape, pedicel, tegula and forewing veins brown; flagellomeres I–VII brown to dark brown; pronotal lobe black; fore leg: coxa apically, base and apex of femur, tibia largely, tarsi fulvous, remainder brown to dark brown; mid leg: fulvous except middle of trochanter and tibia dark brown; hind leg: trochanter and tibia largely dark brown, remainder fulvous; gaster dark brown apically; clypeal margin and mandible with sparse golden setae.

Head. Mandible tridentate apically, median tooth large. Labrum pentagonal, and with two distinct triangular teeth apically (Fig. 4A). Clypeus shiny, slightly convex, and with sparse, midsize punctures; free margin of clypeus slightly produced and with two distinct, cornuted teeth medially, slightly reflected, distinctly emarginated in middle (Fig. 4A). Scapal hollow coriaceous, somewhat shallow, and clearly defined, provided with one vestigial minute tubercle medially, not spined (Fig. 4A). Frontal furrow very fine and weakly impressed, inconspicuously; median and upper frons shiny, with sparse, midsize punctures mixed with several large punctures, gently convex (Fig. 4A). Ocellar triangle area flat, shiny, impunctate, area near eyes with dense, short, impressed lines, opaque area smaller than hind ocellus (Fig. 4B). Vertex shiny, with sparse, large punctures, and with longitudinal line weakly impressed medially (Fig. 4B). Gena shiny, with sparse, midsize to large punctures dorsally; ventral gena shiny, smooth and impunctate. Head from above with temples rarely convergent posteriorly, subquadrate (Fig. 4B). Occipital carina incomplete, not ending to midventral line, suddenly ended at posterior ridge of stomal hollow, dorsal area narrowed, coarsely crenulate, ventral area slightly broadened, distinctly crenate. Inner and outer orbital furrows lacking (Fig. 4A).

Mesosoma. Anterior area of pronotal collar with strong, transverse carina, and with incomplete lateral rugae, only distinct in posterior area, without antero-lateral corner (Fig. 4C). Scutum shiny, with sparse, large punctures; admedian line distinctly impressed, extending to 2/5 of scutum length; notaulus deeply grooved and crenulate, also reaching 2/5 of scutum length; parapsidal line distinctly impressed (Fig. 4C). Scutellum shiny, with sparse, midsize to large punctures, and without longitudinal line (Fig. 4C). Metanotum slightly matt, finely rugulose (Fig. 4C). Mesopleuron shiny, with sparse, midsize punctures, posterior area smooth, without rugae, episcrobal area finely coriaceous; scrobal suture, omaulus and hypersternaulus broadened, distinctly crenate, scrobal suture complete (Fig. 4D). Propodeal enclosure U-shaped medially, and with a longitudinal median rugae and sparse, irregular, transverse rugae, with dense, disorganized, slender rugae laterally; posterior surface of propodeum with sparse, irregular rugae, median groove inconspicuous (Fig. 4E); lateral surface of propodeum moderately matt, smooth anteriorly and medially, with sparse, oblique longitudinal rugae posteriorly (Fig. 4D).

Legs. Outer surface of hind tibia with three long, slender, fulvous to dark brown spines.

Wings. Forewing venation typical for genus *Stigmus*, hindwing media diverging before cu-a.

Metasoma. Dorsal surface of petiole subquadrate, moderately convex and widened toward apex slightly, and with two sturdy oblique, longitudinal carinae forming V-shaped medially, area between carina with dense, irregular, transverse rugae, median and posterior areas with several sturdy, lateral rugae on

each side (Fig. 4F); lateral surface of petiole with two sturdy, longitudinal rugae (Fig. 7E); ventral surface of petiole with a few sturdy, longitudinal rugae posteriorly. Gastral terga shiny, with sparse, midsize punctures, gastral sterna shiny, sterna II–VII with sparse, fine punctures; pygidial area moderately matt, broadly triangular, and with several, midsize punctures basally (Fig. 4G).

Male. Same as female, except: mandible fulvous except reddish brown apically; scape and pedicel fulvous; flagellomeres I–III dark brown; fore leg: inner margin of tibia fulvous, middle of femur dark brown; mid leg: trochanter brown, apex of femur and outer margin of tibia dark brown; hind leg: femur, tibia largely black; setae on clypeus dense, silvery, long (Fig. 4H); mandible bidentate apically; clypeus with dense, tiny punctures; free margin of clypeus slightly produced and nearly truncate medially, with shallow emargination, slightly reflected apically (Fig. 4H); vertex shiny, impunctate, without longitudinal line medially (Fig. 4I); head from above with temples somewhat roundly convergent posteriorly (Fig. 4I); flagellomeres without tyloids, setae normal (Fig. 4I); lateral surface of propodeum with irregular reticulation posteriorly (Fig. 7F); gastral sterna moderately matt, impunctate.

Distribution. China (Yunnan).

Etymology. The name, *rugidensus*, is derived from the Latin *rug-* (= rugae) and the Latin word *densus* (= dense), referring to the propodeal enclosure with dense, disorganized, slender rugae on each side.

***Stigmus sulciconspicus* Li & Ma, sp. nov.**

<https://zoobank.org/AFF9DC36-AD65-416E-BDE6-377FF46CE6BD>

Figs 5A–G, 8B

Type material. Holotype: CHINA • ♀; Baoshan City, Longyang District, Lujiang Country, Gaoligong Mountain; 24°57'N, 98°50'E; 20–21.VII.2006; 938 m elev.; coll. Li Ma; Yellow plate (YNAU). **Paratypes:** CHINA • 1♀, same data as for holotype.

Diagnosis. Distinguished from *S. interruptus* Bashir & Ma, 2019 by the following combination of characters: anterior area of pronotal collar with complete, sturdy, transverse carina; scutum shiny, with sparse, midsize punctures mixed with a few large punctures, without wrinkle; scrobal suture inconspicuous, just single longitudinal striation; in female, pygidial area shiny, impunctate and without striations. *Stigmus interruptus* has the following characters: anterior area of pronotal collar with incomplete, sturdy, transverse carina, narrowly emarginated in middle; mesoscutum moderately matt, with sparse, large punctures, anterior and posterior areas with dense, longitudinal micro-striations; scrobal suture broadened, distinctly crenate; in female, pygidial area with weakly longitudinal striations, basal area with several large punctures.

Description. Female. Measurements. ♀, BL: 4.7 mm; HW: HLD: HLF = 85: 60: 65; HW: EWd: EW: TW: EL = 85: 23: 24: 31: 65; POD: OOD: OCD = 9: 15: 16; length of scape: length of pedicel: length of flagellomere I: width of flagellomere I: length of flagellomere II: width of flagellomere II = 27: 11: 8: 5: 8: 5; PL: PW: LTI: WTI: HFL: HTL = 42: 15: 46: 49: 49: 60.

Color pattern. Body black; clypeus with reddish brown band subapically; mandible yellowish except reddish brown apically; labrum dark brown; palpi yellowish; antenna, tegula, forewing veins and gaster apically fulvous to brown; pronotal lobe white; fore and mid legs: yellowish except coxa largely dark

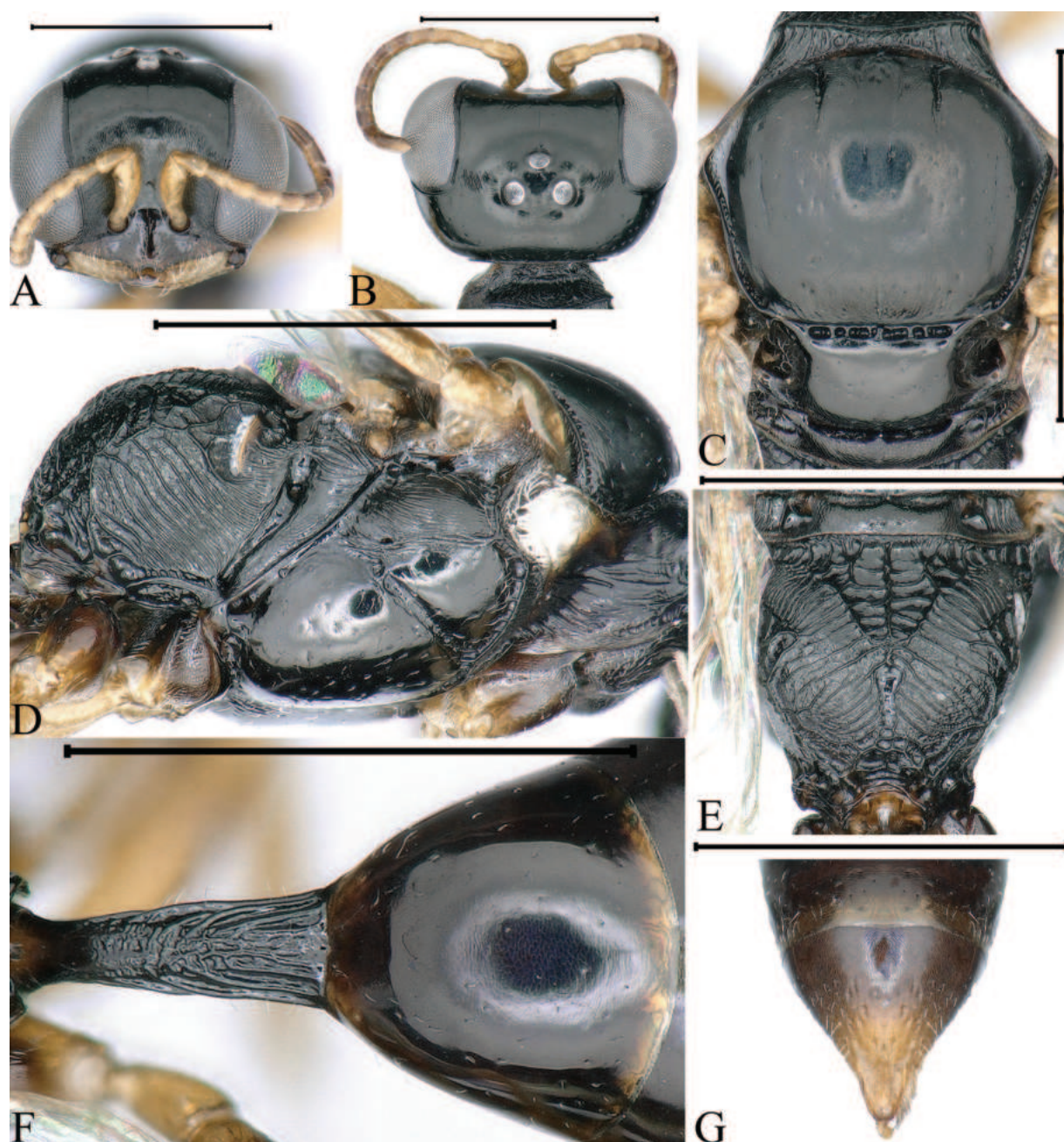


Figure 5. *Stigmus sulciconspicus* Li & Ma, sp. nov. (female) **A** head, frontal view **B** head, dorsal view **C** collar, scutum, scutellum and metanotum, dorsal view **D** thorax, lateral view **E** propodeum, dorsal view **F** petiole, dorsal view **G** pygidial plate, dorsal view. Scale bars: 1 mm.

brown; hind leg: coxa largely and femur medially brown, remainder yellowish; clypeal margin and mandible with sparse golden setae.

Head. Mandible tridentate apically, median tooth large. Labrum with two distinct, triangular teeth apically (Fig. 5A). Clypeus shiny, moderately convex, and with sparse, fine punctures mixed with several large punctures; free margin of clypeus slightly produced and with two distinct, cornuted teeth medially, slightly reflected, slightly emarginated in middle (Fig. 5A). Scapal hollow shiny, shallow, broad, and not clearly defined, provided with one vestigial, minute tubercle medially, not spined (Fig. 5A). Frontal furrow weakly impressed, inconspicuous (Fig. 5A). Median and upper frons slightly matt, finely coriaceous, and with sparse, midsize punctures,

slightly convex (Fig. 5A). Ocellar triangle area flat, shiny, with several fine punctures, area near eyes with dense, short, impressed lines, opaque area larger than hind ocellus (Fig. 5B). Vertex shiny, with sparse, tiny punctures (Fig. 5B). Gena shiny, with sparse, midsize to large punctures dorsally; ventral gena shiny, and with a few midsize punctures. Head from above with temples rarely convergent posteriorly, subquadrate (Fig. 5B). Occipital carina incomplete, not ending to midventral line, suddenly ended at posterior ridge of stomal hollow, without tooth; occipital carina much narrowed, no crenulate. Inner and outer orbital furrows lacking (Fig. 5A).

Mesosoma. Pronotal collar with strong, transverse carina anteriorly, lateral rugae lacking, without antero-lateral corner (Fig. 5C). Scutum shiny, with sparse, midsize punctures mixed with several large punctures; admedian line distinctly impressed, extending to 5/12 of scutum length; notaulus deeply grooved and crenulate, reaching 1/4 of scutum length; parapsidal line distinctly impressed (Fig. 5C). Scutellum shiny, with sparse, tiny punctures, median longitudinal line weakly impressed (Fig. 5C). Metanotum finely coriaceous (Fig. 5C). Mesopleuron shiny, with sparse, midsize punctures, posterior area smooth without rugae, episcrobal area with dense, longitudinal sculptures; scrobal suture inconspicuous, just single longitudinal rugae; hypersternaulus broadened, smooth, not crenate; omaulus broadened, distinctly crenate (Fig. 5D). Propodeal enclosure elongate, U-shaped medially, with one strong, longitudinal, rugae and sparse, irregular, transvers rugae, and with oblique, longitudinal rugae laterally; posterior surface of propodeum with somewhat narrow, shiny, conspicuous, median groove, lateral area of median groove with sparse, oblique, longitudinal rugae, and with sparse, irregular rugae posteriorly (Fig. 5E); lateral surface of propodeum with dense, slender, oblique longitudinal rugae (Fig. 5D).

Legs. Outer surface of hind tibia with three long, slender, fulvous spines.

Wings. Forewing venation typical for genus *Stigmus*, hindwing media diverging beyond cu-a.

Metasoma. Dorsal surface of petiole subquadrate, gently convex and widened toward apex distinctly, with strong, irregular rugae and with several strong, longitudinal rugae posteriorly (Fig. 5F); lateral surface of petiole with a few sturdy, longitudinal rugae (Fig. 8B); ventral surface of petiole with several sturdy, longitudinal rugae posteriorly. Gastral terga shiny, terga I–V with sparse, fine punctures, tergum VI with sparse, midsize punctures apically (Fig. 5G); gastral sterna shiny, sterna I–VI with sparse, fine punctures, sternum VI with dense, fine punctures (Fig. 5G); pygidial area moderately matt, broadly U-shaped, apex rounded (Fig. 5G).

Male. Unknown.

Distribution. China (Yunnan).

Etymology. The name, *sulciconspicus*, is derived from the Latin *sulc-* (= groove) and the Latin word *conspicus* (= conspicuous), referring to the posterior surface of propodeum with conspicuous median groove.

New record for China

***Stigmus solskyi* Morawitz, 1864**

Figs 6A–M, 8C, D

Stigmus solskyi A. Morawitz, 1864: 462; Tsuneki, 1954: 24; Lomholdt, 1975: 129; Bohart & Menke, 1976: 189.

Stigmus europaeus Tsuneki, 1954: 25. Synonymized with *Stigmus solskyi* by Yarrow, 1954: 239; de Beaumont, 1956: 385; Tsuneki, 1954: 6.

Stigmus verhoeffi Tsuneki, 1954: 6, 26, 36. Synonymized with *Stigmus solskyi* by de Beaumont, 1956: 385.

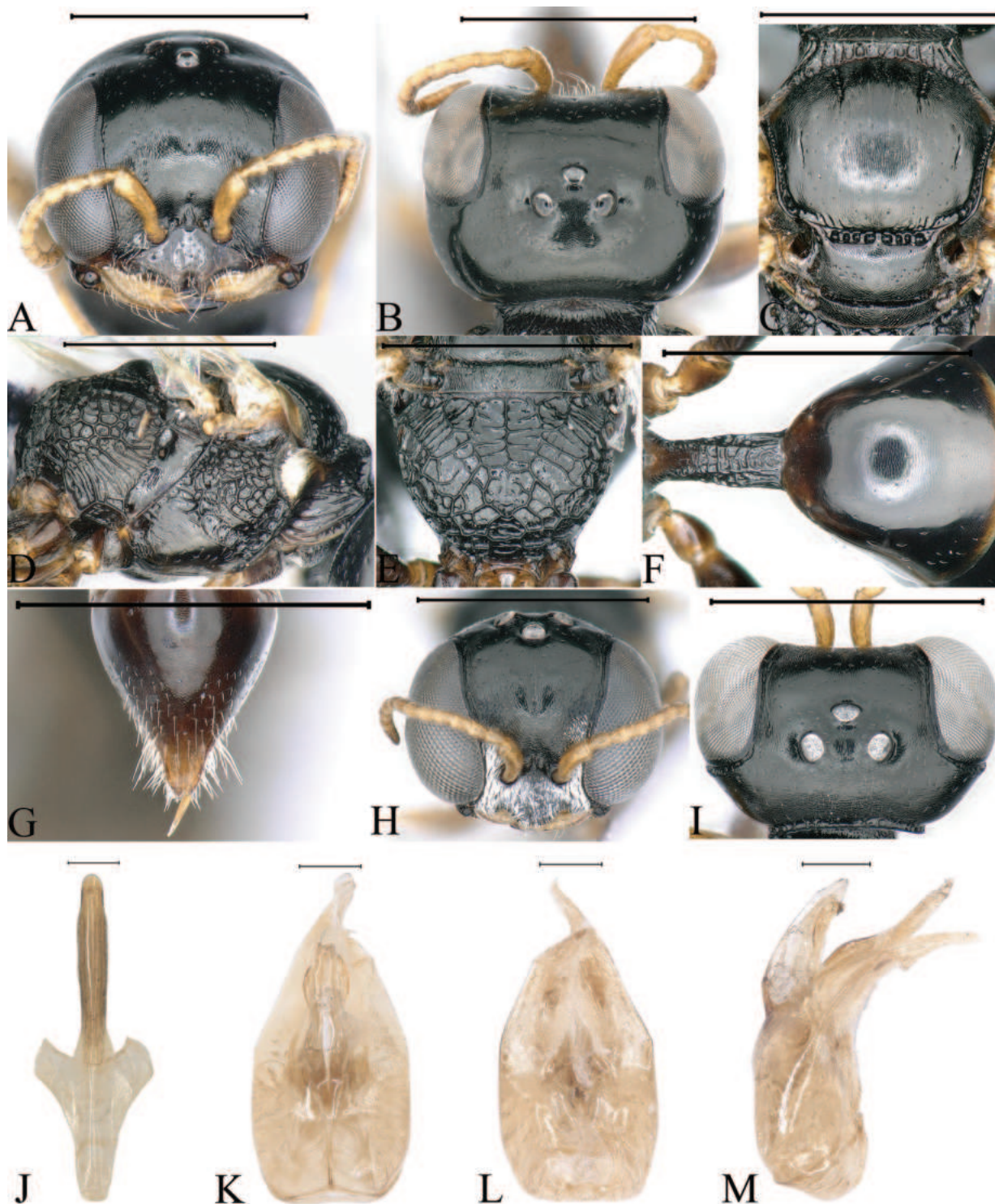


Figure 6. *Stigmus solskyi* Morawitz, 1864. (A–G female H–M male) A, H head, frontal view B, I head, dorsal view C collar, scutum, scutellum and metanotum, dorsal view D thorax, lateral view E propodeum, dorsal view F petiole, dorsal view G pygidial plate, dorsal view J gastral tergum VIII, ventral view K male genitalia, dorsal view L male genitalia, ventral view M male genitalia, lateral view. Scale bars: 1 mm (A–I); 0.1 mm (J–M).

Specimen examined. CHINA • 1♀; Inner Mongolia; 8.VII.2001; coll. Bo Qiu. CHINA • 1♀, 3♂♂; Inner Mongolia, Bayan Nur City; 13.VII.2007.

Distribution. China (Inner Mongolia), Algeria, Europe northwards to Finland, Turkey, Georgia, Kazakhstan, Russia.

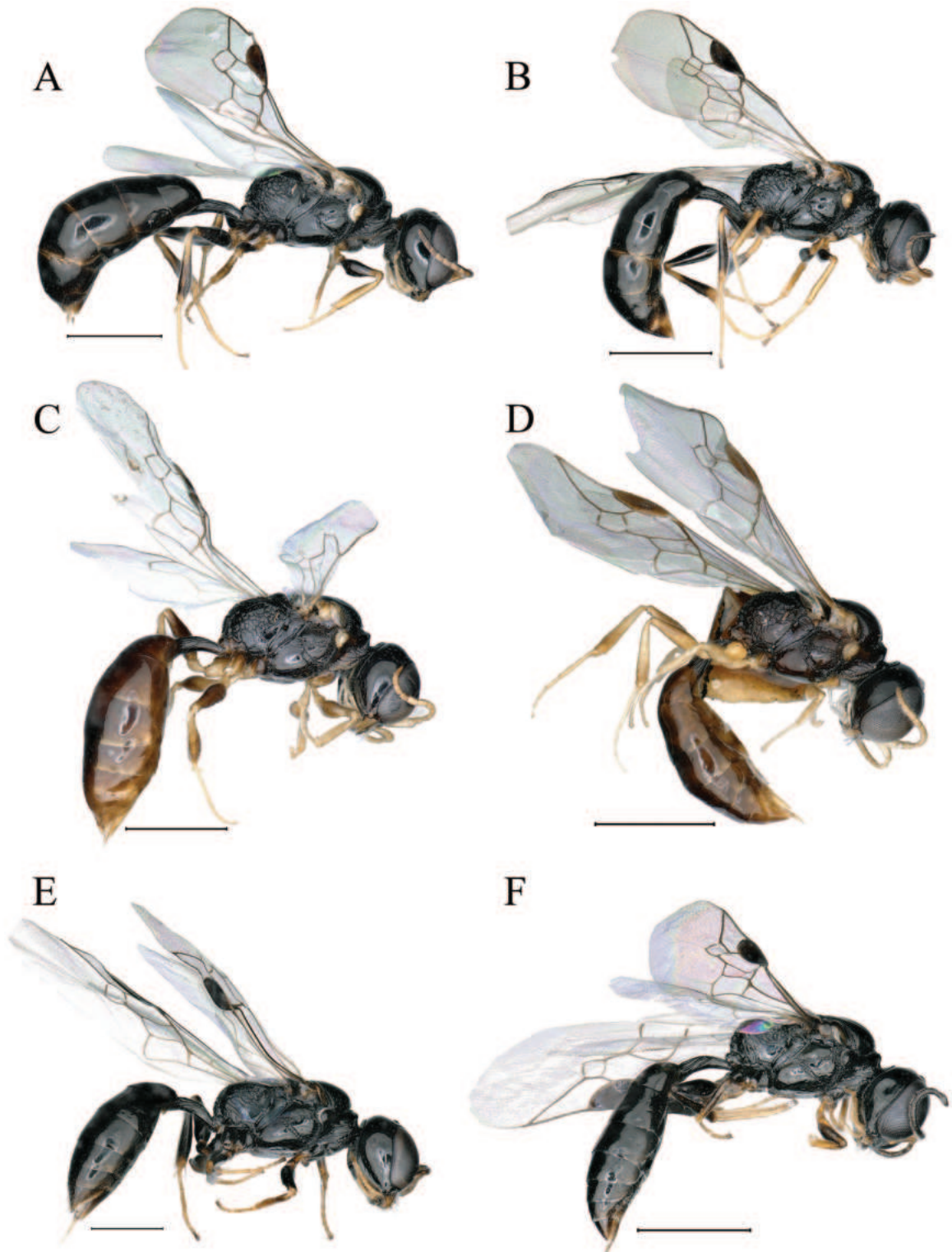


Figure 7. A, B *Stigmus carinannulatus* Li & Ma, sp. nov. (A female B male) C, D *Stigmus clypeglabratus* Li & Ma, sp. nov. (C female, D male) E, F *Stigmus rugidens* Li & Ma, sp. nov. (E female F male) A–F lateral view. Scale bars: 1 mm.

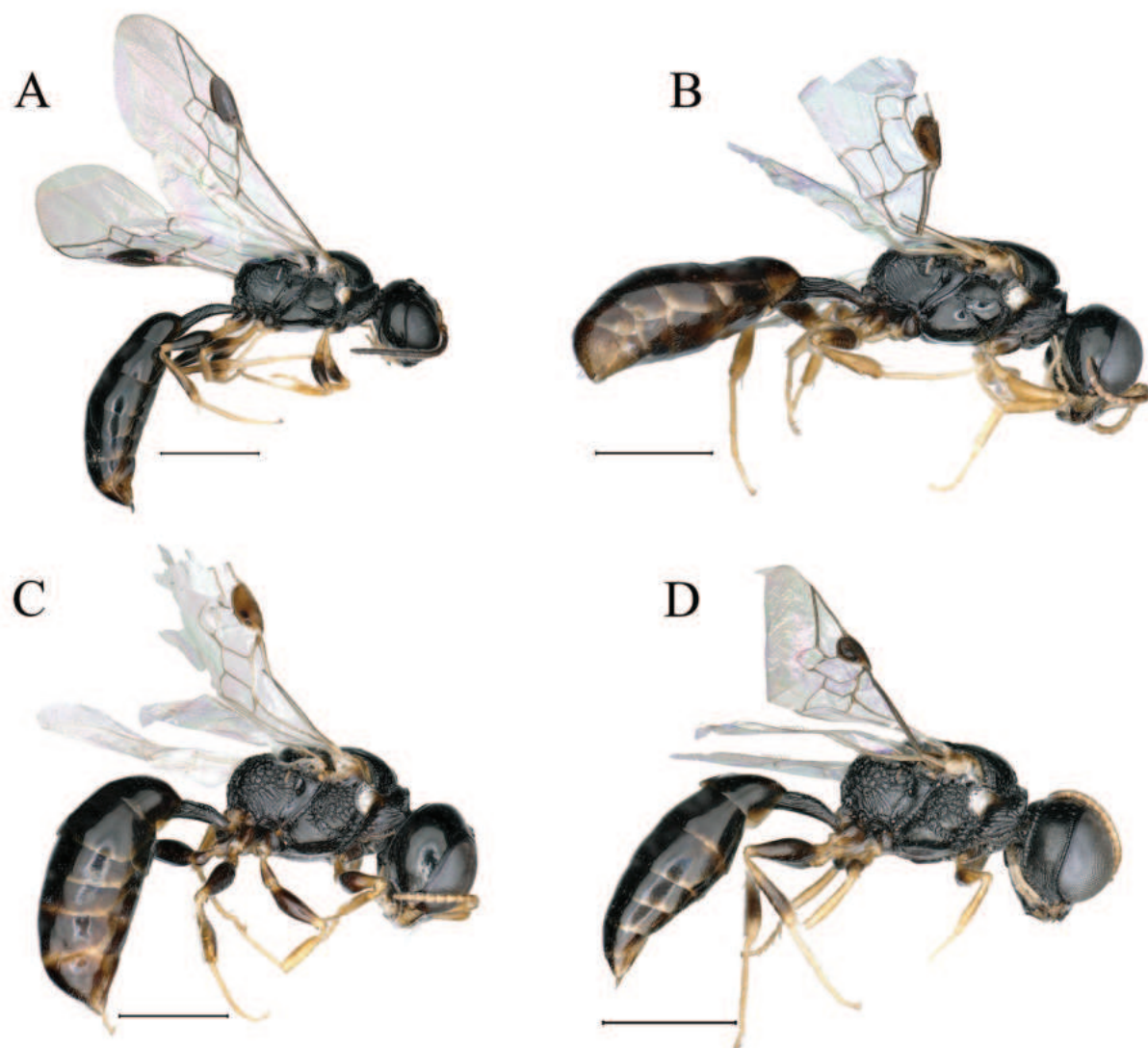


Figure 8. **A** *Stigmus flagellipilaris* Li & Ma, sp. nov. (male) **B** *Stigmus sulciconspicus* Li & Ma, sp. nov. (female) **C, D** *Stigmus solskyi* Morawitz, 1864. (**C** female **D** male) **A–D** lateral view. Scale bars: 1 mm.

Acknowledgements

We express our hearty thanks to Wojciech J. Pulawski (California Academy of Sciences, California) for providing us with many valuable references. We are cordially grateful to section editor and all anonymous reviewers for valuable and constructive comments that helped improve this article.

Additional information

Conflict of interest

The authors have declared that no competing interests exist.

Ethical statement

No ethical statement was reported.

Funding

This work was supported by the National Natural Science Foundation of China under Grant number 32270485 and the Agricultural Basic Research joint project of Yunnan Province under Grant number 202101BD070001-004.

Author contributions

Jinghong Li conducted the investigation (field work), wrote, and revised the manuscript; Qiang Li conceived the study, acquired funding, and revised the manuscript; Li Ma conceived the study, acquired funding, conducted the investigation (field work), and revised the manuscript.

Author ORCIDs

Jinghong Li  <https://orcid.org/0009-0002-3346-5018>

Qiang Li  <https://orcid.org/0000-0001-5950-8843>

Li Ma  <https://orcid.org/0000-0002-3436-1387>

Data availability

All of the data that support the findings of this study are available in the main text.

References

- Allen GW (1987) *Stigmus pendulus* Panzer (Hymenoptera, Sphecidae) new to Britain. *Entomologist's Gazette* 38: 214.
- Amarante STP (2002) A synonymic catalog of the Neotropical Crabronidae and Sphecidae (Hymenoptera: Apoidea). *Arquivos de Zoologia* 37(1): 1–139. <https://doi.org/10.11606/issn.2176-7793.v37i1p1-139>
- Bashir NH, Li Q, Ma L (2019) Review of the genus *Stigmus* Panzer (Hymenoptera, Crabronidae) in China, with description of five new species from the Oriental and Palearctic Regions. *ZooKeys* 843: 51–69. <https://doi.org/10.3897/zookeys.843.31885>
- Bohart RM, Menke AS (1976) Sphecid wasps of the world, a genetic revision. University of California Press, Berkeley, Los Angeles, London, 695 pp. <https://doi.org/10.1525/9780520309548>
- Budrys ER (1987) Digger wasps of the genus *Stigmus* Panzer and *Carinostigmus* Tsunek (Hymenoptera, Sphecidae) of the Far East of USSR. In: Lehr PA, Storozheva NA (Eds) *New data on insect systematic of Russian Far East*. DVO AN SSSR, Vladivostok, 49–56. http://researcharchive.calacademy.org/research/entomology/Entomology_Resources/Hymenoptera/sphecidae/copies/Budrys_1987.pdf
- Budrys ER (1995) Subfamily Pemphredoninae. In: Lehr PA (Ed.) *Key to the insects of Russian Far East*. Vol. 4. Nauka, Sant-Peterburg, 388–406. <https://www.nhbs.com/3/series/keys-to-the-insects-of-the-russian-far-east?qtview=122918>
- Finnamore AT (1995) Revision of the world genera of the subtribe Stigmina (Hymenoptera: Apoidea: Sphecidae: Pemphredoninae), Part 1. *Journal of Hymenoptera Research* 4: 204–284. <http://biodiversitylibrary.org/page/3387491>
- Jones RA (2001) *Stigmus pendulus* (Panzer) (Hymenoptera: Sphecidae) associated with ancient woodlands in south-east London. *British Journal of Entomology and Natural History* 13: 213–214. <https://biodiversitylibrary.org/page/39462229>
- Kohl FF (1892) Neue Hymenopterenformen. *Annalen des k.k. Naturhistorischen Hofmuseums* 7: 197–234. [pls. XIII–XV] <http://biodiversitylibrary.org/page/5745488>

- Kolesnikov VA (1977) Sphecoid wasps (Hymenoptera, Sphecidae) of the Bryansk region and their role as entomophagous insects. *Entomologicheskoye Obozreniye* 56: 315–325. http://researcharchive.calacademy.org/research/entomology/Entomology_Resources/Hymenoptera/sphecidae/copies/Kolesnikov_1977.pdf
- Krombein KV (1955) Miscellaneous prey records of solitary wasps. I (Hymenoptera: Aculeata). *Bulletin of the Brooklyn Entomological Society* 50: 13–17.
- Krombein KV (1958) Miscellaneous prey records of solitary wasps. III (Hymenoptera, Aculeata). *Proceedings of the Biological Society of Washington* 71: 21–26. http://researcharchive.calacademy.org/research/entomology/Entomology_Resources/Hymenoptera/sphecidae/copies/Krombein_1955a.pdf
- Krombein KV (1973) Notes on North American *Stigmus* Panzer (Hymenoptera, Sphecoidea). *Proceedings of the Biological Society of Washington* 86: 211–230. https://researcharchive.calacademy.org/research/entomology/Entomology_Resources/Hymenoptera/sphecidae/copies/Krombein_1973_Stigmus.pdf
- Krombein KV (1984) Biosystematic studies of Ceylonese wasps, XIV: a revision of *Carinostigmus* Tsuneki (Hymenoptera: Sphecoidea: Pemphredonidae). *Smithsonian Contributions to Zoology* 396(396): 1–37. <https://doi.org/10.5479/si.00810282.396>
- Melo GAR (1999) Phylogenetic relationships and classification of the major lineages of Apoidea (Hymenoptera), with emphasis on the crabronid wasps. *José Luis Meilán Gil* 14. <https://doi.org/10.5962/bhl.title.4053>
- Mokrousov M (2017) To the knowledge of digger wasps of subfamily Pemphredoninae (Hymenoptera: Crabronidae) of Russia. *Far Eastern Entomologist [= Dal'nevostochnyi Entomolog]* 337: 1–16. <https://doi.org/10.25221/fee.337.1>
- Morawitz A (1864) Verzeichniss der um St.-Petersburg aufgefundenen Crabroninen. *Bulletin de l'Académie Impériale des Sciences de St.-Petersbourg* 7: 451–465. <https://biodiversitylibrary.org/page/33683794>
- Packard AS (1867) Revision of the fossorial Hymenoptera of North America. I. Crabronidae and Nyssonidae. *Proceedings of the Entomological Society of Philadelphia* 6: 39–115 (1866), 353–444 [6 June 1867]. <http://biodiversitylibrary.org/page/3831118>
- Panzer GWF (1804) *Faunae insectorum germanicae initiae oder Deutschlands Insecten*, H, 86. [24 pls] <https://biodiversitylibrary.org/page/15488140>
- Pulawski WJ (2024) *Stigmus*: Catalog of Sphecidae. https://researcharchive.calacademy.org/research/entomology/entomology_resources/hymenoptera/sphecidae/genera/Stigmus.pdf
- Ratzlaff CG (2016) Checklist of the spheciform wasps (Hymenoptera: Crabronidae & Sphecidae) of British Columbia. *Journal of the Entomological Society of British Columbia* 112: 19–46. http://researcharchive.calacademy.org/research/entomology/Entomology_Resources/Hymenoptera/sphecidae/copies/Ratzlaff_2015.pdf
- Rohwer SA (1911) Descriptions of new species of wasps with notes on described species. *Proceedings of the United States National Museum* 40(1837): 551–587. <https://doi.org/10.5479/si.00963801.1837.551>
- Smith MR (1923) Unusual damage to the floors of a house by a species of pemphredinid wasp, *Stigmus fulvicornis* Rohwer. *Journal of Economic Entomology* 16: 553–554. http://researcharchive.calacademy.org/research/entomology/Entomology_Resources/Hymenoptera/sphecidae/copies/Smith_M_1923b.pdf
- Terayama M (2012) Taxonomic guide to the Japanese Aculeate wasps. 12. Subfamily Pemphredoninae. Tribe Pemphredonini: keys to the species. *Tsunekibachi* 22: 1–31.

- http://researcharchive.calacademy.org/research/entomology/Entomology_Resources/Hymenoptera/sphecidae/copies/Terayama_2012.pdf
- Tsuneki K (1954) The genus *Stigmus* Panzer of Europe and Asia, with description of eight new species (Hymenoptera, Sphecidae). *Memoirs of the Faculty of Liberal Arts, Fukui University (Series II, Natural Science)* 3: 1–38. http://researcharchive.calacademy.org/research/entomology/Entomology_Resources/Hymenoptera/sphecidae/copies/Tsuneki_1954a.pdf
- Tsuneki K (1970) Gleanings on the bionomics of the East-Asiatic non-social wasps (Hymenoptera). V. Some species of Pemphredoninae. *Etizenia* 42: 1–20. http://researcharchive.calacademy.org/research/entomology/Entomology_Resources/Hymenoptera/sphecidae/copies/Tsuneki_1970d.pdf
- Tsuneki K (1971) Studies on the Formosan Sphecidae (XIII). A supplement to the subfamily Pemphredoninae (Hym.) with a key to the Formosan species. *Etizenia* 57: 1–21. http://researcharchive.calacademy.org/research/entomology/Entomology_Resources/Hymenoptera/sphecidae/copies/Tsuneki_1971j.pdf
- Uffen RWJ (1997) Exhibit of *Stigmus pendulus* from Welwyn, at BENHS meeting 8 October 1996. *British Journal of Entomology and Natural History* 10: 181. <https://biodiversitylibrary.org/page/36266245>
- Uffen RWJ (1998) Exhibit of *S. pendulus* from Tyttenhanger, at BENHS Annual Exhibition 2 November 1996. *British Journal of Entomology and Natural History* 10: 181. <https://biodiversitylibrary.org/page/36266245>

Two new species of *Bamazomus* Harvey, 1992 from southern China (Schizomida, Hubbardiidae)

Tao Zheng^{1,2}, Jiaxian Gong³, Feng Zhang^{1,2}

¹ Key Laboratory of Zoological Systematics and Application, College of Life Sciences, Hebei University, Baoding, Hebei 071002, China

² Hebei Basic Science Center for Biotic Interaction, Hebei University, Baoding, Hebei 071002, China

³ College of Bee Science and Biomedicine, Fujian Agriculture and Forestry University, Fuzhou, Fujian 350002, China

Corresponding author: Feng Zhang (dudu06042001@163.com)

Abstract

Two new schizomid species belonging to *Bamazomus* Harvey, 1992 are described from China: *B. shanghang* sp. nov. (♂♀) from Fujian Province and *B. songi* sp. nov. (♂♀) from Guangdong Province. In addition to their descriptions, illustrations and diagnoses, a distribution map is provided. These are first *Bamazomus* species from the mainland China and the northernmost in continental Asia.

Key words: Asia, morphology, short-tailed whipscorpions, taxonomy

Introduction

Schizomida is an understudied arachnid order mainly distributed in tropical and subtropical areas. The order is a homogeneous group of 372 species unequally divided between Hubbardiidae Cook, 1899 and Protoschizomidae Rowland, 1975. In addition, there are 14 fossil species currently placed in Calcitronidae Petrunkevitch, 1945 (two species) and Hubbardiidae (12 species). Hubbardiidae, which is distributed worldwide, is the largest schizomid family with 356 species placed in 69 genera; among them there are three genera and four species recorded from China (WSC 2024).

The genus *Bamazomus* Harvey, 1992 was erected to receive *B. bamaga* Harvey, 1992. The taxonomically diagnostic characters are female genitalia with a gonopod and numerous lobes and a dorso-ventrally flattened male flagellum. Currently, *Bamazomus* comprises 11 species distributed from Madagascar to Australia, except for one widespread, introduced species, *B. siamensis* (Hansen, 1905), which has been recorded from Hong Kong (China), Hawaii (USA), Ryukyu Islands (Japan), and Bangkok (Thailand) (Cokendolpher and Reddell 1986; Cokendolpher 1988; WSC 2024). It is the only *Bamazomus* species known from China and from continental Asia (Bangkok).



Academic editor: Yuri Marusik

Received: 27 February 2024

Accepted: 20 May 2024

Published: 12 June 2024

ZooBank: <https://zoobank.org/BAE8C8FA-9F46-4C8A-82A8-8F2330EB63AC>

Citation: Zheng T, Gong J, Zhang F (2024) Two new species of *Bamazomus* Harvey, 1992 from southern China (Schizomida, Hubbardiidae). ZooKeys 1204: 337–353. <https://doi.org/10.3897/zookeys.1204.121754>

Copyright: © Tao Zheng et al.

This is an open access article distributed under terms of the Creative Commons Attribution License (Attribution 4.0 International – CC BY 4.0).

Extensive collecting in 2022 and 2023 from southern China helped us gain a deep understanding of the natural habitat of schizomids and allowed us to obtain additional specimens of this group. In this paper, two new *Bamazomus* species, *B. shanghang* sp. nov. and *B. songi* sp. nov. are described from China.

Materials and methods

Specimens are deposited in the Museum of Hebei University (**MHBU**), Baoding, China. All measurements in the text are given in millimetres, and the total length excludes the flagellum. The spermathecae were removed and cleared in a pancreatin solution (Álvarez-Padilla and Hormiga 2007) and then transferred to 75% ethanol for drawing. All specimens are preserved in 75% alcohol. Photographs were taken using the Leica M205A stereomicroscope equipped with a DFC 550 CCD camera and edited with Adobe Photoshop CC 2019. Morphological terminology for legs and palps follows Reddell and Cokendolpher (1995), cheliceral setae nomenclature follows Lawrence (1969) as modified by Villarreal et al. (2016), flagellar setae terminology follows Cokendolpher and Reddell (1992) as modified by Harvey (1992) and Monjaraz-Ruedas et al. (2016), palpal setae terminology follows Monjaraz-Ruedas et al. (2017), spermathecae nomenclature follows Moreno-Gonzalez et al. (2014), and opisthosomal setae nomenclature follows Villarreal et al. (2016).

Abbreviations: **AB** anterior branch of chitinized arch, **AT** accessory tooth of movable finger, **Dm** dorso-median setae of abdomen and flagellum, **DI** dorso-lateral setae of the abdomen and flagellum, **Fe** femur ectally, **Fed** femur dorso-ectally, **Fev** femur ventro-ectally, **Fm** femur mesally, **Fmd** femur dorso-mesally, **Fmv** femur ventro-mesally, **G** setal group numbers of chelicerae, **GT** guard tooth of movable finger, **IA** internal angle of chitinized arch, **L** lobe, **LT** lateral tip of chitinized arch, **Msp** patches of microsetae of the male flagellum, **PB** posterior branch of chitinized arch, **Pe** patella ectally, **Pm** patella mesally, **Pmm** mid mesal part of patella, **Pme** mid ectal part of patella, **S** serrula, **Ter** row of tibia externally, **Tmr** row of tibia medially, **Tir** row of tibia internally, **Vm** ventro-median setae of the abdomen and flagellum, **VI** ventro-lateral setae of the abdomen and flagellum.

Taxonomy

Family Hubbardiidae Cook, 1899

Genus *Bamazomus* Harvey, 1992

Type species. *Bamazomus bamaga* Harvey, 1992 from Queensland.

Comment. *Bamazomus* resembles *Apozomus* Harvey, 1992 and can be distinguished from it by: 1) spermathecae with numerous lobes vs only with two pairs of lobes; 2) flagellum with posterior process in male vs without posterior process. Currently 11 species of the genus are known to occur from Madagascar to Australia. There is only one anthropochorous species, *B. siamensis* (Hansen, 1905), which is known outside of natural range. It is known from Thailand (type locality), Hawaii, Ryukyu Islands, and Hong Kong. Until now only this species was known from the continental part of Asia, namely from Bangkok (WSC 2024).

***Bamazomus shanghang* sp. nov.**

<https://zoobank.org/E6A3A077-5D27-41CF-95E9-2A4EE4287F38>

Figs 1–7, Table 1

上杭巴马加盾

Type material. *Holotype* ♂ (MHBU-2023312-1), CHINA: Fujian Province, Longyan City, Shanghang County, Shanghang National Forest Park, 25.6364°N, 116.9097°E, 672 m elev., 22.VII.2023, leg. T. Zheng, J.-X. Gong. *Paratype*: 1♀ (MHBU-2023312-2), same data as the holotype.

Etymology. The specific name is a noun in apposition, referring to the name of the type locality.

Diagnosis. The new species resembles *B. siamensis* in having three posterior processes and a small, conical protuberance on the posterior margin of flagellum in the male, and spermathecal lobes with several apical apophyses (Cokendolpher and Reddell 1986: figs 2–4; Hansen and Soerensen 1905: pl. 5, fig. 2g, h), but it can be distinguished by: 1) the absence of duct openings of spermathecal lobes and presence of the incomplete anterior branch of chitinized arch (Fig. 7A, B) vs duct openings present and anterior branch complete (Cokendolpher and Reddell 1986: figs 2–4); 2) the posterior dorsal process of

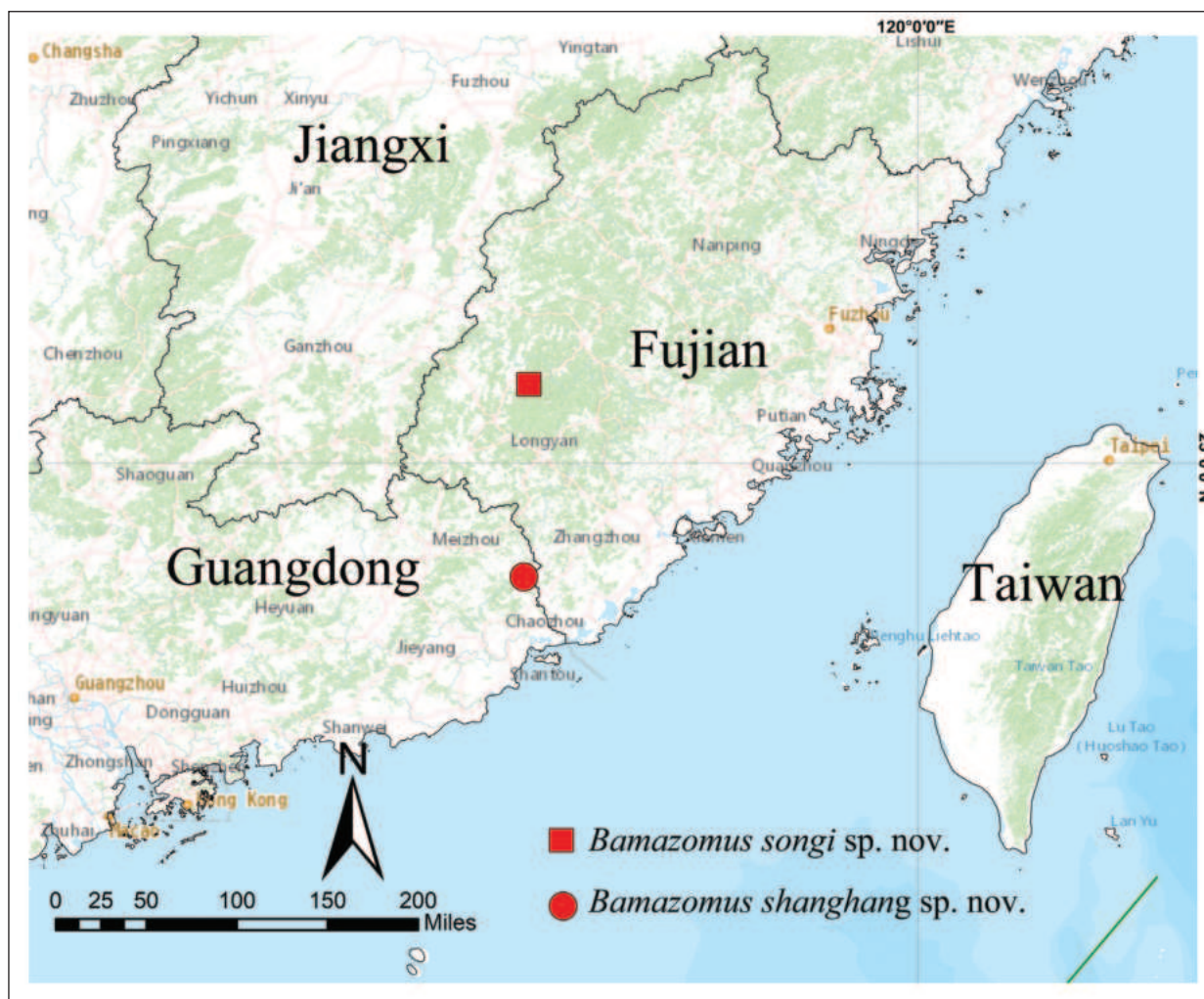


Figure 1. Type localities of *Bamazomus songi* sp. nov. (square) and *B. shanghang* sp. nov. (circle).

XII segment of opisthosoma semi-oval, blunt, and short (Figs 2A, 5A) vs conical, acuminate, and long (Hansen and Soerensen 1905: pl. 5, fig. 2h); 3) the presence of Dm4 on flagellum, with two rows of microsetae placed dorsolaterally next to Dm1, right row with four microsetae, left row with three microsetae

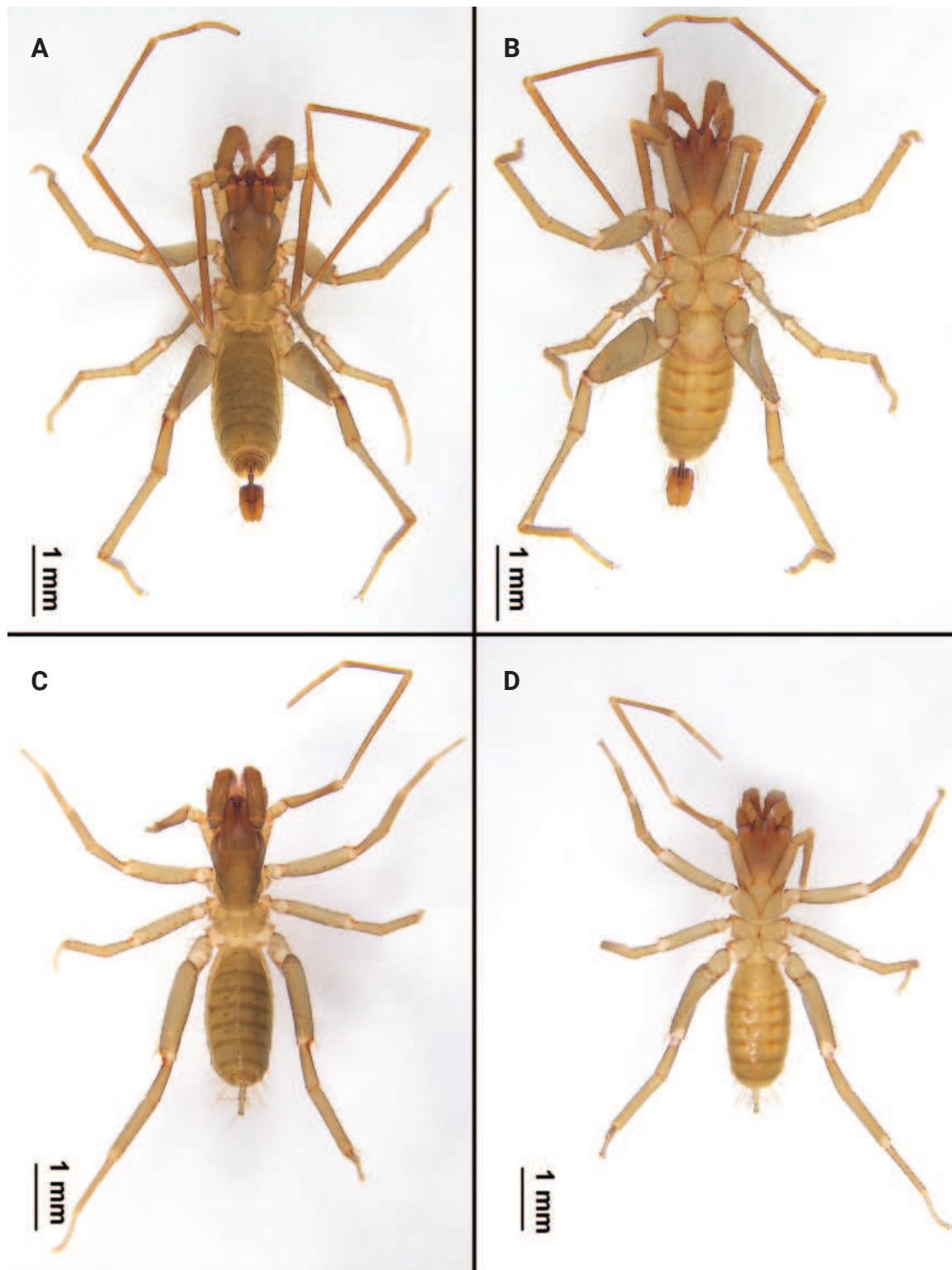


Figure 2. Habitus of *Bamazomus shanghang* sp. nov., holotype male and paratype female A male, dorsal view B same, ventral view C female paratype, dorsal view D same, ventral view.

in the male (Figs 5A–C, 6A–C) vs Dm4 and two row of microsetae are absent (Hansen and Soerensen 1905: pl. 5, fig. 2g, h).

Description. Holotype Male (Fig. 2A, B): measurements as in Table 1. Colour: light brownish. Prosoma: anterior process of propeltidium with three setae (pair of setae followed by a single seta) followed by five pairs of dorsal setae (2+2+2+2+2); eye spots distinct. Mesopeltidia separated. Metapeltidium divided. Anterior sternum with 14 setae (including two sternapophysial setae); posterior sternum triangular with six setae.

Chelicerae (Fig. 3A, B): movable finger: serrula with 17 teeth, guard tooth present, with one prominent accessory tooth at subterminal part of movable finger. Fixed finger with two large teeth and four smaller teeth, proximal tooth with one tiny, blunt lateral tooth. Setation: setal group formula: 3–9–5–4–10–6–1–6. G1 with three spatulate setae; G2 composed of nine smooth setae; G3 with five setae, feathered apically and smooth basally; G4 consisting of four small setae, smooth, basally thick, distally elongated; G5A with 10 similarly

Table 1. Measurements (mm) of *Bamazomus songi* sp. nov. and *B. shanghai* sp. nov.

		<i>Bamazomus shanghai</i> sp. nov.		<i>Bamazomus songi</i> sp. nov.	
		Male (Holotype)	Female (Paratype)	Male (Holotype)	Female (Paratype) MH BU-ZT5-2
Total Length		4.37	4.52	5.41	5.51
Propeltidium	Length	1.45	1.53	1.39	1.49
	Width	0.87	0.87	0.97	0.86
Flagellum	Length	0.67	0.78	0.69	0.49
	Width	0.35	0.09	0.34	0.09
	Height	0.30	0.09	0.30	0.09
Leg I	Coxa	1.00	0.81	1.17	0.73
	Trochanter	0.59	0.46	0.79	0.46
	Femur	2.37	1.51	2.48	1.45
	Patella	3.16	2.03	3.50	1.93
	Tibia	2.38	1.47	2.26	1.44
	Basitarsus	0.64	0.43	0.76	0.44
	Telotarsus	1.48	0.65	0.91	0.55
	Total	11.57	7.36	11.87	7.00
Leg IV	Trochanter	0.64	0.53	0.59	0.51
	Femur	1.84	1.59	2.23	1.58
	Patella	0.90	0.68	0.99	0.66
	Tibia	1.48	1.16	1.68	1.10
	Basitarsus	1.24	0.99	1.46	0.99
	Telotarsus	0.81	0.71	0.88	0.70
	Total	7.39	6.14	8.34	5.98
Pedipalp	Trochanter	0.66	0.65	0.37	0.71
	Femur	0.77	0.74	0.85	0.57
	Patella	0.78	0.73	0.83	0.64
	Tibia	0.73	0.71	0.79	0.62
	Tarsus	0.37	0.28	0.34	0.36
	Total	2.97	2.78	3.28	3.46

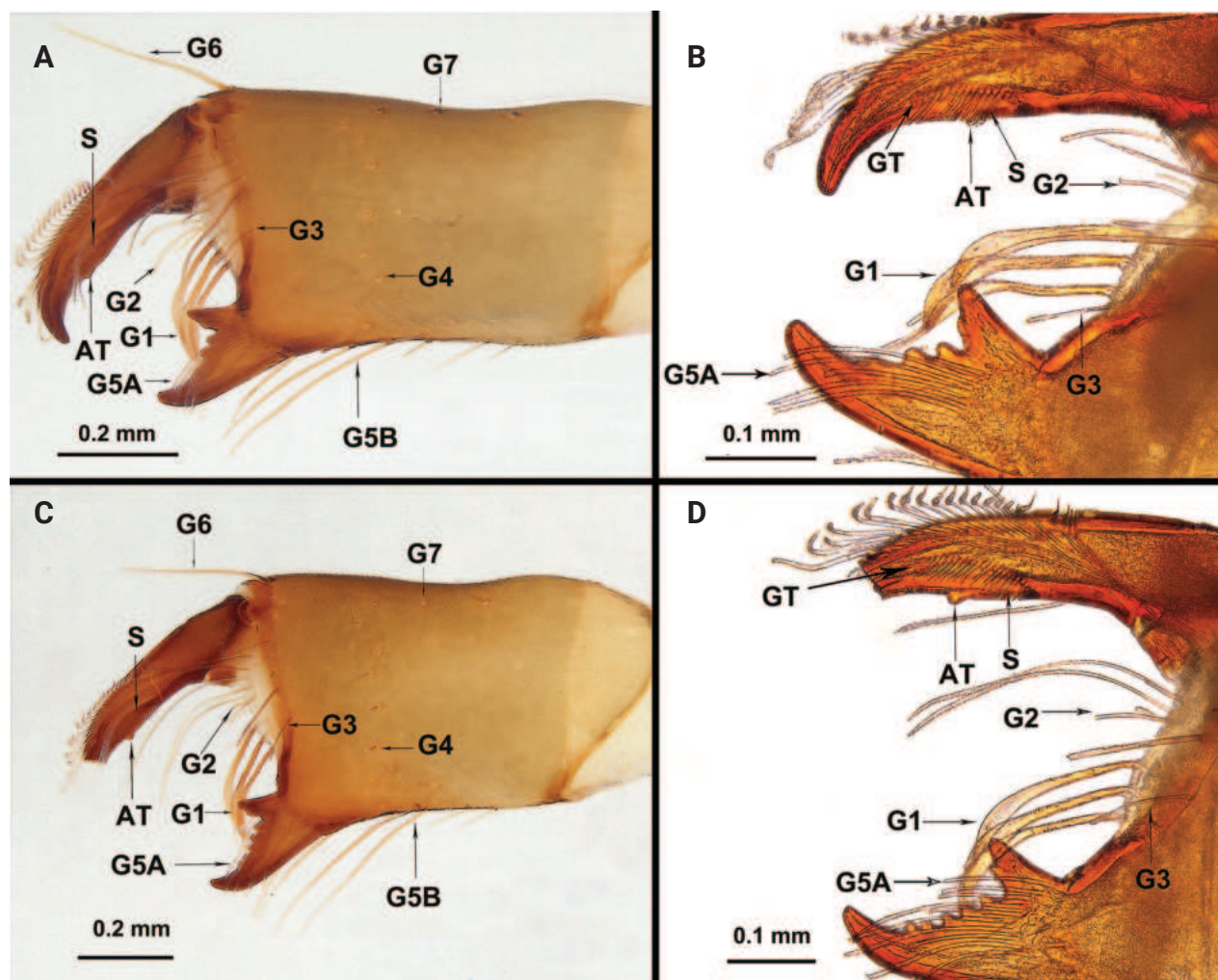


Figure 3. Chelicerae of *Bamazomus shanghang* sp. nov., holotype male and paratype female **A** male, mesal view **B** same, movable finger and fixed finger **C** female (tip broken), mesal view **D** same, movable finger and fixed finger. Abbreviations: AT = accessory tooth of movable finger, G = setal group numbers of chelicerae, GT = guard tooth of movable finger, S = serrula.

sized setae, feathered apically and smooth basally, length almost equal to movable finger; G5B with six setae, basal two short and smooth, apical four longer and feathered; G6 with one smooth seta about 3/5 of movable finger length; G7 with seven smooth setae.

Palps (Fig. 4A, B): 2.05 times longer than propeltidium; trochanter with apical process, blunt apical process with angle of about 70°; mesal surface of trochanter with two setae near ventral margin and two setae near dorsal margin; with one small mesal spur. Femur 1.7 times longer than high; ventral margin on ectal surface with acuminate setae Fe1, Fe5, Fev1, Fev2 and one dorsal seta Fed3; mesal surface with row of four ventral setae (Fmv 1–4) and one dorsal seta Fmd3. Patella with three acuminate setae Pe and one seta Pme1 on ventro-ectal surface; with three feathered setae Pm and one seta Pmm3 on ventro-mesal surface. Setae formula on tibia 3–3–5. Tarsal spurs asymmetrical.

Legs: leg I, basitarsal–telotarsal proportions: 32: 5: 6: 6: 7: 6: 12. Femur IV 3.14 times longer than high.

Opisthosoma: tergite I with three pairs of microsetae anteriorly and one pair of Dm; tergite II with three pairs of microsetae anteriorly and pair of Dm; tergites III–VII with one pair of Dm setae each; tergite VIII with pairs Dm and DI2;

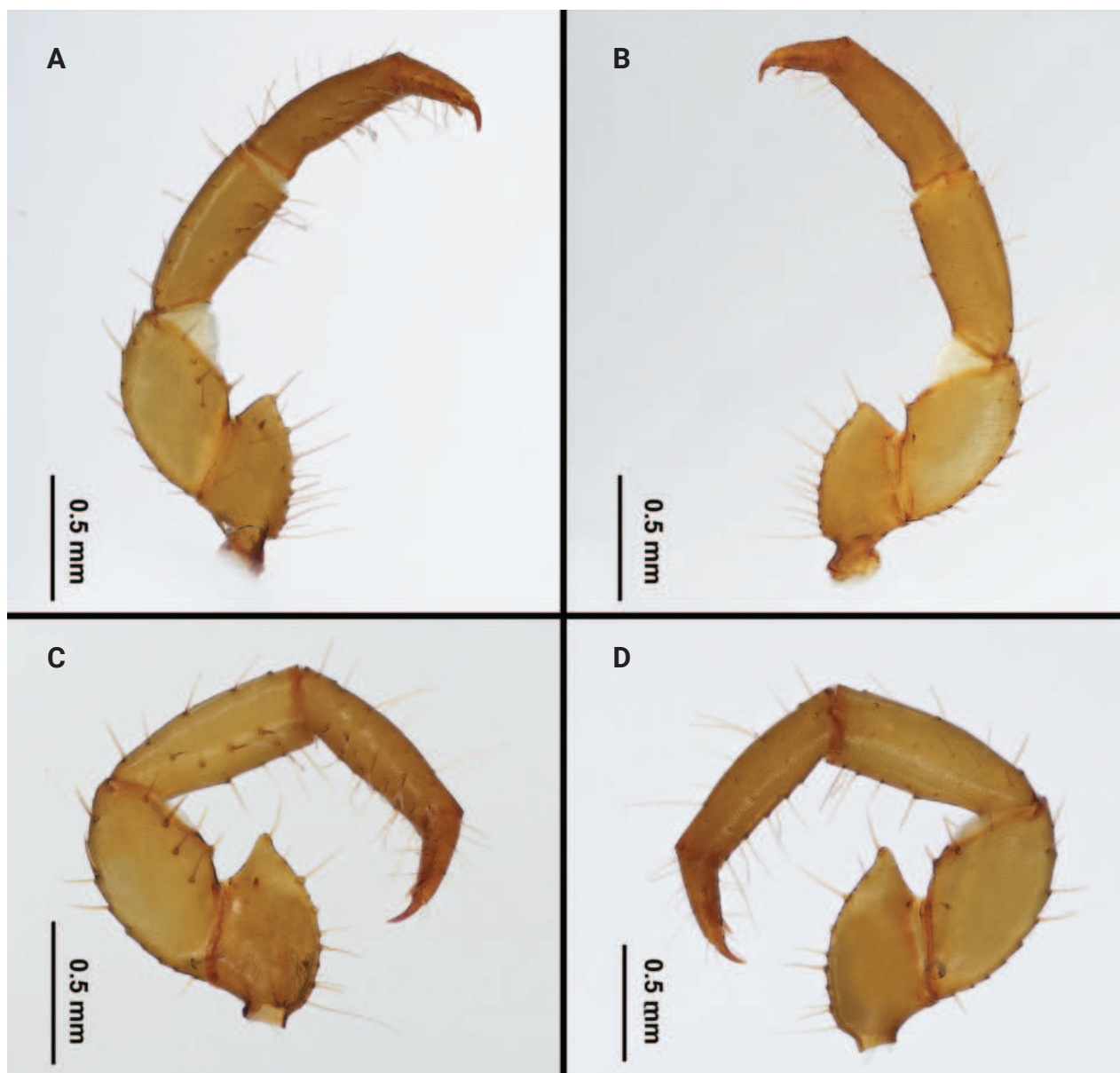


Figure 4. Palps of *Bamazomus shanghang* sp. nov., holotype male and paratype female **A** male, mesal view **B** same, ectal view **C** female, mesal view **D** same, ectal view.

tergite IX with pairs Dm, DI1 and DI2. Segments X, XI telescoped, with setal pairs Dm, DI1, DI2, Vm2, VI1, VI2, and single Vm1; segment XII with Dm, DI1, DI2, Vm2, VI1, VI2, and single Vm1, with posterodorsal process. Sternites II–VII with two irregular rows of setae each; genital plate with scattered setae.

Flagellum (Figs 5A–C, 6A–C): nearly rectangular in shape; 1.94 times longer than wide; posterior margin with three posterior processes; dorsal side with small, conical protuberance; setation: seta Dm1 situate base of bulb, two rows of microsetae located dorsolaterally next to Dm1, right row with four microsetae, left row with three microsetae; Dm4 at same level as DI3; DI2 anterior to Dm4; both sides of pedicel with DI1; Vm1 posterior to Vm2; Vm3 anterior to VI1; Vm5 at same level as VI2; two Msp between VI1 and VI2.

Female. Paratype (Fig. 2C, D): measurements as in Table 1. Colour: light brownish. Palps (Fig. 4C, D) similar to male, 1.82 times longer than propeltidium,

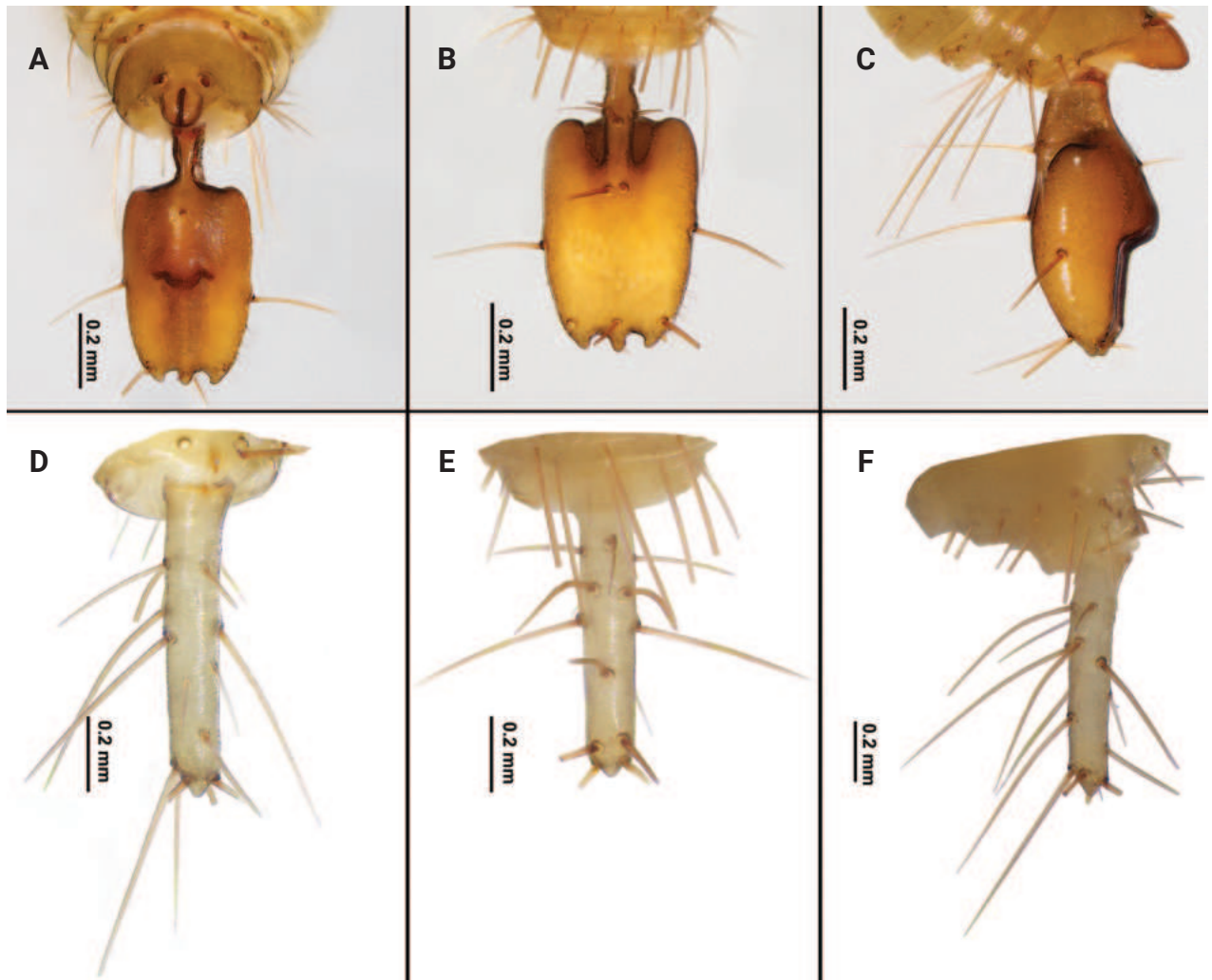


Figure 5. Flagellum of *Bamazomus shanghang* sp. nov., holotype male and paratype female **A** male, dorsal view **B** same, ventral view **C** same, lateral view **D** female, dorsal view **E** same, ventral view **F** same, lateral view.

setae formula on tibia 4–2–3. Prosoma: anterior process of propeltidium with three setae (pair of setae followed by single seta) followed by five pairs of dorsal setae. Flagellum (Figs 5D–F, 6D–F) with three flagellomeres, setation: VI1 anterior to DI2; Vm1 at same level as Vm2; DI4 posterior to Dm4; Vm3 anterior to VI1; DI3 at same level as VI2; DI1 posterior to Vm2; Vm5 posterior to DI2. Spermathecae (Fig. 7A, B) with five or six pairs of lobes, short and thick, with some apical apophyses. Chitinized arch heart-shaped, with a wide LT and with curved, wide and incomplete anterior AB. Gonopod distal bifurcation. Chelicerae (Fig. 3C, D): movable finger with one prominent accessory tooth; serrula with 17 teeth. Fixed finger with two large teeth and six smaller teeth, proximal tooth with one tiny, blunt lateral tooth. Setal group formula 3–9–5–4–10–6–1–6.

Comments. The female of new species has a more pronounced apical process of the palpal trochanter than the male, which is uncommon and generally opposite to other schizomids. Usually, there are two or three G4 on the chelicerae in Hubbardiidae, and these are concentrated in the lower row. G4 are easily confused with G7, but it is believed that G4 can be distinguished by their short setae which are thickened at the base (vs long setae which are not basally thickened), as seen in the new species.

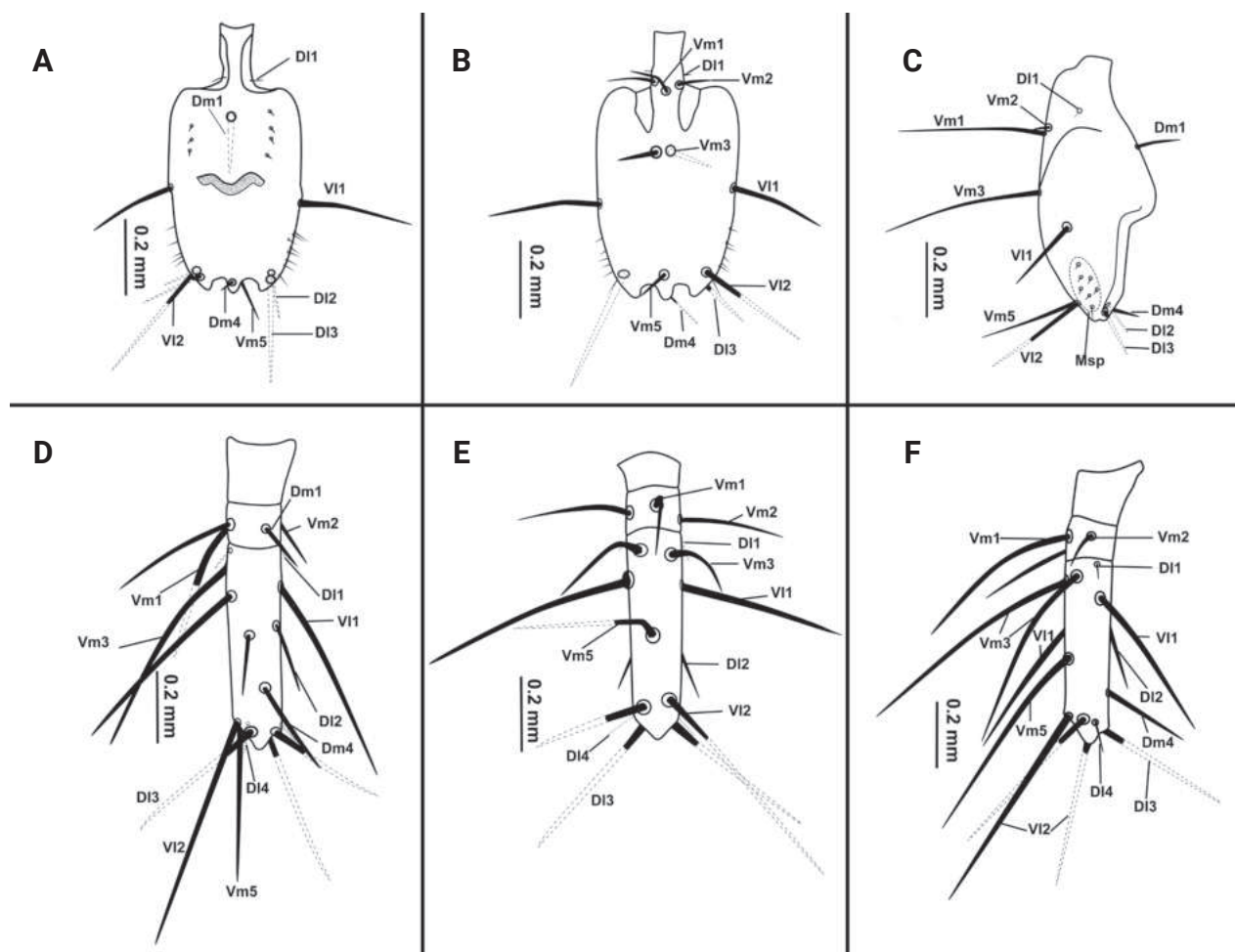


Figure 6. Flagellum of *Bamazomus shanghai* sp. nov., holotype male and paratype female **A** male, dorsal view **B** same, ventral view **C** same, lateral view **D** female, dorsal view **E** same, ventral view **F** same, lateral view. Abbreviations: Dm = dorso-median setae of abdomen and flagellum, DI = dorso-lateral setae of the abdomen and flagellum, Vm = ventro-median setae of the abdomen and flagellum, VI = ventro-lateral setae of the abdomen and flagellum.

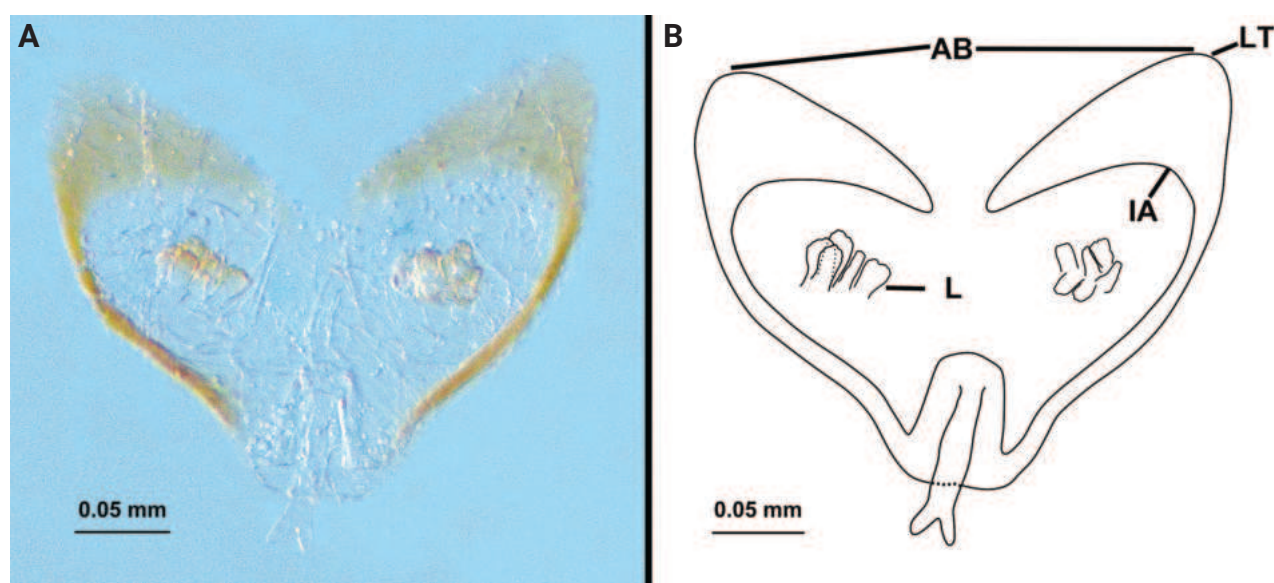


Figure 7. Spermathecae of *Bamazomus shanghai* sp. nov. **A**, **B** female paratype, dorsal view. Abbreviations: AB = anterior or branch of chitinized arch, IA = internal angle of chitinized arch, L = lobe, LT = lateral tip of chitinized arch.

Habitats. The new species was collected under a heap of leaf-covered stones. The female specimen was collected from the underside of a stone, while the male was found in the ground under the stones.

Distribution. This species is known only from the type locality (Fig. 1).

***Bamazomus songi* sp. nov.**

<https://zoobank.org/DD7C1E05-5C3C-4408-9321-20D5367790B6>

Figs 1, 8–13, Table 1

宋氏巴马加盾

Type material. *Holotype* ♂ (MHBU-ZT5-1), CHINA: Guangdong Province, Chaozhou City, Raoping County, Raoyang Town, Gangxia Village, 24.0924°N, 116.8814°E, 177 m elev., 23.VIII.2023, leg. J.-X. Gong. *Paratype*: 2♂ 4♀ (MHBU-ZT5-2), same data as the holotype.

Etymology. The specific name is a patronym in honour of the late academician Daxiang Song (1935–2008), a scholar of arachnology who was the first to describe Schizomida from China.

Diagnosis. *Bamazomus songi* sp. nov. resembles *B. shanghang* sp. nov. in having three posterior processes and a small, conical protuberance on the posterior margin of flagellum in the male, and in having spermathecal lobes with several apical apophyses and an incomplete anterior branch (Figs 5A, B, 6A, B, 7A, B), but can be distinguished by: 1) the presence of seven or eight pairs of spermathecal lobes (Fig. 13A, B) vs five or six pairs of lobes (Fig. 7A, B); 2) the short, proximally gonopod broad and wide chitinized arch (Fig. 13A, B) vs the long, proximally narrow gonopod and narrow chitinized arch (Fig. 7A, B); 3) the Dm4 anterior to the middle dorsal process of flagellum (Figs 11A, 12A) vs Dm4 on the middle dorsal process (Figs 5A, 6A); 4) the Dm4 anterior to DI3 and the Vm5 anterior to VI2 on flagellum, the long, acuminate trochanter apical process on pedipalps in the male (Figs 10A, B, 11A–C, 12A–C) vs the Dm4 posterior to DI3, the Vm5 at same level as VI2, blunt and short (Figs 4A, B, 5A–C, 6A–C).

Description. Holotype Male (Fig. 8A, B): measurements as in Table 1. Colour: brownish. Prosoma: anterior process of propeltidium with three setae (pair of setae followed by single seta) followed four pairs of dorsal setae (2+2+2+2); eye spots distinct. Mesopeltidia separated. Metapeltidium divided. Anterior sternum with 11 setae (including two sternapophysial setae); posterior sternum triangular with six setae.

Chelicerae (Fig. 9A, B): movable finger: serrula with 17 teeth, guard tooth present, with one prominent accessory tooth at subterminal part of movable finger. Fixed finger with two large teeth and four smaller teeth, proximal tooth with one tiny, blunt lateral tooth. Setation: setal group formula: 3–6–4–5–13–10–1–5. G1 with three spatulate setae; G2 composed of six feathered setae; G3 with four setae, feathered apically and smooth basally; G4 consisting of five small setae, smooth, basally thick, distally elongated; G5A with 13 similar sized setae, feathered apically and smooth basally, length almost equal to movable finger; G5B with 10 setae, basal three short and smooth, apical seven longer and feathered; G6 with one smooth seta about 1/2 of movable finger length; G7 with five smooth setae.

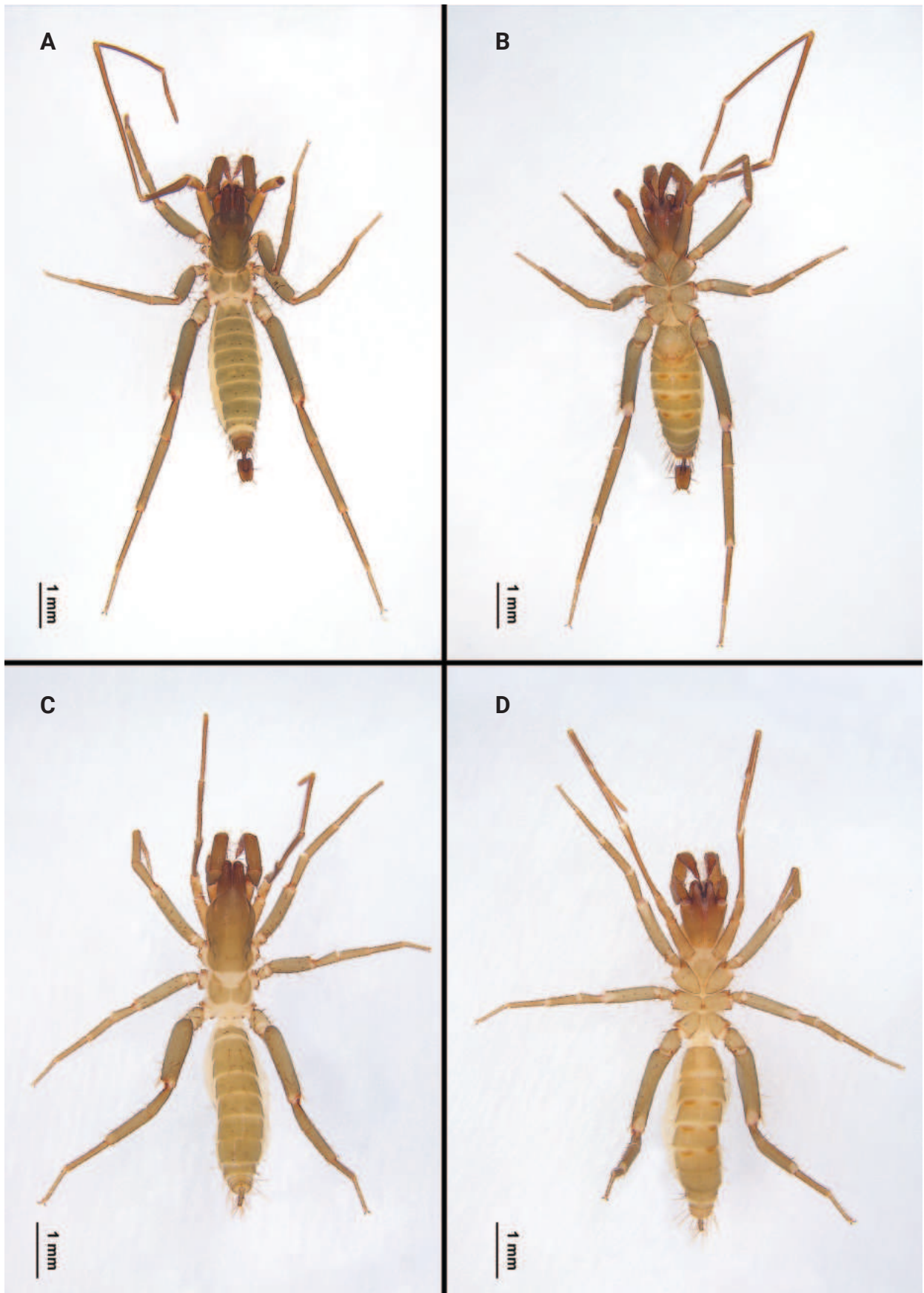


Figure 8. Habitus of *Bamazomus songi* sp. nov., holotype male and paratype female **A** male, dorsal view **B** same, ventral view **C** female paratype, dorsal view **D** same, ventral view.

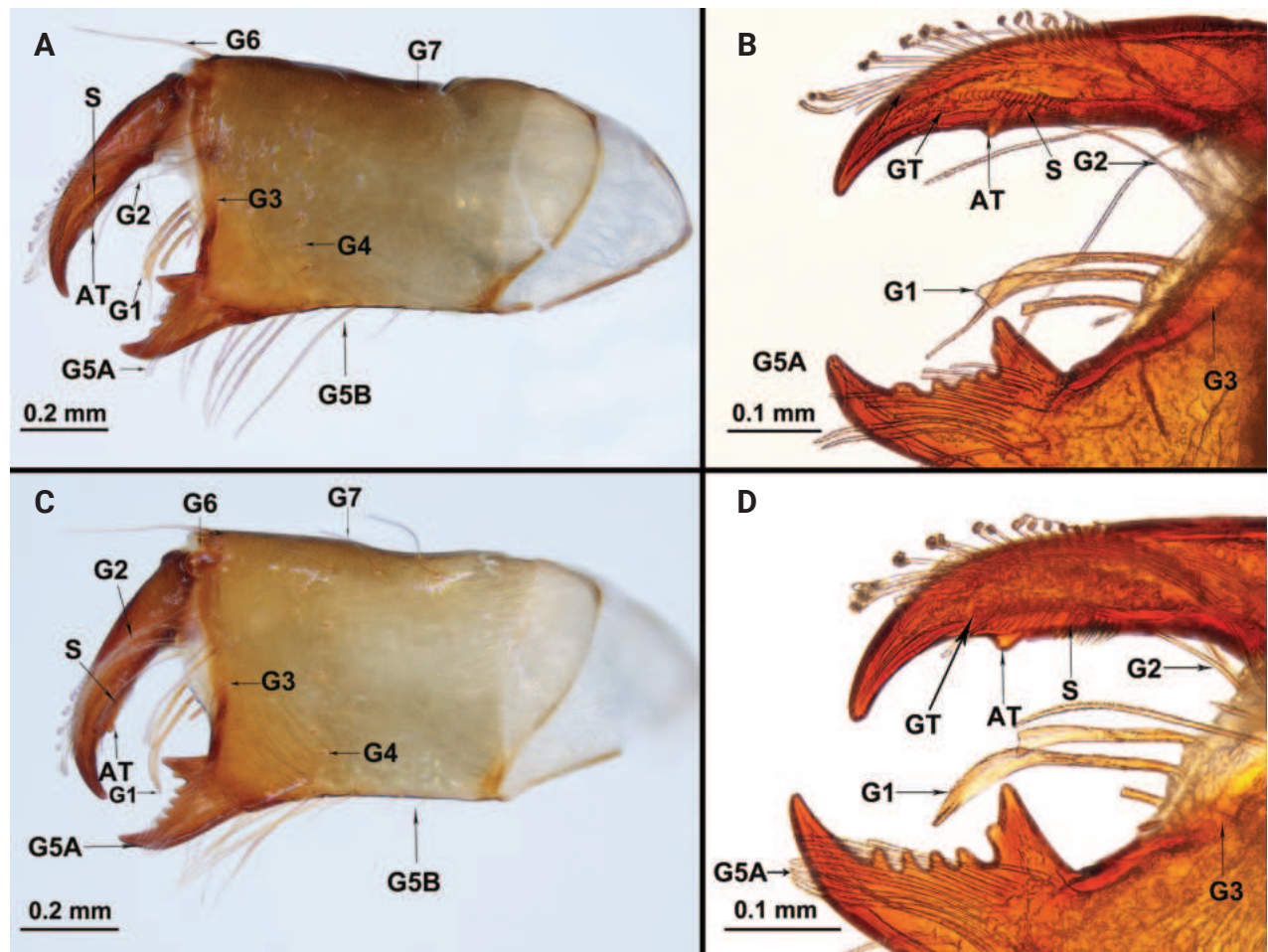


Figure 9. Chelicerae of *Bamazomus songi* sp. nov., holotype male and paratype female **A** male, mesal view **B** same, movable finger and fixed finger **C** female, mesal view **D** same, movable finger and fixed finger. Abbreviations: AT = accessory tooth of movable finger, G = setal group numbers of chelicerae, GT = guard tooth of movable finger, S = serrula.

Palps (Fig. 10A, B): 2.9 times longer than propeltidium length; trochanter with apical process, pointed apical process with angle of about 45°; mesal surface of trochanter with three setae near ventral margin and one seta near dorsal margin; with one small mesal spur. Femur 2.4 times longer than high; ventral margin on ectal surface with acuminate setae Fe1, Fe5, Fev1, Fev2 and one dorsal setae Fed3; mesal surface with a row of four ventral setae (Fmv 1–4) and one dorsal seta Fmd3. Patella with three acuminate setae Pe and one seta Pme1 on ventro-ectal surface; with three feathered setae Pm and one seta Pmm3 on ventro-mesal surface. Setae formula on tibia 5–3–6. Tarsal spurs asymmetrical.

Legs: leg I, basitarsal–telotarsal proportions: 37: 5: 6: 7: 6: 7: 13. Femur IV 3.70 times longer than high.

Opisthosoma: tergite I with three pairs of microsetae anteriorly and pair of Dm; tergite II with three pairs of microsetae anteriorly and pair of Dm; tergites III–VII with one pair of Dm setae each; tergite VIII with pairs Dm and DI2; tergite IX with pairs Dm, DI1, and DI2. Segments X, XI telescoped, with setal pairs DI1, DI2, Vm2, VI1, VI2, and single Vm1; segment XII with Dm, DI1, DI2, Vm2, VI1, VI2, and single Vm1, with posterodorsal process. Sternites II–VII with two irregular rows of setae each; genital plate with scattered setae.

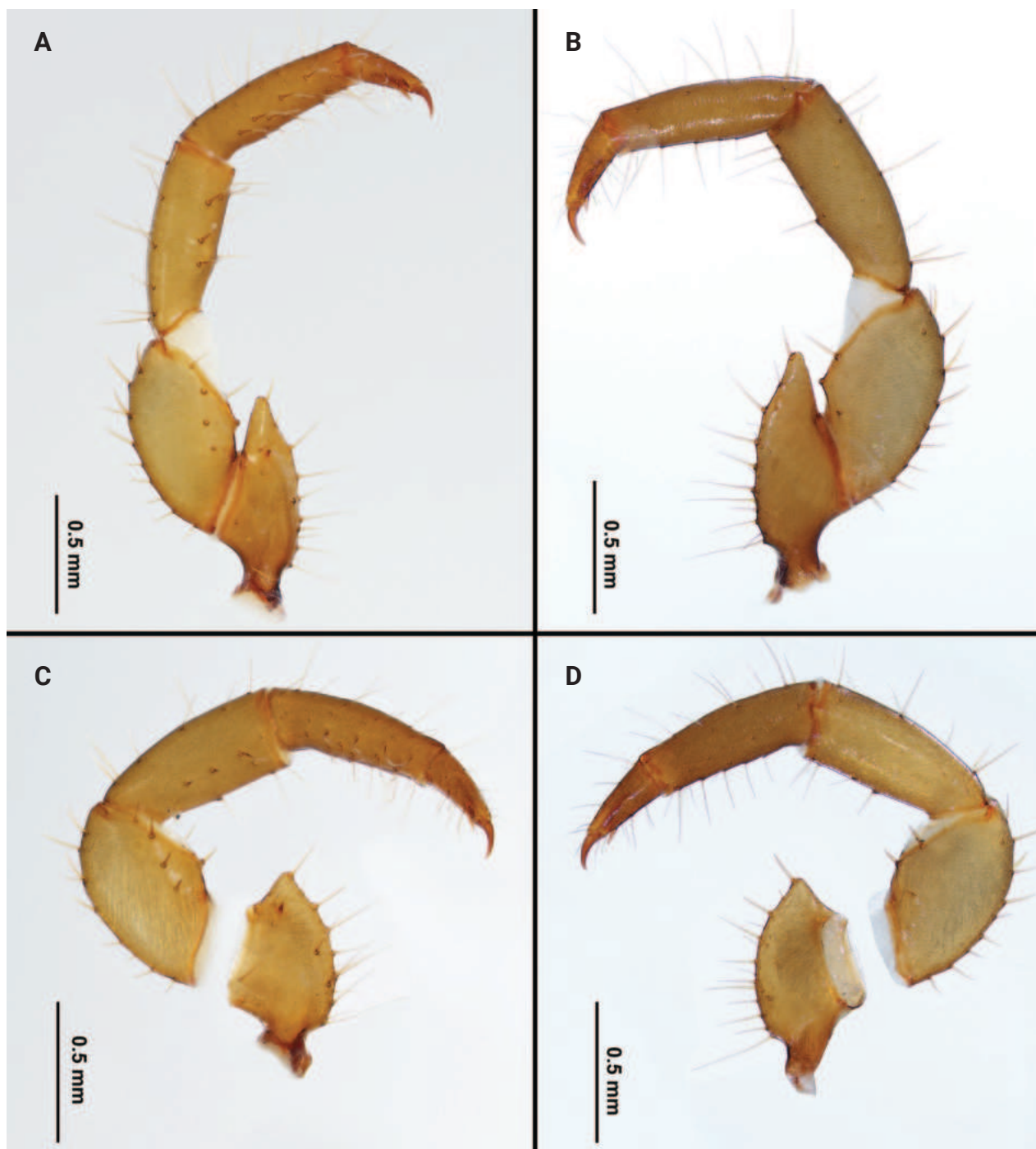


Figure 10. Palps of *Bamazomus songi* sp. nov., holotype male and paratype female **A** male, mesal view **B** same, ectal view **C** female, mesal view **D** same, ectal view.

Flagellum (Figs 11A–C, 12A–C): nearly rectangular in shape; 1.75 times longer than wide; posterior margin of flagellum with three posterior processes; the dorsal side with a small, conical protuberance; setation: seta Dm1 situate base of bulb, two rows of microsetae placed dorsolaterally next to Dm1, each row with three microsetae; Dm4 anterior to DI3; DI2 anterior to Dm4; both sides of pedicel with DI1; Vm1 posterior to Vm2; Vm3 anterior to VI1; Vm5 anterior to VI2; two Msp between VI1 and VI2.

Female. Paratype (Fig. 8C, D): measurements as in Table1. Colour: brownish. pedipalps (Fig. 10C, D) similar to male, 2.30 times longer than propeltidium

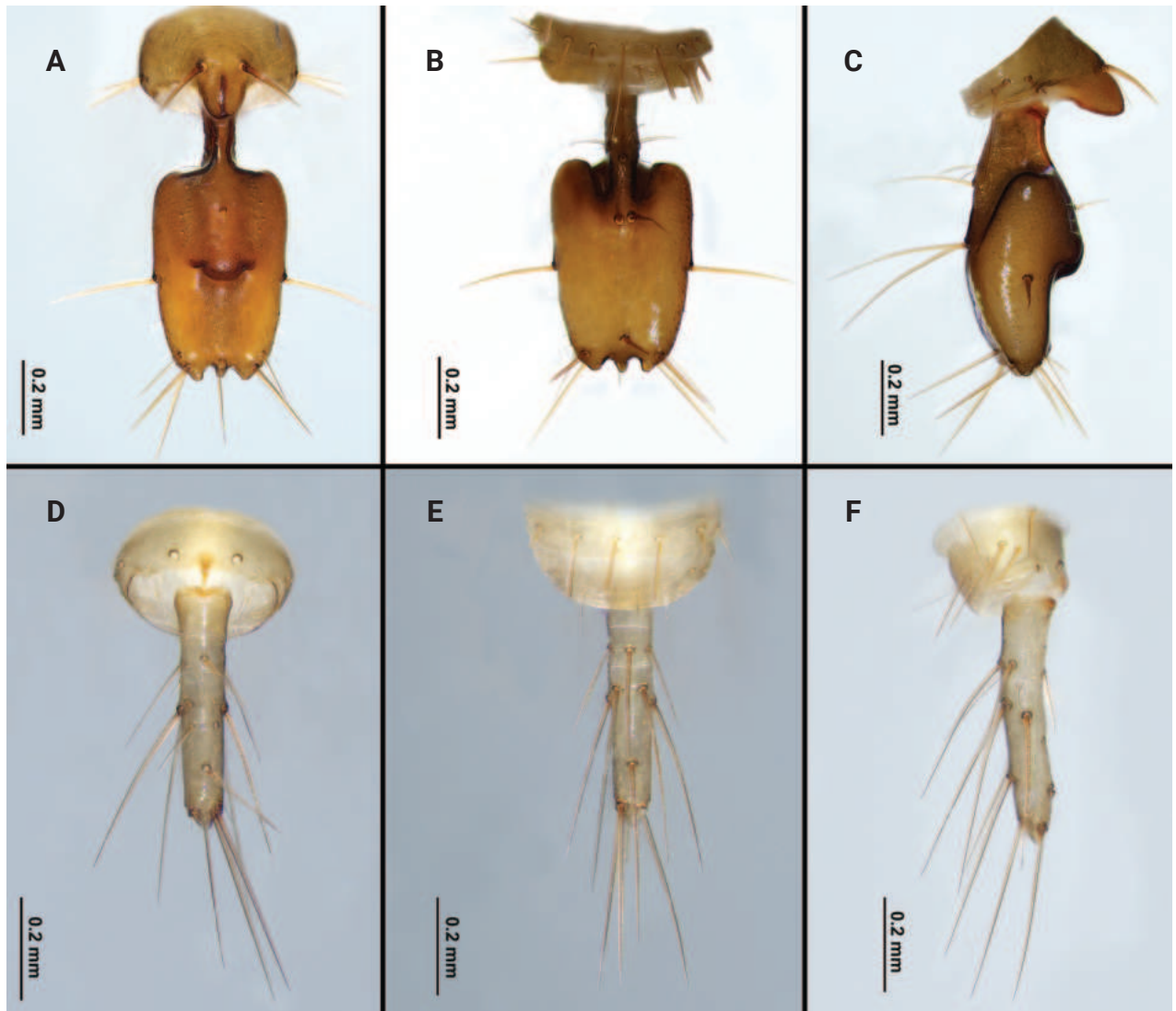


Figure 11. Flagellum of *Bamazomus songi* sp. nov., holotype male and paratype female **A** male, dorsal view **B** same, ventral view **C** same, lateral view **D** female, dorsal view **E** same, ventral view **F** same, lateral view.

length, setae formula on tibia 4–5–4. Prosoma anterior process of propeltidium with three setae (pair of setae followed by single seta) followed by four pairs of dorsal setae. Flagellum (Figs 11D–F, 12D–F) with three flagellomeres. Setation: VI1 anterior to DI2; Vm1 at same level as Vm2; DI4 posterior to Dm4; VI2 anterior to DI3; DI1 anterior to Vm3; Dm4 posterior to Vm5. Spermathecae (Fig. 13A, B) with seven or eight pairs of short, thick lobes; spermathecal lobes with many small apical apophyses and with slight bifurcations. Chitinized arch wide, heart-shaped; with a wide LT and with curved, wide and incomplete AB. Gonopod short and the base broad, with distal bifurcation. Chelicerae (Fig. 9C, D): movable finger with one prominent accessory tooth; serrula with 16 teeth. Fixed finger with two large teeth and five smaller teeth between these, including one tiny, blunt lateral tooth on proximal tooth. Setal group formula 3–6–5–4–11–9–1–5.

Comments. The number of G4 on the chelicerae of both *B. songi* sp. nov. and *B. shanghang* sp. nov. is similar, with all of them exceeding three. Therefore, previous descriptions of some species in the Hubbardiidae might have confused G4 and G7.

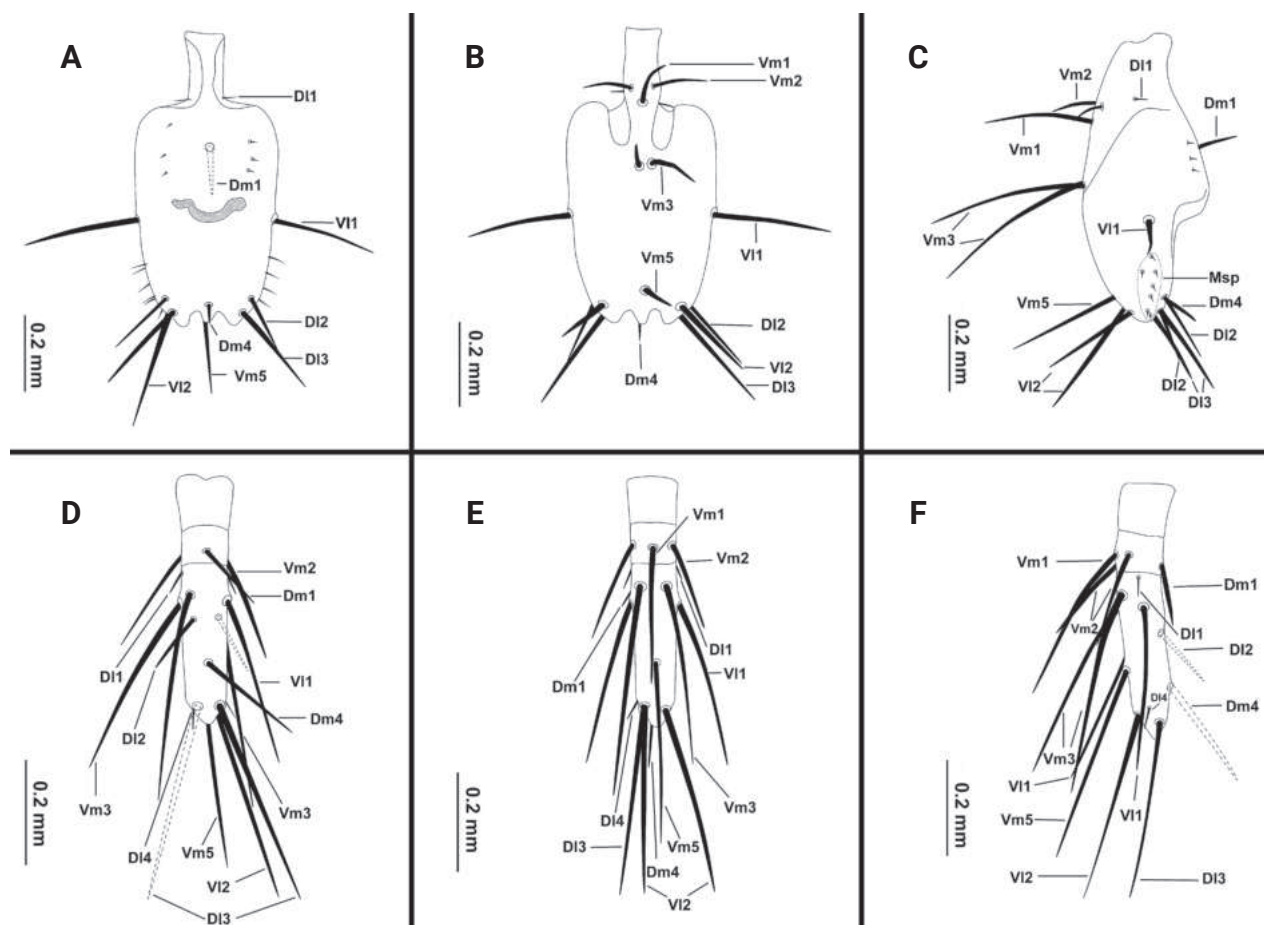


Figure 12. Flagellum of *Bamazomus songi* sp. nov., holotype male and paratype female **A** male, dorsal view **B** same, ventral view **C** same, lateral view **D** female, dorsal view **E** same, ventral view **F** same, lateral view. Abbreviations: Dm = dorso-median setae of abdomen and flagellum, DI = dorso-lateral setae of the abdomen and flagellum, Vm = ventro-median setae of the abdomen and flagellum, VI = ventro-lateral setae of the abdomen and flagellum.

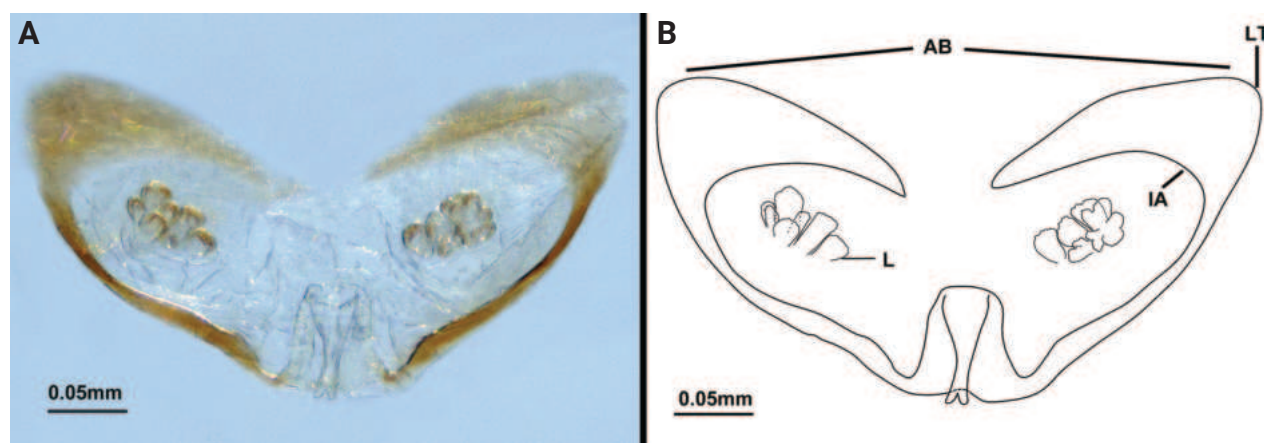


Figure 13. Spermathecae of *Bamazomus songi* sp. nov. **A**, **B** female paratype, dosal view. Abbreviations: AB = anterior branch of chitinized arch, IA = internal angle of chitinized arch, L = lobe, LT = lateral tip of chitinized arch.

Habitats. Specimens of *Bamazomus songi* sp. nov. were collected under leaf-covered, relatively wet stones near a stream.

Distribution. This species is known only from the type locality (Fig. 1).

Acknowledgements

Thanks go to Jiaqi Zhao and Xiaoru Qi (Hebei University, China) for their help during the fieldwork. We are grateful to Lorenzo Prendini (American Museum of Natural History), Mark Harvey (Western Australian Museum), and an anonymous reviewer for their valuable comments on the manuscript, to subject editor Yuri Marusik (Institute for Biological Problems of the North RAS) and copy editor Robert Forsyth for their editorial efforts. We thank Dr Xinping Wang (University of Florida) for reviewing the English in the earlier draft.

Additional information

Conflict of interest

The authors have declared that no competing interests exist.

Ethical statement

No ethical statement was reported.

Funding

This study was supported by the National Natural Science Foundation of China (no. 32170468) and by the Science and Technology Fundamental Resources Investigation Program (grant no. 2022FY202100).

Author contributions

Tao Zheng: writing-original draft the manuscript, Jiaxian Gong: writing, Feng Zhang: review and editing.

Author ORCIDs

Tao Zheng  <https://orcid.org/0009-0000-5936-9097>

Jiaxian Gong  <https://orcid.org/0009-0009-4753-0360>

Feng Zhang  <https://orcid.org/0000-0002-3347-1031>

Data availability

All of the data that support the findings of this study are available in the main text.

References

- Álvarez-Padilla F, Hormiga G (2007) A protocol for digesting internal soft tissues and mounting spiders for scanning electron microscopy. *The Journal of Arachnology* 35(3): 538–542. <https://doi.org/10.1636/Sh06-55.1>
- Cokendolpher JC (1988) Review of the Schizomidae (Arachnida, Schizomida) of Japan and Taiwan. *Bulletin of the National Science Museum, Series A: Zoology* 14(4): 159–171.
- Cokendolpher JC, Reddell JR (1986) *Schizomus siamensis* (Schizomida: Schizomidae) from eastern Asia and Hawaii. *Acta Arachnologica* 35(1): 23–28. <https://doi.org/10.2476/asjaa.35.23>
- Cokendolpher JC, Reddell JR (1992) Revision of the Protoschizomidae (Arachnida: Schizomida) with notes on the phylogeny of the order. *Texas Memorial Museum, Speleological Monographs* 3: 31–74.

- Cook OF (1899) *Hubbardia*, a new genus of Pedipalpi. *Proceedings of the Entomological Society of Washington* 4: 249–261.
- Hansen HJ, Soerensen WE (1905) The Tartarides: a tribe of the order Pedipalpi. *Biodiversity Heritage Library* 2(8).
- Harvey M (1992) The Schizomida (Chelicerata) of Australia. *Invertebrate Systematics* 6(1): 77–129. <https://doi.org/10.1071/IT9920077>
- Lawrence RF (1969) The trichoid structures on the chelicerae of the short-tailed whipscorpions (Schizomida: Arachnida). *Transactions of the Royal Society of South Africa* 38(2): 123–132. <https://doi.org/10.1080/00359196909519080>
- Monjaraz-Ruedas R, Francke OF, Cruz-López JA, Santibáñez-López CE (2016) Annuli and setal patterns in the flagellum of female micro-whipscorpions (Arachnida: Schizomida): hypotheses of homology across an order. *Zoologischer Anzeiger* 263: 118–134. <https://doi.org/10.1016/j.jcz.2016.05.003>
- Monjaraz-Ruedas R, Francke OF, Santibáñez-López CE (2017) The morphological phylogeny of the family Protoschizomidae revisited (Arachnida: Schizomida): setal characters, fossil and paraphyletic genera. *The Journal of Arachnology* 45(1): 99–111. <https://doi.org/10.1636/JoA-S-16-040.1>
- Moreno-Gonzalez JA, Delgado-Santa L, Armas LD (2014) Two new species of *Piaroa* (Arachnida: Schizomida, Hubbardiidae) from Colombia, with comments on the genus taxonomy and the flagellar setae pattern of Hubbardiinae. *Zootaxa* 3852(2): 227–251. <https://doi.org/10.11646/zootaxa.3852.2.4>
- Reddell JR, Cokendolpher JC (1995) Catalogue, bibliography, and generic revision of the order Schizomida (Arachnida). *Texas Memorial Museum. Speleological Monographs* 4: 1–170.
- Villarreal OM, Miranda GS, Giupponi APL (2016) New proposal of setal homology in Schizomida and revision of *Surazomus* (Hubbardiidae) from Ecuador. *PLOS ONE* 11(2): e0147012. <https://doi.org/10.1371/journal.pone.0147012>
- WSC (2024) World Schizomida Catalog. Natural History Museum Bern. <http://wac.nmbe.ch> [Accessed 25 February 2024]

